NASA-CR-205423

JPL Publication 97-13

Proceedings of the Twenty-First NASA Propagation Experimenters Meeting (NAPEX XXI)

and the

Advanced Communications Technology Satellite (ACTS) Propagation Studies Miniworkshop

Held in El Segundo, California
June 11–13, 1997

Nasser Golshan
Editor

August 1, 1997

National Aeronautics and
Space Administration

Jet Propulsion Laboratory
California Institute of Technology
Pasadena, California

JPL Publication 97-13

Proceedings of the Twenty-First NASA Propagation Experimenters Meeting (NAPEX XXI)

and the

Advanced Communications Technology Satellite (ACTS) Propagation Studies Miniworkshop

Held in El Segundo, California
June 11–13, 1997

Nasser Golshan
Editor

August 1, 1997

National Aeronautics and
Space Administration

Jet Propulsion Laboratory
California Institute of Technology
Pasadena, California

This publication was prepared by the Jet Propulsion Laboratory, California Institute of Technology, under a contract with the National Aeronautics and Space Administration.

ABSTRACT

The NASA Propagation Experimenters (NAPEX) meeting is convened each year to discuss studies supported by the NASA Propagation Program. Representatives from the satellite communications industry, academia and government who have an interest in space-ground radio wave propagation are invited to NAPEX meetings for discussions and exchange of information. The reports delivered at this meeting by program managers and investigators present recent activities and future plans. This forum provides an opportunity for peer discussion of work in progress, timely dissemination of propagation results, and close interaction with the satellite communications industry.

NAPEX XXI took place in El Segundo, California on June 11–12, 1997 and consisted of three sessions. Session I, entitled "ACTS Propagation Study Results & Outcome ," covered the results of 20 station-years of Ka-band radio-wave propagation experiments. Session II, "Ka-band Propagation Studies and Models," provided the latest developments in modeling, and analysis of experimental results about radio wave propagation phenomena for design of Ka-band satellite communications systems. Session III, "Propagation Research Topics," covered a diverse range of propagation topics of interest to the space community, including overviews of handbooks and databases on radio wave propagation. The ACTS Propagation Studies miniworkshop was held on June 13, 1997 and consisted of a technical session in the morning and a plenary session in the afternoon. The morning session covered updates on the status of the ACTS Project & Propagation Program, engineering support for ACTS Propagation Terminals, and the Data Center. The plenary session made specific recommendations for the future direction of the program.

PREFACE

The NASA Propagation Experimenters (NAPEX) meeting is convened each year to discuss studies supported by the NASA Propagation Program. The reports delivered at this meeting by program managers and investigators present our recent activities and future plans. Representatives from the satellite communications industry, academia and government who have an interest in space-ground radio wave propagation are invited to NAPEX meetings for discussions and exchange of information. This forum provides an opportunity for peer discussion of work in progress, timely dissemination of propagation results, and close interaction with the satcom industry. NAPEX XXI took place at Embassy Suites Hotel in El Segundo, California on June 11–12, 1997 and consisted of the welcome, opening remarks, and three sessions. Steve Townes, the Manager of Space Communications Technology Program at JPL, welcomed the participants on behalf of our NASA sponsor, Ramon Depaula. Townes commended the close interaction between the program and industry, and called for an even closer partnership and sharing of resources. N. Golshan, the JPL technical manager for the Propagation Program, made the opening remarks, recognizing the outstanding work of the NASA Propagation Experimenters community, excellent participation by the U.S. satellite communications industry, and NASA's foresight for timely investment in this critical technology for utilization of the Ka-band.

Session I, entitled " ACTS Propagation Study Results & Outcome" was chaired by L. Ippolito of Stanford Telecom and covered the results of 20 station-years of Ka-band radio wave propagation experiments. Session II, "Ka-band Propagation Studies and Models" was chaired by F. Davarian of Hughes Space and Communications; it addressed the latest developments in modeling, and analysis of experimental results about radio wave propagation phenomena for design of Ka-band satellite communications systems. Session III, "Propagation Research Topics" was chaired by W. Vogel of University of Texas at Austin, and covered a diverse range of propagation topics of interest to the space community including overviews of handbooks and databases on radio wave propagation. The ACTS Propagation Studies miniworkshop was held on June 13, 1997 and consisted of a technical session in the morning and a plenary session in the afternoon. The morning session was chaired by R. Bauer of NASA LeRC; it covered updates on the status of the ACTS Project & Propagation Program, engineering support for ACTS Propagation Terminals, and the Data Center. The plenary session was chaired by D. Rogers of Communications Research Center and W. Vogel. The plenary session made important recommendations for the future direction of the program.

The success of the meeting owes a lot to the speakers and session chairs and the active participation of all attendees. Special thanks are due S. Townes of JPL and R. Depaula of NASA HQ for the programmatic support of the NASA Propagation Program. I would like to express my thanks to R. Bauer, my counterpart at NASA LeRC for his support of the NASA Propagation Program through the ACTS Project. Last but not least, I would like to thank Mardy Wilkins of JPL for meticulously taking care of many administrative details of the meetings and to C. Cordaro of JPL Technical Information Section for coordinating the publication of this document.

The next ACTS workshop will be held in Boca Raton, Florida on or around November 18,19, 1997. The Next NAPEX meeting will take place in late May or early June of 1997 in Austin,Texas; the exact time and location will be announced by December 1997.

–N. Golshan

CONTENTS

1. ACTS Propagation Study Results and Outcomes

2. Ka-Band Propagation Studies and Models

3. Propagation Research Topics,

4. ACTS Propagation Studies Mini Workshop

CONTENTS (Continued)

1. ACTS Propagation Study Results and Outcomes

IGN OBJECTIVES AND APPROACH

cations Technology Satellite (ACTS) to characterize
:ation by U.S. industry and the space community

at seven sites in North America to receive ACTS
:e measured for subsequent correlation with signal

ıre collected and processed by site PI's
stributed on CD-ROMs for further investigation

: ACTS PROPAGATION CAMPAIGN:

ıttenuation and scintillation

due to propagation

ɔf satellite communications systems

ACTS PROPAGATION STUDIES BACKGROUND AND OBJECTIVES

Nasser Golshan

NASA Propagation Program

Jet Propulsion Laboratory
California Institute of Technology

ACTS PROPAGATION CAMPAIGN OBJECTIVES AND APPROACH

OBJECTIVE:

- To leverage NASA's Advanced Communications Technology Satellite (ACTS) to characterize radiowave propagation at Ka-band for utilization by U.S. industry and the space community

APPROACH:

- ACTS Propagation Terminals are deployed at seven sites in North America to receive ACTS beacon signals at 20 & 27 Ghz; rain-rates are measured for subsequent correlation with signal attenuation
  - Signal attenuation and rain-rate data are collected and processed by site PI's
  - Data from all sites are archived and distributed on CD-ROMs for further investigation

EXPECTED RESULTS & OUTPUTS OF THE ACTS PROPAGATION CAMPAIGN:

- Ka-band propagation data
- Prediction models of rain and atmospheric attenuation and scintillation
- Fade and nonfade distributions
- Frequency scaling models
- Diversity models
- Mitigation schemes for signal impairments due to propagation
- Wet antenna effect model
- Rain climate region map revision
- Revised propagation handbooks for design of satellite communications systems
- Contributions to regulatory organizations

ACTS PROPAGATION CAMPAIGN MILESTONES

• First planning workshop held in Santa Monica, Ca	1987
• Announcement of Opportunity released	1989
• Virginia Polytechnic Institute commissioned to develop the ACTS Propagation Terminal	1989
• Terminals delivered and ACTS launched	1993
• Two years (14 station-years) of ACTS propagation data distributed on CD-ROM	1996
• Work started to use ACTS propagation data to revise propagation models and handbooks	1996
• Three years (20 station-years) of ACTS propagation data distributed on CD-ROM	1997
• Revised propagation models and handbooks to be distributed	1998
• Four years (27 station-years) of ACTS propagation data to be distributed on CD-ROM	1998
• Rain Climate Region Map to be revised	1998-1999
• Contributions to regulatory organizations to be made	1998-1999
• Five years (34 station-years) of ACTS propagation data to be distributed on CD-ROM	1999
• ACTS transitions into inclined orbit	1999

Three Years of Propagation Studies in Alaska

BRADLEY E. JAEGER, DONALD L. HOPKINS, CHARLES E. MAYER

I. INRODUCTION

This report surveys some of the comparisons being made between analyzed propagation data for Fairbanks and established models. Of prime importance to the ACTS propagation campaign is the total attenuation measurements (AFS). Figures 1 and 2 show the yearly attenuation curves versus percentage time for each of the three years of the experiment, for measurement frequencies of 20.2 and 27.5 GHz respectively. Figures 3 and 4 compare the measured attenuation with respect to clear air (ACA = AFS - gaseous absorption) to the predicted attenuation values from the Crane global model and the ITU model.

II. SEVERELY ERRORED SECONDS (SES)

The ITU-T has laid out objectives for digital transmission quality for a hypothetical reference connection (longest length) in recommendation G821. These are in place to suit the needs of high demand services in ISDN. For high grade transmission systems, operating at 64 kbits/s, the severely errored seconds (SES) allocation to a satellite link is 0.03% of available time[1]. The preliminary results in this discussion focus on the propagation effects contribution to predictable severely errored seconds. In particular, three yearly rates of severely errored seconds in Fairbanks are compared to the Matsudo-Karasawa model for the rate of SES due to tropospheric scintillations[2].

The Matsudo-Karasawa model has S(1%) and P_t as arguments. S(1%) is the ratio of fading due to tropospheric scintillations at 1%, $A_s(1\%)$, over approximate total fading at 1%, $A_t(1\%)$,

$$S(1\%)=A_s(1\%)/A_t(1\%) \tag{1}$$

where

$$A_t(1\%) \approx \sqrt{A_r^2(1\%) + A_s^2(1\%)}\,.$$

$A_r(1\%)$ is the fading due to rain. P_t is the percentage of time for which the signal is below a threshold. The model predicts the percentage of severely errored seconds in available time, $P_{s/a}$,

$$P_{s/a} = 10^A \cdot P_t^B \tag{2}$$

where

$$A = 1.42 \cdot S(1\%) - 1.29 \pm \Delta P_{s/a1}$$

$$B = -0.61 \cdot S(1\%) + 1.46 \pm \left(\Delta P_{s/a10} - \Delta P_{s/a1}\right)$$

$$\Delta P_{s/a10} = 0.179 \cdot \sqrt{1.1 + \left(S(1\%) - 0.459\right)^2 / 0.452}$$

$$\Delta P_{s/a1} = 0.357 \cdot \sqrt{1.1 + \left(S(1\%) - 0.459\right)^2 / 0.452}\,.$$

The ± signs are for computing 95% confidence intervals. It should be noted that $P_{s/a}$ represents the time below a threshold and does not have to be equal to the percentage time of SES. This is because a severely errored second is a one second interval for which the BER exceeds 10^{-3}. For any particular system, the model can still be used to predict SES but the signal level, noise temperature characteristics, modulation, and coding of the communication system must be taken into account.

Figures 5 through 10 show 20.185 GHz or 27.505 GHz $P_{s/a}$ at Fairbanks along with predictions from the Matsudo-Karasawa model. Bias was taken as the natural logarithm of measured $P_{s/a}$ over predicted $P_{s/a}$. Errors are given in table I.

Table I.

	1994	1995	1996
20.185 GHz Avg Bias	-0.48238	0.857016	1.731565
20.185 GHz RMSD Bias	1.437727	1.159328	2.19551
27.505 GHz Avg Bias	-0.37284	1.207129	0.867589
27.505 Ghz RMSD Bias	1.312866	1.390923	1.329941

Within each figure is given a hypothetical table. These tables are intended to illustrate the application of $P_{s/a}$. If a hypothetical receiver has a BER of 10^{-3} with 0 dB fade margin then the tables indicate the availability and $P_{s/a}$ achieved with several low fade margins. As can be seen from the tables such a hypothetical receiver would need a fade margin exceeding 3 dB to meet the ITU-T objective of 0.03% SES in available time.

III. INSTANTANEOUS ATTENUATION RATIO

Attenuation scaling in rain is affected by many things. It is affected by the drop size distribution[3]. Scaling is also a function of temperature because changes in scattering are related to changes in the refractive index of water. The refractive index of water is a function of temperature[4]. It is also affected by the wave polarization since falling rain drops form oblate spheroidal shapes [5]. The terminal velocity of rain drops is important for attenuation scaling with rain rate[6]. Finally, the statistical distribution of rain rate with time along the path is important if scaling is derived from an attenuation prediction model.

In order to eliminate fluctuation due to scintillations, the instantaneous attenuation ratio is calculated as:

$$<ACA27>_{2\text{-min}}/<ACA20>_{2\text{-min}}. \qquad (3)$$

Most models of rain attenuation scaling are statistical in nature and somehow describe the rain profile along the path, using one or two model parameters

The Hodge model makes the assumption that the rainfall along the path is a Gaussian function of position, $R(x)=R_0 \cdot \exp-(x/l_0)^2$ [7]. Using the power law and integrating over the path (over x) $A_1=a_1 R_0^{b1} \cdot l_0 \cdot \sqrt{(\pi/b_1)}$. Solving for R_0 and substituting into $A_2=a_2 R_0^{b2} \cdot l_0 \cdot \sqrt{(\pi/b_2)}$ with the assumption $l_0^{(1-b2/b1)} \approx 1$ simplifies to the result:

$$\frac{A_2}{A_1} = \frac{a_2}{a_1}\left(\frac{A_1}{a_1}\cdot\sqrt{\frac{b_1}{\pi}}\right)^{\left(\frac{b_2}{b_1}-1\right)}\cdot\sqrt{\frac{b_1}{b_2}}. \qquad (4)$$

The Kheirallah model assumes the extent of the rain is given by an apparent rain rate and apparent path length, independent of frequency [8]. This approximation was later shown to have a quantifiable error which could be removed by introducing a two frequency scaling relation. Using the power law, $A_1=a_1 \cdot R^{b1} \cdot l_1 = a_1 \cdot R_{app}^{b1} \cdot l_{app}$ and $A_2=a_2 \cdot R^{b2} \cdot l_2 = a_2 \cdot R_{app}^{b2} \cdot l_{app}$. Solving for $l_2=l_1^{b2/b1} \cdot l_{app}^{1-b1/b2}$ and making the assumption $l_{app}^{1-b1/b2} \approx 1$ then $l_2 \approx l_1^{b1/b2}$. Substituting $R=(A_1/a_1)^{(1/b1)}$ and $l_2 \approx l_1^{b1/b2}$ in A_2, the one frequency scaling relation is:

$$A_2 = a_2 \cdot \left(\frac{A_1}{a_1}\right)^{\frac{b_2}{b1}}. \qquad (5)$$

The Rue model assume a single rain cell with an core of intense rain surrounded by a much larger body of light rain [9]. The core is assumed to be d=3 km, the body of light rain is assumed to be at R_{res}=5 mm/hr and the path length parameter , D, is 27 km or L-3 km which ever is smaller. Using the power law, $A_1=k_1 \cdot R_{res}^{\alpha 1} \cdot D+k_1 \cdot R^{\alpha 1} \cdot d$. Solving for R and substituting into $A_2=k_2 \cdot R_{res}^{\alpha 2} \cdot D+k_2 \cdot R^{\alpha 2} \cdot d$, the scaling relation is:

$$A_2 = k_2 \cdot R_{res}^{\alpha_2} \cdot D + k_2 \cdot d \left\{ \frac{A_1 - k_1 \cdot R_{res}^{\alpha_1} \cdot D}{k_1 \cdot d} \right\}^{\frac{\alpha_2}{\alpha_1}}. \qquad (6)$$

The Bothias or ITU model is intended to be independent of drop size distribution. It was derived by making an empirical fit to all available data [9]. The scaling relation is:

$$A_2 = A_1 \cdot \left(\frac{\varphi_2}{\varphi_1} \right)^{1-H(\varphi_1, \varphi_2, A_1)} \qquad (7)$$

with

$$\varphi(f) = \frac{f^2}{1 + 0.0001 \cdot f^2}$$

$$H(\varphi_1, \varphi_2, A_1) = 0.00112 \cdot \left(\frac{\varphi_2}{\varphi_1} \right)^{0.5} \cdot (\varphi_1 \cdot A_1)^{0.55}.$$

The Fedi model is equivalent to assuming a constant path length of 4 km [9]. Using the power law, $A_1=k_1 R^{\alpha 1} \cdot 4$. Solving for R and substituting into $A_2=k_2 R^{\alpha 2} \cdot 4$, the scaling relation is:

$$A_2 = 4 \cdot k_2 \cdot \left(\frac{A_1}{4 \cdot k_1} \right)^{\frac{\alpha_2}{\alpha_1}}. \qquad (8)$$

Figures 11 through 13 show 27.505/20.185 GHz instantaneous attenuation ratio by base attenuation at Fairbanks. Bias calculations are shown with each chart. Over three years, the data shows the least RMSD variation about the Rue (50%) model.

IV. ATTENUATION WITH RESPECT TO CLEAR AIR (ACA)

To do justice to the variety of models for rain attenuation is beyond the scope of this report. Suffice it to say these models are vital for constructing link budgets and evaluating transmission quality as in the SES model discussed earlier. *Electromagnetic Wave Propagation Through Rain* explains the foundations of rain attenuation models and the Global model and the Two Component model are well developed [10]. The Simple Attenuation Model can be found in *Radio Science* [11]. The ITU-R and COMSAT models are available from JPL [12].

Figures 14 and 15 show yearly cumulative distributions at Fairbanks compared to the models listed above. Bias calculations are given with each chart. The data shows the least RMSD variation about the CCIR '90 model.

A. WORST MONTH

Electromagnetic Wave Propagation Through Rain explains the basis for models for the worst month [10]. The ITU-R model is given in the Green Book [13].

Figures 16 and 17 show worst months for 1994 through 1996 at Fairbanks along with the ITU-R and Two Component Models. The measured average year was used as input to the ITU-R model. Average and RMSD bias values are given in the charts. Figures 18 and 19 show an

alternate presentation of the ITU-R model. These figures show Q, the ratio of worst month to average year. Measure values of Q diverge for average year time percentages less than about 0.01% due to dynamic range limitations.

V. RAIN RATE

Rain rate distributions form an integral part of most attenuation prediction models. The Global rain rate distribution is a fit to available rain rate distributions within each Global model climate zone. It can be found in *Electromagnetic Wave Propagation Through Rain* [10]. The Rice-Holmberg model uses the sum of exponential distributions. Parameters for the Rice-Holmberg model are available from NTIS [14]. The ITU-R model describes the tail of the rain rate distribution given the rain rate at 0.01% of the time and can be found in the Green Book [15].

Figures 20 and 21 show yearly cumulative distributions of rain rate with model distributions. The measured rain rate at 0.01% was used as the input for the ITU-R model. Bias calculations are shown for each model. Figures 18 and 19 show worst month distributions against the ITU model. Model values were calculated by multiplying the average year exceedances by Q [13].

VI. GASEOUS ABSORPTION

In addition to rain, gaseous absorption is needed for link budgets. The ITU-R model for gaseous absorption is an approximation to more complicated calculations. The approximation employs the surface water vapor density and the frequency as inputs [16]. Figures 24 and 25 show 3 year cumulative distributions of gaseous absorption. The differences between measured values and ITU model values probably arise from two sources. First, some error is likely incurred from not precisely calculating absorption from a profile of temperature, pressure, and water vapor density with height. Second, some error likely arises from using the ITU- R approximation at water vapor densities above 12 g/m^3.

VII. SUMMARY

This report has explored SES, instantaneous attenuation ratio, and distributions important for modeling rain attenuation. The application of $P_{s/a}$ has been demonstrated. The three years of instantaneous attenuation ratio showed the least variation about the Rue (50%) model. Yearly cumulative distributions of attenuation showed the least variation about the CCIR '90 model.

REFERENCES

[1] R. W. McLintock and B. N. Kearsey, "Error Performance Objectives for Digital Networks," *British Telecommunications Engineering*, vol. 3, pp. 92-98, Jul. 1984.

[2] T. Matsudo, and Y. Karasawa, "Characteristics and Predictions Methods for the Occurrence Rate of SES in Available Time Affected by Tropospheric Scintillations," *Electronics and Communications in Japan*, vol. 74, no. 8, pp. 89-100, 1991.

[3] T. Ihara, and Y. Furuhama, "Frequency Scaling of Rain Attenuation at Centimeter and Millimeter Waves Using a Path-averaged Drop Size Distribution," *Radio Science*, vol. 16, no. 6, pp. 1365-1372, Nov.-Dec. 1991.

[4] P. Ray, "Broadband Complex Refractive Indices of Ice and Water," *Applied Optics,* vol. 11, no. 8, pp. 1836-1844, Aug. 1972.

[5] T. Oguchi, "Scattering Properties of Pruppacher-and-Pitter Form Raindrops and Cross Polarization Due to Rain: Calculations at 11, 13, 19.3, and 34,8 GHz," *Radio Science,* vol. 12, no. 1, pp. 41-51, Jan.-Feb. 1977.

[6] G. B. Foote and P. S. Du Toit, "Terminal Velocity of Raindrops Aloft," *Journal of Applied Meteorology,* vol. 8, pp. 249-253, Apr. 1969.

[7] D. Hodge, "Frequency Scaling of Rain Attenuation," *IEEE Transactions on Antennas and Propagation,* pp. 446-447, May 1978.

[8] H. Kheirallah et al., "Frequency Dependence of Effective Path Length in Prediction of Rain Attenuation Statistics," *Electronics Letters,* vol. 16, no. 12, pp. 448-450, Jun. 1980.

[9] J. E. Allnutt, *Satellite-to-ground Radiowave Propagation,* London: Peregrinus, 1989, pp. 219.

[10] R. K. Crane, *Electromagnetic Wave Propagation Through Rain,* New York: Wiley-Interscience, 1996.

[11] W. L. Stutzman and K. M. Yon, "A Simple Rain Attenuation Model for Earth-space Radio Links Operating at 10-35 GHz," *Radio Science,* vol. 21, no. 1, pp. 65-72, Jan.-Feb. 1986.

[12] A. Kantak, K. Suwitra, and C. Le, "Database Software for Propagation Models," *Reference Manual-Version 3.0,* JPL D-11843, Jun. 1995.

[13] "Worst-Month Statistics," *Recommendations and Reports of the CCIR-Volume V Propagation in Non-ionized Media,* XVIth Plenary Assembly, Dubrovnik, 1986, pp. 231-239.

[14] E. J. Dutton, "Prediction Variability in the U.S.A. for Microwave Terrestrial System Design," OTR 77-134 (NTIS, Springfield, VA 22151), Aug. 1974.

[15] "Radiometeorological Data," *Recommendations and Reports of the CCIR-Volume V Propagation in Non-ionized Media,* XVIth Plenary Assembly, Dubrovnik, 1986, pp.132.

[16] "Propagation Data and Prediction Methods Required for Earth-space Telecommunication Systems," *Recommendations and Reports of the CCIR-Volume V Propagation in Non-ionized Media,* XVIth Plenary Assembly, Dubrovnik, 1986, pp.392-393.

Fig. 1 - Alaska 20 GHz Yearly Attenuation EDF's

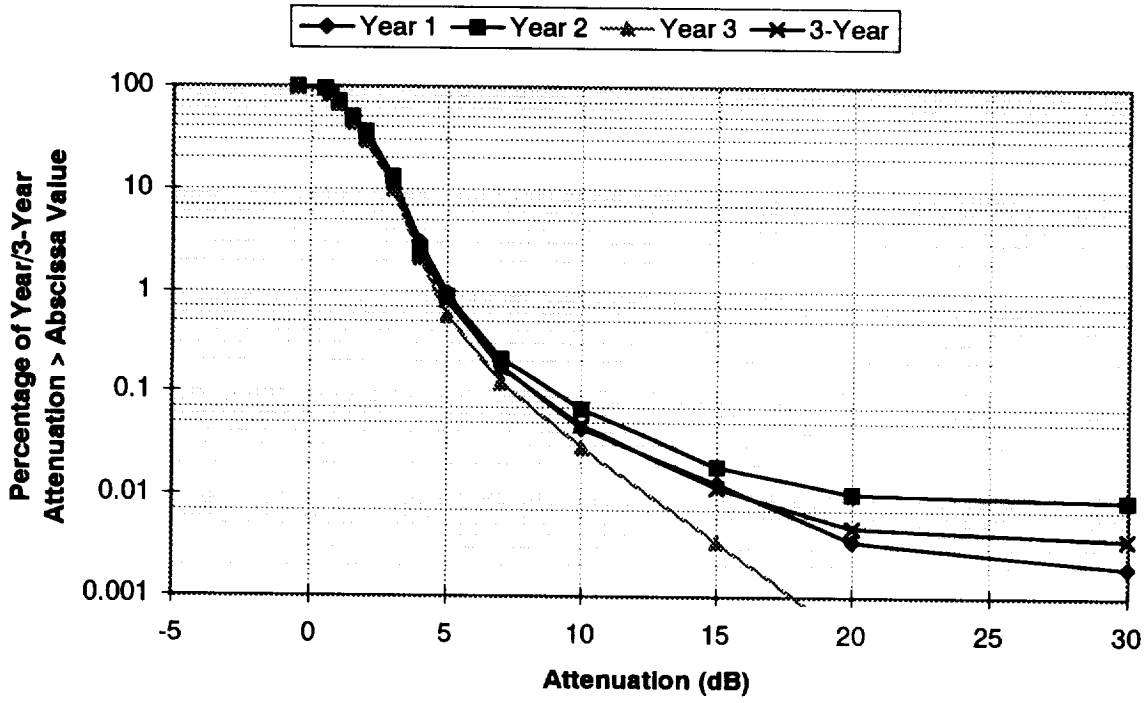

Fig. 2 - Alaska 27 GHz Yearly Attenuation EDF's

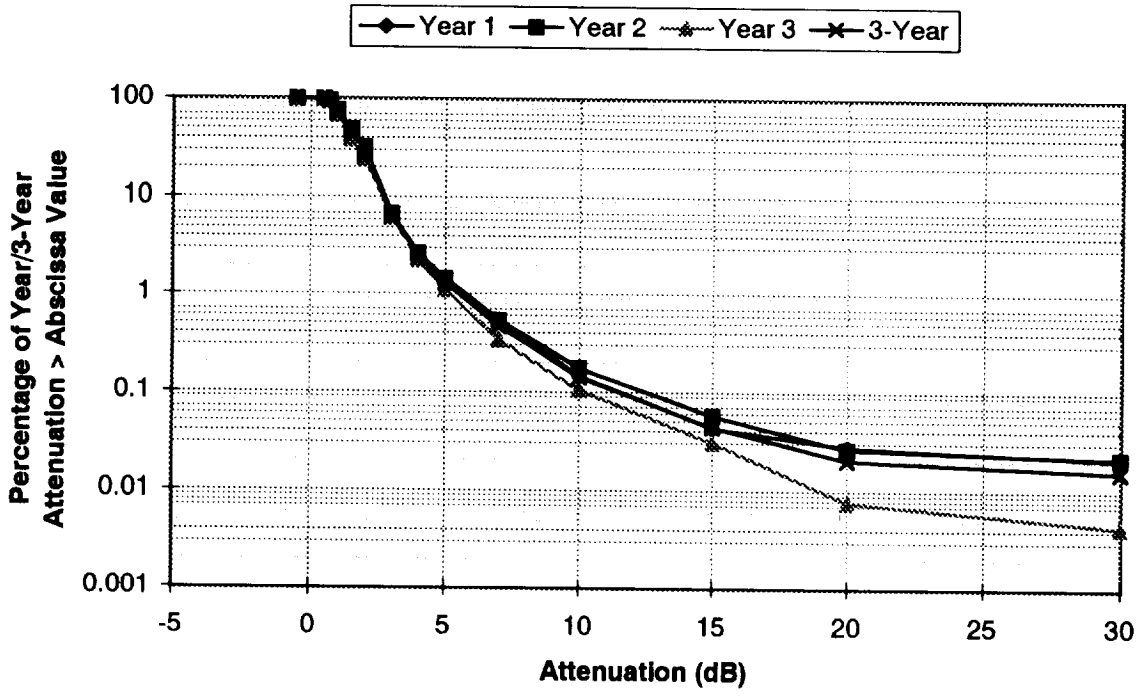

Fig. 3 - Alaska 3-Year 20 GHz Attenuation EDF vs. Models

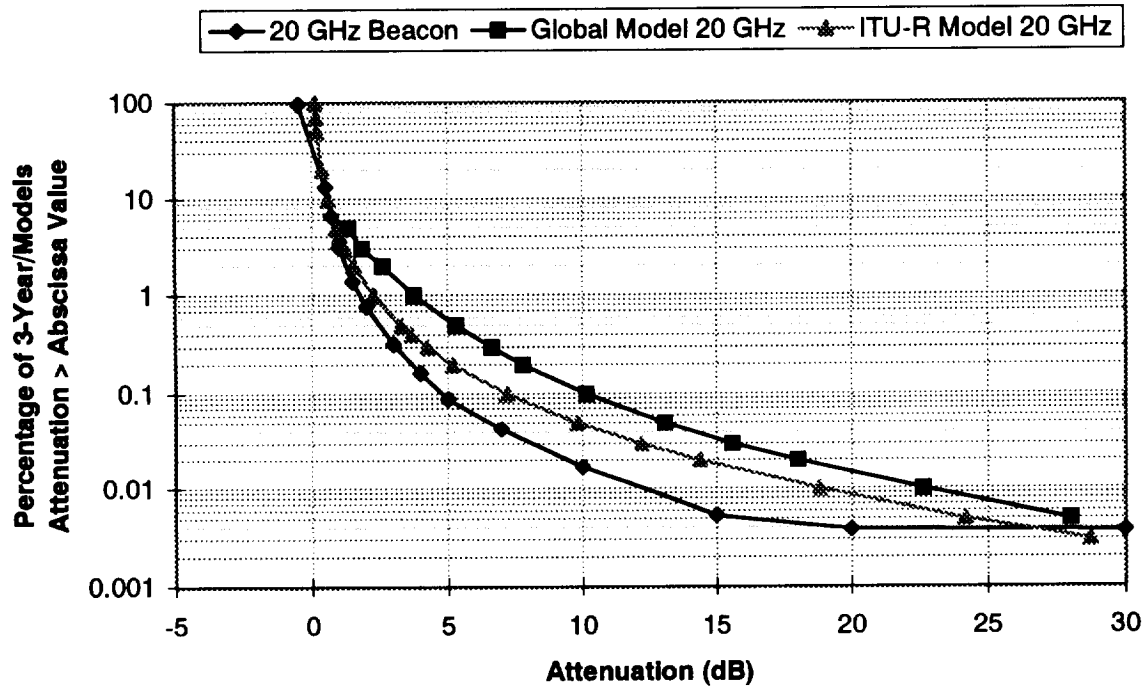

Fig. 4 - Alaska 3-Year 27 GHz Attenuation EDF vs. Models

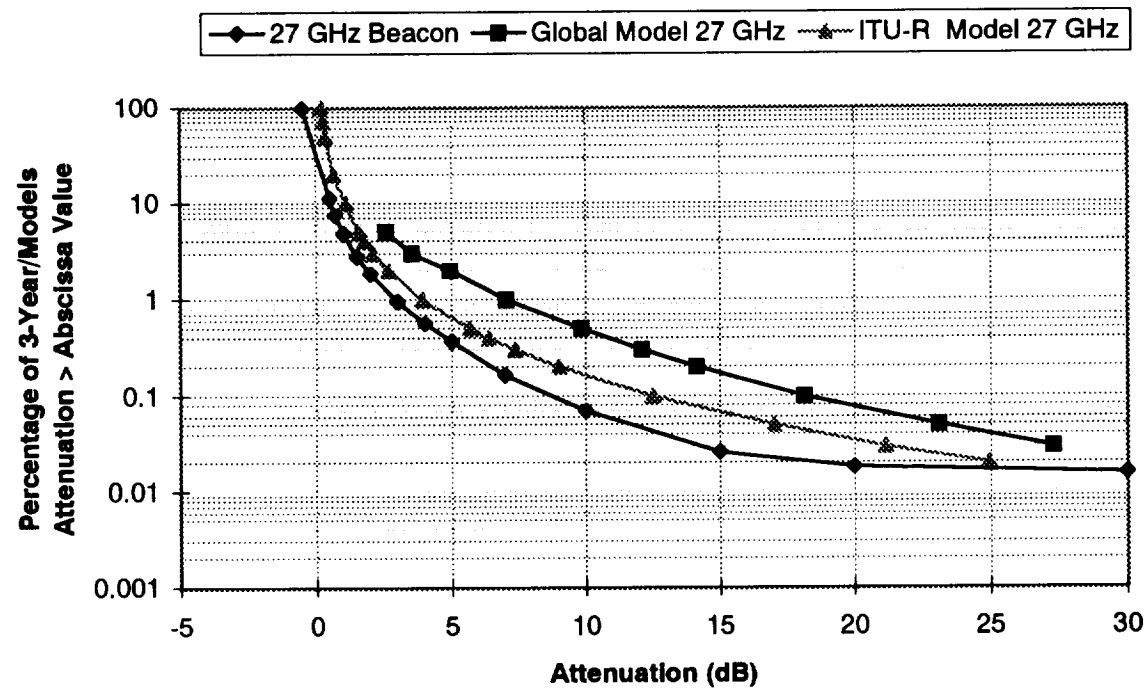

Fig. 5 - Percentage of Severely Errored Seconds (SES) in Available Time
December, 1995 to November, 1996

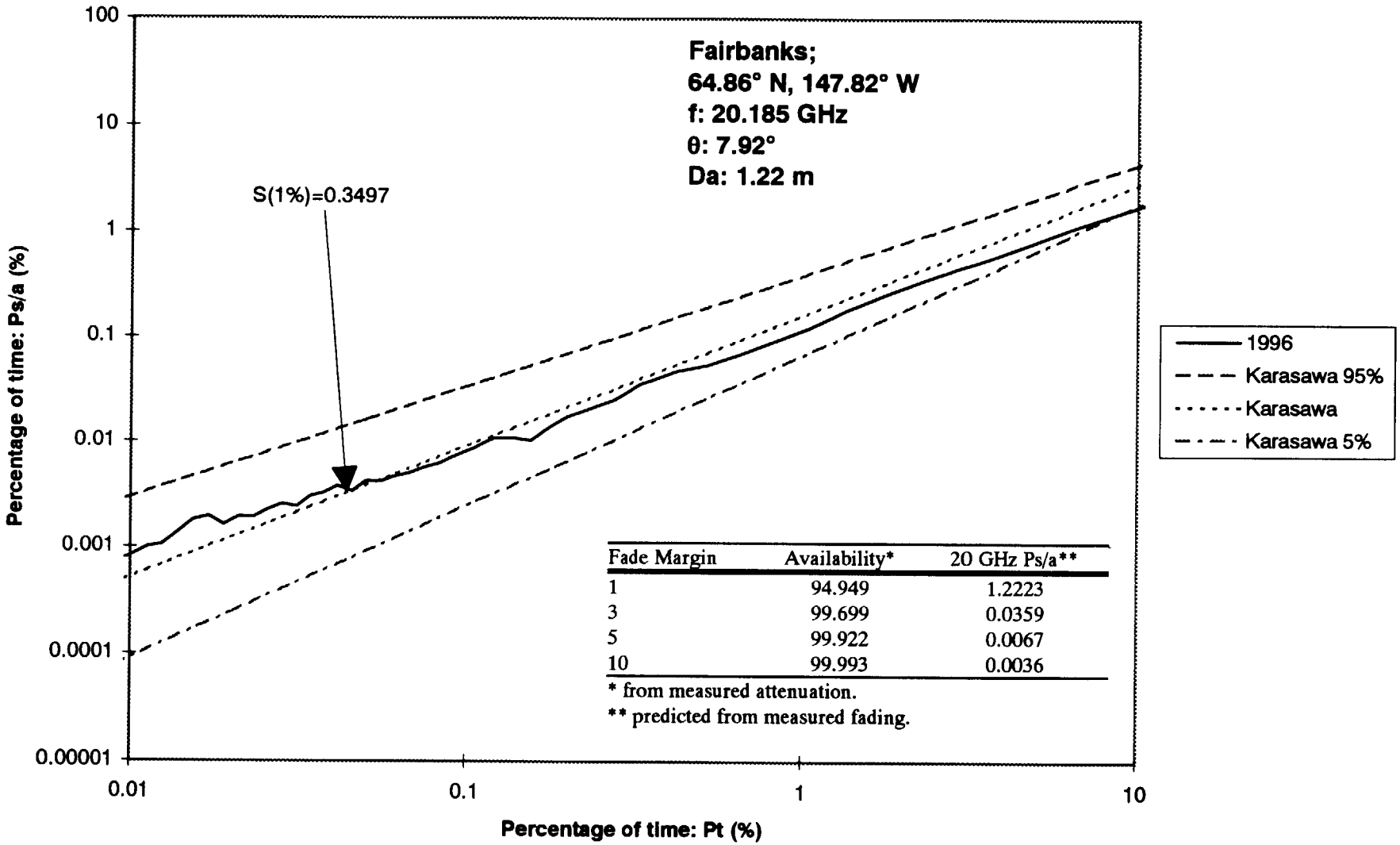

Fade Margin	Availability*	20 GHz Ps/a**
1	94.949	1.2223
3	99.699	0.0359
5	99.922	0.0067
10	99.993	0.0036

* from measured attenuation.
** predicted from measured fading.

Fig. 6 - Percentage of Severely Errored Seconds (SES) in Available Time
December, 1995 to November, 1996

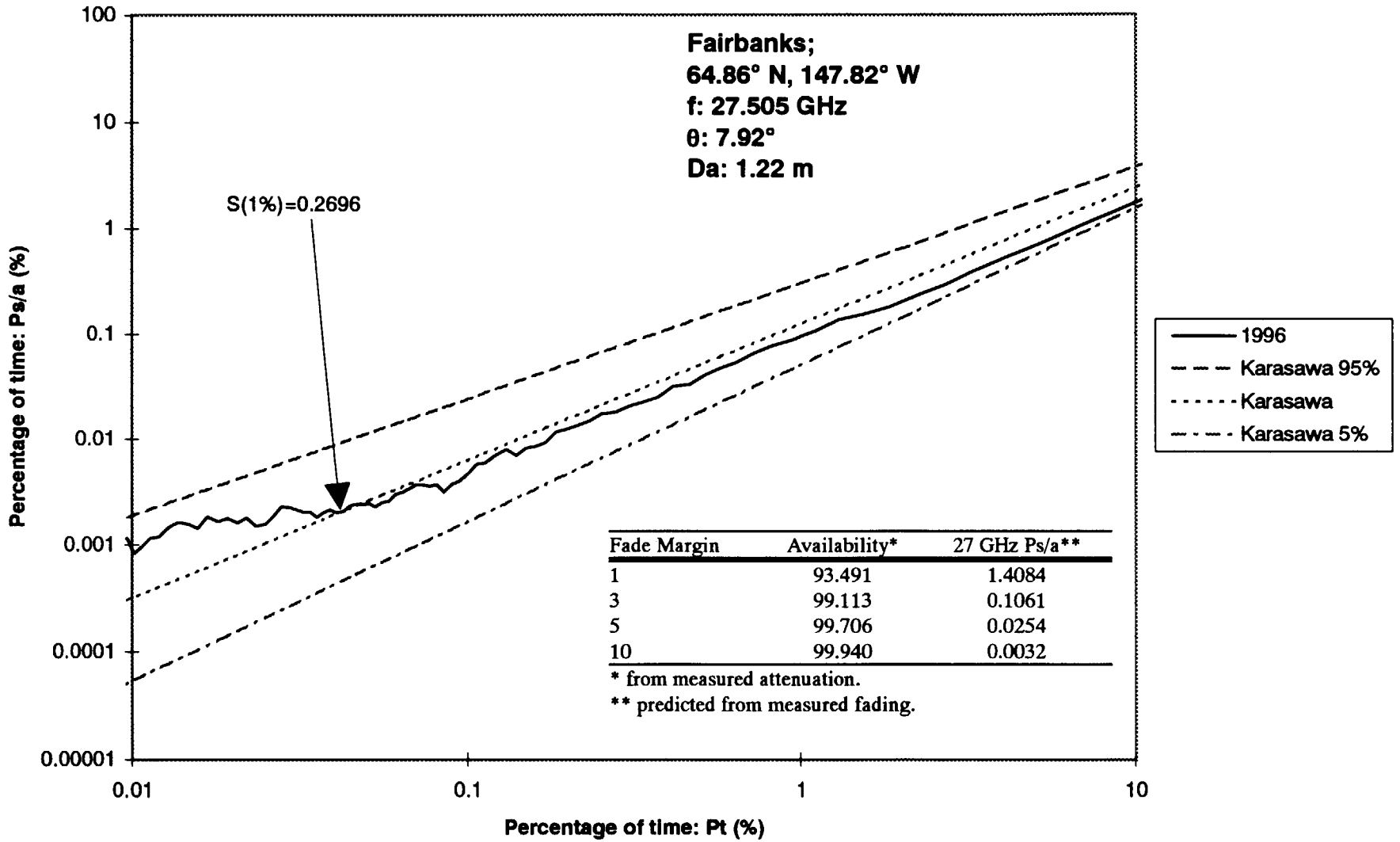

Fade Margin	Availability*	27 GHz Ps/a**
1	93.491	1.4084
3	99.113	0.1061
5	99.706	0.0254
10	99.940	0.0032

* from measured attenuation.
** predicted from measured fading.

Fig. 7 - Percentage of Severely Errored Seconds (SES) in Available Time
December, 1994 to November, 1995

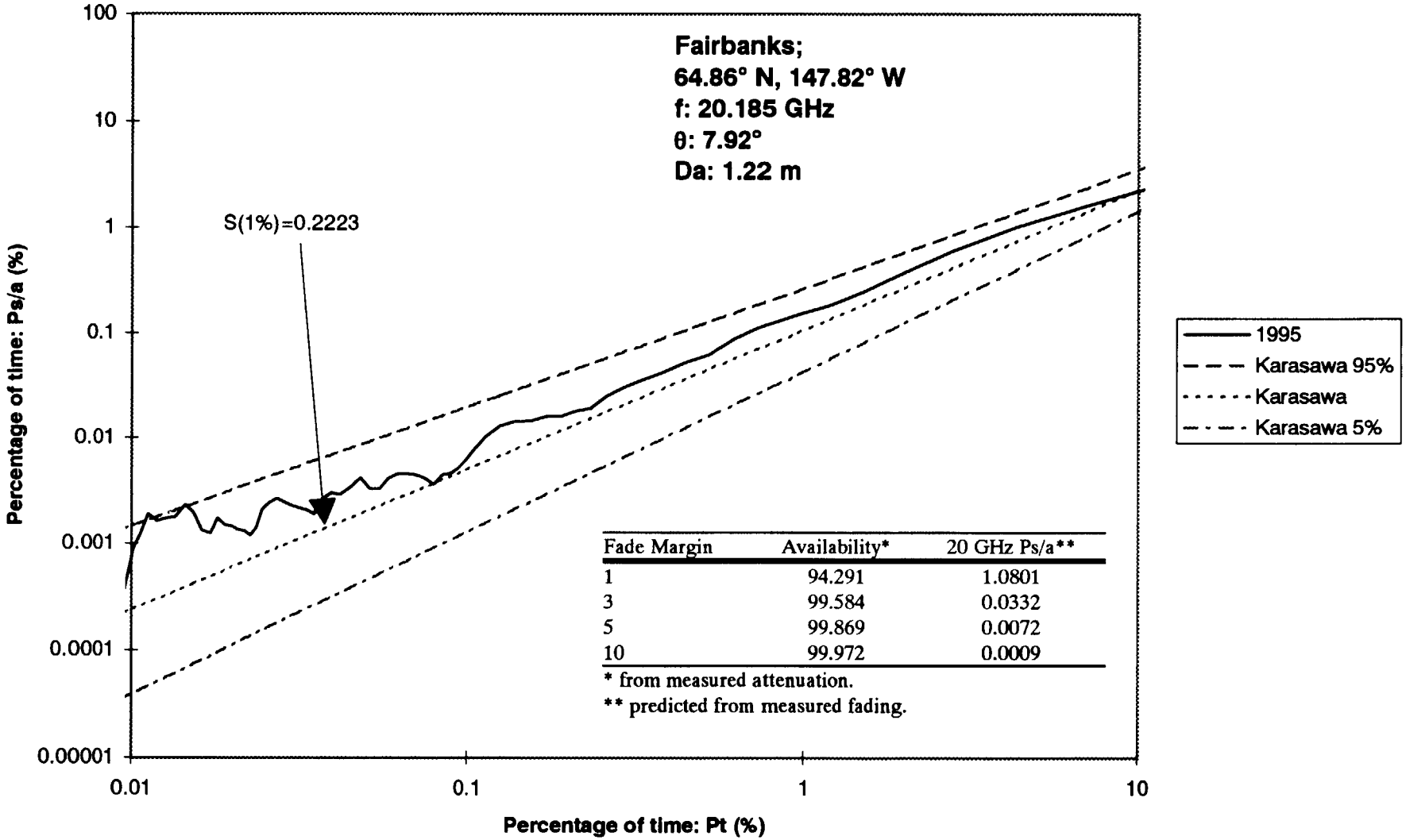

Fade Margin	Availability*	20 GHz Ps/a**
1	94.291	1.0801
3	99.584	0.0332
5	99.869	0.0072
10	99.972	0.0009

* from measured attenuation.
** predicted from measured fading.

Fig. 8 - Percentage of Severely Errored Seconds (SES) in Available Time
December, 1994 to November, 1995

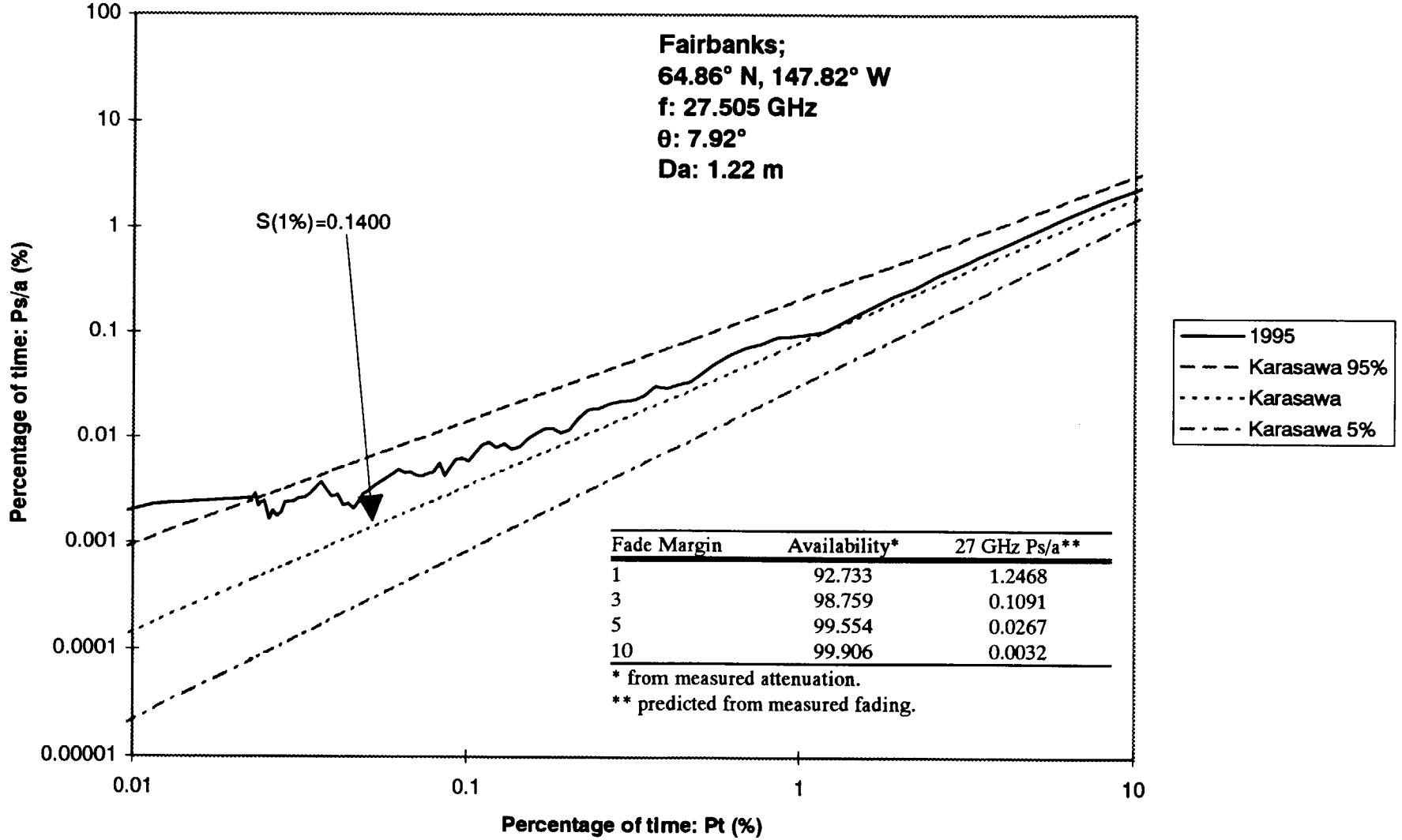

Fade Margin	Availability*	27 GHz Ps/a**
1	92.733	1.2468
3	98.759	0.1091
5	99.554	0.0267
10	99.906	0.0032

* from measured attenuation.
** predicted from measured fading.

Fig. 9 - Percentage of Severely Errored Seconds (SES) in Available Time December, 1993 to November, 1994

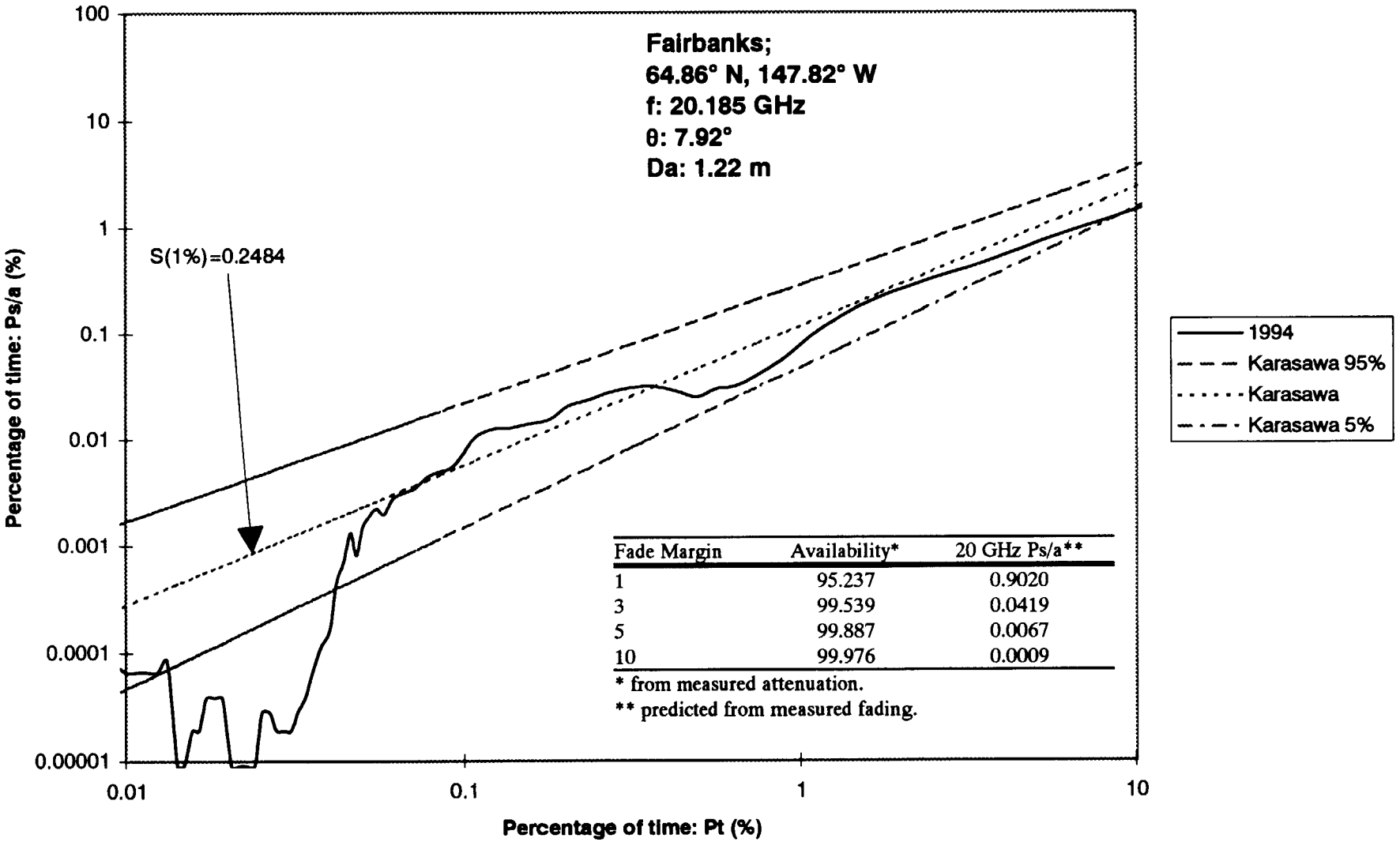

Fade Margin	Availability*	20 GHz Ps/a**
1	95.237	0.9020
3	99.539	0.0419
5	99.887	0.0067
10	99.976	0.0009

* from measured attenuation.
** predicted from measured fading.

Fig. 10 - Percentage of Severely Errored Seconds (SES) in Available Time
December, 1993 to Novemeber, 1994

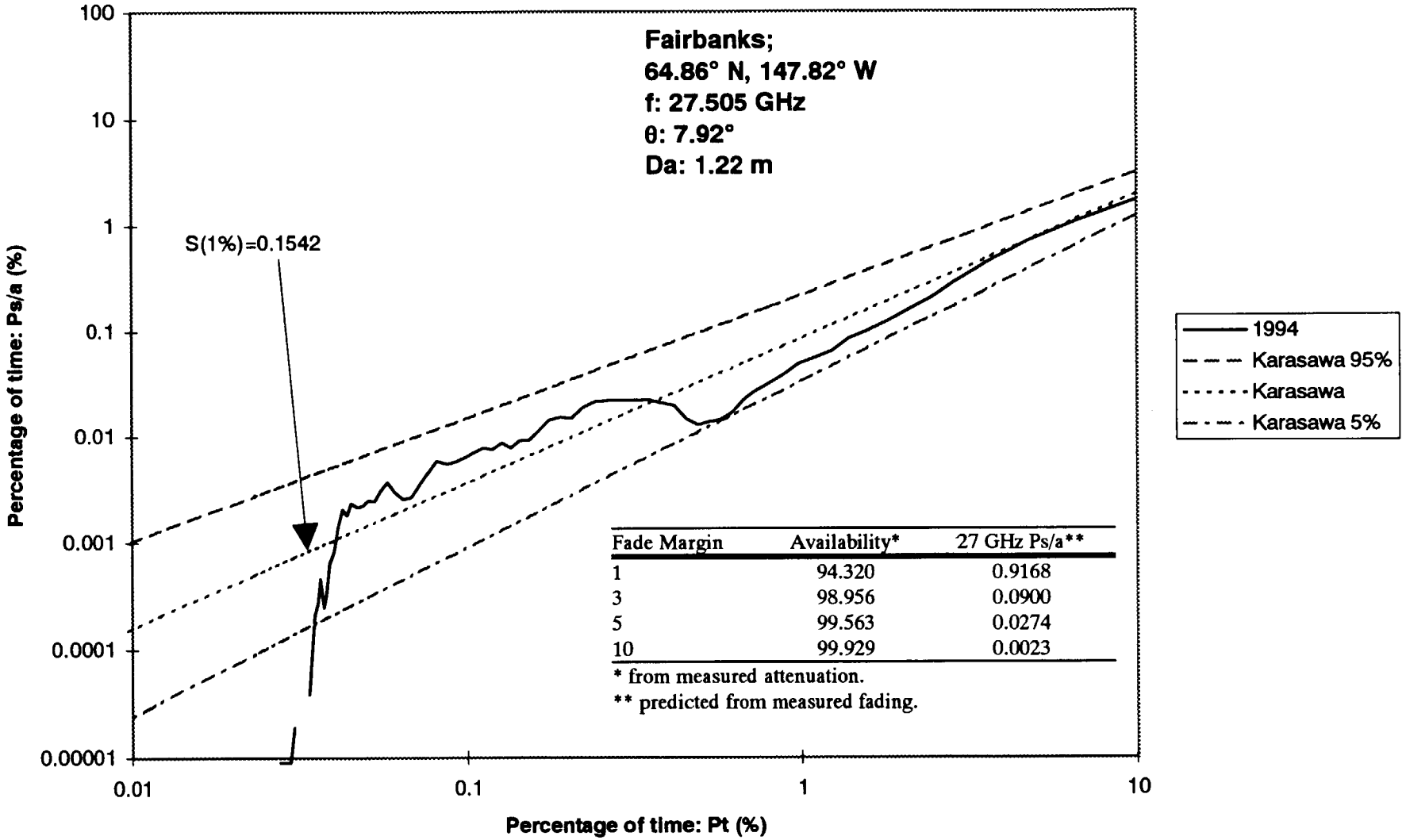

Fade Margin	Availability*	27 GHz Ps/a**
1	94.320	0.9168
3	98.956	0.0900
5	99.563	0.0274
10	99.929	0.0023

* from measured attenuation.
** predicted from measured fading.

Fig. 11 - 27.505/20.185 Instantaneous Attenuation Ratio by Base Attenuation
December, 1995 to November, 1996

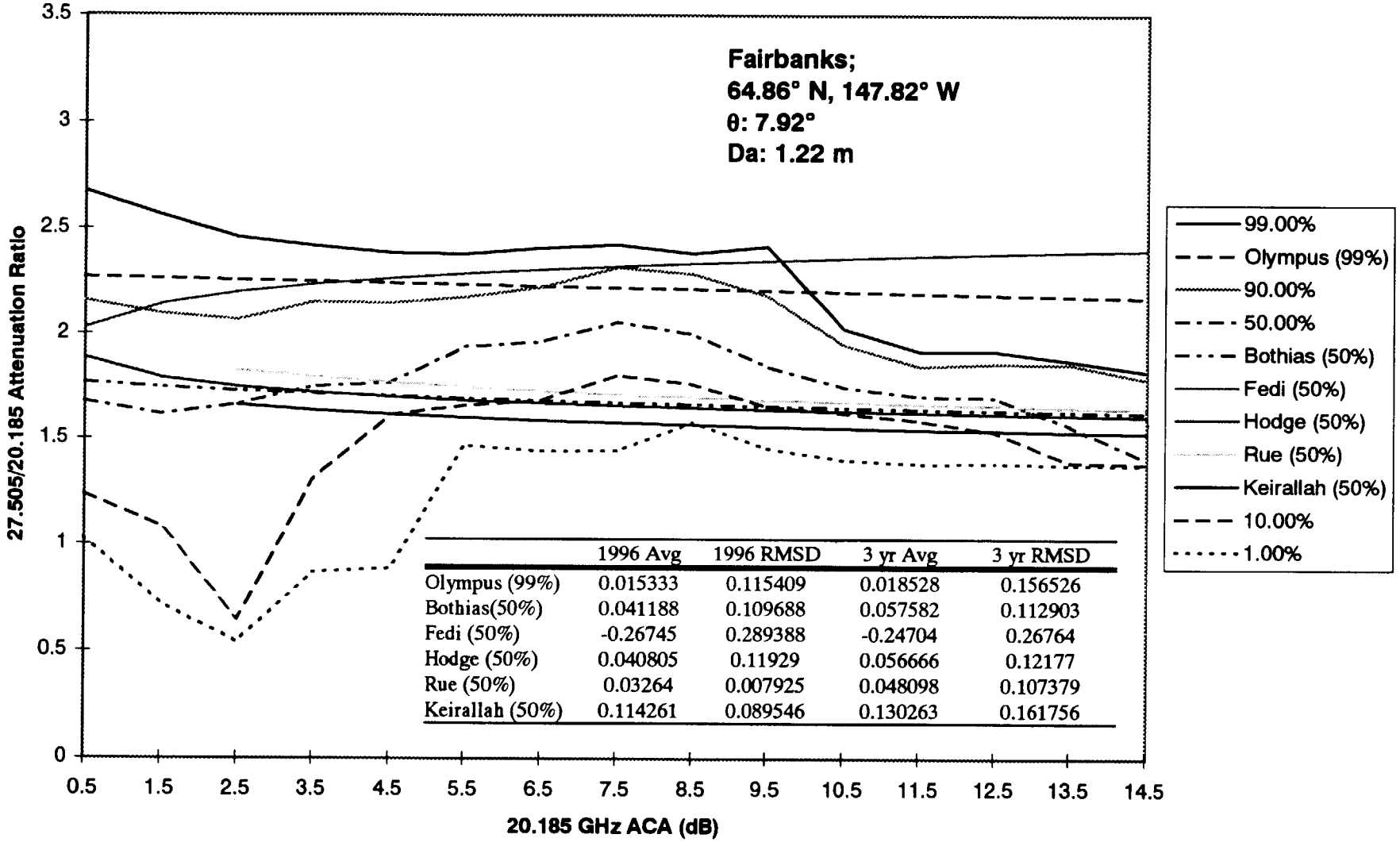

	1996 Avg	1996 RMSD	3 yr Avg	3 yr RMSD
Olympus (99%)	0.015333	0.115409	0.018528	0.156526
Bothias(50%)	0.041188	0.109688	0.057582	0.112903
Fedi (50%)	-0.26745	0.289388	-0.24704	0.26764
Hodge (50%)	0.040805	0.11929	0.056666	0.12177
Rue (50%)	0.03264	0.007925	0.048098	0.107379
Keirallah (50%)	0.114261	0.089546	0.130263	0.161756

Fig. 12 - 27.505/20.185 Instantaneous Attenuation Ratio by Base Attenuation
December, 1994 to November, 1995

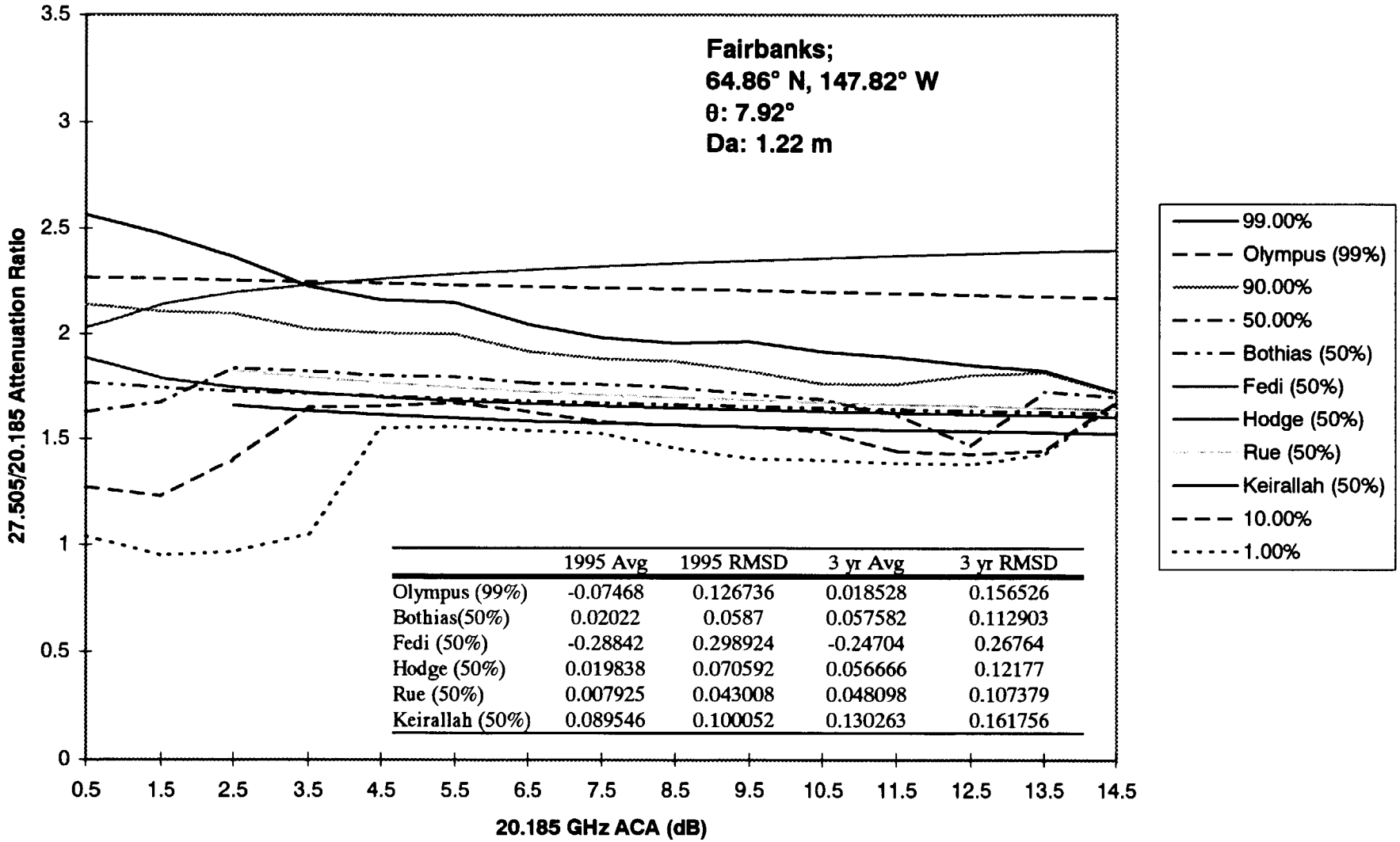

	1995 Avg	1995 RMSD	3 yr Avg	3 yr RMSD
Olympus (99%)	-0.07468	0.126736	0.018528	0.156526
Bothias(50%)	0.02022	0.0587	0.057582	0.112903
Fedi (50%)	-0.28842	0.298924	-0.24704	0.26764
Hodge (50%)	0.019838	0.070592	0.056666	0.12177
Rue (50%)	0.007925	0.043008	0.048098	0.107379
Keirallah (50%)	0.089546	0.100052	0.130263	0.161756

Fig. 13 - 27.505/20.185 GHz Attenuation Ratio by Base Attenuation
December, 1993 to November, 1994

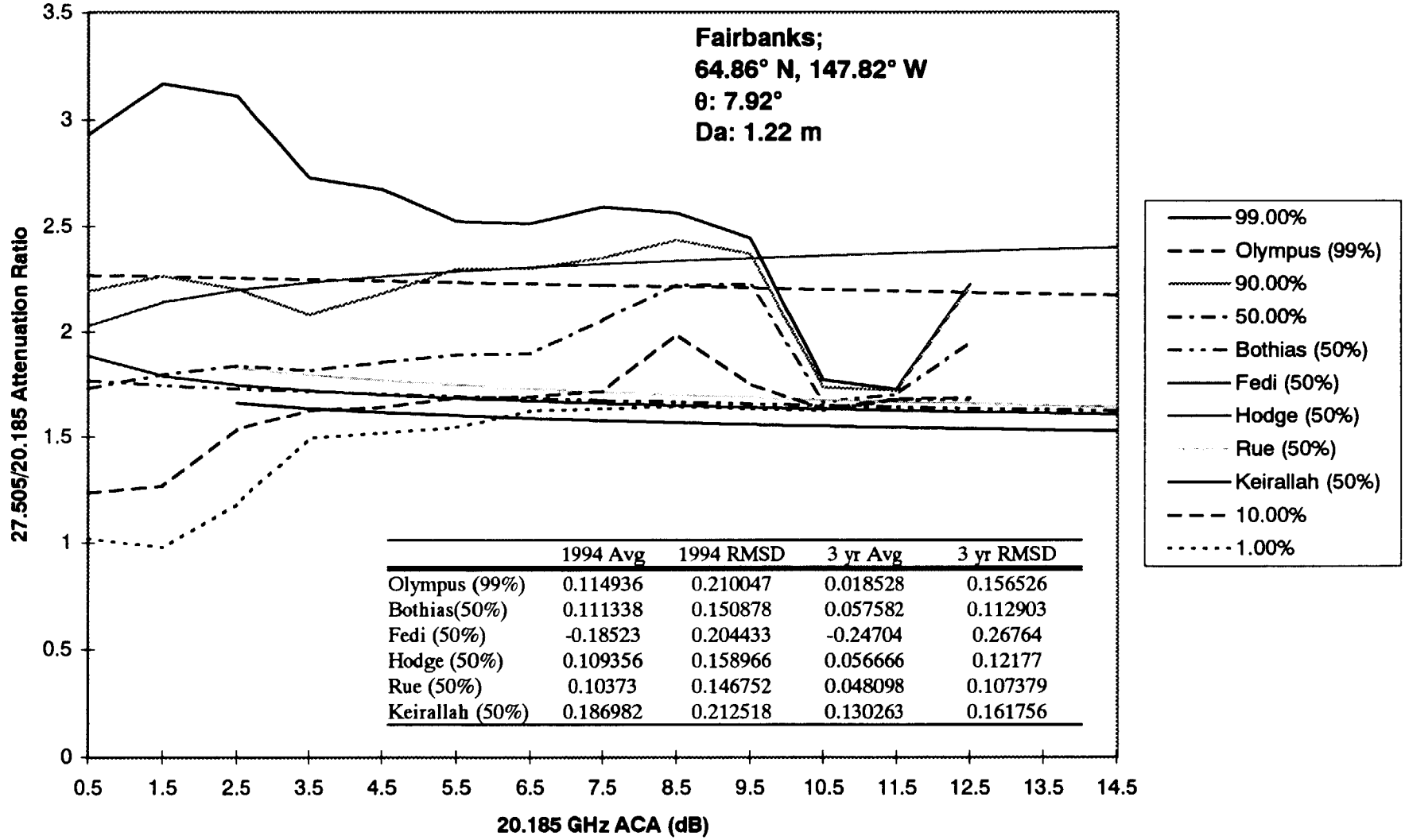

	1994 Avg	1994 RMSD	3 yr Avg	3 yr RMSD
Olympus (99%)	0.114936	0.210047	0.018528	0.156526
Bothias(50%)	0.111338	0.150878	0.057582	0.112903
Fedi (50%)	-0.18523	0.204433	-0.24704	0.26764
Hodge (50%)	0.109356	0.158966	0.056666	0.12177
Rue (50%)	0.10373	0.146752	0.048098	0.107379
Keirallah (50%)	0.186982	0.212518	0.130263	0.161756

Fig. 14 - Yearly Cumulative Distributions
20.185 GHz ACA

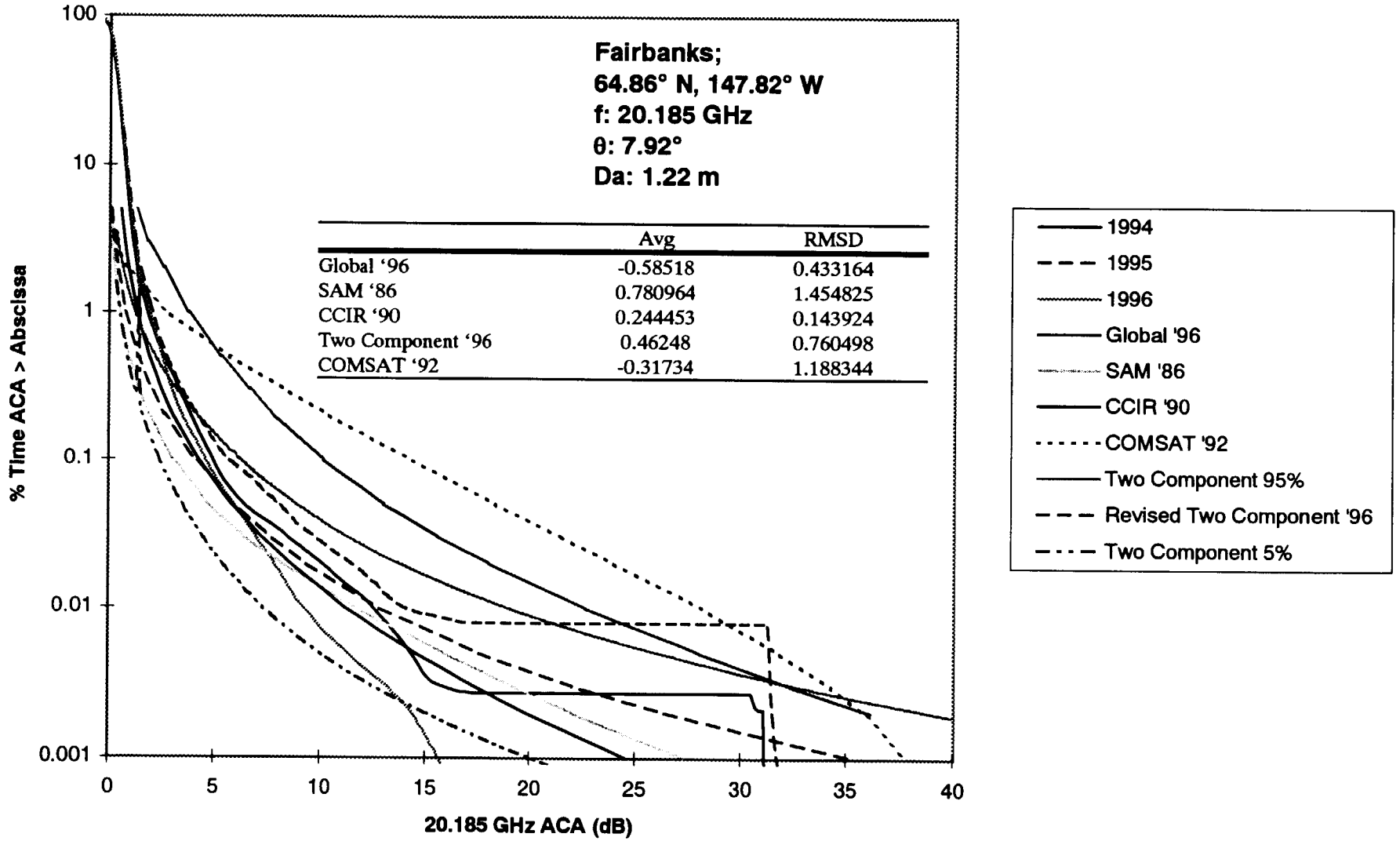

Fig. 15 - Yearly Cumulative Distributions
27.505 GHz ACA

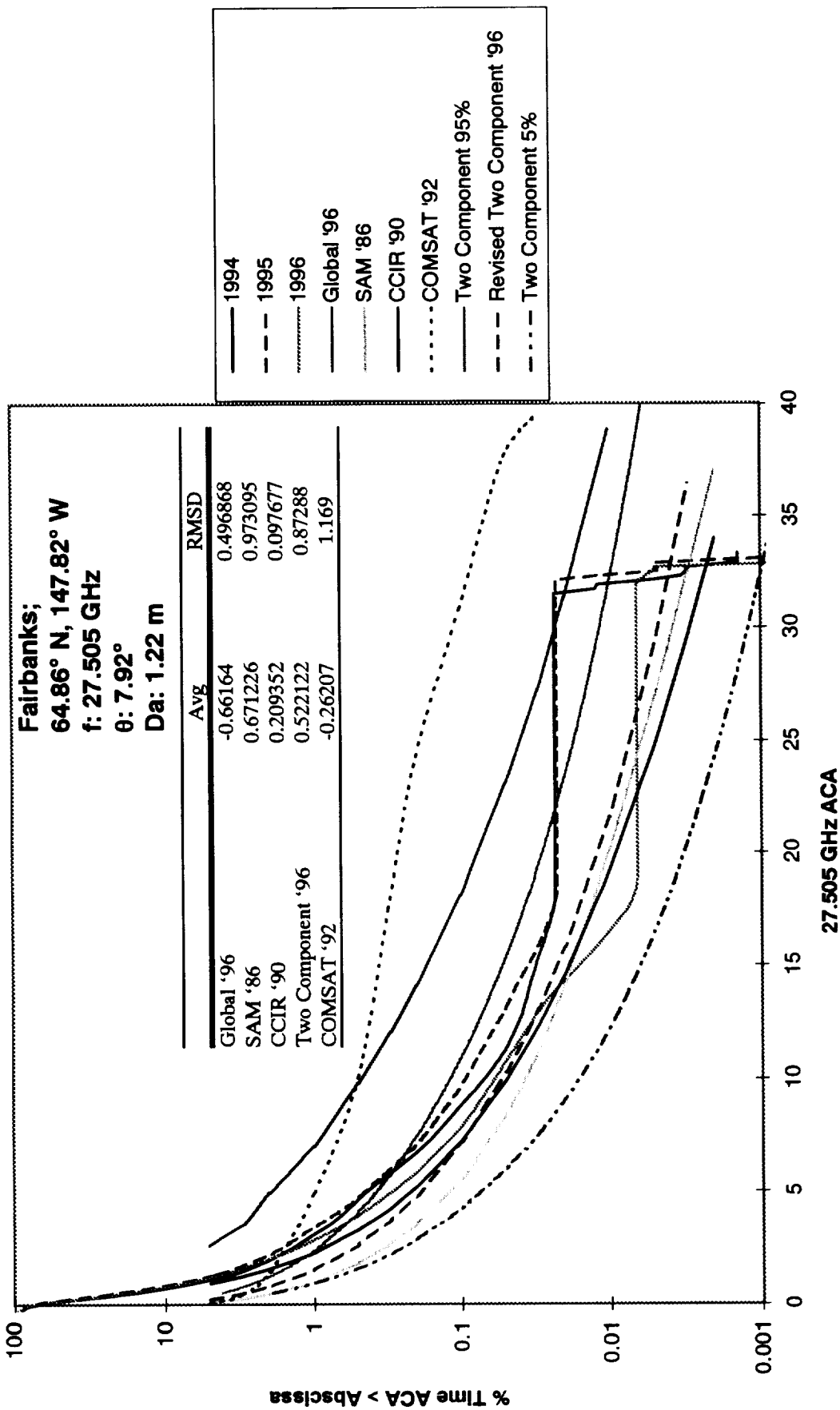

Fig. 16 - Worst Month Cumulative Distributions
20.185 GHz ACA

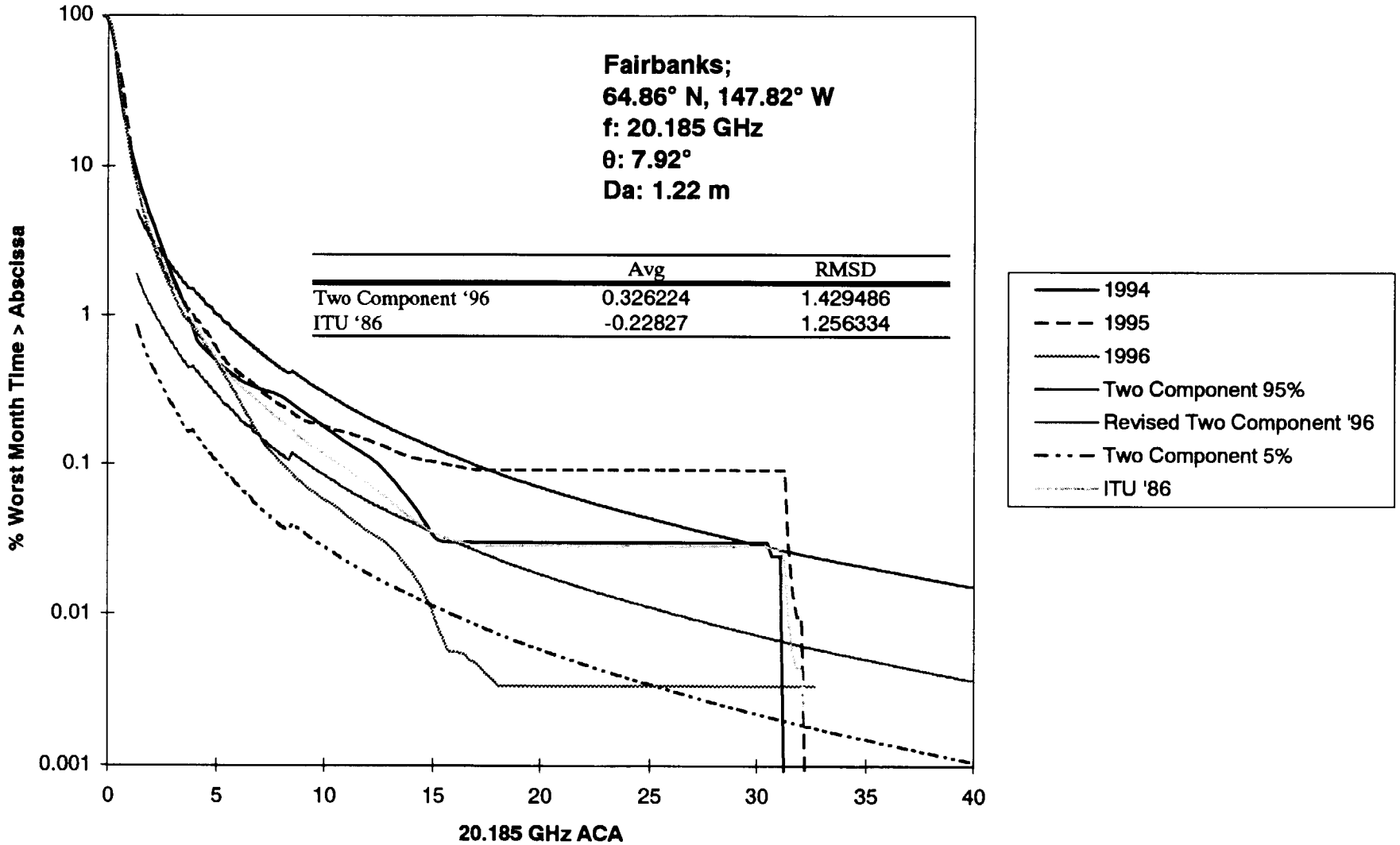

Fig. 17 - Worst Month Cumulative Distributions
27.505 GHz ACA

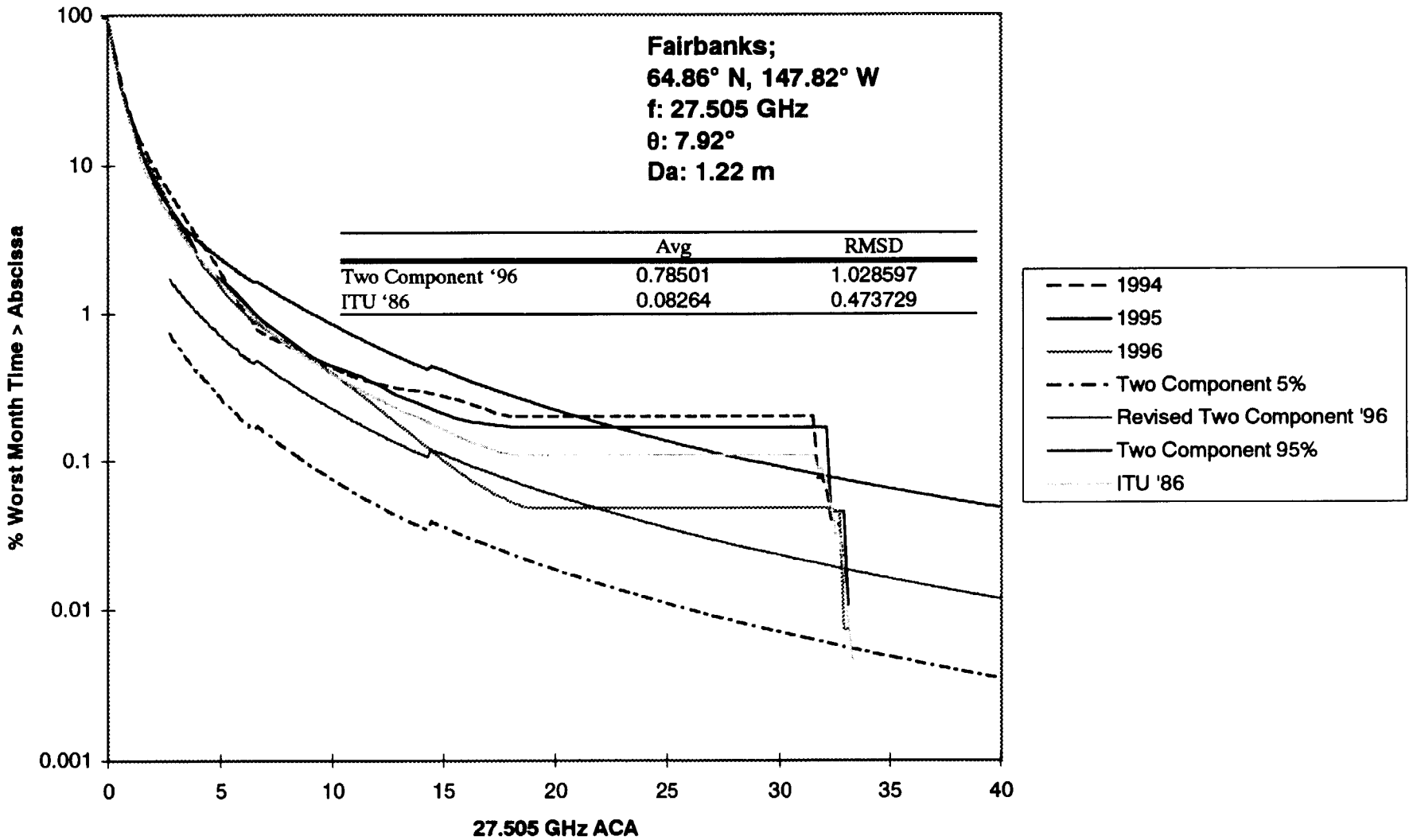

Fig. 18 - Ratio of Worst Month to Average Year, Q
20.185 GHz ACA

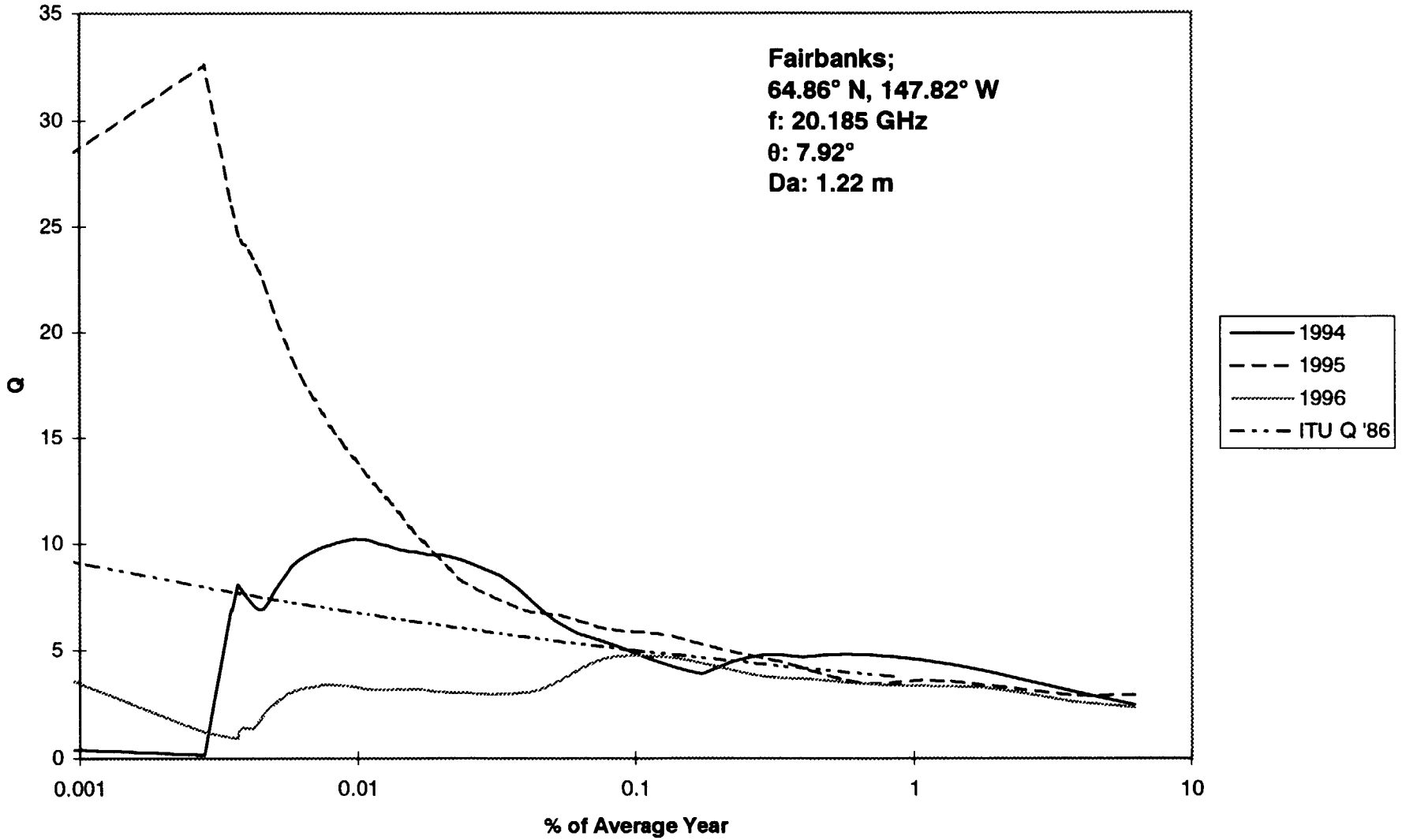

Fig. 19 - Ratio of Worst Month to Average Year, Q
27.505 GHz ACA

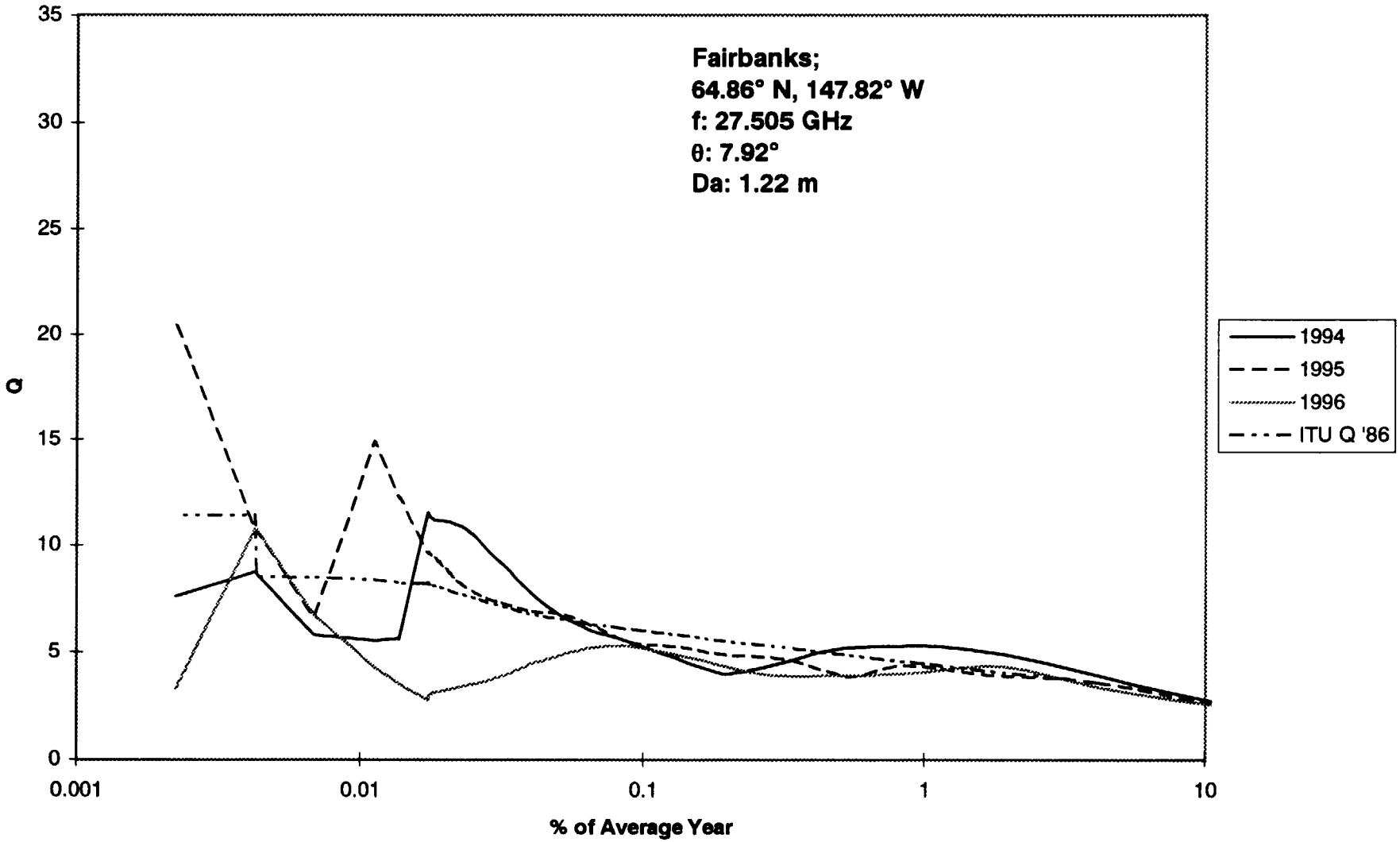

Fig. 20 - Yearly Cumulative Distributions
Capacitive Rain Guage

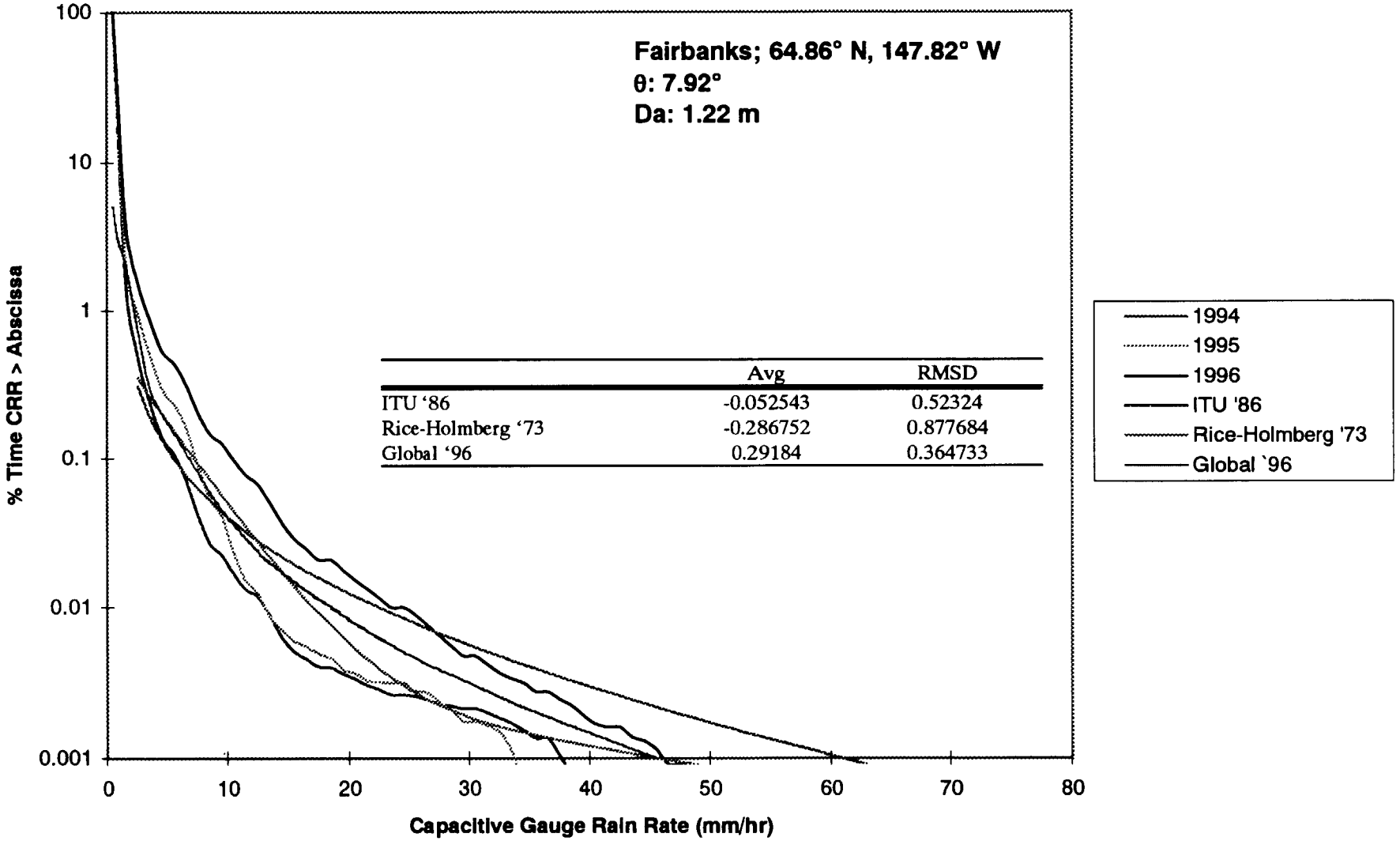

	Avg	RMSD
ITU '86	-0.052543	0.52324
Rice-Holmberg '73	-0.286752	0.877684
Global '96	0.29184	0.364733

Fig. 21 - Yearly Cumulative Distributions
Optical Rain Guage

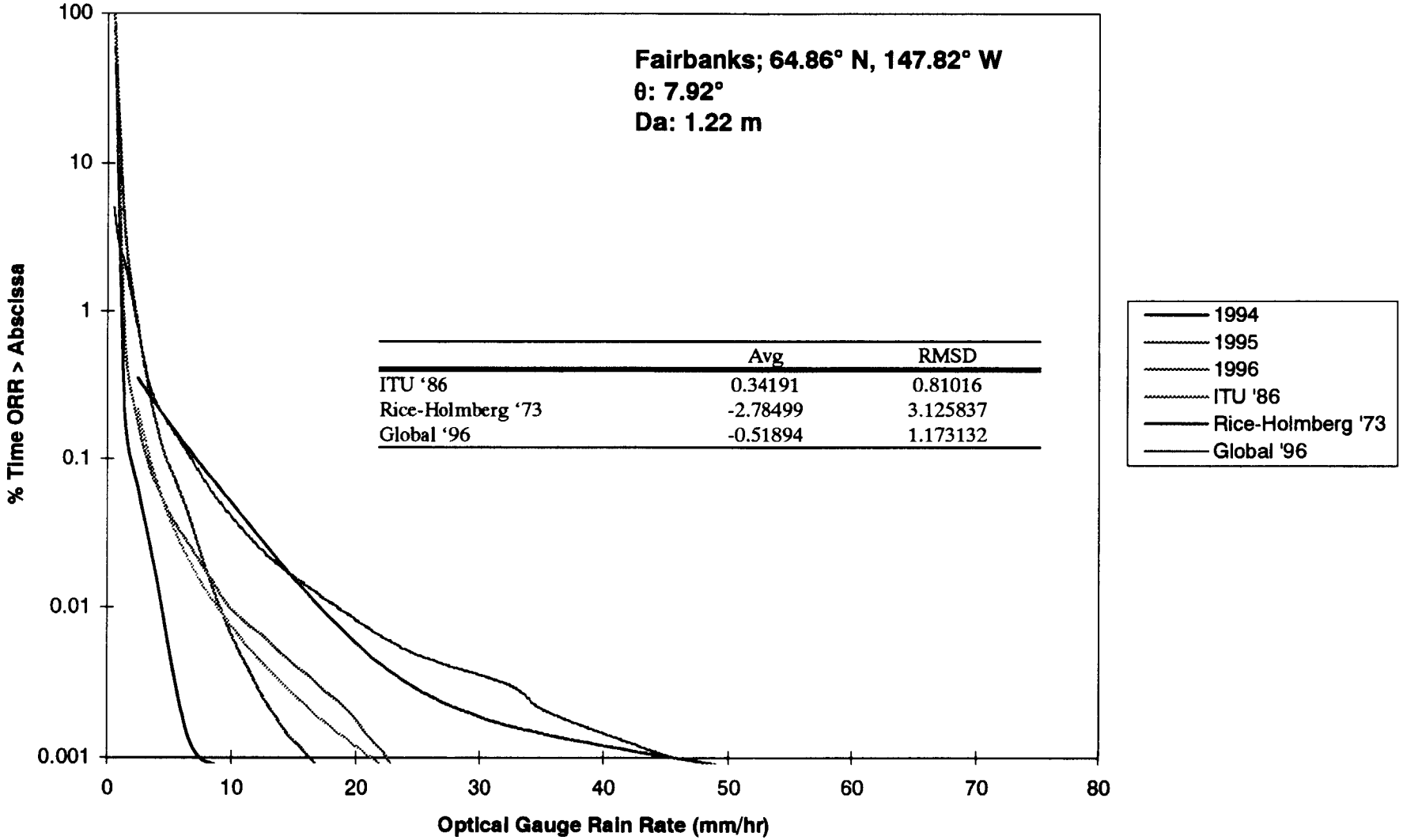

	Avg	RMSD
ITU '86	0.34191	0.81016
Rice-Holmberg '73	-2.78499	3.125837
Global '96	-0.51894	1.173132

Fig. 22 - Worst Month Cumulative Distributions
Capacitive Rain Guage

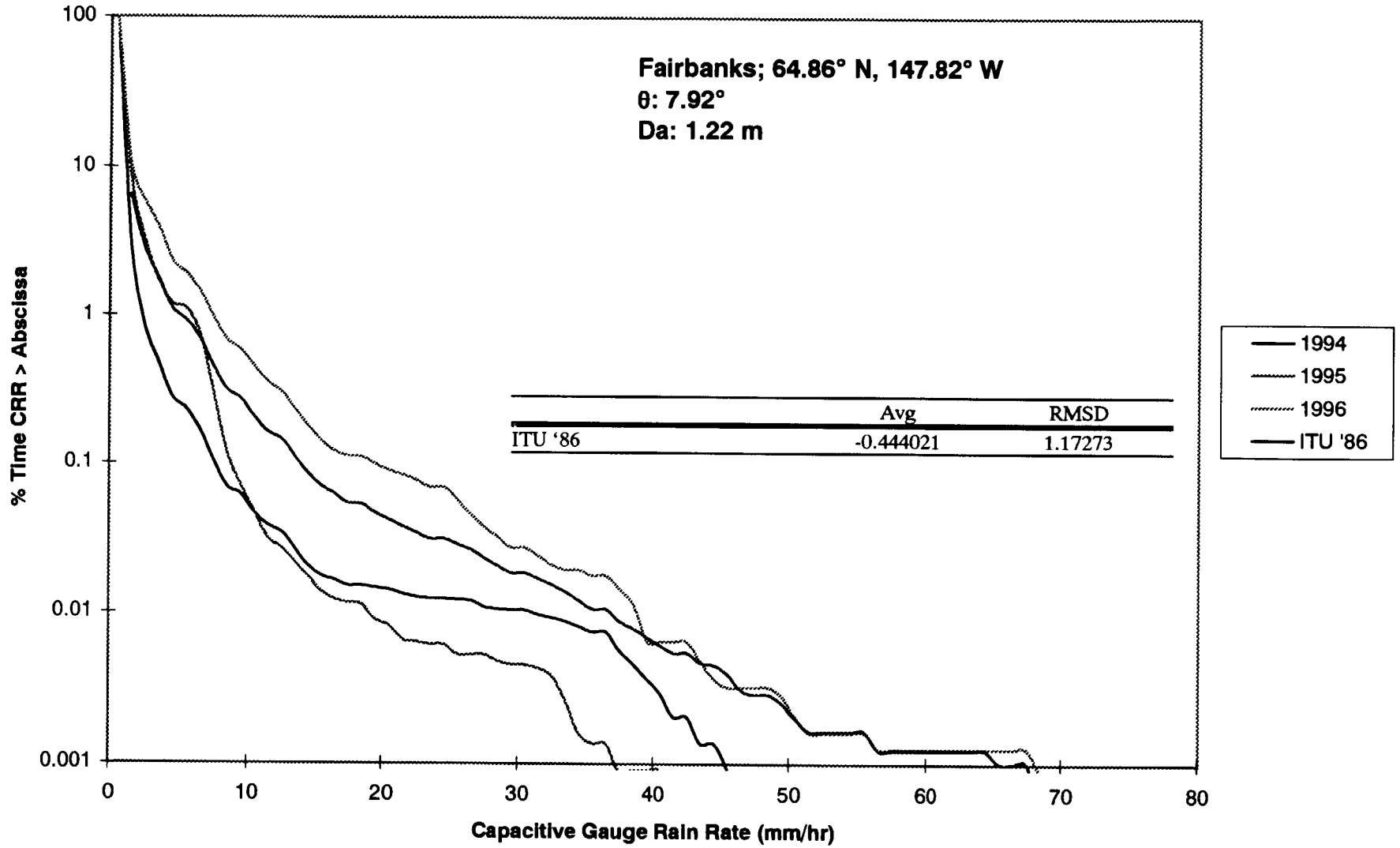

Fig. 23 - Worst Month Cumulative Distributions
Optical Rain Guage

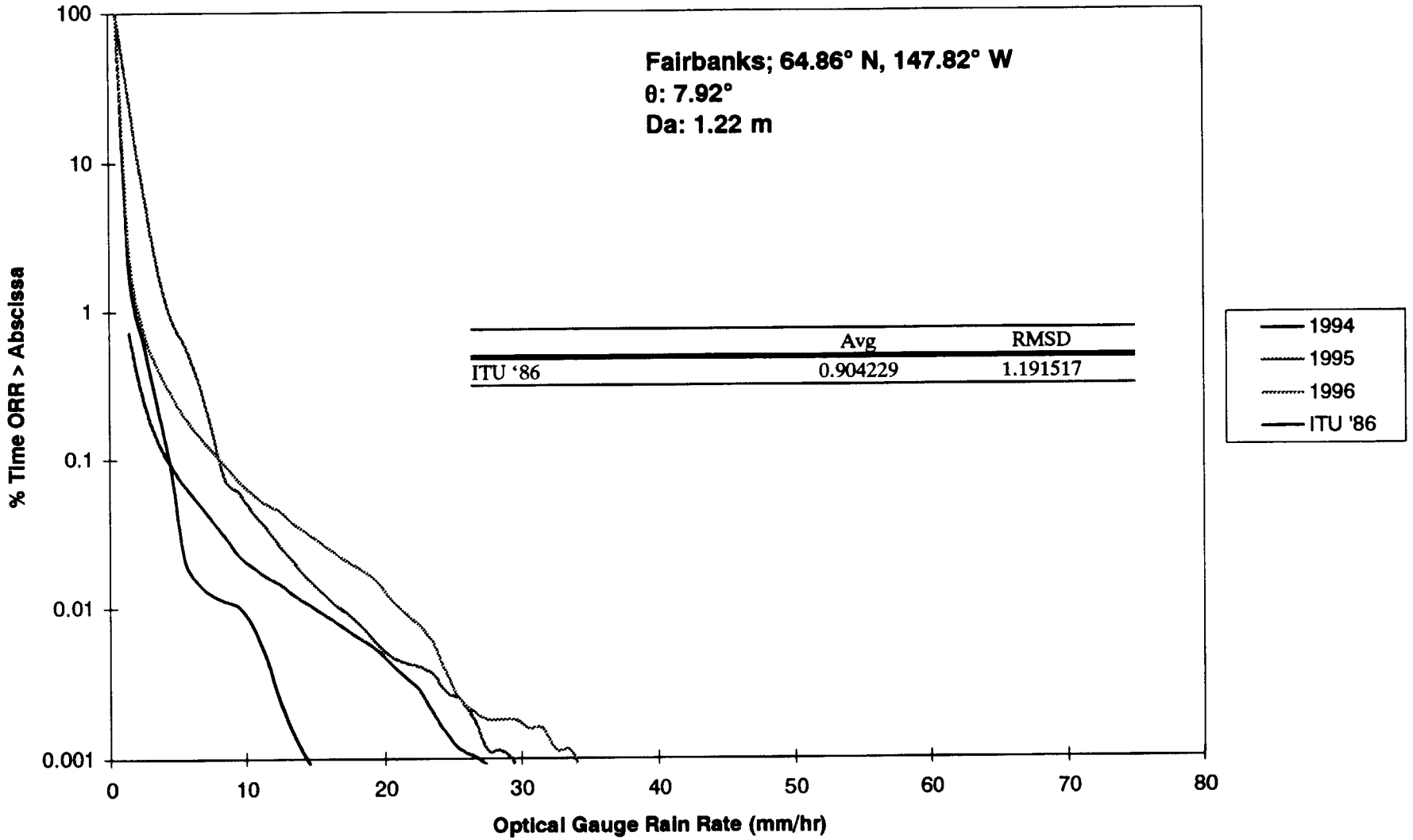

Fig. 24 - 3 Year Cumulative Distributions
20.185 GHz Gaseous Absorption

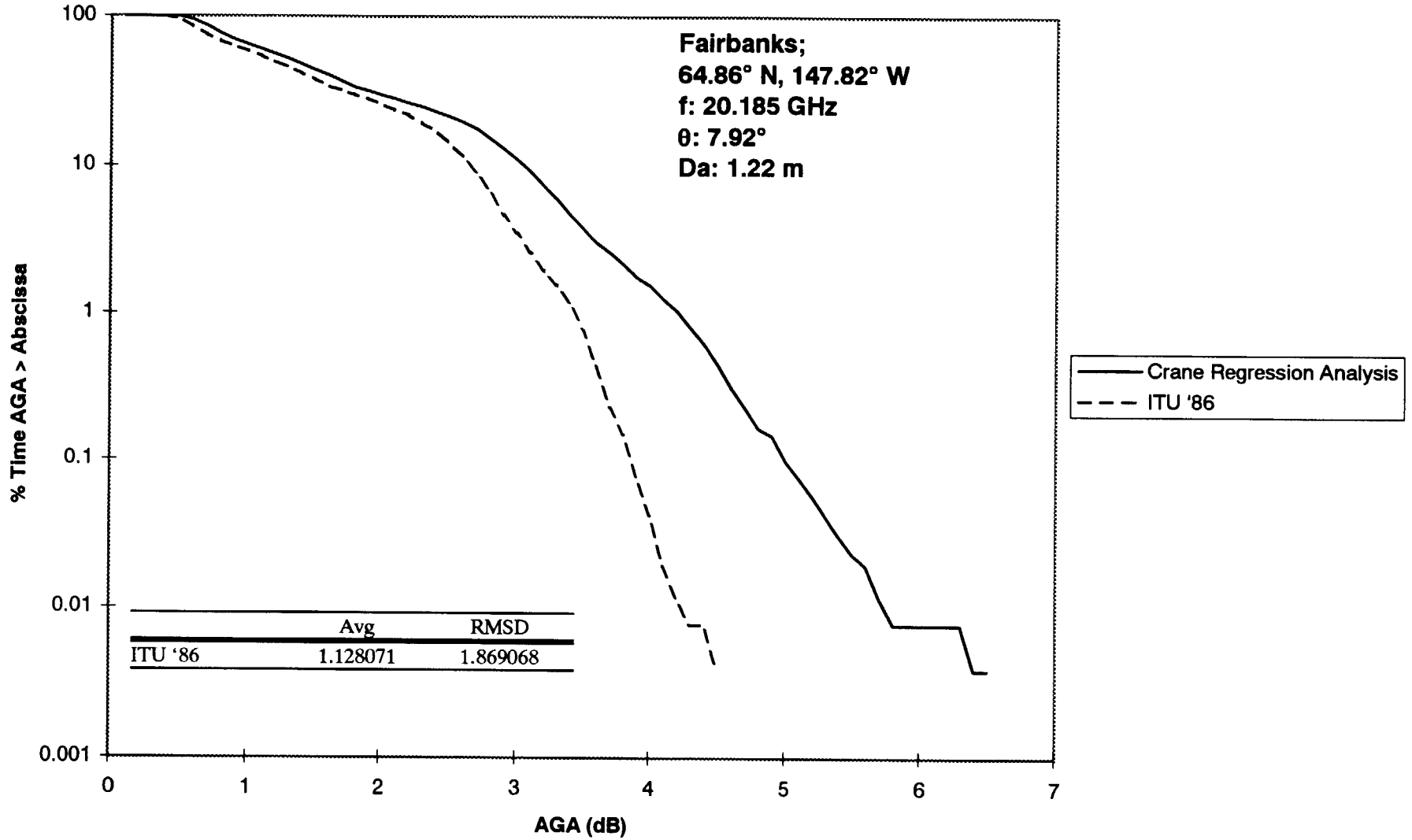

Fig. 25 - 3 Year Cumulative Distributions
27.505 GHz Gaseous Absorption

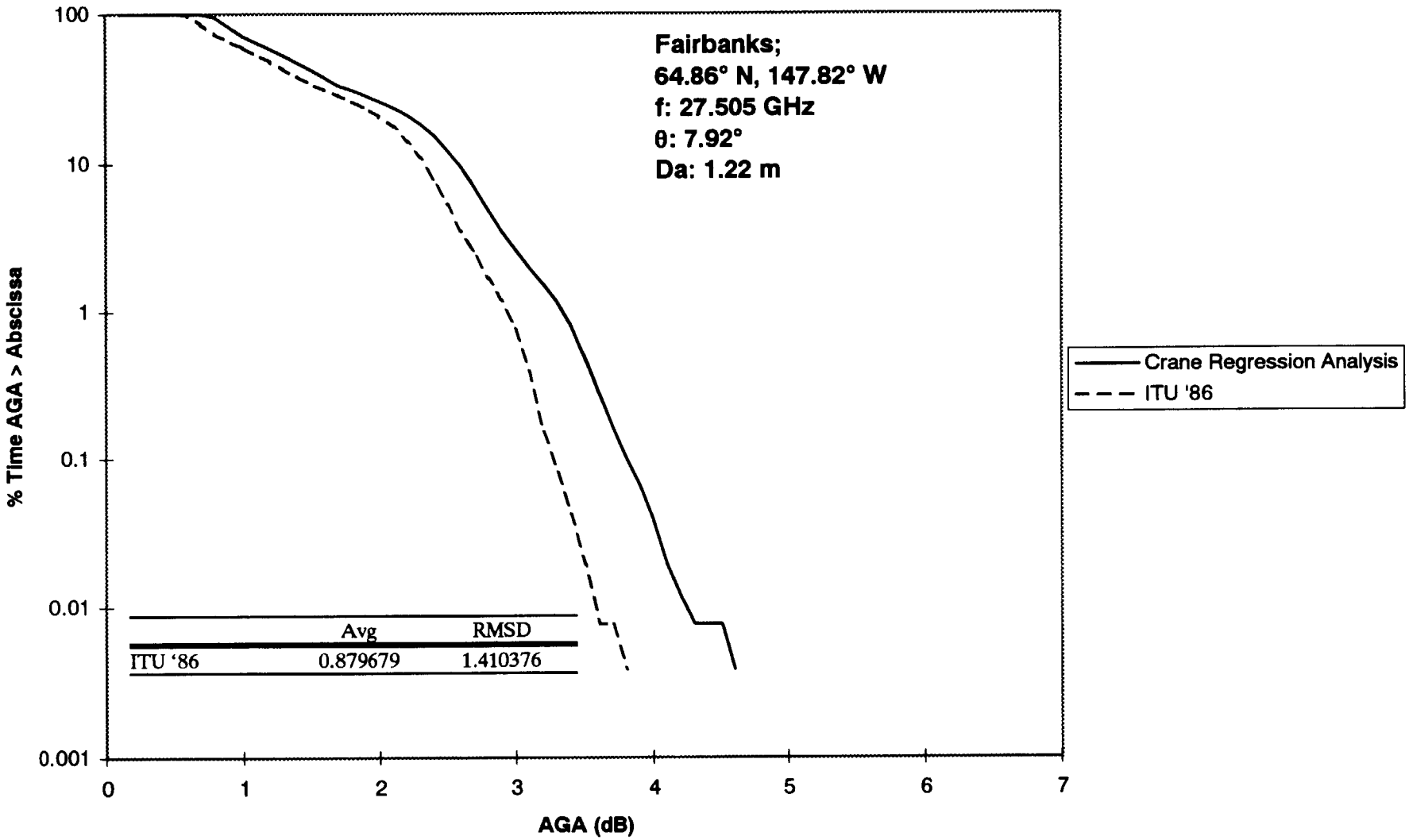

Three Years of ACTS Propagation Measurements at Vancouver, B.C.

Bruce Dow
University of British Columbia
Vancouver, British Columbia

David Rogers
Communications Research Centre
Ottawa, Ontario

Overview

I. Features of the Vancouver Facility:
- Site summary (location, climate, etc.)
- Goals of ACTS measurements at Vancouver

II. Results to Date:
- Structure of fading events
- Example statistics from first two years
- General results

III. Current Status/Plans:
- Areas under investigation at UBC and CRC
- Summary/Conclusions

UBC/ACTS Experiment Configuration

- Site coordinates: 49.25°N latitude, 123.25°W longitude
- Elevation angle 29.3°; Azimuth 150.4° CWN
- Pol. tilt angle of beacon signals: V (18.9° CCW)
- Beacon/radiometer frequencies: 20.2 and 27.5 GHz
- Terminal antenna: 1.2 m diameter, offset fed
- Climate type: Pacific NW maritime (ITU-R rain zone D)

Clear-Sky Link Budgets

	20.2 GHz	27.5 GHz
Beacon EIRP (dBW), *nominal*	15.0	15.0
Free-space Loss (dB)	- 210.3	- 213.0
Clear-sky Loss (dB), *nominal*	- 0.9	- 0.8
Polarization Loss (dB)	- 0.2	- 0.1
Earth Terminal Pointing Loss (dB)	- 0.2	- 0.4
Modulation Loss (dB), *nominal*	- 3.2	0.0
Earth Terminal G/T (dB/K), *nominal*	15.1	17.6
Received Power (dBW)	- 184.7	- 181.7
1/k (dB-Hz K/W)	228.6	228.6
C/N_0 (dB-Hz)	43.9	46.9
C/N in 20 Hz (dB)	30.9	33.9

General Goals

- **Obtain Ka-band propagation data for important class of climate (maritime)**
- **Support Ka-band propagation model development**
- **Investigate melting layer effect on path attenuation**
- **Investigate event details/fade dynamics (development of adaptive-mitigation, resource-sharing strategies)**

➡ ***Support communication system development***

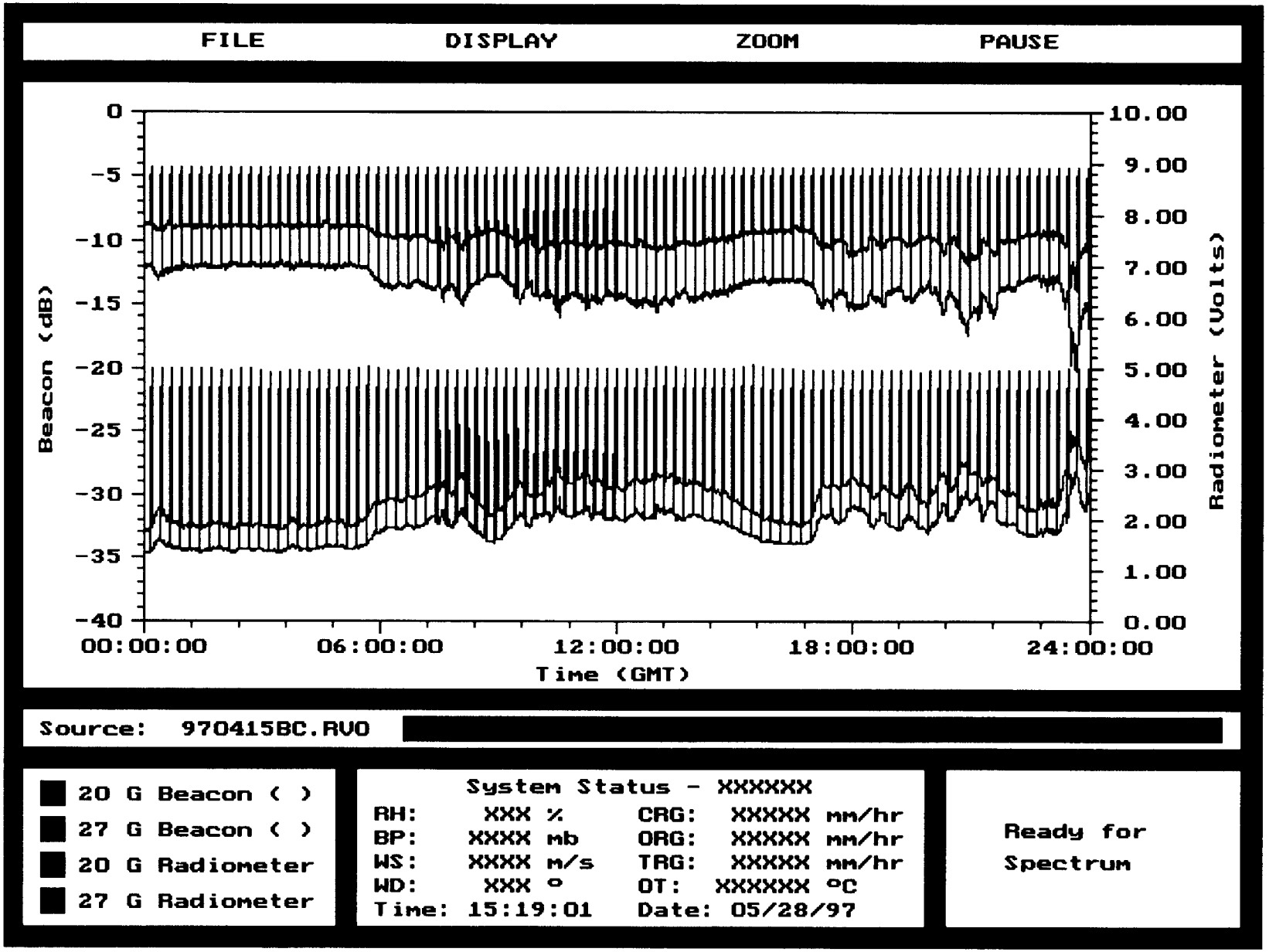
FILE
DISPLAY
ZOOM
PAUSE
0
-5
-10
-15
-20
-25
-30
-35
-40
Beacon (dB)
10.00
9.00
8.00
7.00
6.00
5.00
4.00
3.00
2.00
1.00
0.00
Radiometer (Volts)
00:00:00
06:00:00
12:00:00
18:00:00
24:00:00
Time (GMT)
Source: 970415BC.RVO
20 G Beacon ( )
27 G Beacon ( )
20 G Radiometer
27 G Radiometer
System Status - XXXXXX
RH: XXX %
BP: XXXX mb
WS: XXXX m/s
WD: XXX °
Time: 15:19:01
CRG: XXXXX mm/hr
ORG: XXXXX mm/hr
TRG: XXXXX mm/hr
OT: XXXXXX °C
Date: 05/28/97
Ready for
Spectrum

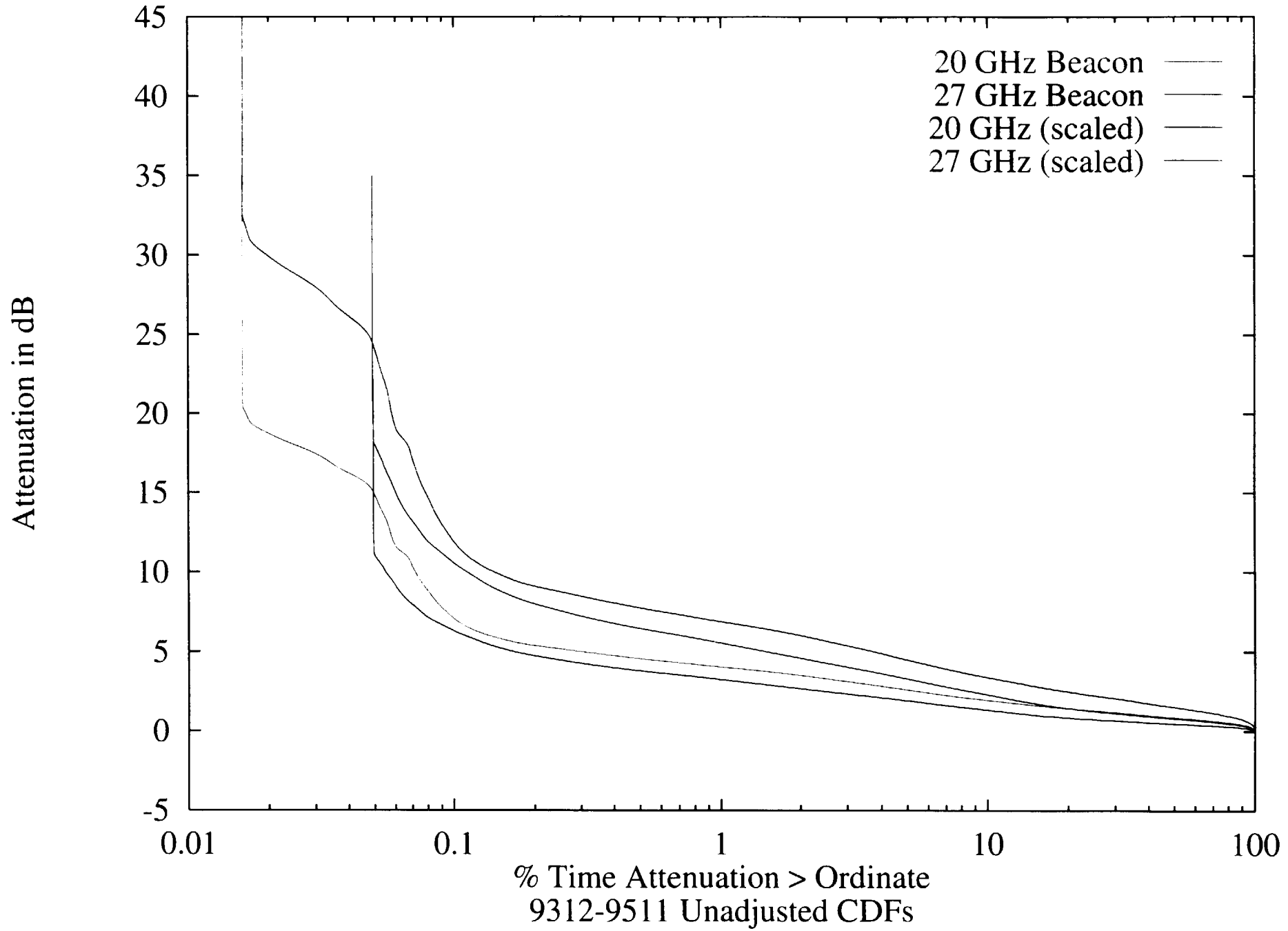
20 GHz Beacon
27 GHz Beacon
20 GHz (scaled)
27 GHz (scaled)
Attenuation in dB
45
40
35
30
25
20
15
10
5
0
-5
0.01
0.1
1
10
100
% Time Attenuation > Ordinate
9312-9511 Unadjusted CDFs

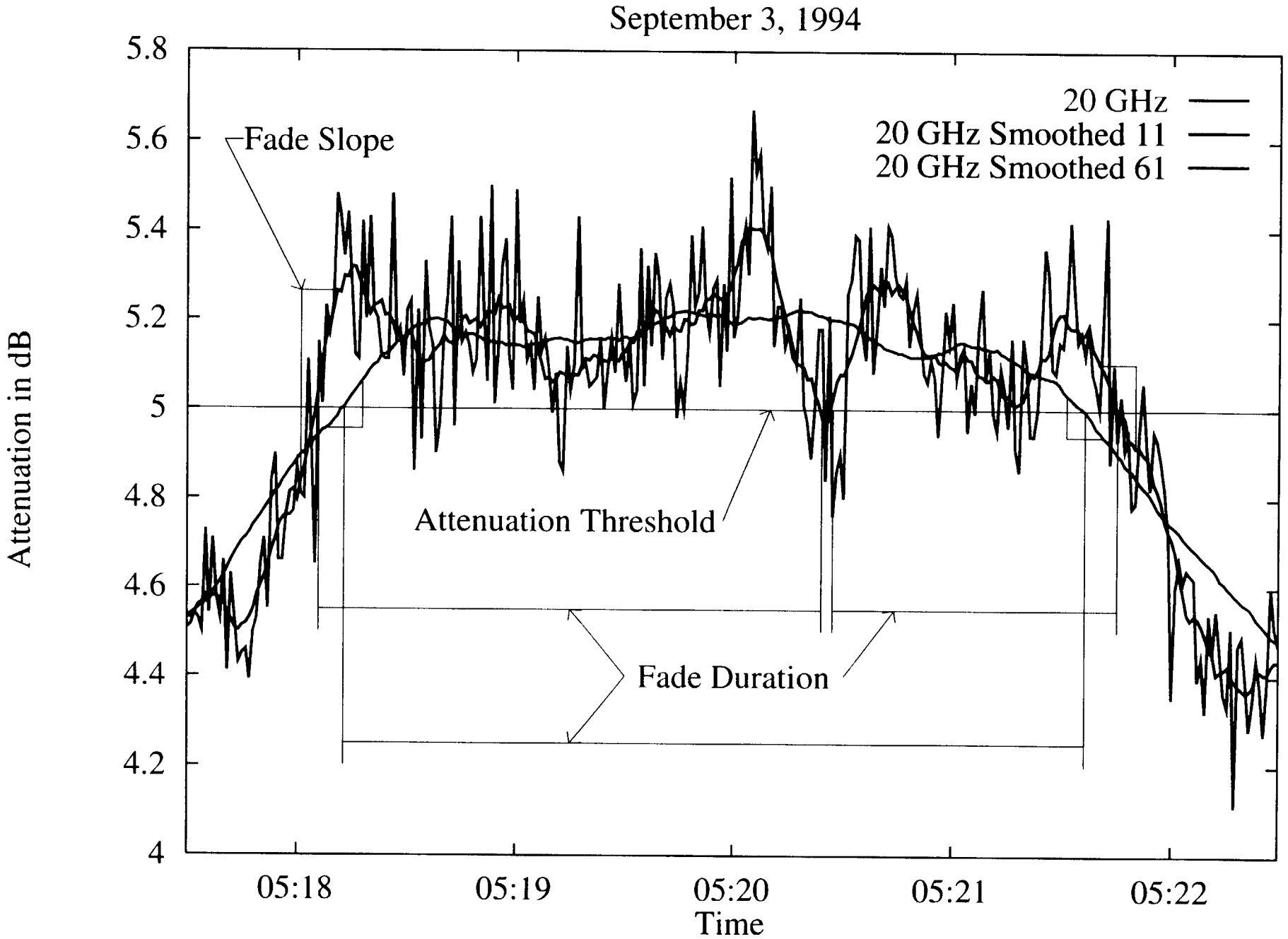
September 3, 1994
20 GHz
20 GHz Smoothed 11
20 GHz Smoothed 61
Fade Slope
Attenuation Threshold
Fade Duration
Attenuation in dB
Time
5.8
5.6
5.4
5.2
5
4.8
4.6
4.4
4.2
4
05:18
05:19
05:20
05:21
05:22

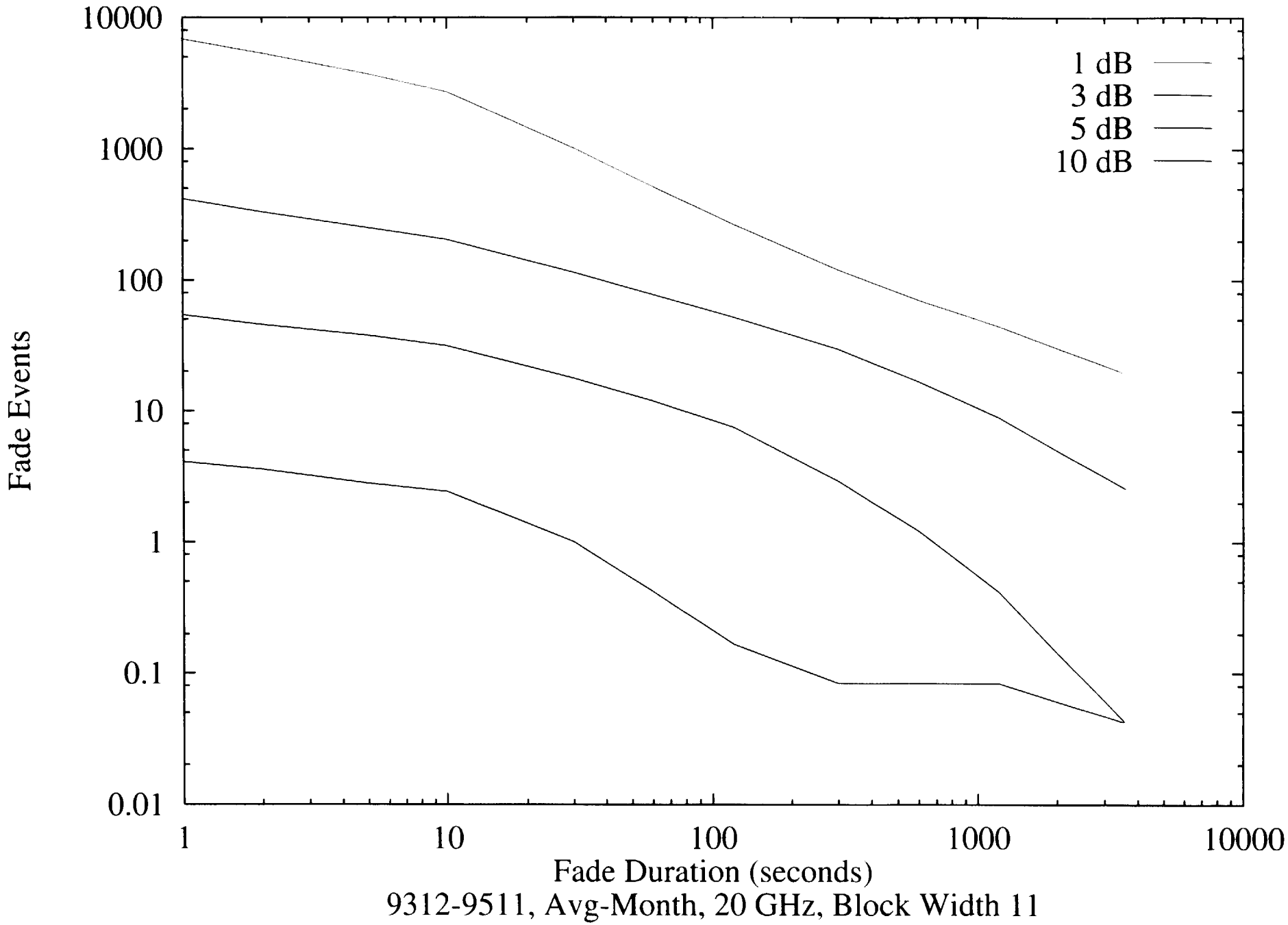
10000
1000
100
10
1
0.1
0.01
Fade Events
1 dB
3 dB
5 dB
10 dB
1
10
100
1000
10000
Fade Duration (seconds)
9312-9511, Avg-Month, 20 GHz, Block Width 11

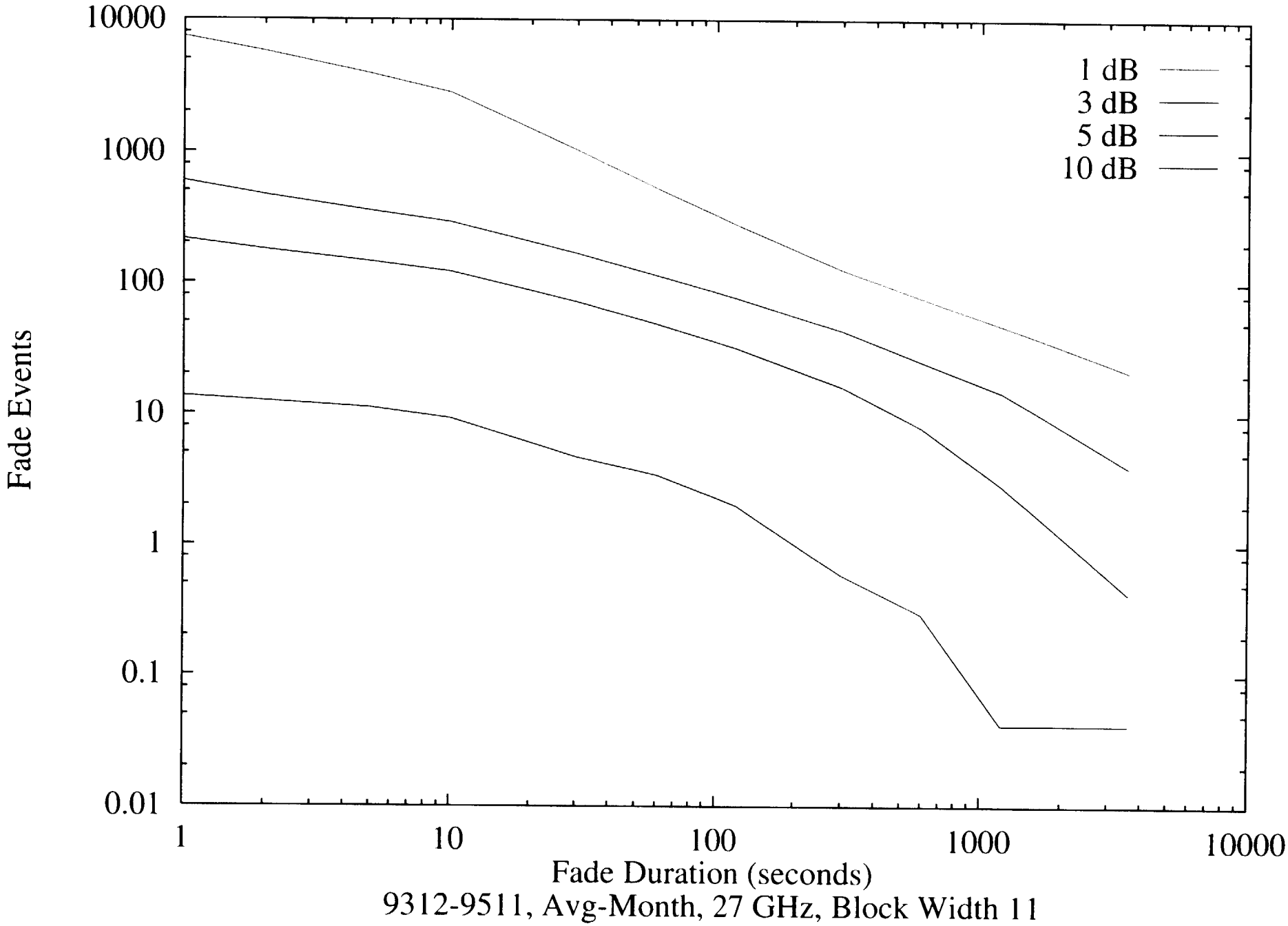
10000
1000
100
10
1
0.1
0.01
Fade Events
1
10
100
1000
10000
Fade Duration (seconds)
1 dB
3 dB
5 dB
10 dB
9312-9511, Avg-Month, 27 GHz, Block Width 11

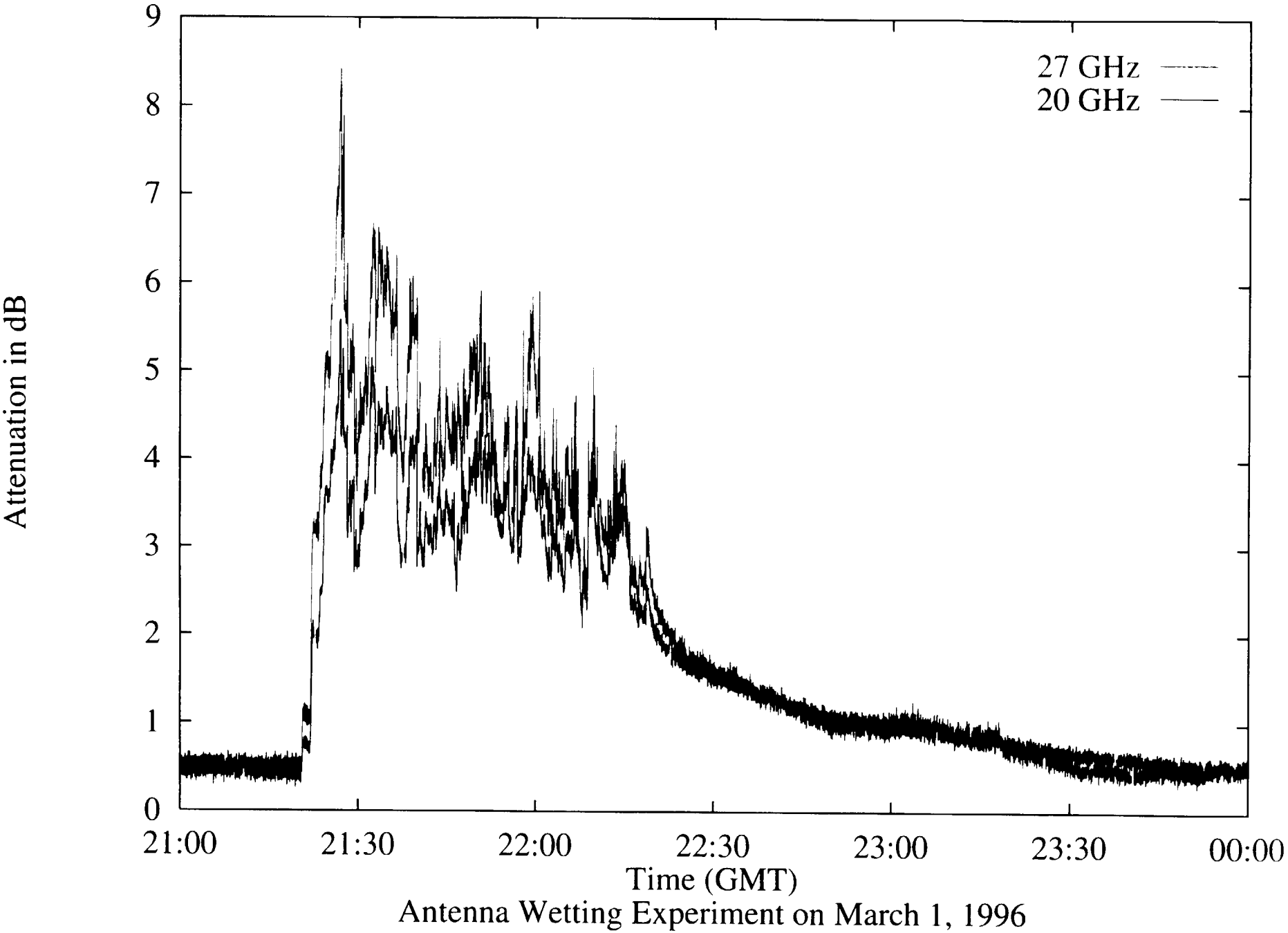
27 GHz
20 GHz
Attenuation in dB
0
1
2
3
4
5
6
7
8
9
21:00
21:30
22:00
22:30
23:00
23:30
00:00
Time (GMT)
Antenna Wetting Experiment on March 1, 1996

Areas of Current Interest

- Possible contributions from snow events
- Effects of moisture penetration into feed
- Calibration issues
- Precipitation on antenna surfaces (most problematic issue; applies for *all* APT sites)
- Accuracy of 20.2/27.5-GHz statistics (related to factors listed above)

Summary

- ACTS measurements continuing at UBC
- UBC operates/maintains APT; inspects and preprocesses the data; contributes expertise in other areas; etc.
- CRC implementing data display, editing and analysis capability to augment ACTS propagation investigations
- UBC/CRC will address data issues (in collaboration with other ACTS experimenters)

Ka-Band Propagation Studies Using the ACTS Propagation Terminal and the CSU-CHILL Multiparameter Radar

Experimenters

Colorado State University

Department of Electrical Engineering

Fort Collins, CO 80523

Investigators

V.N. Bringi, Professor

John Beaver

NASA Propagation Experimenters Meeting
(NAPEX XXI)
and
ACTS Propagation Studies Mini-Workshop
June 11-13, 1996
El Segundo, CA

Outline

- CSU-APT Status Report
  - Terminal Update

- Brief Description of Two New Case Studies for 1997
  - Radar data available from Wyoming King Air

- CSU-APT Attenuation Data
  - 1996 Data
  - Comparisons with 1994 and 1995 data

CSU-APT Site Location

- CSU-APT is located about 30 km southeast of Fort Collins near LaSalle, Colorado (approx. 13 km south of the CSU-CHILL radar)
- APT elevation angle - 43 deg
- APT azimuth angle - 173 deg

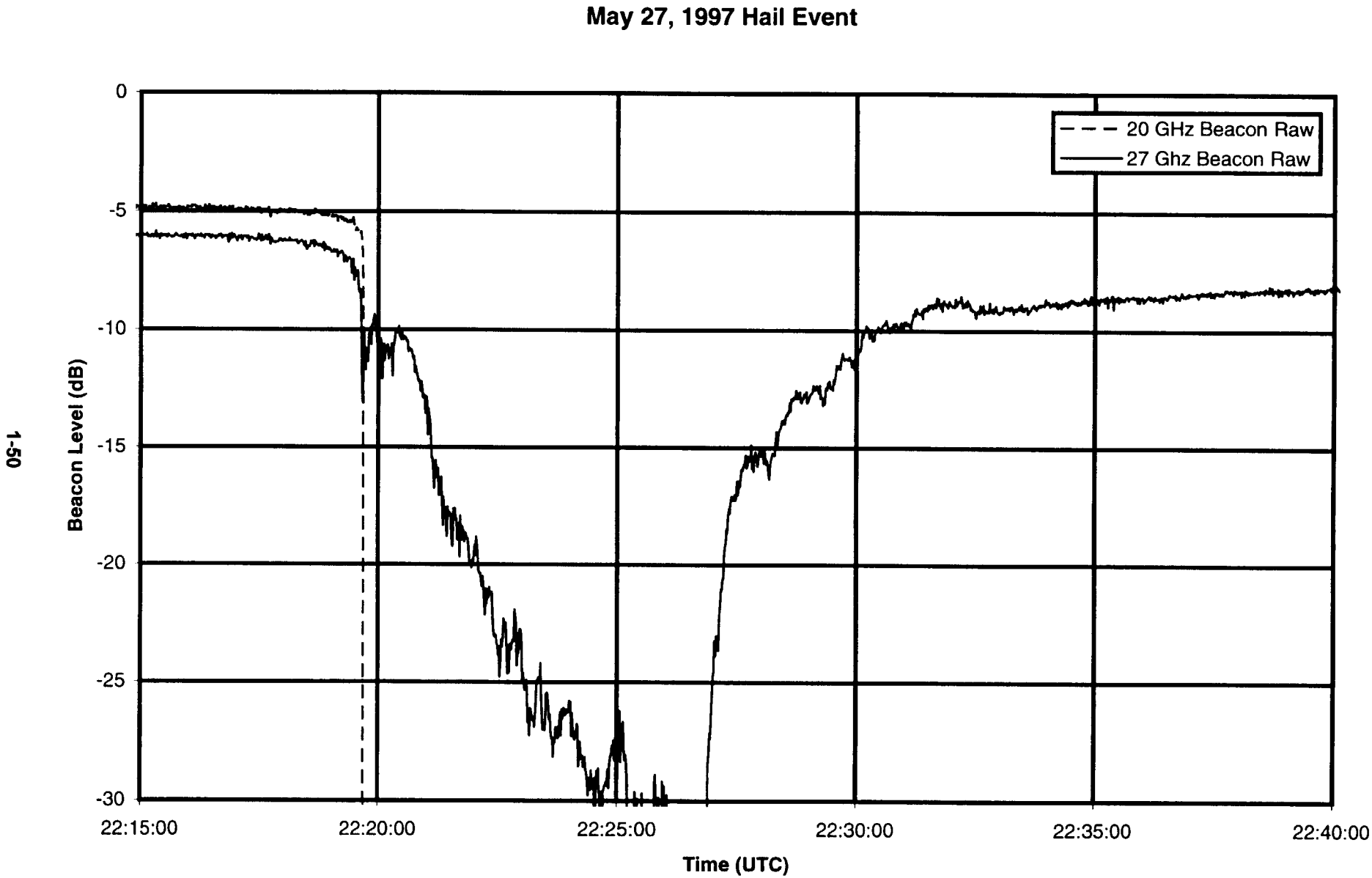
May 27, 1997 Hail Event
20 GHz Beacon Raw
27 Ghz Beacon Raw
Beacon Level (dB)
0
-5
-10
-15
-20
-25
-30
22:15:00
22:20:00
22:25:00
22:30:00
22:35:00
22:40:00
Time (UTC)

CSU-APT Hardware Status

- Severe hail storm directly hit APT site on May 27, 1997
  - Radar reported +60 dBZ near the ground at APT site.
  - Ground observers at site reported hail stones on ground were approximately 2.5 cm in diameter.
- Damage to APT system
  - Feed horn membrane destroyed
  - Heat exchanger fins flattened
  - 20 GHz LNA out of commision

Current Research Projects

- Two case studies with concurrent CSU-CHILL radar data and Wyoming King Air cloud probe and polarimetric radar data
  - Wyoming King Air data
    - Various cloud probes and weather instrumentation
    - 95 GHz polarimetric airborne radar - can be either vertically pointing or horizontally pointing
  - CSU-CHILL radar data
    - 3 GHz polarimetric radar data

- March 13, 1997 stratiform event
  - Wyoming King Air made a pass along the ACTS slant path with radar in a vertically pointing mode
  - CSU-CHILL radar scanning along slant path

- April 2, 1997 event
  - Layer of ice crystals aloft (high Zdr's seen by CHILL and King Air on the order of 4 dB)
  - Scintillation effects and small fades (< 1dB) are noted in ACTS data (no precipitation at ground level)

Statistics

- Cumulative Distribution Function (CDF)
  - For both AFS and ARD data at 20 and 27 GHz
  - No average applied to the data
  - Data is binned from -3.0 to 30.0 dB in 0.1 dB steps

- Attenuation Ratio (RA)
  - 30 second moving average is applied to the data
  - Divide the 27 GHz AFS by the 20 GHz AFS
  - RA values binned from 0 to 10 in 0.05 steps for base attenuation levels greater than 1 dB
  - RA values are also binned from different base attenuation levels ranging from 1 to 30 dB in 1 dB steps

Statistics

- Fade Duration (FD) and Inter-Fade Duration (IF)
  - 30 second moving average is applied to the AFS data
  - threshold levels range from 0 to 30 dB in 1 dB steps
  - fade duration (nonfade duration) bins include 0-1, 1-2, 2-3, 3-5, 5-6, 6-10, 10-15, 15-18, 18-20, 20-30, 30-60, 60-120, 120-180, 180-300, 300-600, 600-1200, 1200-1800, and 1800-3600 seconds

- Fade Slope (FS)
  - 10 second moving average applied to AFS data
  - defined only if attenuation level corsses a threshold for more than 10 seconds (above or below)
  - threshold values range from 0 to 30 dB in 1 dB steps
  - FS data are binned from -1.25 to 1.25 dB/sec in 0.0d dB/sec steps

$$FS_i = (AFS_{i+5} - AFS_{i-5}) / 10.0$$

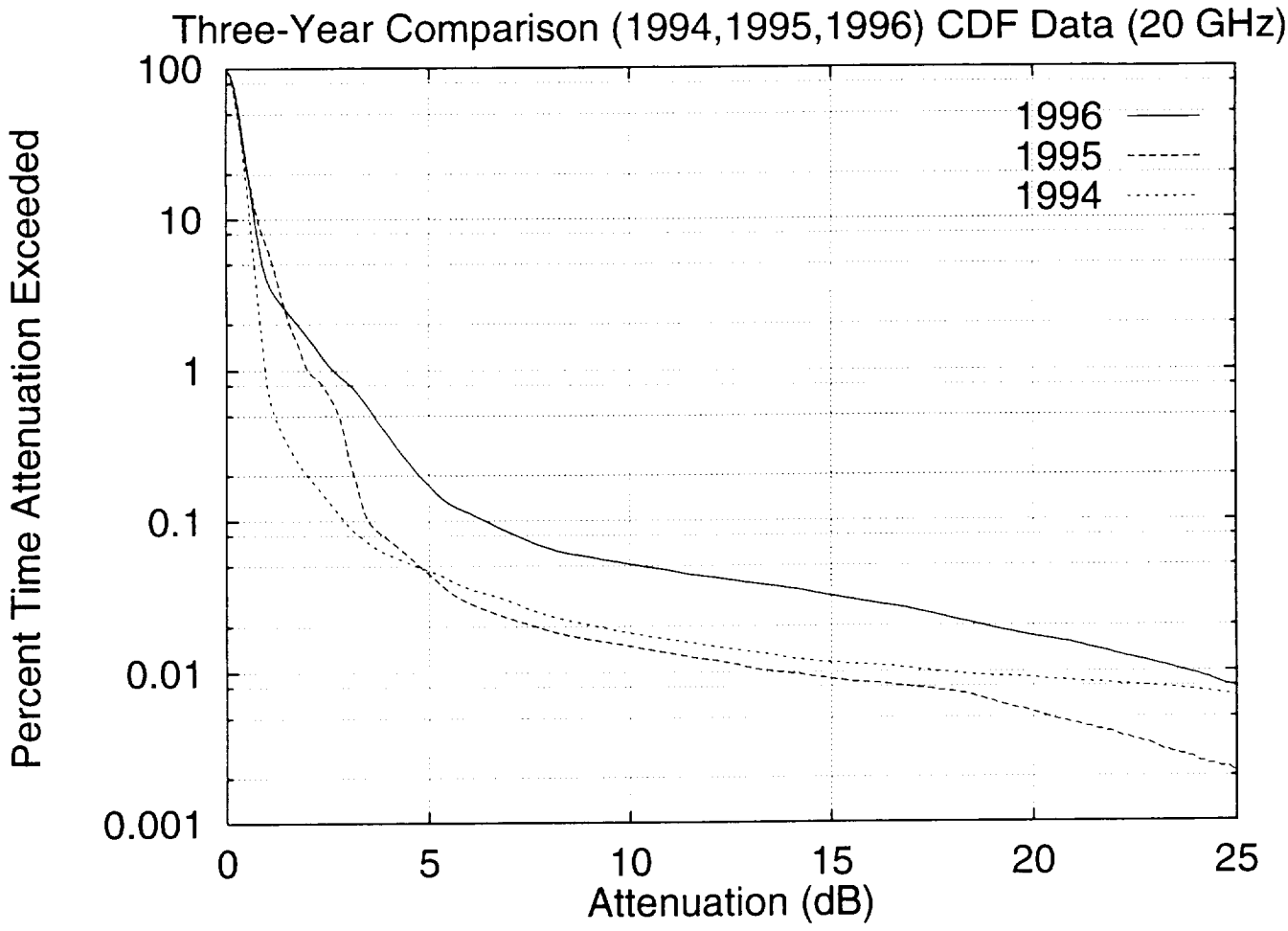
Three-Year Comparison (1994,1995,1996) CDF Data (20 GHz)
Percent Time Attenuation Exceeded
100
10
1
0.1
0.01
0.001
0
5
10
15
20
25
Attenuation (dB)
1996
1995
1994

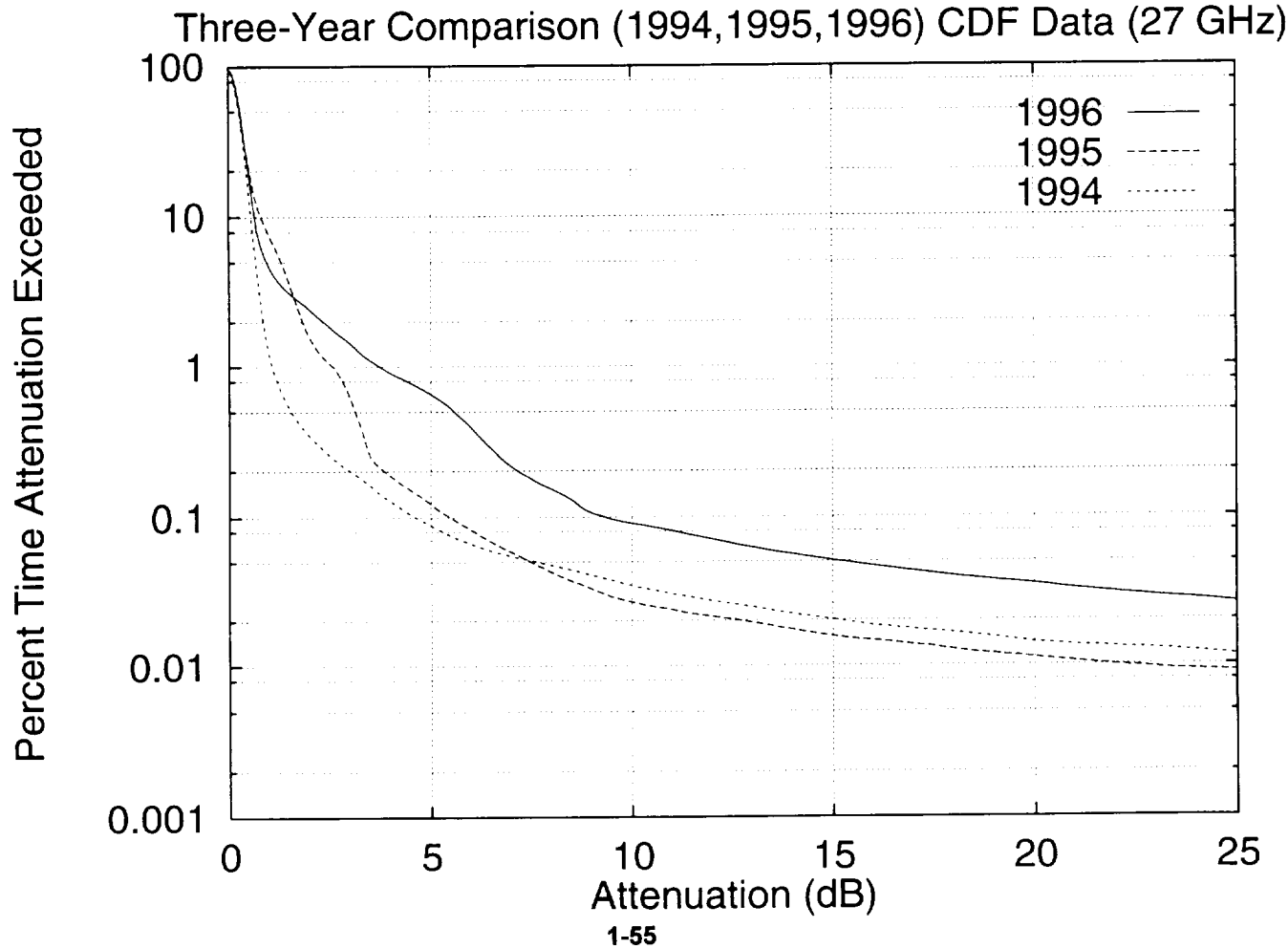
Three-Year Comparison (1994,1995,1996) CDF Data (27 GHz)
Percent Time Attenuation Exceeded
100
10
1
0.1
0.01
0.001
0
5
10
15
20
25
Attenuation (dB)
1996
1995
1994

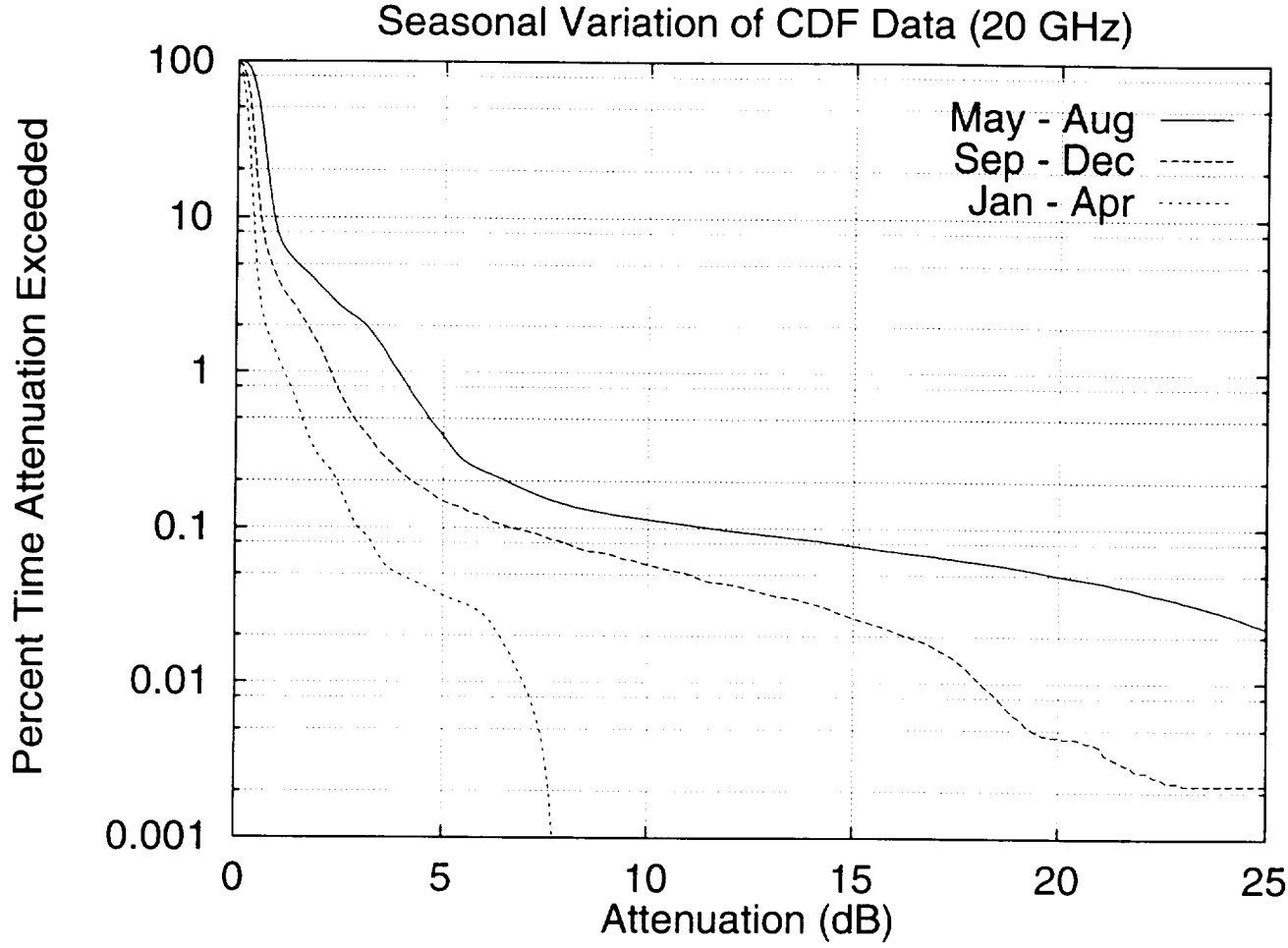
Seasonal Variation of CDF Data (20 GHz)
Percent Time Attenuation Exceeded
100
10
1
0.1
0.01
0.001
0
5
10
15
20
25
Attenuation (dB)
May - Aug
Sep - Dec
Jan - Apr

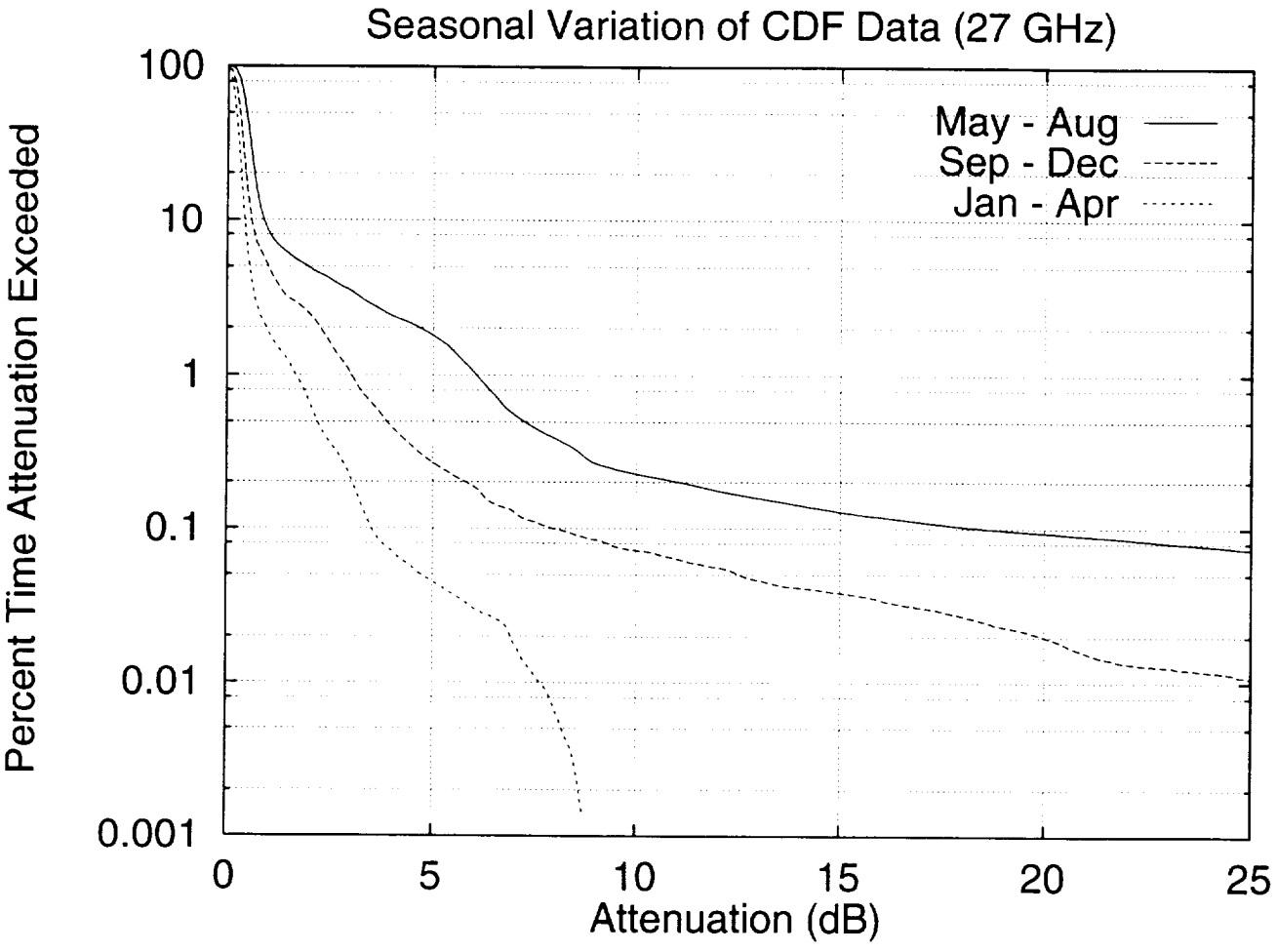
Seasonal Variation of CDF Data (27 GHz)
Percent Time Attenuation Exceeded
100
10
1
0.1
0.01
0.001
0
5
10
15
20
25
Attenuation (dB)
May - Aug
Sep - Dec
Jan - Apr

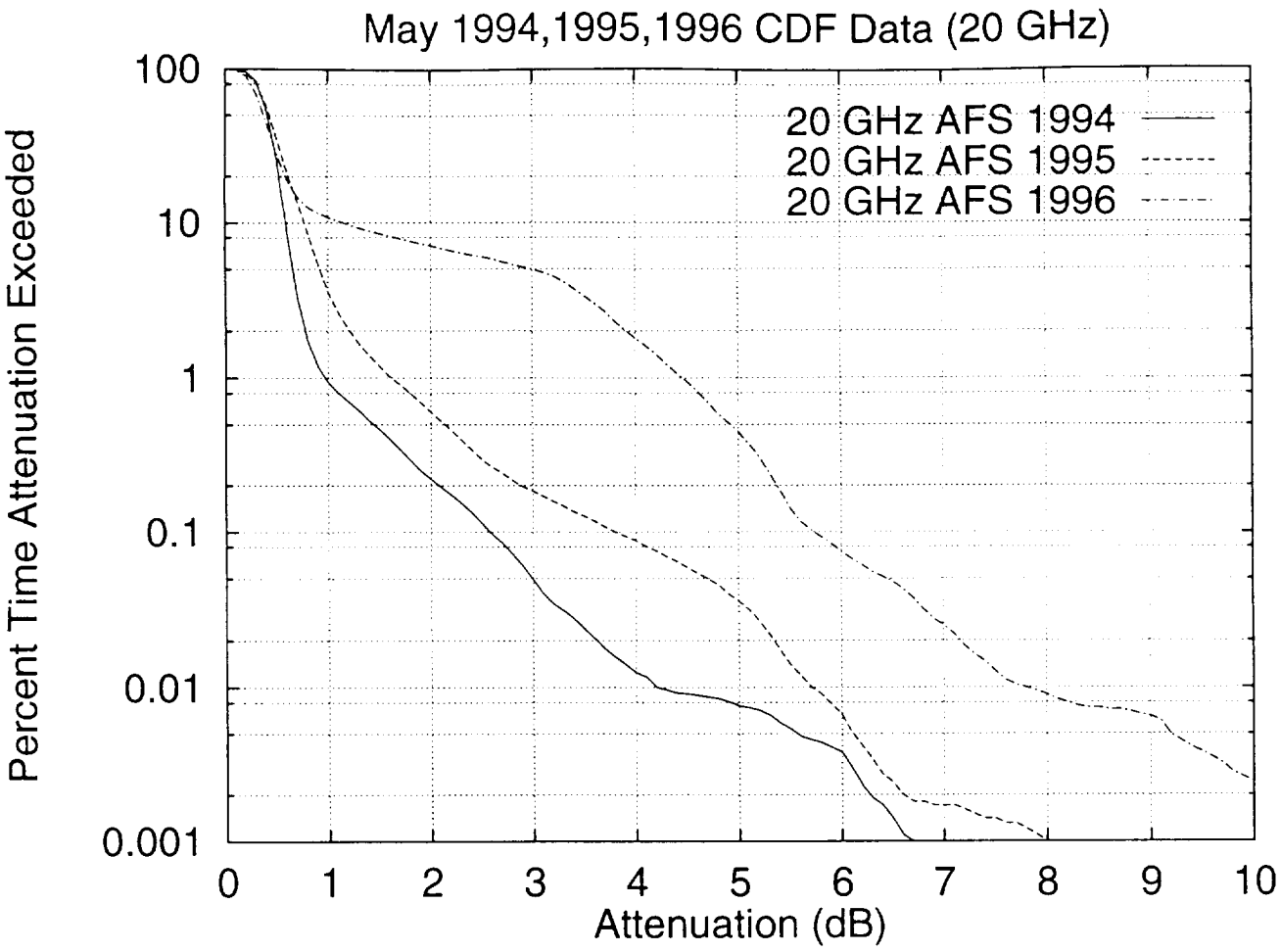
May 1994,1995,1996 CDF Data (20 GHz)
Percent Time Attenuation Exceeded
Attenuation (dB)
20 GHz AFS 1994
20 GHz AFS 1995
20 GHz AFS 1996
100
10
1
0.1
0.01
0.001
0 1 2 3 4 5 6 7 8 9 10

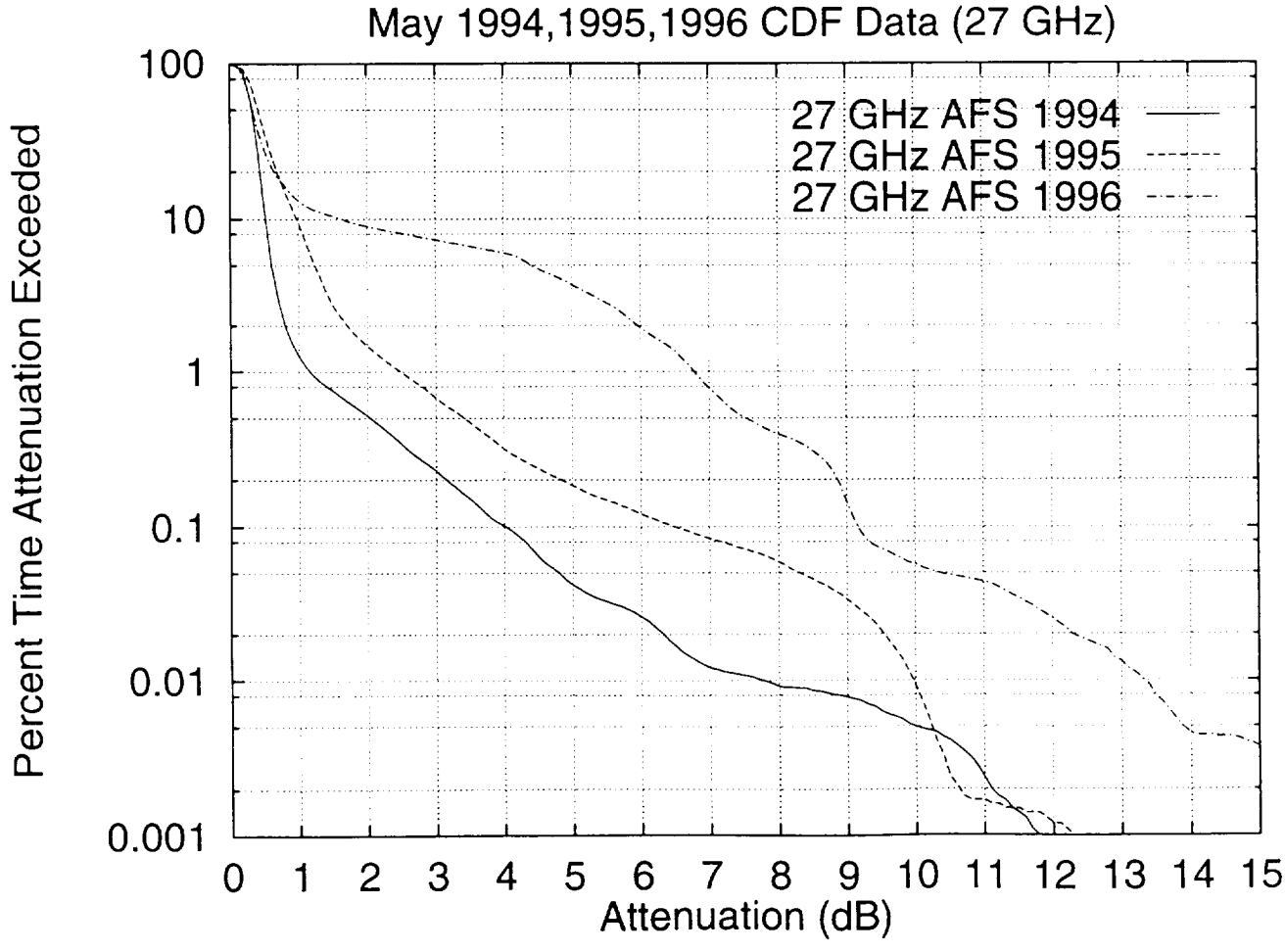
May 1994,1995,1996 CDF Data (27 GHz)
Percent Time Attenuation Exceeded
Attenuation (dB)
27 GHz AFS 1994
27 GHz AFS 1995
27 GHz AFS 1996
100
10
1
0.1
0.01
0.001
0 1 2 3 4 5 6 7 8 9 10 11 12 13 14 15

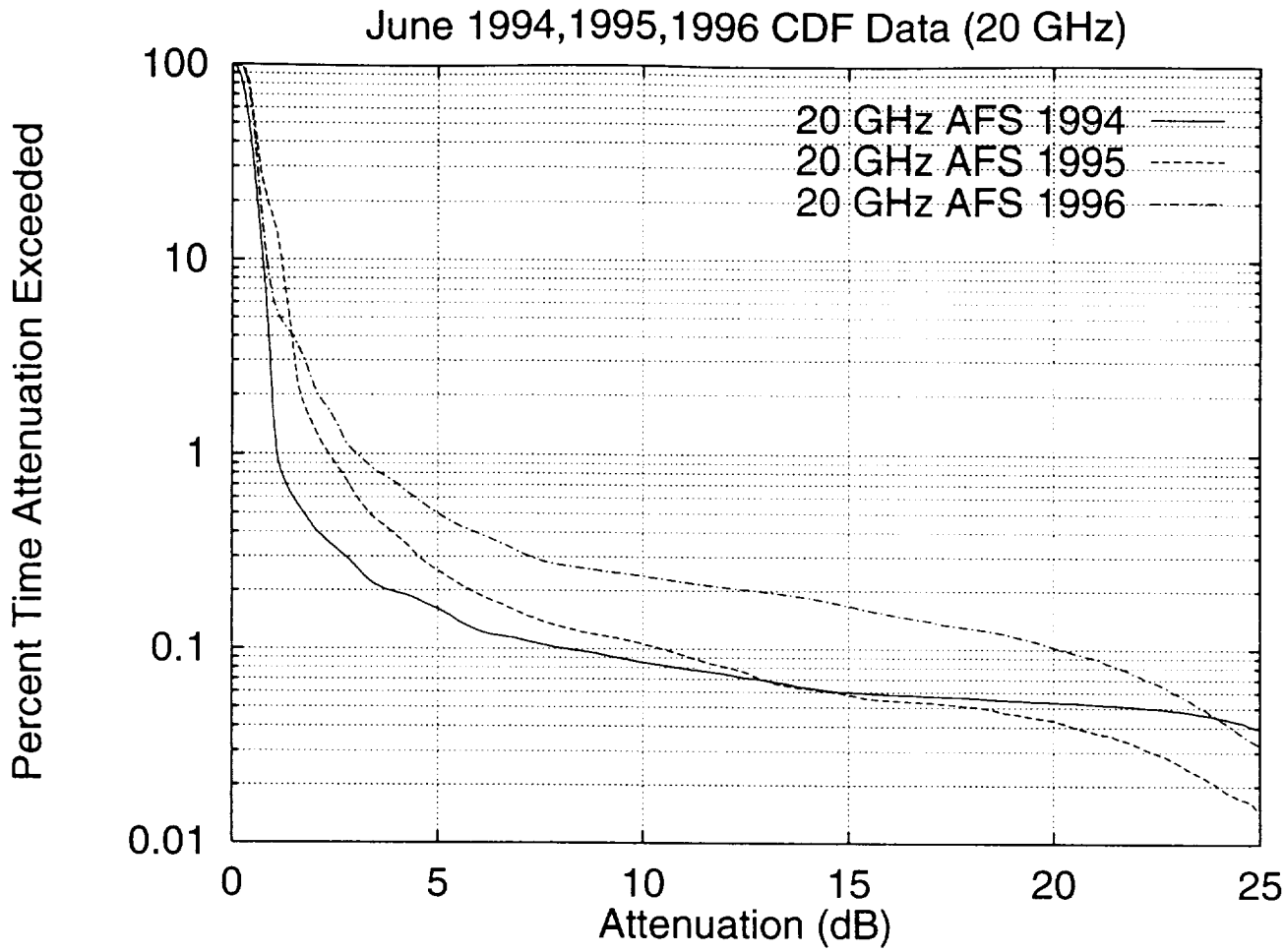
June 1994,1995,1996 CDF Data (20 GHz)
Percent Time Attenuation Exceeded
100
10
1
0.1
0.01
0
5
10
15
20
25
Attenuation (dB)
20 GHz AFS 1994
20 GHz AFS 1995
20 GHz AFS 1996

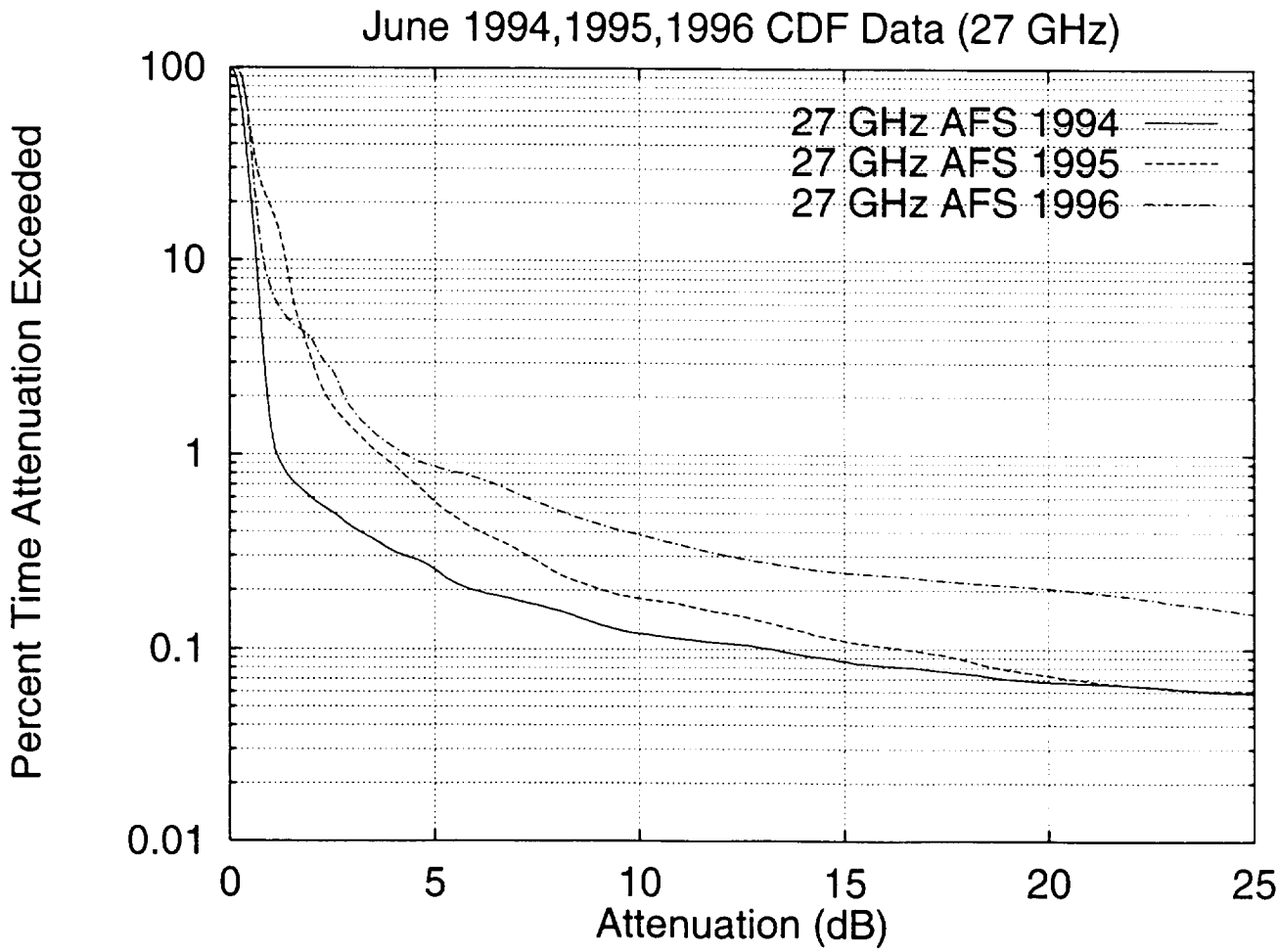
June 1994,1995,1996 CDF Data (27 GHz)
Percent Time Attenuation Exceeded
100
10
1
0.1
0.01
0
5
10
15
20
25
Attenuation (dB)
27 GHz AFS 1994
27 GHz AFS 1995
27 GHz AFS 1996

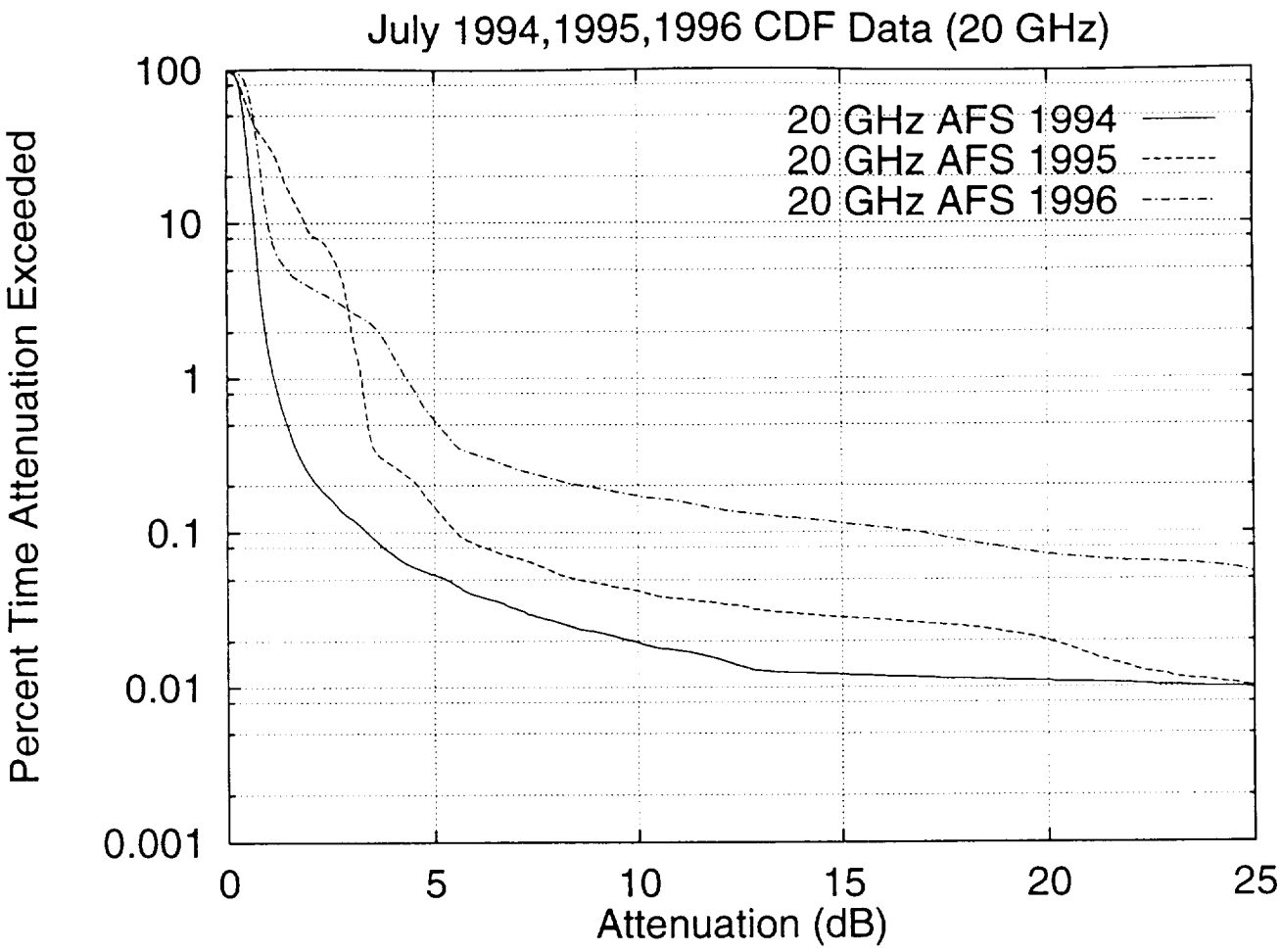
July 1994,1995,1996 CDF Data (20 GHz)
Percent Time Attenuation Exceeded
100
10
1
0.1
0.01
0.001
0
5
10
15
20
25
Attenuation (dB)
20 GHz AFS 1994
20 GHz AFS 1995
20 GHz AFS 1996

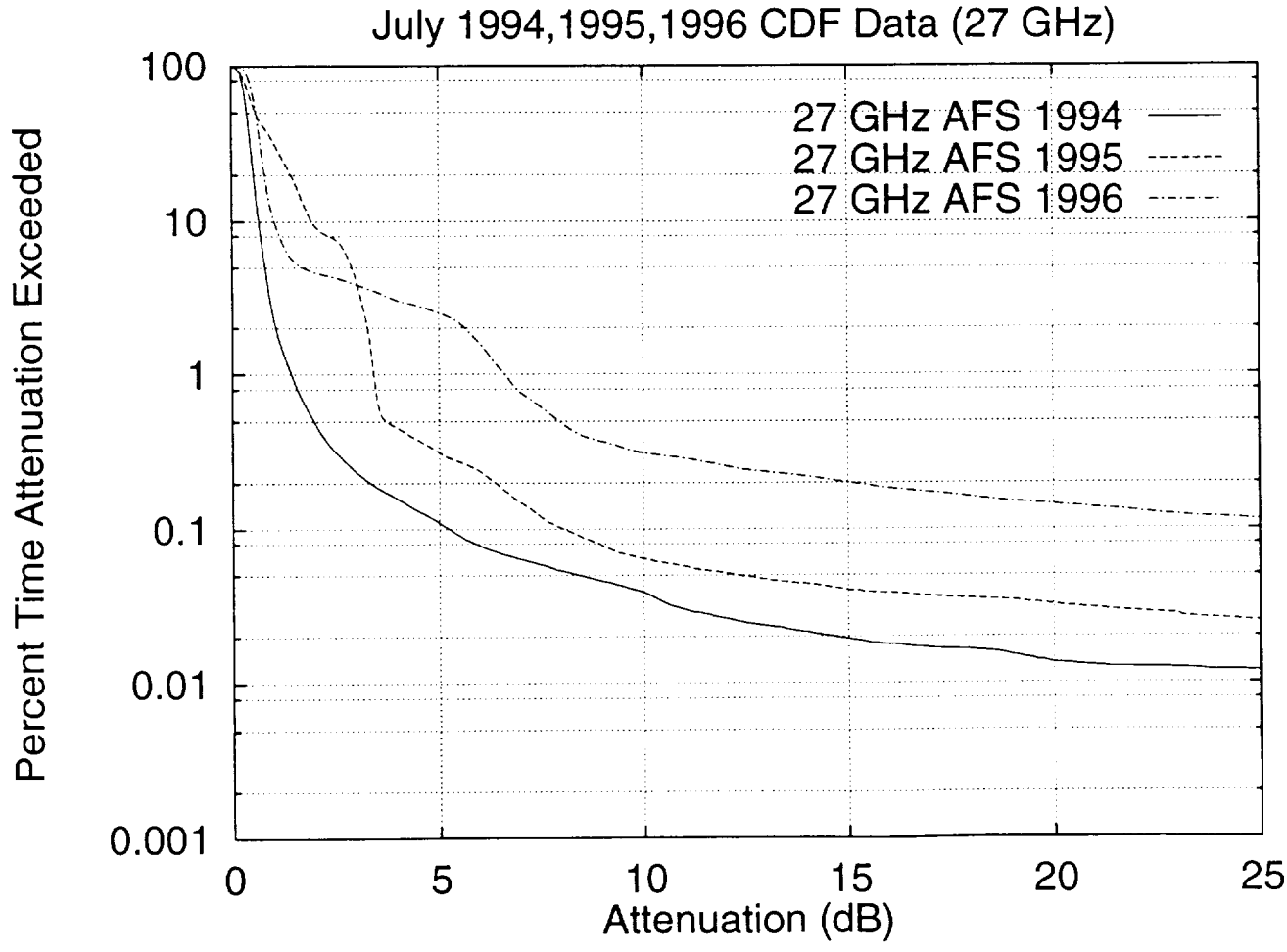
July 1994,1995,1996 CDF Data (27 GHz)
Percent Time Attenuation Exceeded
100
10
1
0.1
0.01
0.001
0
5
10
15
20
25
Attenuation (dB)
27 GHz AFS 1994
27 GHz AFS 1995
27 GHz AFS 1996

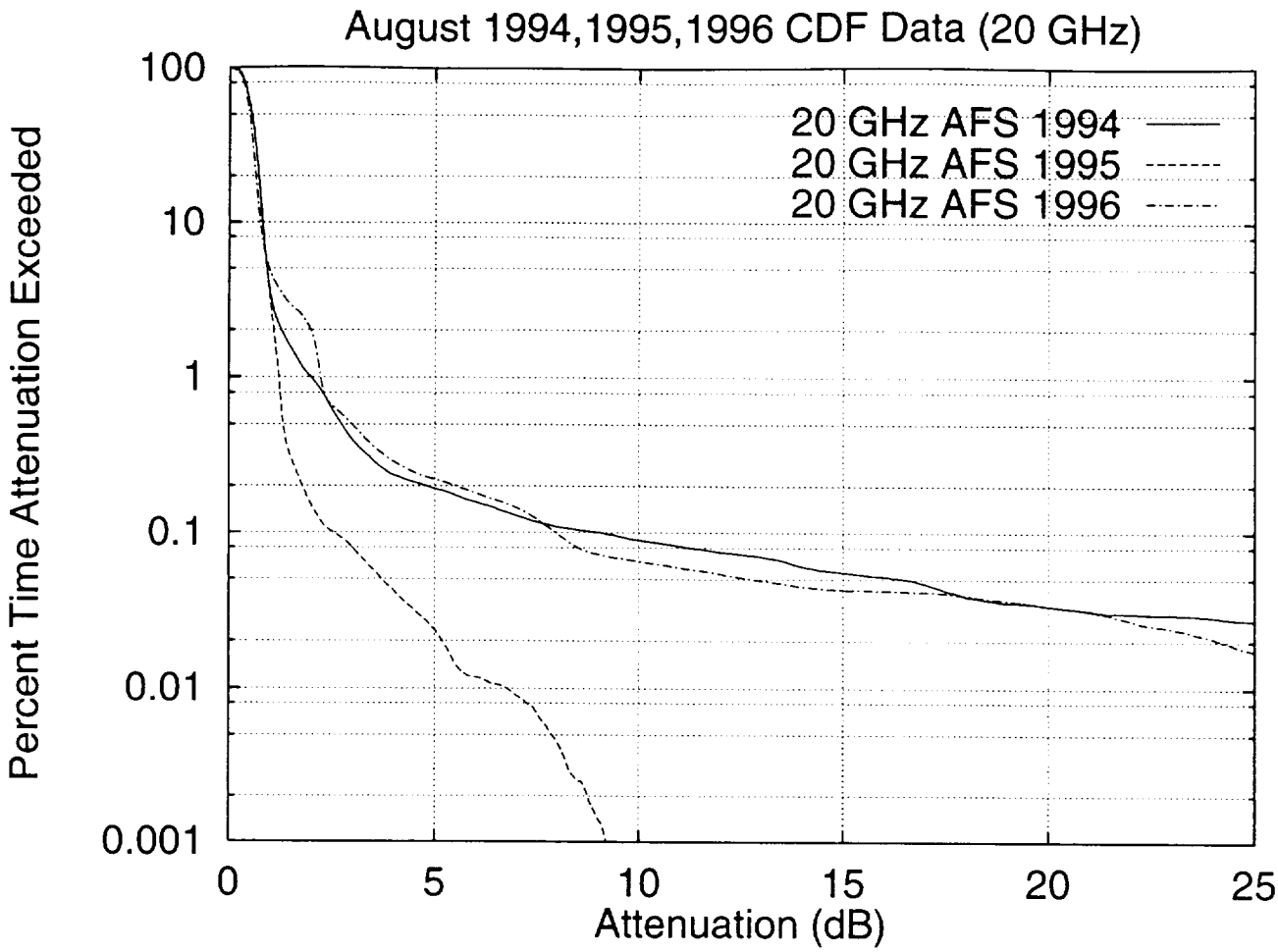
August 1994,1995,1996 CDF Data (20 GHz)
20 GHz AFS 1994
20 GHz AFS 1995
20 GHz AFS 1996
Percent Time Attenuation Exceeded
100
10
1
0.1
0.01
0.001
0
5
10
15
20
25
Attenuation (dB)

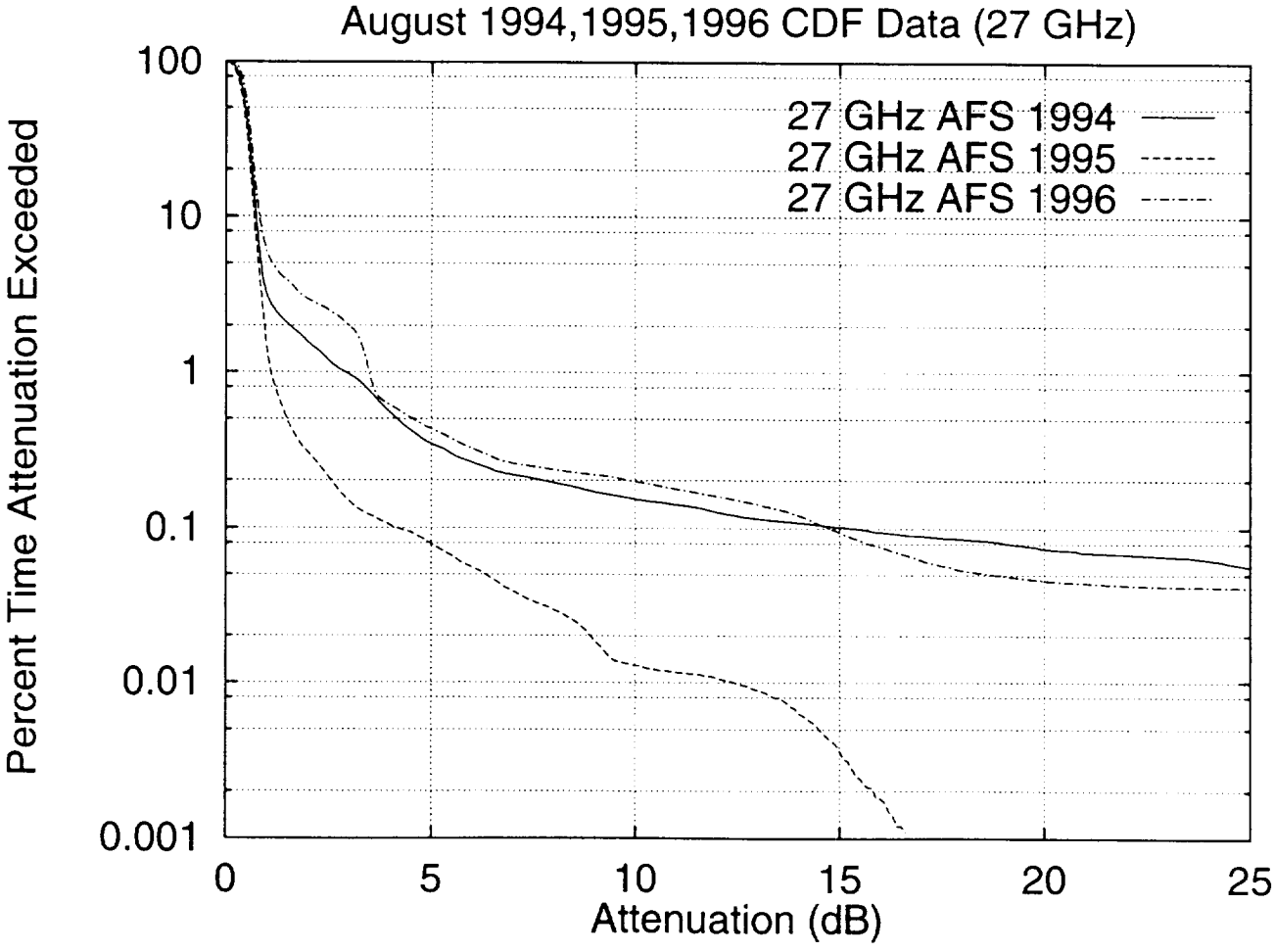
August 1994,1995,1996 CDF Data (27 GHz)
27 GHz AFS 1994
27 GHz AFS 1995
27 GHz AFS 1996
Percent Time Attenuation Exceeded
100
10
1
0.1
0.01
0.001
0
5
10
15
20
25
Attenuation (dB)

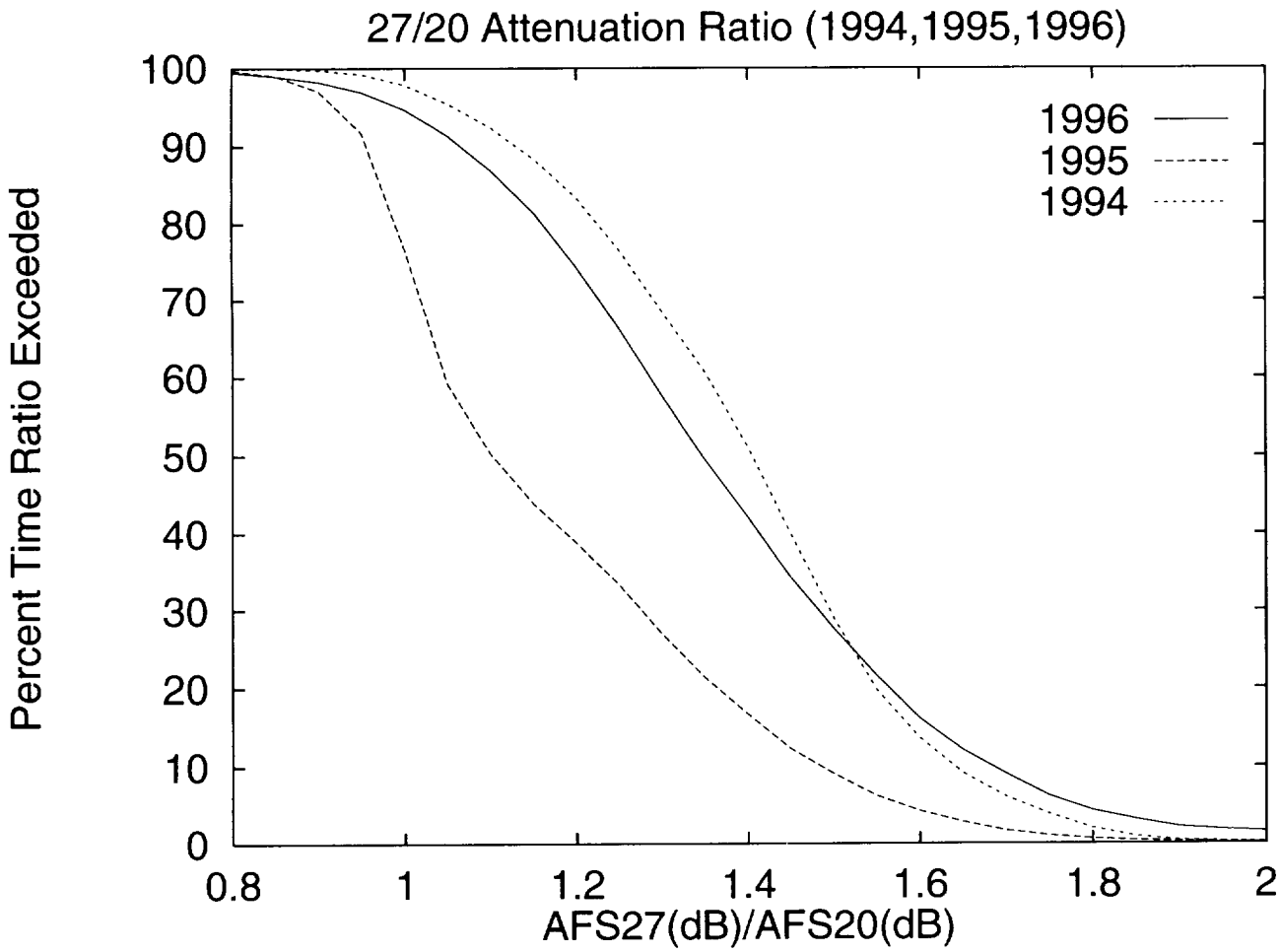
27/20 Attenuation Ratio (1994,1995,1996)
Percent Time Ratio Exceeded
100
90
80
70
60
50
40
30
20
10
0
0.8
1
1.2
1.4
1.6
1.8
2
AFS27(dB)/AFS20(dB)
1996
1995
1994

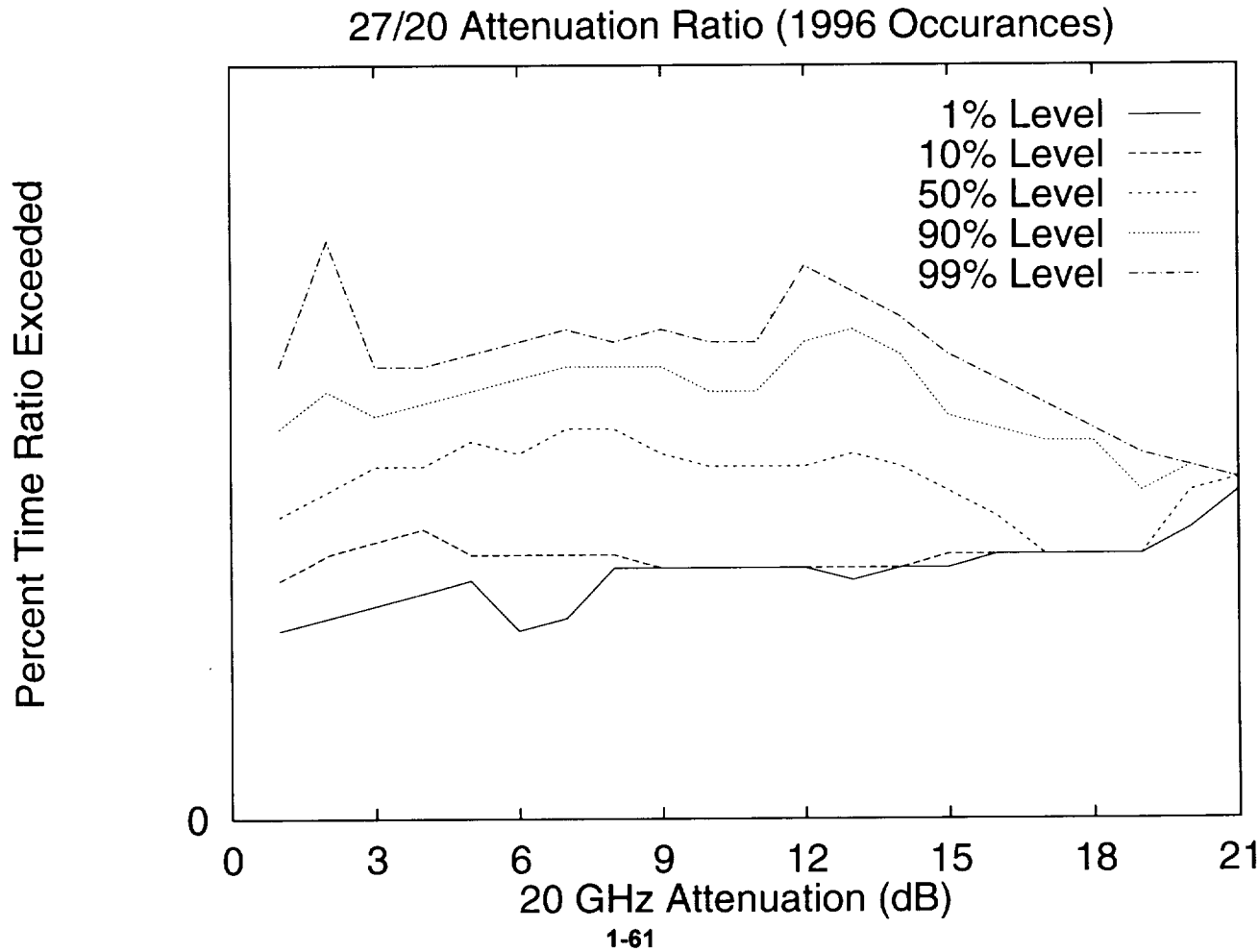
27/20 Attenuation Ratio (1996 Occurances)
Percent Time Ratio Exceeded
0
0
3
6
9
12
15
18
21
20 GHz Attenuation (dB)
1% Level
10% Level
50% Level
90% Level
99% Level

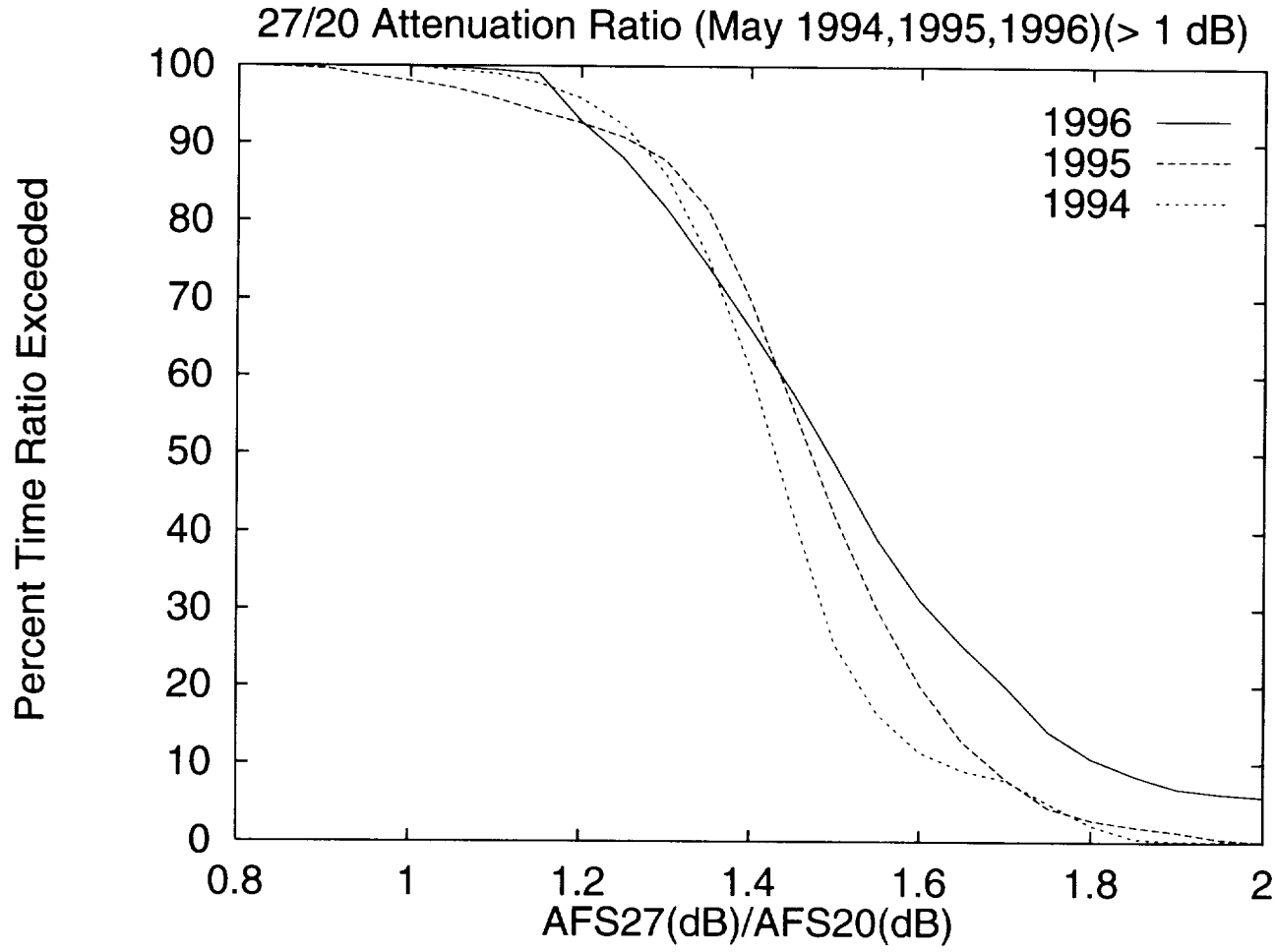
27/20 Attenuation Ratio (May 1994,1995,1996)(> 1 dB)
Percent Time Ratio Exceeded
100
90
80
70
60
50
40
30
20
10
0
0.8
1
1.2
1.4
1.6
1.8
2
AFS27(dB)/AFS20(dB)
1996
1995
1994

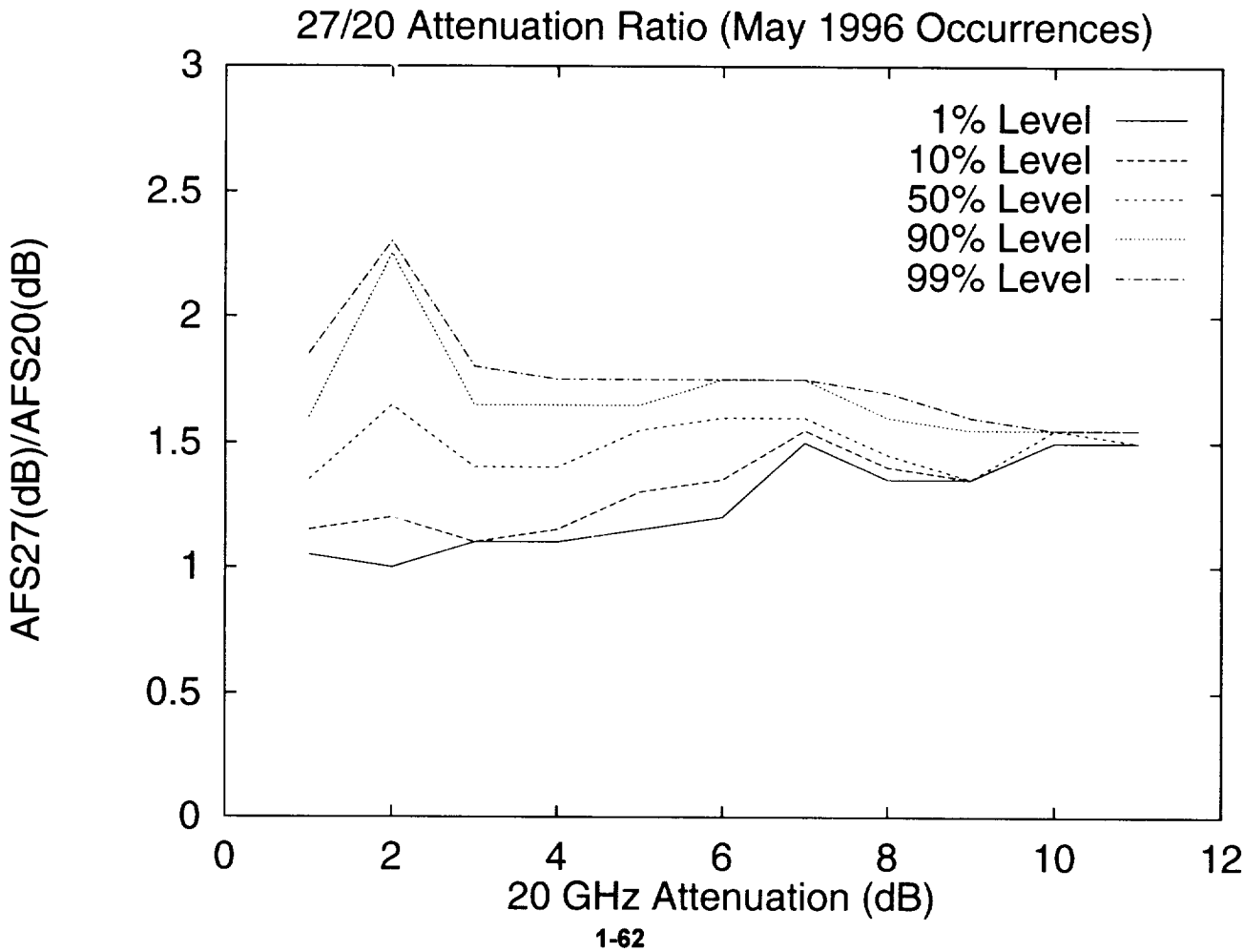
27/20 Attenuation Ratio (May 1996 Occurrences)
AFS27(dB)/AFS20(dB)
3
2.5
2
1.5
1
0.5
0
0
2
4
6
8
10
12
20 GHz Attenuation (dB)
1% Level
10% Level
50% Level
90% Level
99% Level

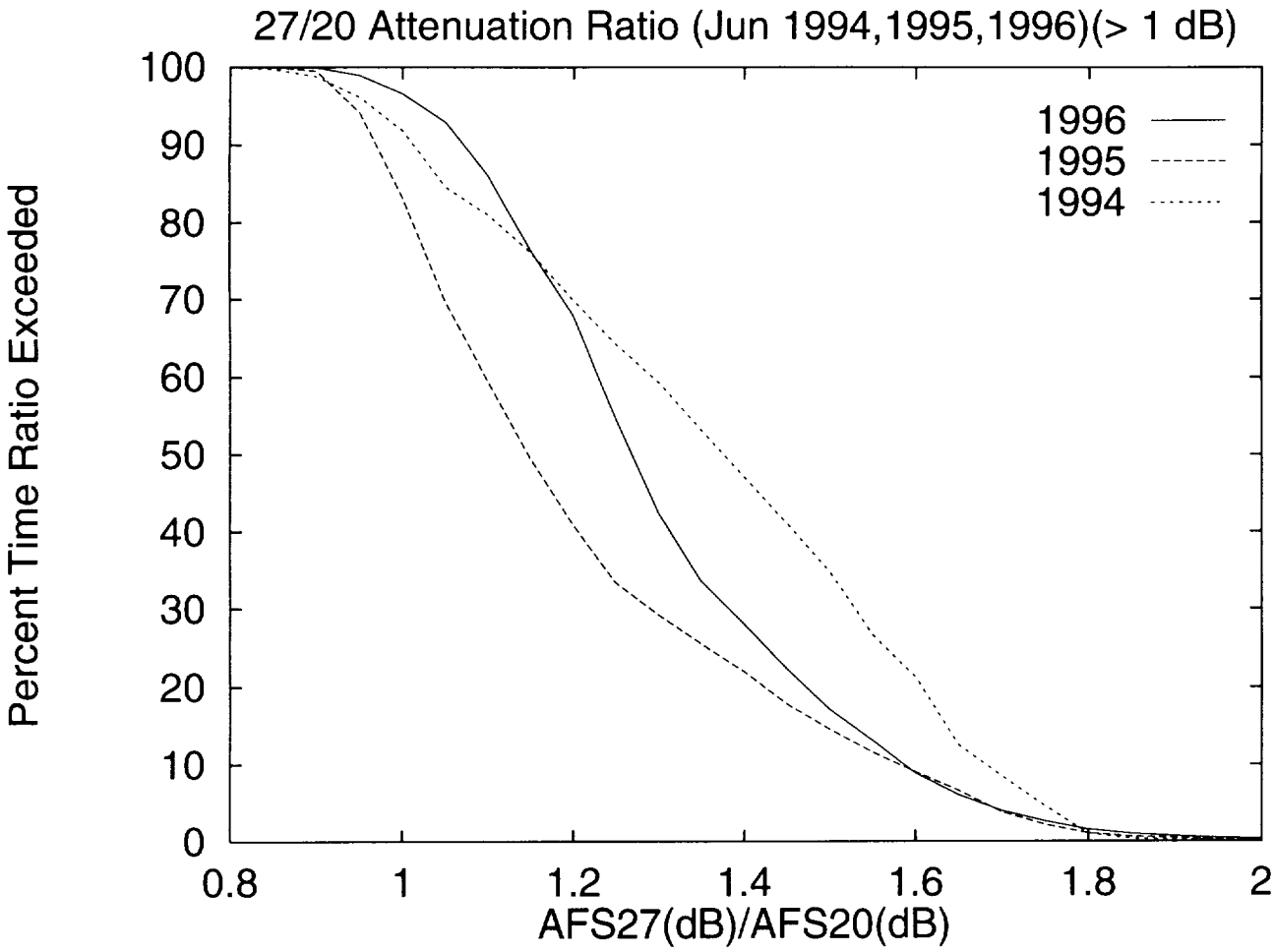
27/20 Attenuation Ratio (Jun 1994,1995,1996)(> 1 dB)
Percent Time Ratio Exceeded
100
90
80
70
60
50
40
30
20
10
0
0.8
1
1.2
1.4
1.6
1.8
2
AFS27(dB)/AFS20(dB)
1996
1995
1994

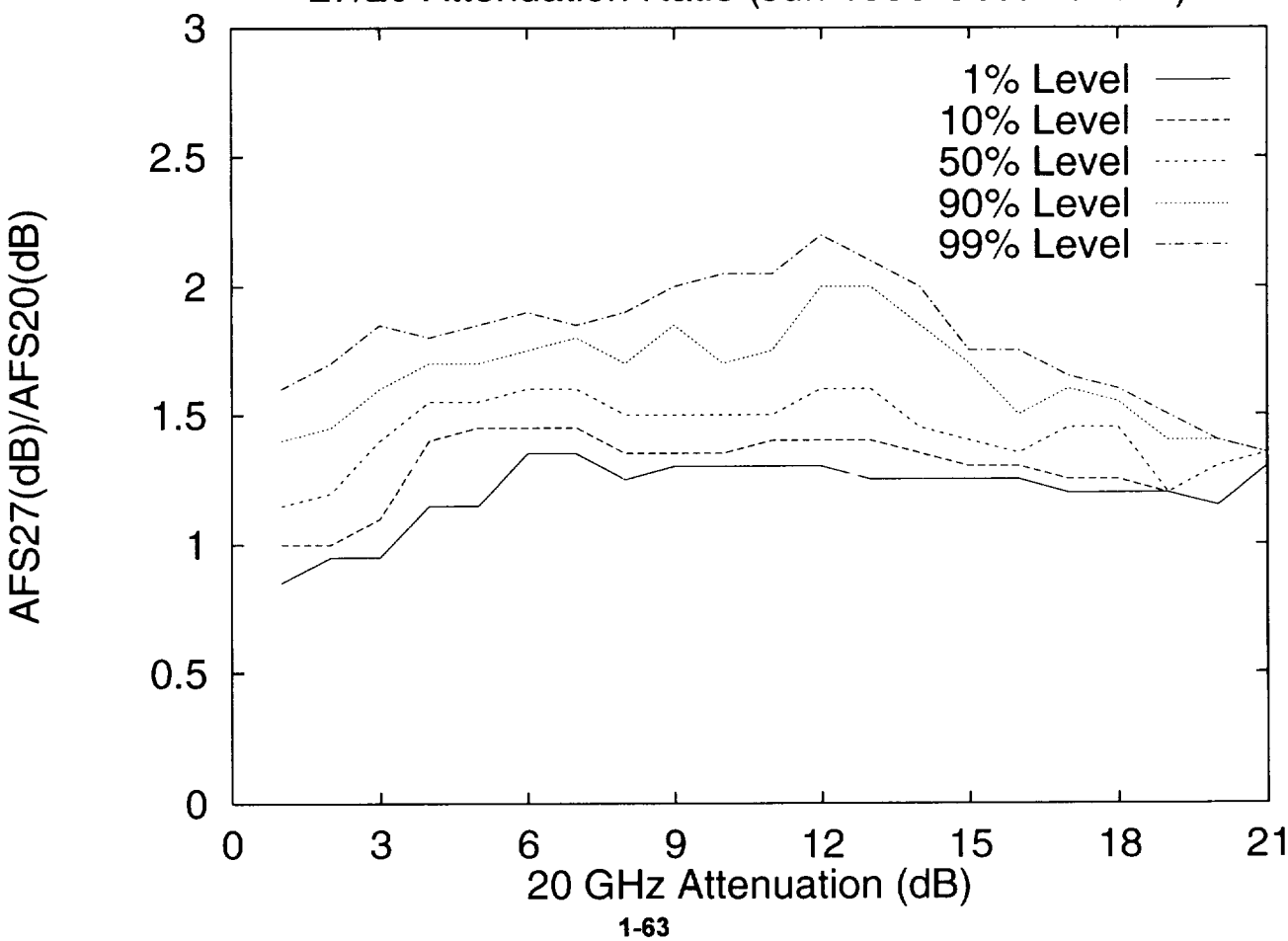
27/20 Attenuation Ratio (Jun 1996 Occurrences)
AFS27(dB)/AFS20(dB)
3
2.5
2
1.5
1
0.5
0
0
3
6
9
12
15
18
21
20 GHz Attenuation (dB)
1% Level
10% Level
50% Level
90% Level
99% Level

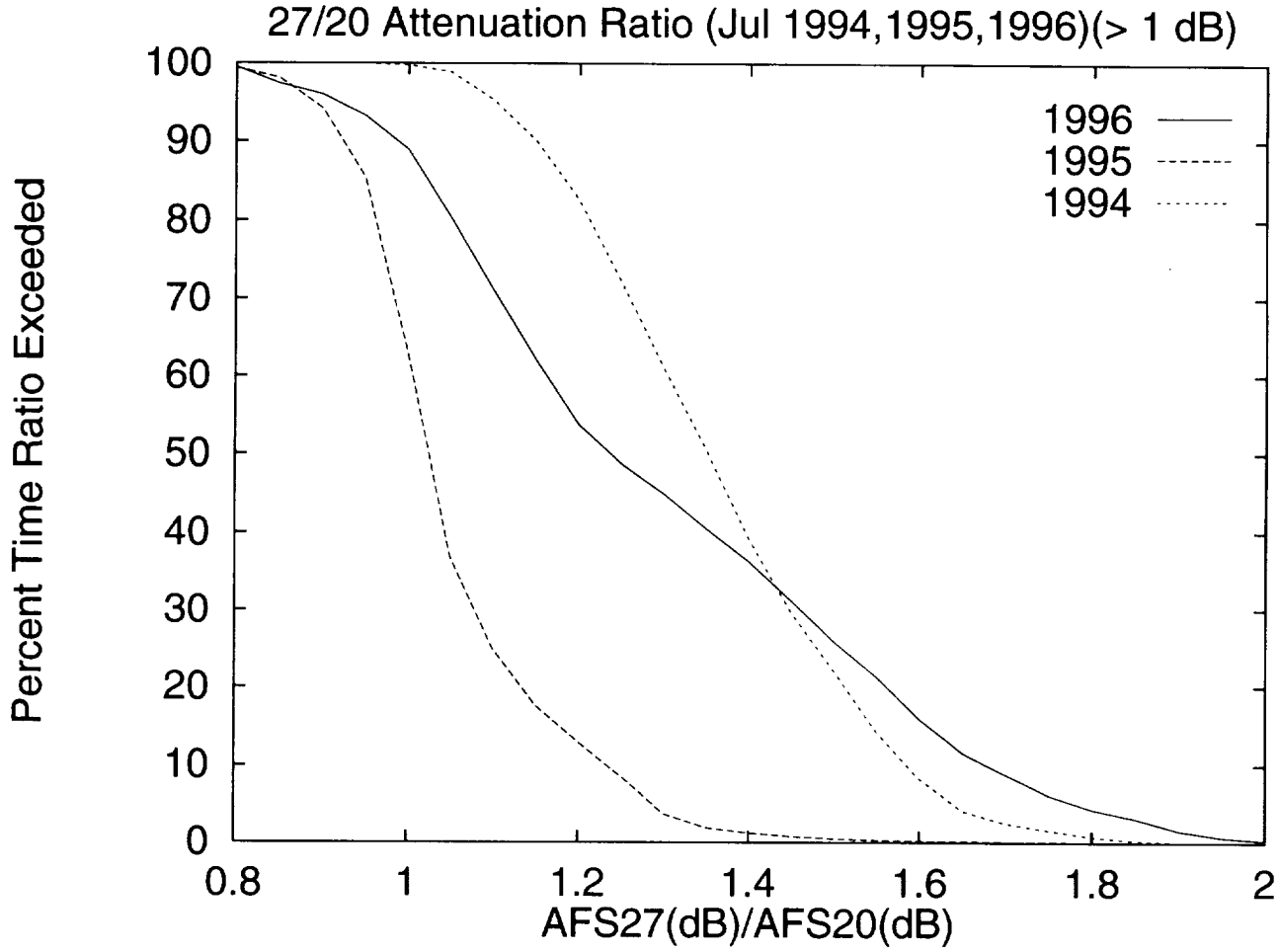
27/20 Attenuation Ratio (Jul 1994,1995,1996)(> 1 dB)
Percent Time Ratio Exceeded
AFS27(dB)/AFS20(dB)
1996
1995
1994
100
90
80
70
60
50
40
30
20
10
0
0.8
1
1.2
1.4
1.6
1.8
2

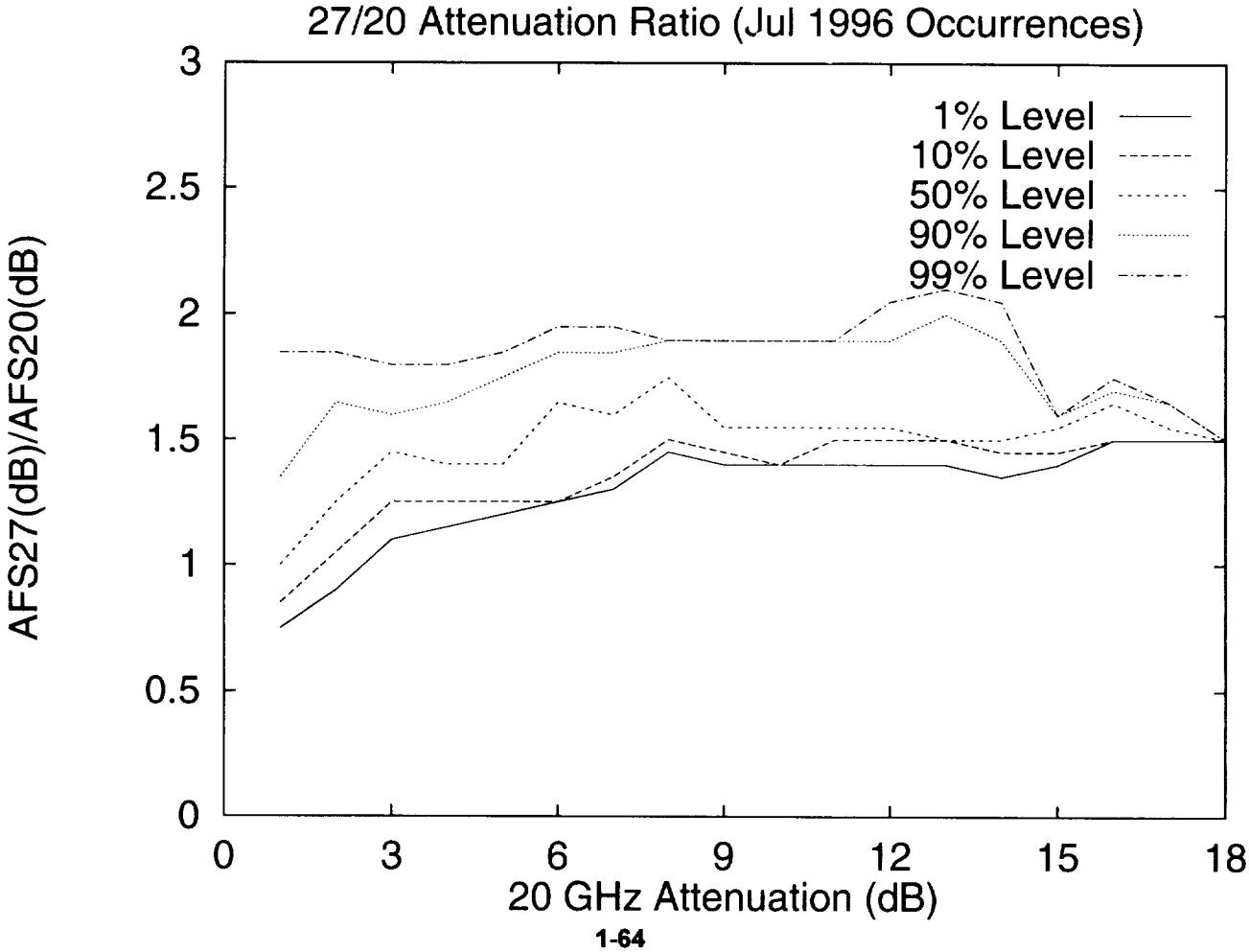
27/20 Attenuation Ratio (Jul 1996 Occurrences)
AFS27(dB)/AFS20(dB)
20 GHz Attenuation (dB)
1% Level
10% Level
50% Level
90% Level
99% Level
3
2.5
2
1.5
1
0.5
0
0
3
6
9
12
15
18

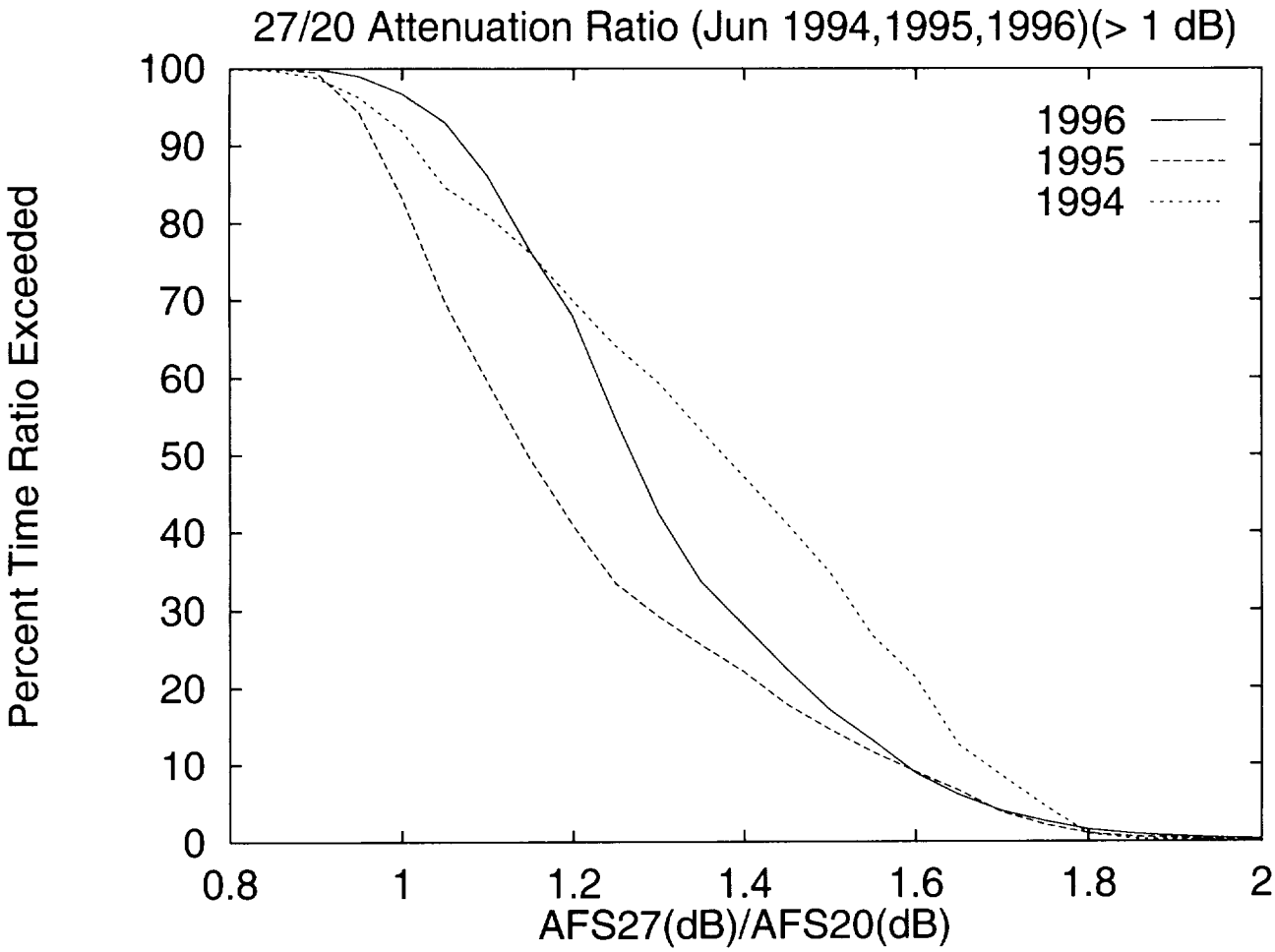
27/20 Attenuation Ratio (Jun 1994,1995,1996)(> 1 dB)
Percent Time Ratio Exceeded
AFS27(dB)/AFS20(dB)
1996
1995
1994
100
90
80
70
60
50
40
30
20
10
0
0.8
1
1.2
1.4
1.6
1.8
2

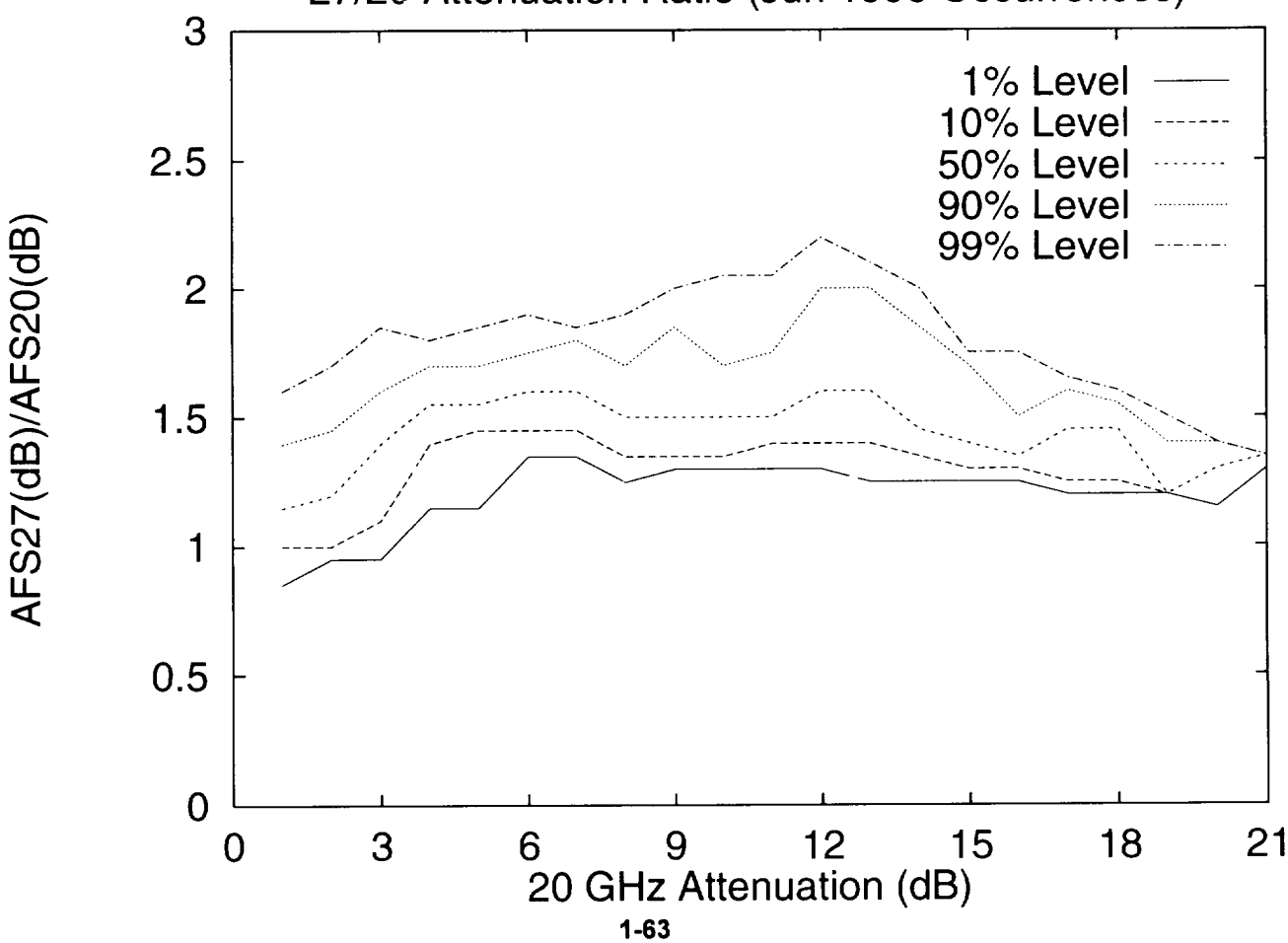
27/20 Attenuation Ratio (Jun 1996 Occurrences)
AFS27(dB)/AFS20(dB)
20 GHz Attenuation (dB)
1% Level
10% Level
50% Level
90% Level
99% Level
3
2.5
2
1.5
1
0.5
0
0
3
6
9
12
15
18
21

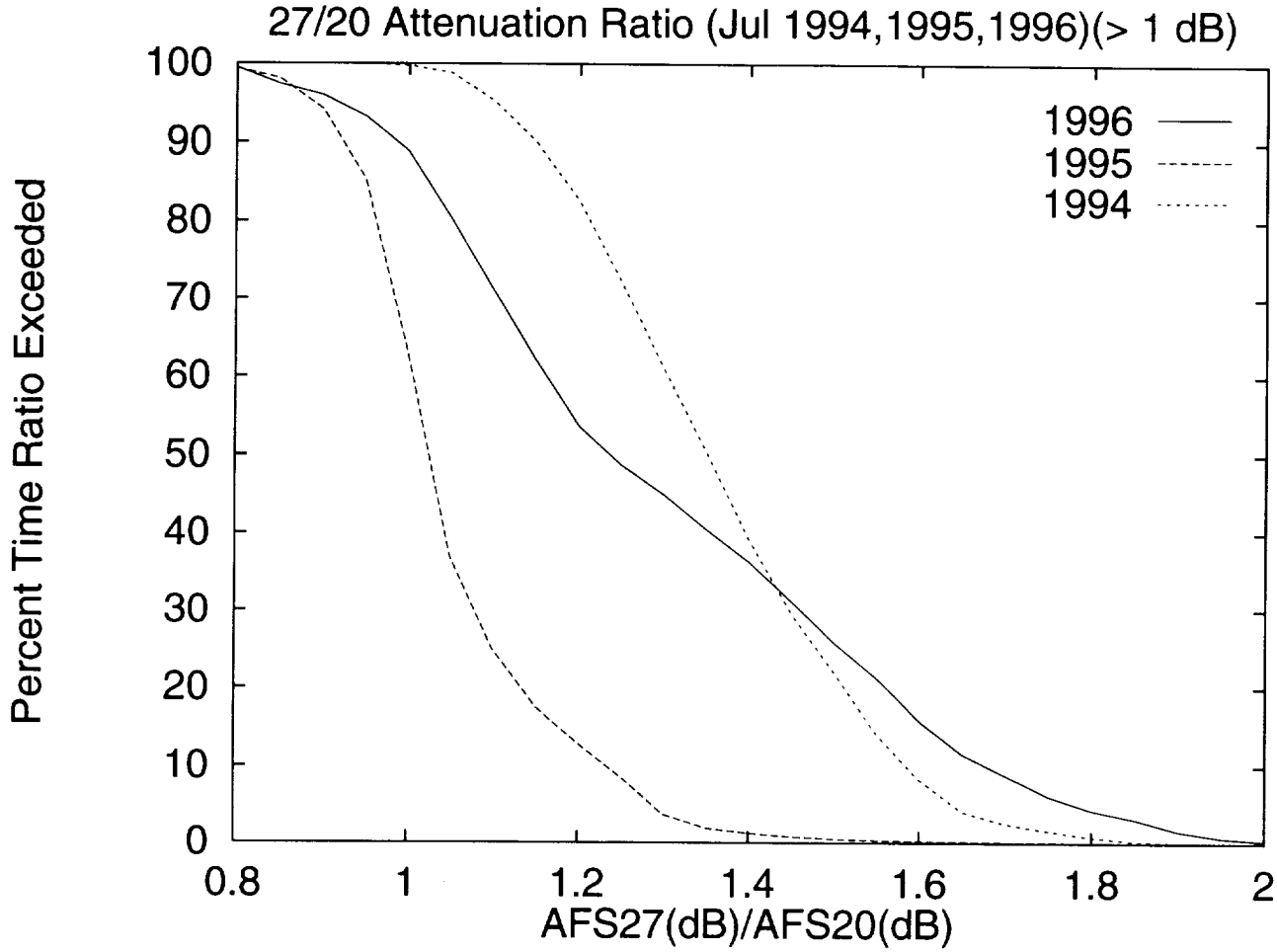
27/20 Attenuation Ratio (Jul 1994,1995,1996)(> 1 dB)
Percent Time Ratio Exceeded
100
90
80
70
60
50
40
30
20
10
0
0.8
1
1.2
1.4
1.6
1.8
2
AFS27(dB)/AFS20(dB)
1996
1995
1994

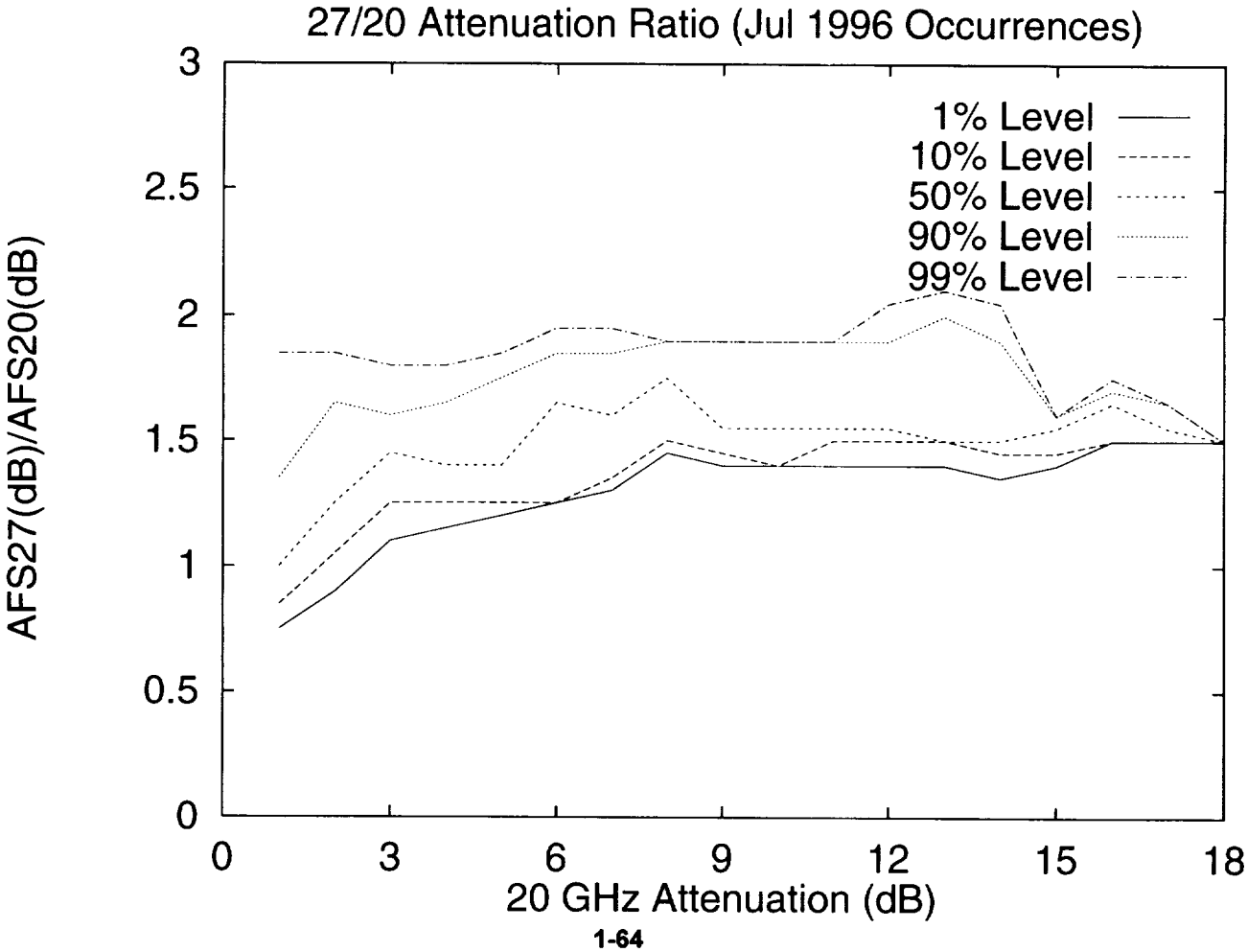
27/20 Attenuation Ratio (Jul 1996 Occurrences)
AFS27(dB)/AFS20(dB)
3
2.5
2
1.5
1
0.5
0
0
3
6
9
12
15
18
20 GHz Attenuation (dB)
1% Level
10% Level
50% Level
90% Level
99% Level

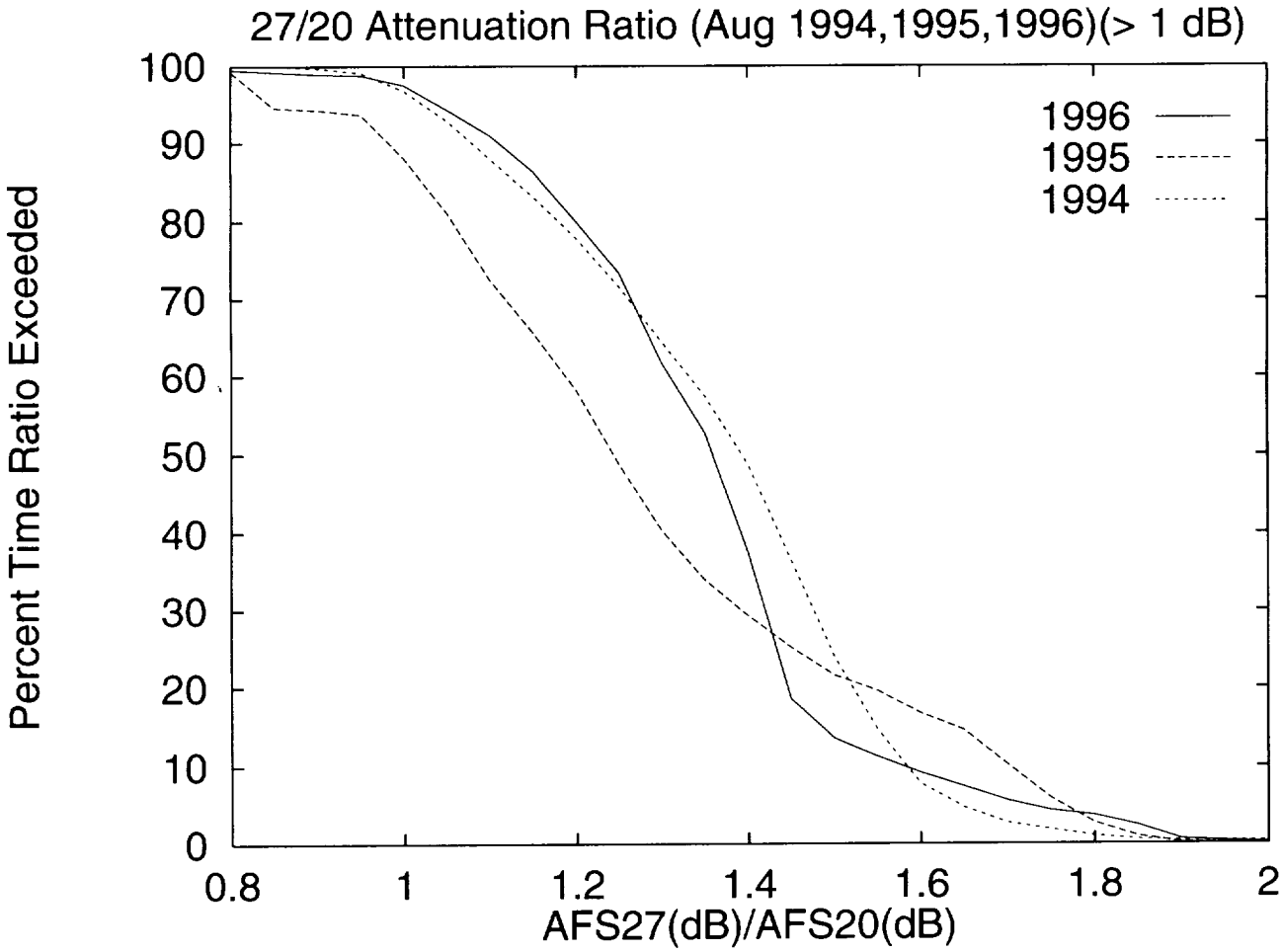
27/20 Attenuation Ratio (Aug 1994,1995,1996)(> 1 dB)
Percent Time Ratio Exceeded
100
90
80
70
60
50
40
30
20
10
0
0.8
1
1.2
1.4
1.6
1.8
2
AFS27(dB)/AFS20(dB)
1996
1995
1994

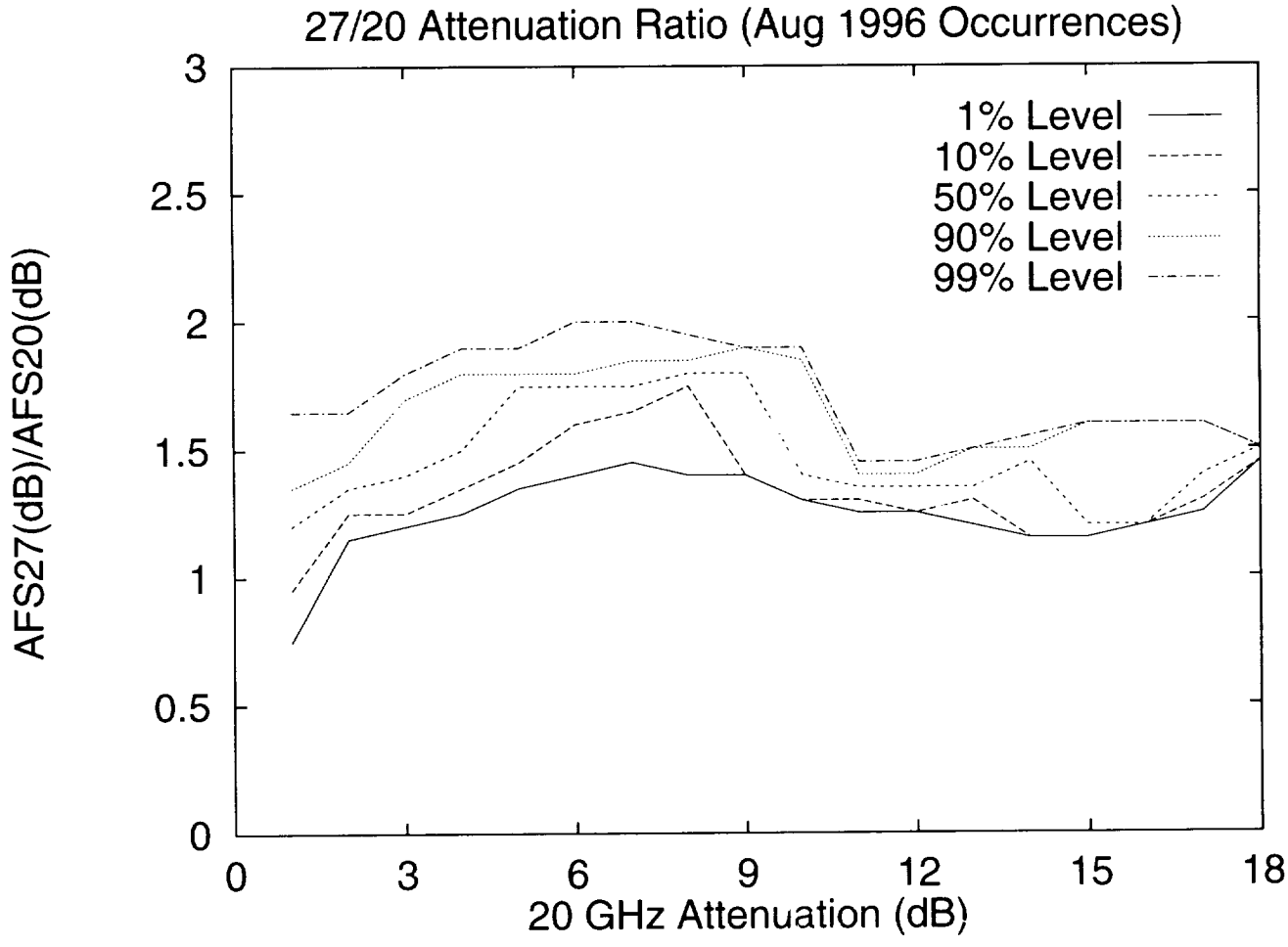
27/20 Attenuation Ratio (Aug 1996 Occurrences)
AFS27(dB)/AFS20(dB)
3
2.5
2
1.5
1
0.5
0
0
3
6
9
12
15
18
20 GHz Attenuation (dB)
1% Level
10% Level
50% Level
90% Level
99% Level

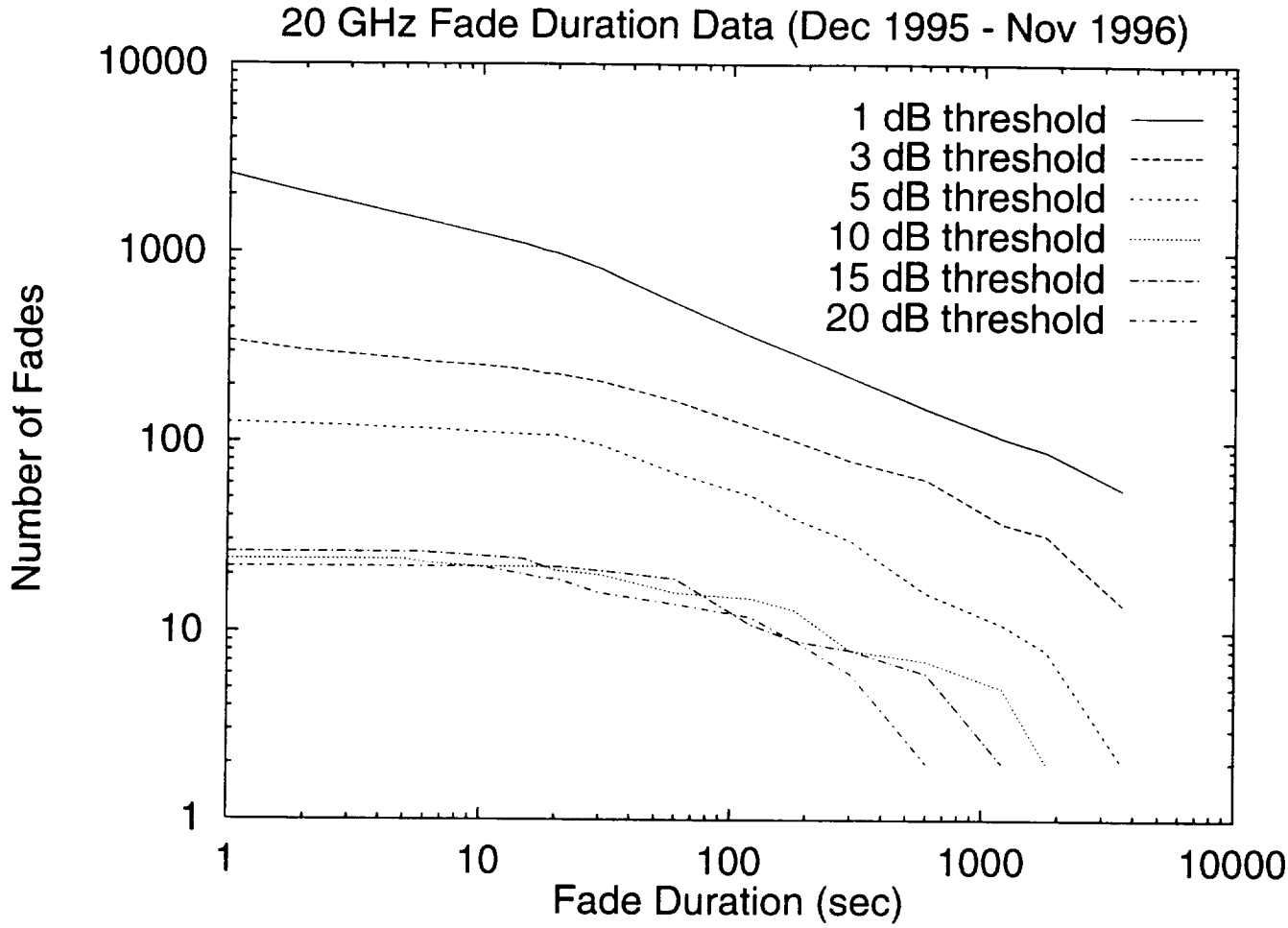
20 GHz Fade Duration Data (Dec 1995 - Nov 1996)
Number of Fades
Fade Duration (sec)
1 dB threshold
3 dB threshold
5 dB threshold
10 dB threshold
15 dB threshold
20 dB threshold
10000
1000
100
10
1
1
10
100
1000
10000

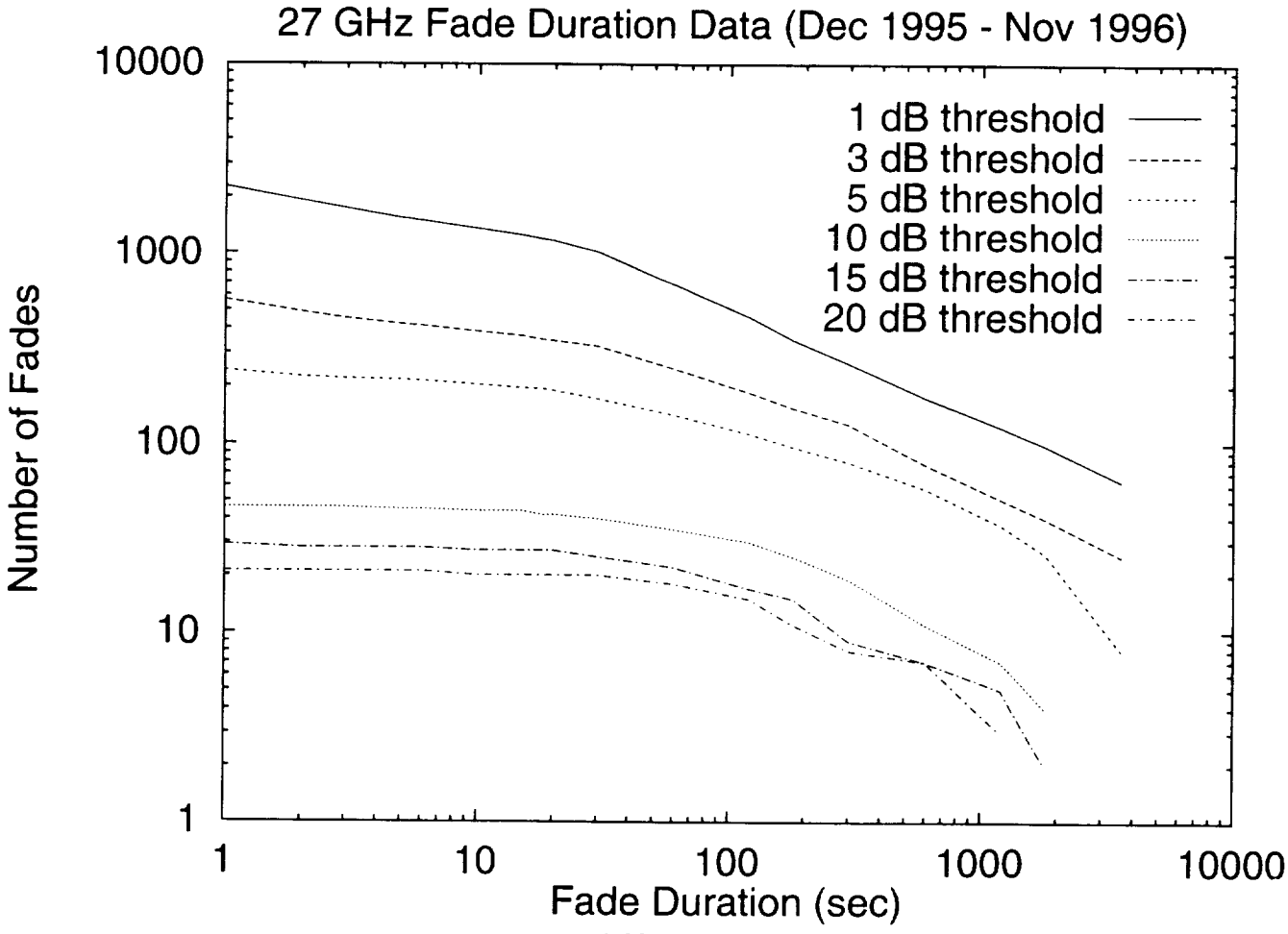
27 GHz Fade Duration Data (Dec 1995 - Nov 1996)
Number of Fades
Fade Duration (sec)
1 dB threshold
3 dB threshold
5 dB threshold
10 dB threshold
15 dB threshold
20 dB threshold
10000
1000
100
10
1
1
10
100
1000
10000

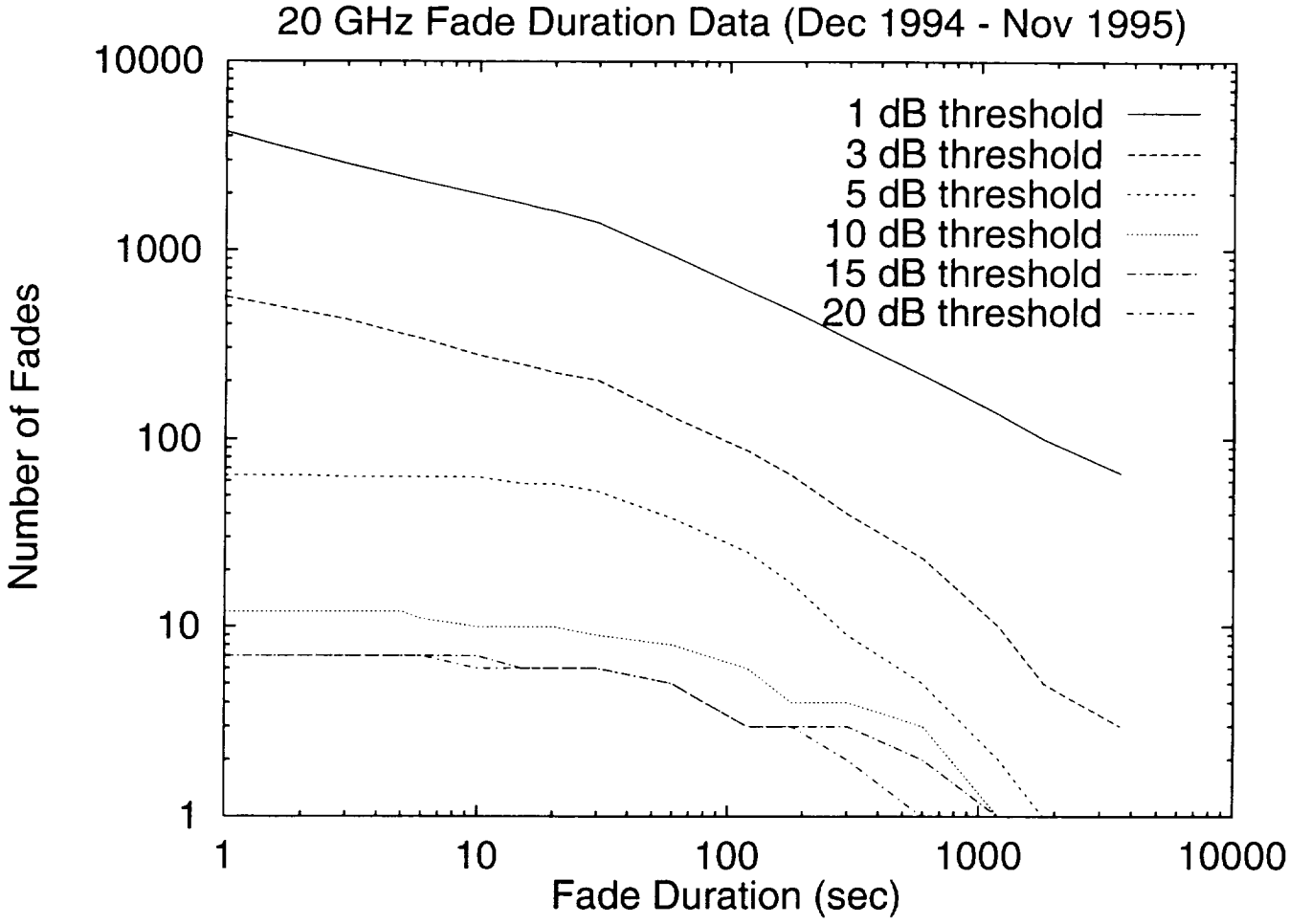
20 GHz Fade Duration Data (Dec 1994 - Nov 1995)
Number of Fades
Fade Duration (sec)
1 dB threshold
3 dB threshold
5 dB threshold
10 dB threshold
15 dB threshold
20 dB threshold
10000
1000
100
10
1
1
10
100
1000
10000

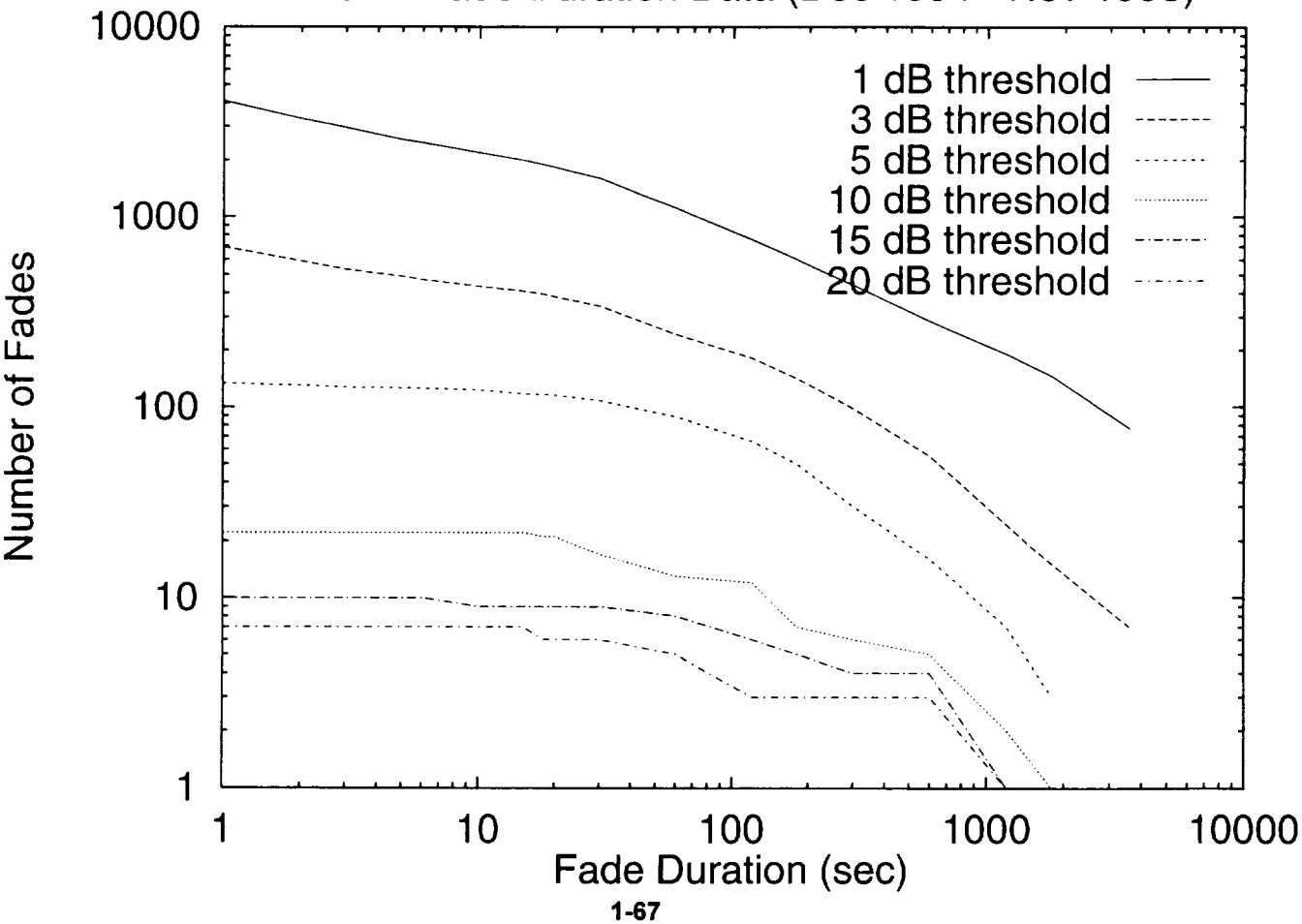
27 GHz Fade Duration Data (Dec 1994 - Nov 1995)
Number of Fades
Fade Duration (sec)
1 dB threshold
3 dB threshold
5 dB threshold
10 dB threshold
15 dB threshold
20 dB threshold
10000
1000
100
10
1
1
10
100
1000
10000

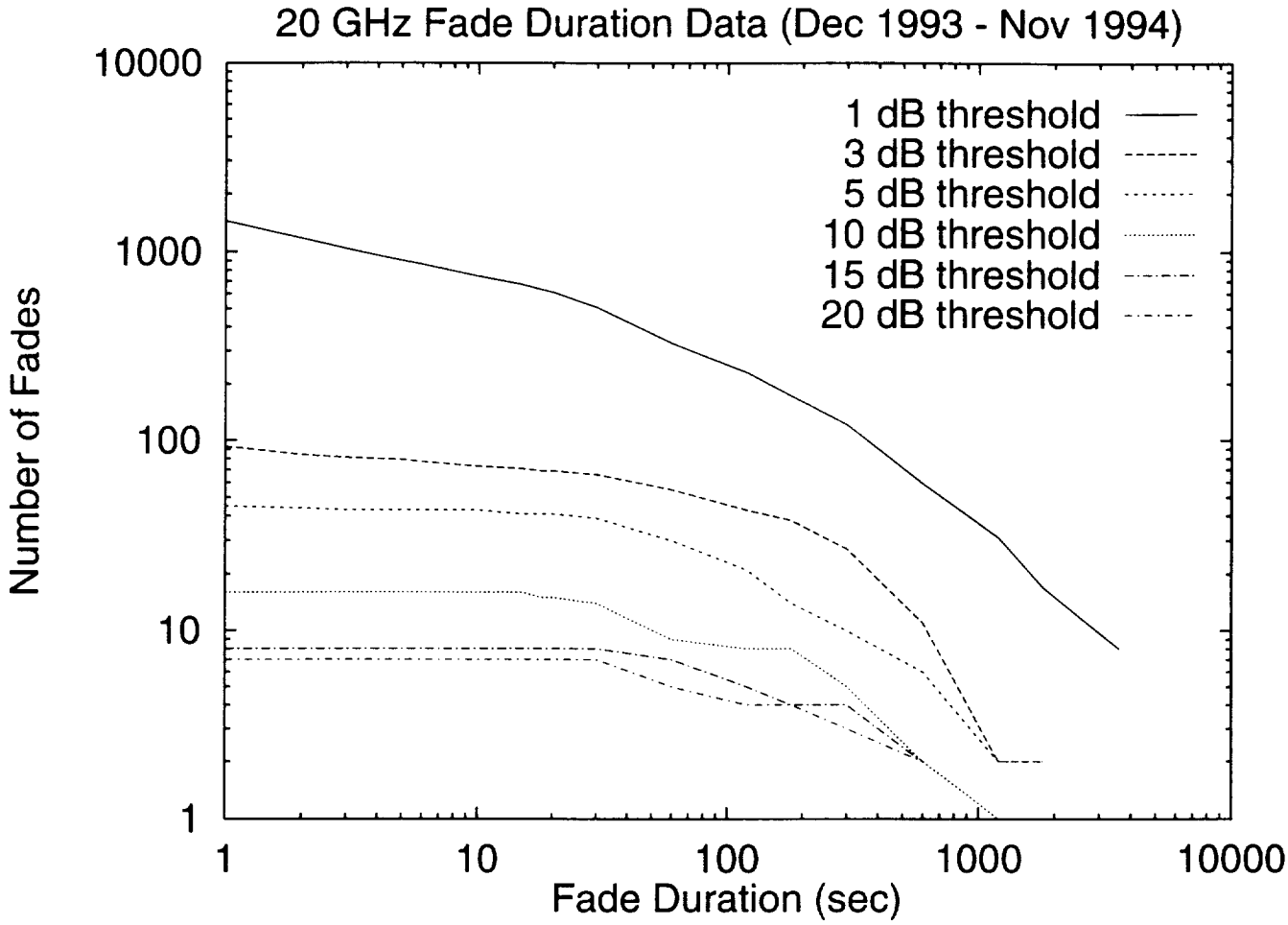
20 GHz Fade Duration Data (Dec 1993 - Nov 1994)
Number of Fades
Fade Duration (sec)
1 dB threshold
3 dB threshold
5 dB threshold
10 dB threshold
15 dB threshold
20 dB threshold
10000
1000
100
10
1
1
10
100
1000
10000

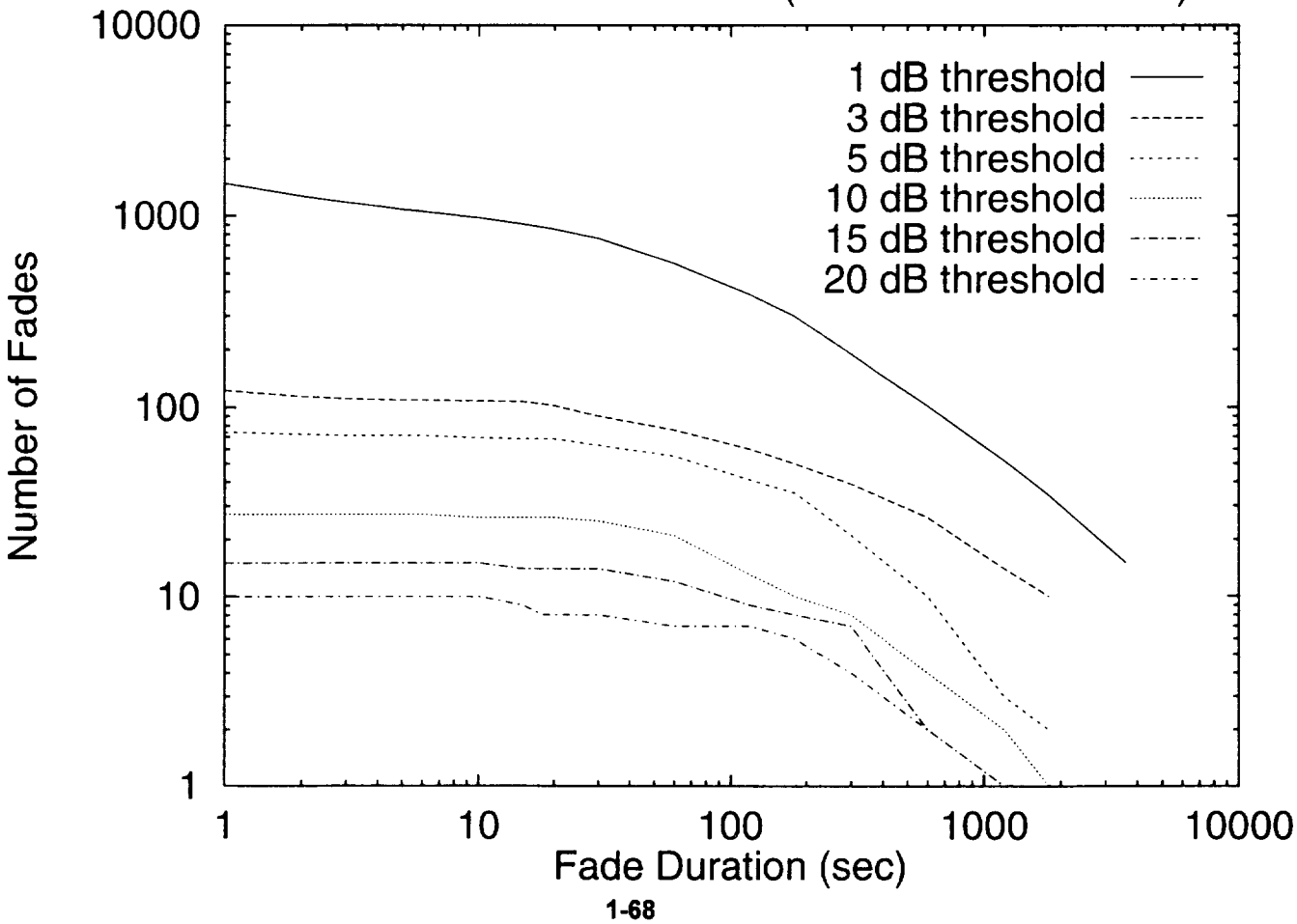
27 GHz Fade Duration Data (Dec 1993 - Nov 1994)
Number of Fades
Fade Duration (sec)
1 dB threshold
3 dB threshold
5 dB threshold
10 dB threshold
15 dB threshold
20 dB threshold
10000
1000
100
10
1
1
10
100
1000
10000

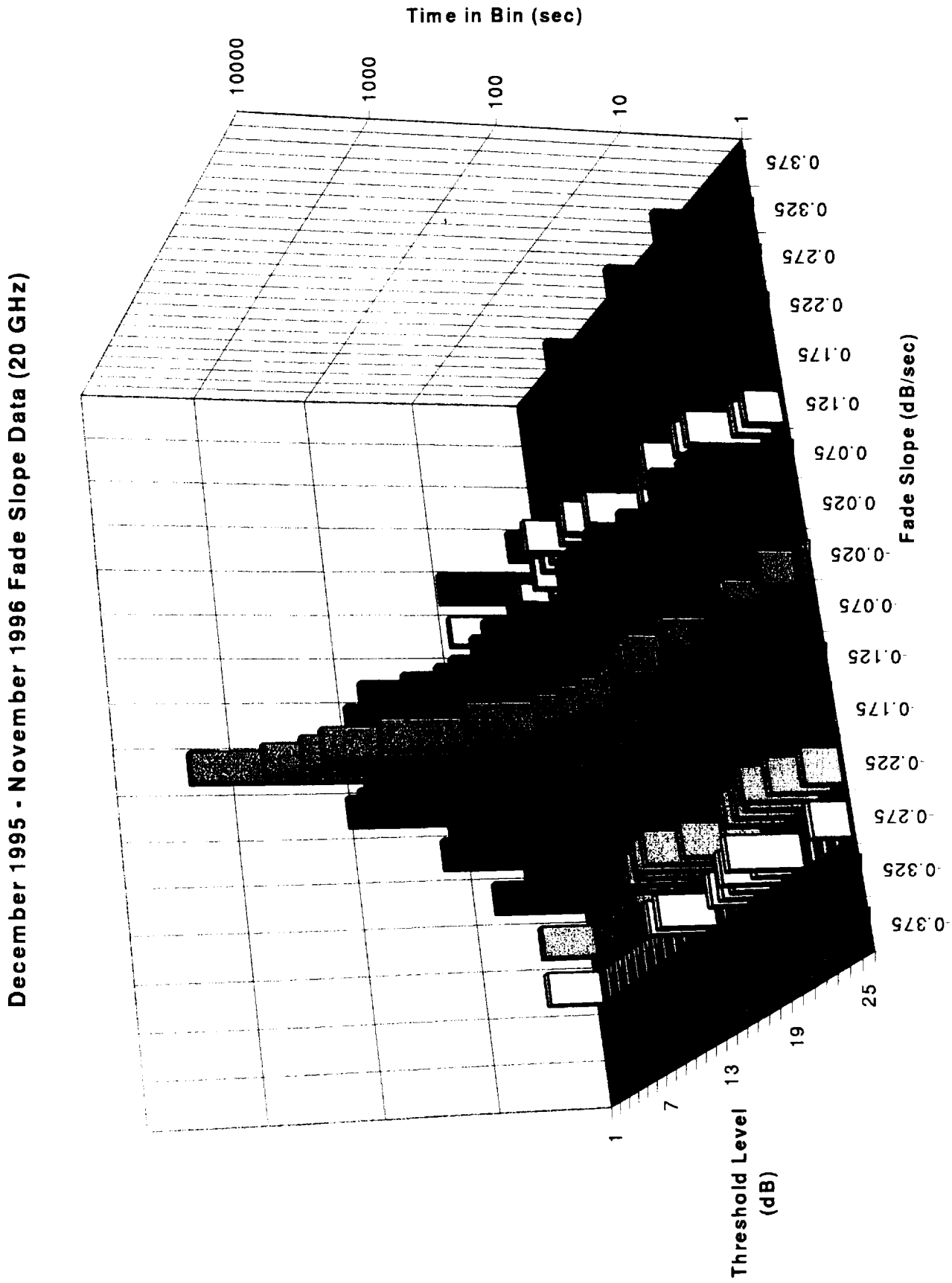
December 1995 - November 1996 Fade Slope Data (20 GHz)
Time in Bin (sec)
10000
1000
100
10
1
Fade Slope (dB/sec)
0.375
0.325
0.275
0.225
0.175
0.125
0.075
0.025
-0.025
-0.075
-0.125
-0.175
-0.225
-0.275
-0.325
-0.375
Threshold Level (dB)
1
7
13
19
25

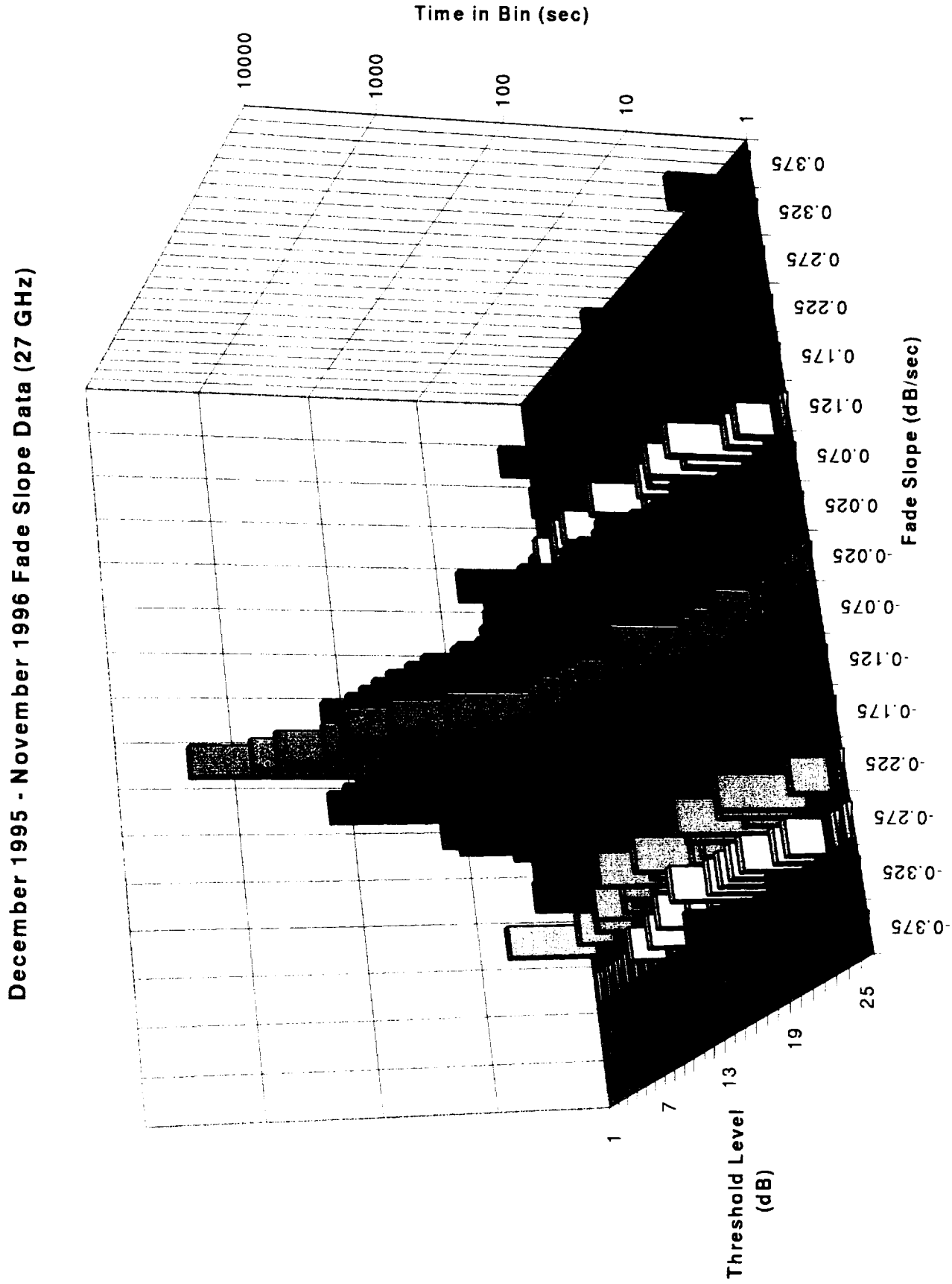
December 1995 - November 1996 Fade Slope Data (27 GHz)
Time in Bin (sec)
10000
1000
100
10
1
Fade Slope (dB/sec)
0.375
0.325
0.275
0.225
0.175
0.125
0.075
0.025
-0.025
-0.075
-0.125
-0.175
-0.225
-0.275
-0.325
-0.375
Threshold Level (dB)
1
7
13
19
25

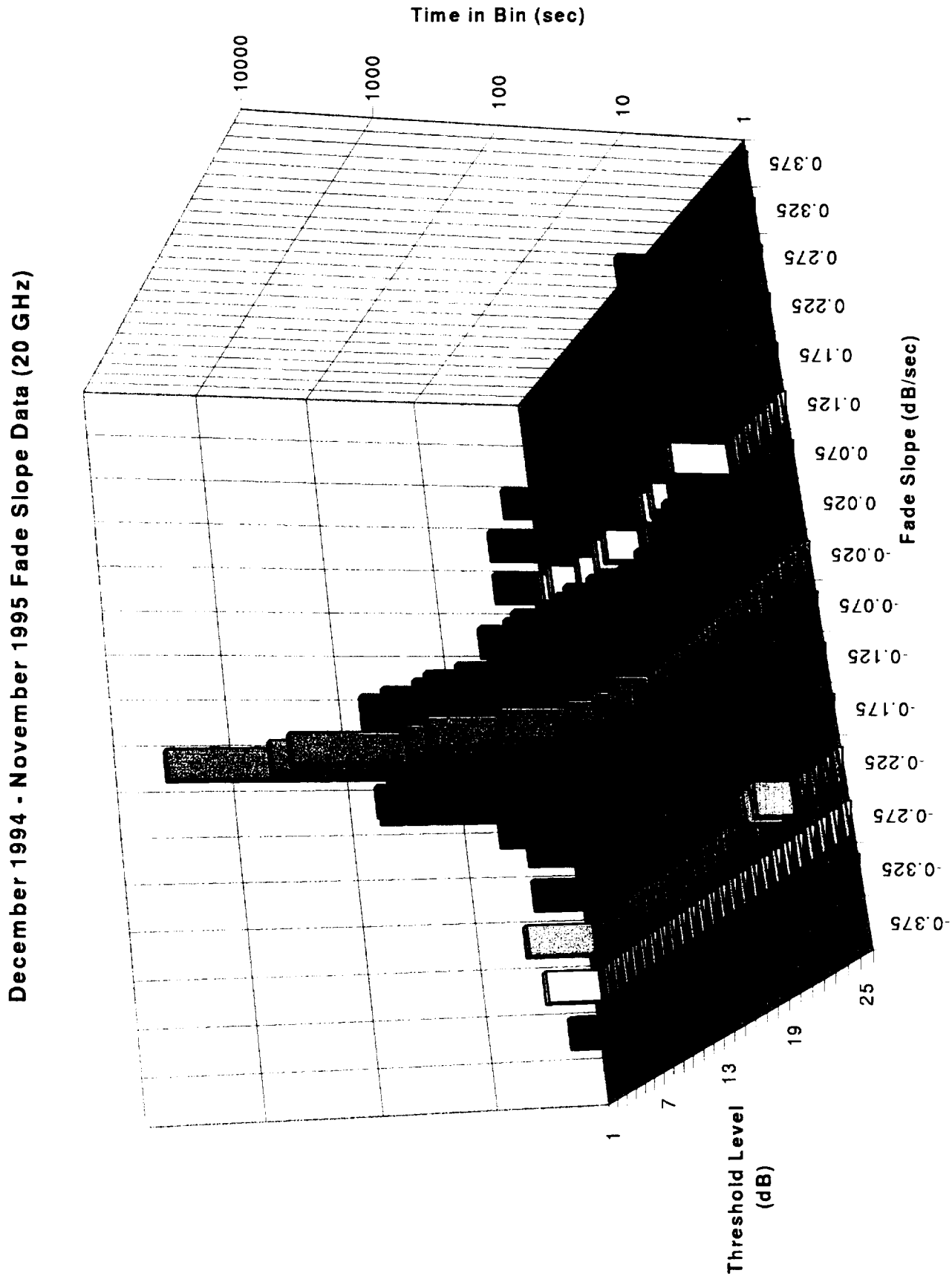
December 1994 - November 1995 Fade Slope Data (20 GHz)
Time in Bin (sec)
10000
1000
100
10
1
Fade Slope (dB/sec)
0.375
0.325
0.275
0.225
0.175
0.125
0.075
0.025
-0.025
-0.075
-0.125
-0.175
-0.225
-0.275
-0.325
-0.375
Threshold Level (dB)
1
7
13
19
25

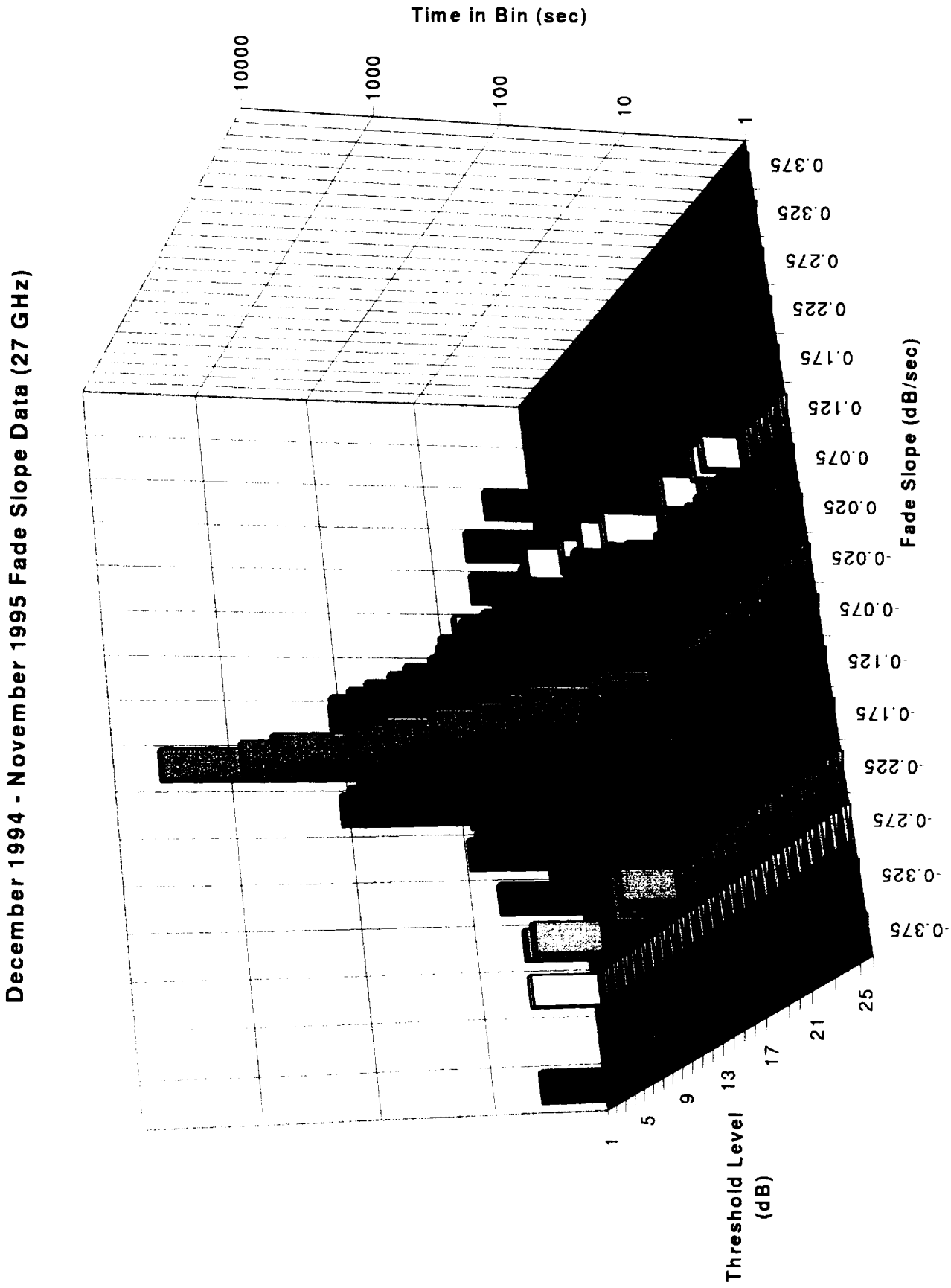
December 1994 - November 1995 Fade Slope Data (27 GHz)
Time in Bin (sec)
10000
1000
100
10
1
Fade Slope (dB/sec)
0.375
0.325
0.275
0.225
0.175
0.125
0.075
0.025
-0.025
-0.075
-0.125
-0.175
-0.225
-0.275
-0.325
-0.375
Threshold Level (dB)
1
5
9
13
17
21
25

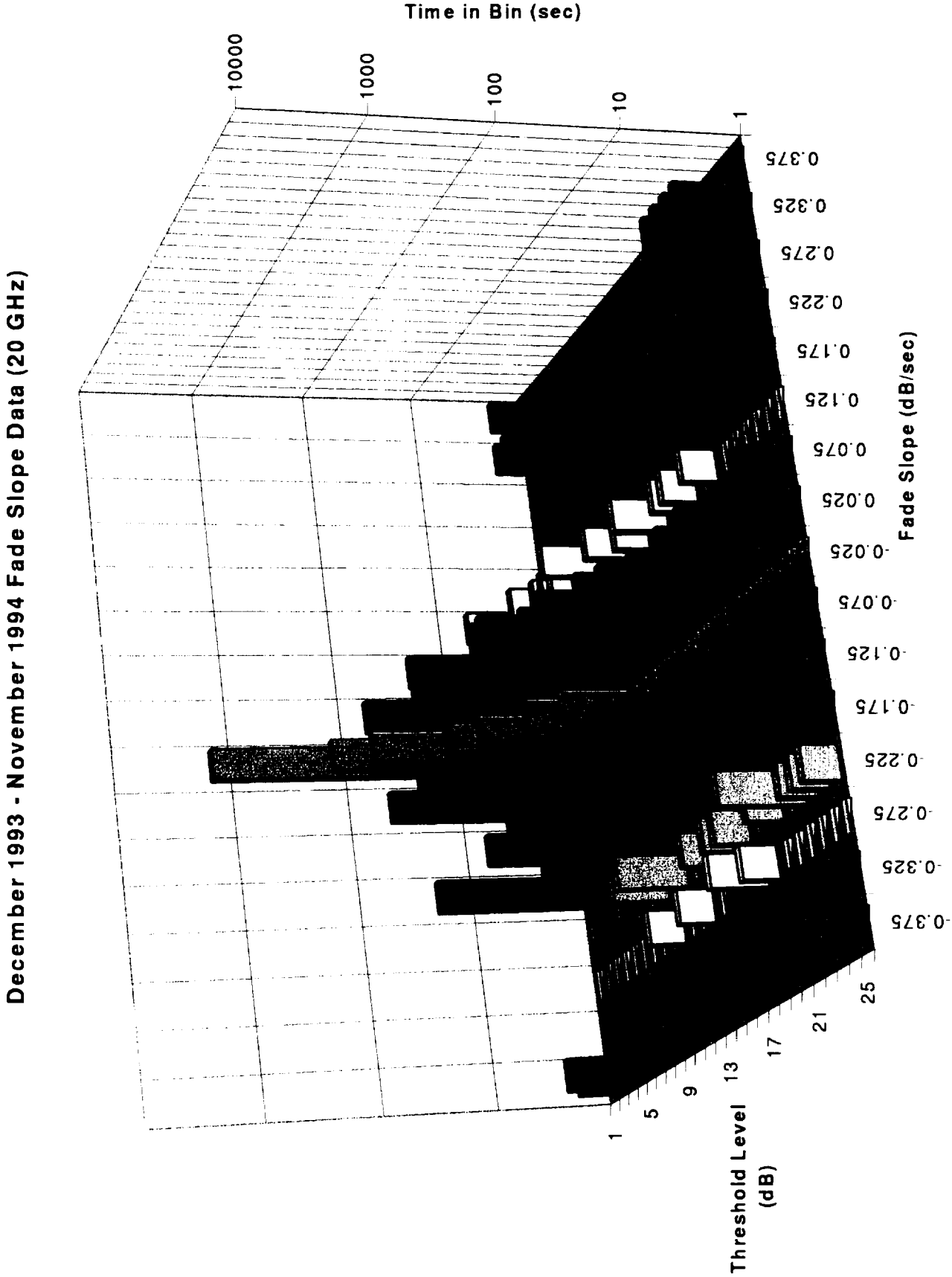
December 1993 - November 1994 Fade Slope Data (20 GHz)
Time in Bin (sec)
10000
1000
100
10
1
Fade Slope (dB/sec)
0.375
0.325
0.275
0.225
0.175
0.125
0.075
0.025
-0.025
-0.075
-0.125
-0.175
-0.225
-0.275
-0.325
-0.375
Threshold Level (dB)
1
5
9
13
17
21
25

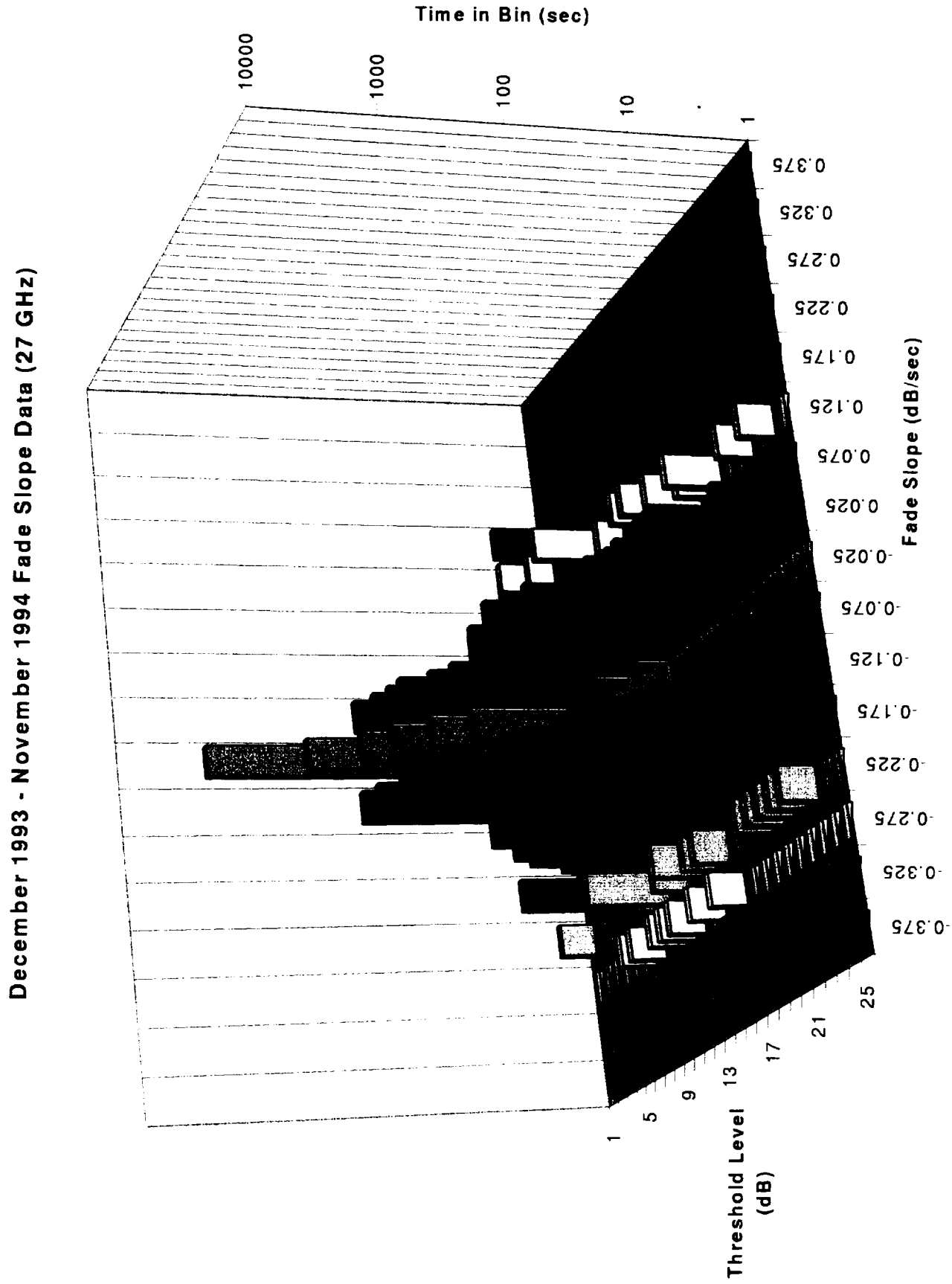
December 1993 - November 1994 Fade Slope Data (27 GHz)
Time in Bin (sec)
10000
1000
100
10
1
Fade Slope (dB/sec)
0.375
0.325
0.275
0.225
0.175
0.125
0.075
0.025
-0.025
-0.075
-0.125
-0.175
-0.225
-0.275
-0.325
-0.375
Threshold Level (dB)
1
5
9
13
17
21
25

299305
P16

Space Communication Technology Center
(SCTC)

PROPAGATION MEASUREMENTS IN FLORIDA

HENRY HELMKEN
FLORIDA ATLANTIC UNIVERSITY (FAU)

&

RUDY HENNING
UNIVERSITY OF SOUTH FLORIDA (USF)

June 11, 1997

3 Years of ACTS Propagation Studies in Florida

ACTS PROPAGATION MEASUREMENTS

- NASA Propagation Terminal in Tampa, Florida:
  University of South Florida (USF) Campus
  - CCIR Rain Zone N
  - Global Rain Region E
  - ACTS Elevation Angle: 52.1 Degrees
    ACTS Azimuth Angle: 214.0 Degrees
  - Longitude: 82.42 Degrees W
    Latitude: 28.06 Degrees N

The following comments are applicable to the data/illustrations on the next pages:

Figure 1: The ACTS Propagation Terminal (APT) is physically located on the roof (4th Floor) of the University of South Florida's College of Engineering Building. The university is located in Northeast Tampa (upper right hand corner of Figure 1a) between Interstate 275 and Interstate 75 and between Fowler and Fletcher Avenues (Figure 1b). Site diversity experiments involve a second terminal 42 km away at a cooperating industry's location - Raytheon's E-Systems division in St Petersburg (Figure 1a) and further include a transportable terminal intermittently at two locations, 1.2 km and 4.3 km from the APT. The first is in the "Village", a university dormitory area, and the second at a cooperating industry, GTE Data Services (Figure 1b).

Figure 2: The APT's roof location is shown in figure 2a. Also shown, shaded, is an experimental antenna measurement area currently being added to increase the university's ability to carry out specialized supporting studies such as "wet antenna" research. Figure 2b shows the APT terminal and the FAU-developed transportable terminal used for close-in site diversity measurements next to each other during site diversity equipment calibration tests.

Following Figure 2 is a list of FAU/USF authored papers and presentations relating to this project. This list is followed by a table identifying students who have been/are affiliated with this program. This table also identifies their Thesis topics.

Figure 3 presents a sample of results from a thesis of Eric Wolfe, directed by Dr. Paul Flikkema. This study explored correlation between APT-determined Ka band propagation attenuation data along the ACTS satellite beam's path and S-band doppler radar reflectivity data gathered by a NEXRAD radar located at Ruskin, FL, along the same path. (See figure 1a for geographical positions.) A more detailed report on this study is presented elsewhere in these Proceedings.

Figure 4 portraits the percent operational "on"-time of the APT terminal on a monthly basis for each of the first three years (Dec. 1 1993 to Nov. 30, 1996). Please note that events beyond the control of the Florida APT site, such as loss of beacon signals due to the ACTS satellite switching power during solar eclipse, are excluded from this data. The data does include equipment outages caused by such events as halting data during routine maintenance, hardware failure problems (for example: low noise amplifier failure), power outages beyond the control of the UPS system, data corruption, solar interference with the APT's fiber-optic data link, failure of normal calibrations, etc.

Figure 5 presents the same information on an annual and 3-yr basis.

Figure 6 shows the buildup of additional path attenuation when a layer of dew forms on the antenna during the night. This is determined by increased beacon signal loss as well as by a radiometer-measured increase in sky temperature. Note that the peak of this buildup occurred at 13:00 GMT or 8:00 am local time, shortly after sunrise. Thereafter the dew rapidly evaporated and as a result performance returned to "normal".

Figure 7 presents CDF's for rain-rate on an annual basis for two years, and for the two years (1995 and 1996) combined. Data is based on "tipping bucket" rain gauge measurements. The Florida site's capacitive rain gauge measurements, while giving better instantaneous measurements when the equipment is working, were not used for this statistical data determination due to the gauge's many outages and at times erroneous readings.

Figure 8a presents annual total rainfall for the Tampa location. Due to the number of on-site rain gauge outages, official data taken at Tampa International Airport is judged to give the most dependable monthly and annual data in this case. Winter and summer data shown in Figure 8b is also based on Tampa International Airport data. Note that the precise division into winter and summer intervals is somewhat arbitrary at this point and deserves further study; however the large difference in rainfall appears to make it desirable to separately identify these two periods.

Figure 9 Presents the annual and three-year free space attenuation (AFS) CDFs for the program's 20.185 GHz and 27.5 GHz frequencies for the first three years of the program. Note that in general these CDF's tracked closely from year to year despite significant differences in weather patterns.

Figure 10 presents initial results in CDF format for the site diversity studies of this program. These studies are focusing on the benefits that can be derived even when short site separation distances are used. Note that at smaller fade levels (for example 5 db) a gain of about 1.5 db is realized, while at larger fade levels (for example 15 db or more) this increases to 5 db or more.

Figure 11 illustrates the frequency response of several filters used to remove rapid scintillations from the beacon data measurements.

Figure 12 presents the results of using different filters when processing the experimental data into a statistical format. It reveals that the processing is only affected in a very minor way (if at all) by the type of filtering used. (Observe only the effect for fade depths greater than 3 db, since fades smaller than 3db are often caused by non-rain (scintillation clouds, etc) effects.)

Figure 13 presents results of analyzing fade duration statistics. Figure 13a presents information on the relation of fade duration to fade level on a log-normal basis using 3 years' fade data. (Data for fade durations below 30 seconds is influenced by filter averaging. Low level fades (e.g. 2 db) are driven by variations in AGA and hence not representative of weather phenomena. Figure 13b presents a least squares fit of some of the data when short duration fades are filtered out.

Figure 14 plots 3 years' data of relative occurrence of fade slope (db/sec). Data is normalized to 0 db/sec and taken over a 10 second interval. As fade level increases, occurrence of higher fade slopes becomes more frequent.

file: napexrpt.697

OUTLINE

- FLORIDA PROGRAM OVERVIEW
- OPERATION PERFORMANCE
- ANTENNA MOISTURE
- CDF RESULTS
- DIVERSITY PROGRAM
- DATA FILTER STUDIES
- CONCLUSIONS

3 Years of ACTS Propagation Studies in Florida

FLORIDA PROGRAM GOALS

- Generate CDF's for a Sub-tropical Region
- Sub-tropical Fade Duration Statistics
- Radiometer Development
- Diversity Gain Measurements
- Sub-tropical Rain Models

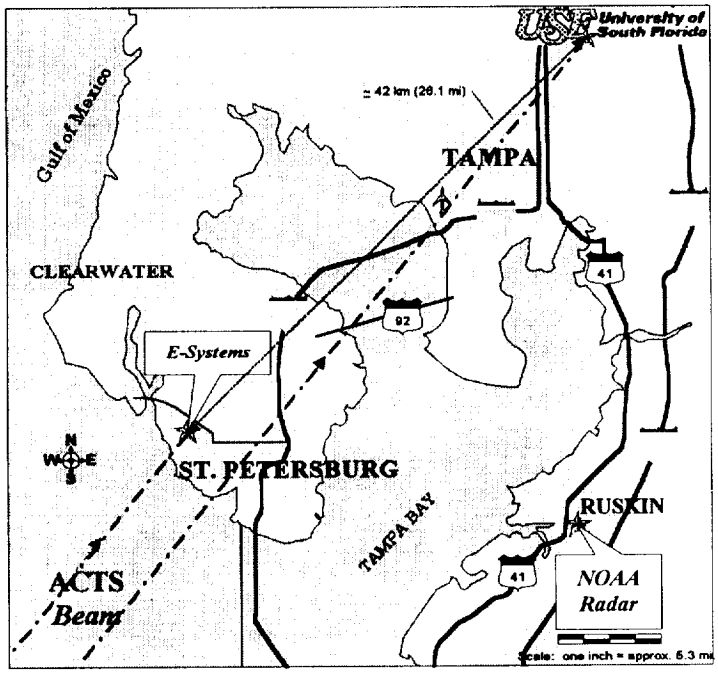

Figure 1a: Tampa Bay Area, Showing Locations of USF, NOAA Radar, and E-Systems

3 Years of ACTS Propagation Studies in Florida

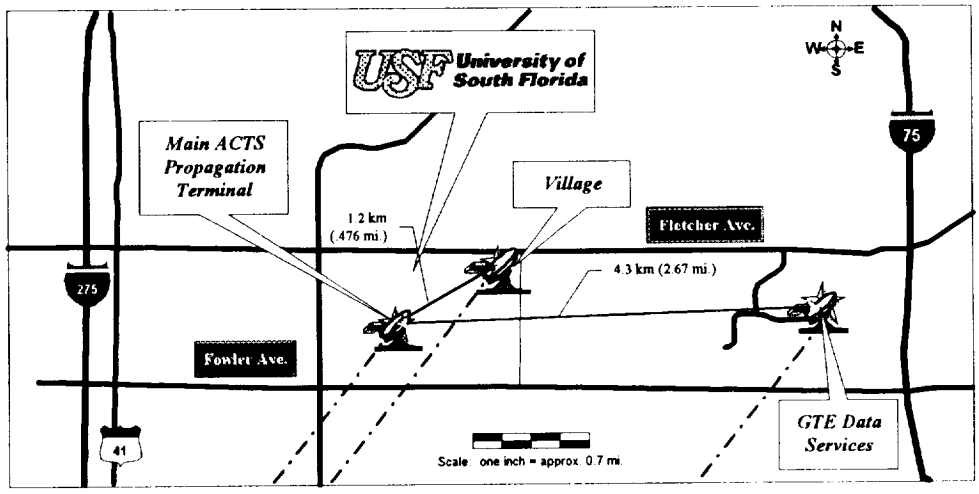

Figure 1b: USF Area, Showing Locations of the APT, the Village, and GTE Data Services

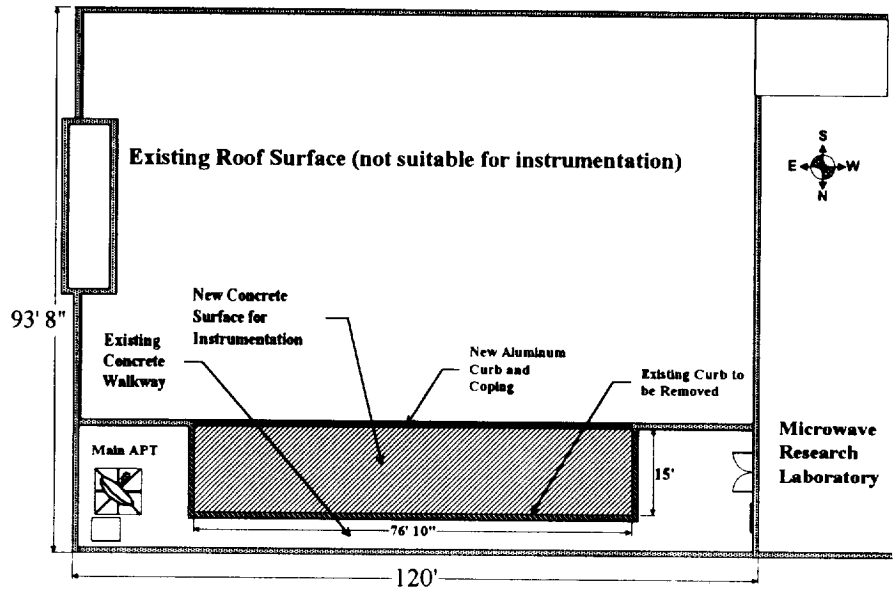

Figure 2a: East Roof of USF's Electrical and CS&E Engineering Building

3 Years of ACTS Propagation Studies in Florida

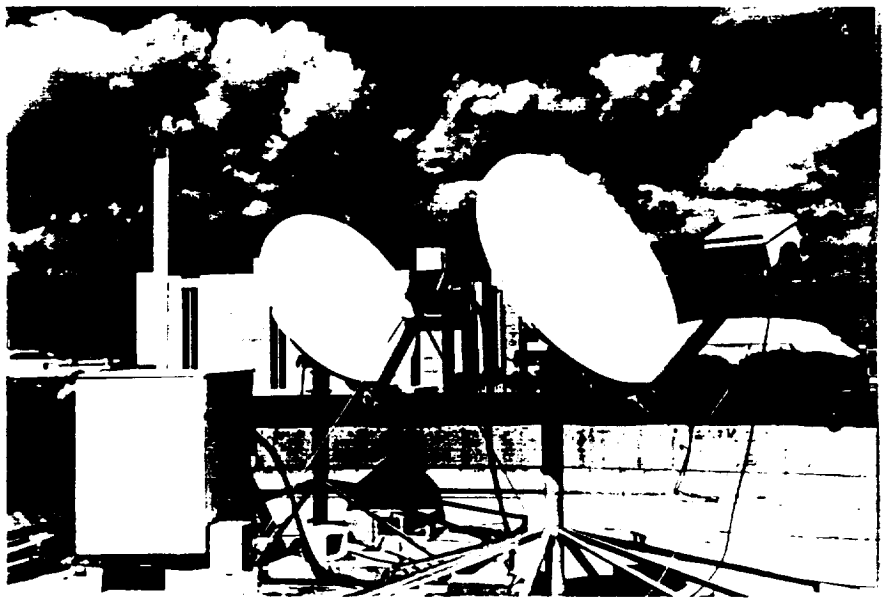

Figure 2b: Main APT and FAU Diversity Terminal on Roof of USF's Electrical and CS&E Engineering Building

ACTS Propagation Program Papers

by Henry Helmken, Florida Atlantic University & Rudy Henning, University of South Florida

1997 (accepted) "Filter Influence on ACTS Fade Duration and Fade Slope Statistics", H. Helmken, R. Henning, J. Feil, C. Mayer, Third Ka-Band Utilization Conference, Sorrento, Italy

1997 (accepted) "ACTS Ka-Band Propagation Measurements in Florida", H. Helmken and R. Henning, 1997 IEEE AP-S International Symposium and URSI North Americal Radio Science Meeting, Montreal, Canada, July 1997

1997 "A Three Site Comparison of Fade Duration Measurements", H. Helmken, R. Henning, J. Feil, L. Ippolito and C. Mayer, Accepted for publication in the Proceedings of the IEEE.

1997 "ACTS Ka-Band Fade Slope Statistics", J. Feil, L. Ippolito, H. Helmken, R. Henning, and C. Mayer, accepted for publication in the Proceedings of the IEEE.

1996 "Ka-Band ACTS Propagation Measurements in Florida", H. Helmken and R. Henning, Proceedings of the Second European Workshop on Mobile/Personal SATCOM, Rome, Italy, October 11, Springer, pgs. 433-442.

1996 "Ka-Band Site Diversity Research in a Subtropical Region Utilizing the ACTS Satellite", R. Henning, S.K. Park and G.M. Szklarz, IEEE Southeastcon '96 Conference Proceedings, Tampa, FL, April 1996.

1996 "Effects of Dew on Millimeter-Wave Propagation", R. Henning and J.R. Stanton, IEEE Southeastcon '96 Conference Proceedings, Tampa, FL, April 1996.

1996 "Florida Propagation Results", H. Helmken and R. Henning, URSI National Radio Meeting, Boulder, CO, January 1996.

1995 "Ka-Band Propagation Results From "Sub-Tropical" Florida", H. Helmken and R. Henning, presented at 20th International Conference on Infrared and Millimeter Waves, Orlando, FL, December 1995.

1995 "Satellite K/Ka-Band Propagation Measurements in Florida", H. Helmken and R.Henning, International Mobile Systems Communications (IMSC) Conference, JPL 95-12, Ottawa, June, 1995 pgs. 140-144.

1995 "Millimeter Propagation Research Using ACTS - A Look At First Year Findings", R. A. Bauer, F. Davarian, H. Helmken and R. Henning, 1995 IEEE National Telesystems Conference Proceedings, Orlando, FL, May 1995.

1995 "ACTS Propagation Measurements in Florida", International Union of Radio Science (URSI), Boulder, January, pg. 27, Jan 1995.

1994 "ACTS Propagation Research - A Key to Increased Satellite Communications Capacity", R.A. Bauer, F. Davarian, H. Helmken and R. Henning, 1994 IEEE National Telesystems Conference Digest, San Diego, CA, May 1994.

1994 "ACTS Propagation Measurements in Florida", Invited Paper, URSI National Radio Science Meeting, January, pg. 27.

File: reh\prop-ppr.597

3 Years of ACTS Propagation Studies in Florida

Degrees Received or Currently Pursued by Research Assistants

Name	Thesis Title	Degree/ Date	Current Employer
Peter J. Bartels	TBA	MSEE/ Expected '98	USF
Monique J. Bourgeois	Ka-Band Radiometry in the ACTS System	MSE/ April '97	Available
Joey A. Duvall	TBA	MSEE/ Expected '98	USF
Zlata Koro	Ka-Band Rain Models Rain Gauge Data Storage Device	MSE/ Dec. '97 Sr. Project/ '95	Teledesic
Ritsuko Pollard	TBA	MSE/ Expected '98	FAU
John Raymond Stanton	Microwave Radiometer Calibration Techniques	MSEE/ May '96	Texas Instruments
Gina Marie Szklarz	Ka-Band Site Diversity in a Sub-tropical Region Utilizing NASA's ACTS Satellite	MSEE/ Dec. '96	Motorola
Eric Wolfe	Correlation of Ka-Band Propagation Attenuation and S-Band Doppler Radar Reflectivity	MSEE/ April '97	Motorola

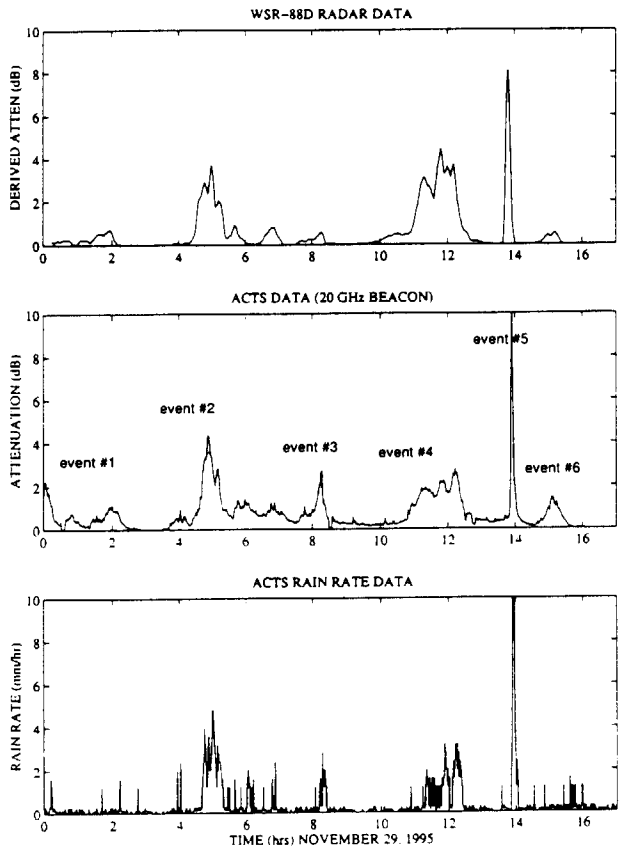

Figure 3: Derived (estimated) attenuation, measured attenuation, and rain rate; 29 Nov. 1995

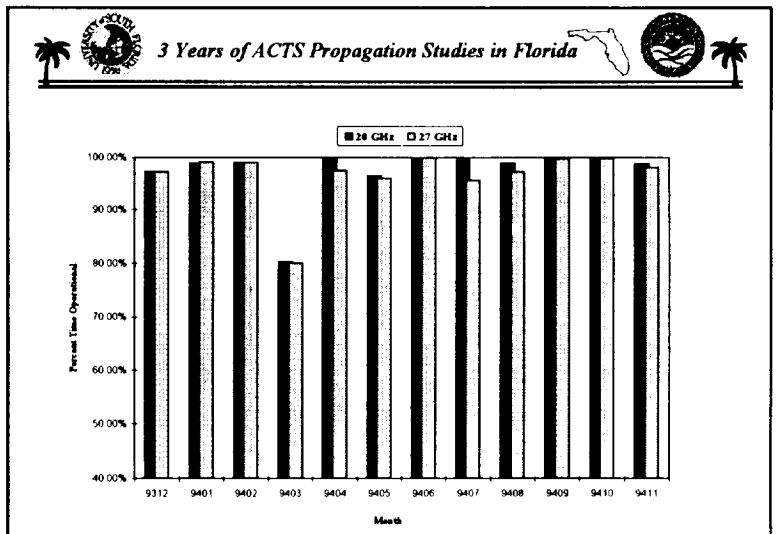

Figure 4a: First-Year (12/93-11/94) Operational Status of Receiver/Radiometer

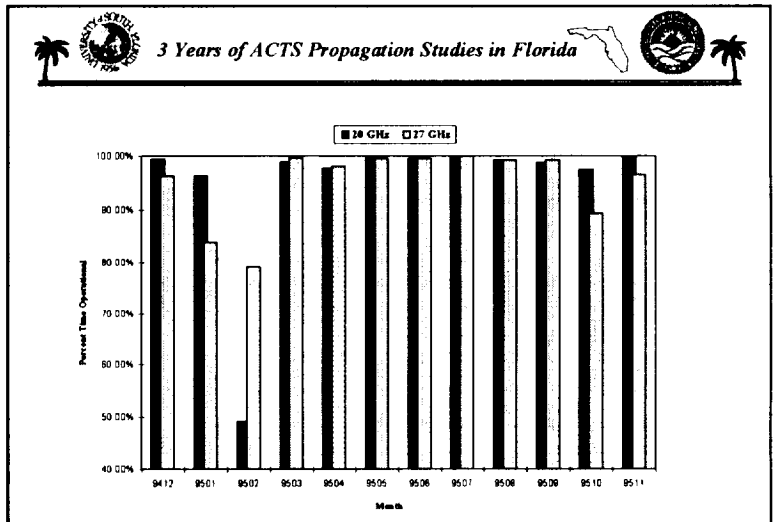

Figure 4b: Second-Year (12/94-11/95) Operational Status of Receiver/Radiometer

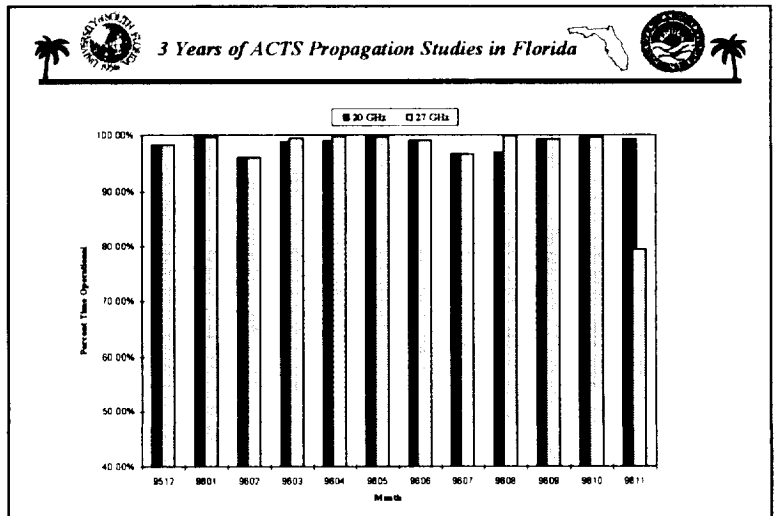

Figure 4c: Third-Year (12/95-11/96) Operational Status of Receiver/Radiometer

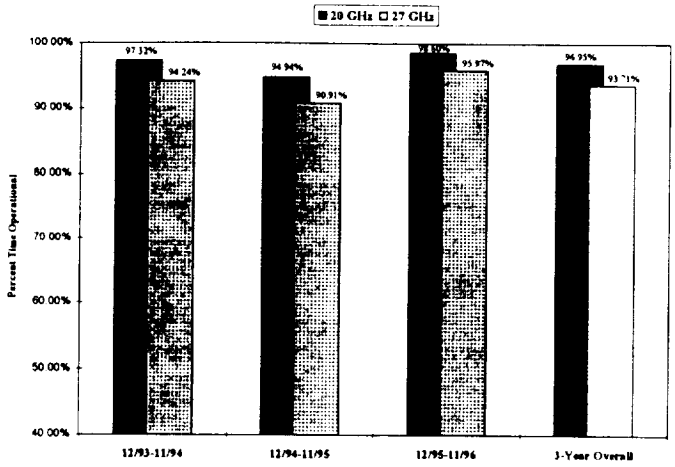

Figure 5: Average *Annual* and *Three-Year* Operational Status of Receiver/Radiometer

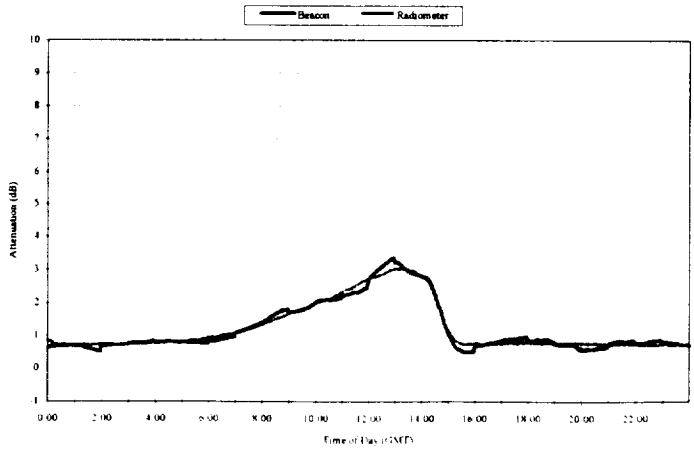

Figure 6: Attenuation Resulting from Dew on Antenna (27 GHz channel) -- 14 January 1996

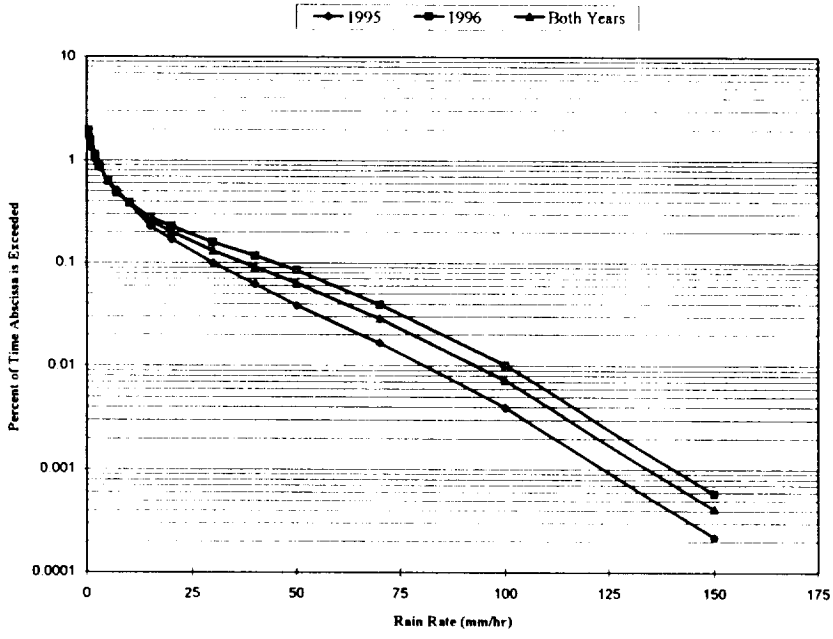

Figure 7: Annual Rain CDF for 1995-1996, from Tipping Bucket Rain Gauge Data

	1994	1995	1996	Three-Yr. Average
December (of previous year)	1.28	1.57	1.02	1.29
January	3.9	3.51	5.52	4.31
February	0.42	2.02	3.04	1.83
March	0.66	2.02	4.65	2.44
April	3.43	1.48	4.2	3.04
May	0.06	1.67	1.45	1.06
June	5.98	9.79	8.96	8.24
July	11.3	10.22	2.72	8.08
August	8.37	13.75	7.39	9.84
September	9.16	2.8	5.44	5.80
October	3.29	4.71	3.12	3.71
November	0.24	1.16	0.91	0.77
Total	**48.09**	**54.70**	**48.42**	**50.40**
Winter Summary (Nov-Apr)				**13.68**
Summer Summary (May-Oct)				**36.73**

source: Tampa International Airport Weather Data

Figure 8a: Tampa Bay Area Annual Rainfall Statistics (1994-1996)

3 Years of ACTS Propagation Studies in Florida

	Winter			Summer		
	1994	1995	1996	1994	1995	1996
December	1.28	1.57	1.02			
January	3.9	3.51	5.52			
February	0.42	2.02	3.04			
March	0.66	2.02	4.65			
April	3.43	1.48	4.2			
May				0.06	1.67	1.45
June				5.98	9.79	8.96
July				11.3	10.22	2.72
August				8.37	13.75	7.39
September				9.16	2.8	5.44
October				3.29	4.71	3.12
November	0.24	1.16	0.91			
Total	**9.93**	**11.76**	**19.34**	**38.16**	**42.94**	**29.08**
Winter Summary		**13.68**				
Summer Summary		**36.73**				
Three-Year Average		**50.40**				

source: Tampa International Airport Weather Data

Figure 8b: Tampa Bay Area Seasonal Rainfall Statistics (1994-1996)

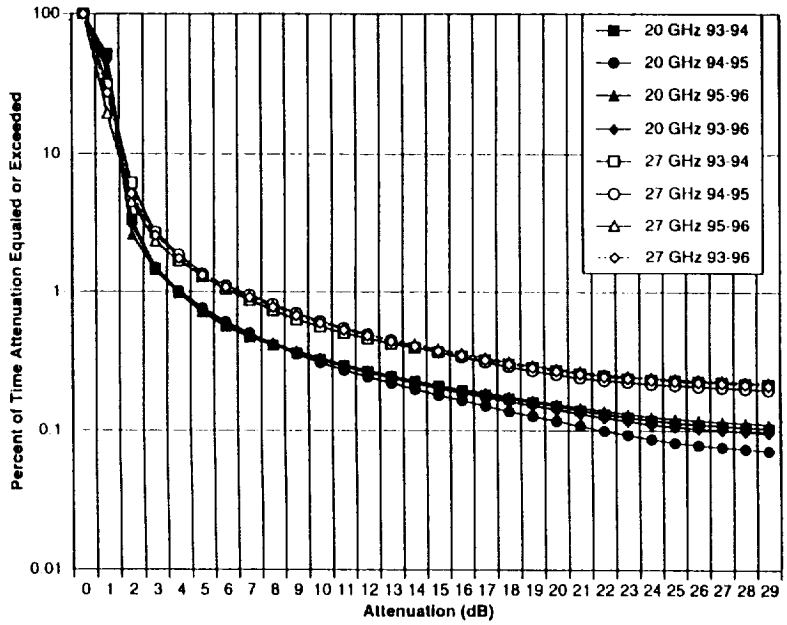

Figure 9: 1993 - 1996 Florida AFS CDF Summary

DIVERSITY PROGRAM

- Diversity Improvement in the Florida Sub-tropical Region
  Focus on short baseline Diversity Improvement
  < 5 km -- greatest commercial interest

- 20 GHz Transportable Terminal
  1.2m APT Dish
  Downconvert to 70 MHz at Feed
  APT Digital Receiver
  Thermal Control
  Easily Replicated

- Operation Validated Adjacent to APT Terminal

- To Continue for Duration of ACTS Program

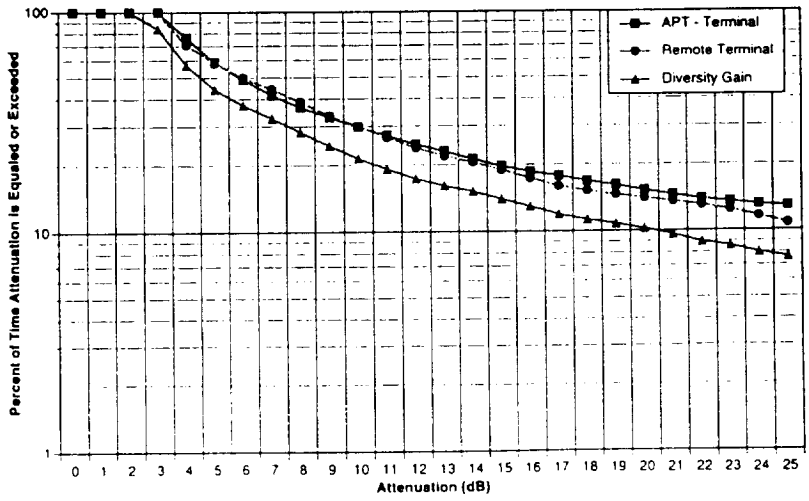

Figure 10: Diversity Enhancement at 1.2 km for May-June, 1996

DATA FILTER STUDIES

- Analyze Beacon and Radiometer Data via FIR Filter Approach

- Filter Options
  Data Representation: Log (dB), Power, or Voltage

- Filter Length
  User-Defined

- Filter Shapes
  Average, Low Pass, Triangular, Cosine Squared,
  McClellan-Parks FIR Design

- Applied to
  CDF Statistics, Fade Duration, Time Duration and
  Fade Slope Statistics

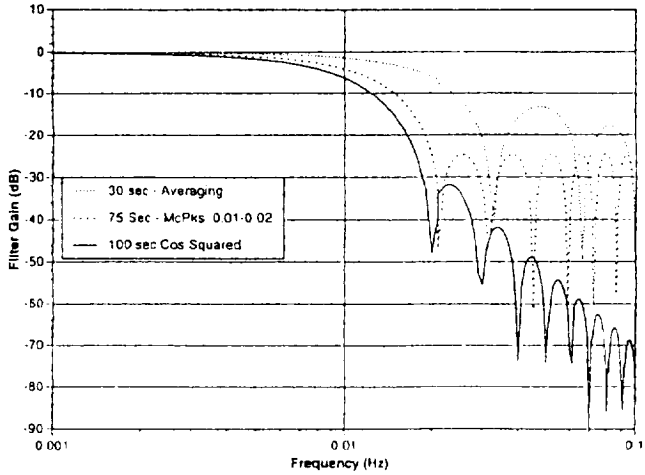

Figure 11: Data Filter Frequency Responses

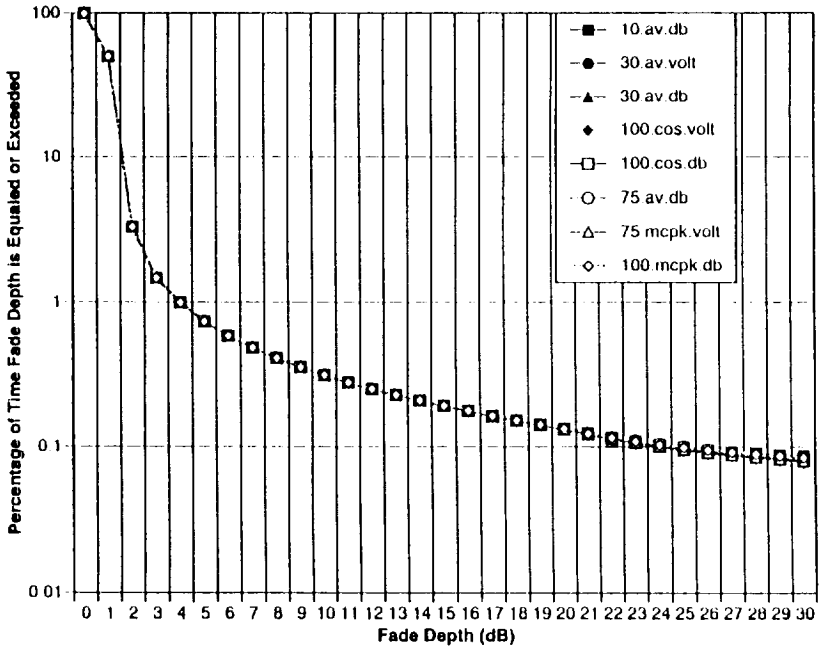

Figure 12: Florida 20 GHz AFS Filter Comparison

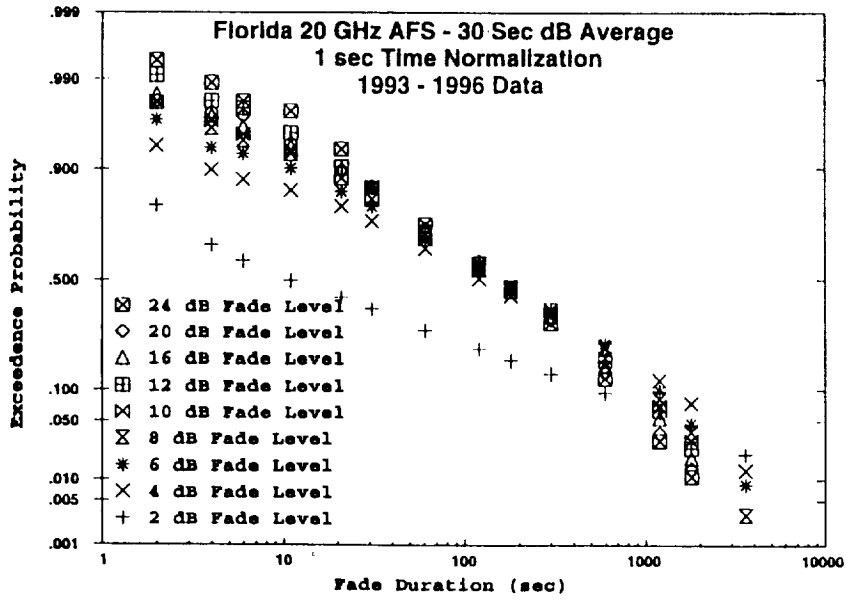

Figure 13a: Log Normal Fade Duration CDF

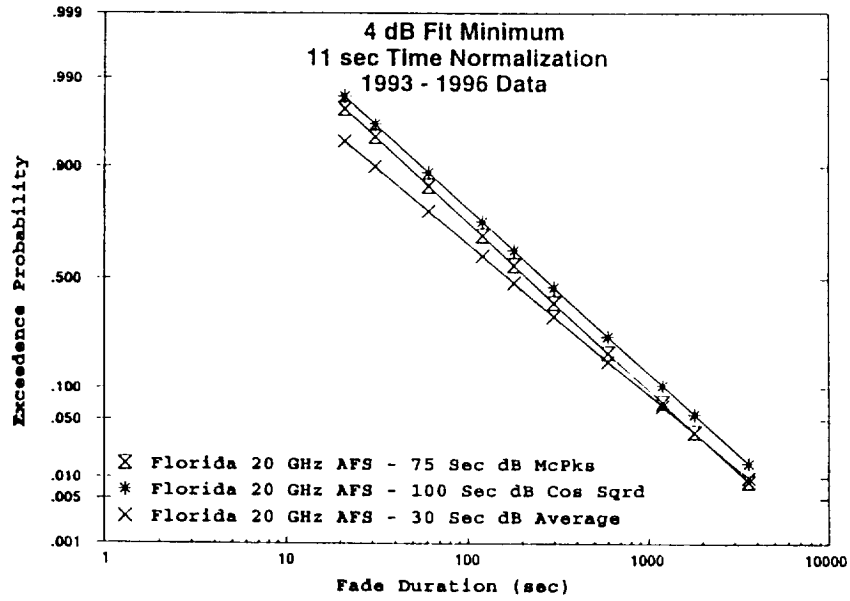

Figure 13b: Log Normal Fade Duration Least Squares Fit

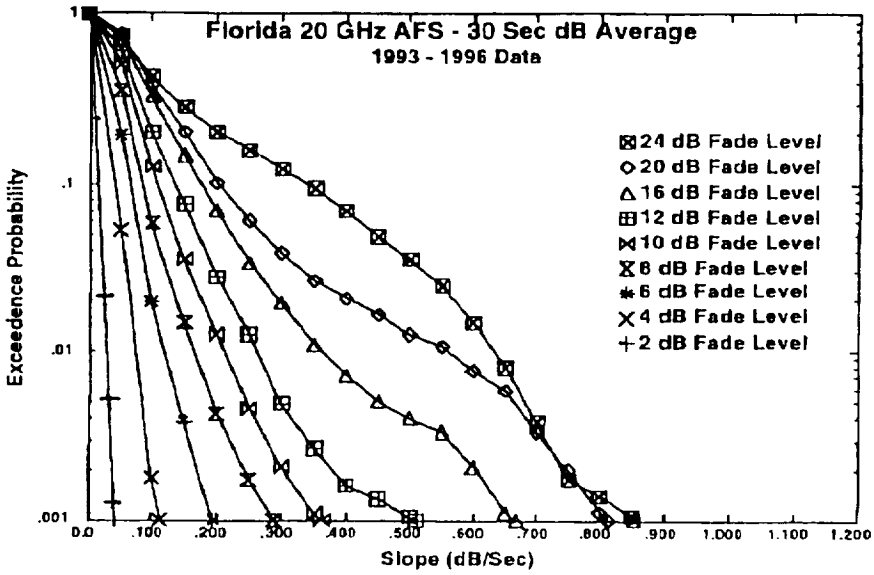

Figure 14: Slope Cumulative Distribution Functions

3 Years of ACTS Propagation Studies in Florida

CONCLUSIONS

- SUCCESSFUL 3.5 + Year Operational Period
  Uniform, Expanding Data Base
- Robust Analysis Software
  Extending Analysis to Other Sites
- Continuing Diversity Program
- Data Filter Studies
  Negligible Effect on CDF's
  Quantifiable on Fade, Time, and Slope Statistics
- All Systems "GO" for Continued Operation

ACTS Propagation Measurements in Maryland and Virginia

Asoka Dissanayake and K. T. Lin

COMSAT LABORATORIES ACTS Propagation Measurements

Introduction

- ACTS propagation measurements are being conducted at three sites in Washington DC area.

- Main objectives of the measurements are:
  - · collect long-term propagation data
  - · investigate multiple site diversity
  - · development of propagation models
  - · investigation of fade mitigation techniques

Measurement Site Configuration

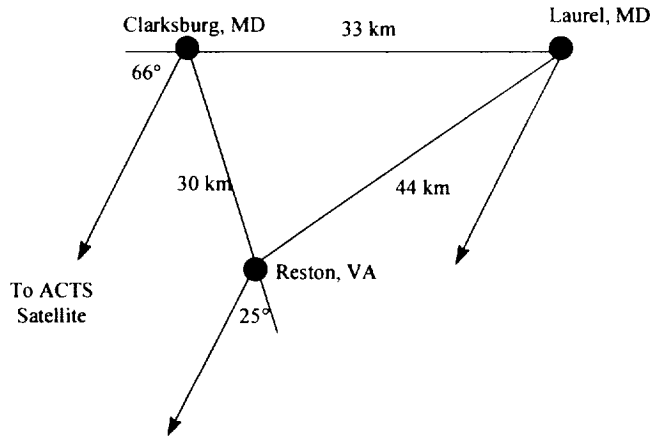

Program Status

- Data collection:
  - Clarksburg: 43 months complete
  - Reston: 39 months complete
  - Laurel: 33 months complete

- Data analysis:
  - Clarksburg: 33 months
  - Reston: 24 months

Attenuation Statistics

- Single site attenuation statistics for the two years from March 1994 through February 1996 are presented.
- For the same 12 month period distribution of attenuation for the two sites are very similar.
- Considerable year-to-year variability seen in the data.
- Model predictions fall within the annual variation.

COMSAT LABORATORIES ACTS Propagation Measurements

Cumulative Distribution of Rain Rate: Clarksburg

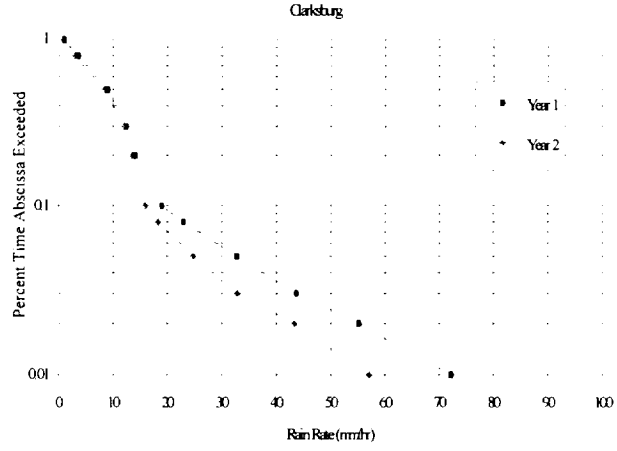

Cumulative Distribution of Attenuation: Reston

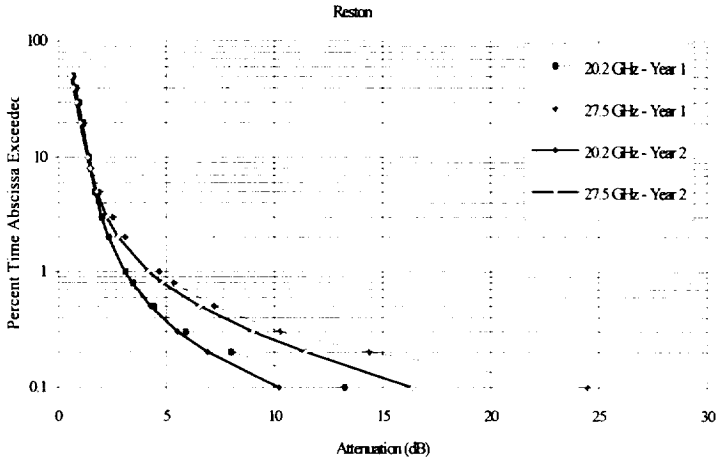

COMSAT LABORATORIES ACTS Propagation Measurements

Cumulative Distribution of Attenuation: Clarksburg

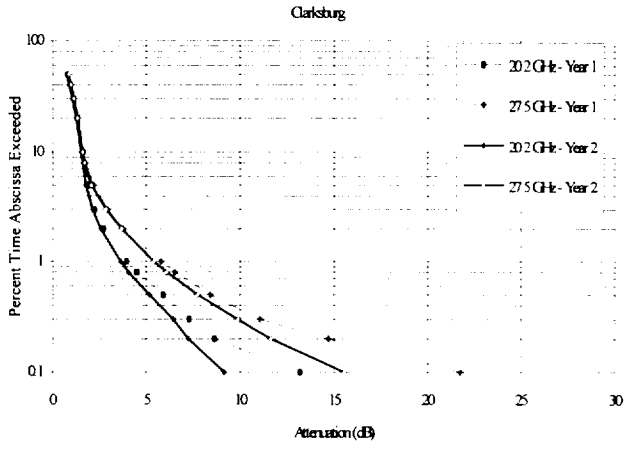

Cloud Attenuation

- Cloud attenuation can be identified from the dual frequency fade measurements. Simultaneous rain measurements are also required.

- Cloud attenuation does not appear to vary appreciably from year to year.

- At 27.5 GHz cloud attenuation levels up to 2 dB have been observed.

COMSAT LABORATORIES ACTS Propagation Measurements

Cloud Attenuation Distribution at Clarksburg

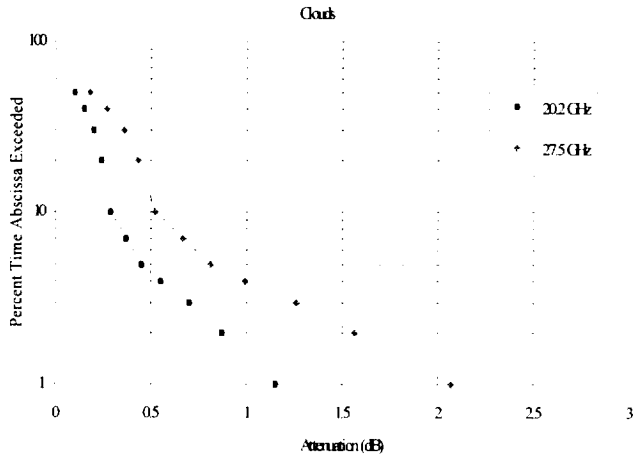

Diversity Analysis

- Diversity statistics derived for the two site configuration Clarksburg and Reston.

- Very little variation between joint statistics for the two measurement years.

- Diversity prediction model appears to under estimate diversity gain.

Joint Attenuation Statistics at 20.2 GHz

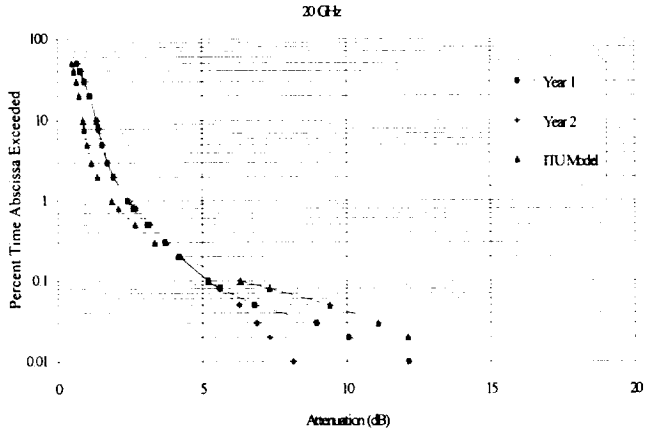

Joint Attenuation Statistics at 27.5 GHz

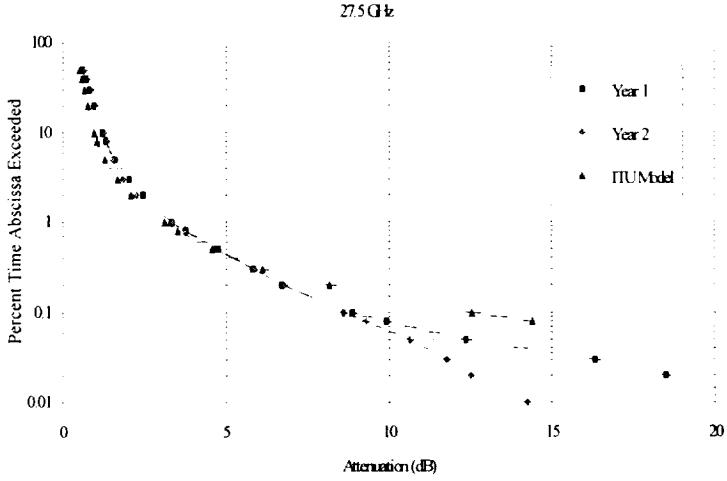

COMSAT LABORATORIES ACTS Propagation Measurements

Fade Slopes

- Fade slopes calculated after removing scintillation effects using a 20 s moving average filter.
- Positive and negative going slopes symmetrically distributed.
- Fade slopes appear to be relatively insensitive to fade threshold.
- 1 dB/s represents a reasonable upper bound to fade slopes.

Fade Slope Histogram: 20.2 GHz

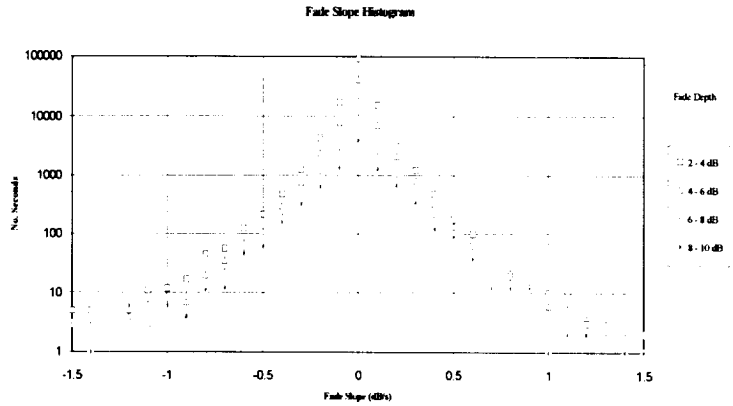

COMSAT LABORATORIES ACTS Propagation Measurements

Fade Slope Distribution: 20.2 GHz

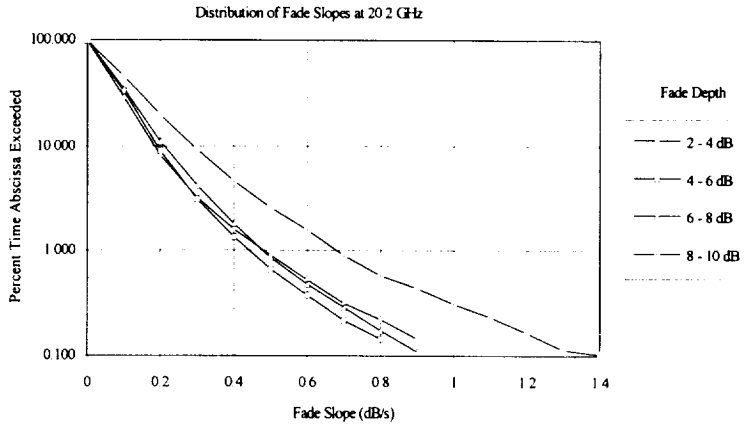

Fade Slope Distribution: 27.5 GHz

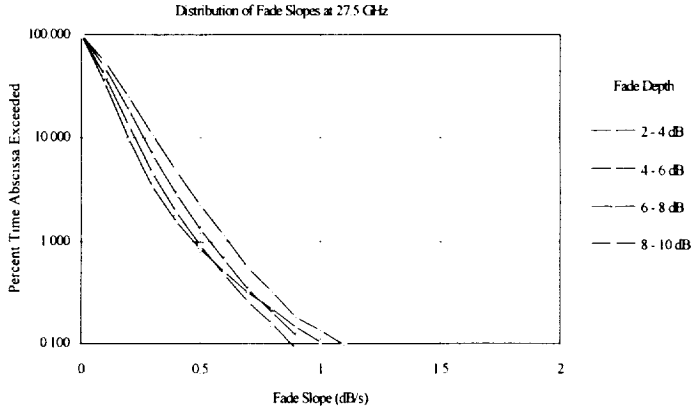

COMSAT LABORATORIES ACTS Propagation Measurements

Antenna Wetting

- Experiment conducted by using two closely spaced antenna systems. One of the antenna reflectors covered with a water repellant cloth cover. Two systems used to receive the 20 GHz ACTS beacon signal.

- Under test conditions the covered antenna fared significantly better than the uncovered antenna.

- Under rainy conditions the covered antenna produced slightly more attenuation than the uncovered antenna.

Reflector Wetting Loss: 20 GHz

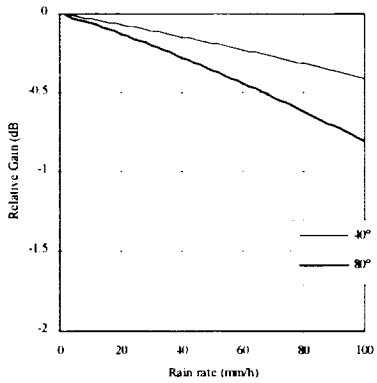

Feed Wetting Loss: 20 GHz

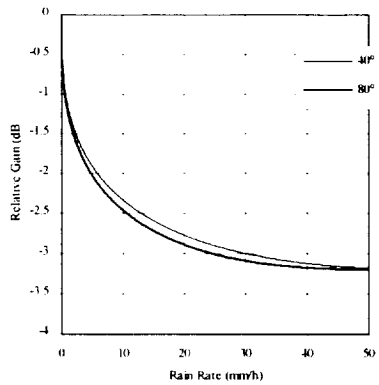

COMSAT LABORATORIES ACTS Propagation Measurements

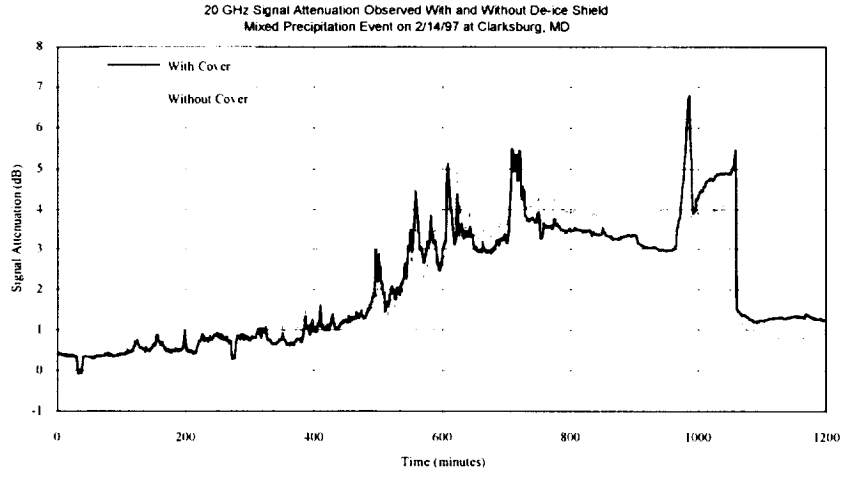

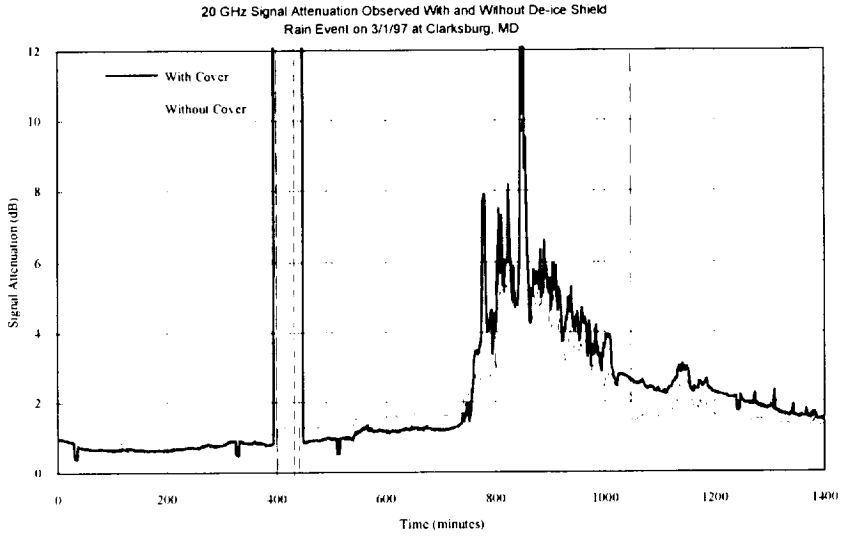

COMSAT LABORATORIES ACTS Propagation Measurements

Conclusions

- ACTS beacon data from Maryland and Virginia used to derive long-term statistics of attenuation and parameters required for the design of fade mitigation techniques.

- Further analysis required to validate/improve propagation models.

- Fourth year of data collection in progress.

New Mexico ACTS Propagation Terminal Status

Stephen Horan, Frank Paulic, and
Atle Borsholm

New Mexico State University

June 1997

NM APT

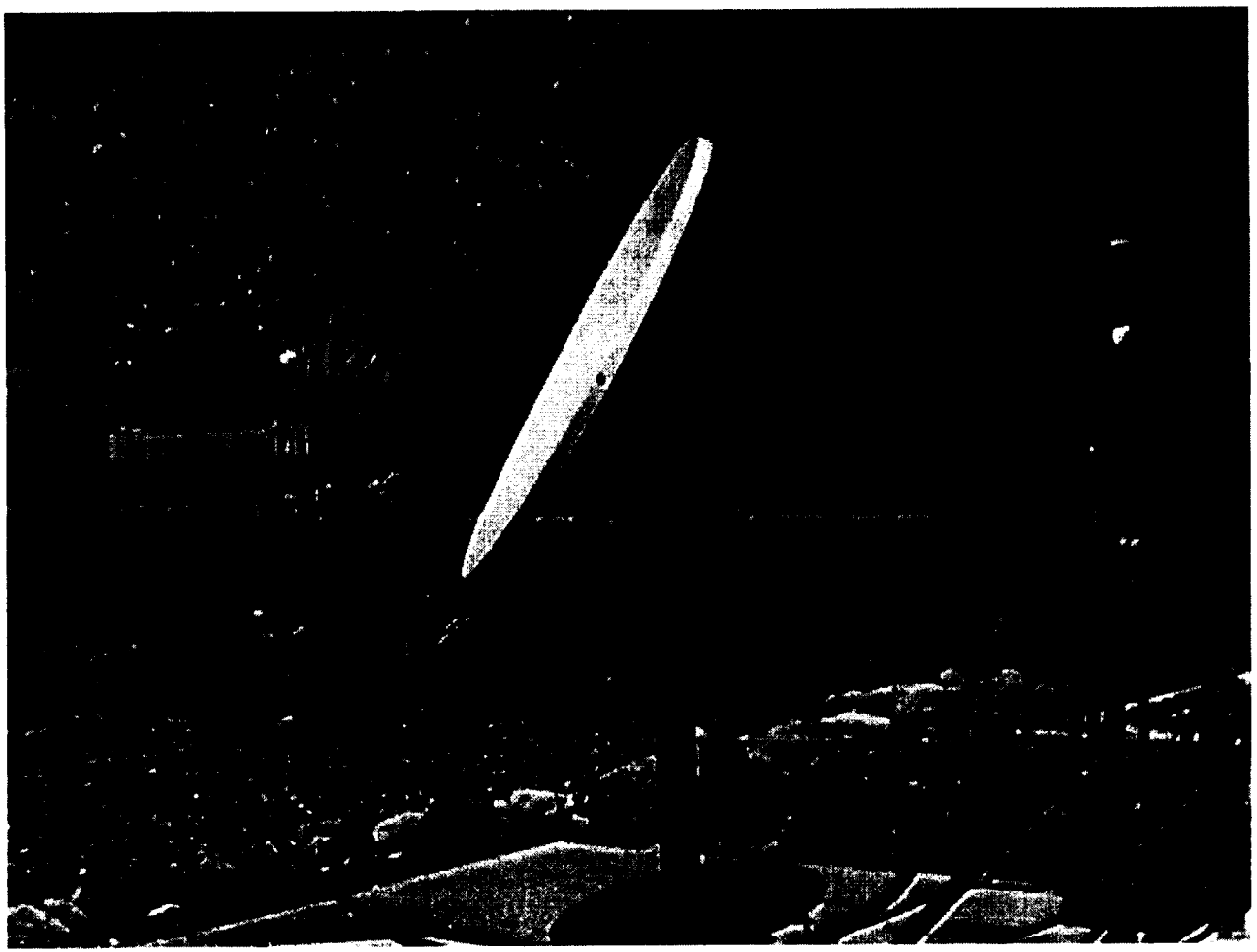

Topics

- Changes
- Availablity
- Antenna Wetting
- Rain Statistics

1-105

Changes

- Replaced WWV active antenna element on 28 January 1997
- Installed ZIP drive and SCSI controller on 1 February 1997
- Replaced power splitter at input to receiver and radiometer on 20 GHz channel on 29 April 1997
- Replaced relative humidity gauge on 19 May 1997

1-106

Changes

- With ZIP drive, the SCSI controller drivers must not be loaded on system re-boot if the drive itself is not physically present. If the ZIP drive is not present physically when the system re-boots, then the system will hang.
- Cure: Need to install drivers only when using drive!

1-107

Changes

- Power Splitter appears to have been causing a level shift (glitch) in both the radiometer and beacon levels
- Editing the data by hand was required to remove the glitches
- Usually, there are nor more than one or two shifts per day. However, March 28 had approximately 100 level shifts in one day!

1-108

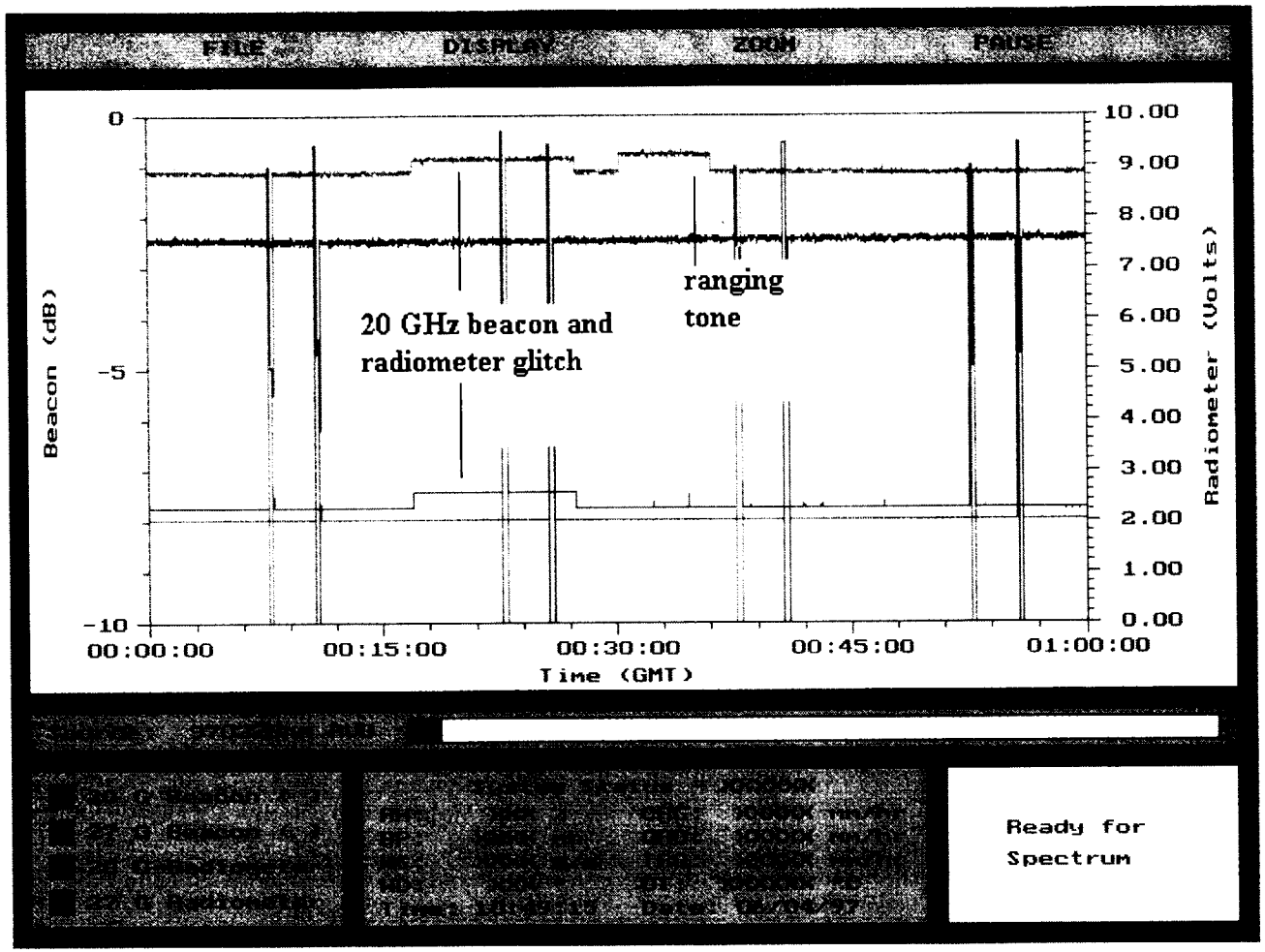

glitch and ranging tone on the 20 GHz channel

Availability

		Total Time			
Month	**Status**	**Days**	**Hours**	**Minutes**	**% of Total**
November	Up	28	20	54	96.24%
	Down	1	3	6	3.76%
December	Up	24	6	9	78.25%
	Down	6	17	51	21.75%
January	Up	28	0	50	90.43%
	Down	2	23	10	9.57%
February	Up	26	17	36	86.24%
	Down	1	6	24	4.09%
March	Up	31	0	0	100.00%
	Down	0	0	0	0.00%
April	Up	26	7	41	84.90%
	Down	3	16	19	11.87%
May	Up	31	0	0	100.00%
	Down	0	0	0	0.00%
Total	Up	196	5	10	92.55%
	Down	15	18	50	7.45%

Antenna Wetting

- Two Experiments
  - hand-held squirt bottle
  - "wetting machine" using the UBC design
- Experimental Observations
  - effect of a wet dish alone
  - effect of wet feed horn alone
  - effect of "rain field" on vicinity of dish and feed

1-111

NM APT with UBC-type rain maker

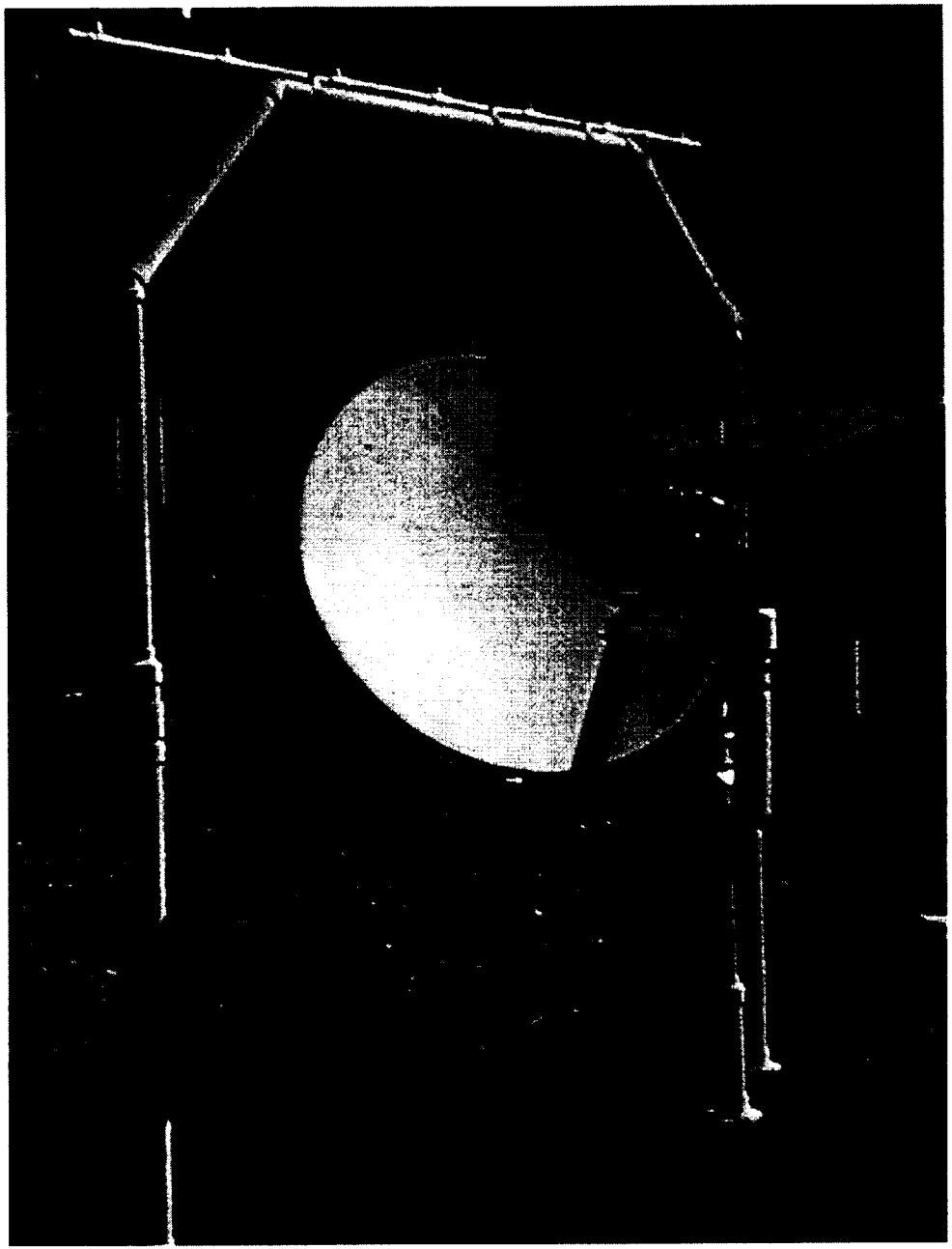

1-112

Antenna Wetting

- Squirt Tests
  - wet feed with mist from spray bottle
    - dish to remain dry
  - wet dish with mist from spray bottle
    - feed to remain dry
  - wet both dish and feed with dry air between both (residual moisture on both surfaces)

1-113

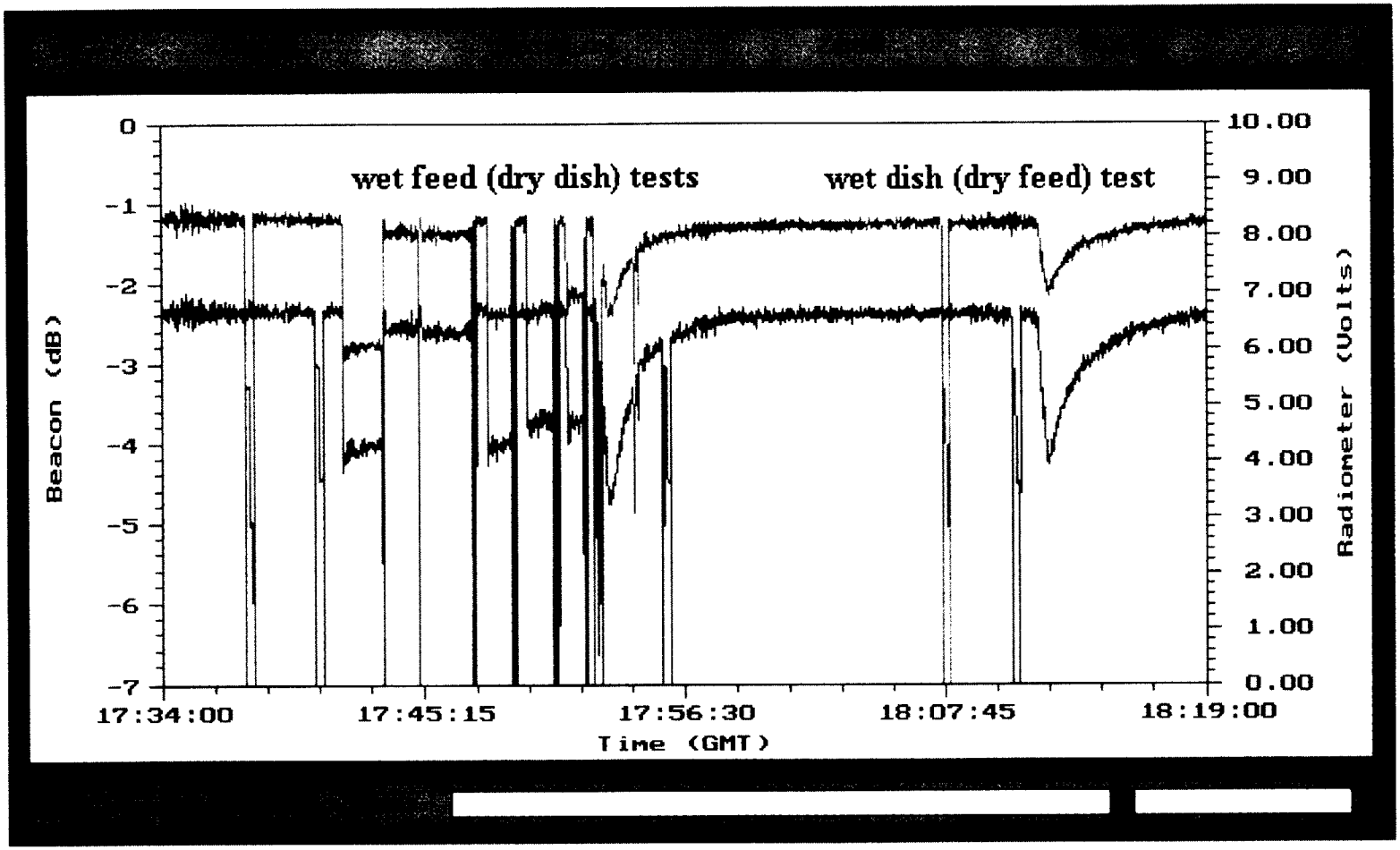

1-114

experimental run #1 using a squirt bottle

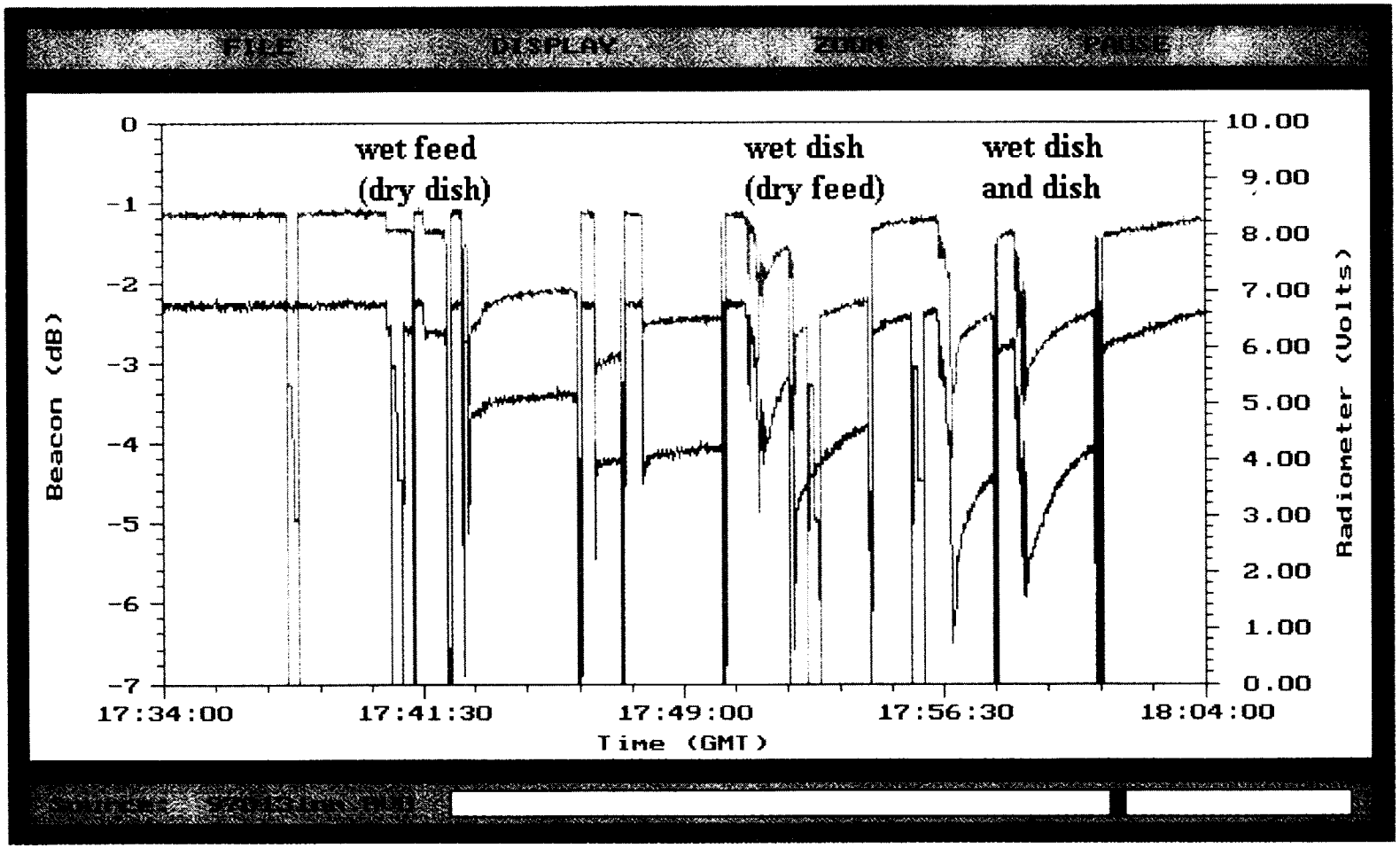

1-115

experimental run #2 using a squirt bottle

Antenna Wetting

- Results
  - wet feed alone: 1.5 dB effect
  - wet dish alone: 1.5 dB effect
  - both wet: 3 - 4 dB effect

1-116

Antenna Wetting

- Rain Machine Tests
  - used different water pressures to vary "rain" rate
  - did not attempt to shield feed from water
  - no coatings aplied to antenna surface

1-147

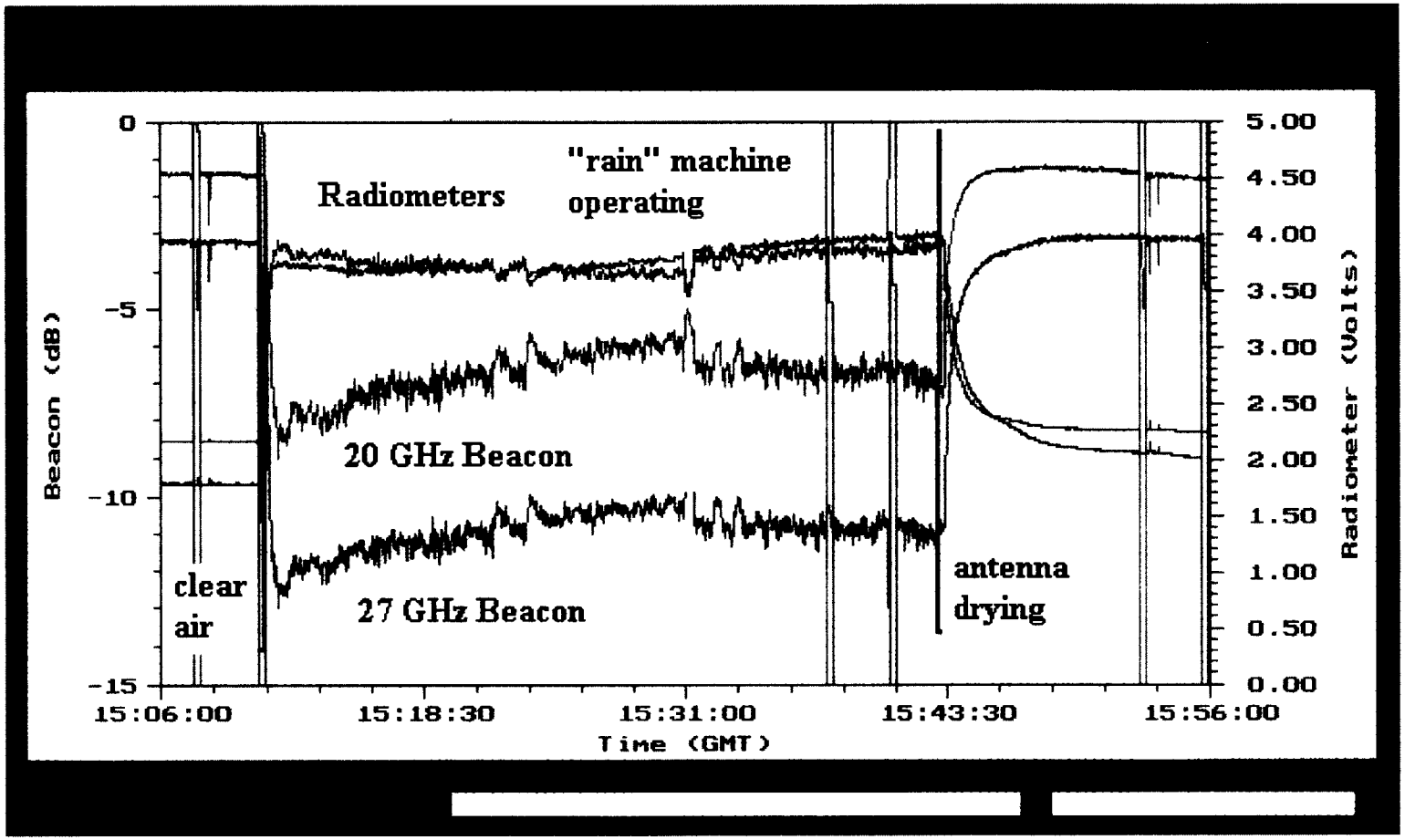

experimental run using the “rain machine”

970602 Rain Rate vs 20 Beacon

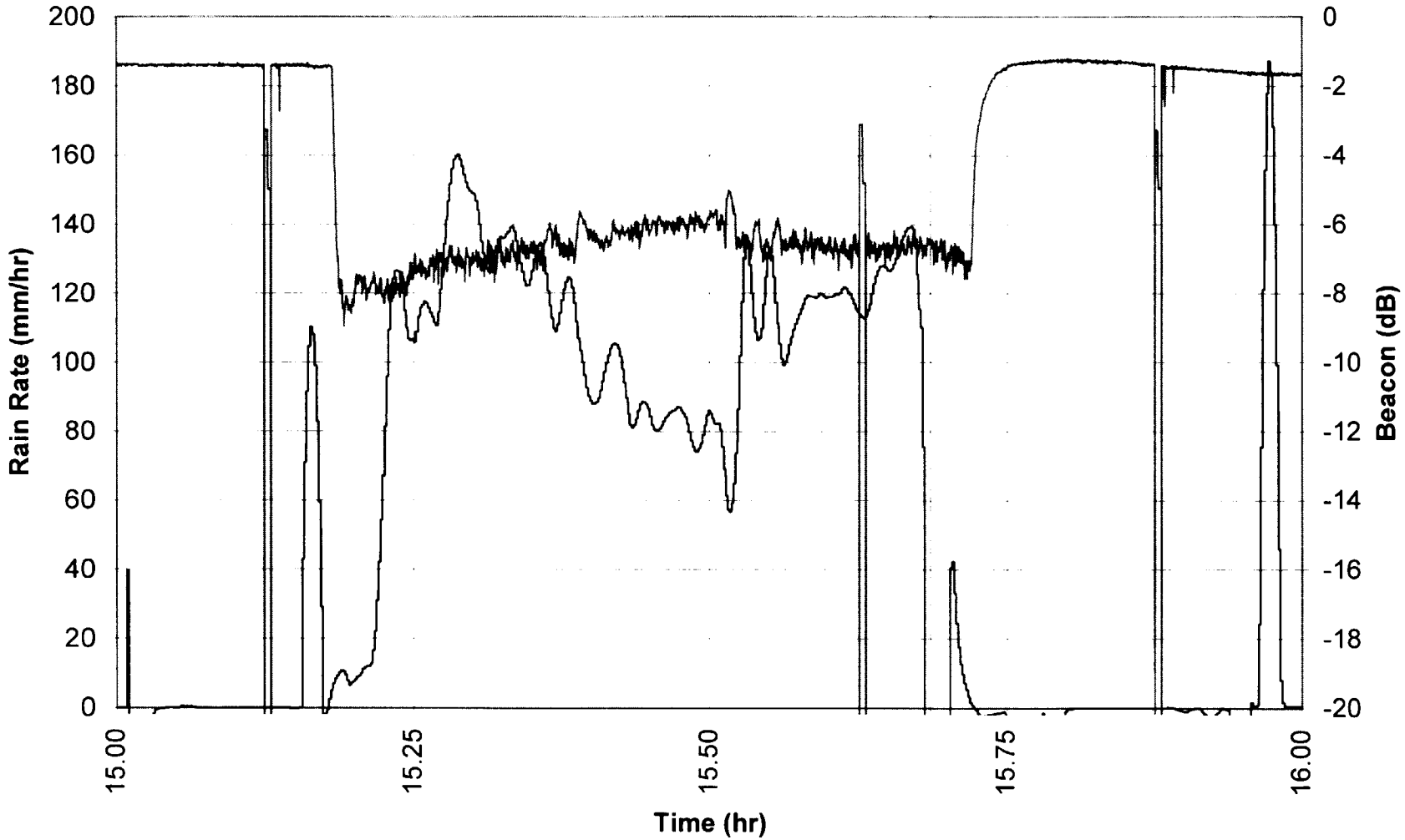

970602 Rain Rate vs 27 Beacon

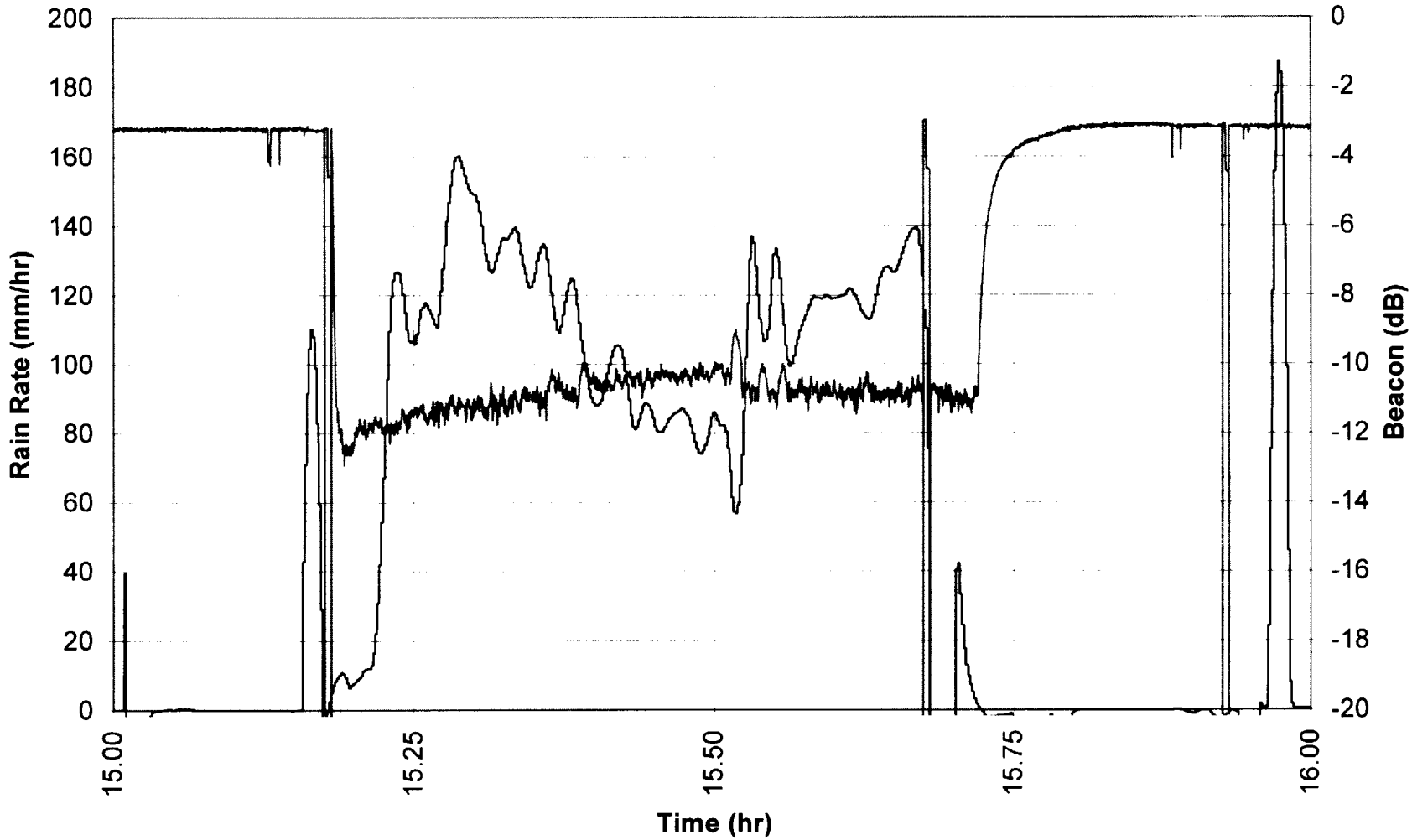

Antenna Wetting

- Results
  - 5 - 7 dB effect for non-coated dishes
  - some variation (~ 0.5 dB due to "rain" rate) in overall attenuation

1-121

Rain Statistics

- Third full year of rain statistics will be complete in August 1997
- NM APT is located in the Crane Global Model Region F
- NM APT is located in the ITU Region E (near the E/M boundary)

Rain Statistics

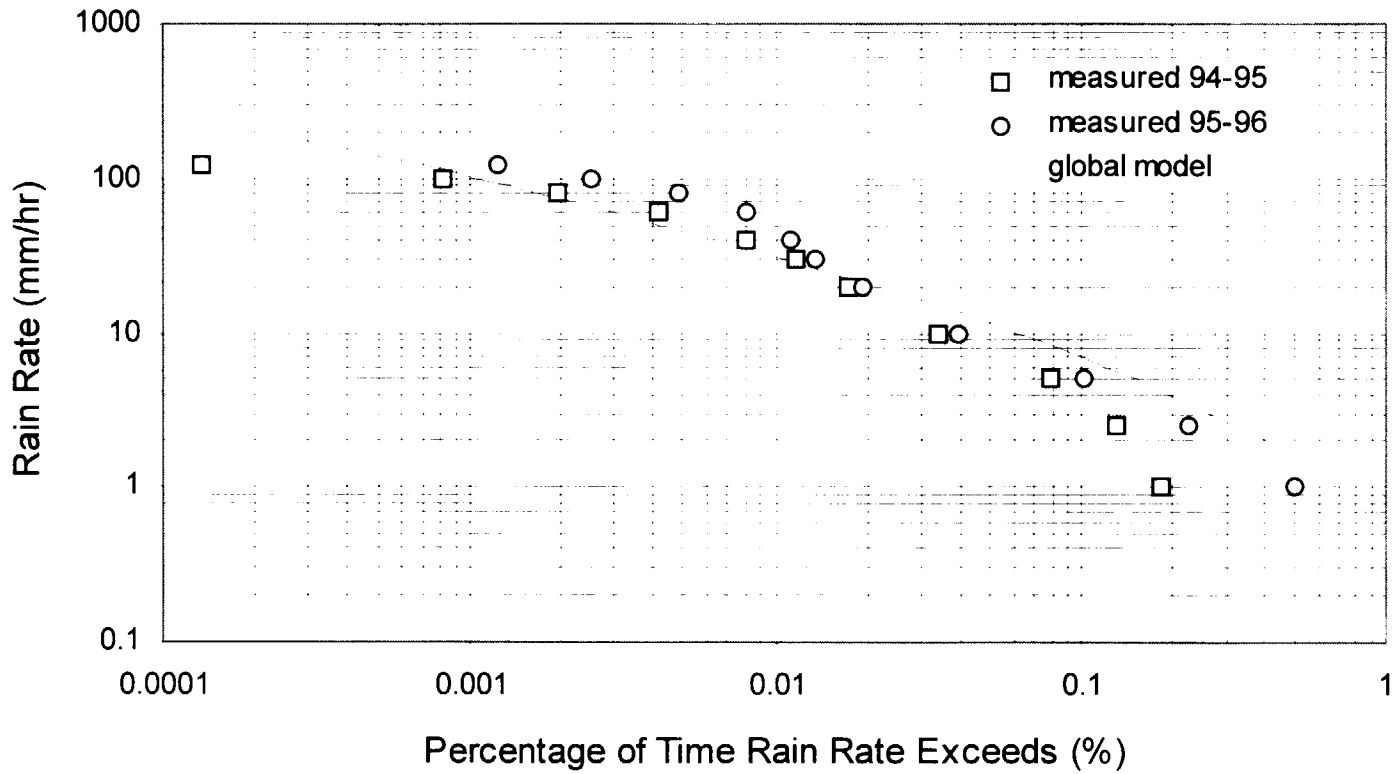

1-123

Rain Statistics

- In 1996
  - total annual precipitation = 6.20 in; 1961-1990 average precipitation = 9.40 in
  - warmest February since 1957 (second warmest since 1892)
  - for May 1996, a new May record high mean temperature and driest May since 1974
  - driest December since 1980

Rain Statistics

- In 1996
  - second warmest year on record (63.6 degrees) behind 1994 (63.9 degrees) and above the 1961 - 1990 average (60.7 degrees)
  - 24 new daily maximum temperature records set during 1996

1-125/126

ACS
Stanford Telecom

Stanford Telecom / New Mexico State University

ACTS Propagation Measurements Program

Data Analysis Summary

Julie H. Feil
Louis J. Ippolito
Stephen Horan
Jennifer Pinder
Frank Paulic
Atle Borsholm

NAPEX XXI & APSW XI
June 11-13, 1997
Los Angeles, CA

ACS
Stanford Telecom

Agenda

- **Introduction**
  - ➢ Experiment objectives & configuration
- **NM ACTS K_A band measurements and analysis**
  - ➢ Three year (12/93-11/96) propagation statistics
  - ➢ Annual model comparisons
  - ➢ Seasonal statistics
- **Summary and future activities**
- **New Mexico State University: Station status and wet antenna measurements**

STel ACTS Propagation Experiment Objectives

- **Measure and evaluate K_A band propagation effects and link performance for New Mexico**

- **Develop long-term statistics and prediction modeling techniques for New Mexico climate region for advanced satellite system planning and design**

ACS
Stanford Telecom

New Mexico APT

- **Elevation angle: 51°**

- **Measured parameters**
  - ➢ Beacons: 20.185 GHz and 27.505 GHz
  - ➢ Radiometers: 20 GHz and 27.505 GHz
  - ➢ Rain rate (CRG, TBG)
  - ➢ Temperature, Relative Humidity, Wind Vector, Barometric Pressure

ACS
Stanford Telecom

New Mexico ACTS K_A Band Measurements Summary

- Three years of data processed
- Three year weather statistics
- Comparison of old and new processing techniques for three year propagation measurements
- Annual model comparisons
- Statistical attenuation ratio
- Fade duration
- Seasonal statistics
- Worst actual month (in three years): July 1996

ACS
Stanford Telecom

Three Year Weather Effects

Temperature December 1, 1993 - November 30, 1996

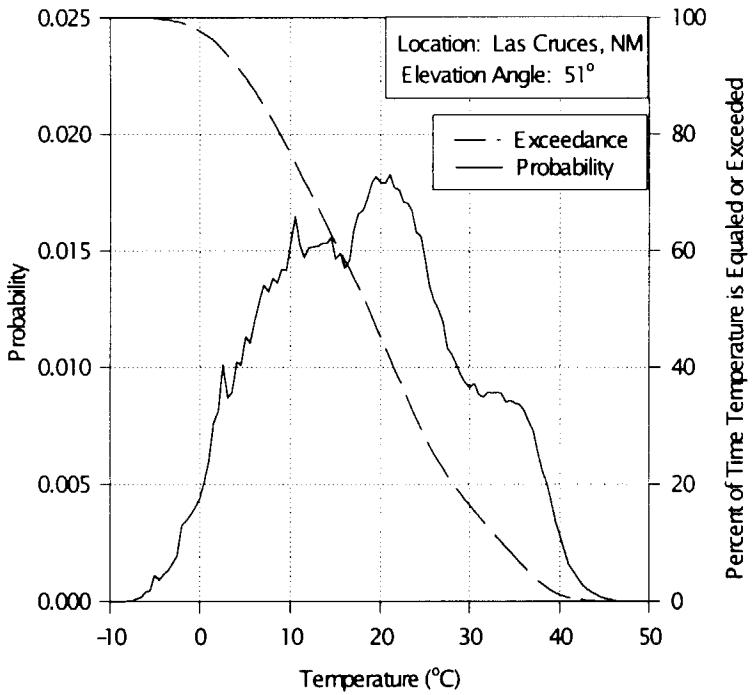

Relative Humidity December 1993 - November 1996

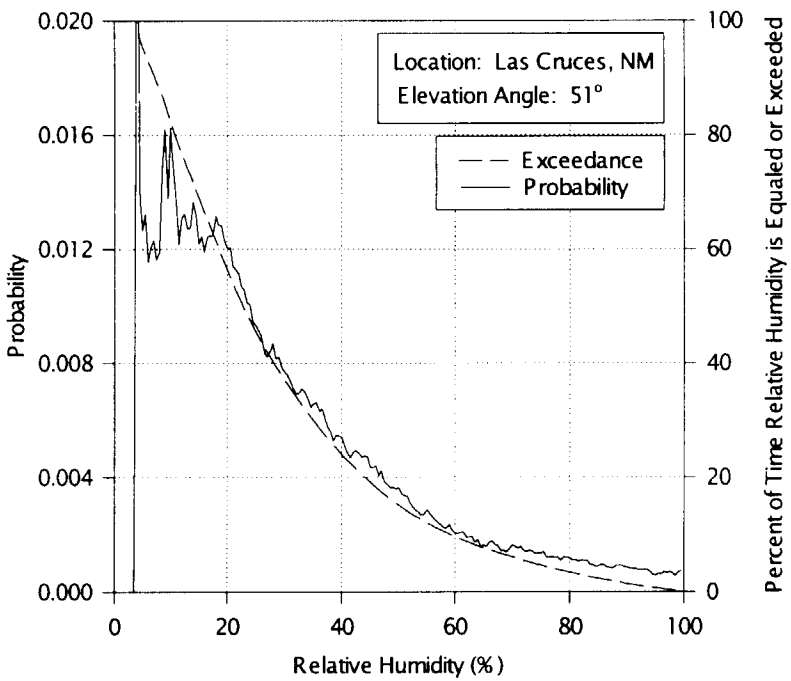

Comparison of Processing Techniques

- **36 Months Statistics: December 1993 -November 1996**
  - From *.pv0 processing (ACTSEDIT)
  - From *.pv2 processing (ACTSPP)

- **Minor differences between two processing techniques**
  - Monthly Statistics are within 1 dB
  - Gaseous absorption is less for *.pv2 than for *.pv0 processing

Definition of Attenuation Terms

- **AFS: Attenuation wrt Free Space**

  Difference between the received beacon level and the received level if in a vacuum. AFS includes attenuation due to atmospheric absorption, rain, clouds, and scintillation.

- **ARD: Radiometrical Derived Attenuation**

  Attenuation measurements from radiometers. Comparable to AFS.

- **ACA: Attenuation wrt Clear Air**

  The difference between the received beacon level and the expected level due to atmospheric absorption (AGA). ACA includes rain, clouds, and scintillation. ACA=AFS-AGA.

- **ARS: Statistical Attenuation Ratio**

  Ratio of equiprobable attenuation levels at two frequencies of interest.

ACS
Stanford Telecom

Three Year Attenuation wrt Free Space (AFS) via ACTSPP

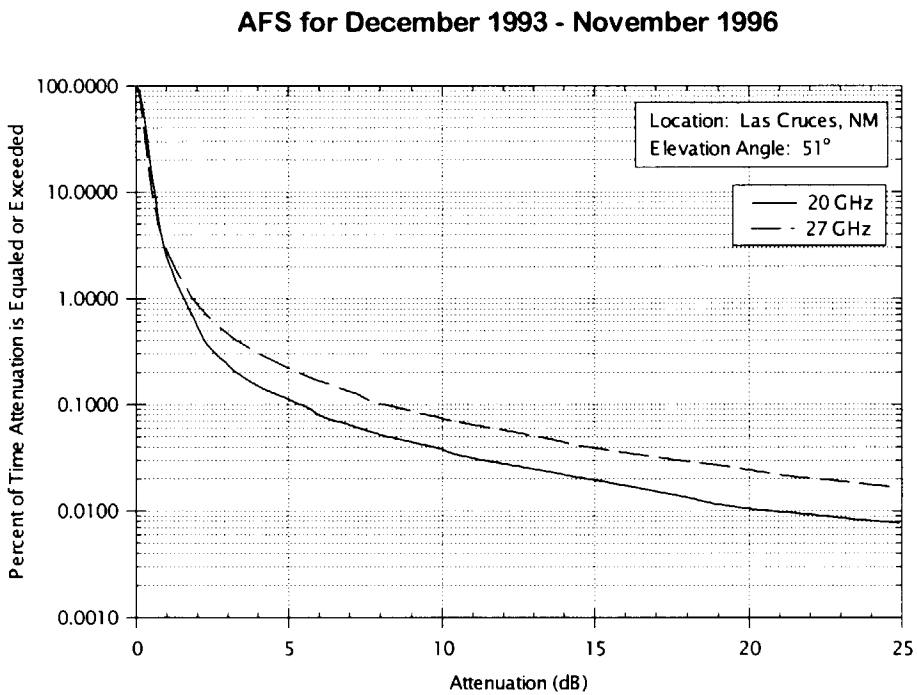

From *.pv2 files

1-135

ACS
Stanford Telecom

Three Year Attenuation wrt Free Space (AFS) via ACTSEDIT

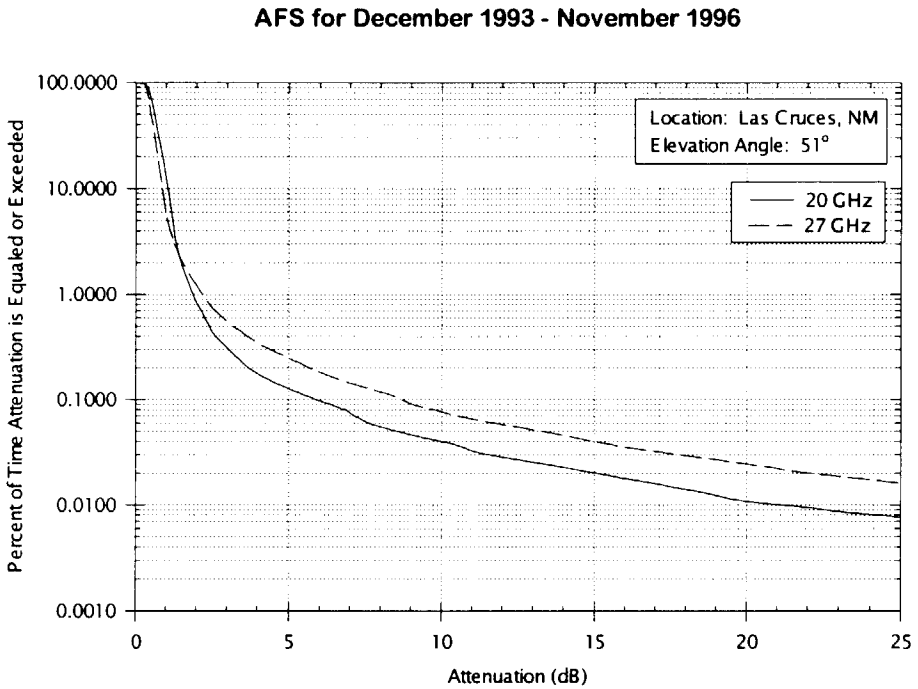

From *.pv0 files

1-136

ACS
Stanford Telecom

Three Year Radiometric Derived Attenuation (ARD) via ACTSPP

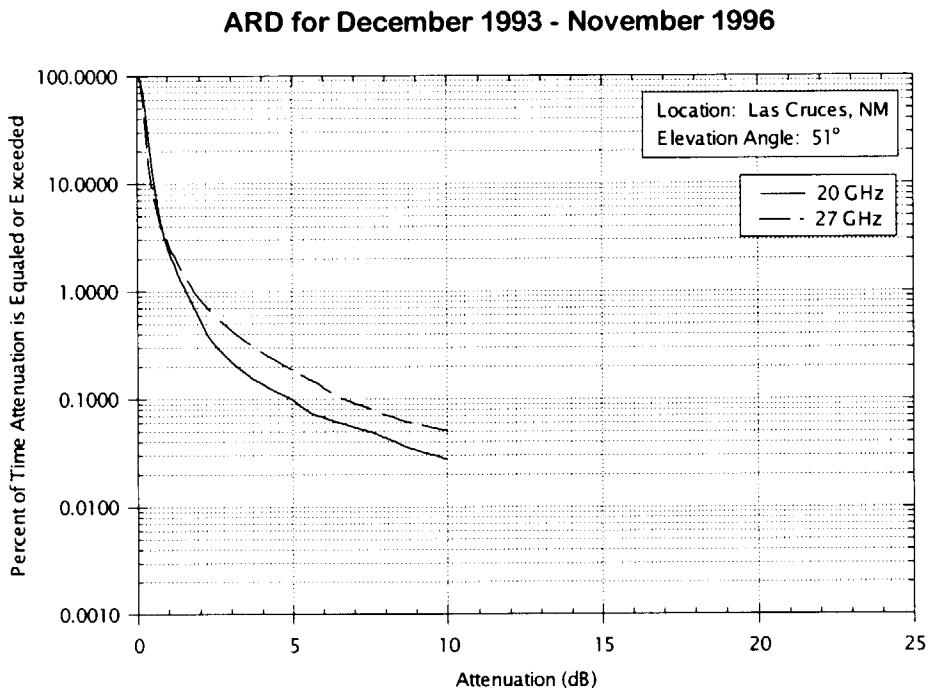

From *.pv2 files

ACS
Stanford Telecom

Three Year Radiometric Derived Attenuation (ARD) via ACTSEDIT

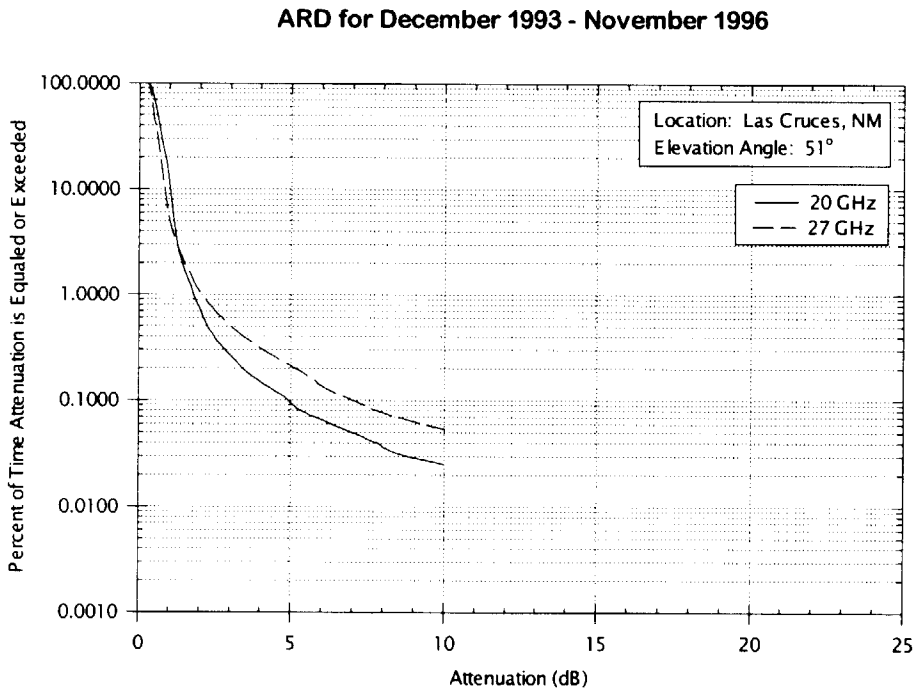

From *.pv0 files

1-138

Three Year Attenuation wrt Clear Air (ACA) via ACTSPP

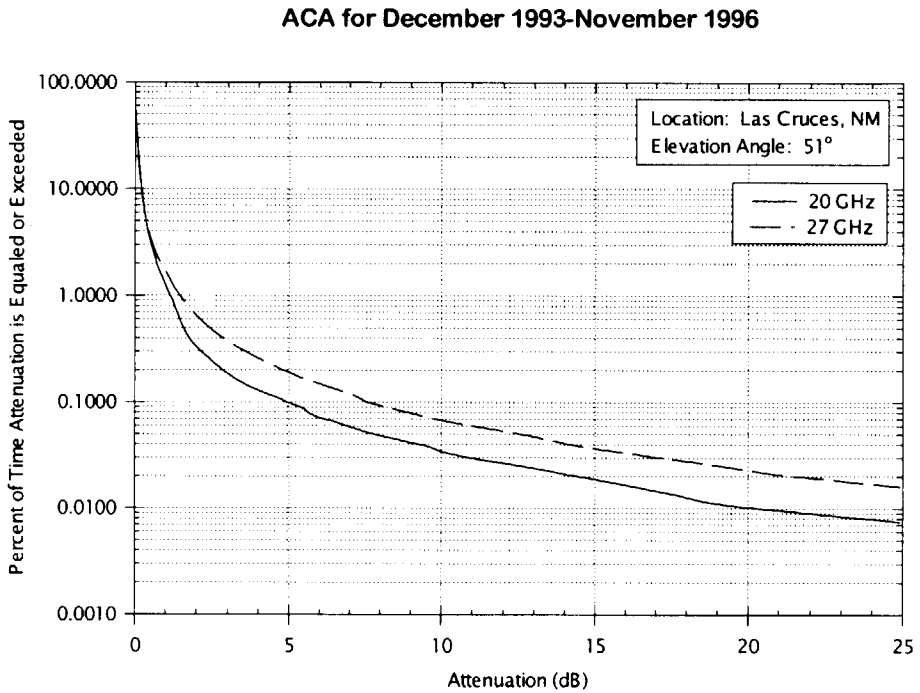

From *.pv2 files

ACS
Stanford Telecom

Three Year Comparison 20 GHz Cumulative Distribution

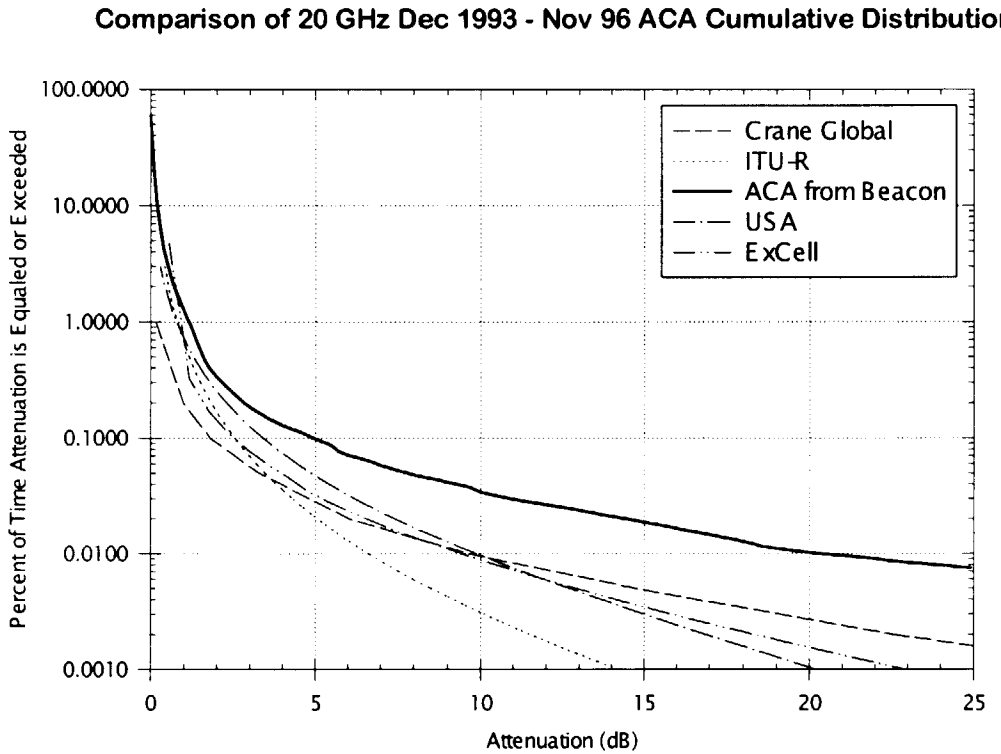

From *.pv2 files

ACS
Stanford Telecom

Three Year Comparison of 27 GHz Cumulative Distribution

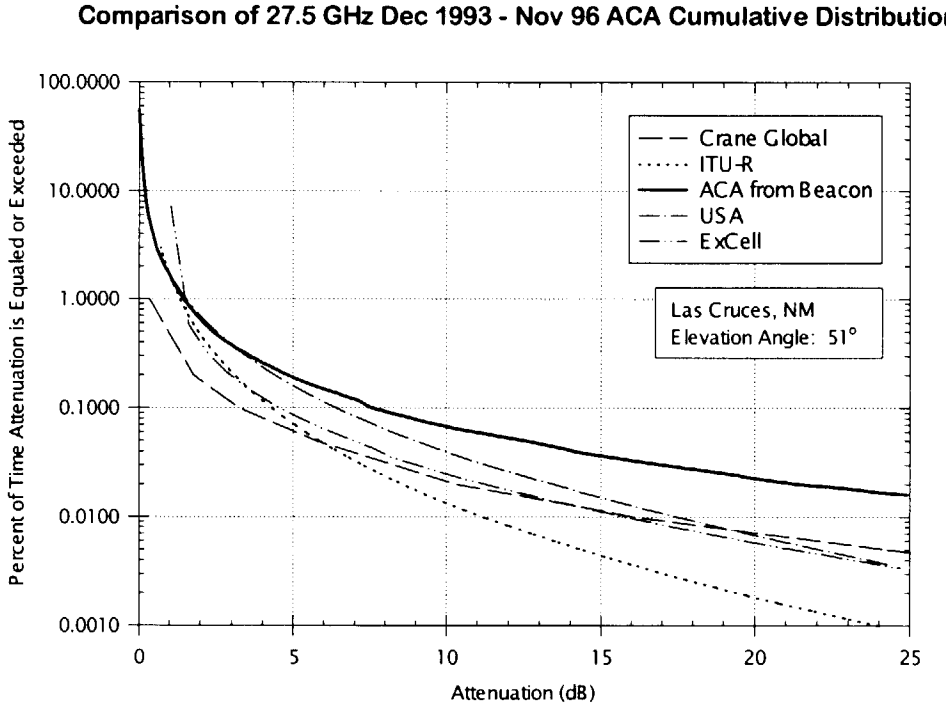

From *.pv2 files

1-141

2 Year Rain Rate Statistics

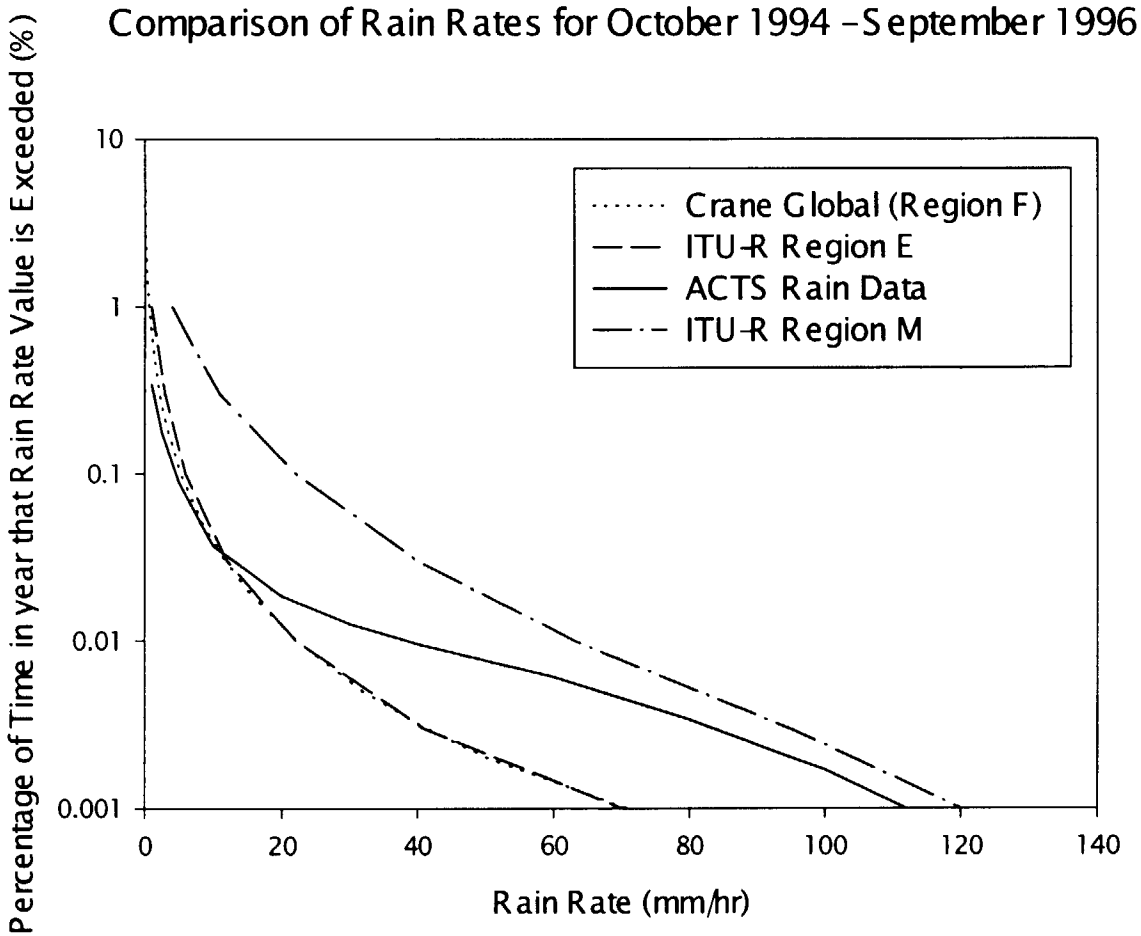

The first six months of the NM ACTS experiment the rain gage did not work.

ACS
Stanford Telecom

Comparison of 2 Year ACA and Global Model with Local Rain Statistics

2 Years: October 1, 1994 through September 30, 1996

20 GHz

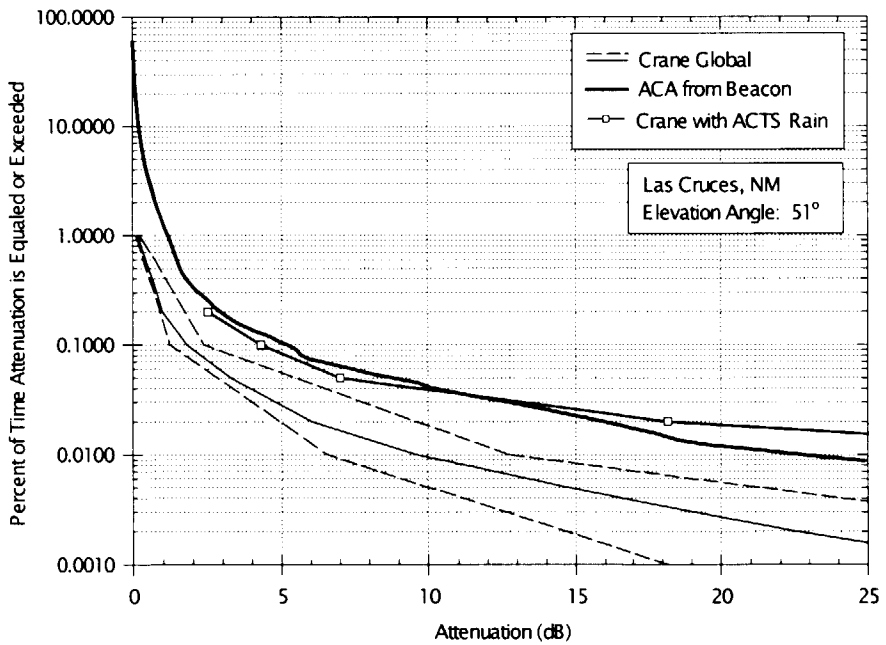

27.5 GHz

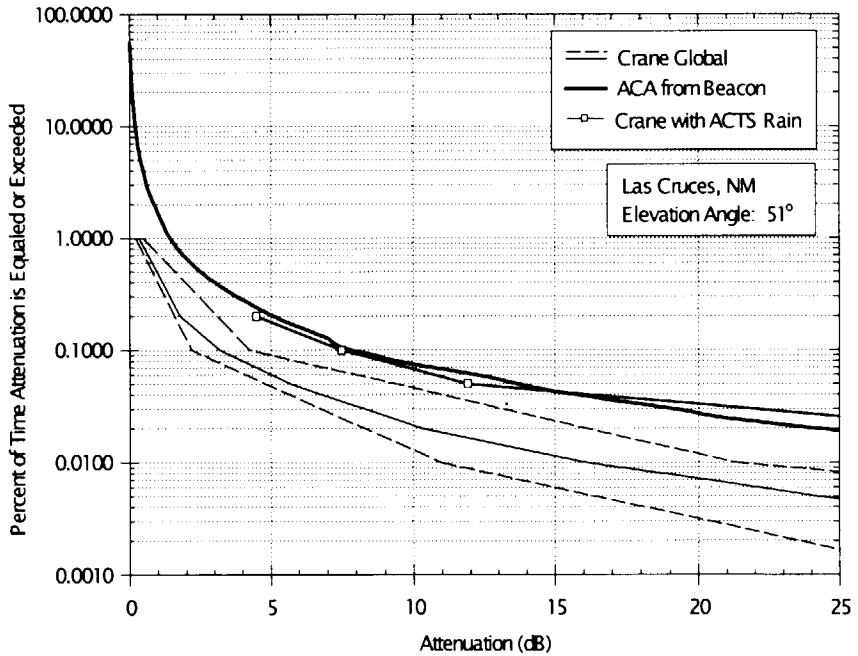

From *.pv2 files
10/1/94-9/30/96

1-143

ACS
Stanford Telecom

Comparison of 2 Year ACA and ITU Model with Local Rain Statistics

2 Years: October 1, 1994 through September 30, 1996

20GHz

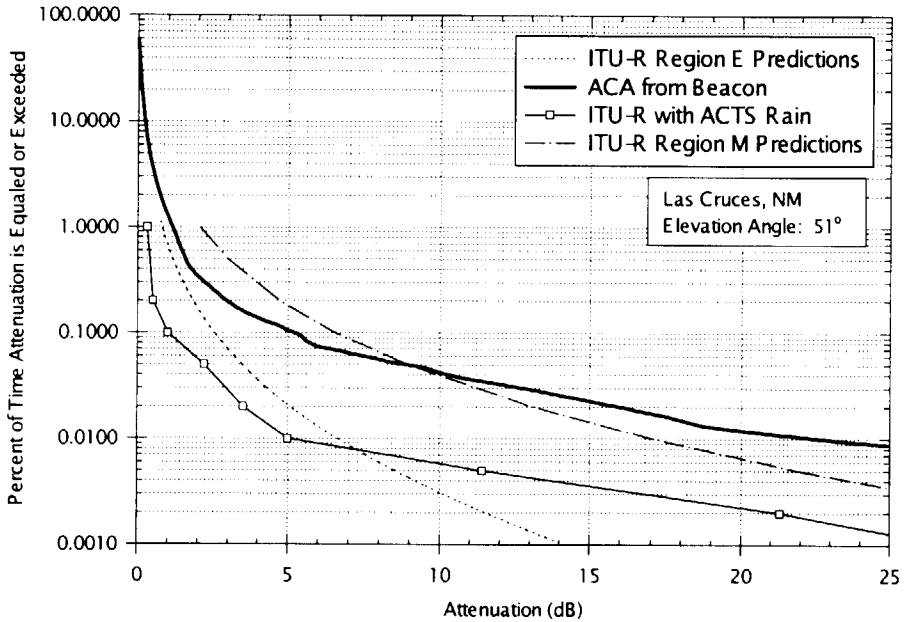

27.5 GHz

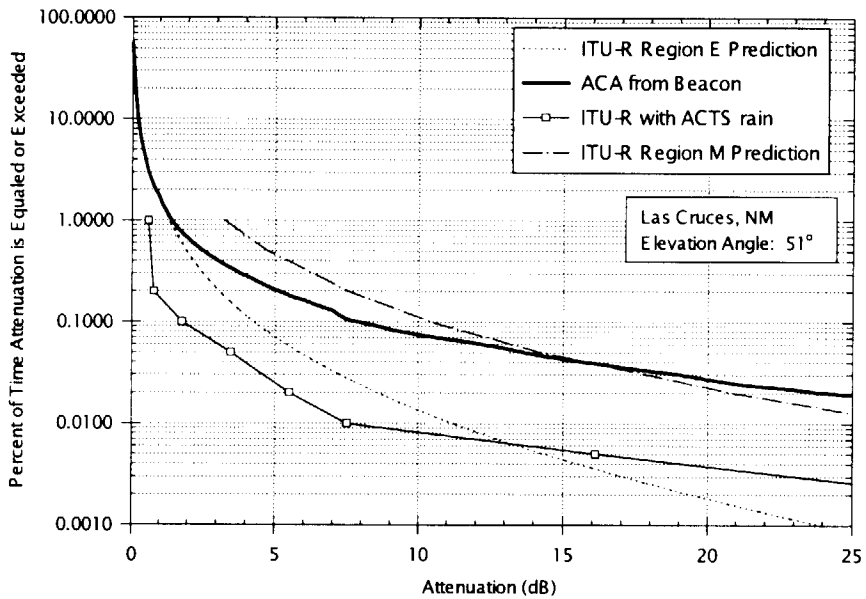

From *.pv2 files
10/1/94-9/30/96

1-144

ACS
Stanford Telecom

Statistical Attenuation Ratio for ACA

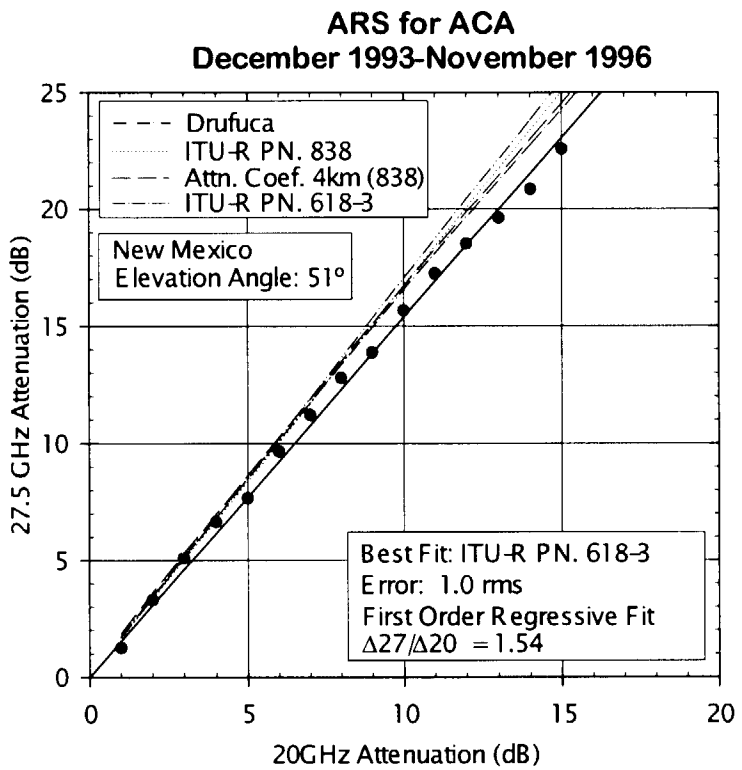

From *.pv2 files

ACS
Stanford Telecom

Statistical Attenuation Ratio for AFS

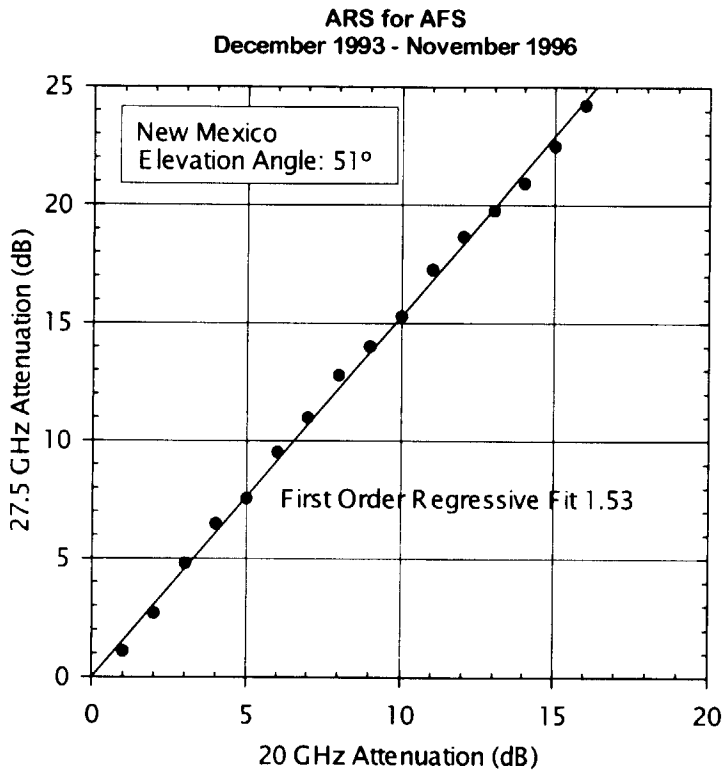

From either *.pv2 or *.pv0 files

ACS
Stanford Telecom

Three Year Fade Duration

200 GHz

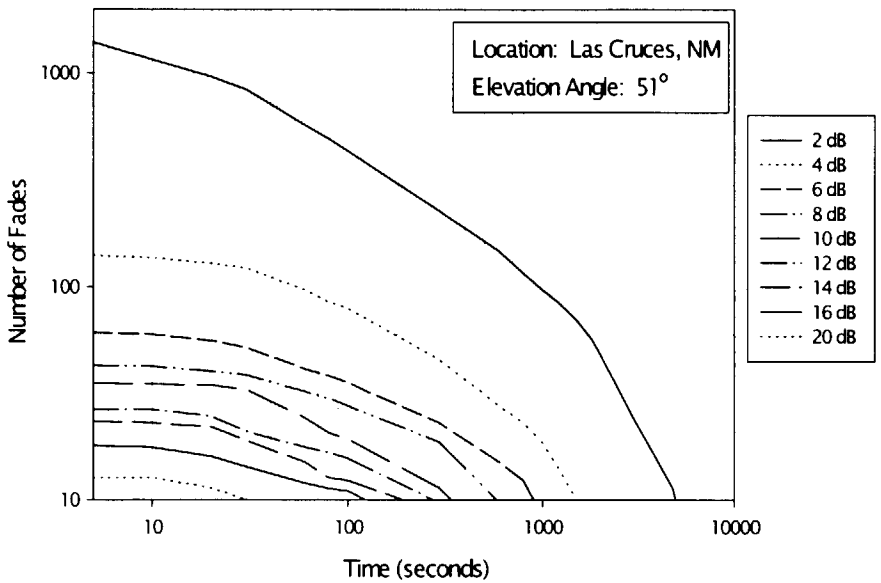

27.5 GHz

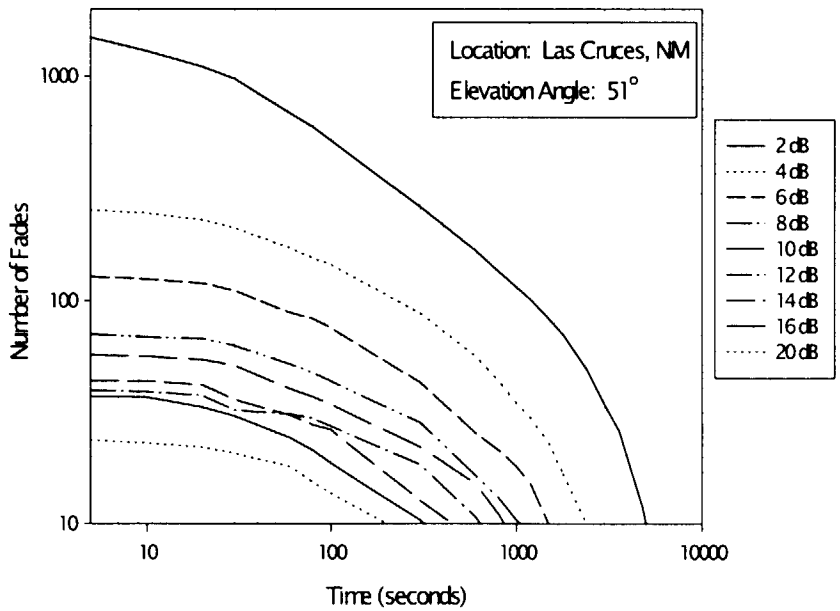

1-147

ACS
Stanford Telecom

Three Year Winter AFS Statistics

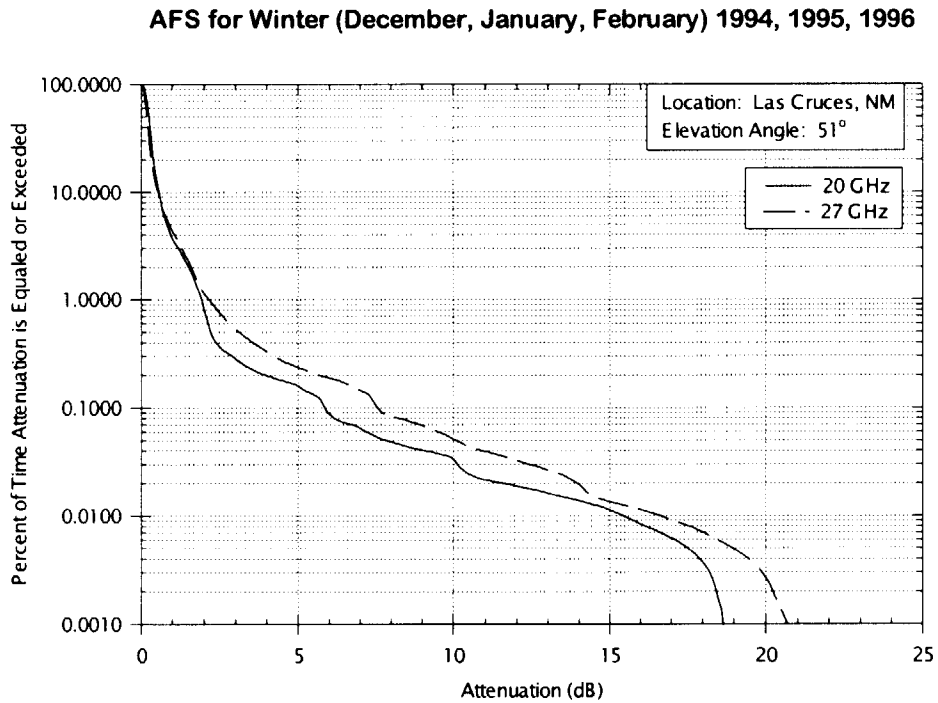

From *.pv2 files

1-148

ACS
Stanford Telecom

Three Year Spring AFS Statistics

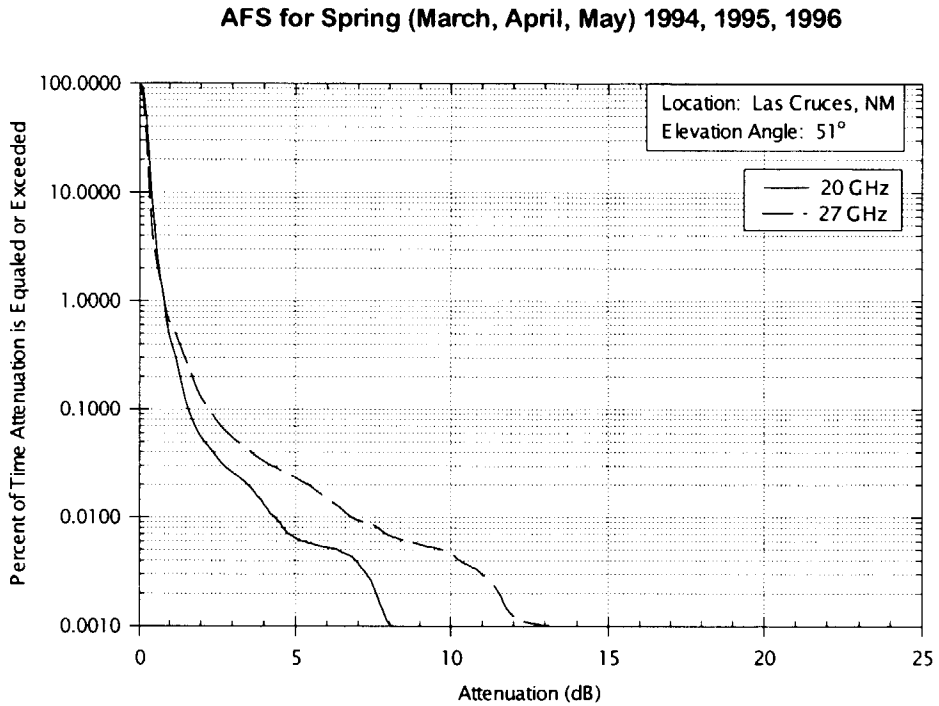

From *.pv2 files

1-149

ACS
Stanford Telecom

Three Year Summer AFS Statistics

AFS for Summer (June, July, August) 1994, 1995, 1996

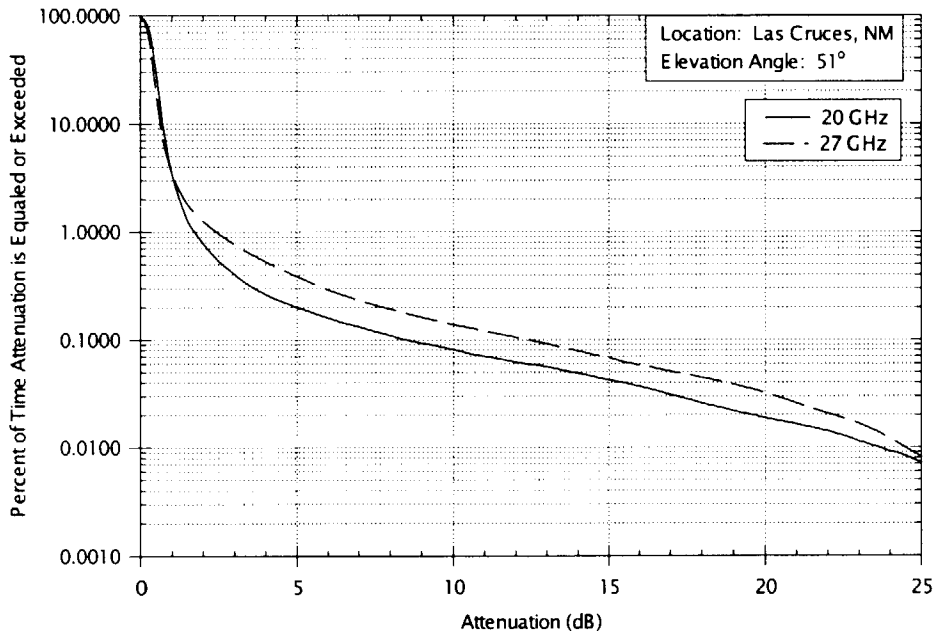

From *.pv2 files

1-150

ACS
Stanford Telecom

Three Year Fall AFS Statistics

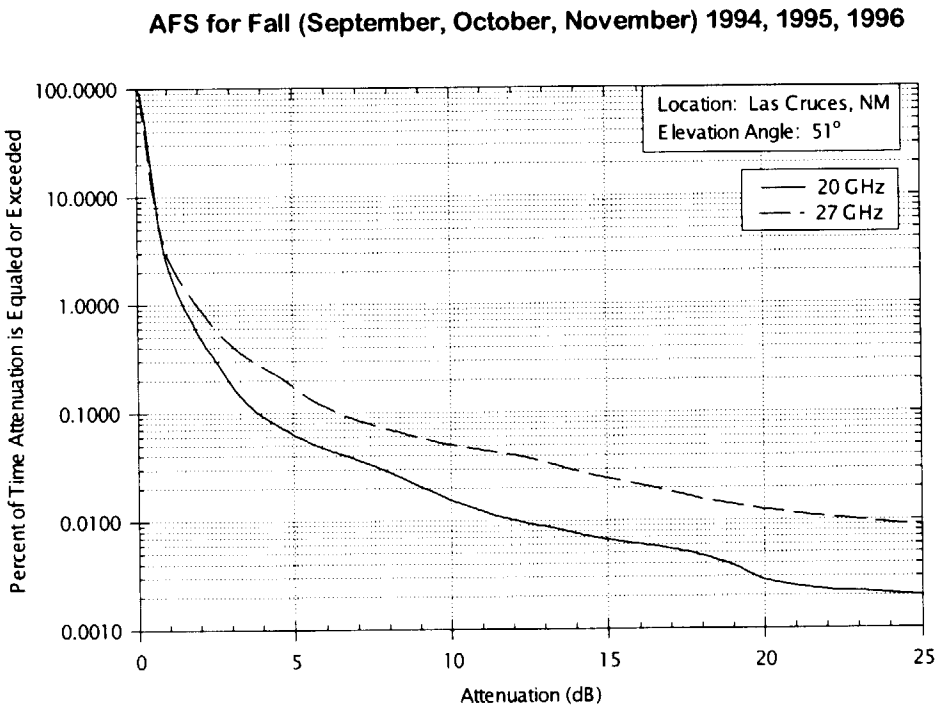

From *.pv2 files

1-151

ACS
Stanford Telecom

Actual Worst Month: July 1996 Attenuation wrt Free Space (AFS)

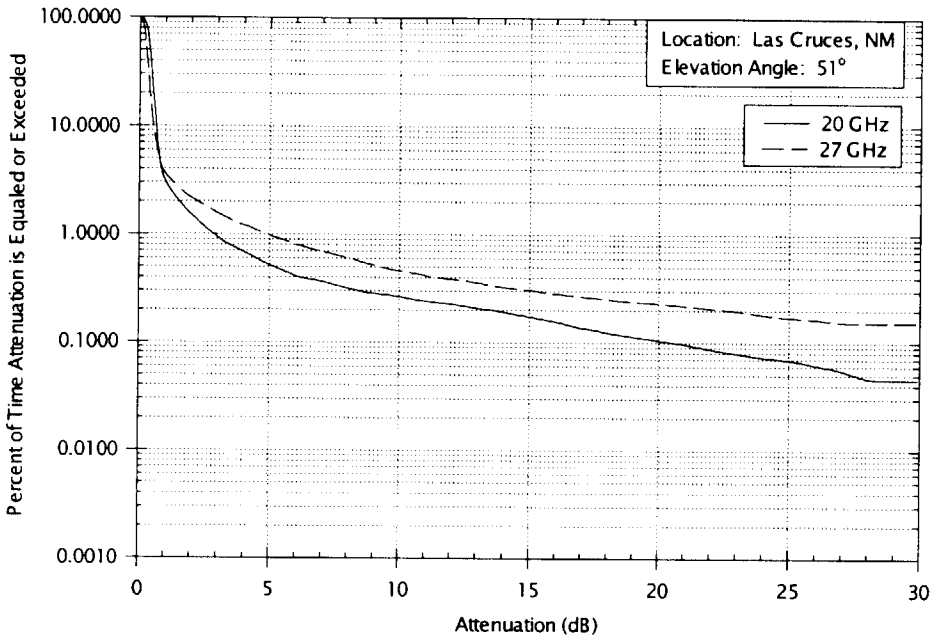

From *.pv2 files

1-152

ACS
Stanford Telecom

New Mexico ACTS Statistics Summary

- **Comparison of pv0 and pv2 processing for 36 months have minor differences (< 1 dB) in attenuation distributions**
- **Measured link performance for three year period (*.pv2)**

Annual Link Availability (%)	20 GHz (dB)	27.5 GHz (dB)
99	1.6	1.8
99.5	2.1	2.8
99.9	5.4	8.1
99.95	8.3	13.1
99.99	20.8	> 25

New Mexico ACTS Statistics Summary (Cont.)

- **According to the National Climatic Data Center**
  - ➢ Above average temperature
  - ➢ Average humidity
  - ➢ Slightly below average precipitation
- **Rain attenuation model prediction comparisons**
  - ➢ Best model prediction dependent on desired availability
    - ✦ For availabilities <99.9%, USA model is best comparison
    - ✦ For availabilites >99.9%, ITU-R model is best comparison
  - ➢ Implementing local rain statistics did improved Crane, but did not improve ITU predictions
- **Attenuation ratio predicted well by models until 10 dB**
- **Worst actual month (in three years): July 1996**

ACS
Stanford Telecom

Stel Future ACTS Activities

- Complete 4 year cumulative distributions from *.pv0 preprocessing
- Complete 4 year cumulative distributions from *.pv2 preprocessing
- Contract renewal to complete fourth and fifth year statistics

1-155/156

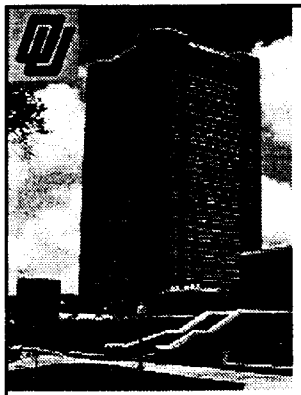

ACTS Propagation Studies in Oklahoma

Xuhe Wang
Deepak Ramachadran
Paul Robinson
Robert K. Crane

School of Meteorology, University of Oklahoma

NAPEX XXI
El Segundo, CA
June 12-13, 1997

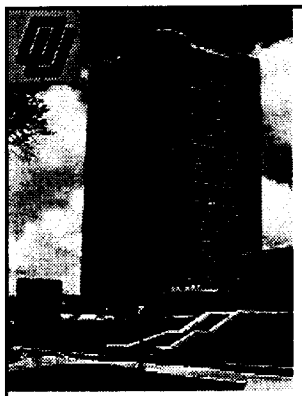

Outline

- OK APT Status and Data Preprocessing
- Scintillation Studies
- Wet Antenna Studies
- OK ACTS Home Page
- Data Summary of All Sites

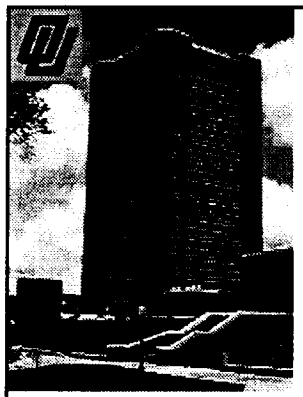

OK APT Status and Data Preprocessing

- OK APT has been operating normally since we replaced the 20 GHz LNA and the cracked feedhorn on July 19, 1996.
- First three years data have been preprocessed and sent to ACTS Data Center.
- Calibration constants are being adjusted for the first four month data of 1997 .

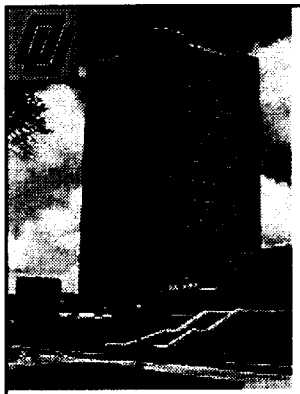

Scintillation Studies Using ACTS 20Hz Sampling Data

- Radiosonde data and radar wind profiler data form the sounding stations near our ACTS terminal were used to estimate the heights and transport speeds of turbulent layers.
- Actshdr3.exe is used to generate the scintillation power spectra from the ACTS 20 Hz sampling data.
- The normal ACTS 1 Hz data are also used to expand the spectra in case the turbulence fluctuation frequency is lower than 0.01 Hz.
- Variance of the logarithm of the amplitude scintillation is calculated from the spectra and compared with Tatarski's theoretical predictions and the CCIR model.

Vertical wind shear profile from radiosonde data of 8/5/96 00Z, OUN (Norman, OK)

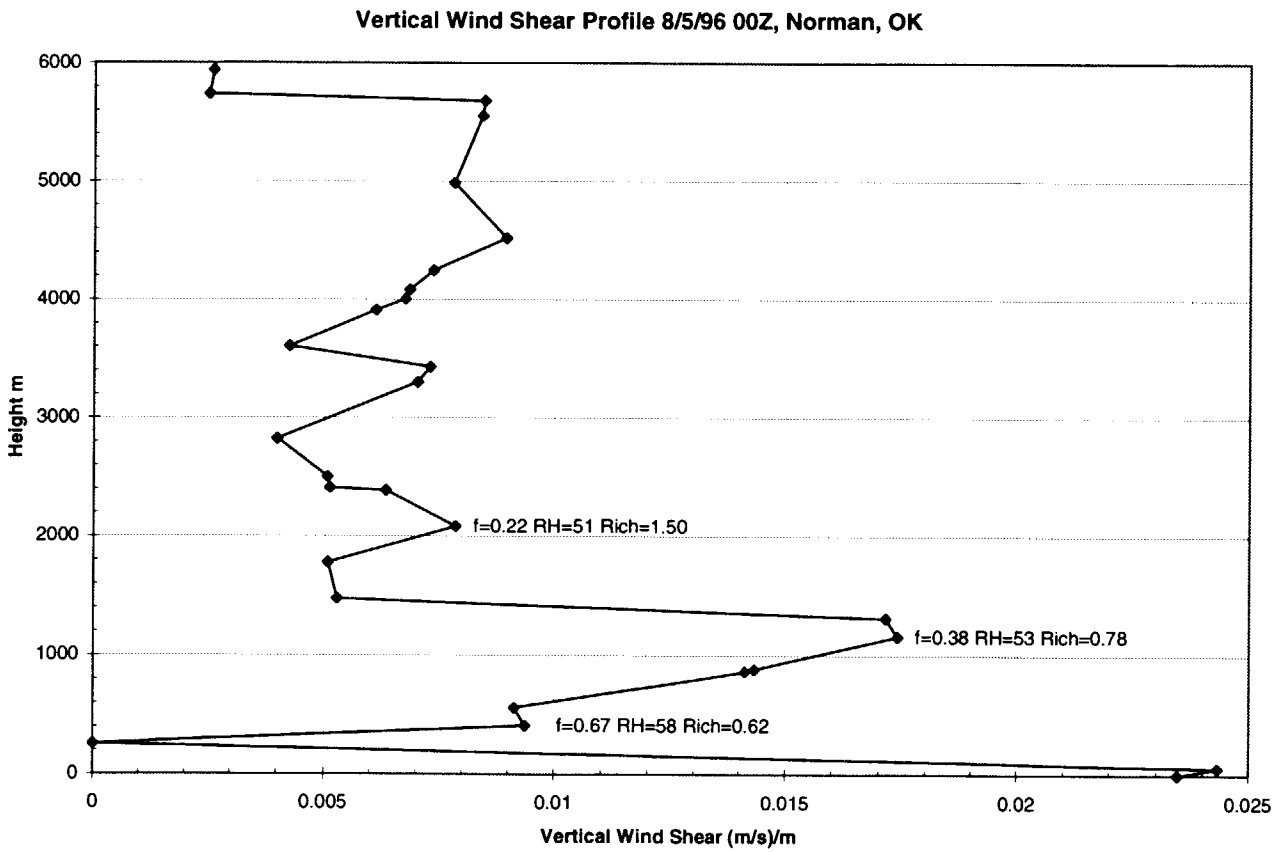

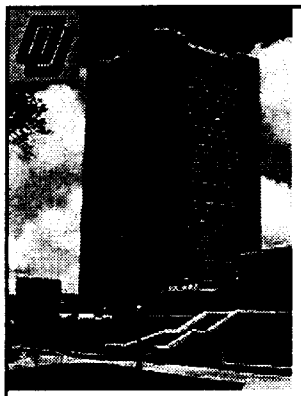

Scintillation Spectrum of 8/5/96 0:11 - 0:12
Norman, OK

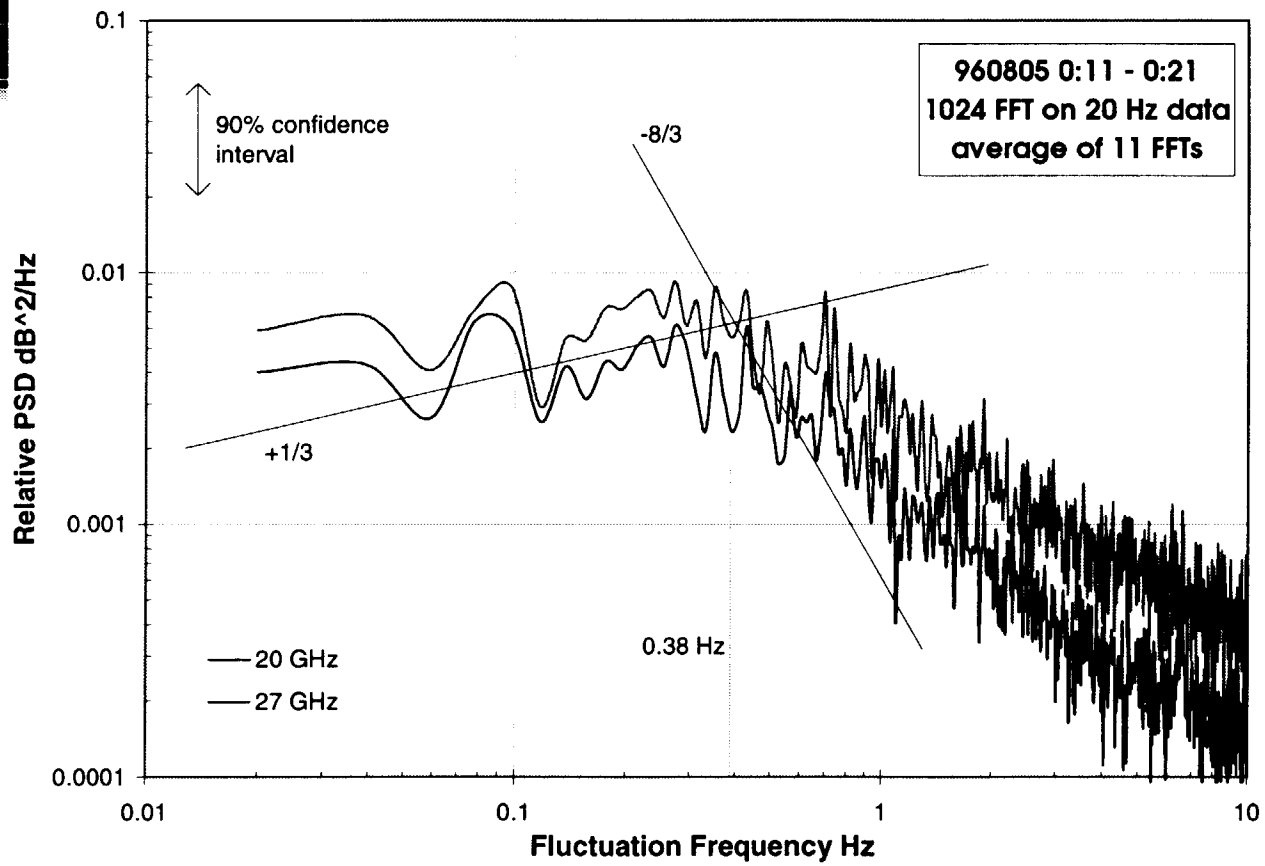

Radar Wind Profile of 5/12/97, Purcell, OK

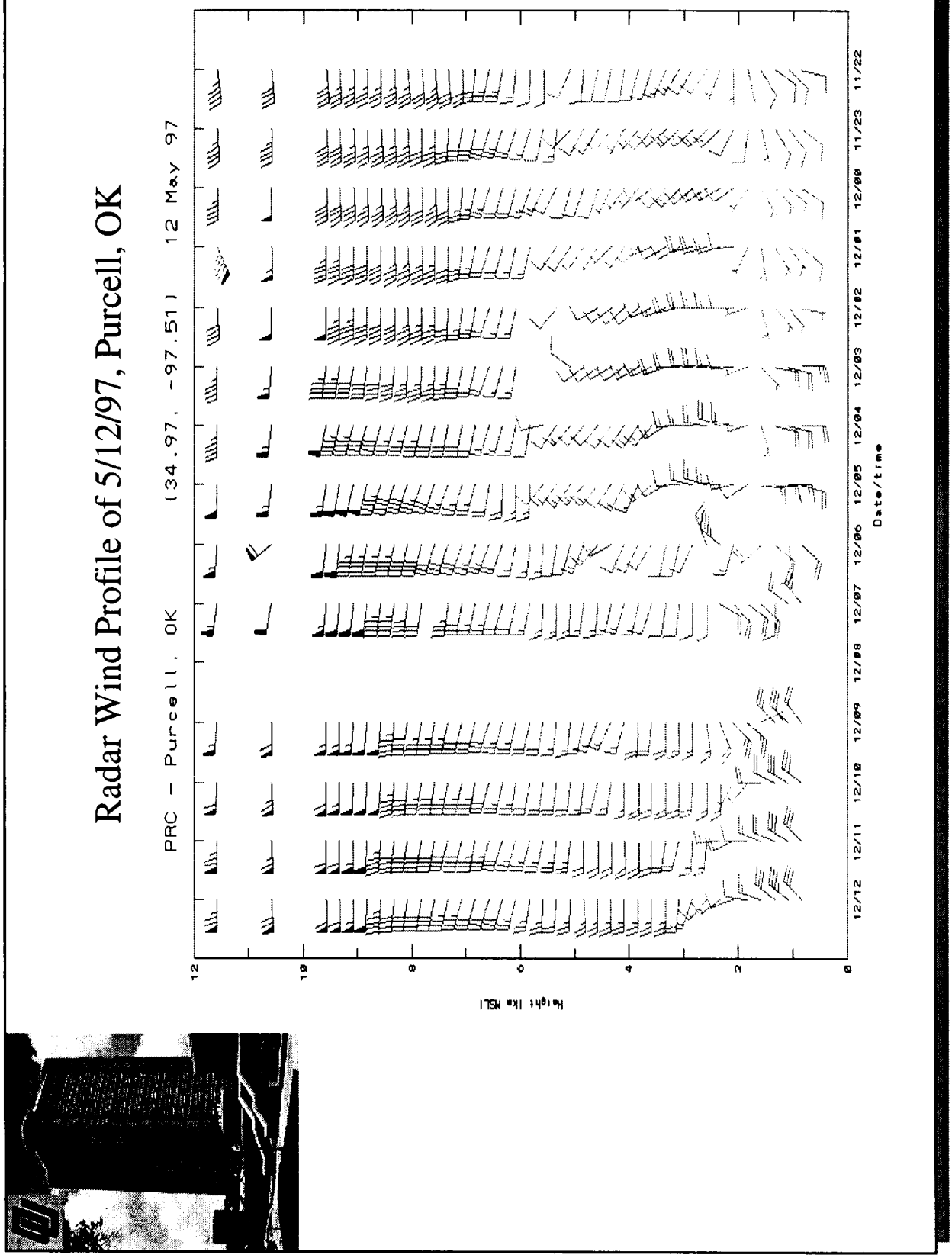

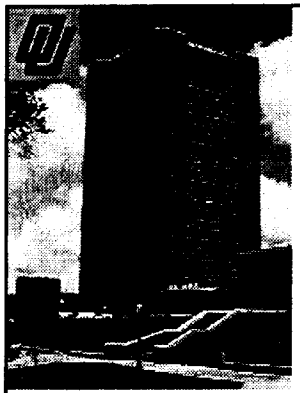

Power Spectra of 5/12/97 1Z - 12Z ACTS 20 Hz Data
Norman, OK

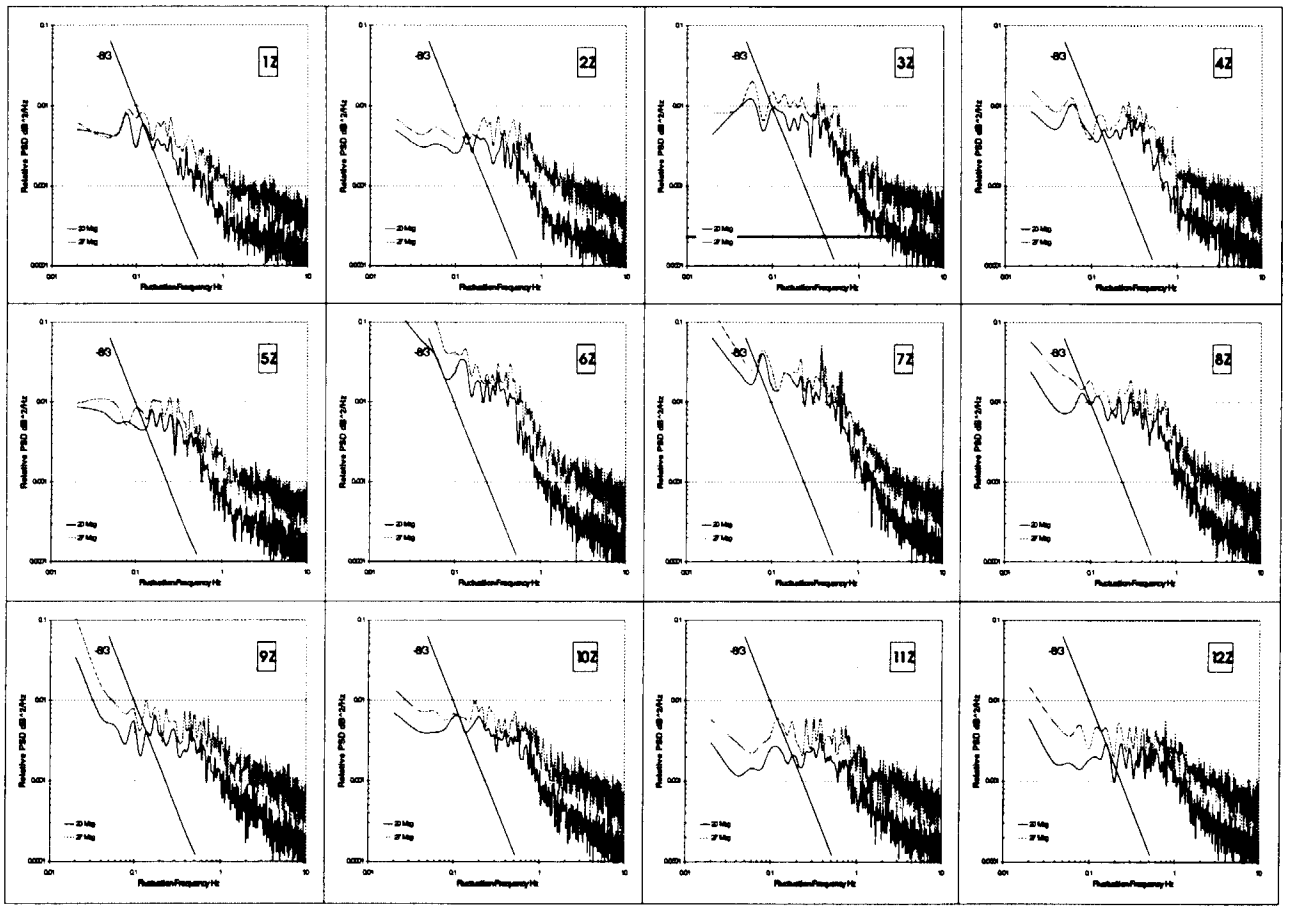

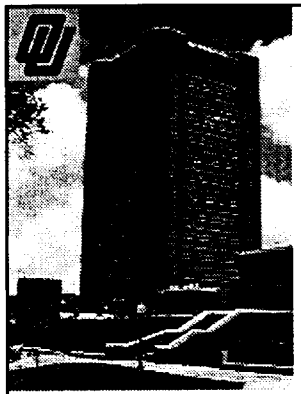

Frequency Dependence of Scintillation Variance

Comparison Scintillation Variance Measured at Two Frequences during 11 - 21 Minute at Each Hour for 960601 - 960930 Oklahoma Site

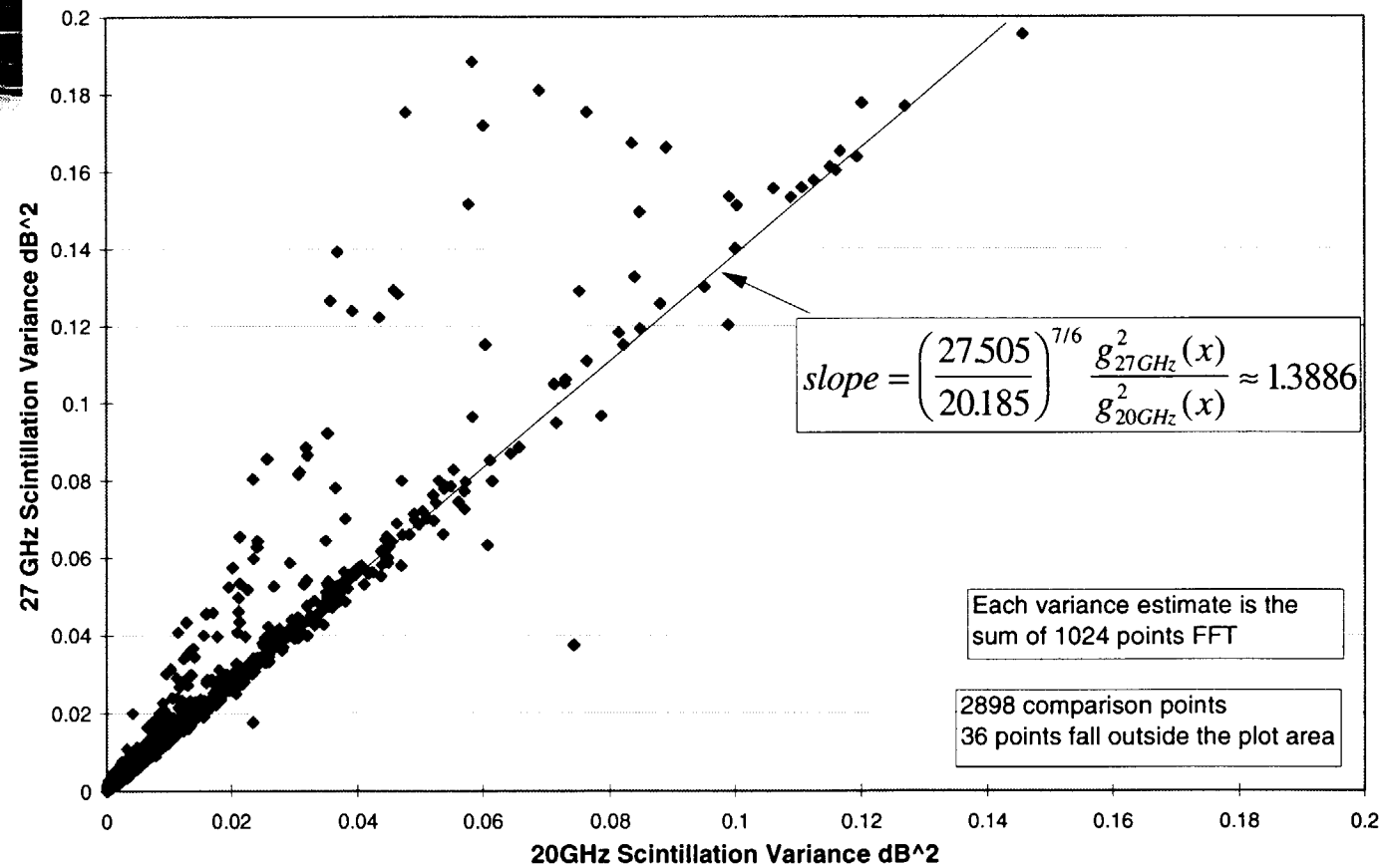

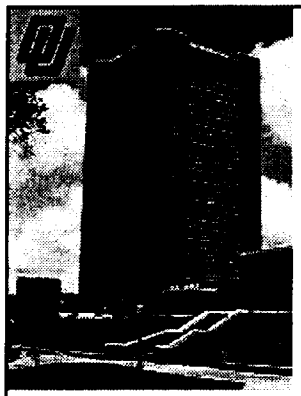

Oklahoma ACTS Home Page

- http://rossby.metr.ou.edu/~actsrain/ (created by Deepak Ramachadran)

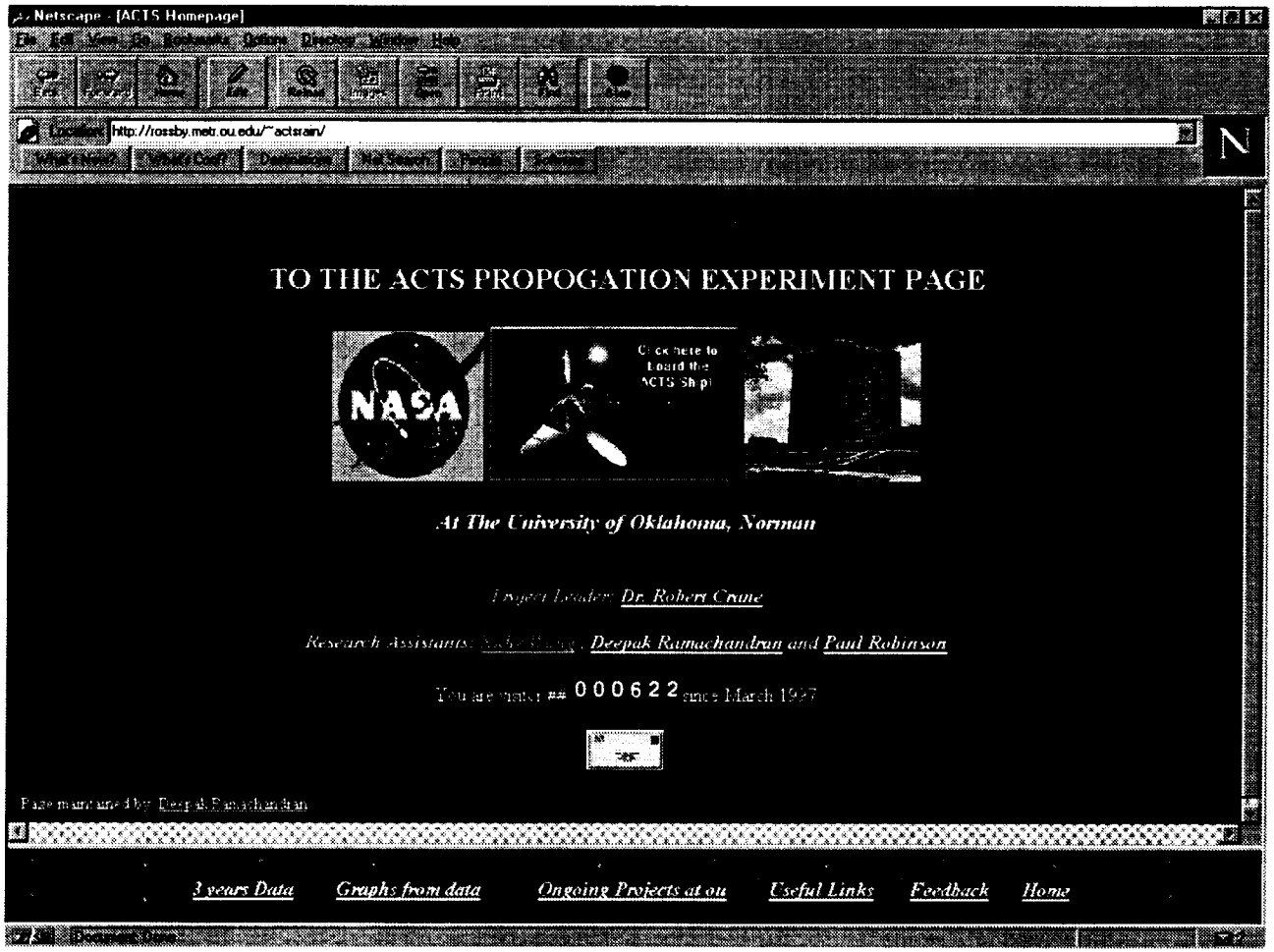

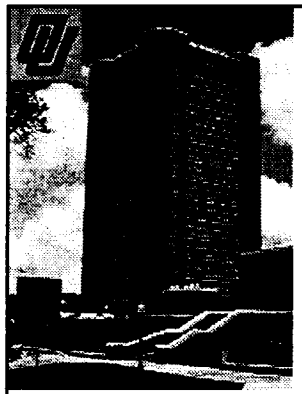

Oklahoma ACTS Home Page: Data

Netscape - [ACTS Homepage]

3 years Data for the 7 stations

Note: *These files are in MS Excel format. You need to have the application MS Excel. Also on your browser (Netscape for example), you need to choose* ***Options*** *from the menubar, then choose* ***General Preferences*** *and finally choose* ***Helpers*** *and scroll down to* ***Application/msexcel*** *and set the action to* ***Excel****(You can browse to the location of this application on your machine).*

ACTS	ALASKA	BRITISH COLUMBIA	COLORADO	FLORIDA	MARYLAND	NEW MEXICO	OKLAHOMA
ATTENSKY	Download	Download	Download	Download	Download	Download	Download
ATTENMIN	Download	Download	Download	Download	Download	Download	Download
ATTENSEC	Download	Download	Download	Download	Download	Download	Download
FADEDUR	Download	Download	Download	Download	Download	Download	Download
IFADEDUR	Download	Download	Download	Download	Download	Download	Download
RAINRATE	Download	Download	Download	Download	Download	Download	Download
STDEV	Download	Download	Download	Download	Download	Download	Download

3 years Data | Graphs from data | Ongoing Projects at ou | Useful Links | Feedback | Home

Document: Done

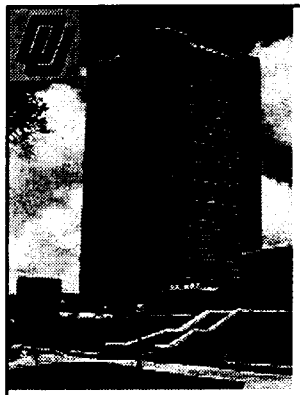

Oklahoma ACTS Home Page: Data

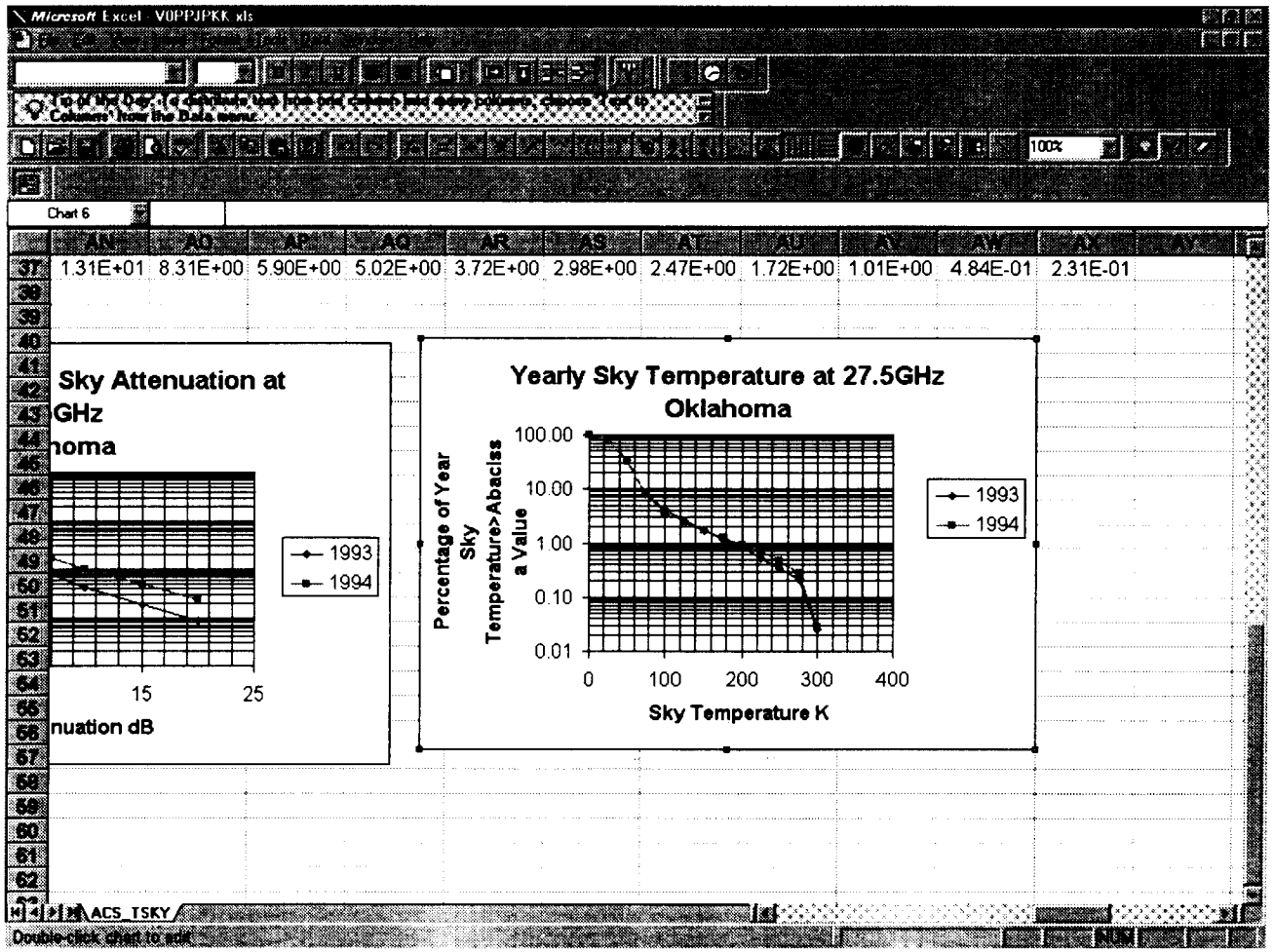

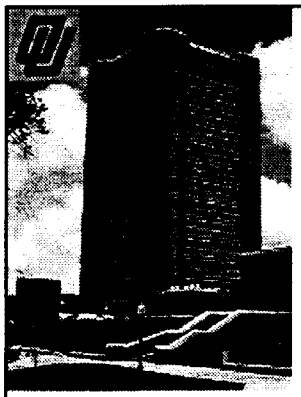

Oklahoma ACTS Home Page: Graphs

Netscape - [ACTS Homepage]

File Edit View Go Bookmarks Options Directory Window Help

Back Forward Home Edit Reload Images Open Print Find Stop

Location: http://www.okstate.edu/OSU_Proper/acts.html

What's New? What's Cool? Destinations Net Search People Software

GRAPHS from the 3 years data

Useful especially if you could not see the data itself in Excel format!

ACTS	ATTENSKY	ATTENMIN	ATTENSEC	FADEDUR	IFADEDUR	RAINRATE	STDEV
ALASKA	Click Here	Click Here	Click Here	Click Here	Click Here	Click Here	Click Here
BRITISH COLUMBIA	Click Here	Click Here	Click Here	Click Here	Click Here	Click Here	Click Here
COLORADO	Click Here	Click Here	Click Here	Click Here	Click Here	Click Here	Click Here
FLORIDA	Click Here	Click Here	Click Here	Click Here	Click Here	Click Here	Click Here
MARY LAND	Click Here	Click Here	Click Here	Click Here	Click Here	Click Here	Click Here
NEW MEXICO	Click Here	Click Here	Click Here	Click Here	Click Here	Click Here	Click Here
OKLAHOMA	Click Here	Click Here	Click Here	Click Here	Click Here	Click Here	Click Here

3 years Data | Graphs from data | Ongoing Projects at ou | Useful Links | Feedback | Home

Document Done

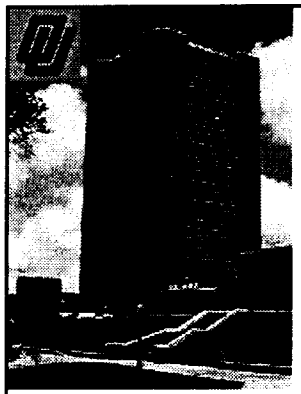

Oklahoma ACTS Home Page: Graphs

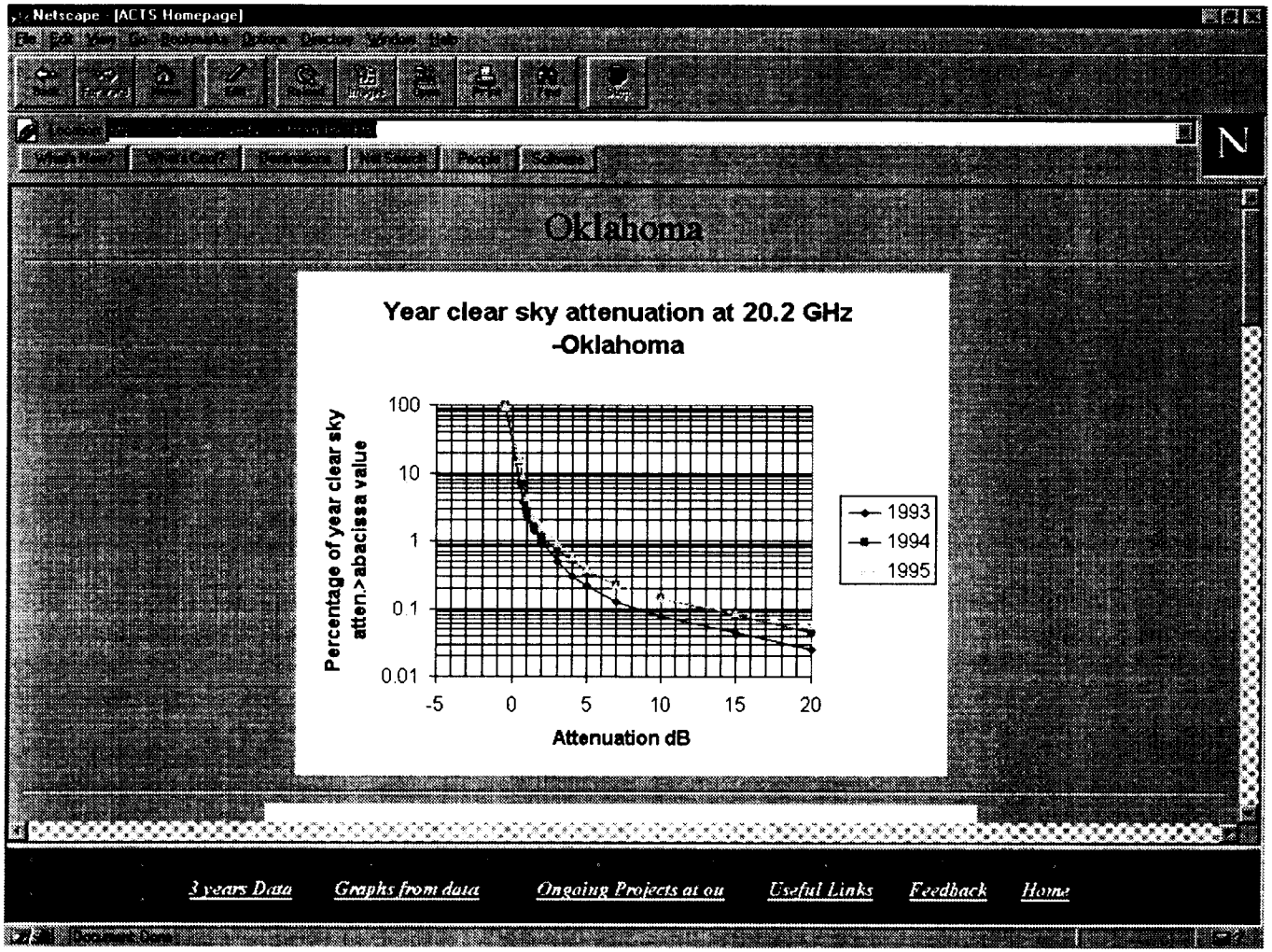

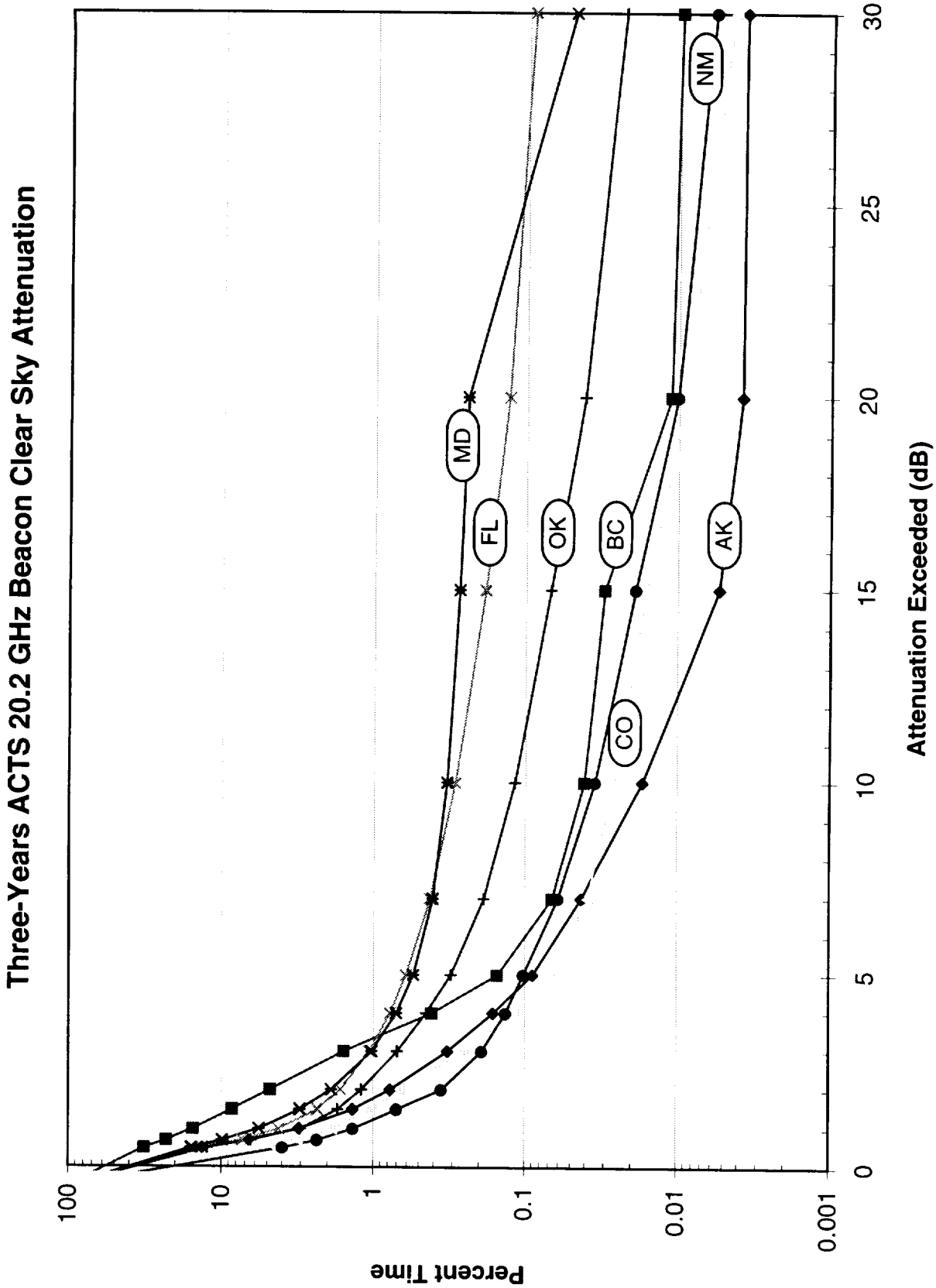
Three-Years ACTS 20.2 GHz Beacon Clear Sky Attenuation
Percent Time
100
10
1
0.1
0.01
0.001
0
5
10
15
20
25
30
Attenuation Exceeded (dB)
MD
FL
OK
BC
CO
AK
NM

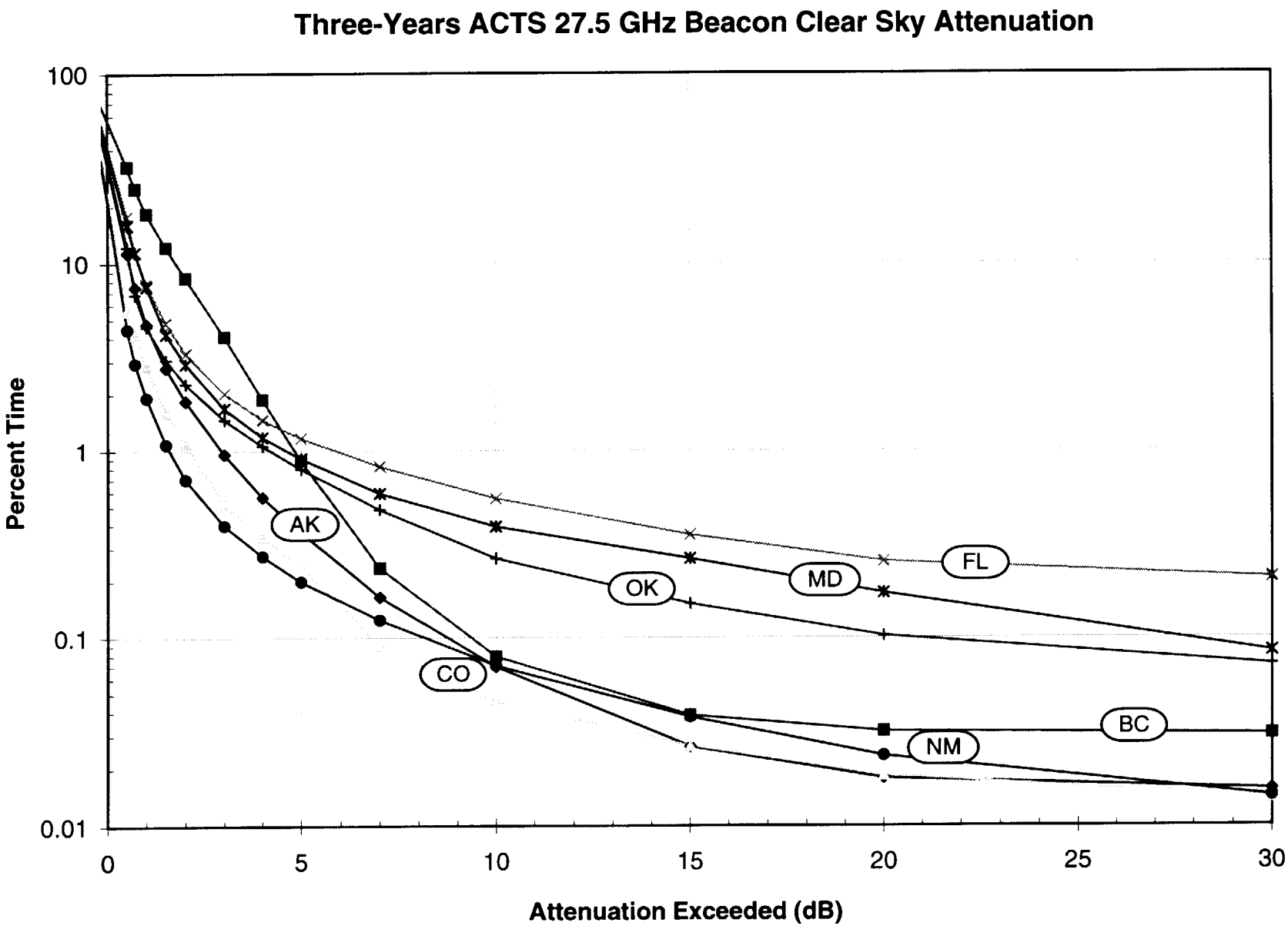
Three-Years ACTS 27.5 GHz Beacon Clear Sky Attenuation
Percent Time
100
10
1
0.1
0.01
0
5
10
15
20
25
30
Attenuation Exceeded (dB)
AK
CO
OK
MD
FL
BC
NM

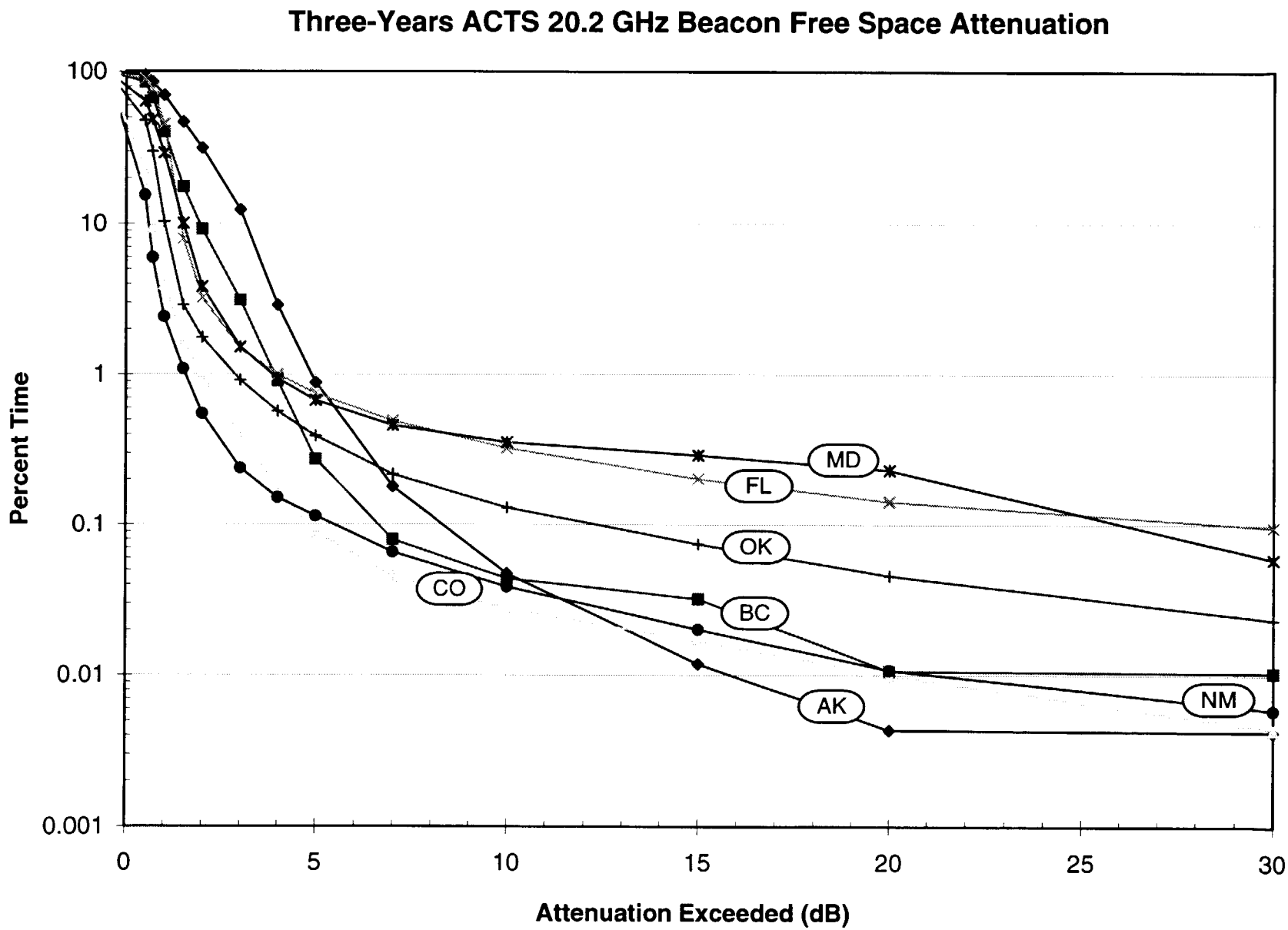
Three-Years ACTS 20.2 GHz Beacon Free Space Attenuation
Percent Time
100
10
1
0.1
0.01
0.001
0
5
10
15
20
25
30
Attenuation Exceeded (dB)
MD
FL
OK
CO
BC
AK
NM

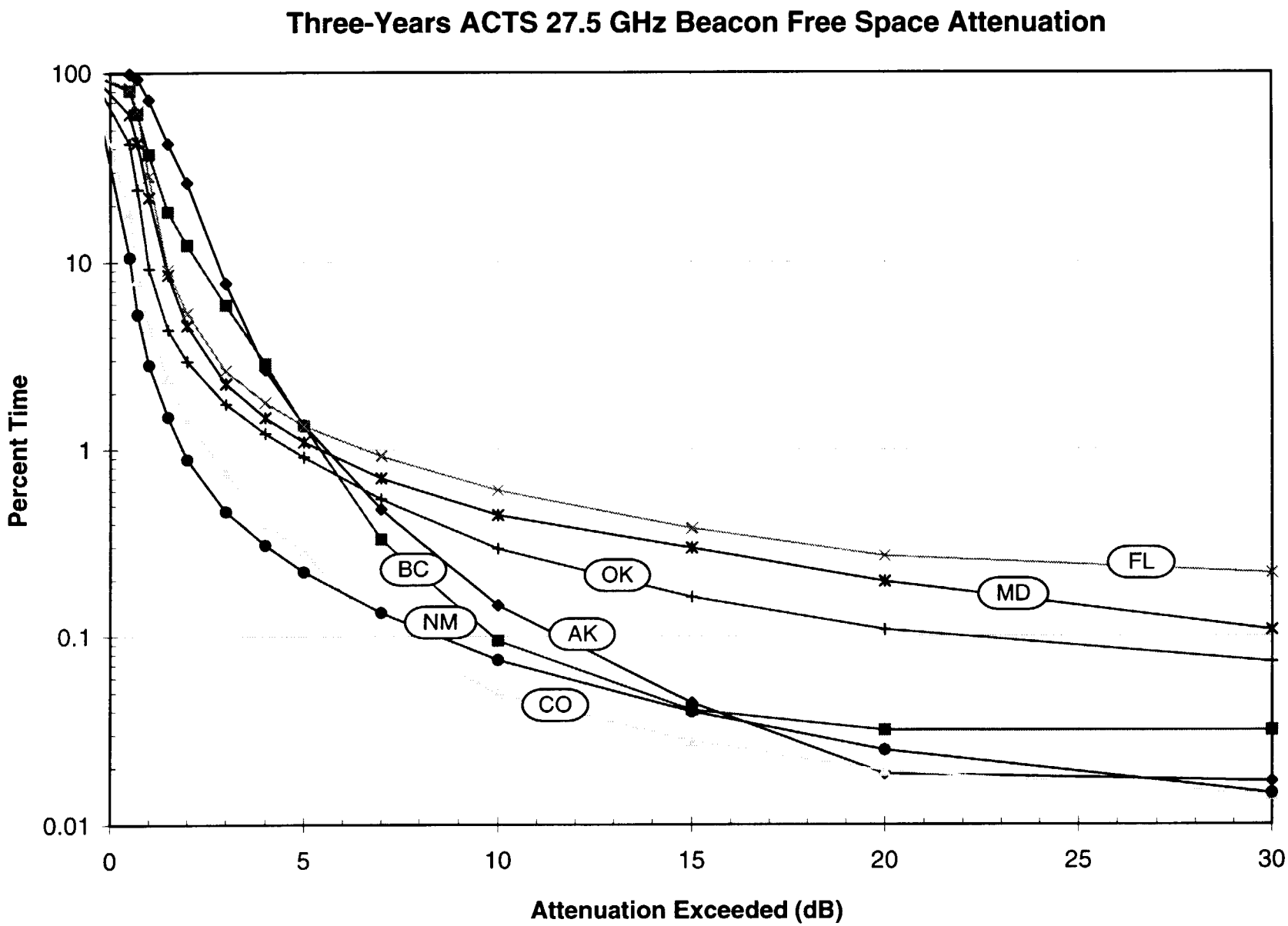
Three-Years ACTS 27.5 GHz Beacon Free Space Attenuation
Percent Time
100
10
1
0.1
0.01
0
5
10
15
20
25
30
Attenuation Exceeded (dB)
BC
NM
CO
AK
OK
MD
FL

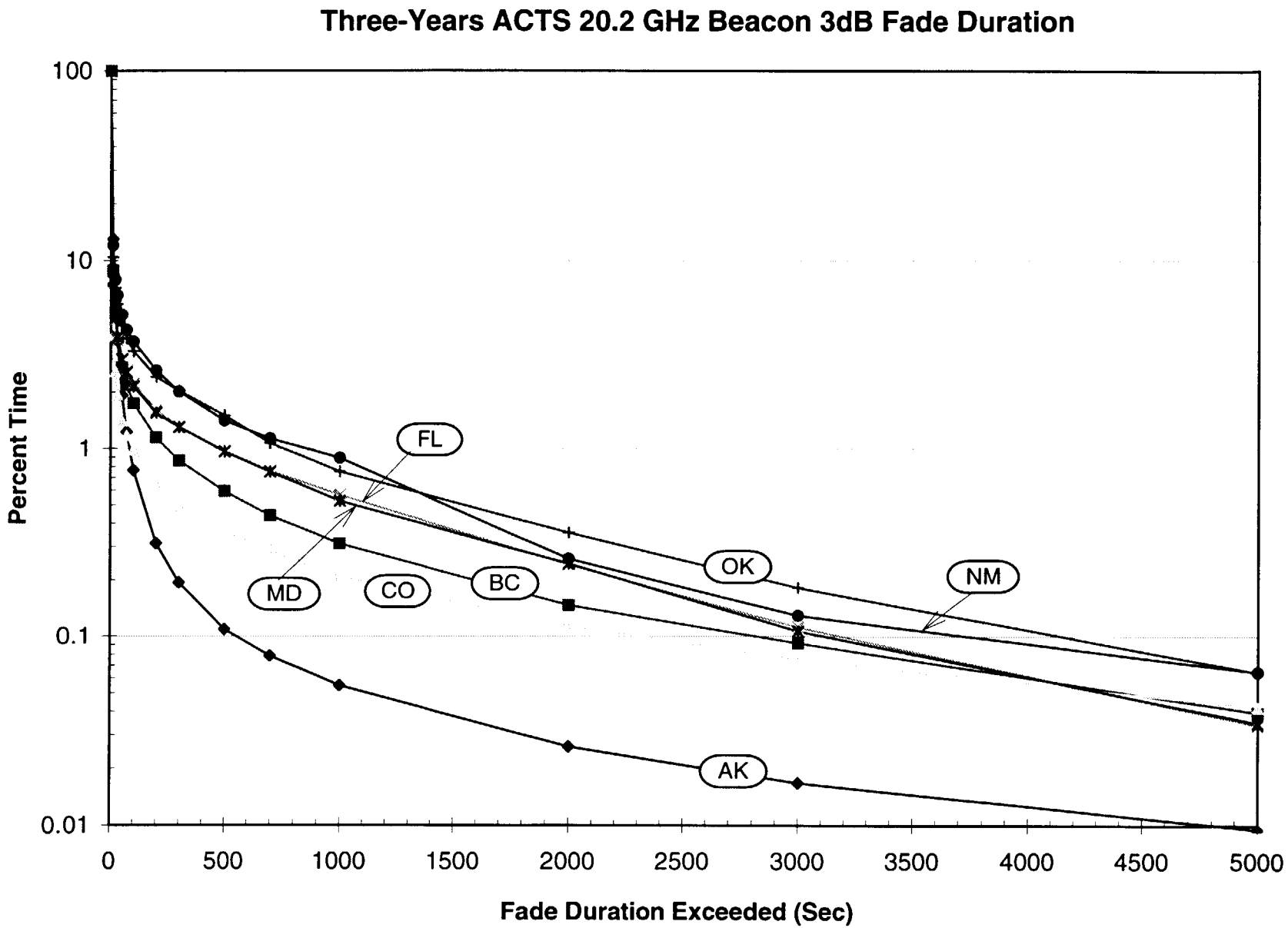
Three-Years ACTS 20.2 GHz Beacon 3dB Fade Duration
Percent Time
100
10
1
0.1
0.01
0
500
1000
1500
2000
2500
3000
3500
4000
4500
5000
Fade Duration Exceeded (Sec)
FL
OK
NM
MD
CO
BC
AK

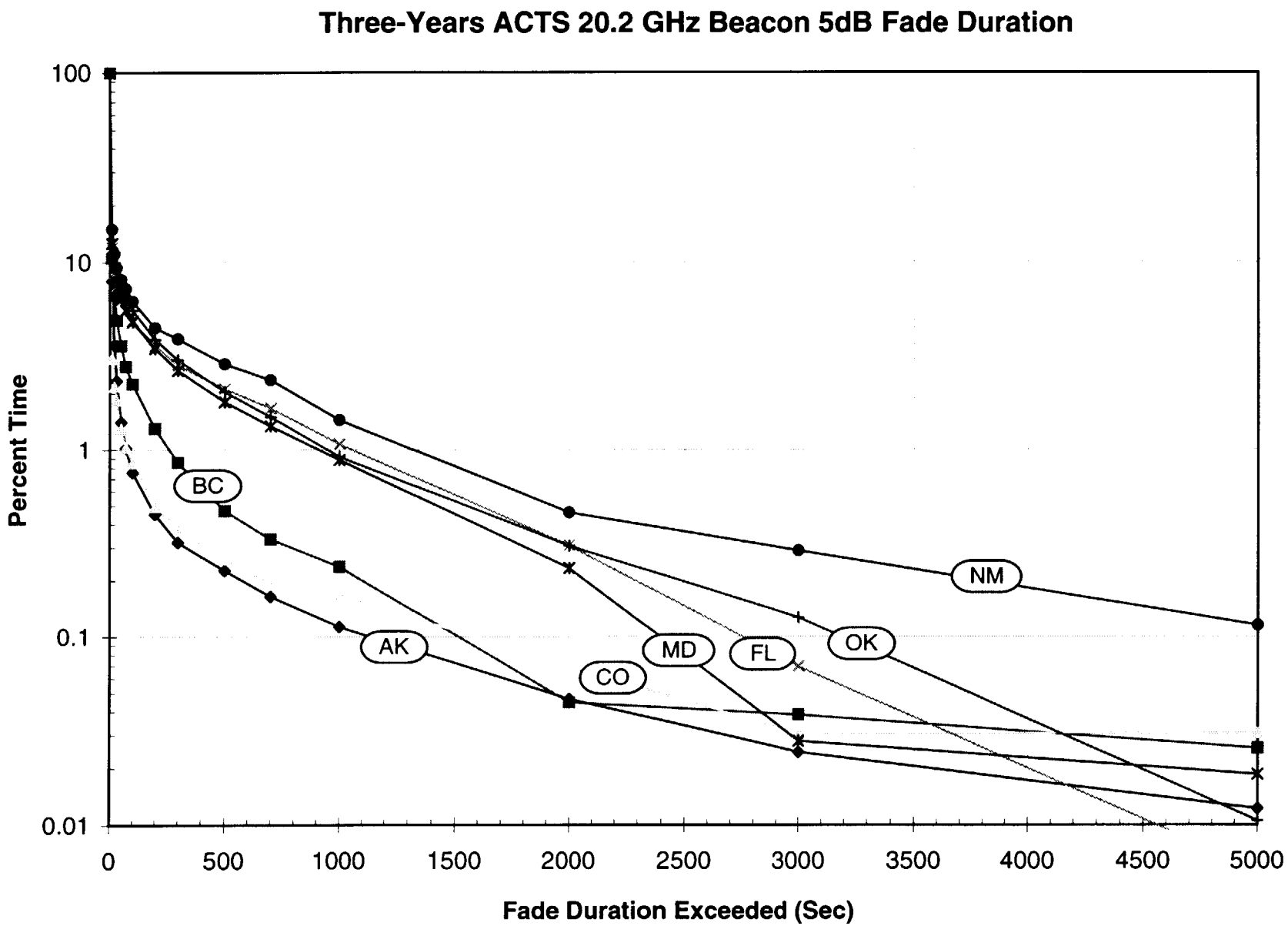
Three-Years ACTS 20.2 GHz Beacon 5dB Fade Duration
Percent Time
100
10
1
0.1
0.01
0
500
1000
1500
2000
2500
3000
3500
4000
4500
5000
Fade Duration Exceeded (Sec)
BC
AK
CO
MD
FL
OK
NM

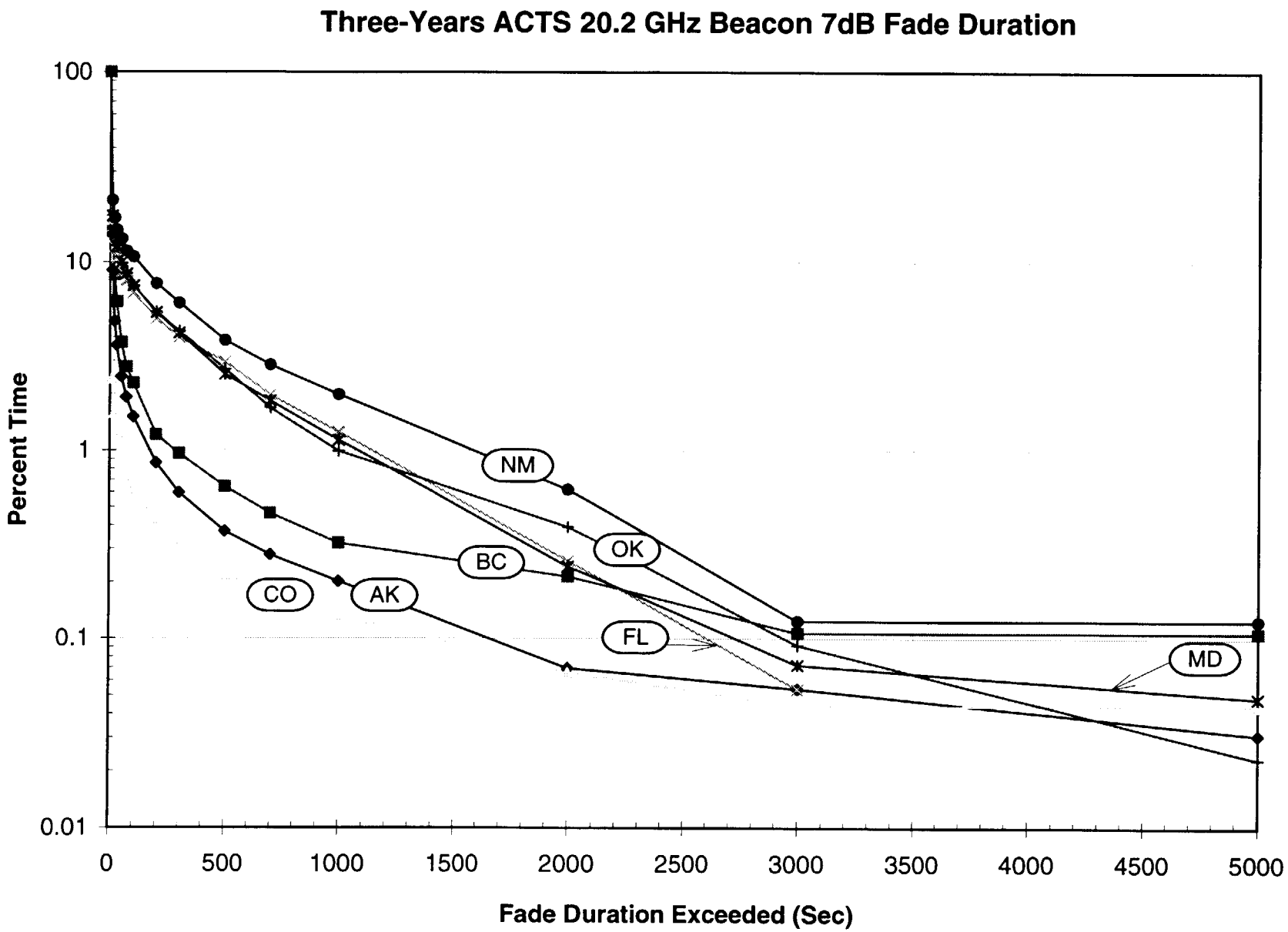
Three-Years ACTS 20.2 GHz Beacon 7dB Fade Duration
Percent Time
100
10
1
0.1
0.01
0
500
1000
1500
2000
2500
3000
3500
4000
4500
5000
Fade Duration Exceeded (Sec)
NM
OK
BC
CO
AK
FL
MD

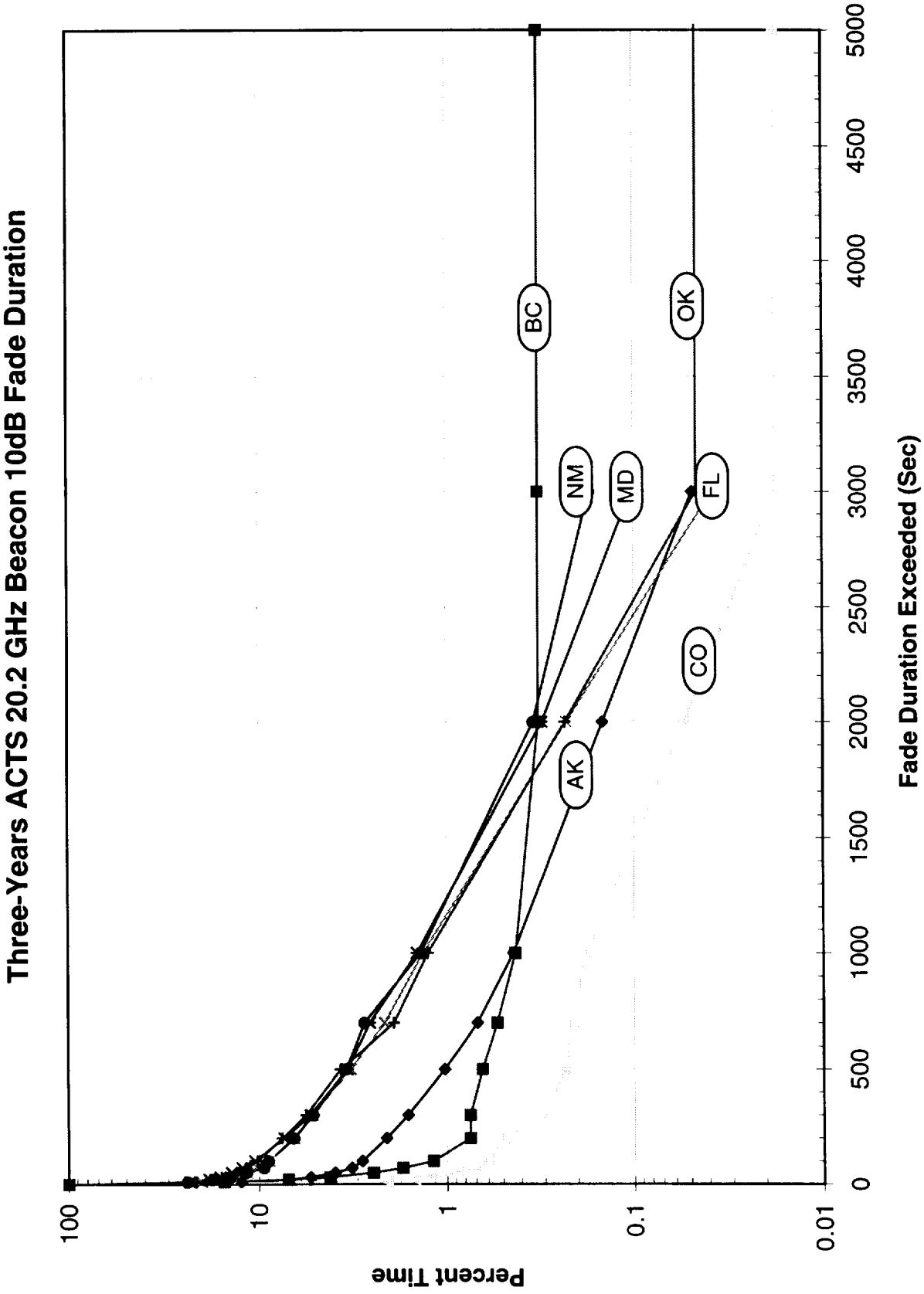
Three-Years ACTS 20.2 GHz Beacon 10dB Fade Duration
Percent Time
100
10
1
0.1
0.01
Fade Duration Exceeded (Sec)
0
500
1000
1500
2000
2500
3000
3500
4000
4500
5000
BC
NM
MD
OK
FL
CO
AK

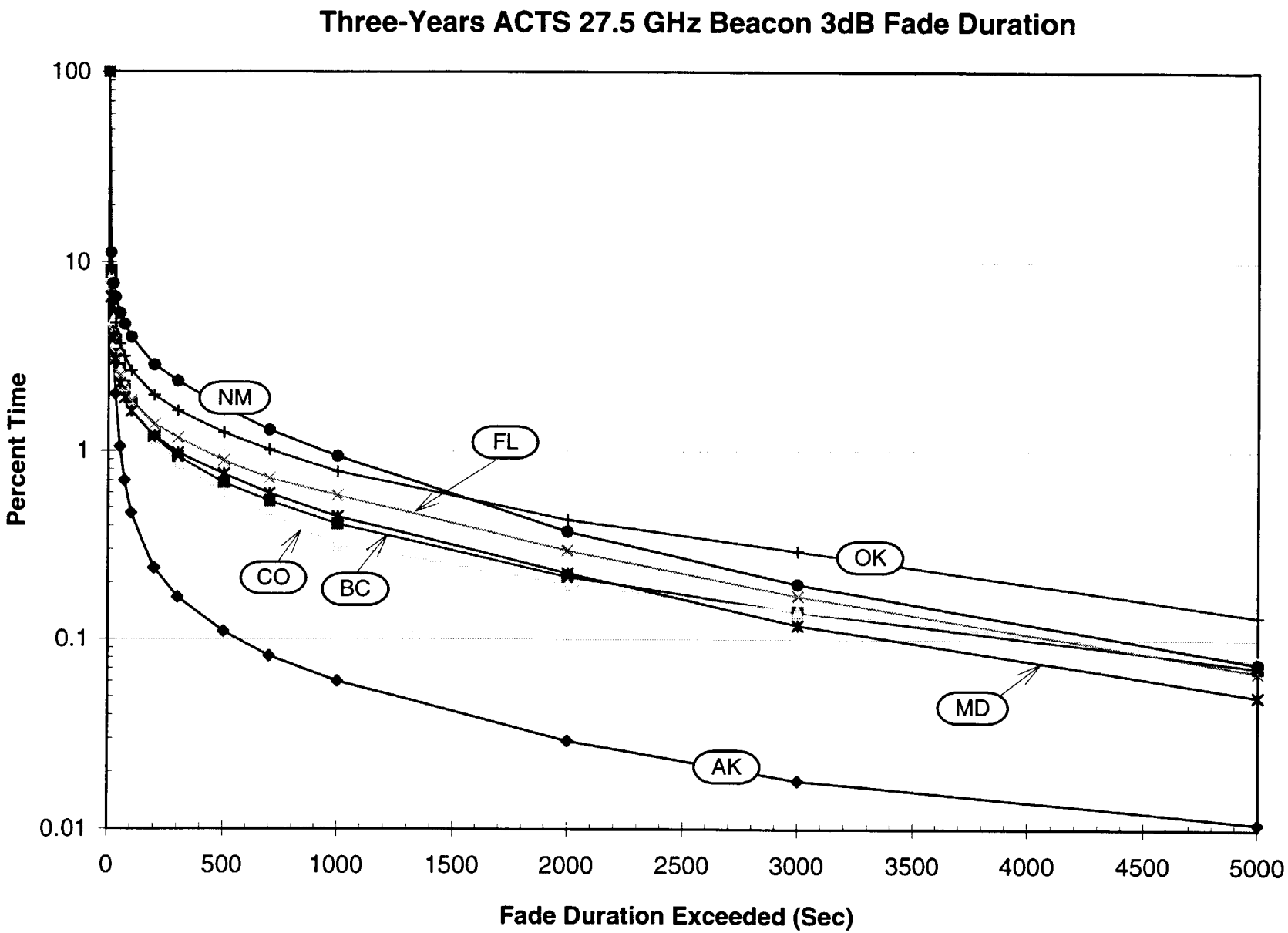
Three-Years ACTS 27.5 GHz Beacon 3dB Fade Duration
Percent Time
100
10
1
0.1
0.01
0
500
1000
1500
2000
2500
3000
3500
4000
4500
5000
Fade Duration Exceeded (Sec)
NM
FL
CO
BC
OK
MD
AK

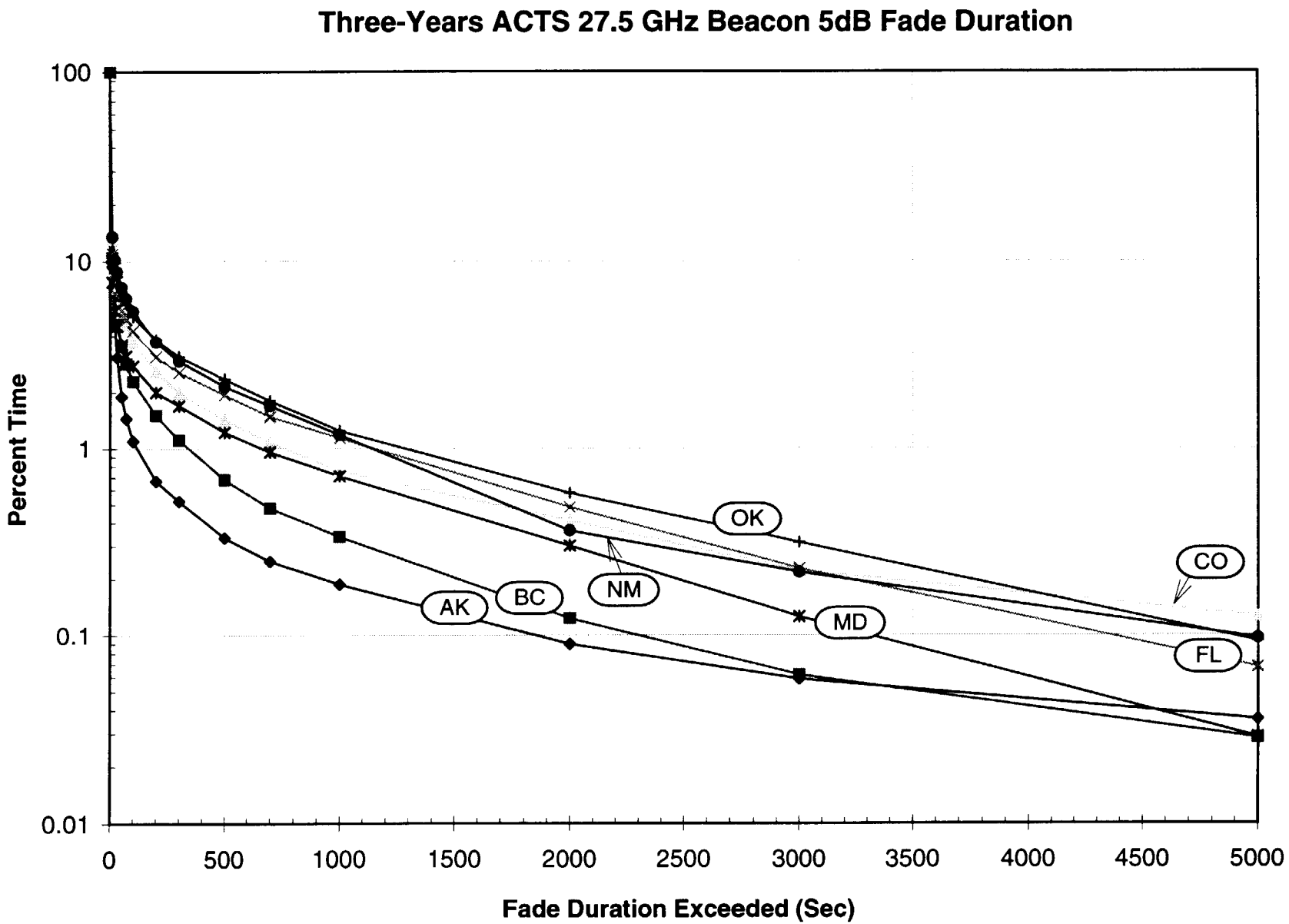
Three-Years ACTS 27.5 GHz Beacon 5dB Fade Duration
100
10
1
0.1
0.01
Percent Time
0
500
1000
1500
2000
2500
3000
3500
4000
4500
5000
Fade Duration Exceeded (Sec)
OK
CO
NM
BC
AK
MD
FL

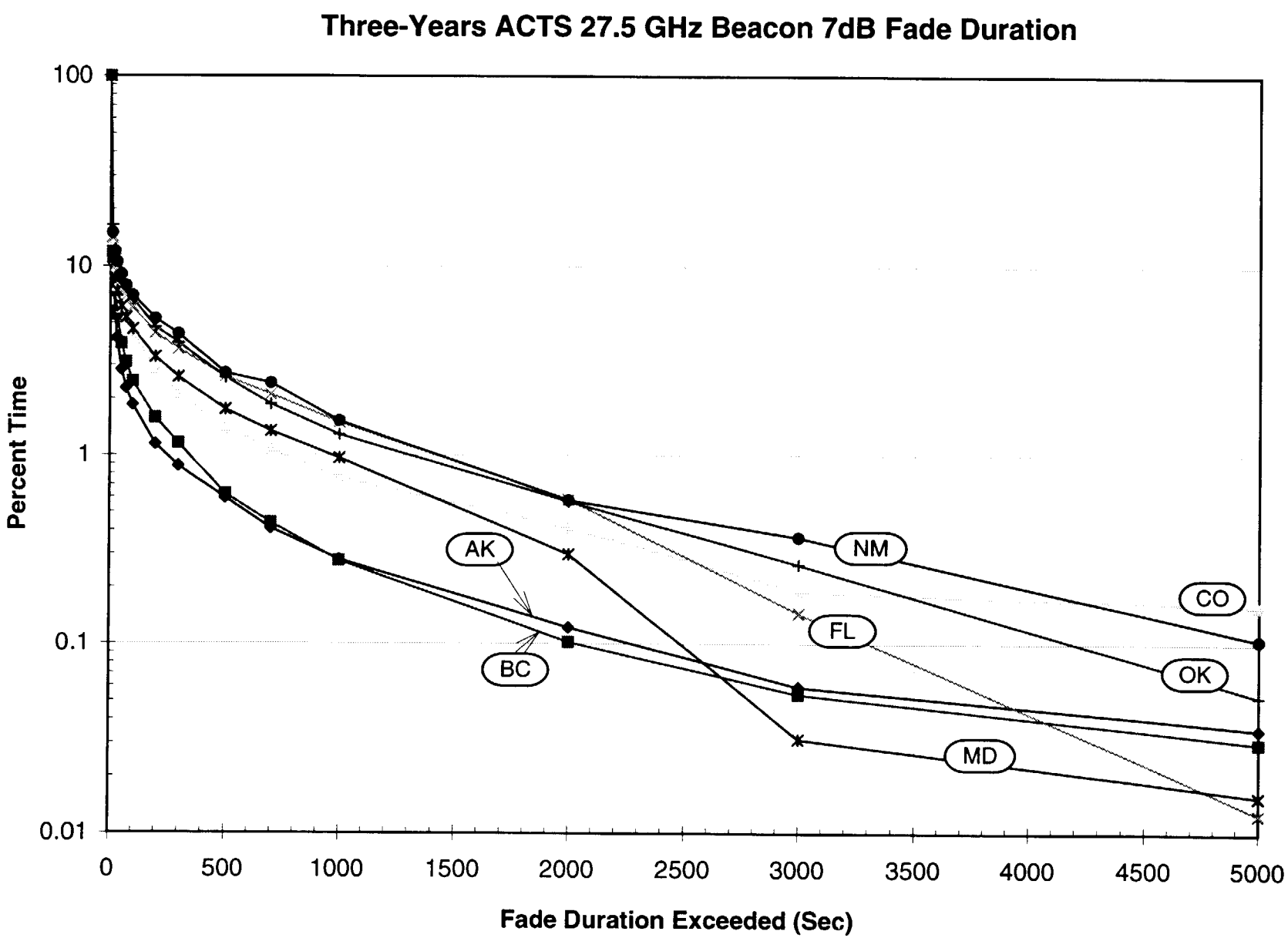
Three-Years ACTS 27.5 GHz Beacon 7dB Fade Duration
Percent Time
100
10
1
0.1
0.01
0
500
1000
1500
2000
2500
3000
3500
4000
4500
5000
Fade Duration Exceeded (Sec)
AK
BC
NM
CO
FL
OK
MD

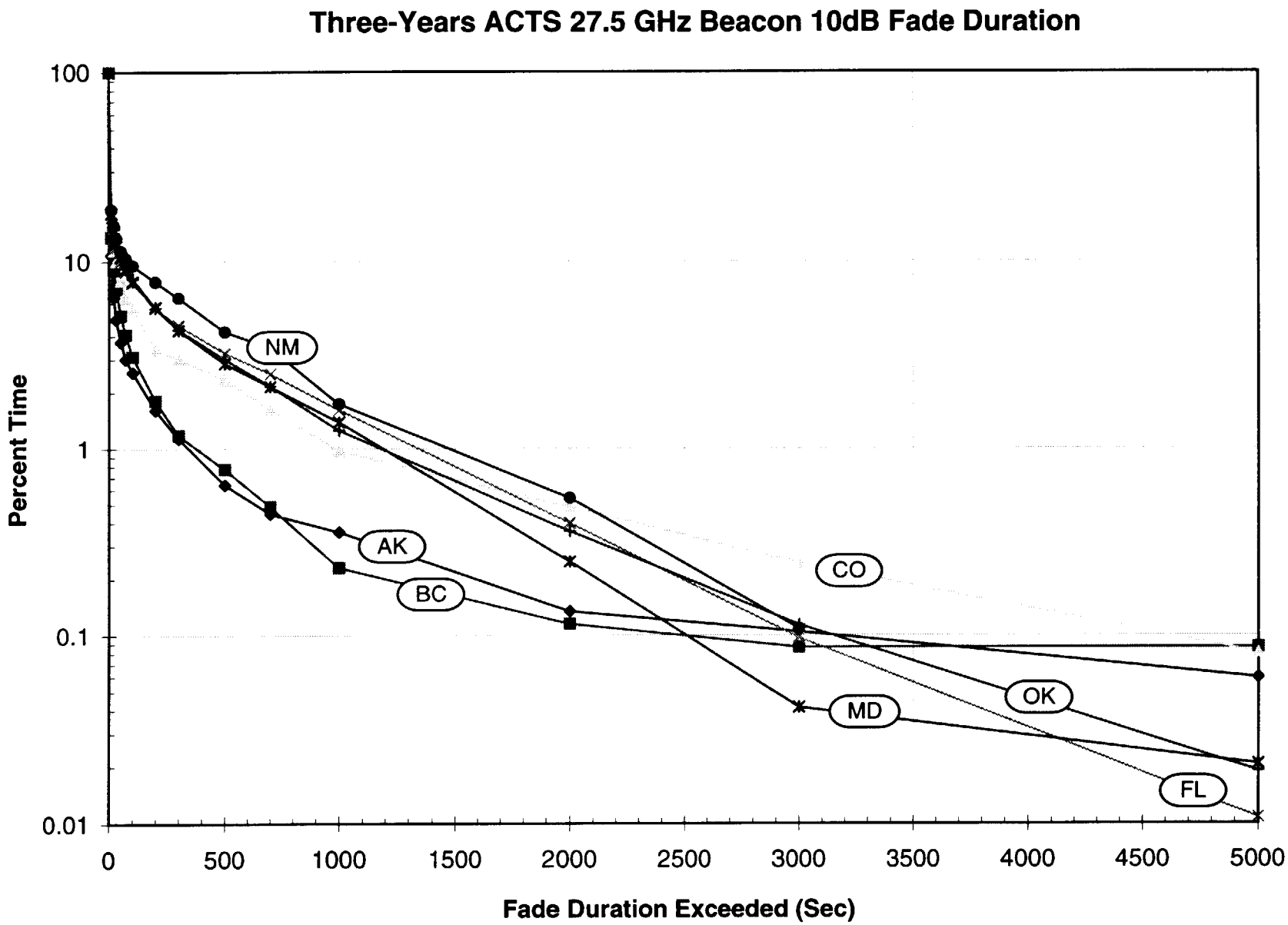
Three-Years ACTS 27.5 GHz Beacon 10dB Fade Duration
100
10
1
0.1
0.01
Percent Time
NM
AK
BC
CO
OK
MD
FL
0
500
1000
1500
2000
2500
3000
3500
4000
4500
5000
Fade Duration Exceeded (Sec)

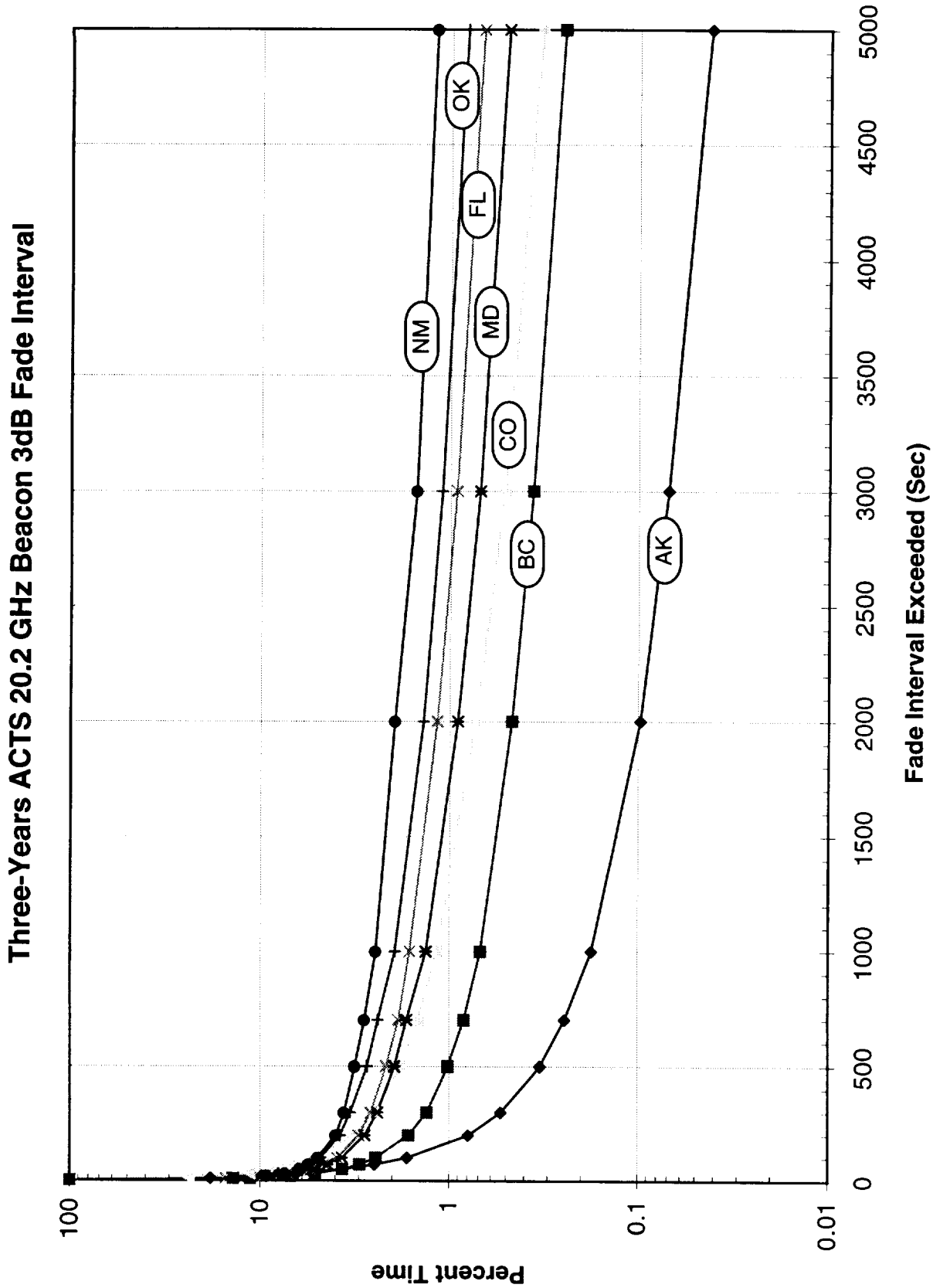
Three-Years ACTS 20.2 GHz Beacon 3dB Fade Interval
Percent Time
100
10
1
0.1
0.01
Fade Interval Exceeded (Sec)
0
500
1000
1500
2000
2500
3000
3500
4000
4500
5000
NM
OK
FL
MD
CO
BC
AK

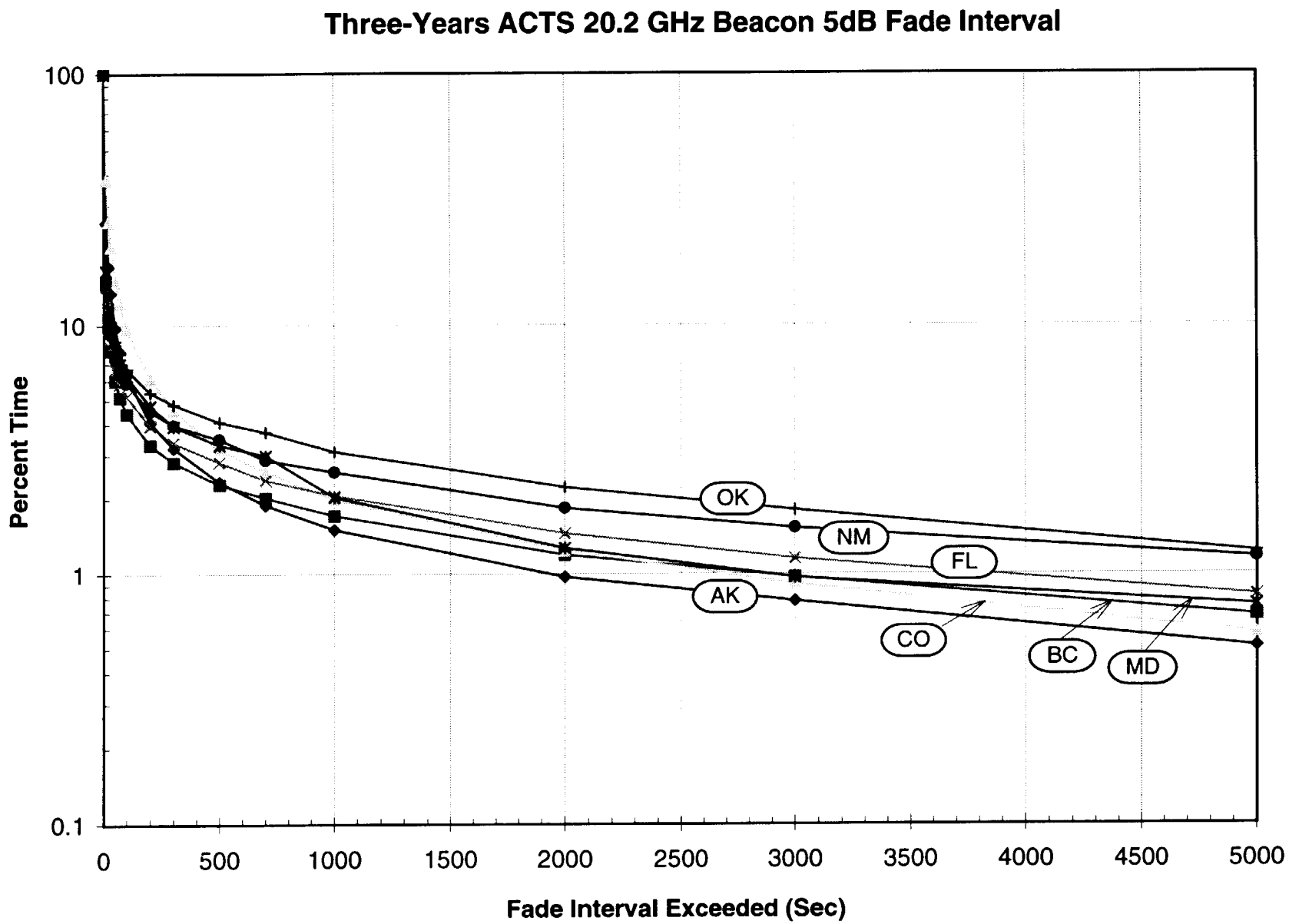
Three-Years ACTS 20.2 GHz Beacon 5dB Fade Interval
Percent Time
100
10
1
0.1
0
500
1000
1500
2000
2500
3000
3500
4000
4500
5000
Fade Interval Exceeded (Sec)
OK
NM
FL
AK
CO
BC
MD

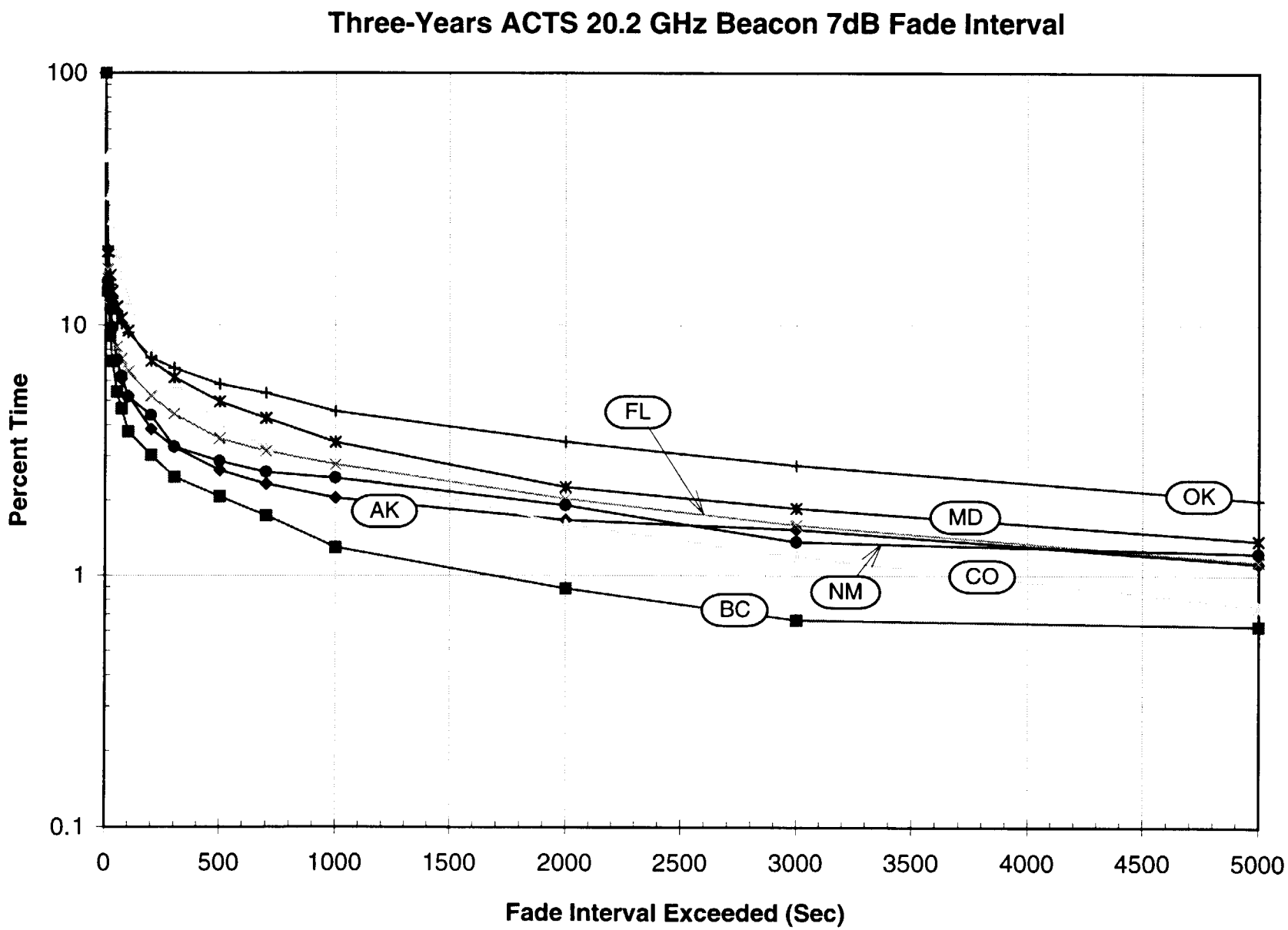
Three-Years ACTS 20.2 GHz Beacon 7dB Fade Interval
Percent Time
100
10
1
0.1
0
500
1000
1500
2000
2500
3000
3500
4000
4500
5000
Fade Interval Exceeded (Sec)
FL
AK
OK
MD
CO
NM
BC

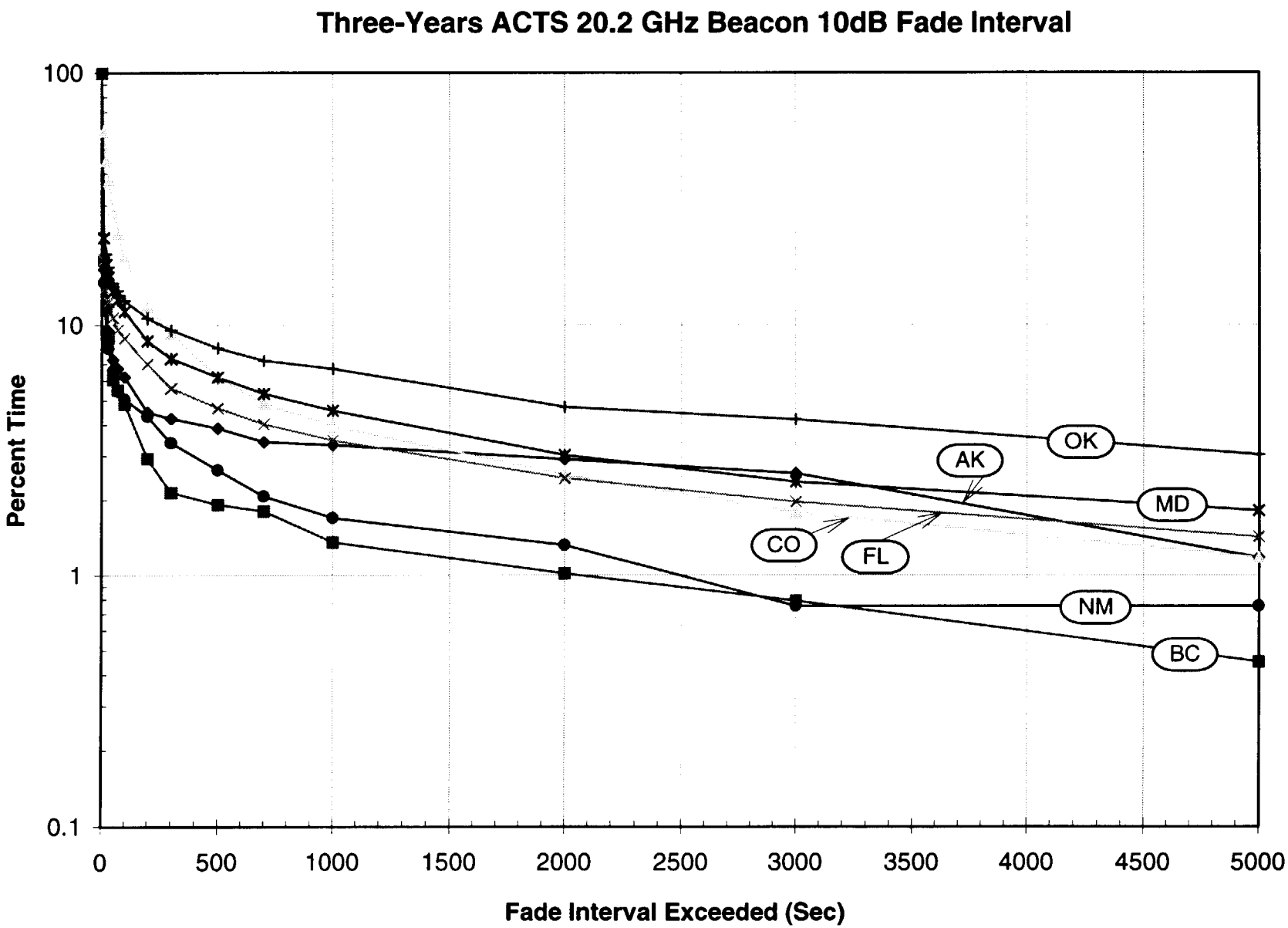
Three-Years ACTS 20.2 GHz Beacon 10dB Fade Interval
100
10
1
0.1
Percent Time
0
500
1000
1500
2000
2500
3000
3500
4000
4500
5000
Fade Interval Exceeded (Sec)
OK
AK
MD
CO
FL
NM
BC

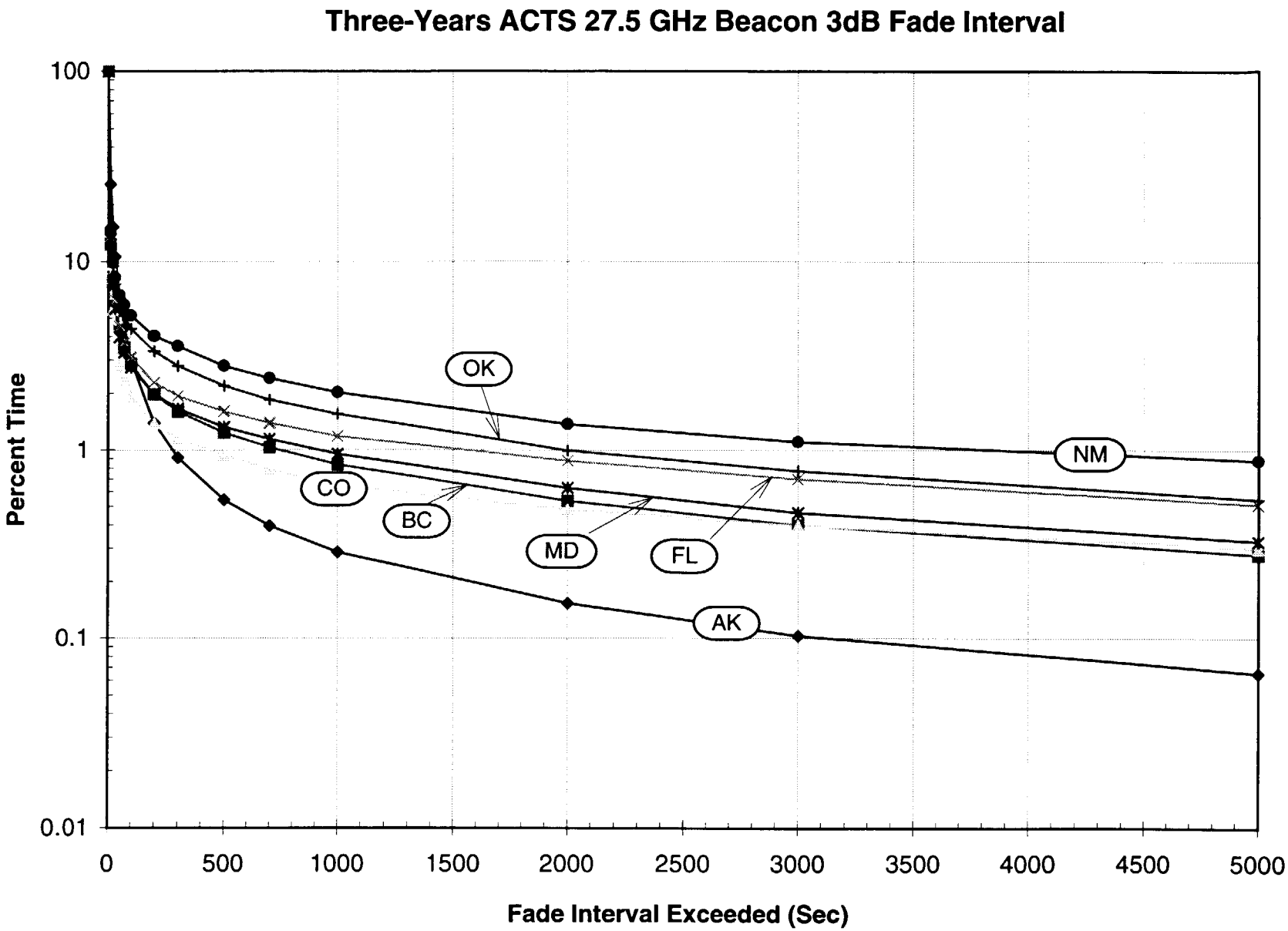
Three-Years ACTS 27.5 GHz Beacon 3dB Fade Interval
Percent Time
100
10
1
0.1
0.01
0
500
1000
1500
2000
2500
3000
3500
4000
4500
5000
Fade Interval Exceeded (Sec)
OK
NM
CO
BC
MD
FL
AK

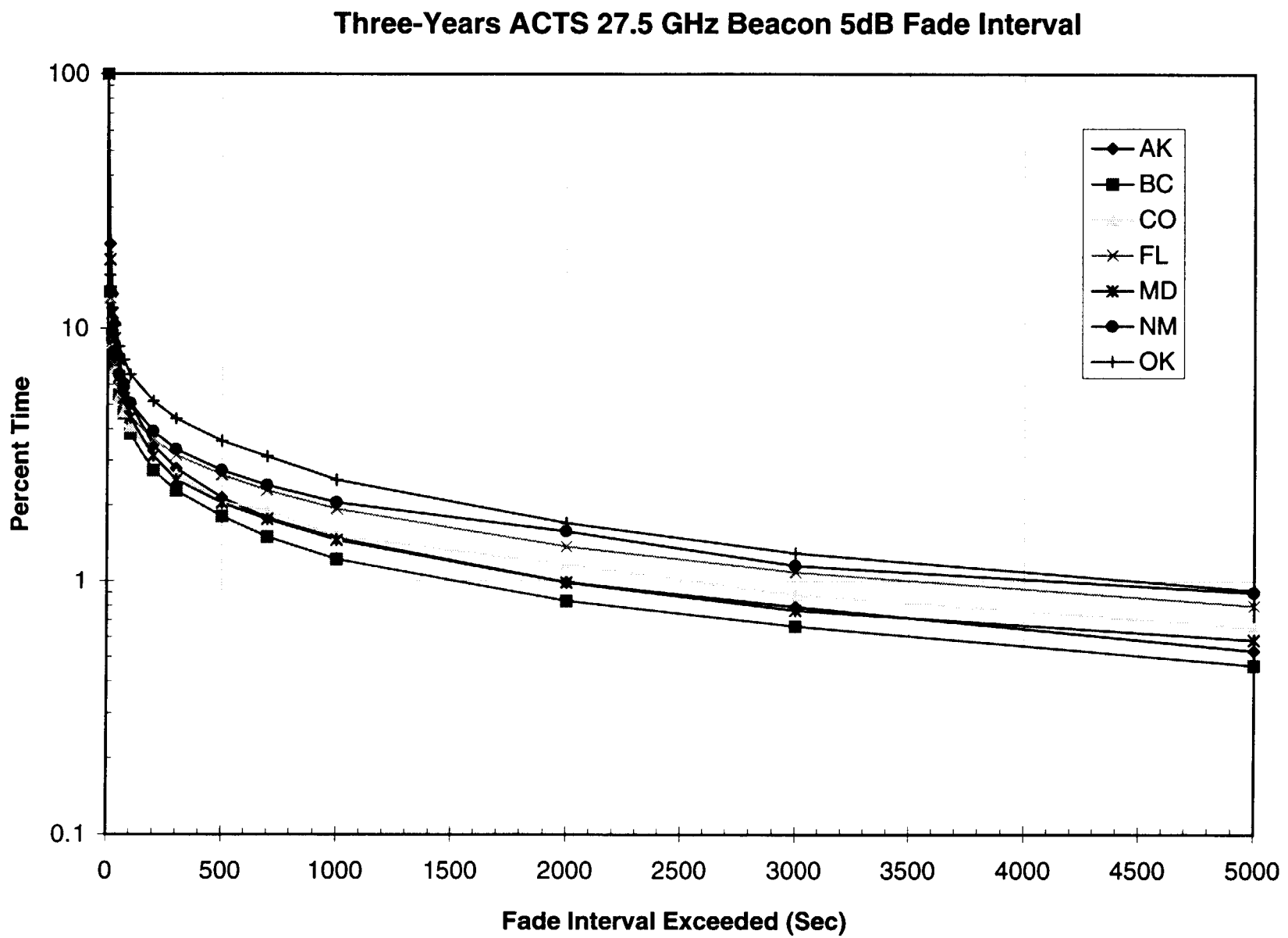
Three-Years ACTS 27.5 GHz Beacon 5dB Fade Interval
100
10
1
0.1
Percent Time
0
500
1000
1500
2000
2500
3000
3500
4000
4500
5000
Fade Interval Exceeded (Sec)
AK
BC
CO
FL
MD
NM
OK

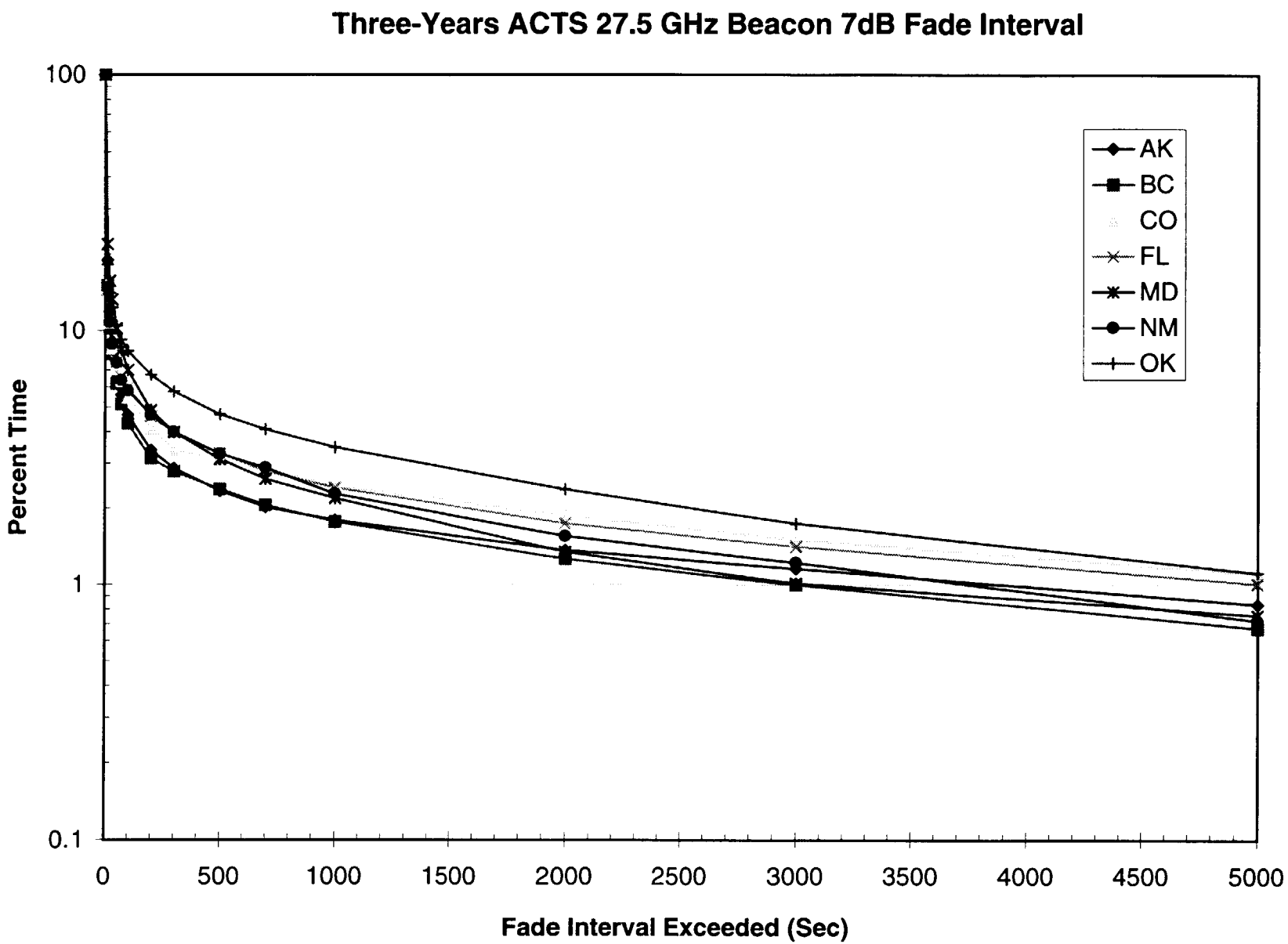
Three-Years ACTS 27.5 GHz Beacon 7dB Fade Interval
100
10
1
0.1
Percent Time
0
500
1000
1500
2000
2500
3000
3500
4000
4500
5000
Fade Interval Exceeded (Sec)
AK
BC
CO
FL
MD
NM
OK

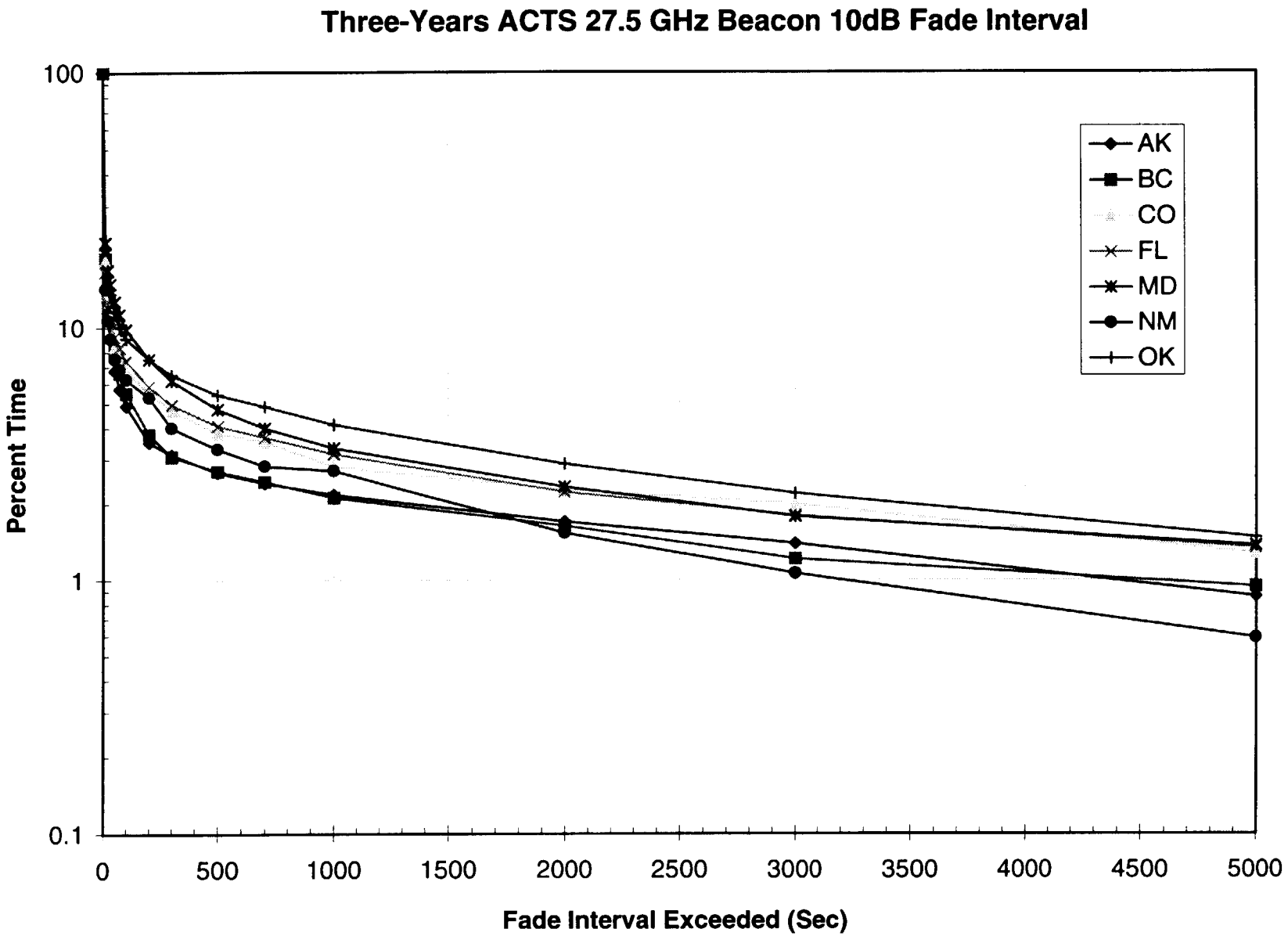
Three-Years ACTS 27.5 GHz Beacon 10dB Fade Interval
100
10
1
0.1
Percent Time
0
500
1000
1500
2000
2500
3000
3500
4000
4500
5000
Fade Interval Exceeded (Sec)
AK
BC
CO
FL
MD
NM
OK

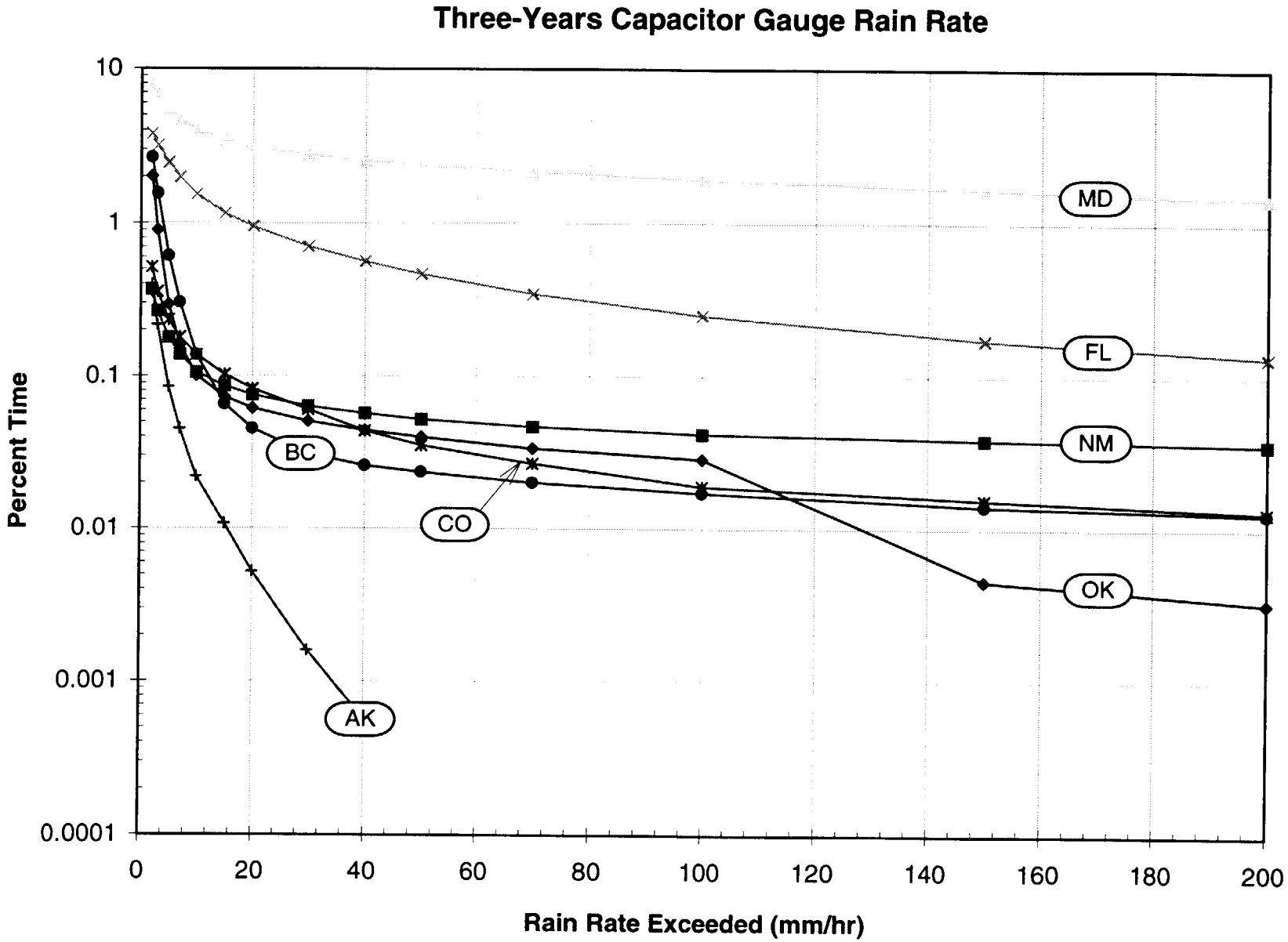
Three-Years Capacitor Gauge Rain Rate
Percent Time
10
1
0.1
0.01
0.001
0.0001
0
20
40
60
80
100
120
140
160
180
200
Rain Rate Exceeded (mm/hr)
MD
FL
NM
OK
BC
CO
AK

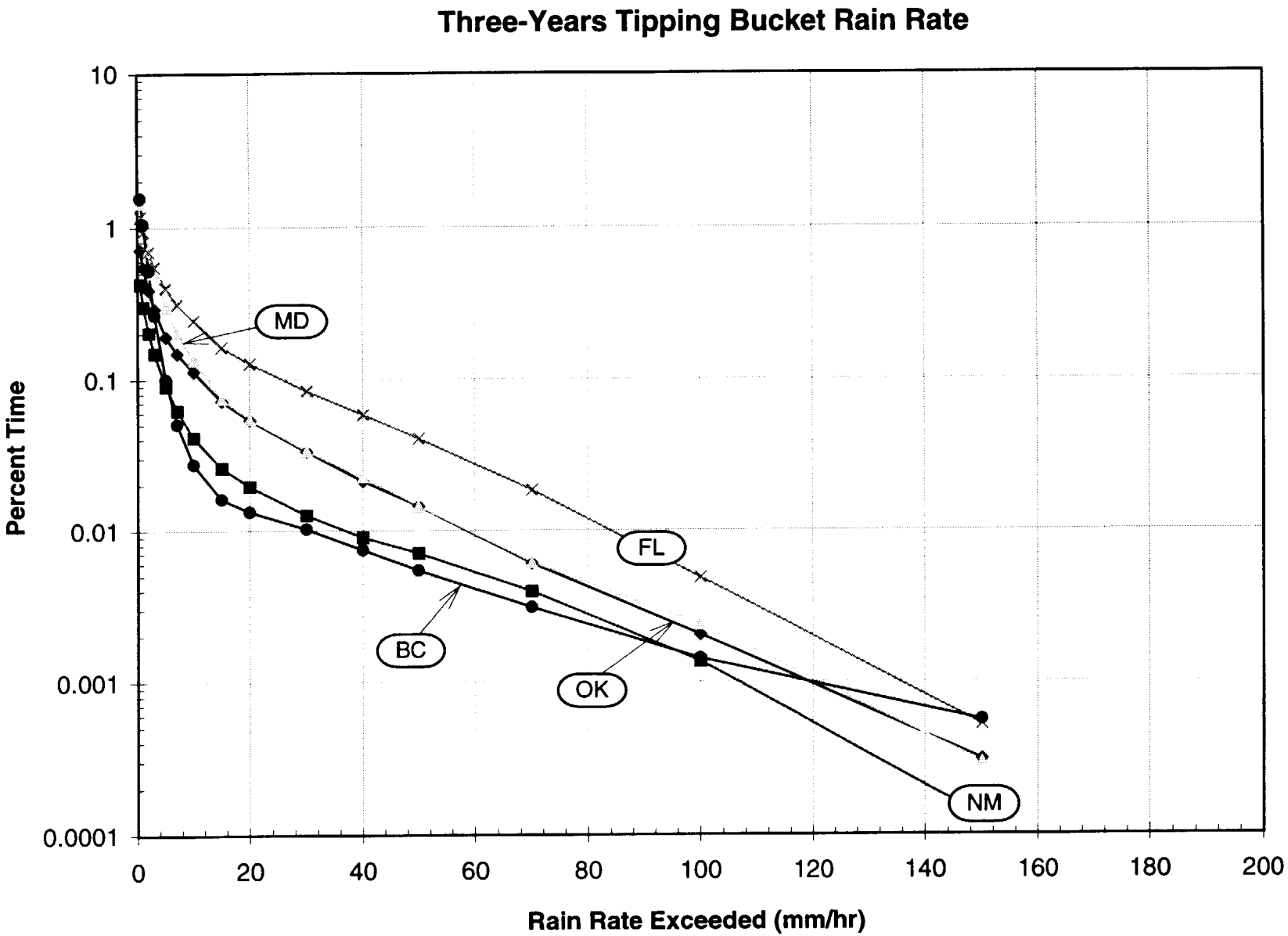
Three-Years Tipping Bucket Rain Rate
Percent Time
10
1
0.1
0.01
0.001
0.0001
0
20
40
60
80
100
120
140
160
180
200
Rain Rate Exceeded (mm/hr)
MD
FL
BC
OK
NM

ACTS PROPAGATION MEASUREMENTS AT OTTAWA, CANADA

D.V. Rogers and K.S. McCormick*
Communications Research Centre
Industry Canada
Ottawa, Ontario, Canada K2H 8S2

1. INTRODUCTION

Measurements of the signal strengths of the Advanced Communications Technology Satellite (ACTS) beacons are being made at the Communications Research Centre to enlarge the Canadian Ka-band rain attenuation data base, to support propagation modeling and model evaluation at these frequencies, and to acquire data needed to investigate propagation features (such as fade dynamics) expected to be important for the design of newer satellite communication systems and for the development of adaptive impairment-mitigation technologies. Ka-band propagation data are also necessary to permit efficient utilization of the spectrum at these frequencies.

Path signal-level data at 20.2 and 27.5 GHz have been collected since August 1995 at Ottawa, Canada, using earth terminals located at 45.35°N and 75.89°W. The path elevation angle is 32.6° and azimuth angle is 212.2° CWN to the geostationary ACTS satellite at 100°W longitude. The tilt angle of the received linear polarization is 22° CW from vertical. Radiometric sky noise data are also collected at 12, 20 and 29.5 GHz for use in supplemental analyses.

The ACTS beacon signals are received using 2.4 m diameter Cassegrain antennas, and the signal power measurements are accomplished by monitoring the level of the down-converted signals with programmable HP Selective Level Meters, under control of a personal computer. The 12, 20 and 29.5 GHz sky noise data are obtained with "dual-slope" radiometers manufactured by Diversitel Inc., using a focus-fed antenna of 1.2m and Cassegrain antennas of 0.6m and 0.5m, respectively. Data are retrieved from the beacon and radiometer receivers with the same PC that is used for system control, and stored for subsequent analysis.

Thus far, the analysis has concentrated on path rain attenuation statistics as measured with the beacon receivers and the 12-GHz radiometer. A variety of techniques has been developed to display, edit and process the data, including methods to select/edit arbitrary segments of the data time series, establish a signal level baseline to remove diurnal variations, and treat questionable data. This paper describes the data processing and analysis procedures, and presents some typical results, including monthly and annual cumulative statistics of 12/20/30-GHz rain attenuation. (In the paper, frequencies are often given as 20 or 30 GHz, instead of their more precise values.)

---

* Retired

2. EXPERIMENTAL CONFIGURATION

The ACTS experiment configuration at CRC is depicted in Fig. 1. The beacon receivers are designed to track and monitor the ACTS beacon transmitters, while the radiometers supply supplementary remotely-sensed data, independent of the satellite, that can enhance the propagation analyses. The 12-GHz radiometer data also provide a good indication of path attenuation at Ku-band to assist in comparing the Ka-band results with existing Ku-band propagation data.

The down-converters for the beacon receivers, designed and fabricated at CRC, use mixers with an integral local-oscillator frequency doubler (20.2 GHz) or tripler (27.5 GHz), and low-noise IF preamplifiers. As the cross-polar isolations of the ACTS beacon antennas are generally poor (likely worse than 22 dB for both beacons when viewed from Ottawa [1]), and as previous analyses at CRC [2] indicate that systems operating at frequencies above 20 GHz will typically be attenuation dominated, cross-polarization measurements are not attempted in the experiment.

Clear-Sky Link Budgets (Ottawa)	20 GHz	30 GHz
Beacon EIRP (dBW), nominal	16.6	15.1
Free-space Loss (dB)	- 210.2	- 212.9
Clear-sky Loss (dB), nominal	- 0.8	- 0.7
Polarization Loss (dB)	- 0.2	- 0.1
Earth Terminal Pointing Loss (dB)	- 0.2	- 0.4
Earth Terminal Antenna Gain (dBi)	(51.6)	(54.3)
Earth Terminal G/T (dB/K), nominal	20.0	20.0
Modulation Loss (dB), nominal	- 3.2	0.0
Received Power (dBW)	- 177.8	- 179.0
1/k (dB-Hz K/W)	228.6	228.6
C/N0 (dB-Hz)	50.8	49.6
C/N in 65 Hz (dB)	32.7	31.5

Table 1. Link budgets for the ACTS beacon measurements.

The consequent simplification to monopolarized reception allows the use of commercial programmable Selective Level Meters (HP 3586C) as frequency-tracking IF receivers [3], under control of a personal computer deployed at the site. The SLMs have an effective detection bandwidth of 65 Hz, and thus the carrier frequency must be tracked fairly carefully to maintain the carrier within this passband. In general, updates of the frequency are performed every 2 minutes, except during the vernal and autumnal equinoxes, when large frequency excursions of the beacons are encountered due to switches to and from the onboard batteries. During equinoctial periods, carrier frequency updates are performed every 30 sec.

The radiometers were manufactured by Diversitel Communications Inc. and use the "dual-slope" technique, originally developed at CRC, to estimate sky noise. In this implementation, the noise power received by the radiometer antenna is accumulated for a fixed time period, which is then compared to the time required to accumulate the same power from a noise diode reference. It can be shown that the ratio of these time periods is proportional to the antenna temperature. These same devices were used in prior Olympus Ka-band measurements at CRC [4], [5]. The 12-GHz radiometer has operated almost continuously during the measurement period. A failed PIN-diode switch caused some loss of data for the 20-GHz radiometer. Early in the measurements, the 29.5-GHz radiometer malfunctioned, and has only recently been returned to service after repair by the manufacturer. At present, all units are operating normally.

The 2.4 m beacon receive antennas have on-axis gains of 51.6 dBi at 20.2 GHz and 54.3 dBi at 27.5 GHz, with respective half-power beamwidths (HPBWs) of 0.44° and 0.32°. The nominal satellite range is 38,400 km. Link budgets for the beacon receive paths are supplied in Table 1. The HPBWs

of the radiometer antennas are: 1.5° for the 1.2 m antenna used at 12-GHz; 1.75° for the 0.6 m antenna at 20-GHz; and 1.5° for the 0.46 m antenna at 29.5-GHz.

3. DATA COLLECTION, PROCESSING AND ANALYSIS

The beacon signal level data are sampled at 1 Hz by interrogating the SLMs at this rate. The data are stored on the computer hard disk for subsequent retrieval and processing. Radiometer data are sampled every 0.5 sec, then integrated and stored every 2 sec. The radiometer data can be further filtered during data sampling by creating a selectable running average of 1 to 30 samples. Presently, a 10-sample (5 sec) running average is used for each radiometer. Sky noise data are accumulated and blocked into 1-h records by a microprocessor in the radiometer for later retrieval.

Data processing activities to date have built on software developed for a Ku-band radiometer experiment previously performed jointly with several ASEAN countries [6]. As an example of the processing capabilities, Fig. 2 shows time series of both beacon signal levels over a period of 24 hours. In order to reduce the effects of system noise, the signals were low-pass filtered with a cutoff of 0.2 Hz at processing time. At 30 GHz, a diurnal variation of received signal strength is clearly visible. The solid lines superimposed on the plot are sine curves with a period of 24 hours. The average level, phase and amplitude of these sine waves has been adjusted visually to establish a reference baseline for the derivation of signal attenuations. (This was done using the two small squares, or "handles", which may be visible on each sine curve.) Fig. 3 shows the resulting event structure, with the baseline removed, for the period 12 to 17 hours. The satisfactory performance of this approach is quite evident.

Due to the several judgments required during the data editing and processing, as well as expected contributions to the statistics caused by equipment noise that gets reflected in the recorded data, it is prudent to verify that the net effect on the propagation statistics is essentially unbiased. For these data, this aspect was checked by computing "attenuation densities" for each data channel, defined as the number of seconds observed in a specified 0.1 dB attenuation bin over the course of a month. Such a presentation is given in Fig. 4, upon which 30-GHz beacon attenuation densities are plotted for August, September and October of 1995. The peaked shape of the densities at zero decibels provides evidence that there is negligible net bias in the data processing procedures.

4. EXAMPLE RESULTS

Fig. 5 illustrates concurrent time series plots of measured signal attenuations for the beacon signals and derived attenuation values for the 12- and 20-GHz radiometer channels for a 12-hour period, collected on 19 January 1996. Just before 1400 GMT (0900 Eastern Standard Time), rain began and was registered in each of the channels. The behavior among the channels approximately follows the expected frequency dependence for rain, and individual features among the time series are observed to be well correlated.

At about 1900 GMT (1400 EST), the precipitation changed to snow, and divergence among the channels increased. For example, very little correlation is observed between the 12- and 20-GHz radiometers at about 2000 GMT. This behavior has been noted several times and is attributed to the different antenna feed types: The 12-GHz focus-fed feed is protected from accumulations of

precipitation on the feed window, while the 20-GHz Cassegrain feed is very susceptible to such effects. Precipitation is also observed on the beacon receive antenna surfaces and feed windows, but a feed-blower assembly keeps the beacon antenna feed windows generally free of precipitation. The corresponding apparent path losses can be relatively large for wet snow, but appear to be less severe for water droplets.

As already noted, the time series outputs of the various sensors are edited and processed to obtain cumulative fade statistics. Table 2 gives the percentage uptimes for each of the three equipments by month. This table should be taken into account in assessing the likely validity of the attenuation distributions which are discussed below. Fig. 6 shows cumulative path attenuation statistics as derived from the 20-GHz beacon data for the first few months of operation, August - September 1995, as well as annual statistics for the one-year period comprised of the months November 1995 through October 1996. Experiment uptime for the first couple of months was poor, but the fading activity for the last three months of 1995 was modest in any case.

Time Period	12 GHz Radiom	20 GHz Beacon	30 GHz Beacon
August 1995	0.0	45.5	46.4
September 1995	0.0	38.6	38.6
October 1995	33.5	95.8	95.7
November 1995	64.3	85.5	85.5
December 1995	78.1	85.7	85.7
January 1996	92.1	95.0	95.1
February 1996	97.8	92.1	92.1
March 1996	80.1	74.6	74.2
April 1996	94.0	0.0	97.9
May 1996	97.6	0.0	80.1
June 1996	96.7	0.0	96.4
July 1996	74.2	16.7	67.3
August 1996	96.8	96.6	96.6
September 1996	80.0	62.6	68.9
October 1996	96.8	94.2	94.2
Nov 1995 - Oct 1996	87.4	51.6	86.1

Table 2. Monthly time percentages that valid data were obtained for the 12-GHz radiometer and the 20- and 30-GHz ACTS signal beacons, for the period November 1995 to October 1996.

Fig. 7 displays a similar plot derived from the 30-GHz beacon data, with very similar general features (and experiment uptimes) as those of Fig. 6 for the 20-GHz channel, except that the monthly distributions for September 1995 do not appear to be consistent with respect to fading at the smallest time percentages. Such discrepancies are investigated by reviewing the time series data, especially after editing, to determine the events that cause the observed features.

By way of example, Fig. 8 displays the cumulative fade distributions derived from the 12-GHz sky noise data for the months July-October 1996, along with annual statistics for November 1995 through October 1996. The behavior of the monthly distribution for August 1995 appears somewhat unusual (though within bounds for a single month of data). By reviewing time series data for the month, it was established that the monthly distribution is an accurate representation of the fading that occurred during the time period under review.

Fig. 9 supplies distributions for the 12, 20 and 30 GHz channels for the month of August 1996, each based on very similar equipment uptimes. Significant fading was experienced during this month, as reflected in the individual distributions. Furthermore, the individual curves are observed to display broad agreement with the expected characteristics of rain attenuation at the different frequencies.

Fig. 10 provides cumulative distributions of measured 20- and 30-GHz attenuation and 12-GHz derived attenuation for the 12 month period November 1995 to October 1996. The derived 12-GHz attenuation distribution is observed to intersect the 20-GHz curves at a time percentage just below

0.01%, which is clearly unlikely. This discrepancy is likely due to differences in the uptimes for these two channels, plus possibly a nonoptimal choice of the effective medium temperature required to transform the sky noise data into a rain attenuation distribution. Identification and evaluation of such features in the results are necessarily continuing as the experiment progresses.

Also shown in Fig. 10 are 12- and 20-GHz distributions which were frequency scaled from the 30-GHz data using the method of Rec. ITU-R P.618-4 [7]. The 30-GHz data were chosen as the baseline because they form a better statistical data set than the 20-GHz data. The scaled distribution at 20 GHz compares very well with the measured distribution down to a time percentage of 0.01%. The scaled 12-GHz distribution shows poor agreement with the measured data, likely for the same reasons as noted in the previous paragraph.

5. REFERENCES

[1] F. Gargione, private communication, Manager, ACTS Flight Systems, GE AstroSpace Division, Princeton, NJ, 14 December 1989.

[2] D.V. Rogers, "Relative Importance of Path Depolarization and Attenuation in 44/20-GHz Military Satellite Communications," CRC Technical Memorandum DRC-TM-93-3, June 1993.

[3] Hewlett-Packard Company, "Operating Manual, Selective Level Meter HP 3586 A/B/C," Everett, WA, March 1991.

[4] R.L. Olsen *et al.*, "The Canadian Olympus Propagation Experiment," *Proc. IEEE Global Telecommunications Conf.*, pp. 302.5.1-302.5.5, San Diego, Dec. 1990.

[5] D.V. Rogers, "Status of the Olympus Experiment at CRC," *Proc. 16th NASA Propagation Experimenters Meeting (NAPEX XVI) and Advanced Commun. Tech. Satellite (ACTS) Propagat. Studies Workshop*, JPL Publ. 92-16, pp. 166-170, Houston, 29-30 May 1992.

[6] K.S. McCormick, "Canada-ASEAN Cooperation in the Ku-Band Propagation Measurement Programme on Earth Space Paths," CRC Report No. CRC-RP-96-006, Communications Research Centre, Ottawa, Canada, June 1996.

[7] ITU-R Recommendation P.618-4, "Propagation Data and Prediction Methods Required for the Design of Earth-Space Telecommunication Systems," *ITU-R Recommendations*, P Series Fascicle, pp. 249-267, ITU, Geneva, 1995.

Acknowledgment: The authors are grateful to Mr. Neville Reed for his many efforts in implementing, operating and maintaining the ACTS experiment facility.

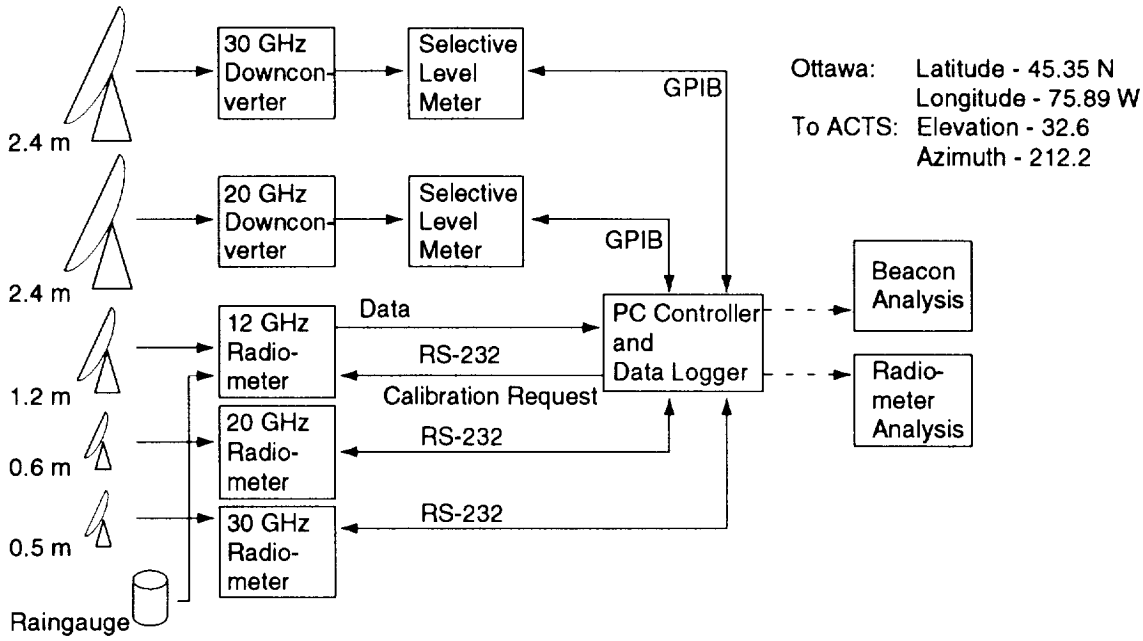

Fig. 1. Experimental configuration for the ACTS beacon measurement program at CRC.

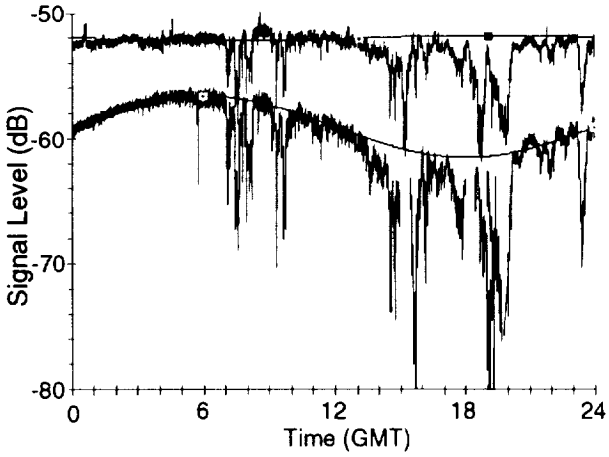

Fig. 2. Signal strength recordings for Oct. 21, 1995. The upper curve is for the 20 GHz beacon, the lower curve for the 27 GHz beacon. Also shown are sine curves with a period of 24 hours used to remove variations in the baseline. The small squares (two on each sine curve) are handles which are used to adjust the average level, the phase and the amplitude of the sine curves.

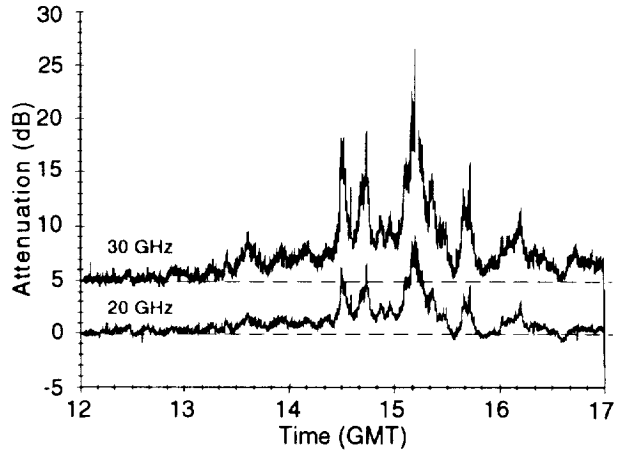

Fig. 3. A portion of the rain attenuation data extracted from the signal strength recordings shown in Fig. 2. The 30 GHz data are offset by 5 dB for clarity.

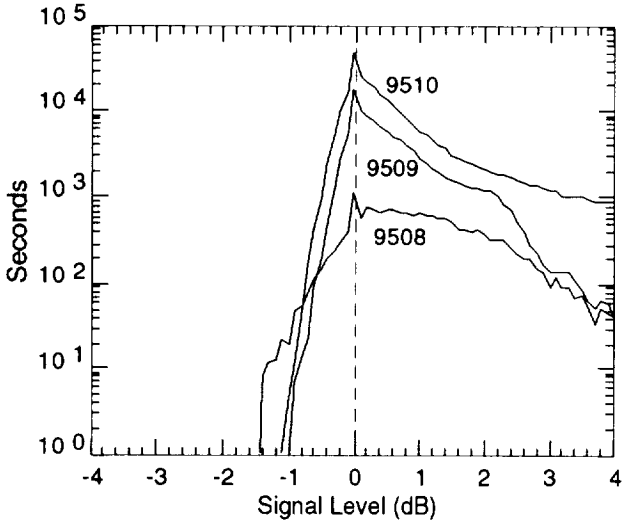

Fig. 4. Density functions of the extracted 30 GHz attenuations for the months of August, September, and October, 1995. The attenuation data were quantized to 0.1 dB, and the plots show the number of seconds the signal was observed in each 0.1 dB bin. The peak in the data at 0 dB gives confidence in the method used to extract the attenuations. The data spread, particularly below 0 dB, is due mainly to signal noise.

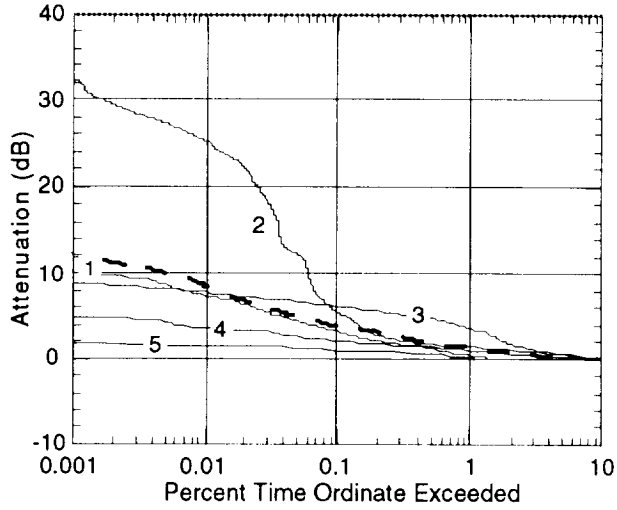

Fig. 6. Monthly cumulative distributions of attenuation derived from the 20 GHz ACTS beacon for: 1 - August; 2 - September; 3 - October; 4 - November; and 5 - December, 1995. The heavy dashed line is the distribution for the year November 1995 through October 1996.

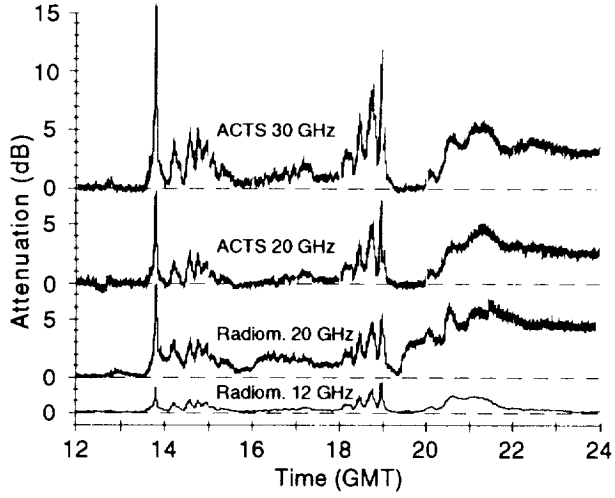

Fig. 5. Concurrent time series plots of measured signal attenuations for the beacon signals and for the derived attenuation values for the 12 and 20 GHz radiometer channels. Data collected on January 19, 1996.

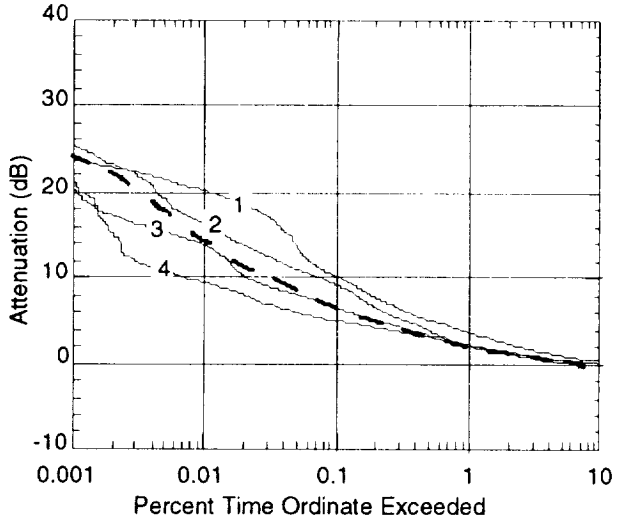

Fig. 7. Monthly cumulative distributions of attenuation beacon derived from the 30 GHz ACTS for: 1 - July; 2 - August; 3 - September; and 4 - October, 1996. The heavy dashed line is the distribution for the year November 1995 through October 1996.

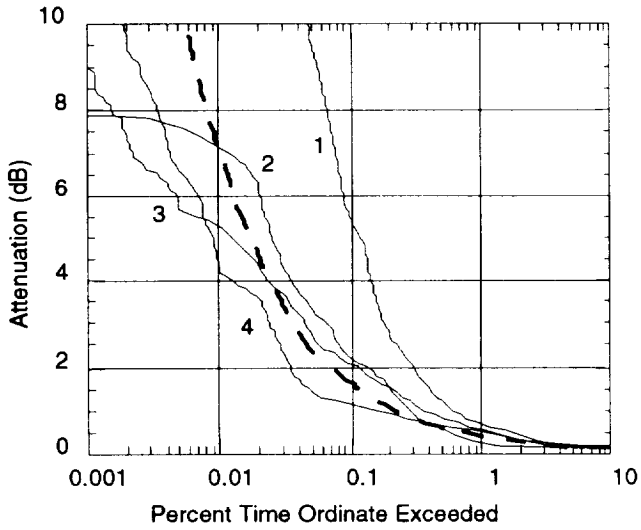

Fig. 8. Monthly cumulative distributions of attenuation derived from the 12 GHz ACTS radiometer for: 1 - July; 2 - August; 3 - September; and 4 - October, 1996. The heavy dashed line is the distribution for the year November 1995 through October 1996. Note the change in attenuation scale.

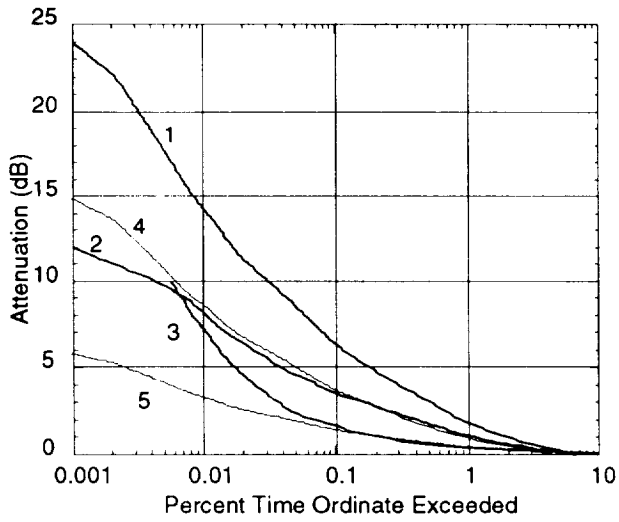

Fig. 10. Comparison of attenuation distributions for the year November 1995 to October 1996: 1 - 30 GHz beacon; 2 - 20 GHz beacon; 3 - 12 GHz radiometer; 4 - 20 GHz scaled from the 30 GHz data; 5 - 12 GHz scaled from the 30 GHz data.

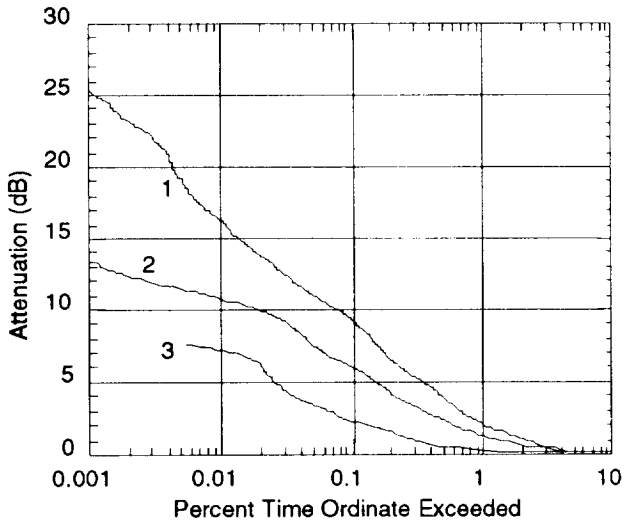

Fig. 9. Comparison of the attenuation distributions for the month of August, 1996: 1 - 30 GHz beacon; 2 - 20 GHz beacon; 3 - 12 GHz radiometer.

EERL / Univ. of Texas

ACTS Propagation Data Base Status

Wolf Vogel

Electrical Engineering Research Laboratory
The University of Texas at Austin

Presented at NAPEX XXI
El Segundo, CA
June 11, 1997

1

EERL / Univ. of Texas

Raw Data Received (06/04/97)

Year	Month	AK	BC	CO	FL	MD	NM	OK
93	Sep	03	10	..	..	..	..	29
93	Oct	31	26	..	..	..	30	31
93	Nov	..	27	..	28	..	15	29
93	Dec	31	31	30	29	..	29	31
94	Jan	31	31	31	31	..	31	31
94	Feb	28	28	28	28	..	25	28
94	Mar	31	31	31	29	17	31	31
94	Apr	30	30	30	30	30	30	30
94	May	31	31	25	30	31	31	31
94	Jun	30	30	30	30	30	30	30
94	Jul	31	31	31	31	31	31	31
94	Aug	31	31	31	31	31	31	31
94	Sep	30	30	29	30	30	30	30
94	Oct	31	31	29	31	31	31	31
94	Nov	27	30	30	30	30	30	30
94	Dec	31	31	31	28	22	31	31
95	Jan	31	31	31	31	19	31	31
95	Feb	28	28	28	28	28	28	28
95	Mar	31	31	31	31	31	31	31
95	Apr	30	30	30	30	28	30	30
95	May	31	31	31	31	31	31	31
95	Jun	30	30	30	30	30	30	30
95	Jul	31	31	31	31	31	31	31
95	Aug	31	31	31	31	31	31	31
95	Sep	30	30	30	30	30	30	30
95	Oct	31	31	31	31	31	31	31
95	Nov	30	30	30	30	30	30	30

Year	Month	AK	BC	CO	FL	MD	NM	OK
95	Dec	31	31	31	31	31	31	31
96	Jan	31	31	31	31	31	31	31
96	Feb	29	29	27	29	29	27	29
96	Mar	31	31	30	31	31	24	31
96	Apr	30	30	30	30	20	30	30
96	May	31	31	31	31	31	31	31
96	Jun	30	30	30	30	30	30	30
96	Jul	31	31	23	31	31	31	31
96	Aug	31	31	31	31	31	31	31
96	Sep	30	30	29	28	30	30	30
96	Oct	31	31	28	31	30	31	31
96	Nov	30	30	30	30	23	30	30
96	Dec	31	31	31	31	31	26	31
97	Jan	31	31	31	..	31	29	..
97	Feb	28	28	28	28	28	28	..
97	Mar	31	..	..	31	31	31	..
97	Apr	..	..	..	..	30	27	..
97	May	..	..	..	..	..	..	..
97	Jun	..	..	..	..	..	..	..

Total Daily RV0 Files: 8448
Total Compressed MegaBytes: 5755

2

EERL / Univ. of Texas

PV2 Data Received (06/04/97)

Year	Month	AK	BC	CO	FL	MD	NM	OK
93	Sep	..	..	..	..	..	..	..
93	Oct	..	..	..	..	..	..	..
93	Nov	..	27	..	..	..	..	29
93	Dec	31	31	30	28	..	29	31
94	Jan	31	31	31	31	..	31	31
94	Feb	28	28	28	28	..	25	28
94	Mar	31	31	31	29	17	31	31
94	Apr	30	30	30	30	30	30	30
94	May	31	31	25	30	31	31	31
94	Jun	30	30	30	30	30	30	30
94	Jul	31	31	31	31	31	31	31
94	Aug	31	31	31	31	30	31	31
94	Sep	30	30	29	30	30	30	30
94	Oct	31	31	29	31	31	31	31
94	Nov	27	30	30	30	30	30	30
94	Dec	31	31	31	28	22	31	31
95	Jan	31	31	31	31	19	31	31
95	Feb	28	28	28	28	28	28	28
95	Mar	31	31	31	31	31	31	31
95	Apr	30	30	30	30	28	30	30
95	May	31	31	31	31	31	31	31
95	Jun	30	30	30	30	30	30	30
95	Jul	31	31	31	31	31	31	31
95	Aug	31	31	31	31	31	31	31
95	Sep	30	30	30	30	30	30	30
95	Oct	31	31	31	31	31	31	31
95	Nov	30	30	30	30	30	30	30

Year	Month	AK	BC	CO	FL	MD	NM	OK
95	Dec	31	31	31	31	31	31	31
96	Jan	31	31	31	31	31	31	31
96	Feb	29	29	27	29	29	27	29
96	Mar	31	31	30	31	31	24	31
96	Apr	30	30	30	30	20	30	30
96	May	31	31	31	31	31	31	31
96	Jun	30	30	30	30	30	30	30
96	Jul	31	31	23	31	31	31	31
96	Aug	31	31	31	31	31	31	31
96	Sep	30	30	29	28	30	30	30
96	Oct	31	31	28	31	30	31	31
96	Nov	30	30	30	30	23	30	30
96	Dec	..	..	..	..	..	..	31
97	Jan	..	31	..	..	..	..	..
97	Feb	..	..	..	..	..	..	..
97	Mar	..	..	..	..	..	..	..
97	Apr	..	..	..	..	..	..	..
97	May	..	..	..	..	..	..	..
97	Jun	..	..	..	..	..	..	..

Total Daily PV2 Files: 7591
Total Compressed MegaBytes: 2915

3

EERL / Univ. of Texas

Miscellaneous Files as of 06-04-1997

Year	Month	AK	BC	CO	FL	MD	NM	OK
93	Sep	.....	.....	.....	.....	.....	.....	.....
93	Oct	.....	.....	.....	.....	.....	.....	.....
93	Nov	.....	LDSRE	.....	.....	.....	.....	LD..E
93	Dec	LDS.E	LDSRE	LDSRE	LDSRE	LDSRE	LDS.E	LD..E
94	Jan	LDS.E	LDSRE	LDSRE	LDSRE	LDSRE	LDS.E	LD..E
94	Feb	LDS.E	LDSRE	LDSRE	LDSRE	.....	LDS.E	LD..E
94	Mar	LDS.E	LDSRE	LDSRE	LDSRE	LDSRE	LDS.E	LD..E
94	Apr	LDS.E	LDSRE	LDSRE	LDSRE	LDSRE	LDS.E	LD..E
94	May	LDS.E	LDSRE	LDSRE	LDSRE	LDSRE	LDS.E	LD..E
94	Jun	LDS.E	LDSRE	LDSRE	LDS.E	LDSRE	LDS.E	LD..E
94	Jul	LDS.E	CLDSRE	LDSRE	LDSRE	LDSRE	LDS.E	LD..E
94	Aug	LDS.E	CLDSRE	LDS.E	LDSRE	LDSRE	LDS.E	LD..E
94	Sep	LDS.E	LDSRE	LDSRE	LDSRE	LDSRE	LDS.E	LD..E
94	Oct	LDS.E	LDSRE	LDSRE	LDSRE	LDSRE	LDS.E	LD..E
94	Nov	LDS.E	LDSRE	LDSRE	LDS.E	LDSRE	LDS.E	LD..E
94	Dec	LDS.E	LDSRE	LDSRE	LDS.E	LDSRE	LDS.E	LD..E
95	Jan	LDS.E	LDSRE	LDSRE	LDS.E	LDSRE	LDS.E	LD..E
95	Feb	LDS.E	LDSRE	LDSRE	LDS.E	LDSRE	LDSRE	LD..E
95	Mar	LDS.E	LDSRE	LDSRE	LDSRE	LDSRE	LDSRE	LD..E
95	Apr	LDS.E	LDSRE	LDSRE	LDSRE	LDSRE	LDSRE	LD..E
95	May	LDS.E	LDSRE	LDSRE	LDSRE	LDSRE	LDSRE	LD..E
95	Jun	LDS.E	LDSRE	LD.RE	CLDSRE	LDSRE	LDSRE	LD..E
95	Jul	LDS.E	LDSRE	LD.RE	CLDSRE	LDSRE	LDSRE	LD..E
95	Aug	LDS.E	LDSRE	LD..E	CLDSRE	LDSRE	LDSRE	LD..E
95	Sep	LDS.E	LDSRE	LD..E	LDSRE	LDSRE	LDSRE	LD..E
95	Oct	LDS.E	LDSRE	LD.RE	LDSRE	LDSRE	LDSRE	LD..E
95	Nov	LDS.E	LDSRE	LD..E	LDSRE	LDSRE	LDSRE	LD..E
95	Dec	LDS.E	LDSRE	LD..E	LDSRE	LDSRE	LDSRE	LD..E
96	Jan	LDS.E	LDSRE	LD.RE	LDSRE	LDSRE	LDSRE	LD..E
96	Feb	LDS.E	LDSRE	LD..E	LDSRE	LDSRE	LDSRE	LD..E
96	Mar	LDS.E	LDSRE	LD.RE	LDSRE	LDSRE	LDSRE	LD..E
96	Apr	LDS.E	LDSRE	LDSRE	LDSRE	LDSRE	LDSRE	LD..E
96	May	LDS.E	LDSRE	LDSRE	LDSRE	LDSRE	LDSRE	LD..E
96	Jun	LDS.E	LDSRE	LDSRE	LDSRE	LDSRE	LDS.E	LD..E
96	Jul	LDS.E	LDSRE	CLDSRE	LDSRE	LDSRE	LDS.E	LD..E
96	Aug	LDS.E	LDSRE	CLDSRE	LD..E	LDSRE	LDS.E	LD..E
96	Sep	LDS.E	LDSRE	LDSRE	LD..E	LDSRE	LDSRE	LD..E
96	Oct	LDS.E	CLDSRE	LDSRE	LDSRE	LDSRE	LDSRE	LD..E
96	Nov	LDS.E	.....	.....	.....	LDSRE	LDSRE	LD..E
96	Dec	.....	.....	.....	.....	.....	.....	LD..E
97	Jan	.....	.....	CLDSRE	.....	.....	.....	.....
97	Feb	.....	.....	.....	.....	.....	.....	.....
97	Mar	.....	.....	.....	.....	.....	.....	.....
97	Apr	.....	.....	.....	.....	.....	.....	.....
97	May	.....	.....	.....	.....	.....	.....	.....
97	Jun	.....	.....	.....	.....	.....	.....	.....

Key: C=CAL, L=LOG, D=DSC, S=SRF, R=RIN, E=EDF

4

EERL / Univ. of Texas

Methods for Submitting Data

in order of preference

- ftp to cancan.eerl.utexas.edu
  - zip monthly files into one ~20 MB file
  - takes ~20 minutes
  - ftp is down during CD-ROM burning
- mail on ZIP drive cartridge
  - zipped or not; cartridges will be returned
- mail on CMS tape
  - arrgghhh

5

EERL / Univ. of Texas

3-YEAR PP CD-ROM Organization

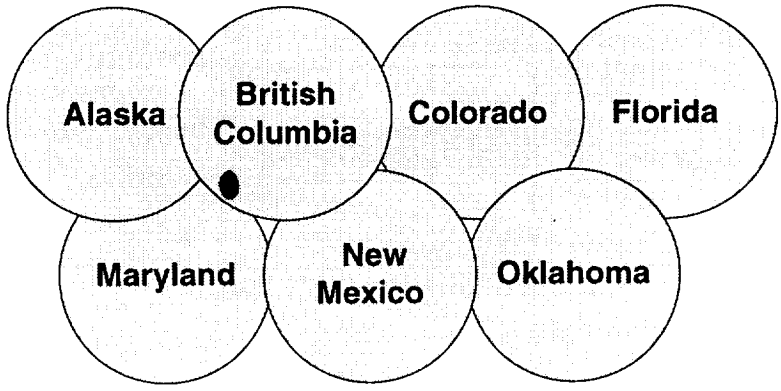

6

EERL / Univ. of Texas

CD-ROM Directory

CD-ROM Volume

YYMM (Year-Month)

PC2 files for month
EDF file for month
misc. files for month

YYMM (Year-Month)

PC2 files for month
EDF file for month
misc. files for month

and so on ....

EERL / Univ. of Texas

PP File Compression & Decompression

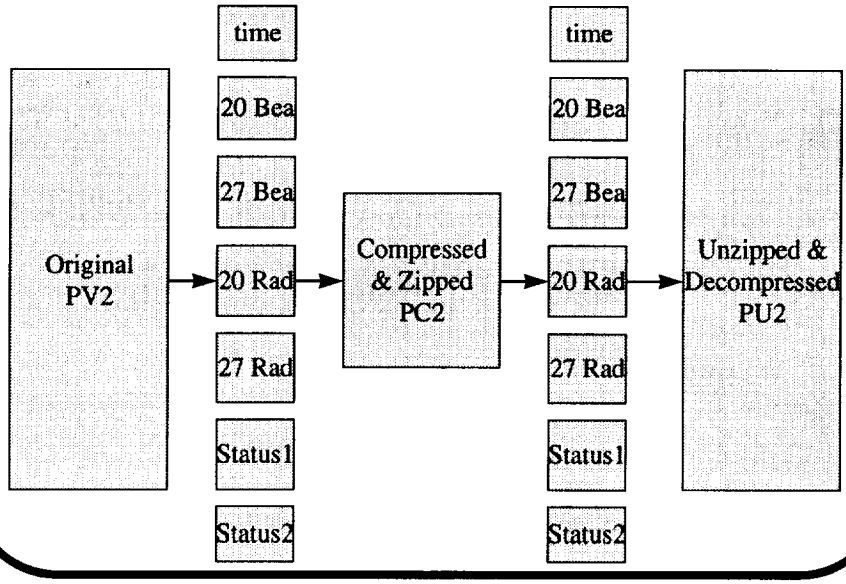

EERL / Univ. of Texas

EERL / Univ. of Texas

Methods for Submitting Data

in order of preference

- ftp to cancan.eerl.utexas.edu
  - zip monthly files into one ~20 MB file
  - takes ~20 minutes
  - ftp is down during CD-ROM burning
- mail on ZIP drive cartridge
  - zipped or not; cartridges will be returned
- mail on CMS tape
  - arrgghhh

5

EERL / Univ. of Texas

3-YEAR PP CD-ROM Organization

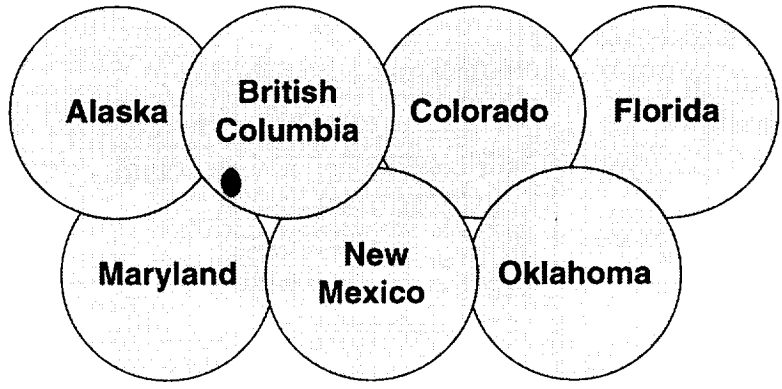

6

EERL / Univ. of Texas

CD-ROM Directory

CD-ROM Volume

YYMM (Year-Month)

PC2 files for month
EDF file for month
misc. files for month

YYMM (Year-Month)

PC2 files for month
EDF file for month
misc. files for month

and so on ....

7

EERL / Univ. of Texas

Diskette Miscellaneous Files

- Information on data file structure and installation
  - Format.txt
- Program installation batch file
  - Run_Me.bat
- Programs for uncompressing data (16 bit OS)
  - directory doswin16
    - » dc.bat, decomp.exe, pkunzip.exe
- Programs for uncompressing data (32 bit OS)
  - directory win32uti
    - » ACTSInst.exe, decomp.exe, pkunzip.exe

8

EERL / Univ. of Texas

Suggested Directory Structure (created by Run_Me.bat)

- C:\
  - ACTS\
    - » EXE\
      - doswin16\
      - win32util\
    - » TMP\

9

EERL / Univ. of Texas

Using ACTSPP Program to Decompress Data

- The ACTSPP program is also available to decompress the data. In addition, this program can produce monthly EDF files using operator-selectable criteria for various 20/27 GHz levels of fade simultaneity definitions and outputs much diagnostic information. This program was used by all seven stations to convert raw data files (RV0 files) to calibrated PV2 files and to produce the monthly EDF files.
- It can be obtained from and is supported by Dave Westenhaver, E-mail: wwwinc@crl.com, Westenhaver Wizard Works, Inc., Tel: 770-925-1091.

10

EERL / Univ. of Texas

PP File Compression & Decompression

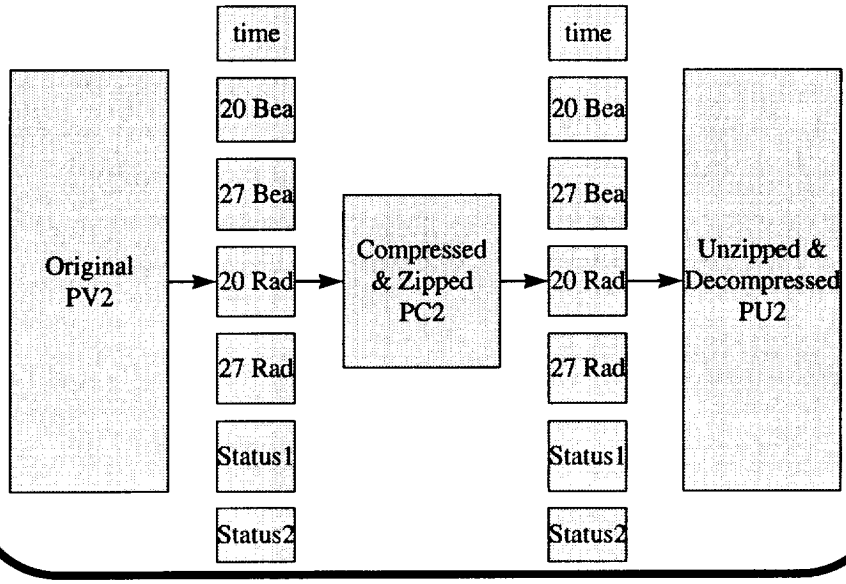

11

EERL / Univ. of Texas

CD-ROM distribution

- Made 14 sets, of which we distributed:
  - 9 Industry/Academic Requests
  - 1 JPL
  - 1 LeRC
  - 1 WWW Inc.
  - 2 ACTS Propagation Data Center
- 1 left to distribute
- More can be made if requested

12

EERL / Univ. of Texas

CD-ROM Requests Filled

- ☒ Ashok Mathur, DirecTV
- ☒ David V Rogers, CRC
- ☒ Zlata Koro, Teledesic
- ☒ Faramaz Davarian, Hughes Space & Communications
- ☒ Rick Leacock, Spaceway
- ☒ Fred I Shimabukuro, The Aerospace Corporation
- ☒ Frederick Solheim, Radiometrics Corporation
- ☒ Hans Kruse, Ohio University
- ☒ Norbert Kleiner, Motorola

13

2. Ka Band Propagation Studies and Models

Industry Needs

F. Davarian,
Hughes Space and Communications Division

Special Issue on Ka-Band Propagation Effects on Earth-Satellite Links

Proceedings of the IEEE, June 1997

1. System Requirements for Ka-Band Earth-Satellite Propagation Data
2. Ka-Band Earth-Space Propagation Research in Japan
3. European Research on Slant Path Propagation
4. Ka-Band Propagation Measurements: An Opportunity with the Advanced Communications Technology Satellite (ACTS)
5. ACTS Propagation Experiment: Experiment Design, Calibration, Data Preparation and Archival
6. ACTS Propagation Experiment: Attenuation Distribution Observation and Prediction Model Comparisons
7. The Application of S-Band Polarimetric Radar Measurements to Ka-Band Attenuation Prediction
8. Cumulative Fade Distributions and Frequency Scaling Techniques at 20 GHz from the Advanced Communications Technology Satellite and at 12 GHz from the Digital Satellite System
9. Comparison of Fade Duration Statistics with Model Prediction
10. Fade Slope Analysis for Alaska, Florida, and New Mexico
11. Ka-Band Scintillations: Measurements and Model Predictions
12. ACTS Propagation Experiment: Rain-Rate Distribution Observation and Prediction Model Comparisons
13. Application of Open Loop Uplink Power Control in Ka-Band Satellite Links
14. Three-Site Space Diversity Experiment at 20 GHz Using ACTS in Eastern United States
15. Channel Characterization and Modeling for Ka-Band Very Small Aperture Terminals

Ka-Band Propagation Studies and Models

- Data
  - Point fade calculations and simulation
- Models
  - Most rain attenuation models are similar in procedure but use different climate maps
  - Fade Dynamics (event based)
- Presentation of Propagation Data and Models
  - Excel user-defined functions
  - Geographic information systems
- Antenna Wetting
- Mitigation Technology

Models for Voice/Data Communications and Satellite Radio Broadcast

- Voice/Data Communications Availability and Signal Quality
  - Handheld receivers (L- and S-band)
    - Antenna effects
    - User motion effects
    - User head effects
    - Multi frequency effects (uplink and downlink frequencies)
- Satellite Radio Broadcast Availability and Signal Quality
  - Vehicular reception (L- and S-band)
- Fade Mitigation
    - Power control
    - Diversity (satellite, time, antenna)
    - Elevation angle
    - Environment and satellite orbit

A New Rain-Rate Distribution Model: Preliminary Version for Annual Statistics

R. K. Crane

School of Meteorology
University of Oklahoma
Norman, OK 73019

Prepared for NAPEX XXI

May 14, 1997

Abstract

The two-component model provides a rain-rate distribution prediction that is based on five parameters. The Crane-Global rain climate zone model provided the five parameters for each rain zone. The new, revised model provides a means to set the five parameters using locally available climate data. This report is preliminary because the procedure developed for setting the parameters requires data that are only available at slightly over 200 stations in the United States. Extension to other climate regions is still required. Because the locations within the United States that have data, have long records, the new model provides a large data base for use in the search for statistical relationships between the model parameters and climate data that are available world wide.

1. Introduction

Models for the prediction of the statistics of attenuation by rain for a particular site and propagation path are based on the predictions of an underlying rain-rate probability distribution model for the site location. Two types of rain-rate distribution prediction models are now available, 1) rain climate zone models for regions of the globe with an expected similarity in rain-rate distribution and 2) parameterized rain-rate distributions with explicit instructions for the use of local climate data to calculate the required distribution parameters. The climate zone was used to collect empirical distributions which were combined to establish the predicted distribution for that region. A climate region (or zone) model does not need an explicit representation for the rain-rate distribution; the tabulated median distribution of the observed distributions is sufficient. Parameterized distributions require the use of either a well defined probability model or a curve-fit model to represent the distribution over a limited probability or rain-rate range.

Early work in rain-rate distribution analysis had suggested the possible use of the following models to represent a rain-rate distribution: 1) a sum of exponential distributions (Rice and Holmberg, 1973), 2) a lognormal distribution (Lin, 1978; Morita and Higuti, 1978), 3) a gamma distribution (Morita and Higuti, 1971) and 4) a power-law distribution (Segal, 1979). In 1982, Crane suggested a two-component model that was the sum of an exponential and a lognormal distribution (Crane, 1982). Since then, the "log-gamma" (Maupfuma, 1985; Flavin, 1994) and Poisson (Tattelman, 1989) distributions have also been proposed.

The earliest distributions were constructed on the basis of simple hypotheses about the statistics of rain intensity. Empirical distribution functions (edfs) were not available for use in curve fitting or in testing the proposed model against observations. Rice and Holmberg used excessive precipitation data to fix one of the exponential distributions (for high rates) and hourly rain-rate accumulation data to fit another of the exponential

distributions (for low rates) and provided a smoothed connection between the high and low intensity regimes. Their distribution was engineered to depend on two climate parameters, the mean annual precipitation accumulation, M, and the ratio of the rain accumulation in the high rain-rate component of the distribution to M, the "thunderstorm" ratio, β. Lin argued for the lognormal distribution on the basis of a multiplicative model for rain production. He used excessive precipitation data to calculate two of the three parameters required for the model and M to establish the third parameter. The recently proposed parameterized distributions generally employ curve-fitting to rain-rate edfs to estimate the distribution parameters and a smoothed mapping to interpolate the parameters to other locations.

In this report, a new model is proposed for the determination of the parameters of the two-component model from locally available climate data. The earlier Rice-Holmberg and Lin models are revisited to explore the utility of those models and of the parameter estimation techniques used to complete each model. When these models were developed, adequate data were not available for model testing and validation. Over the past two decades a considerable body of annual empirical distribution functions have been gathered for use in model validation (ITU-R, 1994a). Sufficient data are now available to test these and other models and to provide a recommendation for the best model to use for rain-rate distribution estimation and in attenuation distribution prediction. This report is preliminary because the model development for the prediction of an annual rain-rate distribution is now complete for over 200 stations in the United States but the extension of the model to cover the rest of the United States and other countries is not finished. Also, a full test of the model using annual edfs from the available data banks must be performed.

2 Early Models

The parameterized Rice-Holmberg and Lin models and the climate zone Crane-Global and ITU-R (1995)models are generally used in attenuation modeling. The first two years of attenuation and rain-rate measurements from the ACTS Propagation Experiment has been used for the testing of the Rice-Holmberg, Crane-Global, and ITU-R models (Crane and Robinson, 1997). Testing results showed that "not one of the model combinations provided good predictions". This result supplies the impetus for this work.

The ACTS Propagation Experiment site with the largest collection of empirical rain-rate distribution functions (rain-rate edfs) for the site and nearby area is Reston, VA. Only one year of data is available from the tipping bucket gauge at the Reston site but three years of data are available from the earlier CTS measurement program at the nearby NASA Goddard Space Flight Center in Greenbelt, MD (Ippolito, 1981) and four more years of

observations are available from measurements at the COMSAT Laboratories in Clarksburg, MD (Kumar, 1984). These annual rain-rate edfs are presented in Figure 1 together with the predictions of the Crane-Global model. While, with the exception of Reston, VA for rain rates less than 5 mm/h and one of the Clarksburg edfs at the highest rain rate, the edfs lay between the upper and lower bounds (expected to enclose 90% of the edf observations) the observations at higher rain rates generally reveal a higher probability of occurrence than predicted. The DAH (Dissanayake et. al., 1996) and ITU-R (1995) attenuation prediction procedures use only the expected rain-rate value at 0.01% of a year. At this probability level, the edfs show higher rain-rate values than predicted. The median of the observed edfs at 0.01% of a year was 61 mm/h while the predicted median value was 49 mm/h. While there is a random, year-to-year variation in rain rate at a fixed probability level, a good model would pass through the center of the distributions (the median value).

2.1 The Rice-Holmberg Model

Rice and Holmberg did not have access to rain-rate edfs constructed from short term (one-minute average) observations (Rice and Holmberg, 1971). They did have the hourly precipitation data and excessive precipitation data from the National Climate Data Center. They used the hourly data to generate a model for the low rain-rate regime and the excessive precipitation data for high rain rates to engineer a plausible rain-rate distribution. They postulated that the highest 5-, 10-, 15-, 20-, 30-, 45- and 60-minute observations in a single excessive precipitation event were obtained from nested time intervals. They could then construct a segment of the rain-rate distribution for each year of observations that could be valid over the 0.001 to 0.01% of a year range. They analyzed more than 20 years of observations at 48 sites. They found 1) the high rain-rate distribution segments that they constructed could be modeled as exponential distributions and 2) the average rain-rate for the exponential distributions could be approximated as 33.3 mm/h for all the sites they considered.

Rice and Holmberg constructed empirical distributions from the hourly observations available at a large number of sites. They also modeled these low rain-rate (hourly) distributions by a second exponential distribution. Between the high and low rain-rate regimes, they fit a third exponential which would combine with the other two to produce a smooth distribution estimate. The average annual integrated rain accumulation produced by the highest rain-rate exponential distribution was identified as "thunderstorm" rain and the average annual accumulation produced by the triple exponential distribution was the average annual attenuation. With the average rain rate for each exponential segment fixed to either their average value for a number of sites and years or to an intermediate value that

smoothly interpolated between the high and low rain-rate regimes, only two parameters are needed to completely determine the entire distribution, M and β. For the sites and years used in constructing the distribution model, each of the exponential distributions could be set from the observations. Rice and Holmberg (1971) calculated the average M and β values for each of these sites. Figure 2 displays the result for Washington, DC together with the observations depicted in Figure 1.

The Rice-Holmberg model performs better that the Crane-Global model for this set of observations. At 0.01% of a year, it predicts a slightly higher rain rate than observed. The median of the observed edfs at 0.01% of a year was 61 mm/h while the predicted median value was 64 mm/h. Considering that the model was developed without the wealth of short term rain-rate edfs now available, it was a remarkable achievement.

A problem with this model is making predictions at sites different from any of the 48 sites used in generating the model. Rice and Holmberg sought proxy variables that could be used in the estimation of M and β without requiring the long (and generally unavailable) data records needed to generate the model. For world-wide application of the model, data available from national weather record centers would be needed. The average annual precipitation accumulation, M, is available in most countries but the thunderstorm ratio, β, is not generally available. They first tried the ratio of thunderstorm to rainy days. The thunderstorm day and rainy day statistics are available for many countries. Unfortunately the ratio did not prove to provide a good estimate of β. They found that they required an additional climate parameter, the largest monthly precipitation accumulation in 30 years to improve the estimate. The latter can be found in the Global Historical Climatology Network (GHCN) Global Climate data base available from the National Climate Data Center.

2.2 The Lin Model

Lin and his colleagues at Bell Laboratories also made use of the excessive precipitation data for the estimation of the expected rain-rate distribution. Lin used some of the same high rain-rate data as employed by Rice and Holmberg but applied a different methodology. The excessive precipitation data contains observations of the highest 5-minute precipitation values for each year. Extreme value statistics can be used to analyze such data (Gumbel, 1958). The high value extremes of observations from exponential, normal, or lognormal distributions, the highest value for each observation interval (i.e. a year or month), follow a type I extreme value distribution. If the number of samples in

each interval is known, the parameters of the distribution within an interval can be established. Lin used the properties of the type I extreme value distribution and the assumption of a lognormal distribution within an interval to obtain the parameters of the average rain-rate distribution within a year interval. The average number of samples in a year was obtained iteratively by requiring the average rain rate computed from the lognormal distribution times the number of samples to equal M, the annual average precipitation accumulation.

The results presented in Figure 3 were obtained using the procedure described by Lin (1978) and a 31-year excessive precipitation data set for Washington, DC. In this case, the model does not fit the observations. The median of the observed edfs at 0.01% of a year was 61 mm/h while the predicted median value was 77 mm/h. It produced a good fit to the data for rain rates above 80 mm/r but did poorly at lower rates. The problem is that the underlying probability distribution model for the higher rain-rate values is not lognormal. As used by Lin, the modeling errors were not important because, for the design of terrestrial radio relay systems, all but the extreme values of attenuation would be within the large system margins needed to accommodate atmospheric multipath. The Lin model cannot be used in the design of lower margin satellite communication systems.

3. The Revised Global Rain-Rate Model

The two-component model uses an exponential probability distribution model to provide predictions at high rain rates and a lognormal model for predictions at low rates. Extreme value statistics were used to set the parameters of the exponential component of the two-component model, the cell component.

3.1 The Cell Component, Predictions at High Rain Rates

Figure 4 presents the ordered distribution of the highest 5-minute accumulation in a year for two data sets from Washington, DC. The long record spans 31 years while the shorter record is for the last 8 years in the 31 year record. For this figure, the accumulation scale is linear as required to represent the extreme value distribution for either an exponential or a normal distribution (or a Weibull or a gamma distribution). The reduced variate is for the type I extreme value (double exponential) distribution. If the type I extreme value distribution were the correct distribution for the accumulation values, the ordered distribution would lie along a straight line. The ordered distribution is itself a random variable. To help judge agreement with the hypothesized distribution, the expected median (50%), upper (95%) and lower (5%) bounds for edfs drawn from the extreme value distribution are also plotted. The parameters for the extreme value distribution (α and

U of Gumbel, 1958; $\sigma_E = 1/\alpha$, μ_E = U of Bury, 1984) were computed using the unbiased estimation procedure developed by Kimball as reported by Bury. The upper and lower bounds can be used for a hypothesis test at the 0.1 significance level. If the 31-year ordered distribution lies entirely within the upper and lower bounding curves the hypothesis that the proposed model is the correct model cannot be rejected at the 0.1 significance level. The bounding curves for the 8-year distribution are further apart so, the correct model hypothesis cannot be rejected for either distribution.

The curve marked "Fit" in Figure 4 is the result of a linear regression analysis of accumulation on the reduced variate. The best "Fit" parameters were not used in the calculation of the median and bound curves. If the data had been censored the "Fit" parameters would have been used. The reporting procedures for excessive precipitation data were changed in 1973. Prior to 1973, the maximum observed accumulations in the several time intervals were reported for each excessive precipitation event. After 1972, the tabulated data were the maximum short duration precipitation observations, the highest accumulation values for each time interval in each month and year. The yearly extreme values used in this analysis can be obtained from either data set as long as an excessive precipitation event occurs every year. In the older data, no data were recorded if an excessive precipitation event did not occur. The observations were then censored at the low accumulation end of the extreme value distribution.

The two data points labeled NWS HYDRO-35 were extracted from maps of the extreme values expected with 2- and 100-year return periods for the central and eastern United States (Frederick et. al., 1977). The 100-year return period value is within the expected bounds for Washington, DC but the 2-year return period is not within bounds. The mapped values were averaged over a 4° latitude by 4° longitude region before the contour lines were drawn. The mapped values cannot be used to estimate the parameters of the underlying distribution.

Parameter estimation for the exponential model component of the annual distribution is straight forward. The slope of the Est. curve, when expressed as the average rain rate over a 5-minute interval rather than the accumulation within the interval, σ_E = 26.4 mm/h, is the average rain rate for the cell component, Rc, of the two-component model. It is also the best estimate of the average rain rate for the high rain-rate exponential distribution of the Rice-Holmberg model. The intercept, when expressed in mm/h, is the expected rain rate at 5-minutes per year (~0.001% of a year). From the exponential distribution assumption, the probability of a cell, Pcell, can be calculated from the slope, intercept and the ratio of 5-minutes to the length of an average year in minutes. Using Pcell and Rc, the

"thunderstorm" accumulation can be calculated and, given the annual accumulation, M, an improved estimate of β for the Rice-Holmberg model can also be calculated.

The extreme value distribution also applies if the underlying distribution is the lognormal distribution. In this case, the ordered distribution of the logarithm of the 5-minute accumulations must be plotted. Figure 5 presents the results. The 31-year ordered distribution strays outside the upper and lower bounds. Therefore, use of this model can be rejected at the 0.1 significance level. For this site, the lognormal model should not be used to represent the high rain-rate observations.

3.3 Predictions at Low Rain Rates

The two-component model uses the lognormal distribution for predictions at low rain rates. Rice and Holmberg employed the hourly data for the construction of the low rate distribution. Recently, 15-minute accumulation data have become available for over 4000 NWS and cooperative observer sites. These data were used to estimate the parameters of the lognormal component of the two-component distribution. Three parameters are needed, the median rain rate, the standard deviation of the logarithm of the rain rate and the probability of occurrence of this component of the two-component model. These parameters were calculated from the average rain accumulation in a 15-minute interval for an integral number of years, the standard deviation of the 15-minute accumulation values for an integral number of years and the average annual count of the number of 15-minute intervals that contain an accumulation value (one or more rain gauge tips). In determining the fraction of time it rains, the result must be adjusted for the quantization of the observations in tips per 15-minute interval. The lowest rain rate that can be observed is 1 mm/h so that only the fraction of time with rates greater than 1 mm/h can be obtain from the average count value. Using the lognormal model hypothesis, the total time that it rains can be obtained from the time with rain greater than 1 mm/h and the time with rain in the cell component of the model.

The spatial correlation function for the logarithm of the rain rate (the lognormal component of the rain-rate process) was obtained from weather radar observations (Crane, 1989). This component of the rain process is highly correlated over distances measured in kilometers. The correlation coefficient for the logarithm of rain rate is higher than 0.8 for distances less than 10 km. At normal rain translation velocities, the temporal correlation function remains high over intervals of 5 to 15 minutes. Therefore, the 15-minute accumulation values provide good estimates of the average and standard deviation values for the lognormal component of the process.

3.3 The Complete Model

Figure 6 presents the results of using the excessive precipitation and 15-minute accumulation data to provide the local climate information needed to calculate the parameters of the two-component model. The new model prediction compares favorably with the observed rain-rate edfs over the entire range of rain-rate values. At 0.01% of a year it predicted the median value for the edfs with an error of 1 mm/h.

4.0 Conclusions and Future Work

The new procedure for estimating the parameters of the two-component model provides a good estimate of the expected rain-rate distribution for a small area about Washington, DC. This is but one site in the United States. Next, the model must be tested against the rest of the ACTS Propagation Experiment data and data in the ITU-R rain-rate data base.

To extend the model for use at locations far from a first order NWS observing station within the United States, a set of proxy variables must be established that can be used to calculate the two-component model parameters. This problem is simplified because the maximum short duration precipitation data are now available for monthly intervals from over 200 sites in the United States and the 15-minute accumulation data are available from a denser network of gauges. These data can be used to estimate the two-component model parameters for each location with data and to determine statistical relationships between these parameters and the long-term climate data that are available world wide.

References

Bury, K. V. (1986): *Statistical Models in Applied Science*, Krieger Publ. Co., Malabar, FL, Chapter 11.

Crane, R. K. (1982): "A two-component rain model for the prediction of attenuation statistics", *Radio Science*, **17(6)**, 1371-1387.

Crane, R. K. and H-C Shieh, (1989): "A two-component rain model for the prediction of site diversity improvement performance", *Radio Science*, **24**(6), 641-655.

Crane, R. K. and P. Robinson, (1997): "ACTS Propagation Experiment: Rain-Rate Distribution Observations and Prediction Model Comparisons", *Proc IEEE*, accepted for publication.

Dissanayake, A. W. , J. E. Allnutt and F. Haidara, (1996): "A prediction model that combines rain attenuation and other impairments along earth-space paths", *IEEE Trans Antennas and Propagat*, submitted, 1996.

Flavin, R. K. (1994): Modelling of Rainfall Rate Distributions for Various Cities in Australia, Rept 8292, Telecom Australia Research Laboratories, Clayton, VIC 3168.

Frederick, R. H., A. A. Myers and E. P. Auciello, (1977): Five- to 60-minute Precipitation Frequency for the Eastern and Central United States, NOAA Tech. Memo. NWS HYDRO-35, NOAA Office of Hydrology, Silver Spring, MD.

Gumbel, E. J. (1958): *Statistics of Extremes*, Columbia Univ. Press, New York.

Ippolito, L. J., (1981): "Radio propagation for space communication systems, *Proc IEEE*, **69**, 697-722.

ITU-R, (1994a): Acquisition, presentation and analysis of data in studies of tropospheric propagation, Recommendation ITU-R PN.311-7, 1994 PN Series Volume Propagation in Non-Ionized Media, International Telecommunications Union, Geneva.

ITU-R, (1994b): Characteristics of precipitation for propagation modeling, Recommendation ITU-R PN.837-1, 1994 PN Series Volume, Propagation in Non-Ionized Media, International Telecommunications Union, Geneva, 1994.

ITU-R, (1995): Propagation data and prediction methods required for earth-space telecommunication systems, Recommendation ITU-R P.618-4, 1995 P Series Fascicle Radiowave Propagation, International Telecommunications Union, Geneva.

Kumar, P. (1984): Private communication.

Lin, S. H. (1978): "More on Rain rate Distributions and Extreme Value Statistics", *Bell Sys. Tech. Jour.*, **57(5)**, 1545-1568.

Morita, K. and I. Higuti, (1971): "Statistical studies in electromagnetic wave attenuation due to rain", *Rev. Elect. Comm. Lab (Japan)*, **19**, 789-842.

Morita, K. and I. Higuti, (1978): "Statistical studies on rain attenuation and site diversity effect on earth to satellite links in microwave and millimeter wavebands", *Trans. Inst. Electron. Commun. Eng. Jpn.)*, **E61**, 425-432.

Moupfuma, F, (1985): "Model of rainfall rate distribution for radio system design", *IEE Proc*, **132H(1)**, 39-43.

Rice, P. L. and N. R. Holmberg (1971): Unpublished Appendix A on Cumulative Time Statistics of Surface Rainfall Rates

Rice, P. L. and N. R. Holmberg (1973): "Cumulative Time Statistics of Surface-Point Rainfall Rates", *IEEE Trans Commun.*, **COM-21(10)**, 1131-1136.

Segal, B., (1979): High-intensity rainfall statistics for Canada, CRC Rept 1329-E, Communications Research Centre, Ottawa.

Tattelman, P., (1989): "New rain rate analyses to assess rain attenuation on satellite EHF communications", *I. Jour. Satellite Commun.*, **7**, 23-35.

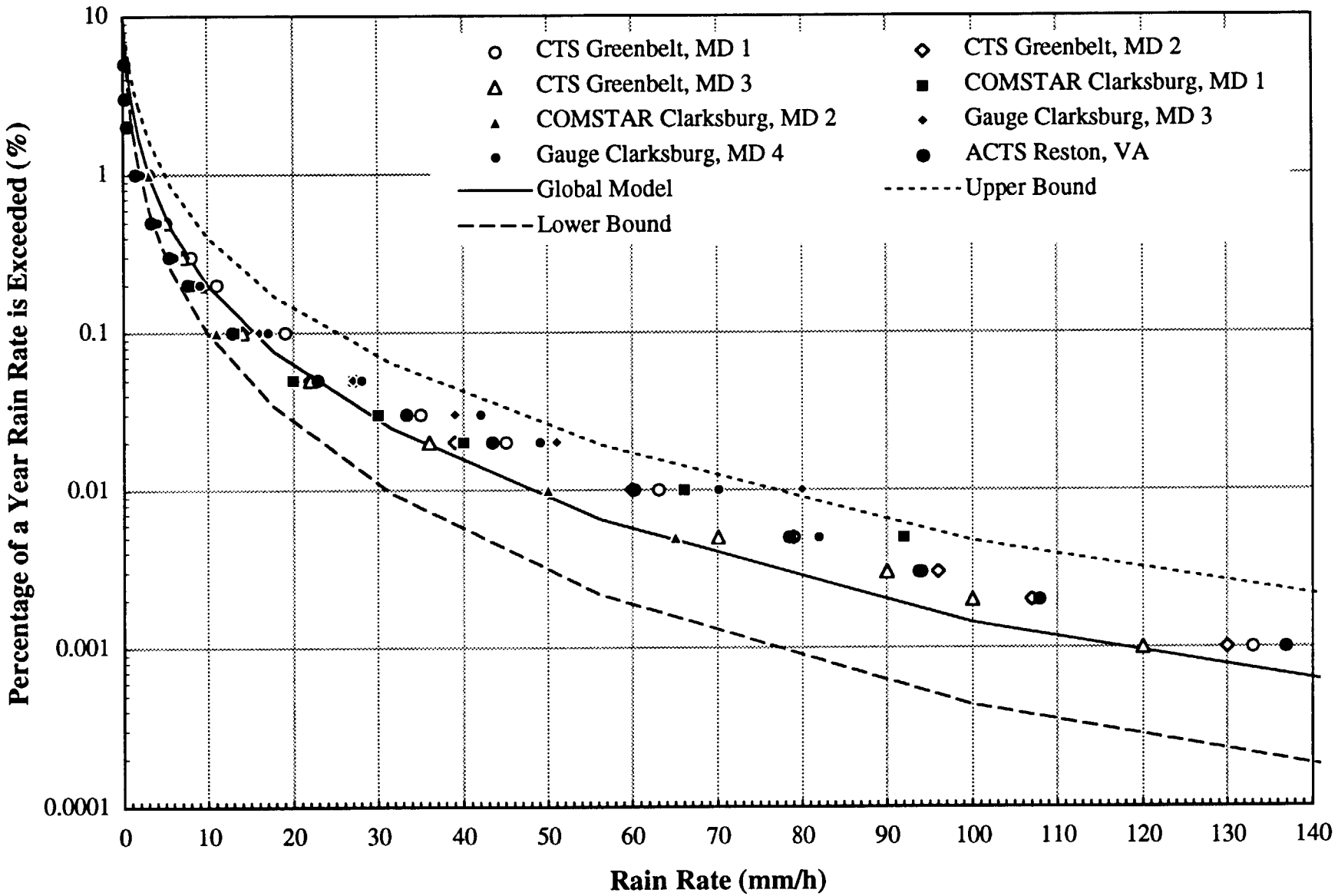

Figure 1 Rain rate empirical distribution functions for the Washington, DC area and Crane-Global model predictions

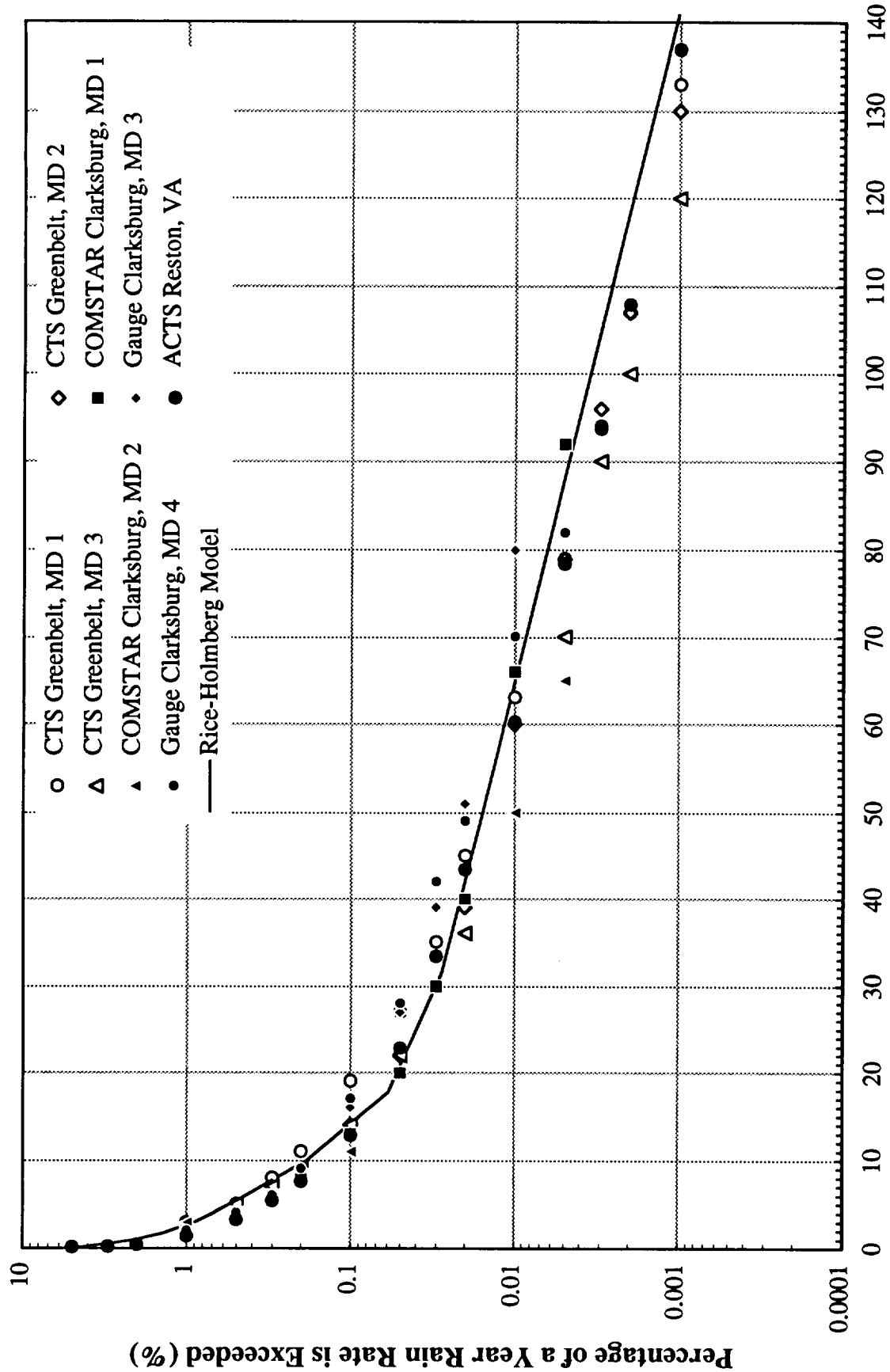

Figure 2 Rain rate empirical distribution functions for the Wasgington, DC area and Rice-Holmberg model predictions

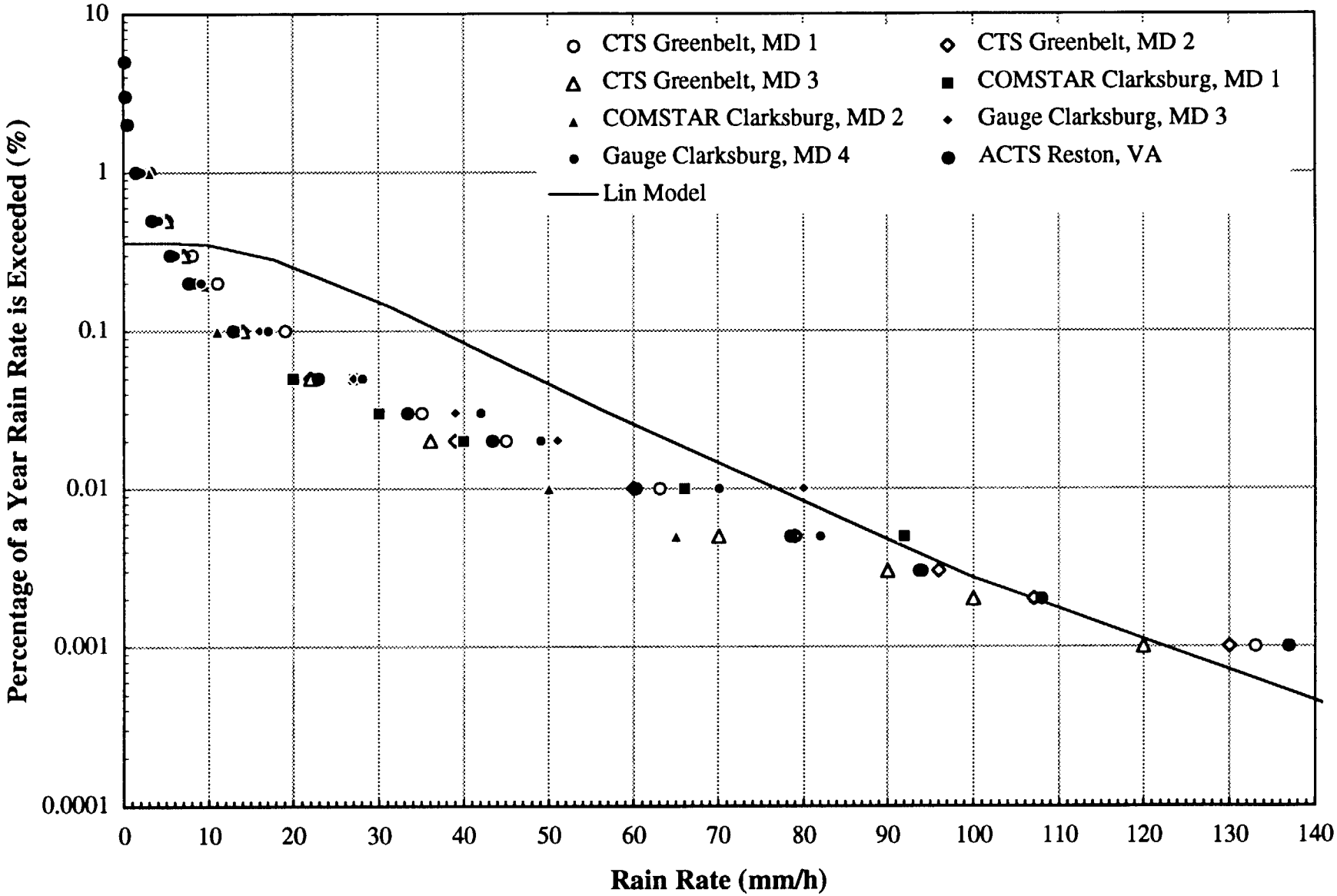

Figure 3 Rain rate empirical distribution functions for the Washington, DC area and Lin model predictions

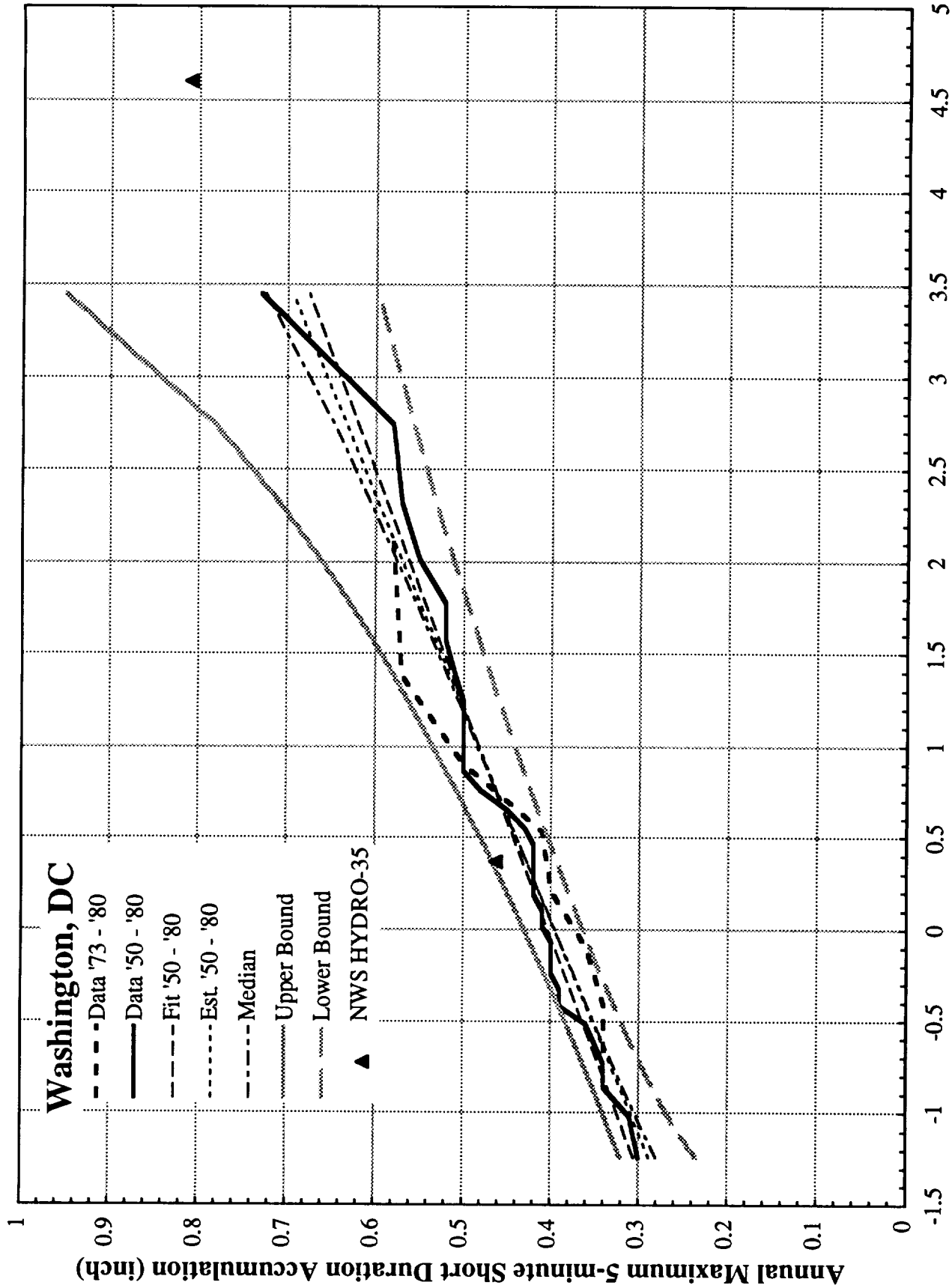

Figure 4 Ordered distribution of the annual maximum 5-minute short duration precipitation values for Washington, DC

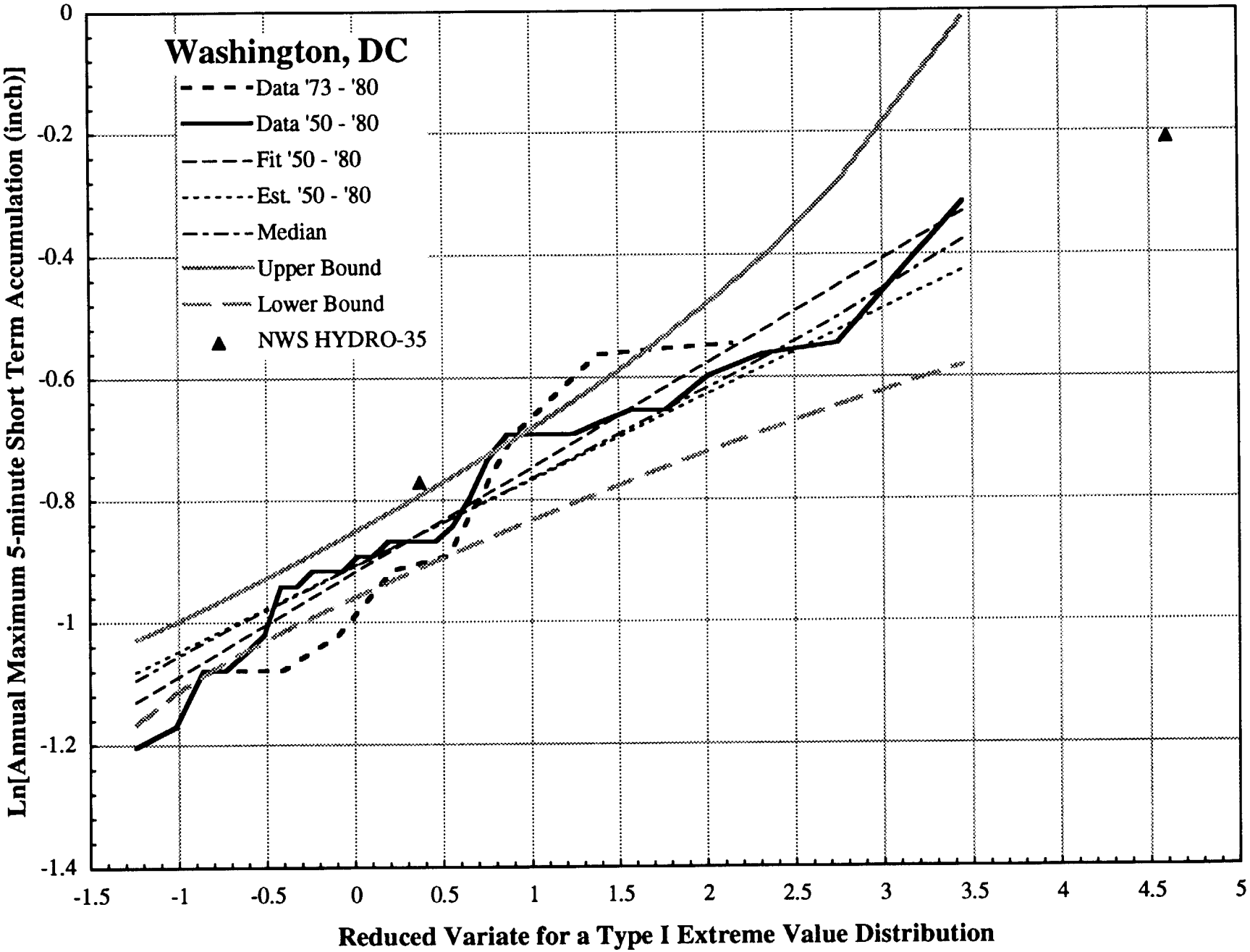

Figure 5 Ordered distribution of the Ln[annual maximum 5-minute short duration precipitation] values for Washington, DC

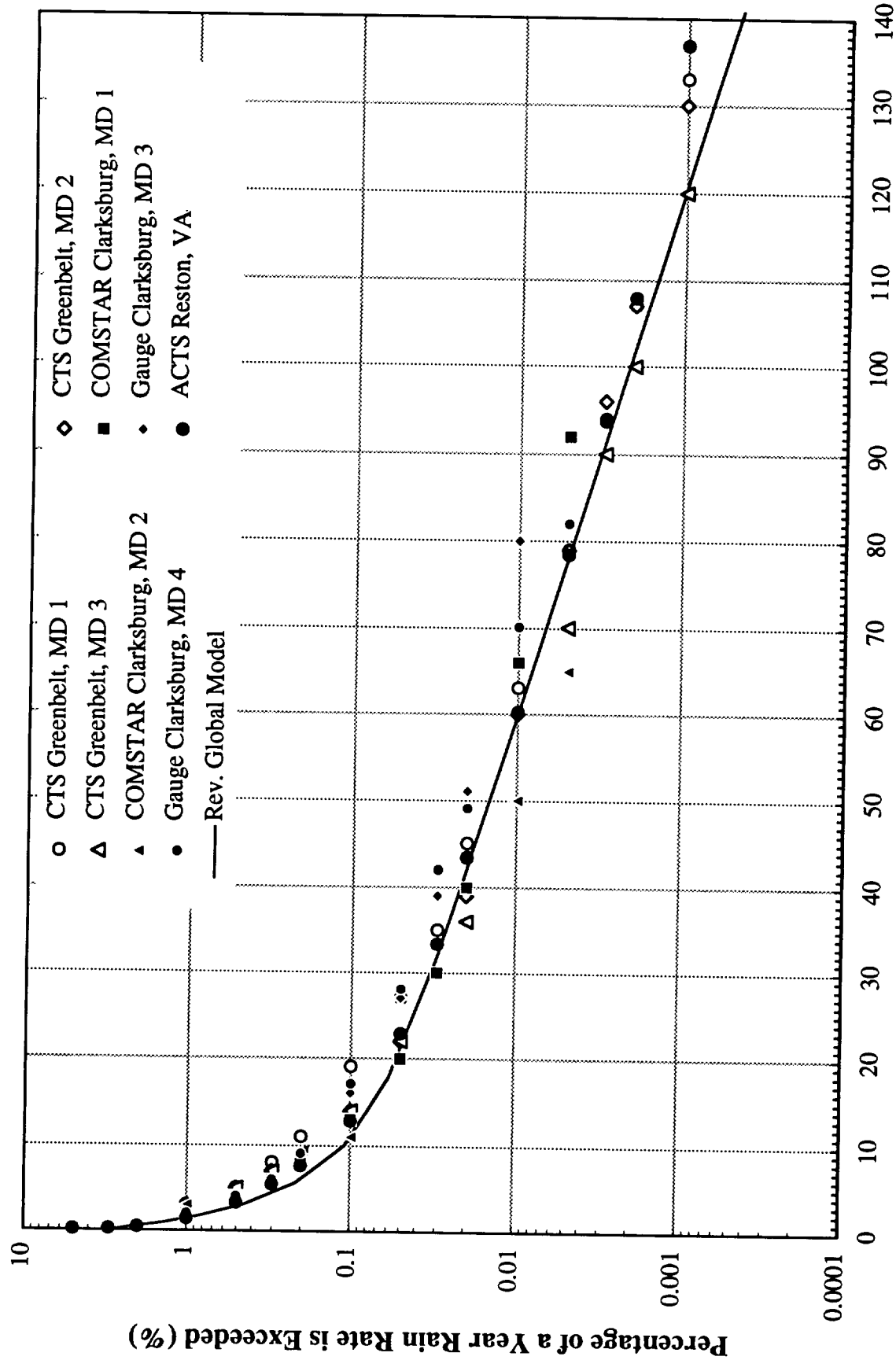

Figure 6 Rain rate empirical distribution functions for the Washington, DC area and the revised global model predictions

FADE DYNAMICS AND ITS EVOLUTION: THE OTHER PART OF THE ACTS RAIN PREDICTION MODEL

Robert M. Manning
Space Communications Office
National Aeronautics and Space Administration
Cleveland, OH 44135

Introduction

The inception of the Advanced Communication Technology Satellite (ACTS) Project has required a similarly advanced statistical mathematical modeling formalism to describe the behavior of the 30/20 GHz links emanating to and from the earth terminals through the deleterious effects of the earth's atmosphere. The resulting ACTS Rain Attenuation Prediction Model has been thoroughly described in [*Manning*, 1990]. In the present paper, the basic rudiments of this model will be reviewed; Section 1 covers the static or time-independent portion of the model and Section 2 covers the dynamic or time-dependent portion. The results of Section 2 are then applied to a new approximate solution of the famous problem of the time duration τ of a fade of a random process below some threshold. This is known as the fade duration. The new approximate solution was published in Russian [*Denisenko*, 1975] and, unfortunately, was never published into English. Hence, this work is restated following [*Denisenko*, 1975] in Section 3 which is immediately applied to the random rain fade process. The results for all five ACTS propagation sites as well as Tampa, FL are then given.

1. A Brief Review of the Description of Time-Independent Rain Attenuation

As discussed in the original work [*Manning*, 1990], appeal is made to physical considerations that dictate a conditional log-normal probability density function governing the log-rainrate:

$$p(\ln R|\text{Rain at Point}) = \sqrt{\frac{1}{2\pi\sigma^2_{\ln R}}}\exp\left(\frac{(\ln R - \ln R_m)^2}{2\sigma^2_{\ln R}}\right) \qquad (1)$$

for the occurrance of rain at a point on the ground. Hence, the corresponding cumulative probability distribution for the rainrate r being less then a given rainrate R is given by

$$P(r<R)=P_0\left[1-\frac{1}{2}\mathrm{erfc}\left(\frac{\ln R-\ln R_m}{\sqrt{2}\sigma_{\ln R}}\right)\right] \tag{2}$$

Here, P_0 is the probability of rain occurring at the point, R_m is the mean rainrate, and $\sigma_{\ln R}$ is the standard deviation of the logarithm of the rainrate; all three of these quantities ate strongly dependent on the location of interest. The analogous description for the specific attenuation is easily found to be

$$P(\gamma<\Gamma)=P_0\left[1-\frac{1}{2}\mathrm{erfc}\left(\frac{\ln\Gamma-\ln\Gamma_m}{\sqrt{2}\sigma_{\ln\Gamma}}\right)\right] \tag{3}$$

where the associated mean and standard deviation are

$$\Gamma_m=aR_m^b \tag{4}$$

and

$$\sigma_{\ln\Gamma}=b\sigma_{\ln R} \tag{5}$$

where a and b are the frequency dependent quantities that originate in the "aR^b relationship" for specific attenuation. Finally, one can obtain the associated probabilistic description for total path attenuation. It has the form of the foregoing, viz.,

$$P(a<A)=P_0(L,\theta)\left[1-\frac{1}{2}\mathrm{erfc}\left(\frac{\ln A-\ln A_m}{\sqrt{2}\sigma_{\ln A}}\right)\right] \tag{6}$$

where $P_0(L,\theta)$ is the probability of rain on the extended propagation path and is given by

$$P_0(L,\theta)=1-(1-P_0)\left[1+\frac{L^2\cos^2\theta}{21.5}\right]^{-0.014} \tag{7}$$

where θ is the elevation angle of the link. The variance of the log-attenuation is related to previously defined quantities by

$$\sigma^2_{\ln A}(L,\theta) = \ln\left[P_0(L,\theta)\left\{ K(L,\theta)\left(\frac{\exp\left(\sigma^2_{\ln\Gamma}\right)}{P_0} - 1 \right) + 1 \right\} \right] \qquad (8)$$

which also employs $K(L,\theta)$, the spatial correlation coefficient for rain cells,

$$K(L,\theta) = \left(\frac{2}{L^2} \right) L_C \sec\theta \left[L - L_C \sec\theta \left\{ 1 - \exp\left(-\frac{L\cos\theta}{L_C} \right) \right\} \right] \qquad (9)$$

where the fundamental correlation length is $L_C = 4.0\,\text{km}$. Finally, the mean attenuation is related to previously defined quantities by

$$A_m(L,\theta) = \frac{P_0 L \Gamma_m}{P_0(L,\theta)} \exp\left(\frac{\sigma^2_{\ln\Gamma} - \sigma^2_{\ln A}}{2} \right) \qquad (10)$$

Equations (2)-(10) essentially constitute the time-independent (or static) rain attenuation prediction model developed for the ACTS Project. The model yields excellent results with observation [*Manning*, 1990]. The parameters, P_0, R_m, and $\sigma_{\ln R}$ are all location-dependent and must be extracted from the long-term meteorological record [*Manning*, 1990]. Such a situation prevents the ability to obtain the temporal evolution of rain fade on a link; that is, the temporal evolution of rainrate (and thus attenuation) on time scales of seconds or minutes is lost due to the climatological record-keeping process that has been used in this country for over 80 years.

2. A Brief Review of the Description of Time-Dependent Rain Attenuation

It is assumed that the random process that 'drives' the rainrate is a Markov process (or a process without aftereffect). Thus, assuming that the time dependent rainrate $R(t)$ observed at a point is a first order Markov process allows one to write the following first order stochastic differential equation governing the process at this point:

$$\frac{dR(t)}{dt} = f(R,t) + g(R,t)\xi(t) \qquad (11)$$

Here, the deterministic functions $f(R,t)$ and $g(R,t)$, commonly known as the drift and diffusion coefficients, respectively, are in the most general case, functions of both R and t. The function $\xi(t)$ is taken to be a Gaussian random process that satisfies the conditions

$$\langle \xi(t) \rangle = 0, \quad \langle \xi(t_1)\xi(t_2) \rangle = \delta(t_1 - t_2) \tag{12}$$

which define a white noise process. Since $R(t)$ in Eq.(11) is also a random function, one can only deal with statistical parameters that describe its behavior. One of the most important of these parameters is the transition probability density function (TPDF) $p\left(R(t),t \middle| R(t_0),t_0\right)$ that describes how $R(t)$ evolves from time t_0 to the time t, $t > t_0$. As is well known [*Stratonovich*, 1963], for a Markov process that is given by Eqs.(11) and (12), the associated TPDF $p \equiv p\left(R(t),t \middle| R(t_0),t_0\right)$ is given by

$$\frac{\partial p}{\partial t} + \frac{\partial}{\partial R}\left(f(R,t)p\right) - \frac{1}{2}\frac{\partial^2}{\partial R^2}\left(g^2(R,t)p\right) = 0 \tag{13}$$

which is the Fokker-Planck-Kolmogorov equation for the problem. Finally, the drift and diffusion coefficients are given in terms of the first two conditional moments of the process $R(t)$ by the relations

$$\begin{aligned} f(R,t) &= \lim_{\Delta t \to 0} \frac{\left\langle \left(R(t+\Delta t) - R(t) \middle| R(t)\right)\right\rangle}{\Delta t} \\ g(R,t) &= \lim_{\Delta t \to 0} \frac{\left\langle \left(R(t+\Delta t) - R(t) \middle| R(t)\right)^2 \right\rangle}{\Delta t} \end{aligned} \tag{14}$$

Following the procedures as set forth in the original reference [*Manning*, 1990], one obtains for the TPDF of $R(t)$:

$$\begin{aligned} &\frac{\partial p}{\partial t} - \gamma \frac{\partial}{\partial x_R}\left(x_R p\right) - \gamma \frac{\partial^2 p}{\partial x_R^2} = 0 \\ &p \equiv p\left(x_R(t),t \middle| x_R(t_0),t_0\right) \end{aligned} \tag{15}$$

where

$$x_R(t) = \frac{\ln R(t) - \ln R_m}{\sigma_{\ln R}}$$

which is a well known form in the theory of Brownian motion; the corresponding stochastic differential equation is

$$\frac{dx_R}{dt} = -\gamma x_R + \sqrt{2\gamma}\xi(t) \tag{16}$$

Here, γ is a characteristic temporal decay parameter peculiar to the rainrate process; base on empirical data, γ= 0.111 min^{-1} The solution of the Kolmogorov equation, Eq.(15), yields for the TPDF of rainrate events at a point characterized by the parameters R_m, $\sigma_{\ln R}$, and γ, [*Stratonovich*, 1963]

$$p\left(R(t),t\middle|R(t_0),t_0\right) = \sqrt{\frac{1}{2\pi\sigma^2_{\ln R}(\Delta t)}}\exp\left[-\frac{\left(\ln R(t) - \ln R_m(\Delta t)\right)^2}{2\sigma^2_{\ln R}(\Delta t)}\right] \tag{17}$$

where $\Delta t = t - t_0$ and the time dependent mean $R_m(\Delta t)$ and standard deviation $\sigma_{\ln R}(\Delta t)$ are given by

$$\begin{aligned} R_m(\Delta t) &= R_m^{(1-\exp(-\gamma\Delta t))}R_0^{\exp(-\gamma\Delta t)}, \quad R_0 \equiv R(t_0) \\ \sigma_{\ln R}(\Delta t) &= \sigma_{\ln R}\sqrt{1-\exp(-2\gamma\Delta t)} \end{aligned} \tag{18}$$

As $\Delta t \to \infty$, $R_m(\Delta t) \to R_m$, $\sigma_{\ln R}(\Delta t) \to \sigma_{\ln R}$ and Eq.(17) becomes the conditional PDF governing the static rainrate model of Section 1.

Having secured a temporal description of the rainrate process, one can continue to obtain specific attenuation time statistics. Thus, Eqs.(15) - (18) hold with the transcriptions $R_m \to \Gamma_m = aR_m^b$ and $\sigma_{\ln R} \to \sigma_{\ln\Gamma} = b\sigma_{\ln R}$. In particular, the stochastic differential equation governing Γ is

$$\frac{dx_\Gamma}{dt} = -\gamma x_\Gamma + \sqrt{2\gamma}\xi(t), \quad x_\Gamma \equiv \frac{\ln\Gamma - \ln\Gamma_m}{\sigma_{\ln\Gamma}} \tag{19}$$

The transition from the specific attenuation at a point to the attenuation along an extended path can be difficult and must be done with care. Without the use of a detailed physical description of the structure of the spatial behavior of rainrate along such a path, one at-

tempts to build upon previous knowledge with the desire to keep the prevailing physical assumptions to a minimum. Leaving all essential details to the original work [*Manning*, 1990], one has the following description for attenuation on an extended path. A first-order markov process is again used that employs an associated temporal parameter γ_1 that concactenates only the essential factors into it. This results in

$$\frac{dx_A}{dt} = -\gamma_1 x_A + \sqrt{2\gamma_1}\xi(t) \tag{20}$$

where the above-mentioned parameter γ_1 of this one-dimensional model reflects the smoothing (temporal averaging) process due to the extended propagation path. The value for γ_1 is found from the transcendental equation

$$\exp(-\gamma T) + \exp(-\gamma_S T) = \exp(-1) \tag{21}$$

the solution of which gives the value of T, which, in turn, yields the corresponding value for $\gamma_1 = 1/T$. The temporally-smoothed parameter γ_S, which connects the relavent link parameters as well as the temporal parameter $\gamma = 1/\tau$ for the point rainrate process is found from

$$\tau_S = \tau\sqrt{\left(1 + \frac{2L\cos\theta}{\pi R_C}\right)}$$

where $\gamma_S = 1/\tau_S$.

This finally completes the review of the rain attenuation prediction model formulated seven years ago. It now remains to discuss in depth the topic of rain fade durations and show how a solution to this problem issues from a new approximate soluition of the well-known problem of fades and surges of random processes.

3. Derivation of an Expression for Fade Duration.

As is well-known, the time duration τ of a surge or fade of a random process is a random variable. The calculation of the PDF of τ presents severe mathematical difficulties and has a well-known history [*Rice*, 1958]; an exact expression for this PDF of τ for a general random process remaines unknown. An approximation for such a PDF has been obtained in [*Rice*, 1958] but a more usefull, general , and in some

respects, more exact expression has been derived in [*Denisenko*, 1975].

The basis for Denisenko's work is the ability of finding the distribution function of the fade duration by using an estimate of an n-dimentional distribution by the nth power of a one-dimentional distribution based on $n-1$ conditions. Unfortunately, this reference never was translated into the English language and remains largly unknown. Here, this work will be thouroughlly reconstructed with the application of the results established for the dynamics of rain attenuation given in Section 2. For those readers who do not want to pour over such a mathematical discourse, they are referred to the final result below, Eq.(40).

Let $y(t)$ be a stationary random process and let t_Y be the time (as measured from an arbitrary origin) that the magnitude of y exceeds the level Y, i. e., $y(t_Y) > Y$. One can now define the following problem: given that $y(t_Y) > Y$, what is the conditional probability that $y(t) > Y$ for the times $t_Y < t < t_Y + \tau$? Let this conditional probability be given by $P\big(y(t_Y + \tau) > Y(t_Y > Y)\big)$. It is expediant to divide the time interval τ into n intervals such that

$$\tau = n\Delta\tau \tag{22}$$

One can now approximatly write the probability of the single event that $y(t) > Y$ when $t_Y < t < t_Y + \tau$ as a joint probability that the n events $y_n(t) > Y$ occur, each for one of the sub-intervals $\Delta\tau$, i.e., $y_n(t) > Y$ for each t such that $t = t_Y + n\Delta\tau$. Thus, one has

$$P\big(y(t_Y + \tau) \geq Y \big| y(t_Y) \geq Y\big) \approx P\big(y(t_Y + \tau) \geq Y, y(t_Y + 2\tau) \geq Y, \cdots$$

$$\cdots, \geq y(t_Y + n\Delta\tau) \big| y(t_Y) \geq Y\big) \tag{23}$$

Using the simplified notation $y_i \equiv y\big(t_Y + i\Delta\tau\big)$, employing the theorem of joint probability (Bayes' Theorem) gives

$$P\big(y(t_Y + \tau) \geq Y \big| y(t_Y) \geq Y\big) \approx \frac{P\big(y_0 \geq Y, y_1 \geq Y, \cdots y_n \geq Y\big)}{P\big(y_0 \geq Y\big)} \tag{24}$$

Considering the limit $n \to \infty$ where, necessarily, $\Delta t \to 0$, Eq.(23) becomes the equality

$$P\left(y(t_Y+\tau)\geq Y\middle|y(t_Y)\geq Y\right)=\frac{1}{P\left(y_0\geq Y\right)}\lim_{n\to\infty(\Delta\tau\to 0)}P\left(y_0\geq Y,y_1\geq Y,\cdots y_n\geq Y\right) \tag{25}$$

Since the values of y_i, $i=0,1,\cdots,n$ are taken to exceed the level Y during the time interval τ, then the point at which this level Y is crossed where $y_i(t_1)<Y$ will occur at some time $t_1\geq t_Y+\tau$. Therefore, the probability $P\left(y(t_Y+\tau)\geq Y\middle|y(t_Y)\geq Y\right)$ can be taken to be that of the time interval τ that the random process y remains above some fixed level Y. Thus, letting $P_Y\left(t\geq\tau\middle|y\geq Y\right)$ be the conditional probability that a level Y is exceeded for a time interval t that is longer than some given value τ (such an event is called a surge above the level Y), one has

$$P_Y\left(t+\tau\middle|t\geq Y\right)=P\left(y(t+\tau)\geq Y\middle|y(t)\geq Y\right) \tag{26}$$

In order to determine this function, it is necessary to find the value of the limit required in Eq.(25). Hence, one needs an expression that describes the general n-dimensional distribution function for the y_i quantitues. However, even in the simplest case of a normal process (which will be dealt with here), such an expression becomes unwieldy even for $n\geq 3$. Another approximate solution must be used.

The right hand side of Eq.(24) can be written as

$$\frac{P\left(y_0\geq Y,y_1\geq Y,\cdots y_n\geq Y\right)}{P\left(y_0\geq Y\right)}=P(1|0)P(2|1,0)\cdots P(n|n-1,\cdots 1,0) \tag{27}$$

where $P(i|i-1,\cdots 1,0)$ is the conditional probability that the event $y_i\geq Y$ occurs, given that the events $y_{i-1}\geq Y,\cdots y_0\geq Y$ have occurred. Taking into account that

$$P(i|i-1,\cdots,1,0)\leq P(i|i-1) \tag{28}$$

one obtains, from Eq.(27),

$$\frac{P\left(y_0\geq Y,y_1\geq Y,\cdots y_n\geq Y\right)}{P\left(y_0\geq Y\right)}\leq P^n(i|i-1)=P^n\left(y(t+\tau/n)\geq Y\middle|y(t)\geq Y\right) \tag{29}$$

Finally, using equations (25) and (26),

$$P_Y(t \geq \tau | y \geq Y) = \lim_{n\to\infty} P\left[y(t+\tau/n) \geq Y | y(t) \geq Y\right]^n$$

$$= \lim_{n\to\infty} \frac{P\left[y(t+\tau/n) \geq Y | y(t) \geq Y\right]^n}{P(y(t) \geq Y)} \tag{30}$$

where the last line follows from application of Bayes' Theorm once again. Equation (30) represents a solution to the problem of the probability of the time interval τ that a random process y remains above some given level Y. This solution essentially estimates an n-dimensional distribution by the n-th power of a one dimensional distribution based on $n-1$ conditions; in the limit that $n \to \infty$, the distribution of $P_Y(t \geq \tau | y \geq Y)$ is obtained. The statistics of the process $y(t)$ enters into the problem through the expression for the joint probability distribution $P(y(t \geq \tau/n) \geq Y, y(t) \geq Y)$. In the case considered here, the process is the attenuation due to rain that occurs on a communications link and the prevailing statistics are, as mentioned in Section 1, log-normal. What is the same thing, the process $y(t)$ can be taken to be the logarithim of attenuation for which the statistics are normally distributed. In this later case, one can write, using the well known equation for the bivariate normal distribution and making the identifications $y(t) \equiv \ln A(t)$ and $Y \equiv \ln A_0$, one has

$$P\left[a(t+\tau/n) \geq A_0, a(t) \geq A_0\right] = P_0(L,\theta) P\left[a(t+\tau/n) \geq A_0, a(t) \geq A_0 \,|\, \text{Rain on Link}\right]$$

$$= P_0(L,\theta)\left(\frac{1}{2\pi\sigma^2_{\ln A}\sqrt{1-R^2(\Delta\tau)}}\right) \cdot$$

$$\cdot \int_{\ln A_0}^{\infty}\int_{\ln A_0}^{\infty} \exp\left[\frac{(x_1-a)^2 - 2R(\Delta\tau)(x_1-a)(x_2-a) + (x_2-a)^2}{2\sigma^2_{\ln A}\sqrt{1-R^2(\Delta\tau)}}\right] dx_1 dx_2 \tag{31}$$

where $R(\Delta\tau)$ is the temporal correlation coefficient of the attenuation process that , in general, can be a function of the time interval $\Delta\tau = \tau/n$ and all other parameters that have been previously defined. If $\Delta\tau$ is small, the conditional joint probability

$$P_C(\Delta\tau) \equiv P\left[a(t+\Delta\tau) \geq A_0, a(t) \geq A_0 | \text{Rain on Link}\right)$$

can be expanded about the point $R(0)$ in a Taylor series, i.e.,

$$P_C(\Delta\tau) = P_C(0) + \left[\frac{dP_C(\Delta\tau)}{dR(\Delta\tau)} \frac{dR(\Delta\tau)}{d(\Delta\tau)}\right]_{\Delta\tau=0} \Delta\tau + \cdots$$

Performing the required calculations, simplifying, and noting that

$$P_C(0) = P\left[a(t) \geq A_0, a(t) \geq A_0 | \text{Rain on Link}\right] =$$
$$= P\left[a(t) \geq A_0 | \text{Rain on Link}\right]$$

one obtains

$$P_C(\Delta\tau) \approx P\left[a(t) \geq A_0 | \text{Rain on Link}\right] + \frac{(-R''(0))^{1/2}}{2\pi} \exp\left(\frac{(\ln A_0 - \ln A_m)^2}{2\sigma_{\ln A}^2}\right)\Delta\tau \tag{32}$$

where $R''(\Delta\tau)$ denotes the second time-derivative of $R(\Delta\tau)$. Substituting Eq.(32) into (30) and noting the first line of Eq.(31) gives, after simplification,

$$P_{A_0}\left(t \geq \tau | a \geq A_0\right) = \lim_{n\to\infty}\left[1 - \alpha\frac{\tau}{n}\right]^n$$
$$= \exp(-\alpha\tau) \tag{33}$$

where

$$\alpha \equiv \frac{P_0(L,\theta)(-R''(0))^{1/2} \exp\left[-(\ln A_0 - \ln A_m)^2 / 2\sigma_{\ln A}^2\right]}{2\pi P\left(a(t) \geq A_0\right)} \tag{34}$$

since one has that

$$P\left(a(t) \geq A_0\right) = P_0(L,\theta) P\left[a(t) \geq A_0 | \text{Rain on Link}\right]$$

and, as was shown in Section 1,

$$P(a(t) \geq A_0 | \text{Rain on Link}) = \frac{1}{2}\text{erfc}\left(\frac{\ln A_0 - \ln A_m}{\sqrt{2}\sigma_{\ln A}}\right)$$

Equation (34) can now also be written as

$$\alpha \equiv \frac{(-R''(0))^{1/2}\exp\left[-(\ln A_0 - \ln A_m)^2/2\sigma_{\ln A}^2\right]}{\pi\,\text{erfc}\left[\ln A_0 - \ln A_m/\sqrt{2}\sigma_{\ln A}\right]} \tag{35}$$

It now remains to find the value for the second derivative of $R(\Delta\tau)$ evaluated at $\Delta\tau = 0$. For this, one must go back to the stochastic differential equation adopted to describe the attenuation process, viz., Eq. (20). To find the correlation function of the process defined by Eq.(20), one makes use of the Wiener-Khintchine Theorem: Taking the temporal Fourier transform of Eq.(20), forming the normalized power spectrum and inverse transformong the result yields

$$R(\Delta\tau) = \exp(-\gamma_1\Delta\tau) \tag{36}$$

Following the prescription given in [*Beckmann*, 1967] for obtaining the second derivative of Eq.(36) and setting $\Delta\tau = 0$ finally gives

$$R''(0) = -\gamma_1^2$$

Substituting this result into Eq.(35) and using the definitions of Eq. (20) gives

$$\alpha = \frac{\gamma_1}{F(X_0)} \tag{37}$$

where

$$F(X_0) \equiv \pi\,\text{erfc}\left(\frac{X_0}{\sqrt{2}}\right)\exp\left(\frac{X_0^2}{2}\right), \qquad X_0 \equiv \frac{\ln A_0 - \ln A_m}{\sigma_{\ln A}} \tag{38}$$

Combining Eqs.(33) and (37) gives

$$P_{A_0}(t \geq \tau | a \geq A_0) = \exp\left(-\frac{\gamma_1\tau}{F(X_0)}\right) \tag{39}$$

It now remains to multiply this conditional probability by the cumulative probability $P(a \geq A_0)$ to obtain the desired result, i. e.,

$$P_{A_0}(t \geq \tau) = \frac{1}{2} P_0(L,\theta) \operatorname{erfc}\left(\frac{X_0}{\sqrt{2}}\right) \exp\left(-\frac{\gamma_1 \tau}{F(X_0)}\right) \qquad (40)$$

The application of Eq.(40) will be made for six locations in the continental U.S. This relation is in fact built into the software package that implements the ACTS Rain Model, viz., the LeRC-SLAM Program [*Manning*, 1989]. This program, with some slight modifications, was used to obtain the graphical results shown in Figures 1 through 6. It is important to note that, by definition, $P_{A_0}(t \geq 0)$, i.e., τ=0, is the annual non-availability that prevails for the particular site. This "annual distribution" is noted in each case. Fade duration's of 20, 40, and 60 minutes are also displayed.

REFERENCES

Beckmann, P., Probability in Communication Engineering, Harcort Brace and World, New York, NY, 1967, pp. 224-226.

Denisenko, A. N., "Estimate of the distribution of surge durations of random process", *Radiotekh. Elecktron.* **20**, pp. 1529-1532 (1975).

Manning, R. M., 'The NASA Lewis Research Center satellite link attenuation model program (LeRC-SLAM) version 1.1", University of Georgia, NASA Software for Industry (1989).

Manning, R. M., A unified statistical rain-attenuation model for communication link fade predictions and optimal stochastic fade control design using a location-dependent rain-statistics database", *Int. J. Satell. Comm.* **8**, pp. 11-30 (1990).

Rice, S. O., "Distribution of the duration of fades in radio transmission: Gaussian Noise Model", *Bell Syst. Tech. J.* **37**, pp. 581-635 (1958).

Stratonovich, R, L., *Topics in the Theory of Random Noise*, Vol.1. Gordon and Breach, New York, NY, 1963, Chap. 4.

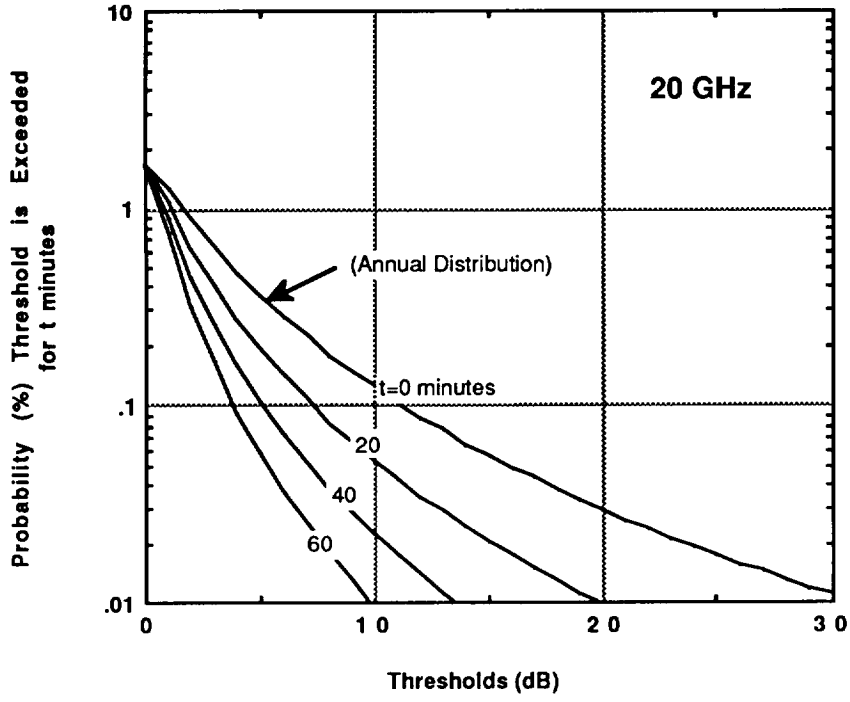

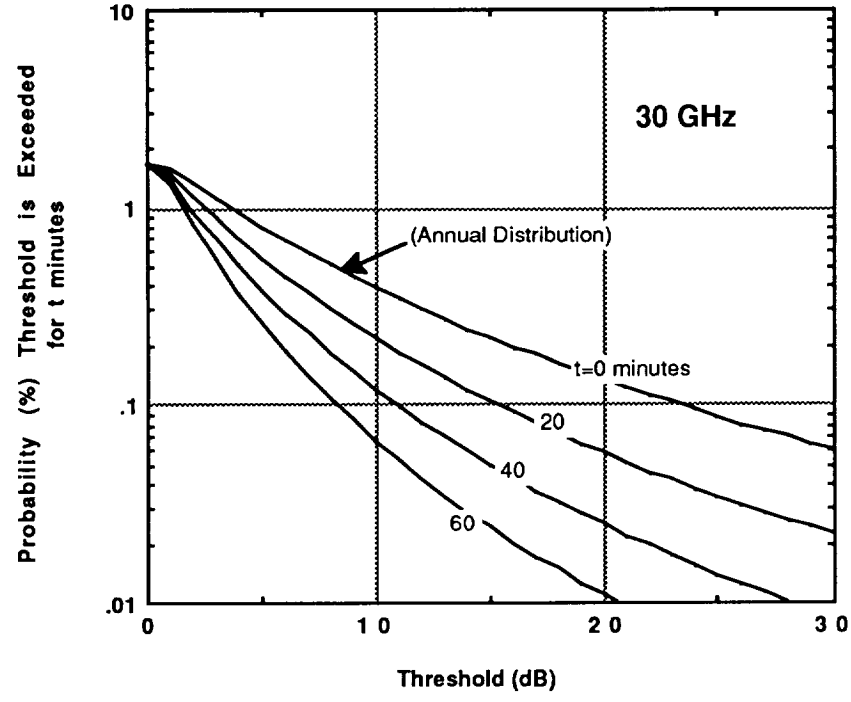

FIGURE 1. CLARKSBURG, MD

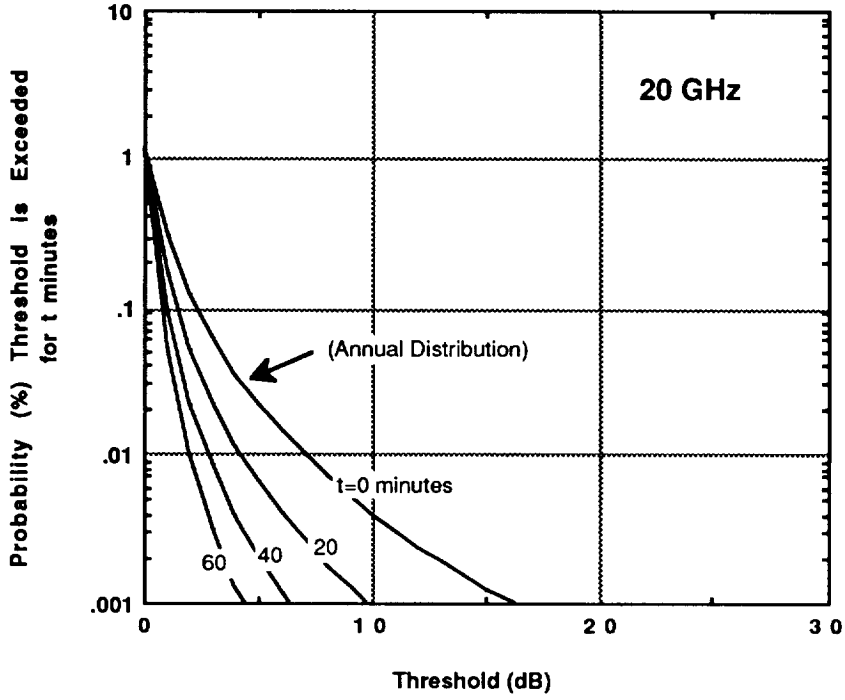

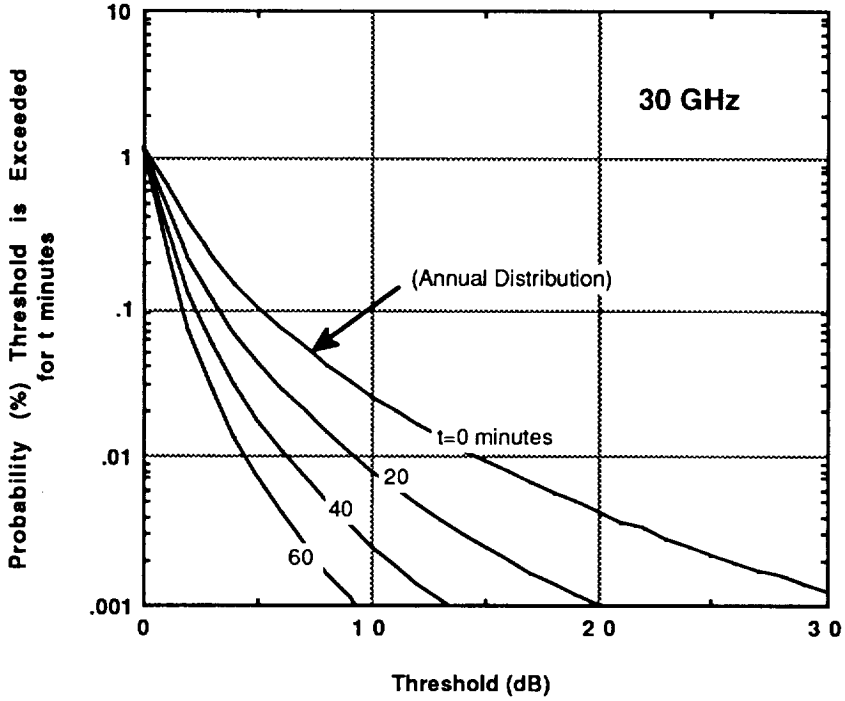

FIGURE 2. FT. COLLINS, CO.

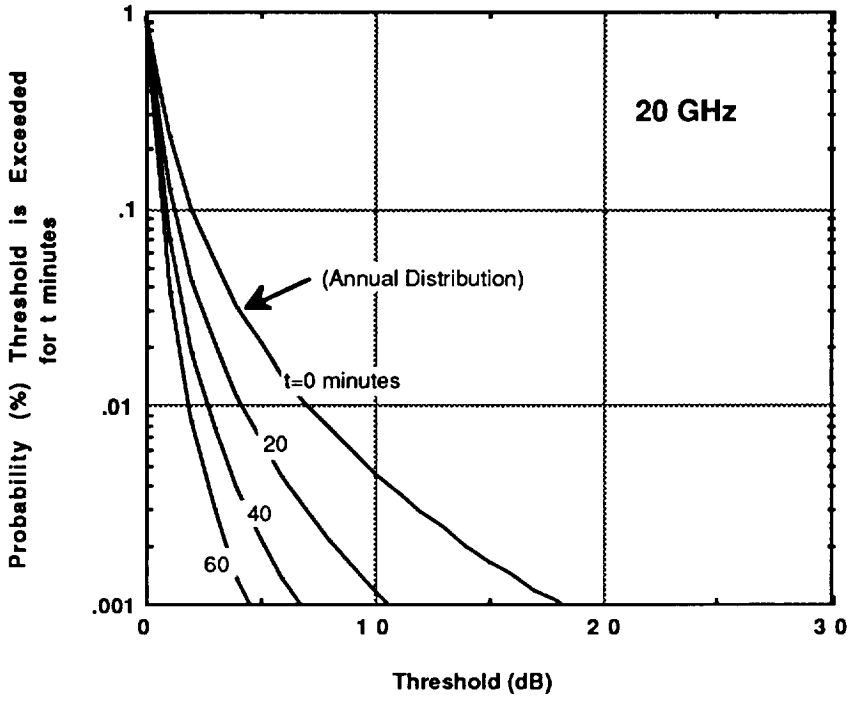

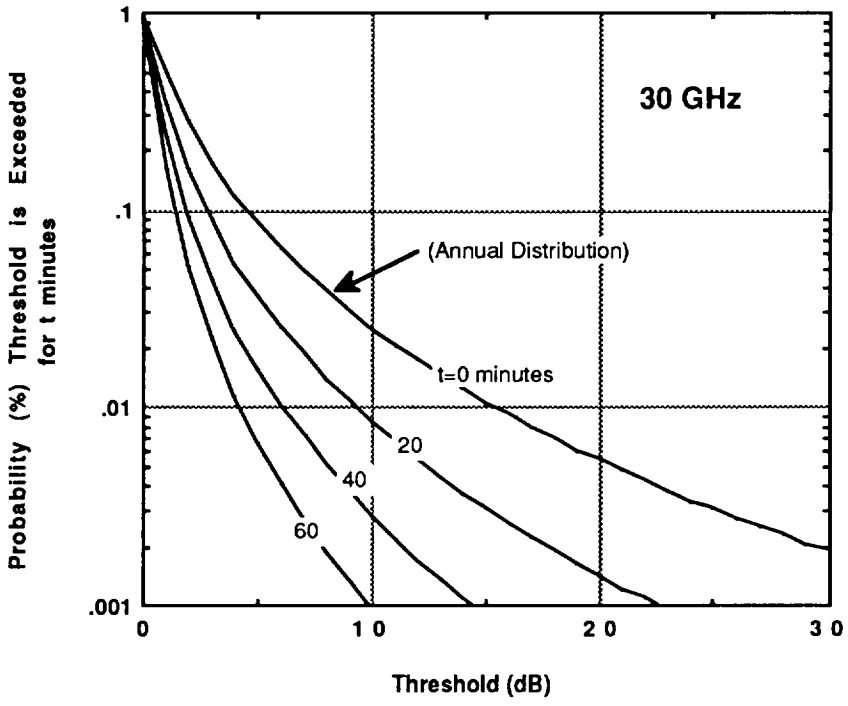

FIGURE 3. LAS CRUCES, NM

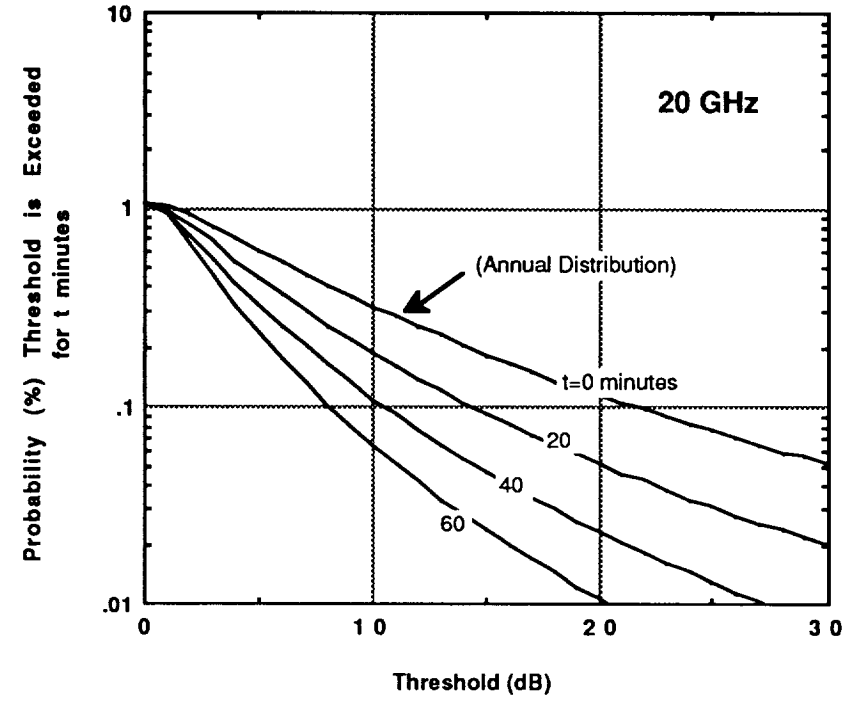

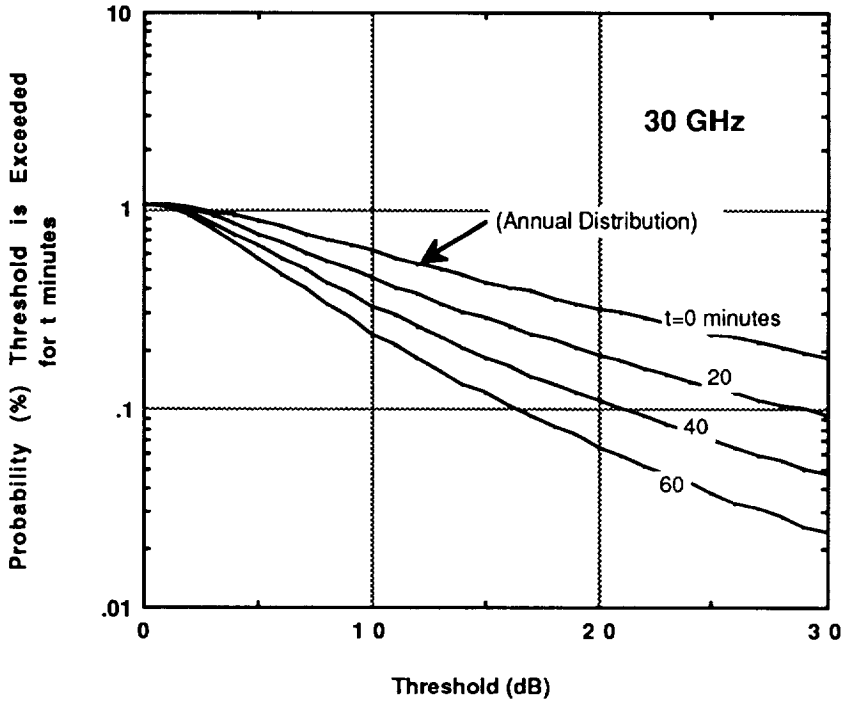

FIGURE 4. MIAMI, FL

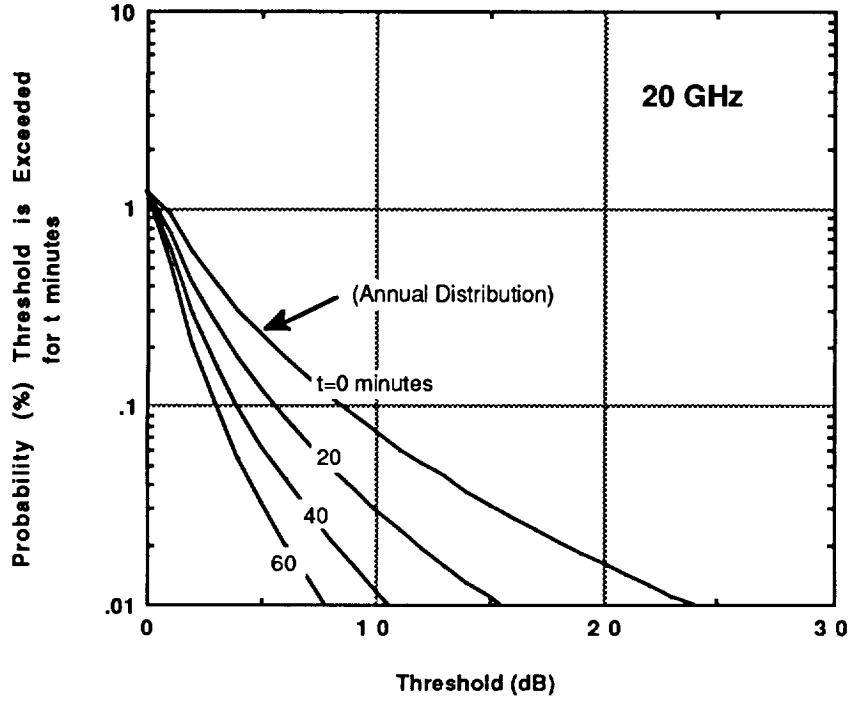

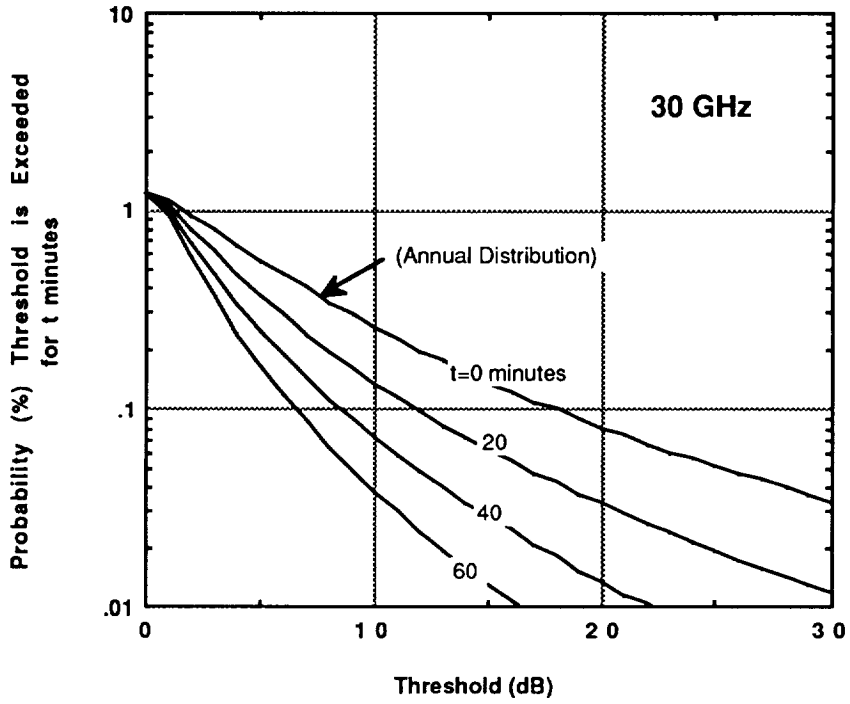

FIGURE 5. NORMAN, OK

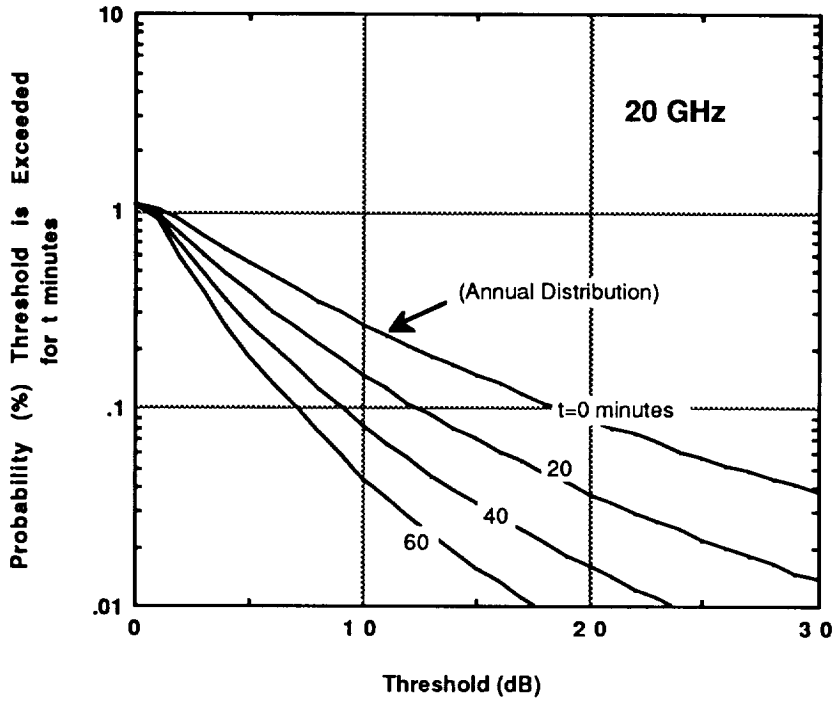

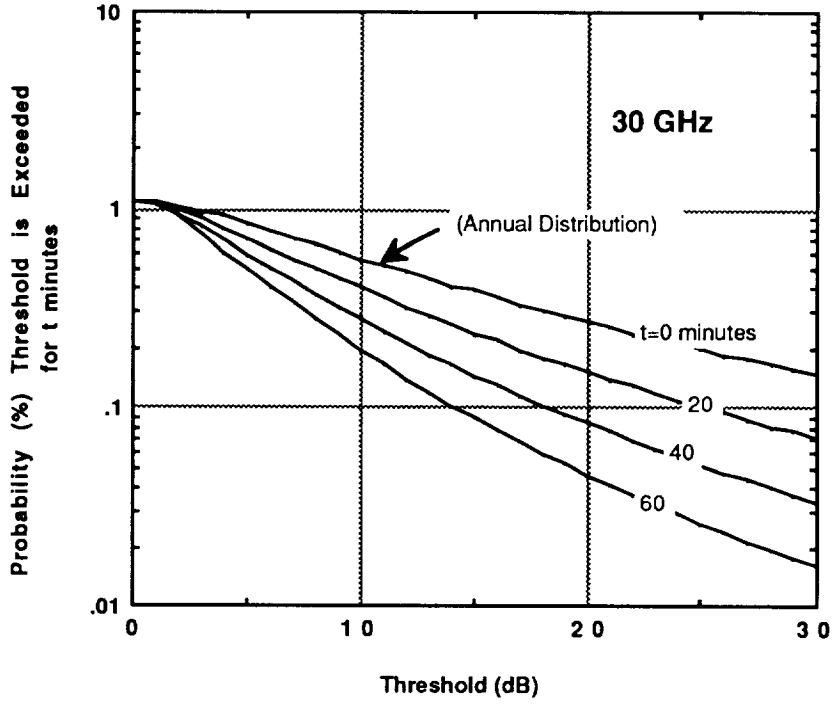

FIGURE 6. TAMPA, FL

Wet Antenna Studies at LeRC

Roberto J. Acosta, Richard Reinhart
Dave Kifer and Carol Emrich

NASA Lewis Research Center
Cleveland Ohio, 44145

Outline

1. Motivation
2. The Wet Antenna Concept
3. Experiment Description
4. Analysis
5. Summary
6. Future Work

MOTIVATION

- What is the relative effect of antenna wetness on different antenna sizes and designs.
- What is effect of a wet antenna on system margin and system availability.
- What is the effect of a wet antenna on fade depth, fade duration, and fade rate.
- Can the effect of a wet antenna be predicted analytically?
- Can the wet antenna effects be characterized for a given antenna design ?

Experiment Description

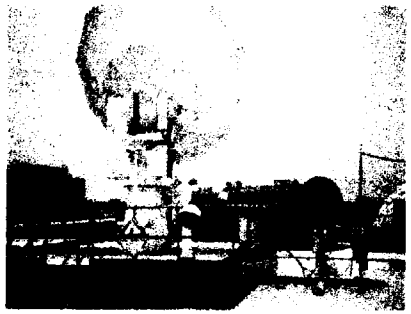

NGS (5.5 m)

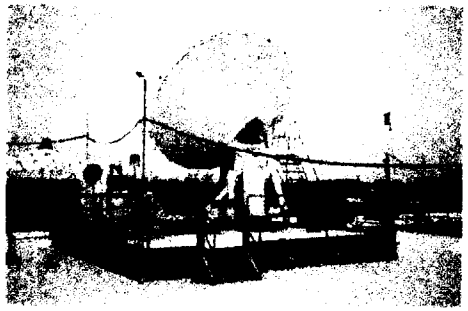

LET (4.7 m)

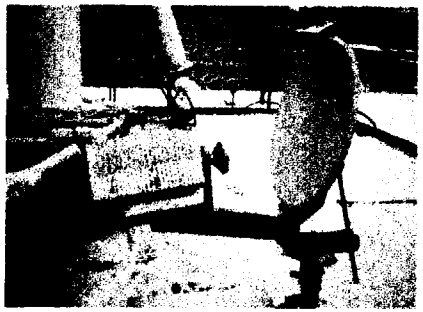

USAT (0.35 m)

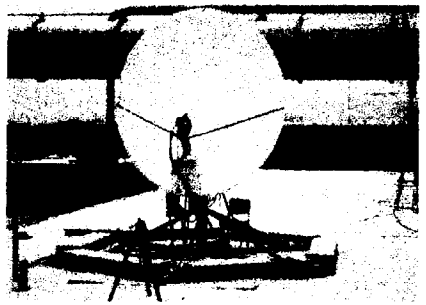

T1VSAT (2.4 m)

Antenna Diameter	5.5 m	4.7 m	3.4 m	2.4 m	1.2 m	0.6 m	0.35 m
F/D	0.40	0.20	0.60	0.60	0.60	0.60	0.60

WET ANTENNA CONCEPT

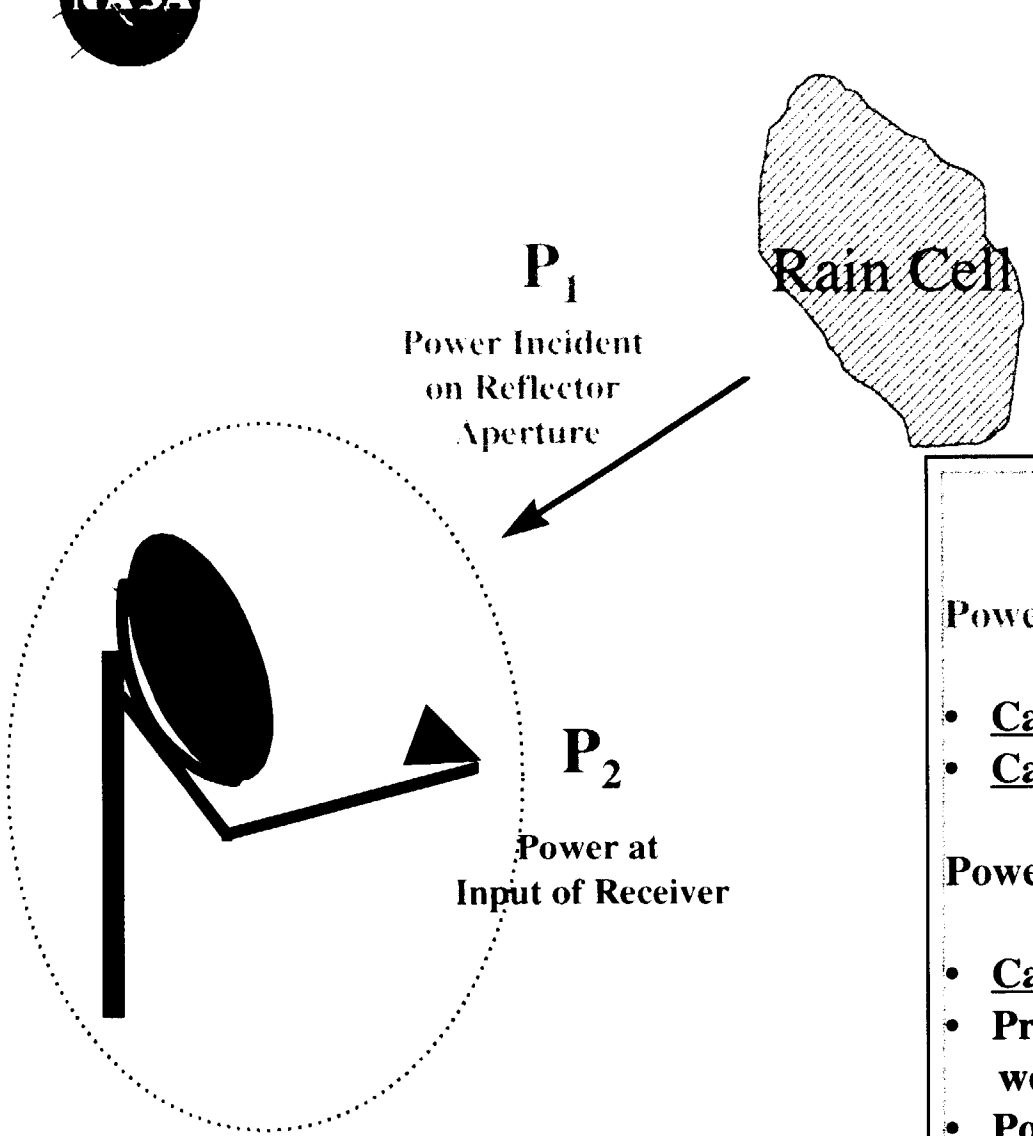

Problem Statement

Power at P1 :

- Can be predicted by propagation models
- Can not be easily Measured

Power at P2 :

- Can not be predicted with good accuracy.
- Propagation models does not include antenna wettness
- Power is easily measured
- This is the power used for comparison with propagation models.

Definition of Antenna Wettness Factor

TWO IDENTICAL ANTENNAS

USAT 1: Enviromentally *Protected*

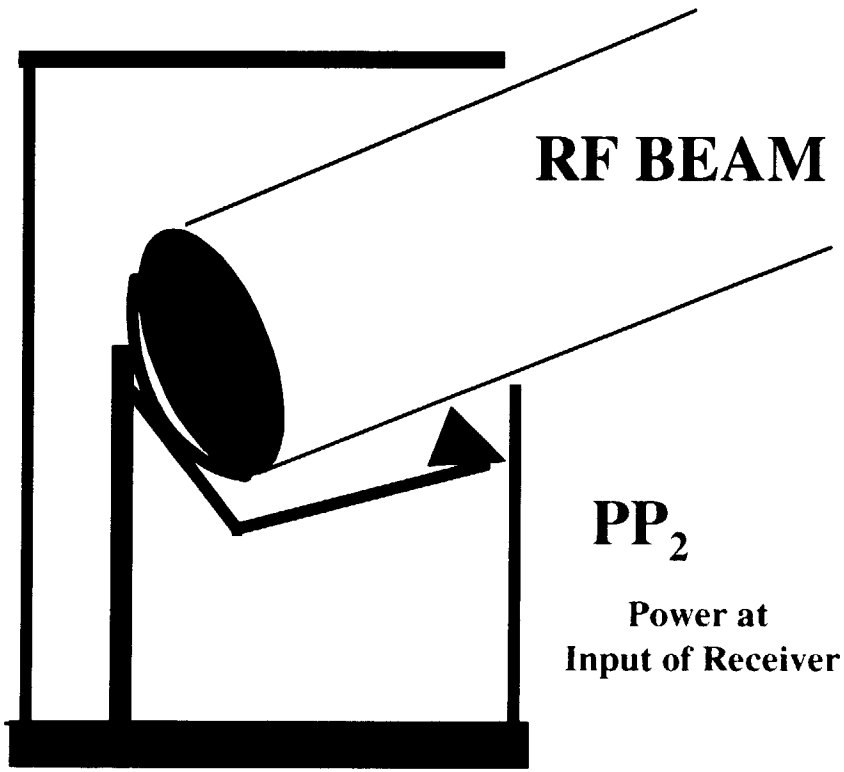

USAT 1: *Not Protected* Enviromentally

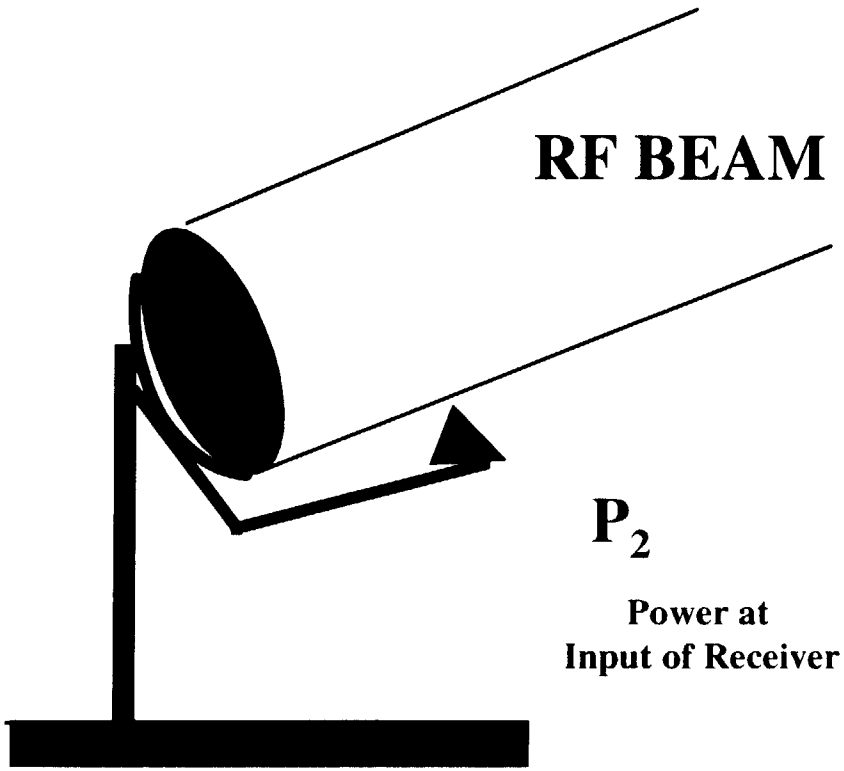

PP_2 - P_2 = Antenna Wettness Factor

Theory vs. Experiment (Test Case #1)

Objective : To Quantify the effect on received power (20 GHz) of a water cell (spherical) of volume V on the main beam, on the reflector surface, in between the feed and reflector and on the feed aperture.

Assumptions

L_1 : **Main Beam Location**

L_2 : **On-Reflector Location**

L_3 : **Between Reflector and Feed**

L_4 : **On -Feed Location**

P_{rec} (dbm) : **Power Received at 20GHz**

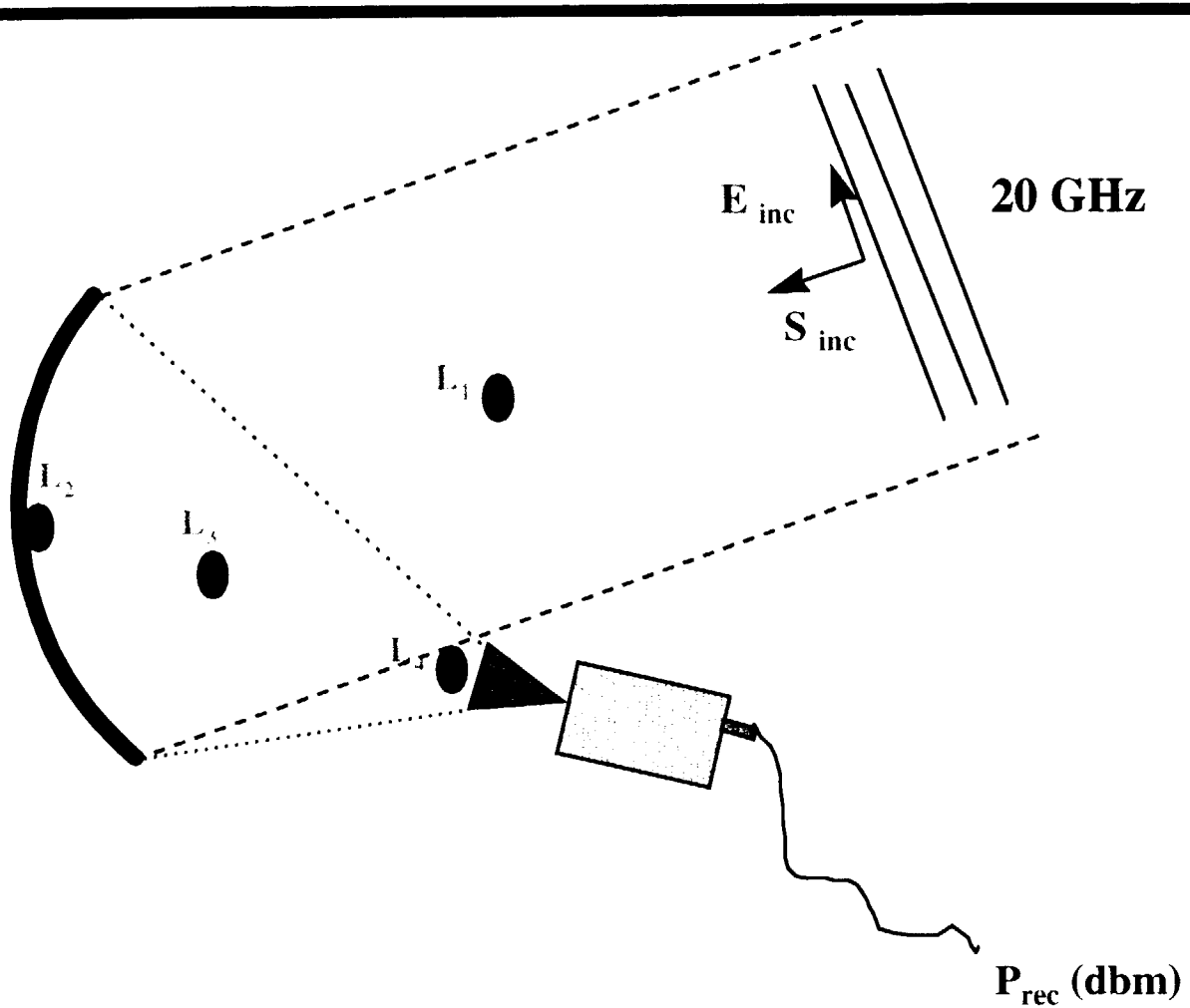

Figure 1. Geometry of Experiment

Test Case #1 : Results

Wet Antenna - Static Case

Location of Water Cell	Measured Attenuation (dB)
L1	-0.25
L2	-0.44
L3	-1.13
L4	-9.50

Test Conditions:

- *** T = 29 °**
- *** Rel Humidity = 81 %**
- *** Volume = 1.56 in ^{3}**
- *** Diameter = 0.35 m**
- *** F/D = 0.6**

Note: Theoretical model in progress

Theory vs Experiment : Test Case #2

Wet Antenna - Dynamic Simulation (0.35 m and 0.6 m Ref.)

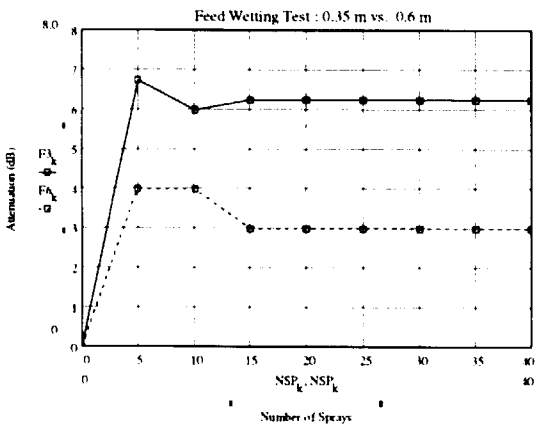

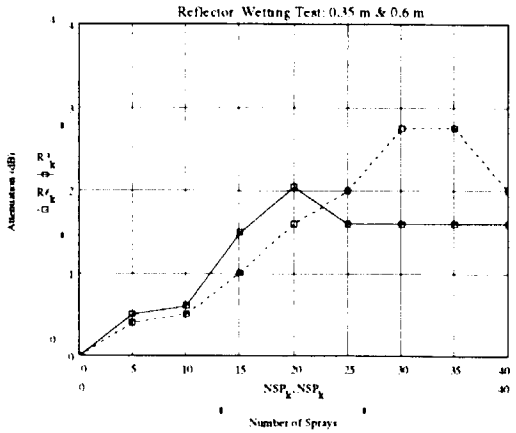

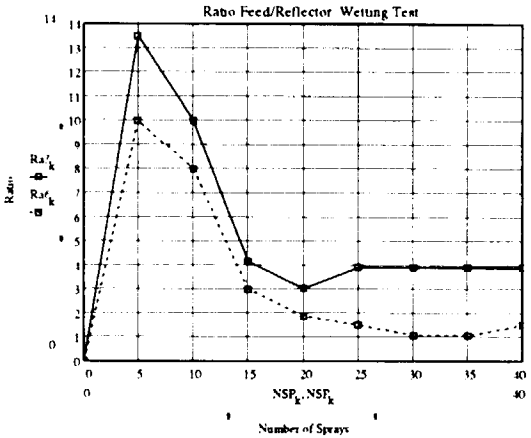

Assumptions:
- * Simulated Rain Rate = 38 mm/hr
- * Volume of Water per Spray = 0.06 in 3
- * Distance of Sprayer from feed = 12 inches
- * Distance of Sprayer from Reflector = 12 inches

Test 2 :
- * T = 75 °
- *Rel Humidity = 65 %

Blue : 0.6 m (F/D = 0.6)
Red : 0.35 m (F/D = 0.6)

Fade Distribution for Different Antenna Sizes

Black : 4.7 m (F/D= 0.20)
Red : 0.35 m (F/D = 060)
Blue : 0.60 m (F/D = 0.60)

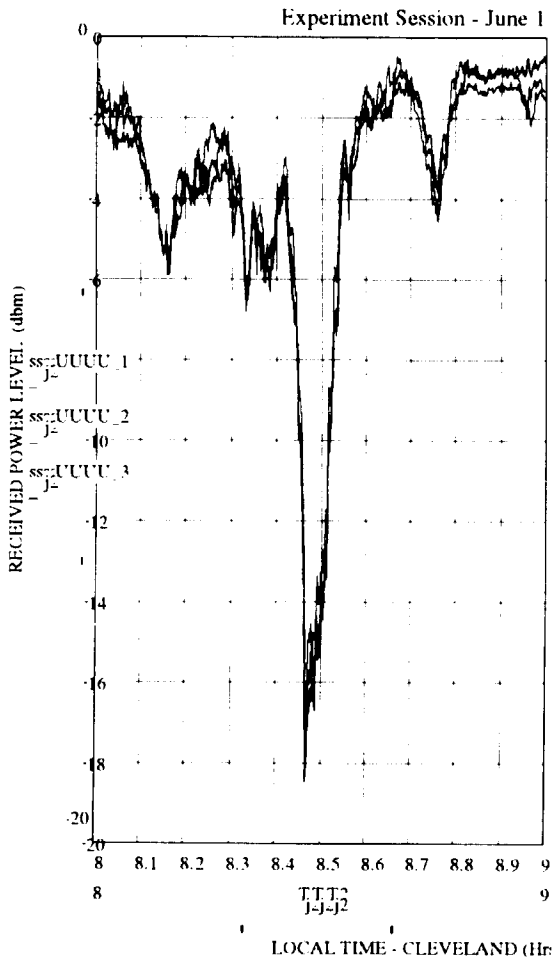

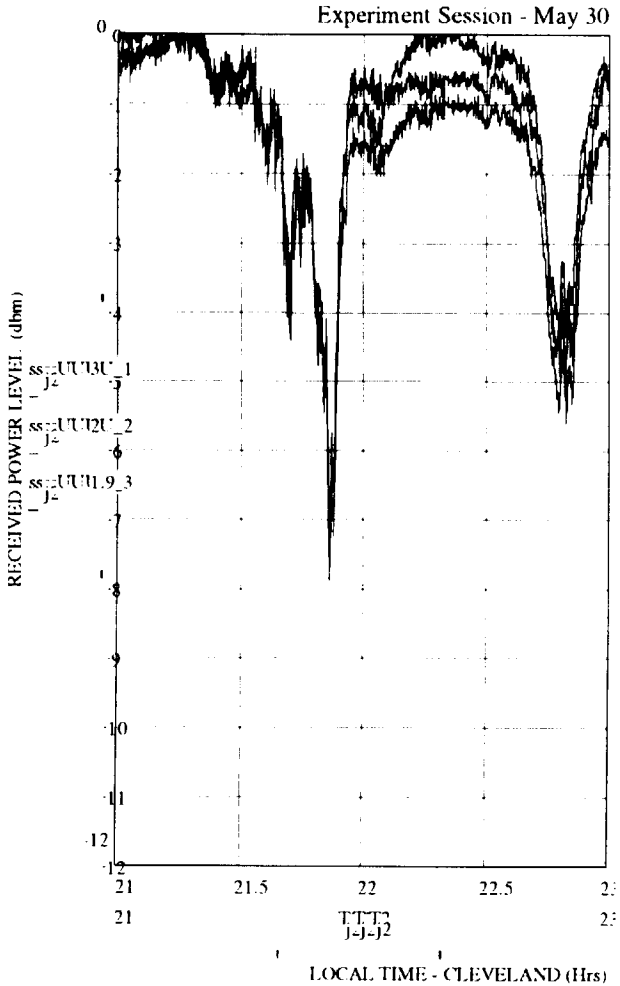

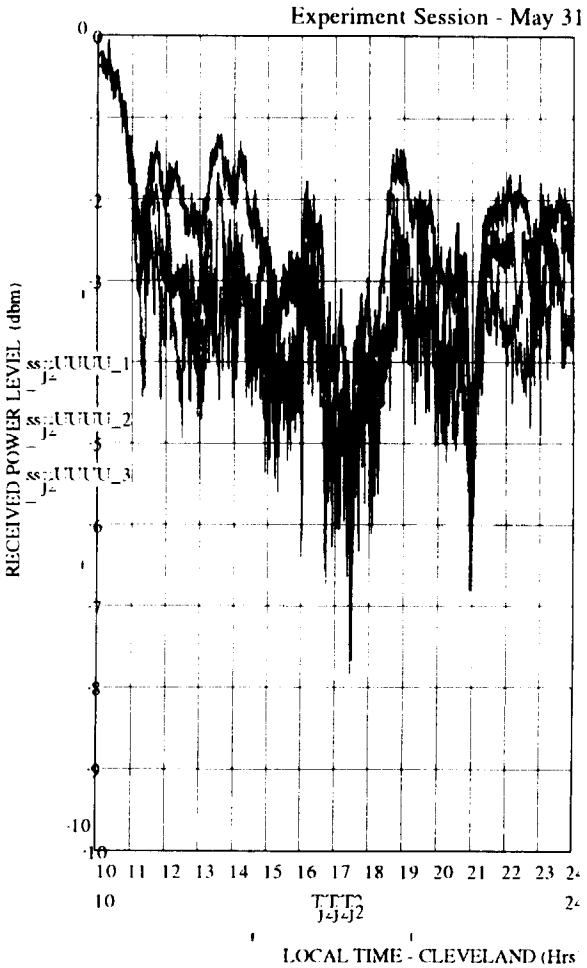

Assumptions: * Sample Spacing 0.5 sec
*** Same physical location**

Fade Distribution for Two Identical Antennas

CLEAR SKY - May 28

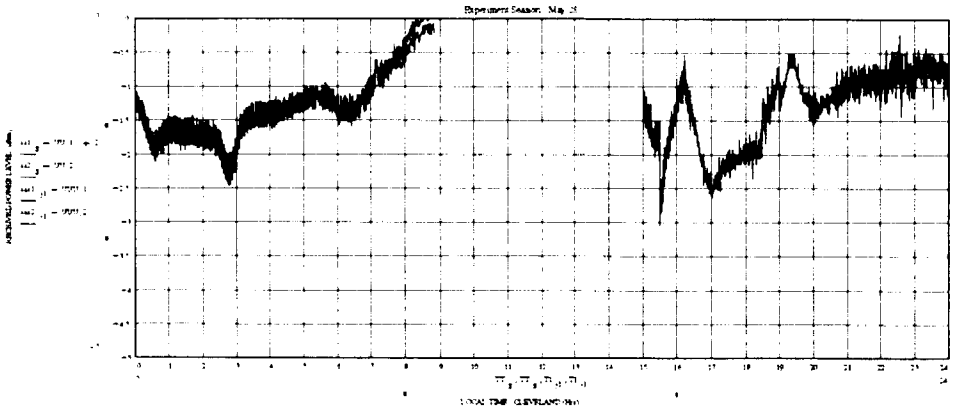

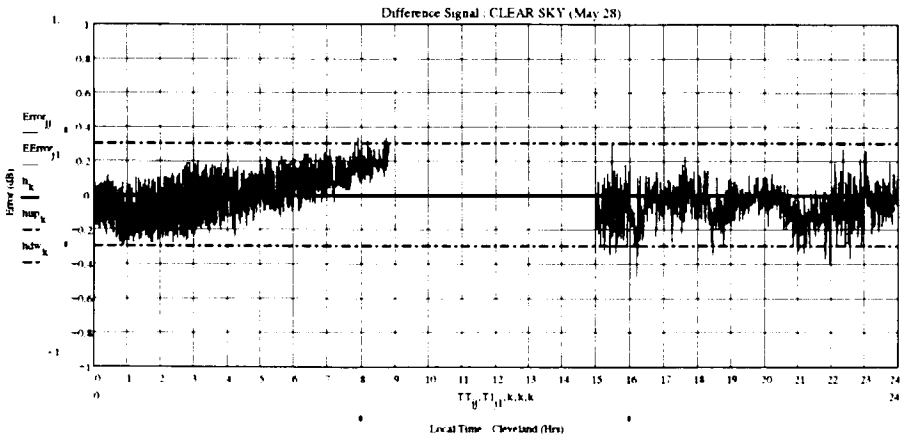

Antena Size = 0.35 m
F/D = 0.6 m

Fade Distribution for Two Identical Antennas

Rainy Day - May 5

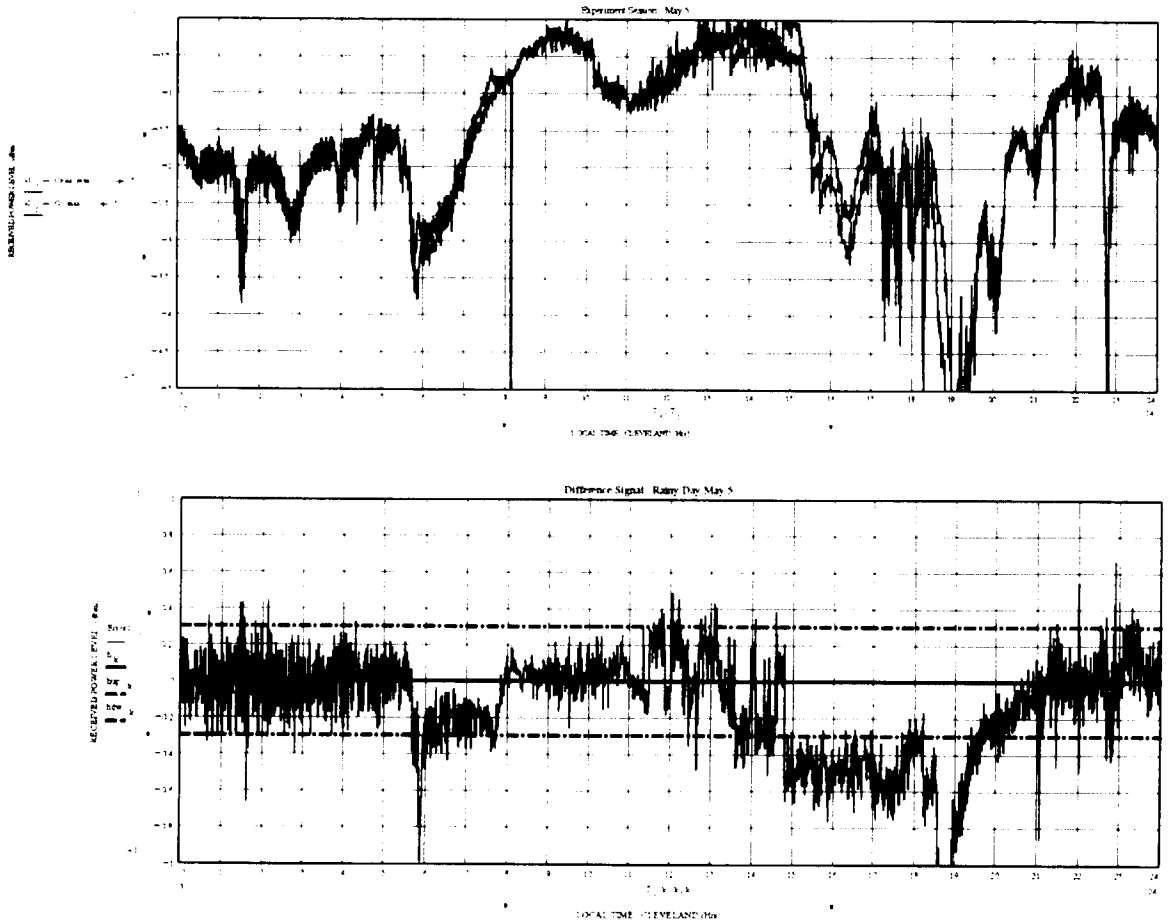

FADE RATE ANALYSIS
Results

Fourier Series

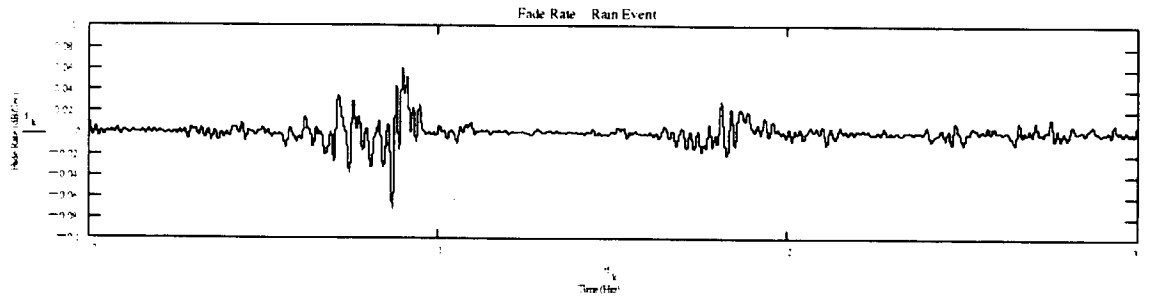

Central Difference h^2

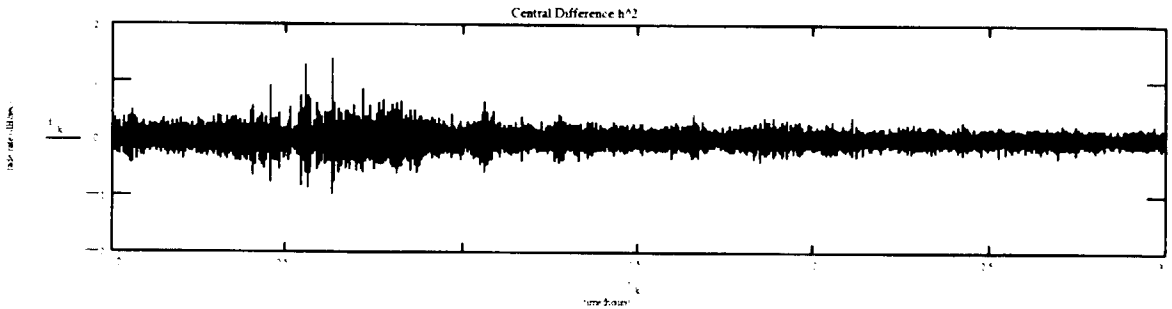

Central Difference h^4

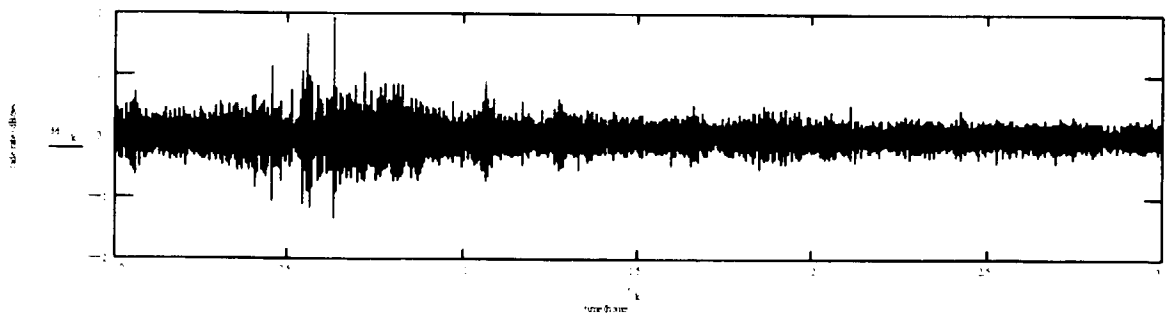

FADE RATE ANALYSIS METHODOLOGY

- FOURIER SERIES

$$d_k := \left(\frac{2\cdot\pi}{T}\right)\cdot\left[\sum_{n=1}^{200}\left(-a_n\cdot n\cdot\sin\left(n\cdot 2\cdot\frac{\pi}{T}\cdot tf_k\right)+b_n\cdot n\cdot\cos\left(n\cdot 2\cdot\frac{\pi}{T}\cdot tf_k\right)\right)\right]$$

- FINITE DIFFERENCE

$$d_k := \frac{Sig_{k+1} - Sig_{k-1}}{2\cdot\Delta}$$

$$dd_k := \frac{-Sig_{k+2} + 8\cdot Sig_{k+1} - 8\cdot Sig_{k-1} + Sig_{k-2}}{12\cdot\Delta}$$

SUMMARY

(Lessons Learned)

- Wet antenna factor (definition establish)
- Static Test : Wet feed attenuates signal by factor of 8 times from wet reflector.
- Dynamic Test: Wet feed attenuates signal by a factor of 10 - 14 times (depending on reflector size) from wet reflector.
- Larger reflector attenuates signal more than smaller reflector.
- Fades for several antenna sizes showed a variance of about 1 dB during (ligth to medium rain).
- Larger antenna showed a larger fade depth.
- For ligth rain (constant rate) the fade depth appears to be random.
- The two identical antenna test shows tracking good performance under clear sky and under rain (ligth) conditions.
- Fourier method to be used for calculating fade rates and fade duration during experiments.

FUTURE WORK

- Investigate wet antenna factor for at least two different antenna design under varying rain conditions.
- Investigate how wet antenna affects fade depth, fade duration fade rates for various rain conditions.
- Investigate the look angle dependance on the wet antenna .

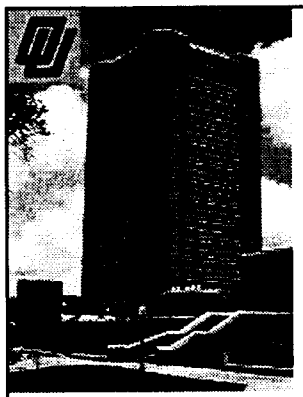

Wet Antenna Studies
by Deepak Ramachadran

- The surface considered is similar to that of a Parabolic dish.
- A theoretical analysis was made on a "**Wet Antenna**", for one without a plastic and paint coating and then a similar analysis was made for one with a plastic and paint coating.
- It is a problem of "Reflection at multiple dielectric interfaces", the interfaces being air-water-paint-plastic-conductor. Wave equations were constructed for every medium and boundary conditions were applied at each boundary to get a set of equations. These equations were solved using a computer and simple Cramer's rule to estimate the attenuation.

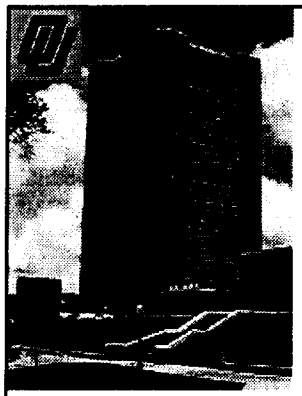

Wet Antenna Studies by Deepak Ramachadran

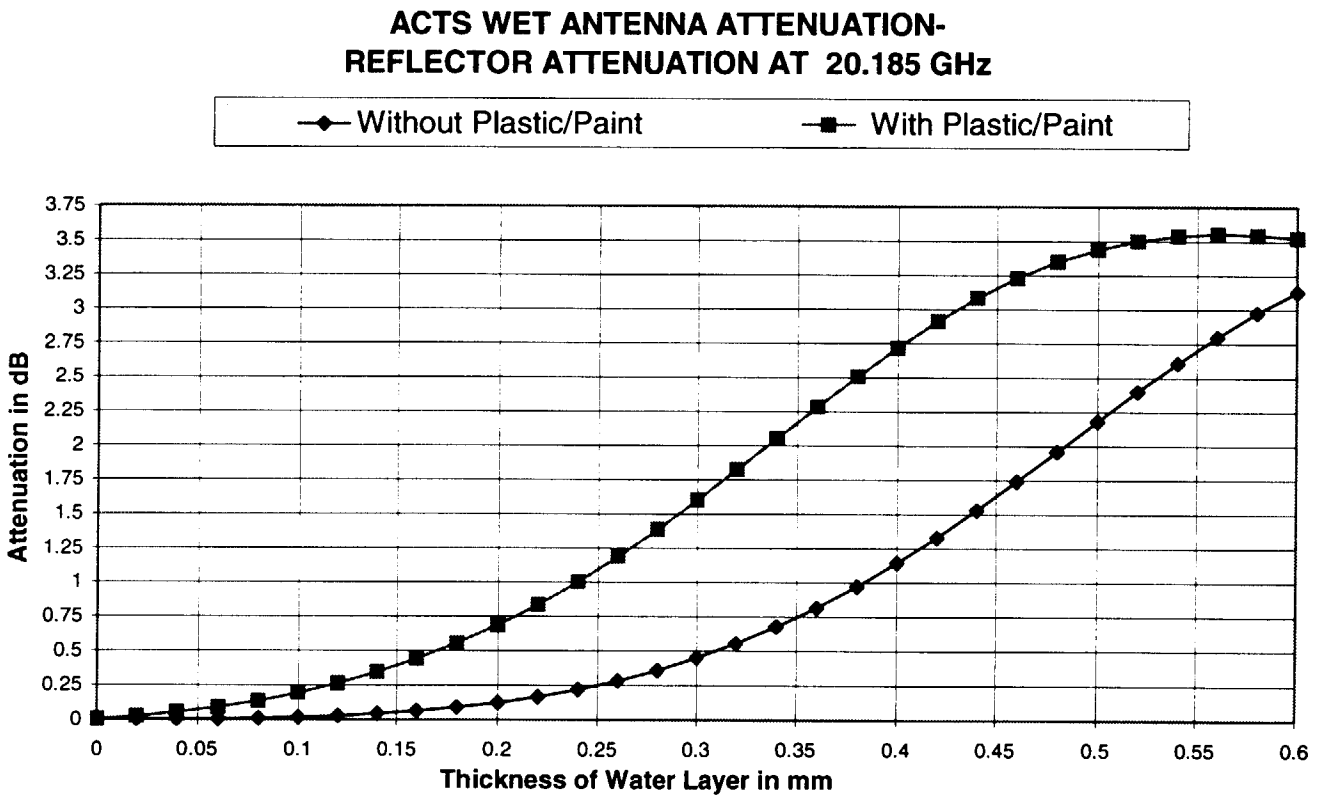

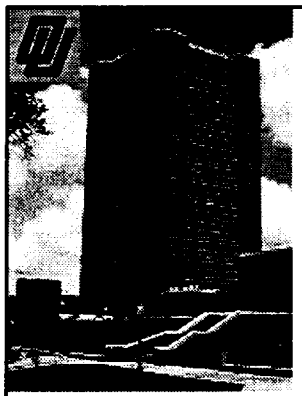

Wet Antenna Studies by Deepak Ramachadran

ACTS WET ANTENNA ATTENUATION-
REFLECTOR ATTENUATION AT 27.5 GHz

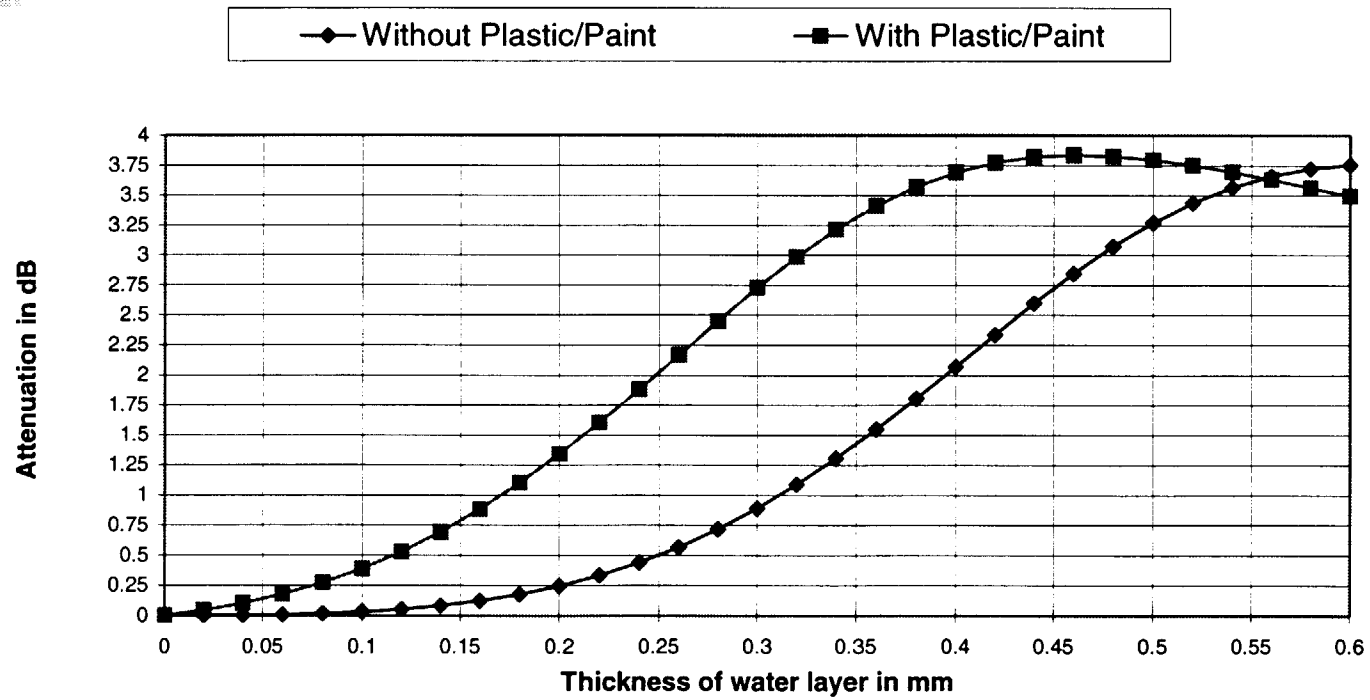

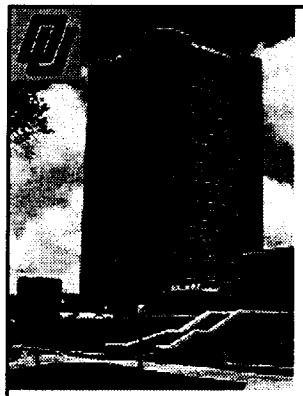

Wet Antenna Studies by Deepak Ramachadran

Thickness vs Difference at 20.185GHz

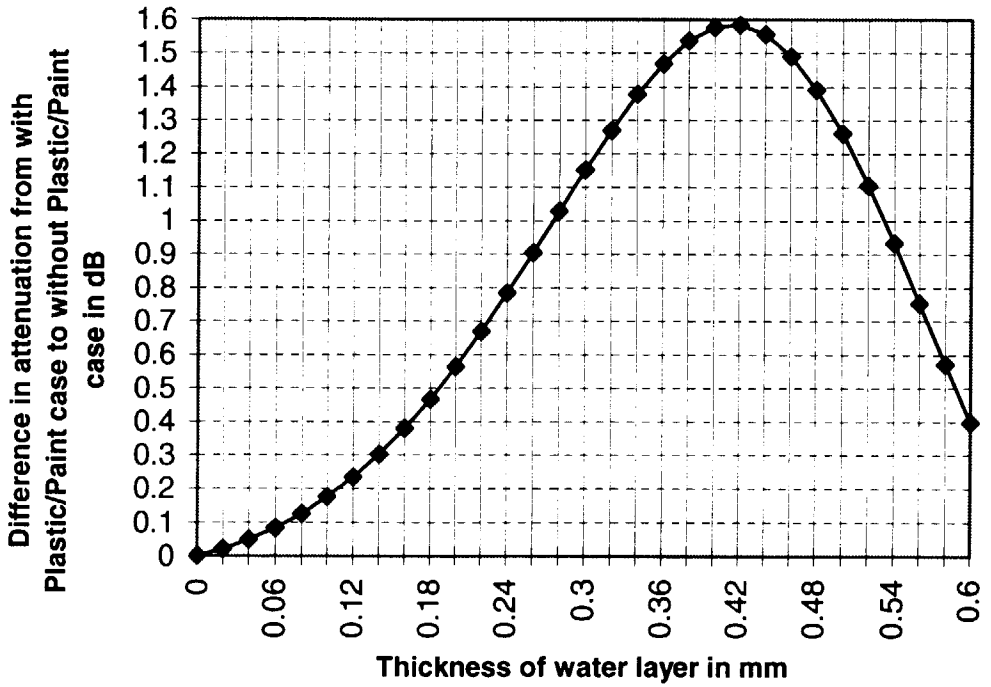

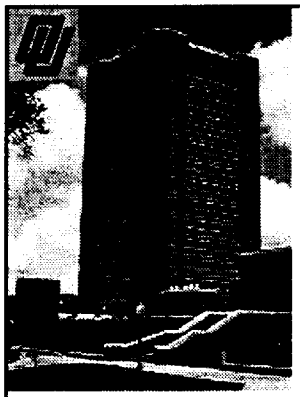

Wet Antenna Studies by Deepak Ramachadran

Thickness vs Difference at 27.5GHz

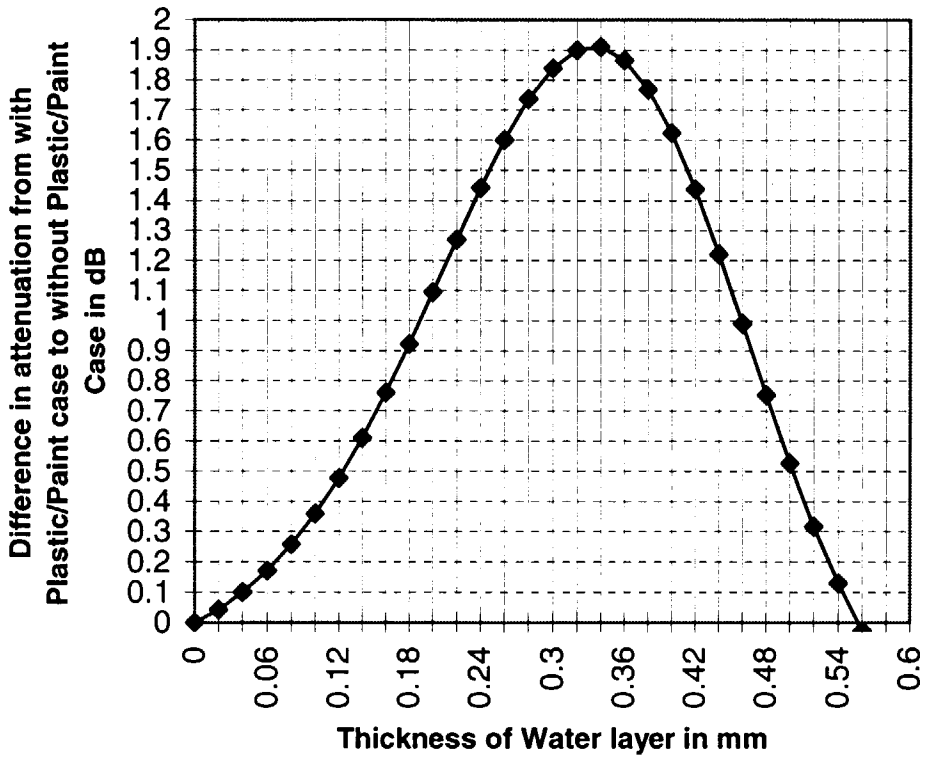

299311
P.10

PC21 UN/AC0010

ACS Stanford Telecom

Fade Slope Analysis for Alaska, Florida, and New Mexico ACTS Propagation Data

Julie H. Feil
Louis J. Ippolito
Henry Helmken
Charles Mayer
Stephen Horan
Rudolf Henning

NAPAX XXI & APSW XI
June 11-13, 1997
Los Angeles, CA

PC21 UN/AC0010

ACS Stanford Telecom

Fade Slope Analysis Agenda

- ❑ **Definition & Calculations**
- ❑ **Time Composite Statistics**
  - ➢ Two years of ACTS data from Alaska, Florida, and New Mexico
- ❑ **Comparison of fade slope probabilities for rain periods**
  - ➢ Investigation of dependent parameters
- ❑ **Summary and Future Work**

ACS Stanford Telecom

What is Fade Slope?

- **Measurement of the attenuation rate of change with respect to time (dB/s).**
  - ➢ Measurement of slow-varying rain attenuation rather than fast-vary scintillation
- **System designers utilize fade slope statistics to develop power control algorithms and forward error correction techniques to compensate for rain fades.**
- **VPI (Nelson and Stutzman) proposed a model based on VPI Olympus data only.**
  - ➢ Dependent parameters: transmission frequency and fade level

ACS Stanford Telecom

Instantaneous Example

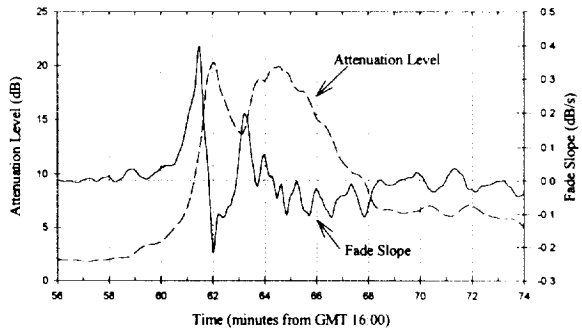

20 GHz beacon data from New Mexico ACTS propagation terminal
September 28, 1995

ACS Stanford Telecom

Exaggerated Fade Slope Calculation

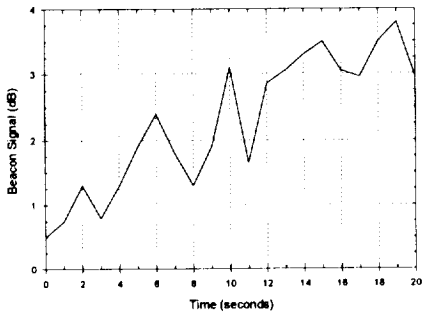

This data has been created to illustrate the fade slope calculation; this data is not actual experimental data.

$$fade\_slope = \frac{signal_{t,s} - signal_{t,s}}{10}$$

$$fade\_slope(t=10) = \frac{signal_{t=15} - signal_{t,5}}{10} = \frac{330 - 180}{10} = 0.15 dB/s$$

ACS Stanford Telecom

Relationship between Attenuation and Fade Slope

- **Fade slope can be thought of as the first derivative of fade level with respect to time.**
- **Fade slope is dependent on rain dynamics.**
- **Sweeney and Bostian (from VPI) proposed that**
  - Fade slope is maximum when first fresnel zone is half full (change in rain dynamics or greatest change in attenuation).
  - Fade slope is minimum when first fresnel zone is full (peak rain and peak attenuation) or empty (clear air or minimal attenuation).

PC21

UN/AC0010

ACS Stanford Telecom

Relationship for Idealized Path

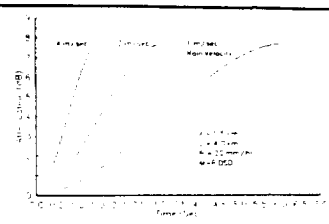

Attenuation versus time for rain velocities of 1, 2, and 4 m/s

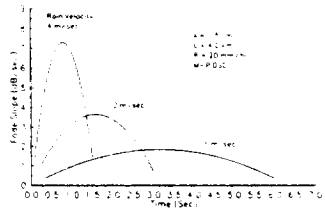

Fade slope versus time for rain velocities of 1, 2, and 4 m/s

rom Sweeney and Bostian, IEEE APS Transactions March 1992

PC21

UN/AC0010

ACS Stanford Telecom

Analysis

- Alaska, Florida, New Mexico ACTS propagation Data.

APT Terminal	Principle Investigators	ITU-R Rain Region & 0.01% rate		Global Rain Zone & 0.01% rate		Elevatio Angle
Fairbanks, Alaska	University of Alaska	C	15 mm/hr	A	9.9 mm/hr	8°
Tampa, Florida	Florida Atlantic University and University of South Florida	N	95 mm/hr	E	91.5 mm/hr	52°
White Sands, New Mexico	Stanford Telecom and New Mexico State University	E	22 mm/hr	F	22.2 mm/hr	51°

- Transmission frequencies are 20.185 and 27.505 GHz.
- Two years of data: December 1, 1993 to November 30, 1995
- Data is filtered to remove scintillation effects

ACS Stanford Telecom

Filter Data

- **Filtering data required to remove scintillation effects.**
- **For academic study, each storm filtered separately with its optimum filter. But this methodology does not make sense for real-time systems.**
- **No standard filter or time constant**
  - ➢ Filter shapes: square (moving average), triangle, $\cos^2$
  - ➢ Time constants: 10 seconds to 3 minutes
- **OPEX implemented 100-second $\cos^2$ filter after much investigation**
- **For this analysis implemented both 100-second $\cos^2$ filter and 30-second moving average. Both filters had similar results. The 100-second $\cos^2$ filter was implemented similar to the OPEX analysis.**

ACS Stanford Telecom

Filter Comparison

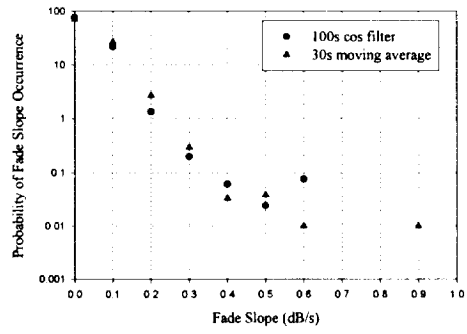

This plot is for Florid 20 GHz Florida data given a 10 dB fade has occurred
This plot is indicative of data for data at other fade levels for all three sites

ACS Stanford Telecom

Analysis Results

- **Annual composite distributions (rain and clear air).**
- **Probability of occurrence for rain only periods.**
  - ➢ Comparison between different transmission frequencies for a given receiver site.
  - ➢ Comparison between different receiver sites for given attenuation level.

ACS Stanford Telecom

Alaska Time Composite Results

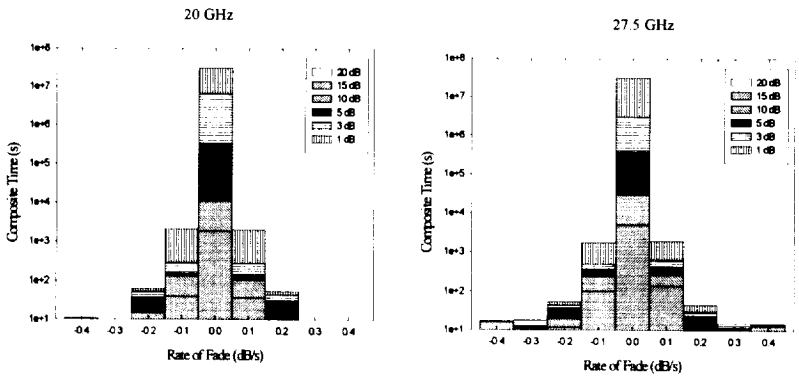

PC21 UN/AC0010

ACS Stanford Telecom

Florida Time Composite Results

20 GHz

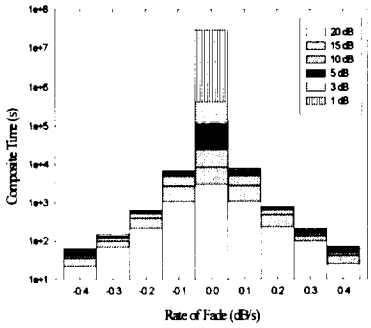

27.5 GHz

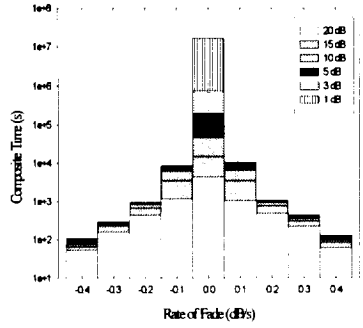

PC21 UN/AC0010

ACS Stanford Telecom

New Mexico Time Composite Results

20 GHz

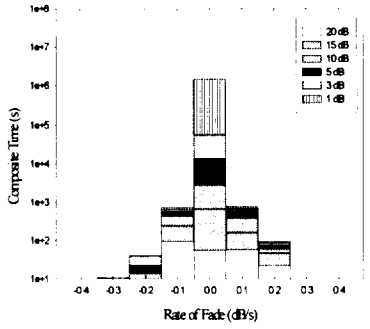

27.5 GHz

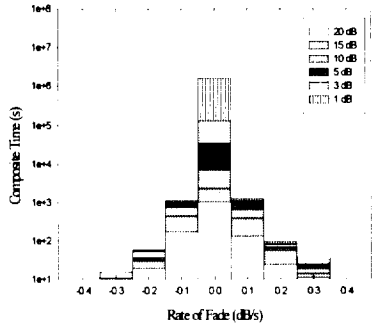

PC21 UN/AC0010

ACS Stanford Telecom

Fade Slope during Rain

- **Conditional probabilities: fade slope occurrence given that it is raining.**
- **Rain periods determined by clear air (gaseous absorption) attenuation threshold from annual attenuation cumulative distributions.**
  - ➢ Alaska: 4 dB
  - ➢ Florida: 3 dB
  - ➢ New Mexico: 1 dB

PC21 UN/AC0010

ACS Stanford Telecom

Rain Statistics

Alaska

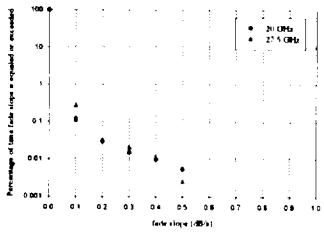

Florida

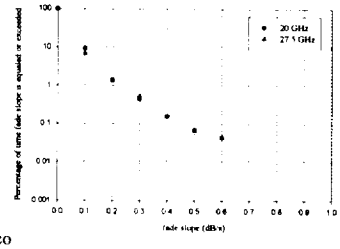

New Mexico

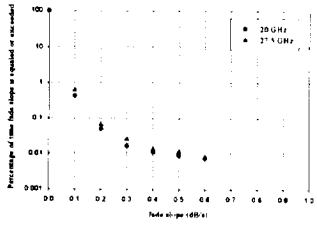

PC21 UN/AC0010

ACS Stanford Telecom

Fade Slope Rain Statistics

- ❑ **Fade slope (during rain) is not directly correlated with transmission frequency.**
- ❑ **Is fade slope correlated with fade level?**

PC21 UN/AC0010

ACS Stanford Telecom

Statistics at Given Fade Level

5 dB

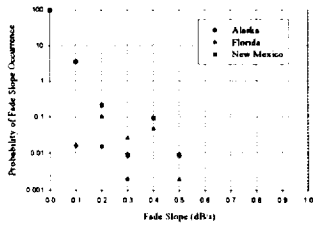

10 dB

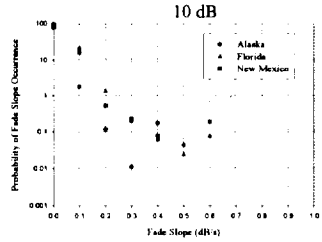

15 dB

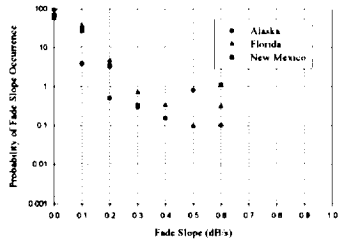

ACS Stanford Telecom

Summary and Future Work

- **Florida and New Mexico data have very similar fade slope statistics at a given fade level even though the two sites are located in very different climatic region!**
- **Fade Slope Summary**
  - ➢ Dependent parameters: elevation angle & fade level.
  - ➢ Not dependent parameters: Transmission frequency & climatic region
- **Future Work**
  - ➢ Additional data collection: 3 to 5 years of data collection since not many fade at 10 and 15 dB.
  - ➢ Additional ACTS sites: British Columbia, Colorado, Maryland, and Oklahoma.
  - ➢ Determine elevation angle & fade level relationship to fade slope.

ACS Stanford Telecom

Literature Reference

This presentation is the results from the paper:

"Fade Slope Analysis for Alaska, Florida, and New Mexico ACTS Propagation Data at 20 and 27.5 GHz"

by Julie Feil, Louis J. Ippolito, Henry Helmken, Charles Mayer, Stephen Horan, Rudolf Henning

In the IEEE Proceedings for ACTS Propagation Experiment

3. Propagation Research Topics

Measurements of K_A-band Amplitude and Phase Scintillation

Scott A. Borgsmiller

Dr. Paul G. Steffes

School of Electrical and Computer Engineering

Georgia Institute of Technology

NAPEX/APSW

Research Objectives

- Measure amplitude and phase spectra of K_a-band carrier signals to determine scintillation magnitude
- Measure bit-error rate of digital spread spectrum signals during scintillation to determine performance degradation
- Extrapolate LEO scintillation effects from measurements with geostationary ACTS

Frequency Spectrum for Scintillation

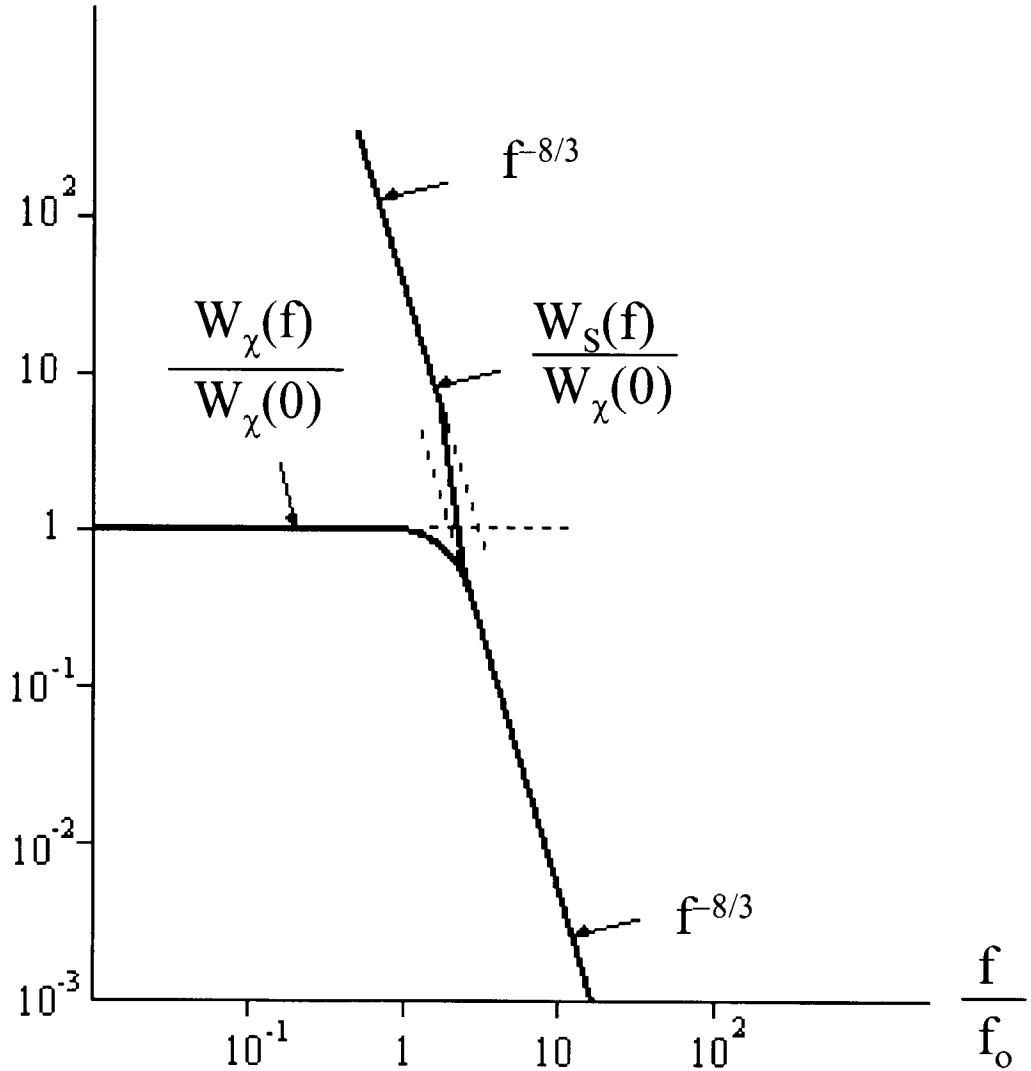

Georgia Tech-ACTS Transceiver

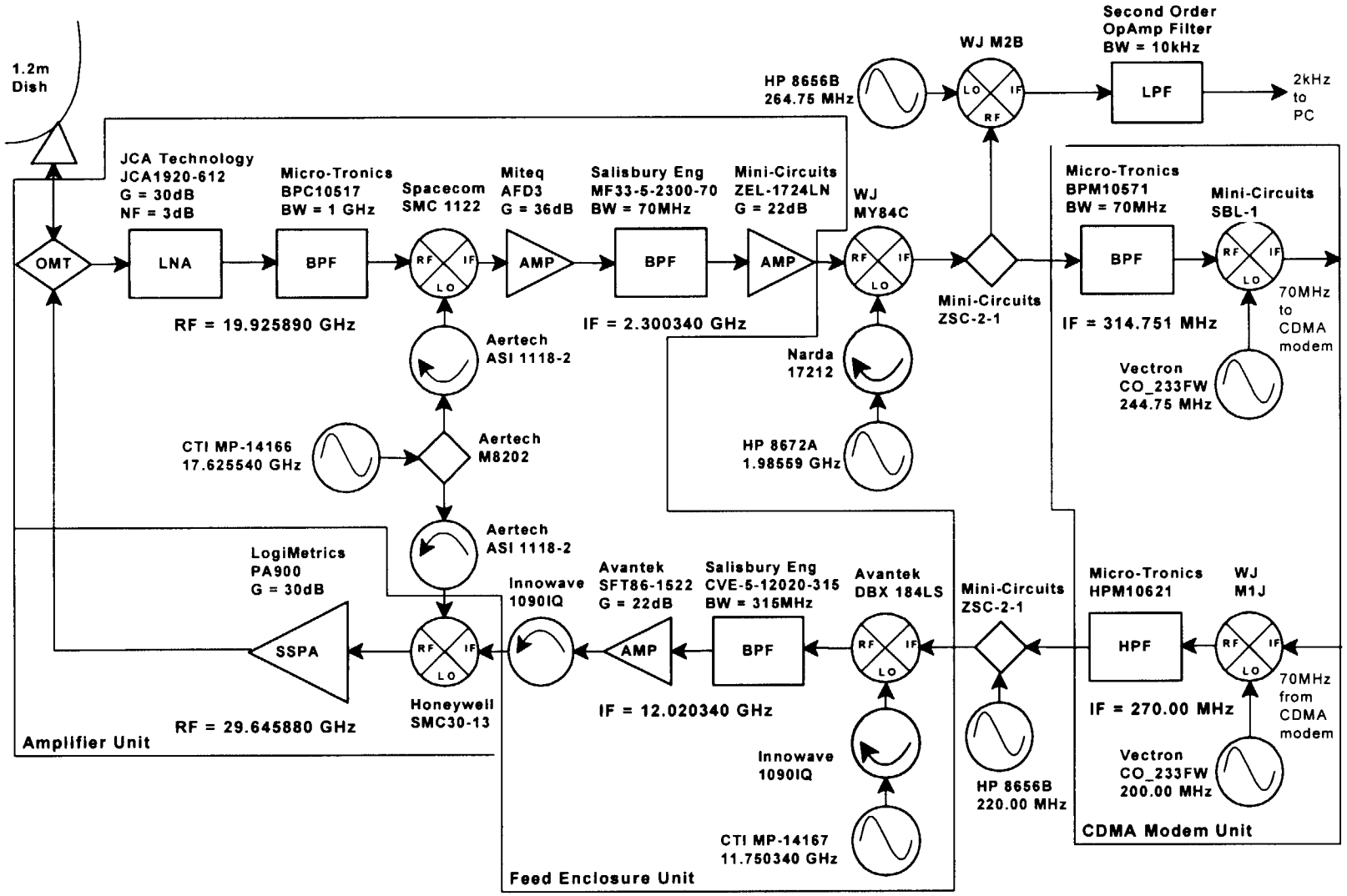

CDMA Modem

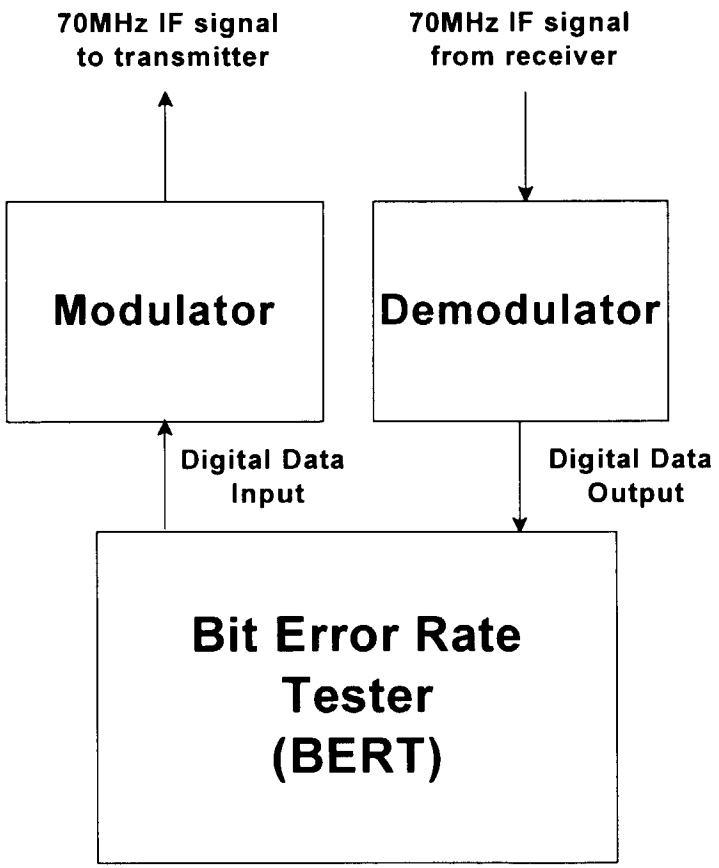

- BPSK, QPSK, MSK, OQPSK, and others
- Data rates to 40Msymbols/sec
- Chip rates to 40Mchips/sec
- 70MHz IF input & output
- ISA board construction

Completed Measurements

- Receive-only measurements of the amplitude and phase spectra of the propagation beacon carrier signal
- Loopback tests with the CDMA modem in clear-air conditions using TWT uplink amplifier

Amplitude Spectra Measurement

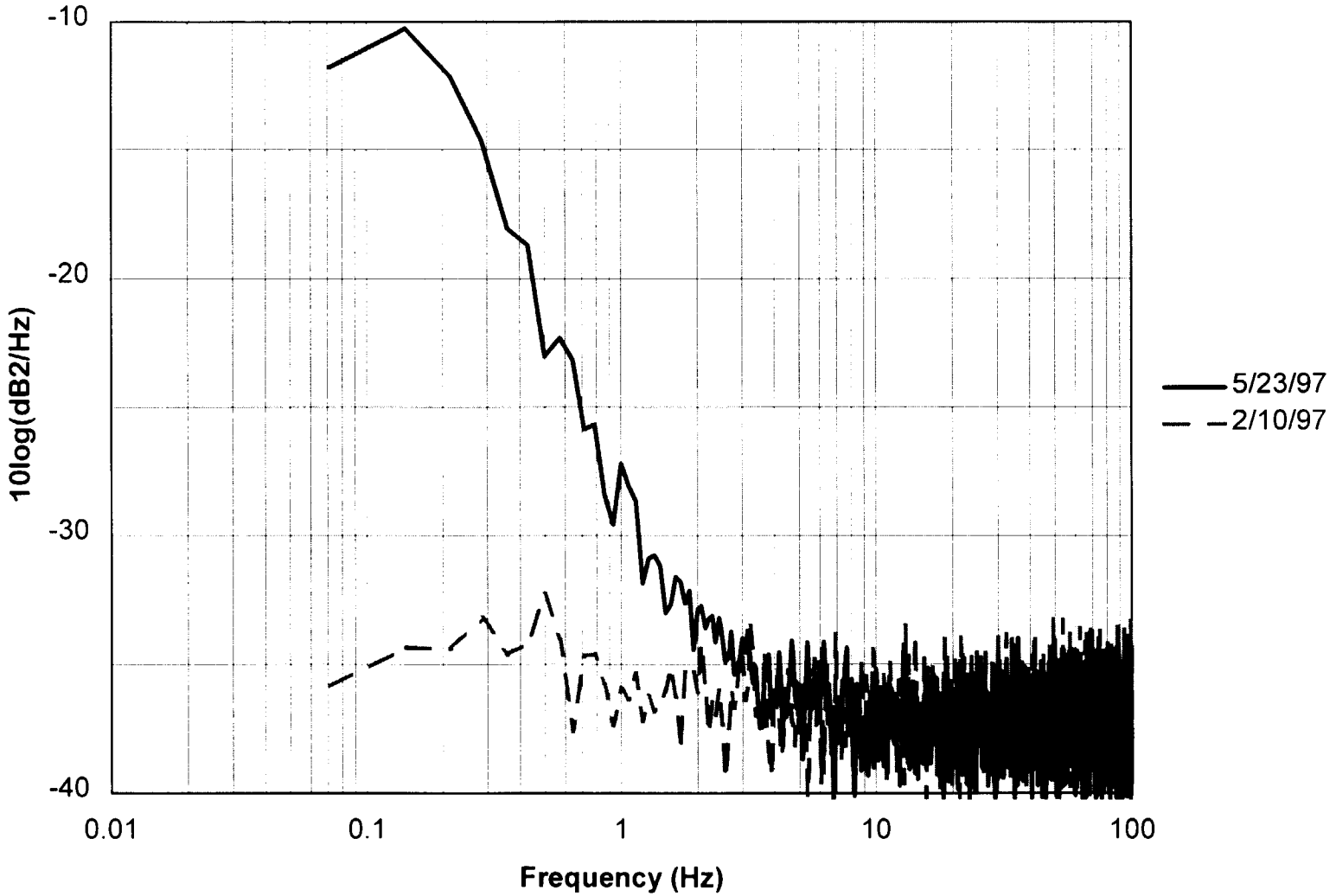

Phase Spectra Measurement

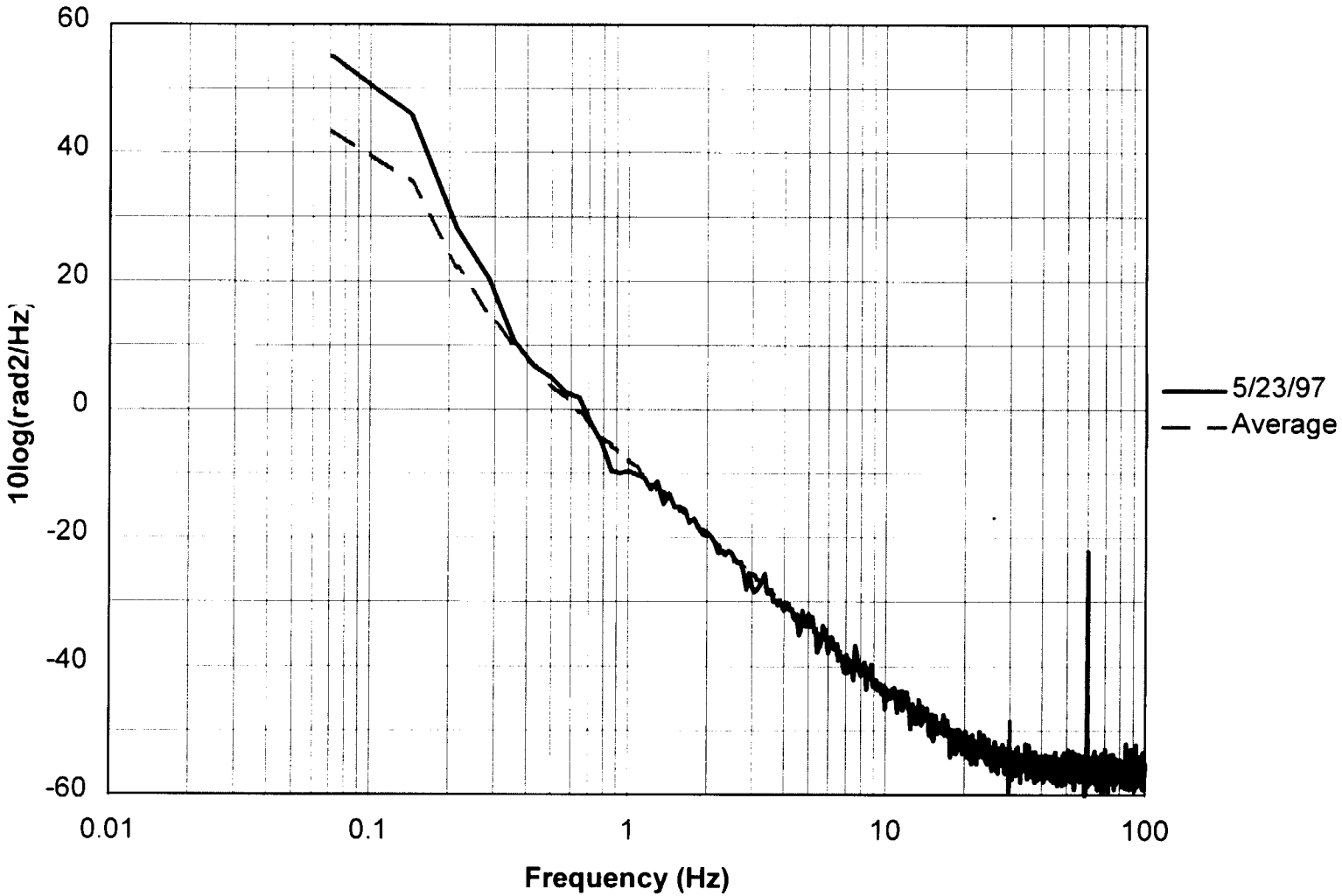

Amplitude Spectra Measurement

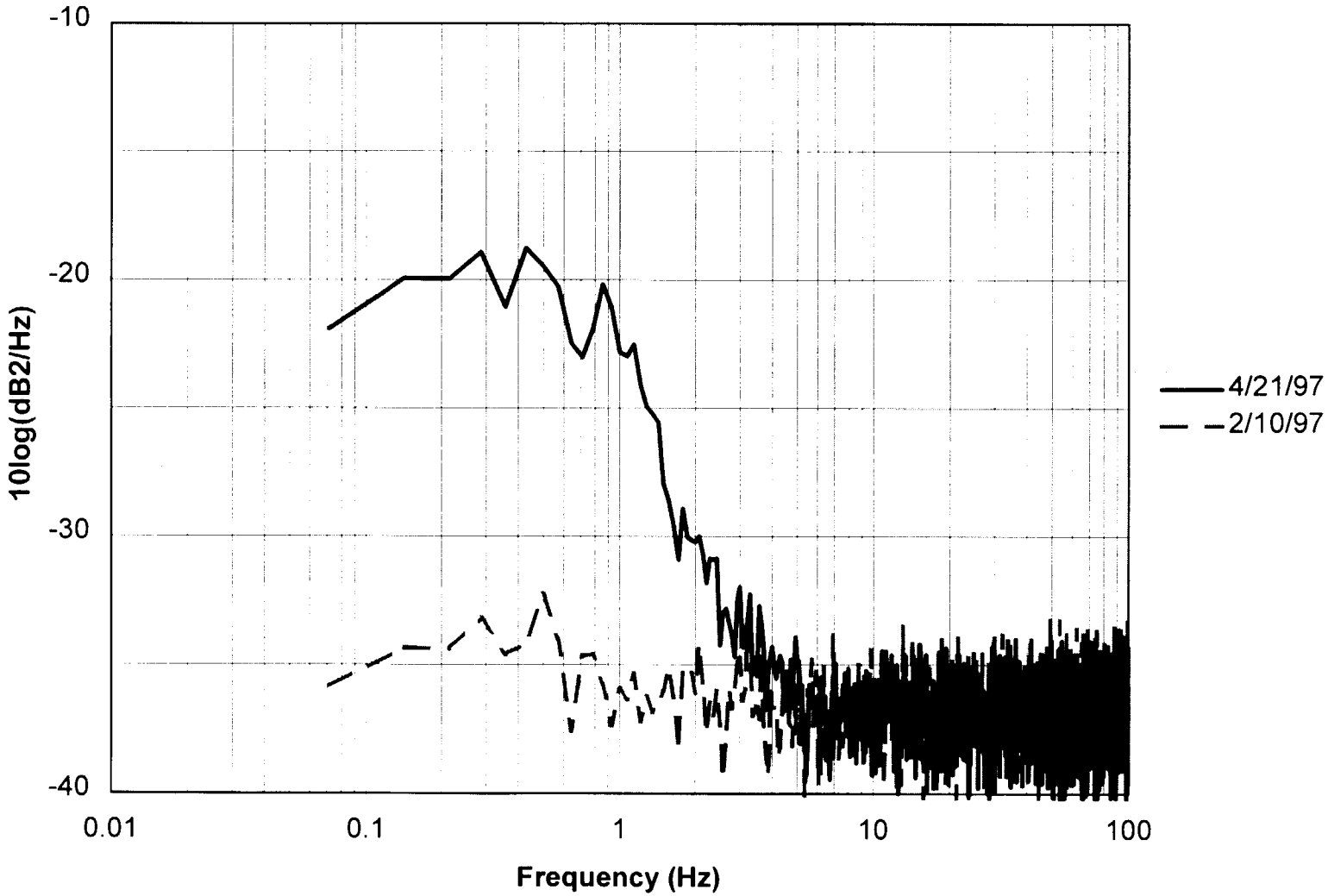

Phase Spectra Measurement

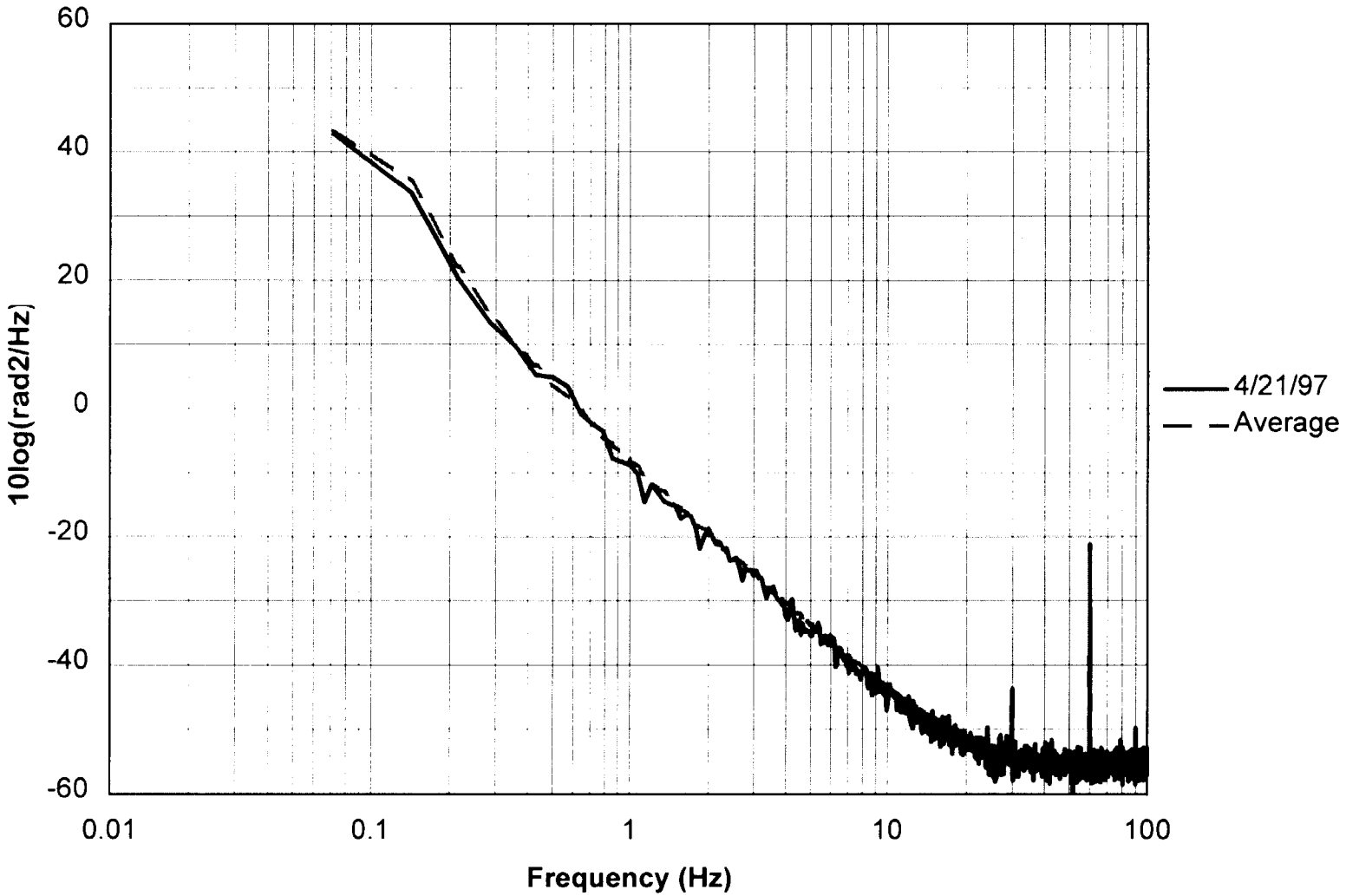

Spread Spectrum Modem Tests

- Modulation set to BPSK
- Data rates set to 1.544 Mbps (T1)
- Chip rate set at 30.88 Mcps
- 20 chips/bit code length
- Clear-air atmospheric conditions

CDMA Modem Performance

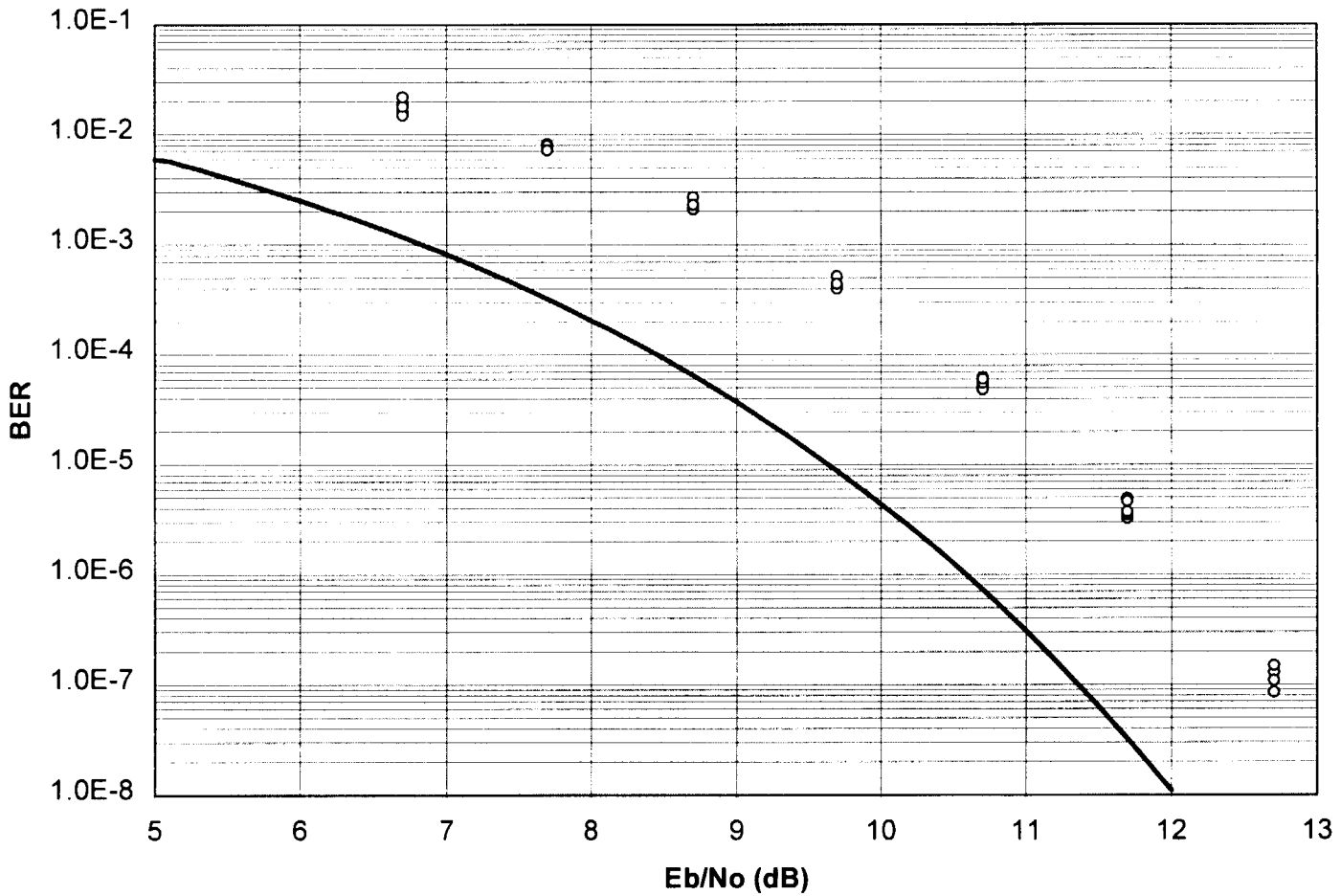

Spread Spectrum Measurements

- Spread spectrum signal will be combined with a carrier tone at the edge of the signal bandwidth
- Receiver will downconvert tone to audio range for digital sampling and processing
- Carrier tone will then be analyzed for C/N variations and scintillation
- Look for deviations from the expected BER during scintillation events

Scintillation in LEO Systems

- Velocity of the propagation path due to the motion of the satellite can be an order of magnitude greater than prevailing wind velocity
- Turbulent intensity (C_n) and path length (L) can no longer be considered constants
- Changes in the path length and velocity can be modeled, and the result used to extrapolate LEO scintillation effects

Conclusions

- Ka-band amplitude and phase scintillation have been measured on the ACTS propagation beacon
- Experiments to be performed will characterize effects of scintillation on the BER of a CDMA transmission
- Estimates of scintillation in a Ka-band LEO system will be obtained by extrapolating from ACTS measurements

CORRELATION OF S-BAND WEATHER RADAR REFLECTIVITY AND ACTS PROPAGATION DATA IN FLORIDA*

Eric E. Wolfe† Paul G. Flikkema, and Rudolf E. Henning

Department of Electrical Engineering
University of South Florida
Tampa, Florida USA

Abstract

Previous work has shown that Ka-band attenuation due to rainfall and corresponding S-band reflectivity are highly correlated. This paper reports on work whose goal is to determine the feasibility of estimation—and, by extension, prediction—of one parameter from the other using the Florida ACTS propagation terminal (APT) and the nearby WSR-88D S-band Doppler weather radar facility operated by the National Weather Service. This work is distinguished from previous efforts in this area by (i) the use of a single-polarized radar, preventing estimation of the drop size distribution (e.g., with dual polarization) and (ii) the fact that the radar and APT sites are not co-located.

Our approach consists of locating the radar volume elements along the satellite slant path and then, from measured reflectivity, estimating the specific attenuation for each associated path segment. The sum of these contributions yields an estimation of the millimeter-wave attenuation on the space-ground link. Seven days of data from both systems are analyzed using this procedure. The results indicate that definite correlation of S-band reflectivity and Ka-band attenuation exists even under the restrictions of this experiment.

Based on these results, it appears possible to estimate Ka-band attenuation using widely available operational weather radar data. Conversely, it may be possible to augment current radar reflectivity data and coverage with low-cost attenuation or sky temperature data to improve the estimation of rain rates.

*Partial support for this work was provided by NOAA and the University Corporation for Atmospheric Research under subaward UCAR-S96-75635 and by NASA under contract NAS3-26412.

†Now with Motorola Space and Systems Technology Group, 8201 E. McDowell Road, Mail Drop H2171, Scottsdale, AZ 85252.

1 Introduction

The purpose of this research is to study experimentally the relationships between S-band signal reflectivity and Ka-band propagation attenuation. Both are linked by atmospheric precipitation with rain rate as the predominant influencing factor. The two systems employed in this study are the Advanced Communications Technology Satellite (ACTS) with an associated ground terminal, and a WSR-88D Doppler weather radar operating in the same vicinity.

The relationship between reflectivity and attenuation is dependent on the drop size distribution (DSD). Previous work [1, 2] has shown that the DSD can be estimated using a dual-polarized radar. One goal of this work was to determine the feasibility of estimating reflectivity from attenuation (and vice versa) using the single-polarized WSR-88D radar employed by the National Weather Service. Even though the correlation of the two can never achieve the accuracy attainable with a dual-polarized radar, the widespread deployment of the WSR-88D poses intriguing possibilities for both propagation measurement and prediction and short-term forecasting.

This paper is organized as follows. In Section 2 we review the underlying theory that serves as the basis for this work. The salient features of the ACTS and WSR-88D systems and the relationships between the ACTS slant path and WSR-88D radar space are discussed in Section 3. Section 4 describes the method used to estimate attenuation from reflectivity data. Section 5 presents and analyzes results and discusses various error sources, and Section 6 provides concluding remarks.

2 Reflectivity and Attenuation

We cite a few well-known results. The rain rate R can be calculated for a given drop size D and drop velocity $W_t(D)$ by [4]

$$R = 6 \cdot 10^5 \pi \int_0^\infty D^3 \cdot W_t(D) dD \qquad \text{mm/hr.} \tag{1}$$

The drop size distribution (DSD) is the core component in determining rain rate R, reflected power Z, and specific attenuation K [3]. The DSD for rainfall $N(D)$ can be modeled with a gamma distribution [4]

$$N(D) = N_0 D^\mu \exp(-\Lambda D) \qquad \text{m}^{-3}\text{mm}^{-1} \tag{2}$$

with parameters N_0 ($\text{m}^{-3}\text{mm}^{-1}$), Λ (mm^{-1}), and μ, that vary according to rain rate, drop shape, and geographic location. Marshall and Palmer [4] determined that by setting $\mu = 0$, $N_o = 8 \cdot 10^3$, and $\Lambda = 4.1 R^{-0.21}$ a close approximation to measured data can be achieved.

The specific attenuation K is a function of the drop size distribution $N(D)$ and the effective drop cross section $\sigma_e(D, \lambda)$ via

$$K = 4.34 \cdot 10^3 \int_0^\infty N(D) \sigma_e(D, \lambda) dD \qquad \text{dB/km.} \tag{3}$$

where D is the drop diameter and λ is the signal wavelength. Similarly, the radar reflectivity factor Z can be expressed as

$$Z = \int_0^\infty N(D) D^6 dD. \tag{4}$$

Since the DSD cannot be determined uniquely from either the reflectivity or the specific attenuation, we turn to single-parameter approximations. By relating Z to R and then R to K, it is possible to take full advantage of previous research in both of these areas. Empirically, Z and R have been shown to be (on average) related by [4]

$$Z = \alpha_1 R^{\beta_1} \qquad \mathrm{mm}^6/\mathrm{m}^3 \tag{5}$$

where α_1, and β_1 are constants. Some empirically derived values for these constants can be found in [4]. Likewise, previous investigations have determined an exponential dependence between K and R [3]

$$K = \alpha_2(f) R^{\beta_2(f)} \qquad \mathrm{dB/km} \tag{6}$$

where $\alpha_2(f)$, and $\beta_2(f)$ are frequency-dependent parameters and K is in dB/km; see [3] for a review of estimates for these constants.

Since reflectivity and specific attenuation are related to the rain rate R via the DSD, Z and K can be directly related by solving (5) and (6) for R and then solving for K

$$K = \alpha_2 \left(\frac{Z}{\alpha_1} \right)^{\frac{\beta_2}{\beta_1}} \qquad \mathrm{dB/Km} \tag{7}$$

Equivalently, we have

$$K = \alpha \left(10^{\frac{Z_{dB}}{10}} \right)^{\beta} \qquad \mathrm{dB/Km} \tag{8}$$

after setting $\alpha = \alpha_2 \alpha_1^{-\frac{\beta_2}{\beta_1}}$ and $\beta = \frac{\beta_2}{\beta_1}$, and where $Z_{dB} = 10 \log_{10}(Z)$. A typical plot of specific attenuation vs. reflectivity using Marshall-Palmer model parameters [4, 3] is shown in Figure 1.

3 Experimental Setup

The ACTS satellite has two Ka-band beacons that transmit at frequencies of 20.185 and 27.505 GHz which are received at ACTS propagation terminals (APTs) in seven U.S. locations (each located in a different climate zone). This study is based on data gathered from the APT based at the University of South Florida (USF) in Tampa, Florida.

The trajectory of the propagating signal between the ACTS and APT is called the slant path. We define the effective slant path as the portion of the slant path that is susceptible to rain attenuation. The highest point above the earth's surface in which atmospheric attenuation from interference can occur is approximately 15 Km. The two end points of the effective slant path

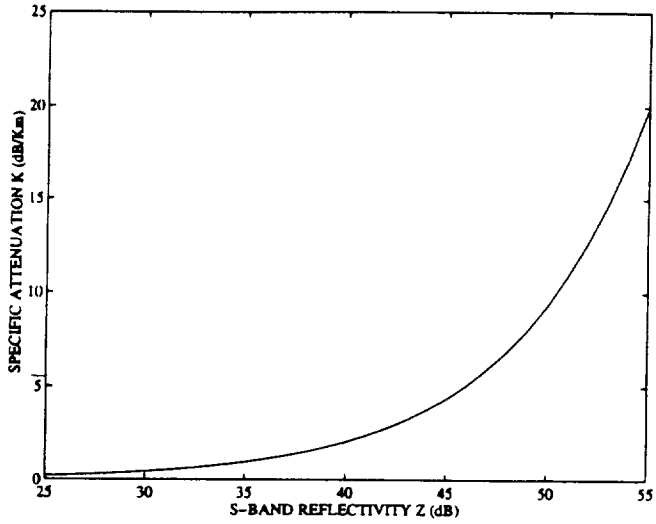

Figure 1: K vs. Z at 27.5 GHz using Marshall-Palmer parameters for α_1, β_1, α_2, and β_2.

are located at the APT antenna and the point on the ACTS slant path 15 Km above the ground respectively.

The NOAA WSR-88D radar used for this study is located in Ruskin FL, approximately 34 Km south of the USF APT. This radar detects precipitation in the atmosphere by transmitting a 2.7 GHz pulse along a radial (an outward radiating vector at specific azimuth and elevation angles) and then measuring the backscattered power from volume elements of the atmosphere. The reflected power received by the radar is measured and averaged over a time interval that coincides with 1,000 meters of range. Thus a volume element is roughly a right circular cone frustum 1,000 m in length (along its radial axis) with diameter increasing with range.

The radar sweeps through azimuth increments of 1° while ranging in elevation from 0.5° to 19.5°. Due to the curvature of the earth, there are undetectable areas below the lowest elevation angle. There are also discontinuities within the operational elevation range of 0.5° to 19.5° depending on the scanning strategy, or volume coverage pattern (VCPs), employed. The data for this study was collected using the most commonly used pattern, called VCP21, which scans 9 elevation angles (with the lower 5 providing contiguous vertical coverage) and requires 6 minutes to complete a full pattern.

4 Approach

In order to relate the two data sets, the effective satellite slant path is located in the radar coordinate system. Ideally, the APT would be co-located with the WSR-88D radial fixed along the ACTS slant path. However, the radar is located 32 Km away, and a complete volume scan requires approximately 6 minutes. Thus temporal and spatial sampling effects are to be expected in rain events due to storms that are concentrated, highly dynamic, or moving quickly.

In order to develop snapshots of the entire slant path, we have found that two approaches have worked well. To overcome the temporal sampling, we employ straightforward linear interpolation of the reflectivity data (at each of the radar volume elements intersecting the slant path). The spatial sampling derives from the fact that the volume coverage patterns are not vertically continuous at higher elevations; only certain intervals along the slant path are sampled by the radar. Our approach to this problem is to divide the effective slant path into contiguous segments each containing a volume element, and further assume that the reflectivity is piecewise constant along each segment.

Our procedure to estimate the total Ka-band attenuation from the S-band reflectivity can be summarized as follows:

1. For each radar volume element i in the effective slant path, determine the reflectivity Z_i from the reflectivity associated with the element.

2. Estimate the most probable specific attenuation K_i from the reflectivity using (8).

3. Compute the millimeter wave attenuation A_i for each segment from the product of K_i and the segment length d_i, and find the total derived attenuation $A_T = \sum_i A_i$ along the slant path.

The approach requires two passes through the data. The first pass is a parameter estimation phase and is based on the total available data. More specifically, the model parameters α and β in (8) need to be fitted to the measured data to reduce the estimation error. Ideally, we would construct a scatter plot of reflectivity Z and the corresponding specific attenuation K, obtaining a fitted curve parameterized by α and β. Unfortunately, the APT measures total attenuation along the ACTS slant path, while each measured reflectivity relates only to the specific attenuation of an effective slant path segment. As an alternate approach we still constructed scatter plots, but plotted the derived total attenuation as a function of the ACTS measured total attenuation. The parameters α and β were then adjusted so that the slope of the line through the mean of the scatterplot is unity. Using this heuristic, we obtained the scatter plot for 20.2 GHz shown in Figure 2. We also used the same approach for the 27.5 GHz beacon. The results for both frequencies are shown in Table 1. In the second pass, the same procedure outlined above is used, except that estimation for individual rain events is performed using the parameters determined in the first pass.

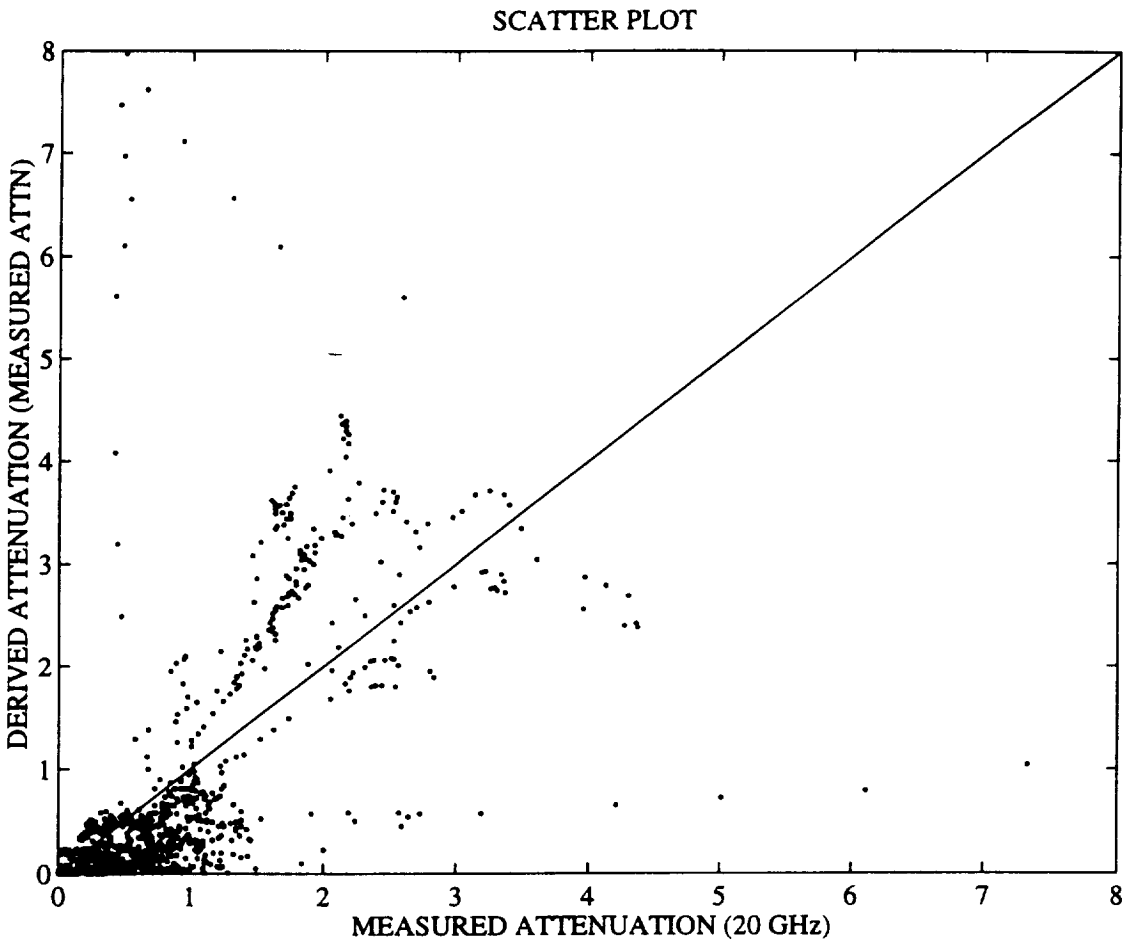

Figure 2: Scatter plot for model parameters: $\alpha = 0.00377$, $\beta = 0.62125$.

Frequency	α	β
20.2 GHz	0.00377	0.6213
27.5 GHz	0.01322	0.5235

Table 1: Established $K - Z$ model parameters.

5 Results

Seven days of data were analyzed using the described correlation procedure. These days and times were chosen to represent various storm intensities and are listed in Table 2. This table also shows the total duration and number of fades (using 20.2 GHz beacon) for thresholds of 1 and 3 dB. To remove as much as possible the attenuation effects not due to rain, the data was filtered with a moving average filter (to smooth scintillations) and thresholds of 1 and 3 dB were applied. Thus the table shows the average difference in dB between derived and measured attenuation for fades greater than 1 dB and 3 dB. The average difference is calculated by summing the absolute differences between the derived and measured attenuation and then dividing by the number of samples. A difference is included in the summation only when at least one of the two values (derived or measured) is above the threshold value.

Date (1995)	GMT Time (min)	Total Time > 1 dB (min)	# fades > 1 dB	Avg Dif (dB)	Total Time > 3 dB (min)	# fades > 3 dB	Avg Diff (dB)
03 Aug	0.01–9.27	76.8	10	1.8	28.0	8	3.5
03 Oct	16.2–24.0	90.5	7	6.3	40.7	5	12.0
04 Oct	13.1–23.9	25.0	4	1.4	3.3	1	9.7
05 Oct	0.1–6.0	62.8	5	2.4	31.0	8	4.8
05 Oct	12.2–16.6	108.5	6	2.2	20.3	3	5.8
08 Nov	0.3–16.0	211.4	13	5.8	57.2	5	13.0
29 Nov	0.3–17.5	214.0	17	1.2	21.3	2	2.2
31 Dec	0.29–23.93	386.3	15	1.6	114.5	15	2.6

Table 2: Summary of data and results.

The accuracy of the estimation depends on several factors. First, the model parameters are based on a global curve fit which is then used for correlation of individual events. Since it is well-known that the parameters vary dramatically even in the same climate zone, some events will be poorly estimated.

Note that in Table 2 the average difference for fades greater than 3 dB is about twice that of the fades greater than 1 dB. This larger difference at deeper fades may be due at least in part to the increased Z-K model sensitivity at higher reflectivities, as shown in Figure 1.

Another effect that has recently become well-known is moisture on the APT antenna surface. This can cause additional attenuation of the millimeter-wave signal by as much as 4 dB [5, 6, 7], which could cause a large underestimation of the total attenuation by the radar. Though the additional wetting loss could be deduced using the rain gage data at the APT, this was not attempted.

Finally, there are several attributes of the radar that will limit accuracy of the estimation. First, as noted earlier, there are elevation gaps in the coverage of the slant path, requiring the piecewise-constant approximation described earlier. Another effect is that of the large radar element volume, implying that the average reflectivity over this element is not necessarily a good representation of reflectivity along the slant path. Additional degradation can occur due to the high temporal sampling interval (approx. 6 minutes) of the radar, which can cause errors for fast-moving or dynamic storms. The radar also does not sample the entire slant path. First, the effective height of the atmosphere is approximately 15 Km. The highest elevation angle provided by the radar is 19.5° which equates to 9,937 km in altitude. Thus, if there is a precipitation event occurring in the ACTS slant path beyond this point (e.g., ice), it will not be detected by the radar but will still be measured as attenuation at the APT. Similarly, the radar's minimum elevation angle implies that even in the best case scenario, in approximate terms it cannot sample the lowest 100 m of the slant path. Finally, though refraction is normally negligible, there can be occasions where it results in signficant ground clutter, corrupting the reflectivity results.

A few cases are discussed here for illustration. Figure 3 shows graphs for November 29, 1995 (20.2 GHz beacon) containing 6 events. The plots consist of the derived attenuation (top), ACTS measured attenuation (middle), and rain rate measured at the APT (bottom). These events are good examples of typical fade scenarios. Figure 4 illustrates event #2. There is a close correlation in both time and fade levels between the derived and measured data. In this case the rain at the APT follows the same pattern implying that most of the attenuation occurred at or near the earth end-point of the ACTS slant path.

The delay between derived and measured data is related to how fast the storm is moving and its direction relative the ACTS slant path. Figure 5 shows event #5, which shows that the radar-derived data peaks 6 minutes before the measured data. We believe, in this case, that even though the storm may not appear in the effective slant path until 13.85 GMT it still occupies a large percentage of the defined volume elements associated with it. Recall that these volume elements are extremely large and may be only partially filled and still show reflectivity at the radar. The low spatial resolution of the radar may also account for the smoothing observed in the derived attenuation data.

Figure 6 illustrates 3 events for October 3, 1995 (20.2 GHz beacon). Event #2 is a very deep but short fade. The rain rate is in excess of 100 mm/hr which is typical for a Florida downpour. Figure 7 shows a closer look at this event. Note that again there is a delay of a few minutes between the detected onset of the rainfall, indicating that the radar volume elements were partially filled prior to the rain cell entering the effective slant path. Note that, though the clipped measured attenuation data appears to indicate APT lost lock at the APT receiver, it was verified that this was not case and thus this shows the true measured attenuation throughout the event.

As described above, inaccuracies can be attributed to the combination of several factors. Figure 8 shows two events for December 31, 1995 (27.5 GHz beacon). The measured data indicated 2 minor fades, one occurring at 7 GMT and the other at 8.5 GMT. The rain gage shows rain for both cases but the derived data did not detect the fade at 8.5 GMT. While this may be caused primarily by

the inability of the radar to sample the complete slant path, further study is warranted.

6 Conclusion

In this study we attempted to determine the feasibility of correlating S-band radar reflectivity with Ka-Band signal attenuation. The results of this study are very encouraging. Most rain events occurring along the ACTS slant path are observed in the derived data, though some events in the derived data appeared earlier or later than the measured data by a few minutes. While many of the smaller fades are underestimated, they are still detected. Occasionally, events detected by one instrument were not detected by the other, which we tentatively attriblute in most cases to spatial and temporal sampling effects at the radar. While these results are only for a small data set, they strongly suggest further study of both short- and long-term correlations between reflectivity and attenuation.

References

[1] J. Beaver, J. Turk, and V. Bringi, "Ka-band propagation studies using the acts propagation terminal and the CSU-chill multiparameter, doppler radar," in *Proceedings of the 1995 27th Conference on Radar Meteorology*, pp. 792–795, 1995.

[2] W. L. Stutzman, T. Pratt, C. W. Bostian, and R. E. Porter, "Prediction of slant path rain propagation statistics using dual polarized radar," *IEEE Transactions on Antennas and Propagation*, vol. 38, pp. 1384–1390, Sept. 1990.

[3] L. Ippolito, *Propagation Effects Handbook for Satellite Systems Design: A Summary of Propagation Impairments on 10 to 100 GHz Satellite Links with Techniques for System Design.* NASA, 1989.

[4] R. Doviak, *Doppler Radar and Weather Observations.* Academic Press, Inc., 1992.

[5] V. N. Bringi and J. Beaver, "Ka-band propagation studies using the ACTS propagation terminal and the CSU-CHILL multiparameter radar," in *Proc. of the Twentieth NASA Propagation Experimenters Meeting (NAPEX XX) and the Advanced Communications Technology Satellite (ACTS) Propagation Studies Miniworkshop*, pp. 85–112, NASA, June 1996.

[6] R. E. Henning and J. R. Stanton, "Effects of dew on millimeter-wave propagation," in *Proceedings of IEEE Southeastcon '96*, pp. 684–687, Apr. 1996.

[7] M. Kharadly, R. Ross, and B. Dow, "Analysis of the ACTS-Vancouver path propagation data," in *Proc. of the Twentieth NASA Propagation Experimenters Meeting (NAPEX XX) and the Advanced Communications Technology Satellite (ACTS) Propagation Studies Miniworkshop*, pp. 67–83, NASA, June 1996.

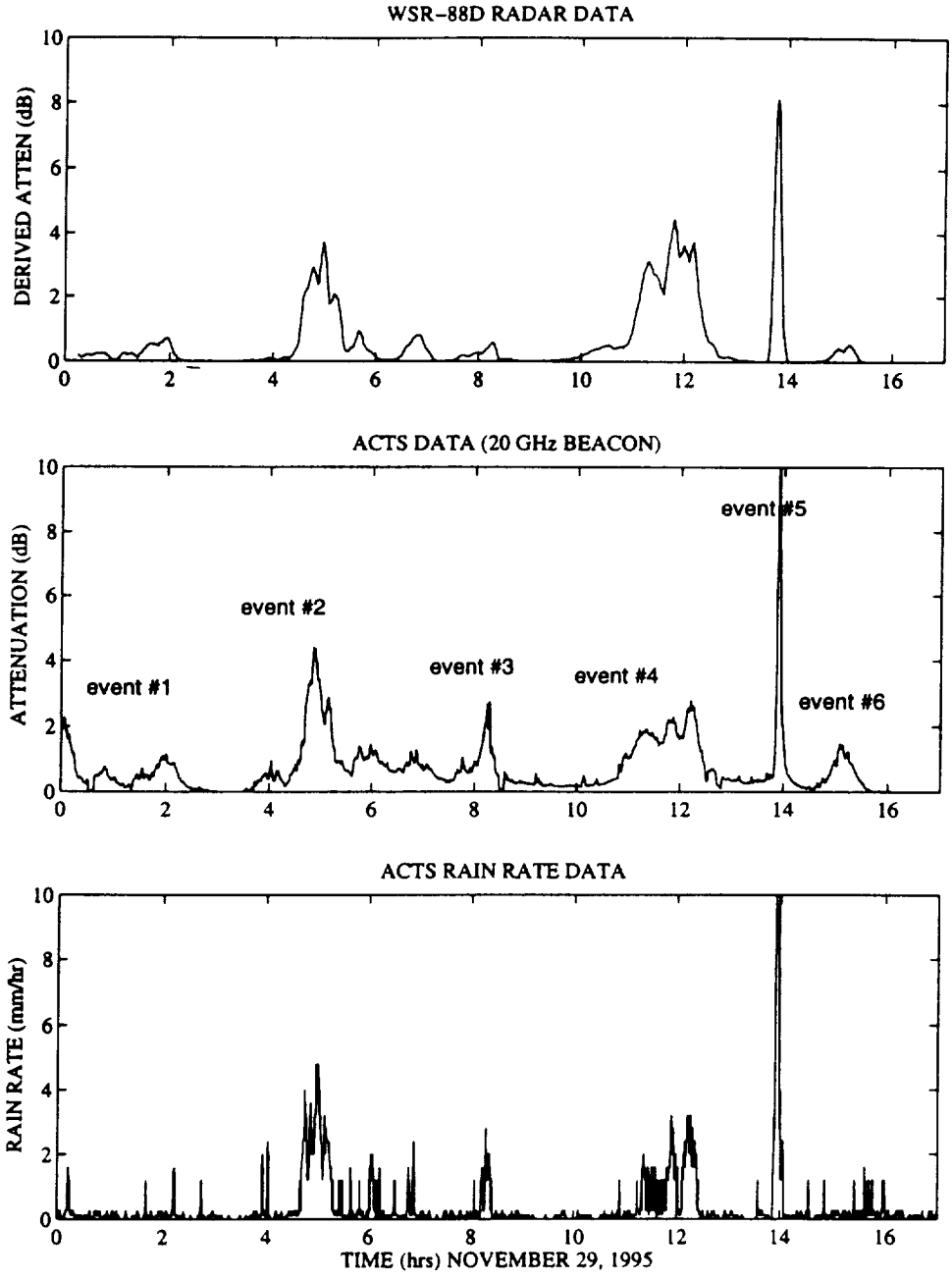

Figure 3: Derived (estimated) attenuation, measured attenuation, and rain rate; Nov. 29, 1995.

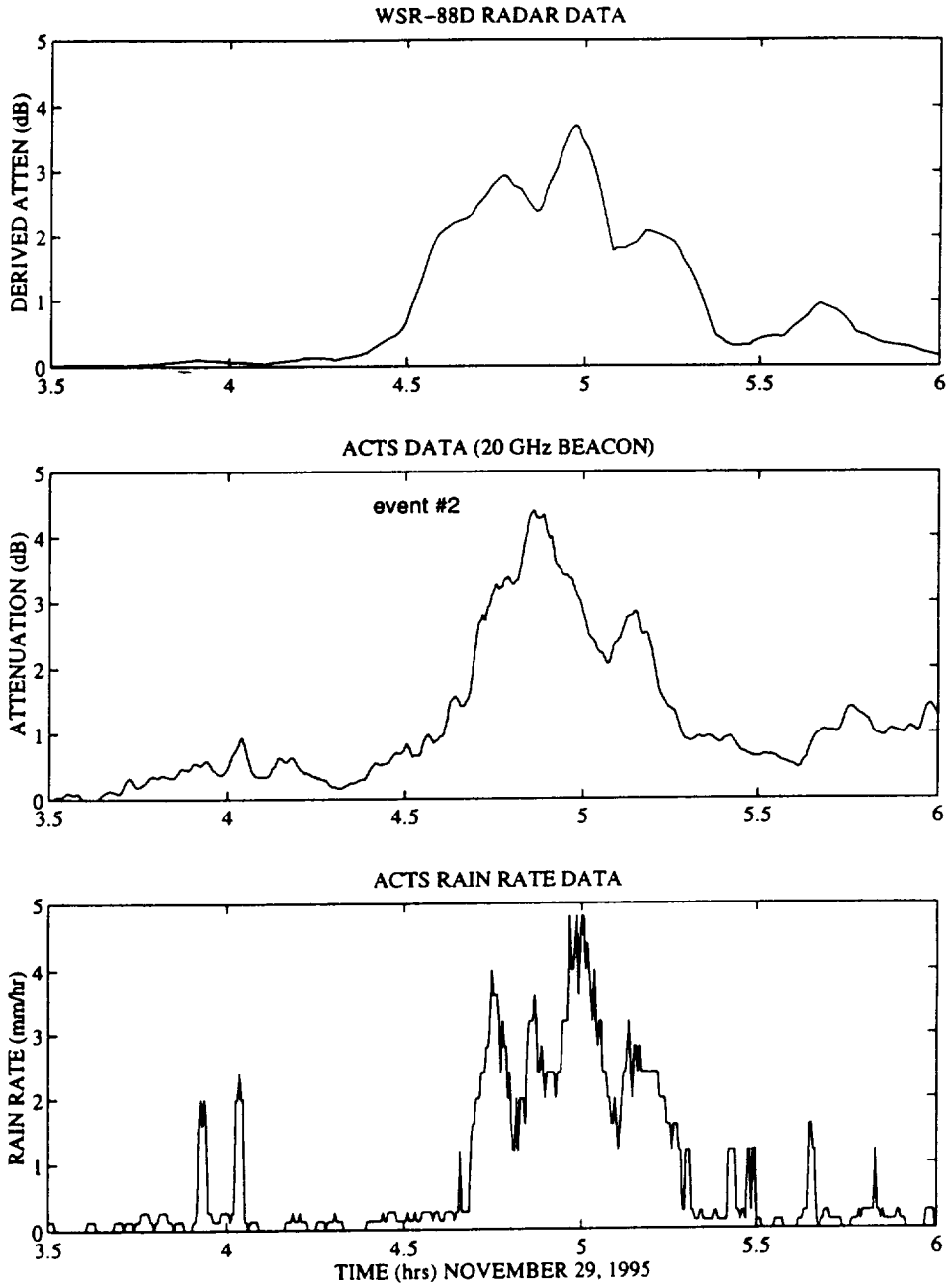

Figure 4: Event #2, Nov. 29, 1995.

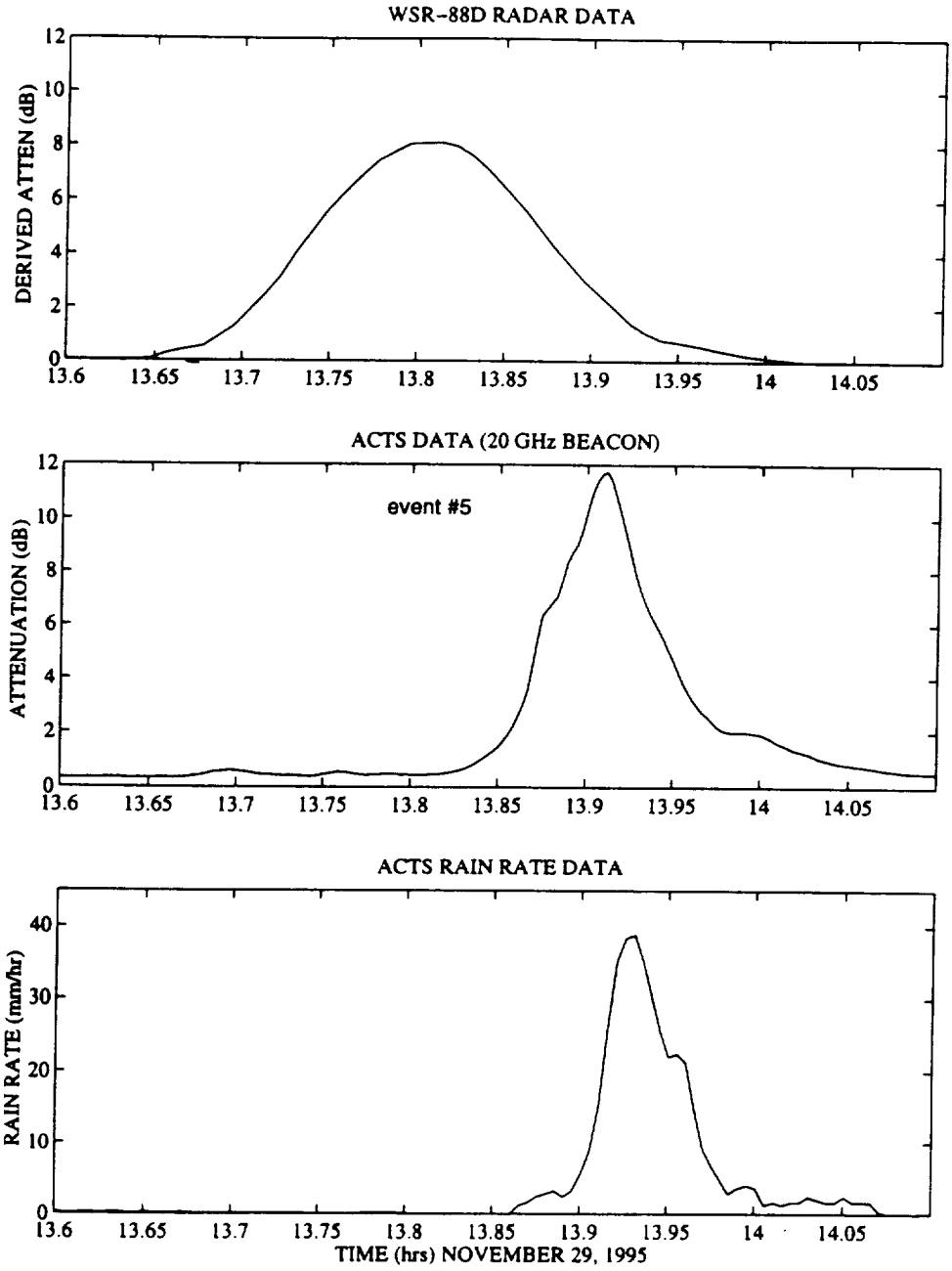

Figure 5: Event #5, Nov. 29, 1995.

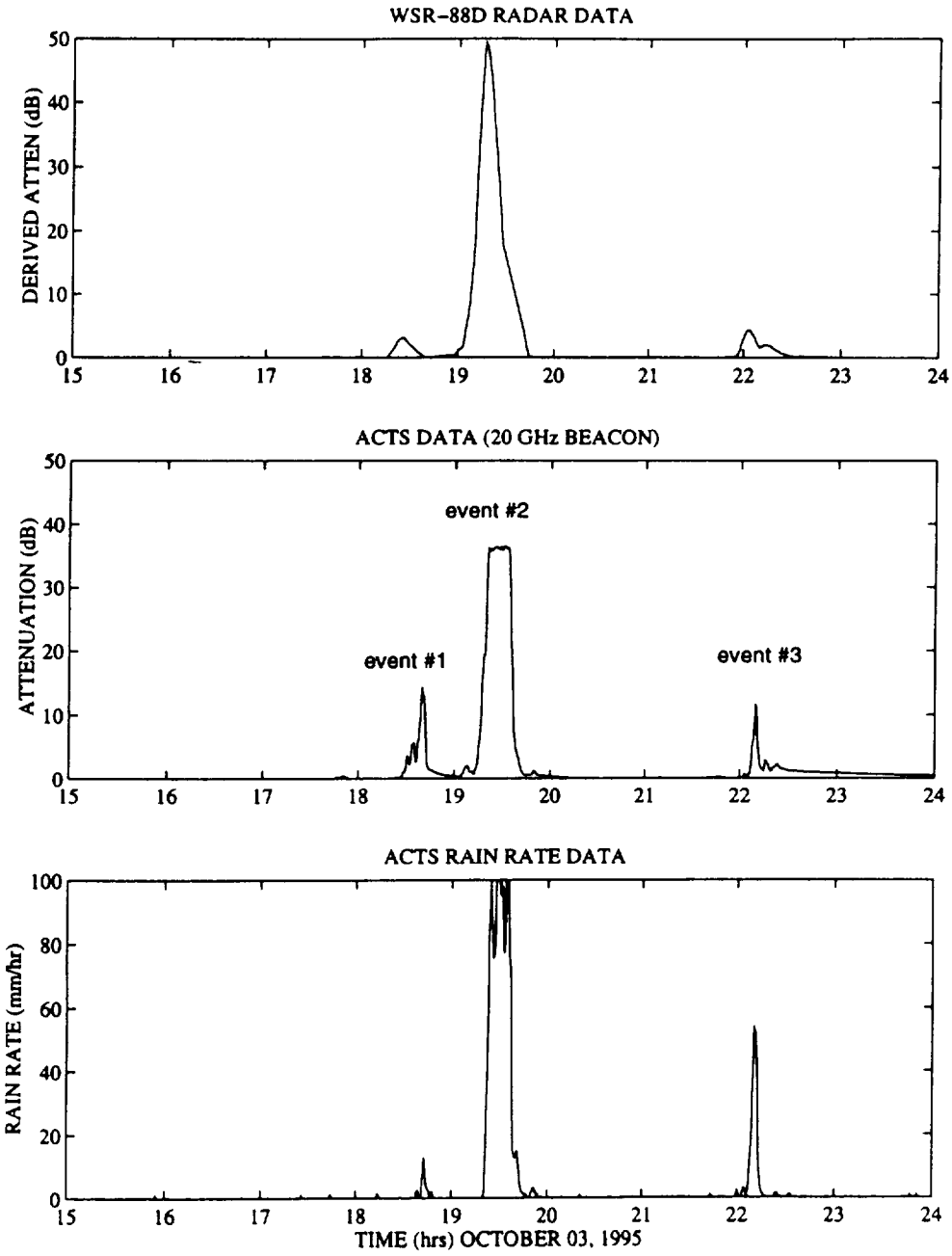

Figure 6: Derived (estimated) attenuation, measured attenuation, and rain rate; Oct. 3, 1995.

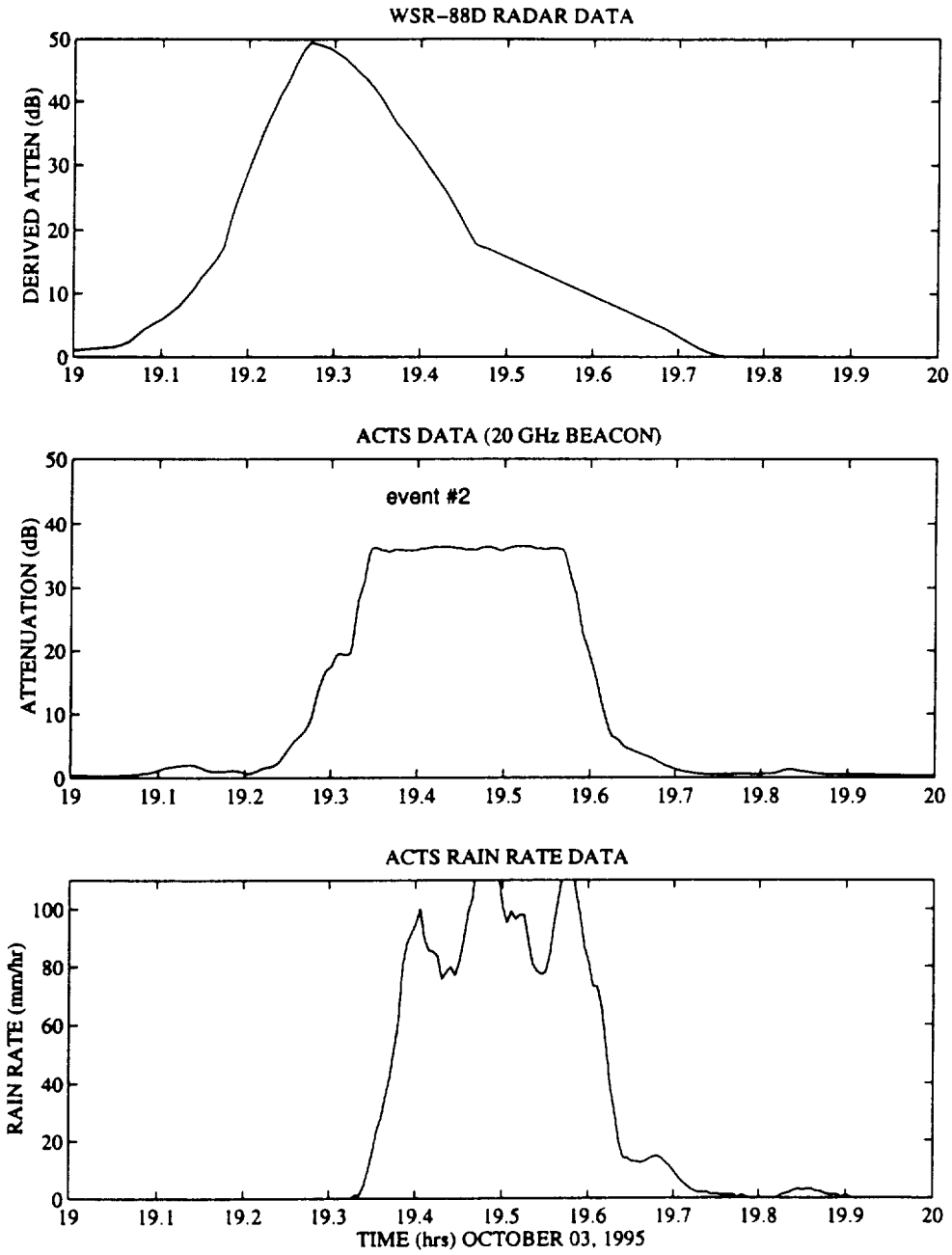

Figure 7: Event #2, Oct. 3, 1995.

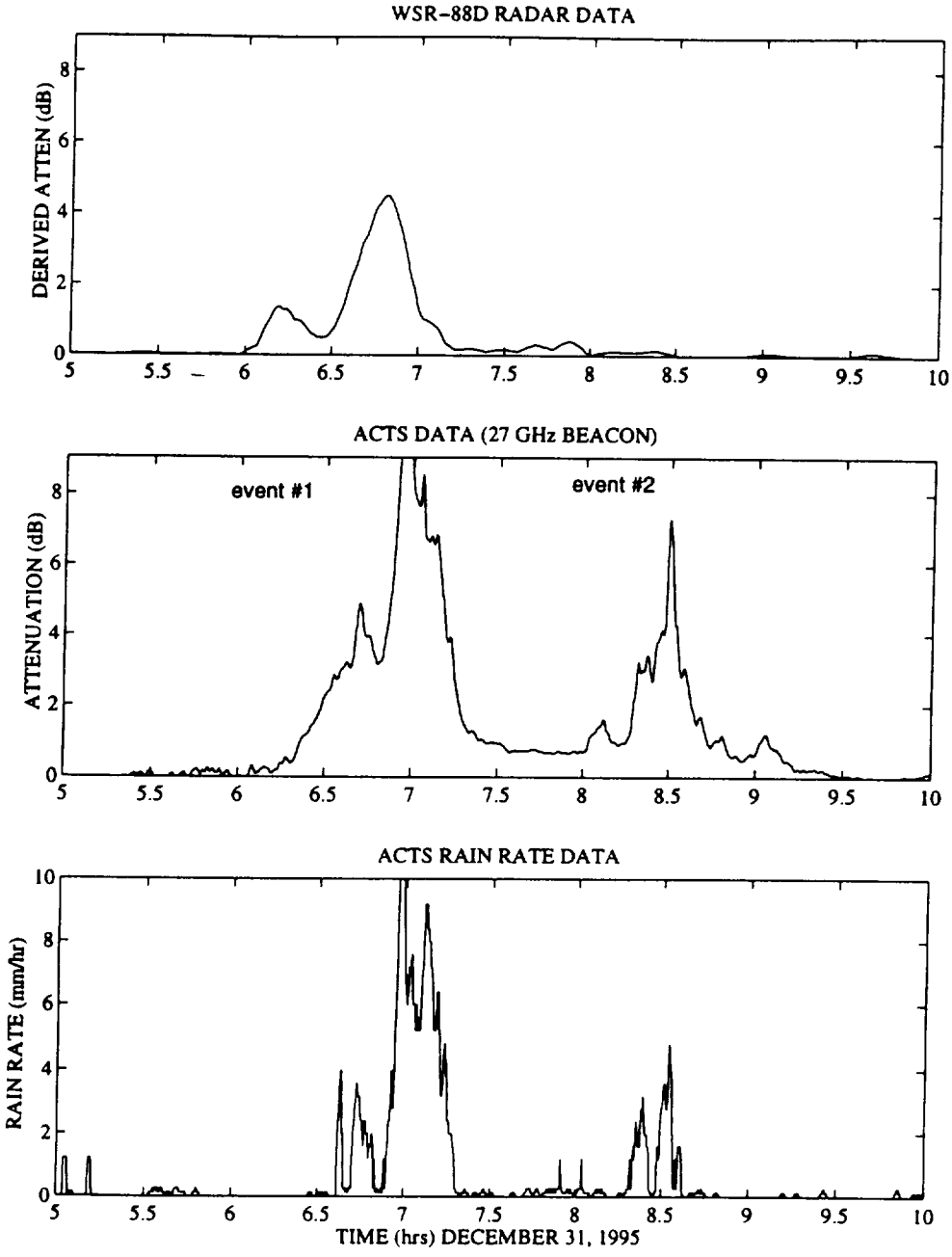

Figure 8: Derived (estimated) attenuation, measured attenuation, and rain rate; two events on Dec. 31, 1995.

S10-32

299318
p 32

Highlights of Revised Mobile Satellite Handbook

Julius Goldhirsh
Applied Physics Laboratory
The Johns Hopkins University
Johns Hopkins Road, Laurel MD 20723-6099
EMAIL: julius_goldhirsh@jhuapl.edu

Wolhard J. Vogel
Electrical Engineering Research Laboratory
The University of Texas at Austin
10100 Burnet Road, Austin TX 78758-44497
EMAIL: wolf_vogel@mail.utexas.edu

Figure #1 Background

In this talk is presented a discussion of the revised mobile satellite handbook. In 1992, the first edition of the handbook was published. This document was entitled, "Propagation Effects for Land Mobile Satellite Systems: Overview of Experimental and Modeling Results," by Julius Goldhirsh and Wolfhard J. Vogel (NASA Reference Publication 1274, February 1992). The text of this document may be acquired on the NASA Propagation Studies world wide web home page (http://propagation.jpl.nasa.gov/). This document contains the results of published information up through approximately 1991 and emphasizes the effects of foliage and terrain for land-mobile satellite scenarios at UHF and L Band. The objective of the revised edition entitled, "Propagation Effects for Vehicular and Personal Mobile Satellite Systems: Overview of Experimental and Modeling Results," is to include the results of published information since 1991 and to broaden the scope of the previous document.

Figures #2: Contents of Talk

In this talk, I'll give a brief review of the chapter titles for the revised handbook, an overview of the status of the text as of this date, followed by a brief description of the contents of each completed chapter. To provide a flavor of the contents of the revised text, an example of new results contained in selected chapters will be presented.

Figures #3 and #4: Chapter Titles

The revised document contains 12 chapters, the titles of which are included here. The asterisk next to the chapter number indicates that this chapter has been completed. The chapter titles are: Chapter 1: Introduction, Chapter 2: Attenuation Due to Individual Trees: Static Case (completed), Chapter 3: Attenuation Due to Roadside Trees: Mobile Case (completed), Chapter 4: Signal Degradation for Line of Sight Communications (completed), Chapter 5: Fade and Non-Fade Durations and Phase Spreads (completed), Chapter 6 Propagation Effects Due to Cross Polarization, Antenna Gain, and Space Diversity (completed), Chapter 7: Land and Mobile Measurements from Different Countries (completed), Chapter 8: Personal Communications Propagation Effects, Chapter 9: Aeronautical and Marine Propagation

Effects, Chapter 10: Optical Methods for Assessing Shadowing and Blockage, Chapter 11: Theoretical Modeling Considerations, and Chapter 12: Recommendations for Further Investigations. Chapters 8, 9, and 10 represent new subject chapters not contained in the previous handbook.. Chapter 8 will contain information related to earth-satellite personal communication scenarios. For example, multipath and attenuation effects from building walls will be given and associated experiments will be reviewed. Chapter 9 will, for example, review multipath effects caused by airplane and or ships structure as well as multipath from the ocean. Chapter 10 will review Wolf Vogel's optical experimental results and methodology to define hemispherical blockage and shadowing effects for mobile satellite scenarios.

Figure #5: Status

As mentioned, six chapters have been completed to date and written in the word processing format of Microsoft Word for Windows 95. These chapters (as of this writing) are awaiting processing by JPL for injection onto the NASA Propagation Studies home page. All chapters should be completed by the fall of 1997.

Figure #6: Chapter 2 Contents: Attenuation Due to Trees: Static Case

In this figure are listed the table of contents for Chapter 2 where the sections marked with an asterisk denote new sections. Each chapter is designed such that it is for the most part independent of the results in other chapters For example, each chapter has its own set of references and its own set of conclusions and recommendations. This particular chapter primarily deals with single tree attenuation at UHF, L Band and K Band, the effects of foliage at these frequencies, foliage versus non-foliage scaling at the different frequencies, and frequency scaling. In the next figure, we cull out Section 2.6.3 entitled "Effects of Foliage at K Band," which describes a model to convert equi-probability fades from shadowing to non-shadowing scenarios, and conversely.

Figure 7: Formulation for Estimating Equal-Probability K-Band Attenuation: Foliage Versus non- Foliage

In this figure is given the empirical formulation for estimating the equal probability attenuation at approximately 20 GHz relating the foliage and non-foliage cases. The static case range of attenuations over which the formulation is valid is given between 5 and 25 dB for the non-foliage case. The formulation is expressed in terms of the indicated power expression. This formulation was derived from two mobile runs along a street in Austin, Texas lined with Pecan Trees. These runs were executed in February and May during which times the trees were without leaves and in full blossom, respectively. The formulation was also found applicable for the static measurement case as is shown in the next figure.

Figure 8: Measured and Predicted Attenuation Distributions at 19.6 GHz for Foliage and Non-Foliage Cases

The solid curves in this figure are the static cumulative fade distributions for a single Pecan tree derived from measurements in Austin, Texas. The curves to the left and right represent the distributions for the non-foliage and foliage scenarios. These distributions were derived

from measurements where a transmitter was placed atop a tower on one side of the tree and the receiver was placed on the opposite side. The receiver was moved laterally to different optically shadowed positions. The dashed distributions correspond to the previously described estimation formulation The right dashed curve predicts the case of the equi-probability foliage attenuation using the non-foliage solid curve, and the left dashed curve is the predicted distribution for the non-foliage case using the foliage solid curve.

Figures 9 and 10: Chapter 3 Contents: Attenuation Due to Roadside Trees: Mobile Case

In Chapter 3 we examine empirical models associated with land-mobile satellite signal attenuation for scenarios in which the vehicle is driven along tree-lined roads. Signal degradation is predominantly due to absorption and scatter from tree canopies. Various models are compared to one another and with measured distributions Examples of major new sections are: Section 3.3 and 3.4 which reviews the Extended Empirical Roadside Shadowing Model and its validation. Section 3.7 (also new) compares the EERS model with other empirical models. In the next three figures we cull out examples regarding these sections.

Figure 11: Features of Extended Empirical Roadside Shadowing Model (EERS)

The Extended Empirical Roadside Shadowing model (EERS) estimates cumulative fade distributions for mobile satellite scenarios in which roadside shadowing gives rise to attenuation. This model is an extension of a former model called the Empirical Roadside Shadowing Model (ERS). The EERS was provisionally accepted by the ITUR on February of 1997. It applies to tree shadowing with a population of trees which range from at least 55% to 75% and is applicable over probabilities from 1% to 80%. It applies to frequencies ranging from 870 MHz to 20 GHz and elevation angles from 7° to 60°. The recent ITUR recommendation suggests methods applicable at L and S bands for extending the angular range to elevation angles above 60°.

Figure 12: Family of L-Band (1.5 GHz) Cumulative Fade Distributions Predicted from Extended Empirical Roadside Shadowing Model

We show here an example of a family of L Band (1.5 GHz) cumulative fade distributions predicted from the EERS model. We note the 1% fade has a range from 8 dB at 60° to 26 dB at 20°. The EERS model states that for angles between 20° to 8°, the 20° distribution may be applied at the smaller elevation angles assuming their is no terrain blockage and no multiple canopy shadowing.

Figure 13: Summary of Empirical Models and Domains of Validity

In this table is given a listing of the major roadside shadowing models and their domains of validity. The ITU-R model denoted here employs a tabulation of high elevation angle measurements between 60° and 80° derived from measurements of Smith, Gardiner and Barton at L and S Band. The EFM model represents the Empirical Fading Model which has a form similar to the ERS model but is applicable between 60° to 80° and at frequencies of 1.3 GHz to 10.4 GHz. The MERS model denotes the Modified Empirical Roadside Shadowing model which gives results that are applicable between 20° and 80° at frequencies

from 1.5 GHz to 2.6 GHz. At L-Band, the MERS model was found to be within 1 dB of the EERS model values at 30°, 45°, and 60°. The CEFM model which stands for Combined Empirical Fading Model combines the ERS model with high elevation angle results above 60°. The CEFM model also agrees with the ERS model to within 1 dB at 30°, 45°, and 60°.

Figure 14: Chapter 4 Contents: Signal Degradation for Line-of Sight Communications
This chapter broaches the question, "What is the LMSS signal degradation for a configuration in which line-of-sight communications are maintained where there is negligible shadowing. The multipath environments may consist of roadside trees, canyon walls, hills, or a body of water. Low elevation effects, and frequencies between UHF and K band are considered. As an example, we describe in the next figures Section 4-6 entitled, "Empirical Multipath Model."

Figures 15 and 16 Empirical Multipath Model (EMM) and Multipath Distributions Derived from Measurements
In Figure 15 are given 12 multipath fade distributions for cases considered in this chapter. These figures span canyon, hills, roadside trees, open fields, and near water measurements. The curves also cover frequencies ranging from 870 MHz to 20 GHz and elevation angles which range between 7° and 45°. The thick solid curve represents the median of these distributions. For probabilities of 2% and greater, the model gives a predictor which is within ± 2 dB of the measured distributions. In this way, a single simple exponential may be considered as a general model which gives an estimator of the multipath. Low elevation angle multipath measurements may give higher values than those shown at 8°. The indicated "near water" measurement was an approximate median of measured distributions for clear line-of-sight scenarios. Figure 16 presents the exponential formulation describing the multipath model. This equation is applicable between 1% to 60% over a fade range of approximately 1 dB to 5 dB.

Figure 17: Chapter 5 Contents: Fade and Non-Fade Durations and Phase Spreads
This chapter reviews fade duration and ITU-R model results for tree-lined roads at L Band for measurements in central Maryland and south-eastern Australia. Phase spread results are also examined. The central Maryland measurements were executed employing a helicopter as the transmitter platform. The south-eastern Australia measurements were obtained using the Japanese ETS-V geostationary satellite. High elevation angle fade duration results (at L Band) of Sforza and Buonomo are described.

Figure 18: Fade Duration Distributions from Different Countries
In this figure are shown L Band fade duration measured distributions (5 dB threshold) for central Maryland at 30°, 45°, and 60° and fade duration distributions (6 dB fade threshold) for measurements made in England by Sforza and Buonoma. Also shown are the ITU-R distributions (solid curve without data points; 5 dB fade threshold) which is based on the Australian measurements at 51°. The durations are expressed in terms of the distance over which the 5 dB threshold is exceeded. The Sforza and Buonoma time duration results were converted to the distance case using their stated average vehicle speed of 8.6 m/s. The differences in the various distributions are due to the foliage characteristics and driving

scenarios when a 5 (or 6) dB fade is exceeded. We may convert to any time fade duration by dividing by the desired vehicle speed.

Figure 19: Polarization, Antenna Gain, and Diversity Considerations

This chapter deals with various L Band and UHF propagation effects associated with land mobile propagation scenarios. These include fading effects related to (1) depolarization, (2) antenna gain, (3) fade reduction due to lane changing, (4) antenna spacing diversity gain, and (5) satellite diversity gain. An important section that is culled out as an example is "satellite diversity."

Figure 20: Imagery Methodology for Determining Satellite Diversity

We briefly describe here a method for determining fade distributions for mobile earth satellite scenario employing optical measurements. The results are described in detail in recent papers by Vogel [1997] and Akturan and Vogel [1997]. The method consists of locating a fisheye lens atop a mobile vehicle and video recording hemispherical scenes. One may then simulate constellations of potentially visible satellite locations for the region of measurement at different times of the day. At each time of day, sets of path states associated with the earth to satellite paths for the satellite constellation may be derived. Each earth-satellite path has associated with it a path state which may be described as: (1) clear, (2) shadowed, and (3) blocked. These are respectively defined as: (1) unobstructed line of sight, (2) a path passing through an attenuating medium such as a tree canopy, and (3) a medium completely blocking the propagation such as a building. Associated with each path state, there is an appropriate theoretical density distribution model. These models are then applied to the measured results and single and joint fade distributions are calculated.

Figure 21: Single and Joint Cumulative Fade Distributions for Tokyo Using Optical Imagery Analysis, Simulated Globalstar Constellation, and Combining Diversity

This figure shows a series of distributions for different look scenarios to the satellite for Tokyo assuming the simulated Globalstar constellation of 48 satellites. In deriving these distributions, 236 images were employed assuming approximately 1000 independent constellations encompassing a 24 hour period (for each image). Hence, an equivalence of 236,000 sets of path states went into the data base, where approximately 50% of the time, three satellites were potentially visible. The distribution labeled "Highest Satellite" represents the distribution associated with the satellite having the greatest elevation angle. This distribution was derived under the condition the mobile antenna transmits or receives radiation from a different satellite position every time a new satellite achieves the highest elevation angle, independent of azimuth. The highest elevation may not necessarily be a "clear" path state but depending upon the scene at the time may be representative of a "blocked" situation. The distribution labeled "Best Satellite" is also derived from multiple satellites where the antenna is pointed to the satellite giving the smallest fade. In calculating this distribution, a decision for "best satellite" was made approximately every 20 seconds before "hand over" was executed. The distribution labeled "2 Best Satellites" represents the joint distribution associated with the two satellites giving jointly the "smallest fades". At any instant of time, different pairs of satellites may fall under the "2 Best Satellite" category. The distributions labeled "3 Best

Satellites" and "4 Best Satellites" are analogously defined. The above joint distributions were derived assuming "combining diversity" where the signals received are "added," as opposed to "hand-off" where the satellite with the "highest" signal is processed. It is apparent that each of the above distributions are calculated from many different satellites at variable elevation and azimuth angles. Using the "Highest Satellite" distribution as the reference, the fade is considerably reduced by switching to the other diversity modes. For example, at the 20% probability, a 17 dB fade for the highest satellite may be compared to 6 dB for the "Best" satellite scenario, giving rise to an 11 dB diversity gain. We note that the higher diversity combinations (e.g., 2, 3, and 4 Best Satellites) do not significantly contribute to an increased diversity gain at percentages greater than 20%. The figure shows that using the "3 Best Satellite" diversity mode, 1% probability gives rise to a 20 dB fade margin for an urban environment. This substantially high fade may preclude voice communications for urban environments at small probabilities even with satellite diversity.

Figure 22: Chapter 7 Contents: Investigations from Different Countries

This chapter provides a compendium of measured cumulative fade distributions for LMSS geometries pertaining to significant experiments in various parts of the world. Emphasis is given to roadside tree environments although suburban environments are also included. Fifty four distributions are plotted pertaining to diverse shadowing conditions which include variable foliage conditions, diverse geographic regions (wooded, forest, rural, mountainous, and highway). Many of the original distributions have been extracted from the original plots using a digitizer and replotted employing the common format of a logarithmic probability scale as the Y-axis and a linear fade scale as the X-axis. The elevation angle range is 5° to 80° and frequency range is 870 MHz to 20 GHz.

Figures 23 and 24: Summary of Fade Ranges for Different Elevation Angles and Frequencies

To provide a further flavor of the diverse results associated with measurements from various countries, we show a summary table in Figures 23 and 24 where the fade distribution entries were culled in terms of frequency and elevation angle given in the first and second columns. The fade range at the 1% and 10% levels are given in the next two columns. The last column gives the number of distributions from which the fade range was compiled. The numbers in parenthesis represent the estimated fade employing the EERS model. The system designer may decide to use the "worst case" fade, the mid-level, or the EERS model which is generally representative of tree shadowing for tree populations which exceed 55%. The EERS model lies generally within the bounds of the measured distributions or is generally within 5 dB of the extremes at P = 1%.

Highlights of Revised Mobile Satellite Handbook

Julius Goldhirsh
Applied Physics Laboratory
The Johns Hopkins University

Wolfhard J. Vogel
Electrical Engineering Research Laboratory
The University of Texas at Austin

Figure 1

Background

1. First edition of mobile satellite handbook published in 1992:

"Propagation Effects for Land Mobile Satellite System: Overview of Experimental and Modeling Results," Julius Goldhirsh, Wolfhard J. Vogel, NASA Reference Publication 1274, February 1992 (NASA Propagation Studies Homepage http://propagation.jpl.nasa.gov/).

2. Revised document entitled,

"Propagation Effects for Vehicular and Personal Mobile Satellite Systems: Overview of Experimental and Modeling Results"

3. Objective of revised document is to include published results since 1991 and to broaden scope.

Figure 2

Contents of Talk

1. Brief review of chapter titles

2. Overview of status of text

3. Brief description of contents of completed chapters
   - Example of new results for each chapter

Figure 3

Chapter Titles

Chapter 1: Introduction

Chapter 2:* Attenuation Due to Individual Trees: Static Case

Chapter 3:* Attenuation Due to Roadside Trees: Mobile Case

Chapter 4:* Signal Degradation for Line of Sight Communications

Chapter 5:* Fade and Non-Fade Durations and Phase Spreads

Chapter 6:* Polarization, Antenna Gain, and Diversity Considerations

Chapter 7:* Land and Mobile Measurements from Different Countries

Chapter 8: Personal Comm. Propagation Effects

Figure 4

Chapter Titles (Continued)

Chapter 9: Aeronautical and Marine Propagation Effects

Chapter 10: Optical Methods for Assessing Shadowing and Blockage

Chapter 11: Theoretical Modeling Considerations

Chapter 12: Recommendations for Further Investigations

Figure 5

Status

1. Six Chapters Completed to Date

2. Documented in Microsoft Word 95

3. Plans to place in NASA Propagation Studies home page:
   http://propagation.jpl.nasa.gov/

4. Completion Date Fall, 1997

Figure 6

Chapter 2 Contents

ATTENUATION DUE TO TREES: STATIC CASE

Figure 7

Formulation for Estimating Equal-Probability K-Band Attenuation: Foliage Versus non- Foliage

$$For\ f \approx 20\ GHz$$

$$For\ 5 \leq A(No\ Foliage) \leq 25\ dB$$

$$A(Foliage) = a + b\ A(No\ Foliage)^{c}$$

$$a = 0.351$$

$$b = 6.825$$

$$c = 0.578$$

Figure 8

Measured and Predicted Attenuation Distributions at 19.6 GHz for Foliage and Non-Foliage Cases

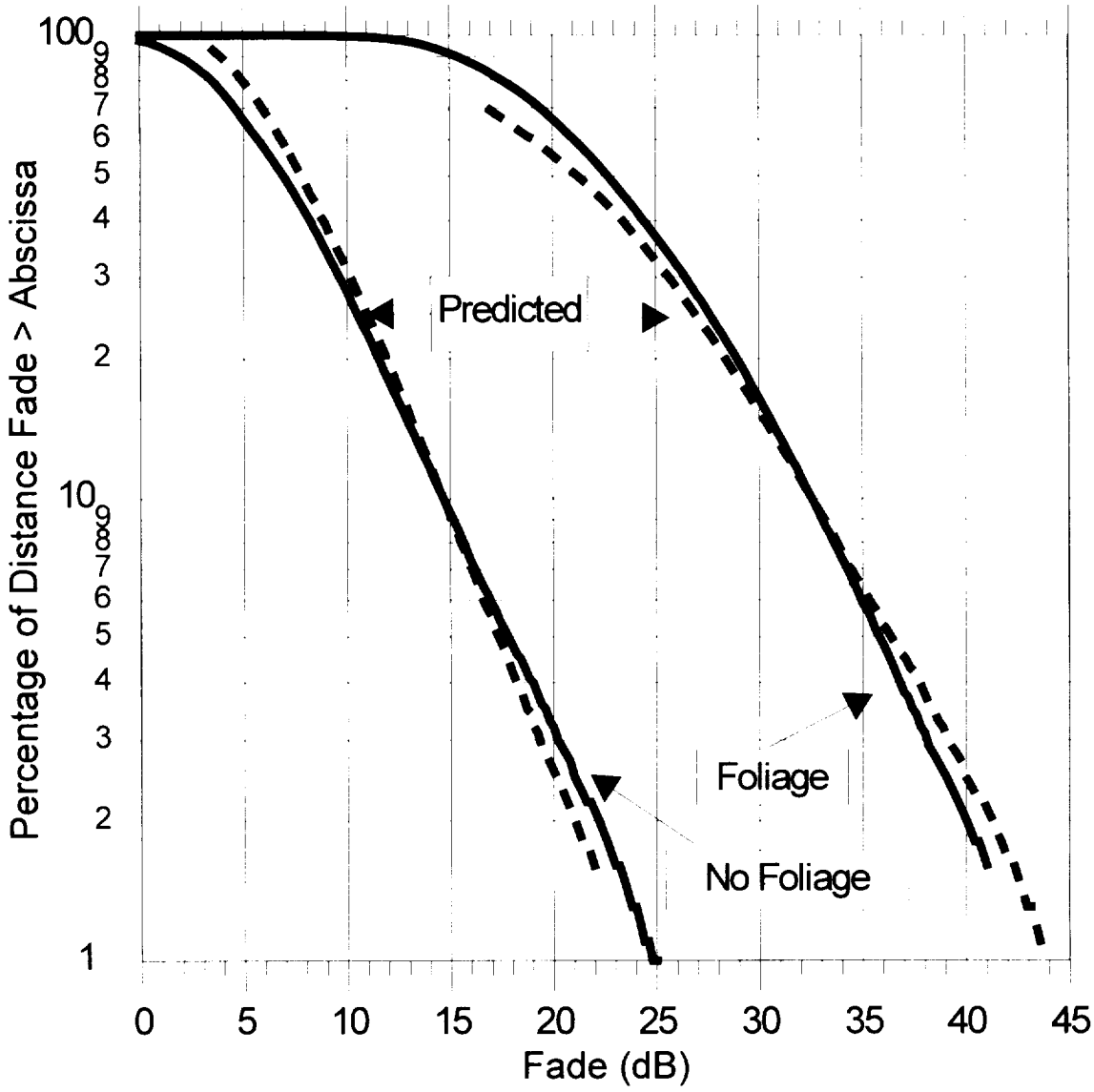

Figure 9

Chapter 3 Contents

ATTENUATION DUE TO ROADSIDE TREES: MOBILE CASE

Figure 10

Chapter 3 Contents (Continued)

Figure 11

Features of Extended Empirical Roadside Shadowing Model (EERS)

1. Estimates cumulative fade distributions
   - Mobile satellite roadside tree shadowing scenarios

2. Extension of Empirical Roadside Shadowing Model

3. Provisionally accepted ITUR Rec. (2/97)

4. Roadside Tree Shadowing POS = 55% to 75%

5. Probabilities from 1% to 80%

6. Frequencies from UHF (870 MHz) to K Band (20 GHz)

7. Elevation Angles from 7° to 60°

8. Higher Elevation Angle Extension (> 60°)
   (L - Band and S - Band; ITUR 2/97)

Figure 12

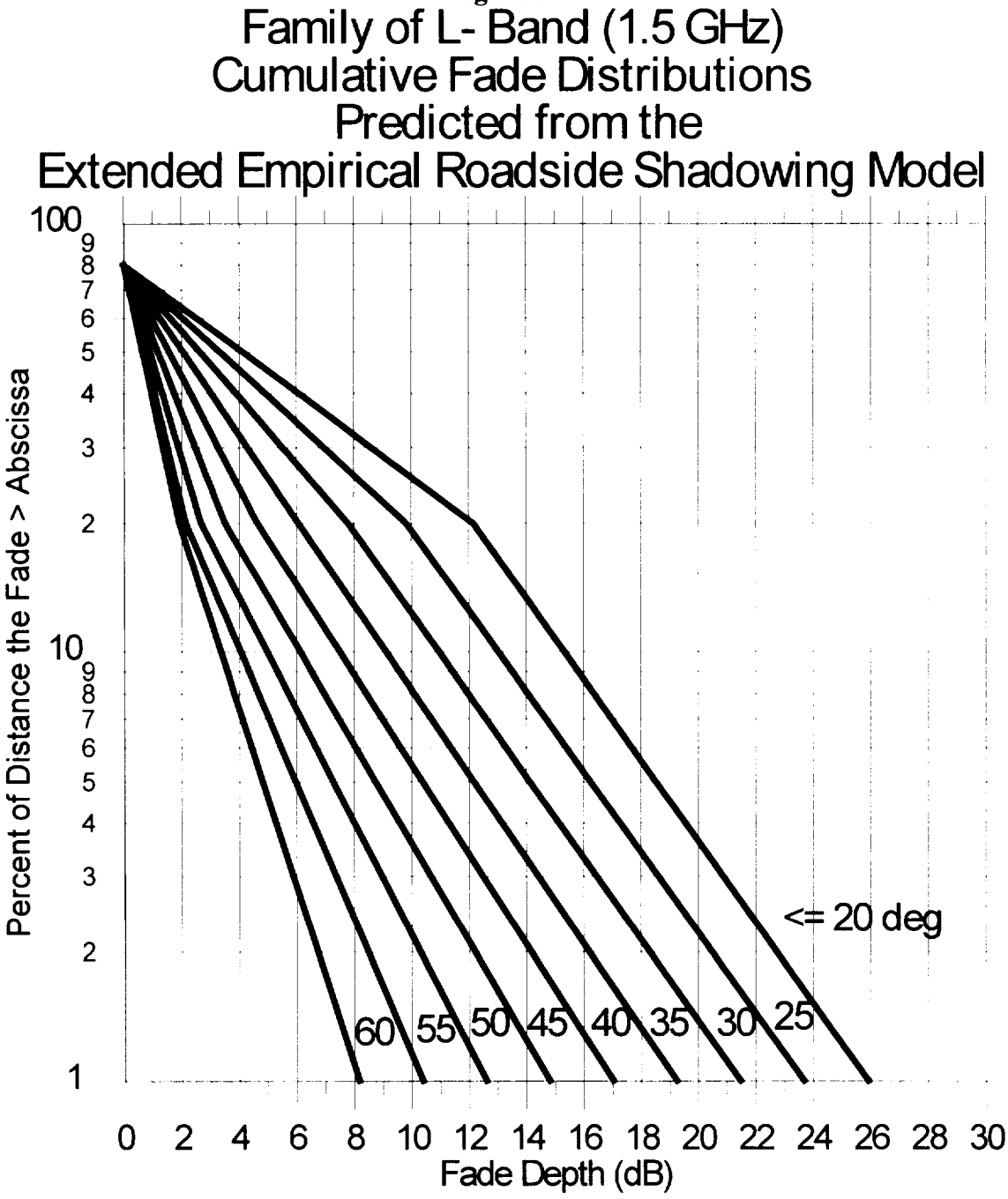
Family of L- Band (1.5 GHz)
Cumulative Fade Distributions
Predicted from the
Extended Empirical Roadside Shadowing Model
Percent of Distance the Fade > Abscissa
100
9
8
7
6
5
4
3
2
10
9
8
7
6
5
4
3
2
1
<= 20 deg
25
30
35
40
45
50
55
60
0 2 4 6 8 10 12 14 16 18 20 22 24 26 28 30
Fade Depth (dB)

Figure 13

Summary of Empirical Models and Domains of Validity

Model Name	% Range	Elevation Angle Range (deg)	Freq. Range (GHz)	Reference
EERS	1-80	7-60	0.87-20	Goldhirsh and Vogel [1995a], ITUR [1997]
ERS	1-20	20-60	0.87-3	Goldhirsh and Vogel [1992] - ITUR [1994]
ITU-R	1-30	60-90	1.6-2.6	ITUR [1997]
EFM	1-20	60-80	1.3-10.4	Parks et al. [1993a]
MERS	1-30	20-80	1.5-2.6	Sforza et al. [1993a]
CEFM	1-20	20-80	1.5-2.6	Butt et al. [1995]

Figure 14

Chapter 4 Contents

Signal Degradation for Line-of-Sight Communications

Figure 15

Empirical Multipath Model (EMM) and Multipath Distributions Derived from Measurements

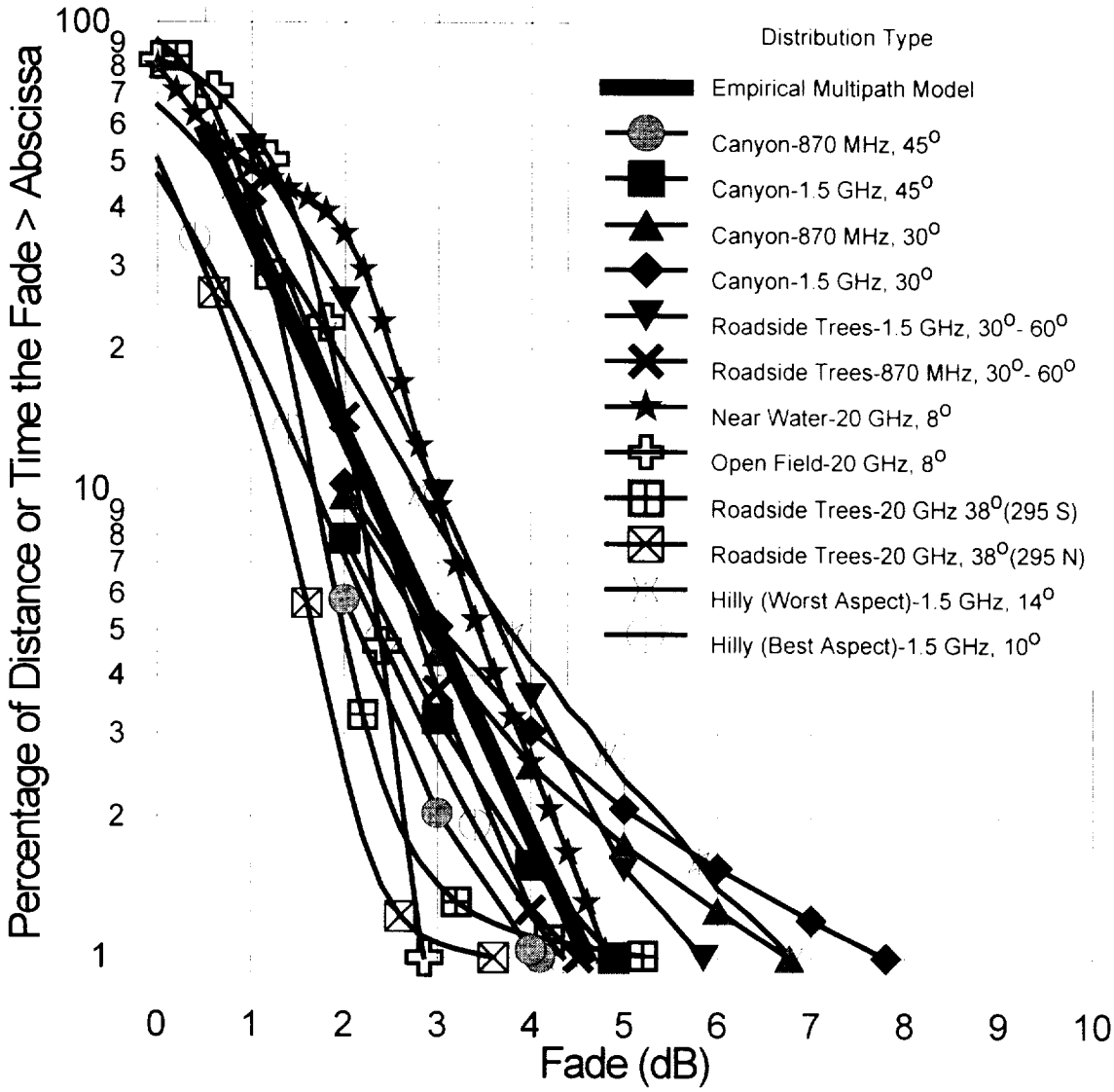

Figure 16

Empirical Multipath Model (EMM)

1. Median of 12 Multipath Distributions
2. Frequency range 870 MHz - 20 GHz
3. Elevation angle range from 8° to 60°

For P = 1% to 60%, A = 1 to 5 dB

$$P = 94.37 \exp(-0.9863\ A)$$

Figure 17

Chapter 5 Contents

Fade and Non-Fade Durations and Phase Spreads

Figure 18

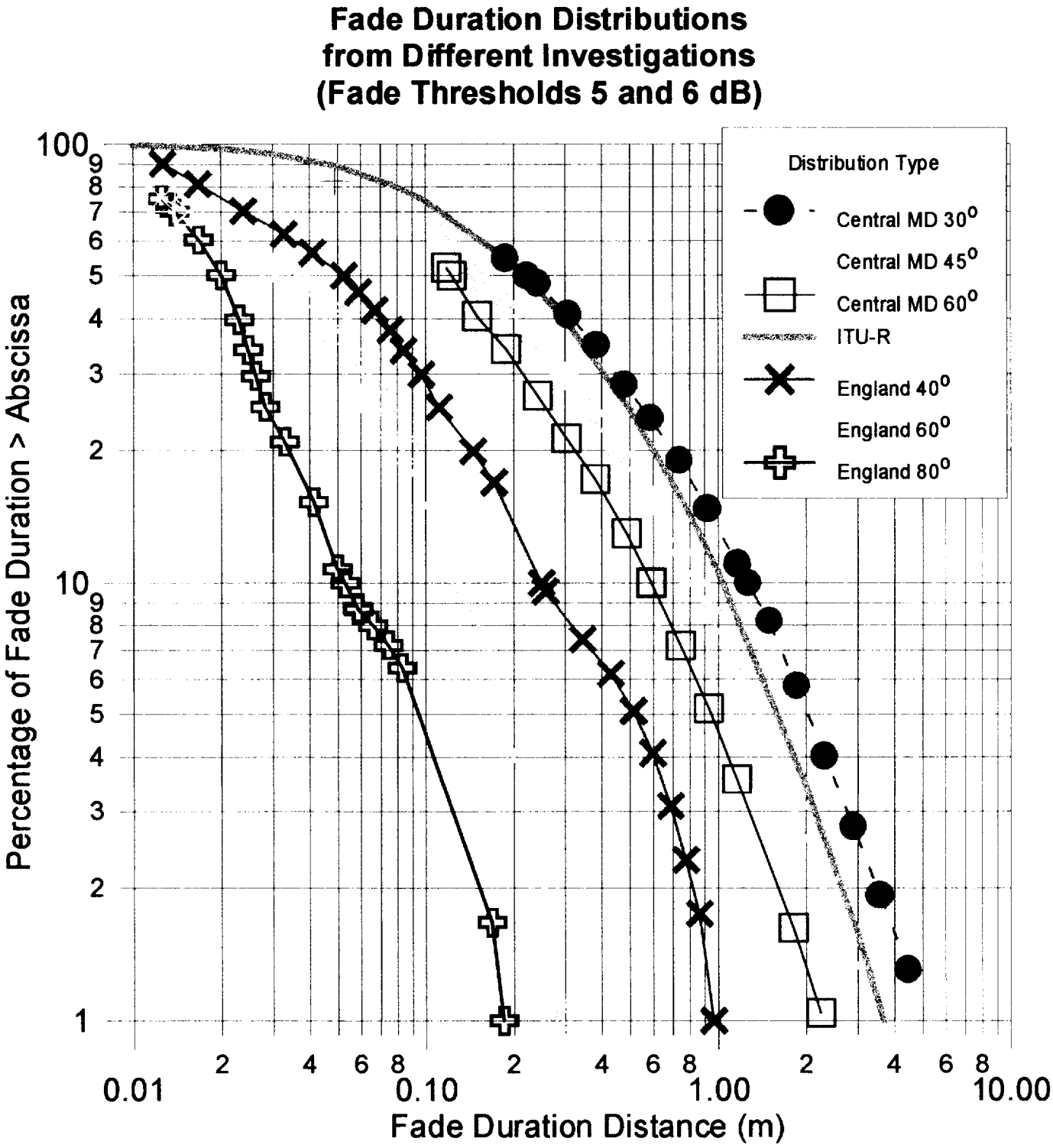
Fade Duration Distributions
from Different Investigations
(Fade Thresholds 5 and 6 dB)
Percentage of Fade Duration > Abscissa
100
9
8
7
6
5
4
3
2
10
9
8
7
6
5
4
3
2
1
0.01
2
4
6
8
0.10
2
4
6
8
1.00
2
4
6
8
10.00
Fade Duration Distance (m)
Distribution Type
Central MD 30°
Central MD 45°
Central MD 60°
ITU-R
England 40°
England 60°
England 80°

Figure 19

Chapter 6 Contents

Polarization, Antenna Gain and Diversity Considerations

Figure 20

Imagery Methodology for Determining Satellite Diversity

1. Method developed and decribed by:
   Vogel, 1997 and Akturan and Vogel, 1997

2. Video Recording of fisheye lens images made

3. Image analysis made of hemispherical scenes

4. Simulation of constellation of "potentially visible" satellite locations (e.g., Globalstar constellation)

5. Extraction of path states (clear, shadowed, blocked)

6. Appropriate density distribution model used for each path state

7. Computation of signal and joint cumulative fade distributions based on model used

Figure 21

Single and Joint Cumulative Fade Distributions for Tokyo Using Optical Imagery Analysis, Simulated Globalstar Constellation, and Combining Diversity (Vogel; 1997)

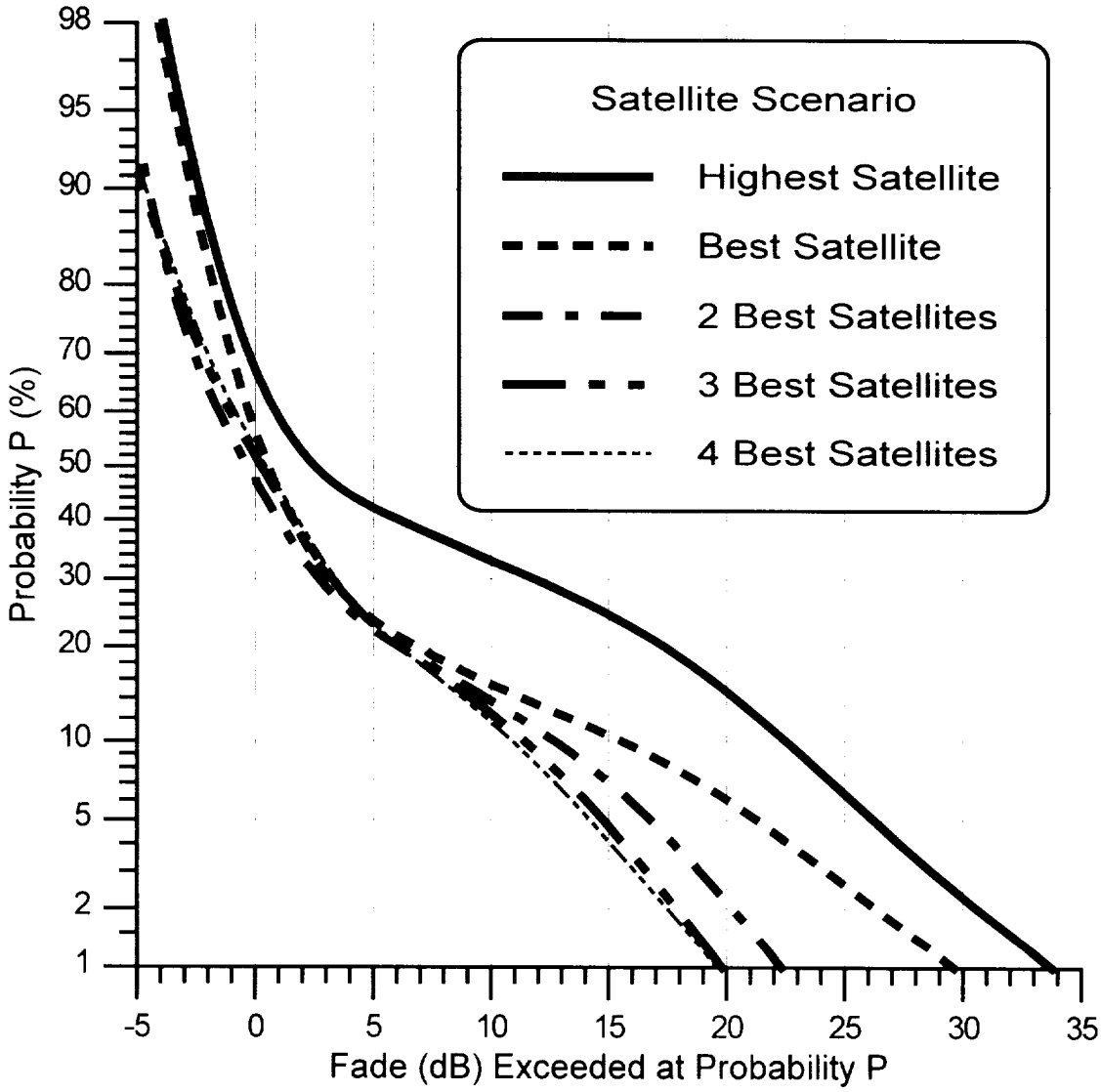

Figure 22

Chapter 7 Contents

Investigations from Different Countries

Figure 23

Summary of Fade Ranges Derived from Measured Distributions

f (GHz)	El (°)	Fade		Number Entries
		P = 1%	P = 10%	
0.87	5	>30 (18)	21.5 (10.5)	1
0.87	15-20	13-18 (18)	5.5-8 (10.5)	2
0.87	30	14-20 (15)	6-10 (7.5)	1
0.87-.893	45	7-15 (10.5)	2-7.5 (4)	2
0.87	60	3-12 (5.5)	2-5 (2.5)	1
1.5	19-26	11-21 (26)	3.5-16 (15.5)	5
1.5-1.55	30	17.5-25 (22)	8-13 (11)	2
1.5-1.6	40-50	2.5-32 (18)	1-20 (8)	7
1.3-1.6	50-60	5-18.5 (13)	2-7.5 (5)	7
1.3-1.6	80	8-12	2-3	3

Figure 24

Summary of Fade Ranges Derived from Measured Distributions (Continued)

f (GHz)	El (°)	Fade		Number
		P = 1%	P = 10%	Entries
2.05-2.09	18-21	>30 (31)	>15 (18.5)	2
2.09-2.66	40-45	12-17.7 (22.5)	7-11.5 (10)	3
2.5-2.6	60	12-22.5 (11)	5-9 (10)	3
2.5-2.6	80	10.5-16	4.5-6	2
10.4	60	27.5-28 (17.5)	13-18.5 (7)	2
10.4	80	24-26	10.5-13	2
20	8	>25 (63)	>25 (37)	1
18.7-20	30-38	21-40 (52)	9-33 (27)	4
20	46	8 to >30 (35)	2-30 (14.5)	3
20	54.5	28 (26)	15 (10)	1

Characterization of HF Propagation for Digital Audio Broadcasting

A. Vaisnys
Jet Propulsion Laboratory - California Institute of Technology
arvydas.vaisnys@jpl.nasa.gov

Abstract - The purpose of this presentation is to give a brief overview of some propagation measurements in the Short Wave (3-30 MHz) bands, made in support of a digital audio transmission system design for the Voice of America. This task is a follow on to the Digital Broadcast Satellite Radio task, during which several mitigation techniques were developed to deal with propagation at S-band. It was hoped that these techniques would be applicable to digital audio in the Short Wave bands as well, in spite of the differences in propagation impairments in these two bands. Two series of propagation measurements were made to quantify the range of impairments that could be expected. An assessment of the performance of a prototype version of the receiver was also made.

I. Introduction

It is well known that propagation in the short wave bands is very variable, with signal fluctuations and distortions which occur both rapidly and slowly. These bands can also contain interference from both nearby and very distant co-channel transmitters. Attempts have been made to produce propagation models, but these can only approximate what really goes on. Propagation prediction programs such as VOACAP are useful in planning the proper frequencies to be used for any particular time of day, in any given month. The fact that VOACAP can produce a 30 dB difference in the predicted mean SNR vs. the 90 percentile SNR, however, shows the variability of propagation at these frequencies.

Two sets of propagation related tests have been accomplished so far; one in October 1996, the other in May 1997. The first one was basically a propagation measurement, using a series of test signals to measure the channel over several propagation paths. The second was more of a performance test of the receiver, but included some test signals to establish the characteristics of the signal path.

II. Test Configuration

VOA transmission facilities at Delano, California were used to transmit the test signals. Reception was accomplished at three sites. (Slide 2).

A typical VOACAP median S/No prediction plot is shown in (Slide 3). The transmit antenna was aimed toward 75 degrees azimuth.

The receiving equipment consisted of a short wave radio whose IF was modified to be at 13 kHz center frequency, which could be recorded on a Digital Audio Tape recorder for post processing. (Slide 4).

III. Propagation Measurement Overview

To stay within the 10 kHz channel, analog test signals (AM modulated) were limited to a 4.5 kHz baseband, while digital signals were pulse shaped and transmitted at 8 ksps. One of the test signals was a 63 bit PN code (8 milliseconds long) used to measure the number of signal delay components.

Snapshots of typical cross-correlation peaks for three paths (October 1996) and a noise free reference are shown in (Slide 5). (Slide 6) shows a 3 minute time segment of the correlation peaks for a (May 1997) Delano to Washington path. Typically there was more than one signal component, and the power in these components varied rapidly. Delay spreads were typically less than 2 milliseconds.

Rapid variations in narrow band fading are illustrated in (Slide 7). (Slide 8) shows a narrow band signal being tuned over the band.

IV. Summary and Conclusions

The digital audio broadcasting system being developed for the VOA is being designed to operate with high orders of modulation in order to transmit a sufficiently high compressed audio data rate through the available 10 kHz channel bandwidth. The receiver employs an equalizer for mitigation of multipath and narrow band fading effects. Other mitigation techniques such as interleaving and coding are being evaluated for effectiveness under short wave propagation conditions. The May 1997 test included a comparison between double sideband AM and 8PSK at the same power level. Results with the digital receiver (Audio Tape) were very favorable.

V. Acknowledgment

The research described in this paper was carried out at the Jet Propulsion Laboratory, California Institute of Technology, and sponsored by the Voice of America (U.S. Information Agency) through an agreement with the National Aeronautics and Space Administration. The digital HF broadcasting project is being managed by Dr. H. Donald Messer of the Voice of America.

VOA/JPL DBS RADIO

DBS-R TECHNOLOGY APPLICATION TO HF BROADCASTING

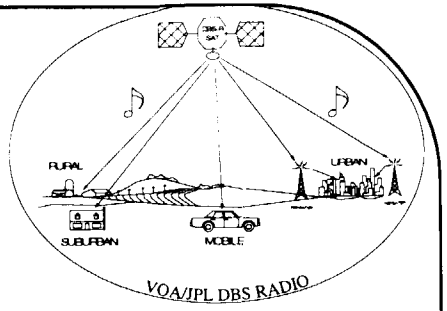

Characterization of HF Propagation for Digital Audio Broadcasting

~~20,000 MHz~~

~~2,000 MHz~~

< 20 MHz

A. Vaisnys
Jet Propulsion Laboratory
California Institute of Technology
arvydas.vaisnys@jpl.nasa.gov

NAPEX XXI
June 12, 1997

VOA/JPL DBS RADIO

DBS-R TECHNOLOGY APPLICATION TO HF BROADCASTING

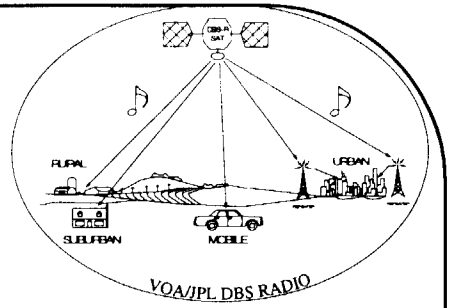

A SERIES OF HF PROPAGATION MEASUREMENTS WAS CONDUCTED IN OCTOBER 1996 TO PROVIDE AN ASSESSMENT OF CHANNEL EFFECTS (INCLUDING TRANSMITTER) ON DIGITALLY MODULATED SIGNALS:

- **TRANSMIT SITE AT DELANO, CA**
- **SIMULTANEOUS RECEPTION AT THREE SITES**
  - **AUSTIN, TEXAS**
  - **WASHINGTON, DC**
  - **TENERIFE, SPAIN**
- **5.9 AND 15.2 MHZ AT BEST TIME OF DAY FOR EACH**

A SECOND SERIES OF TESTS WAS CONDUCTED IN MAY 1997, BETWEEN DELANO AND WASHINGTON DC, AT 17.9 AND 13.7 MHZ. THESE TESTS INCLUDED AN ASSESSMENT OF DIGITAL VS. AM RECEIVER PERFORMANCE.

VOA/JPL DBS RADIO

DBS-R TECHNOLOGY APPLICATION TO HF BROADCASTING

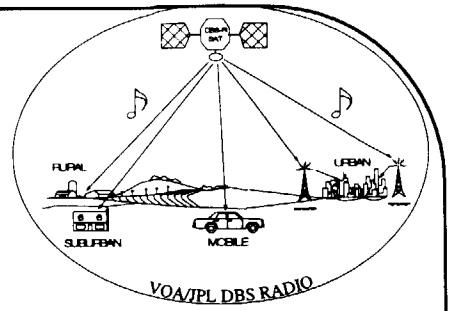

PREDICTED MEDIAN SNR FOR COVERAGE AREA

SNR
default/testhi3.V11

DELANO [HR 4/4/1] 177kW 75deg 19ut 16.000MHz Oct 8ssn

Version 96.0828W

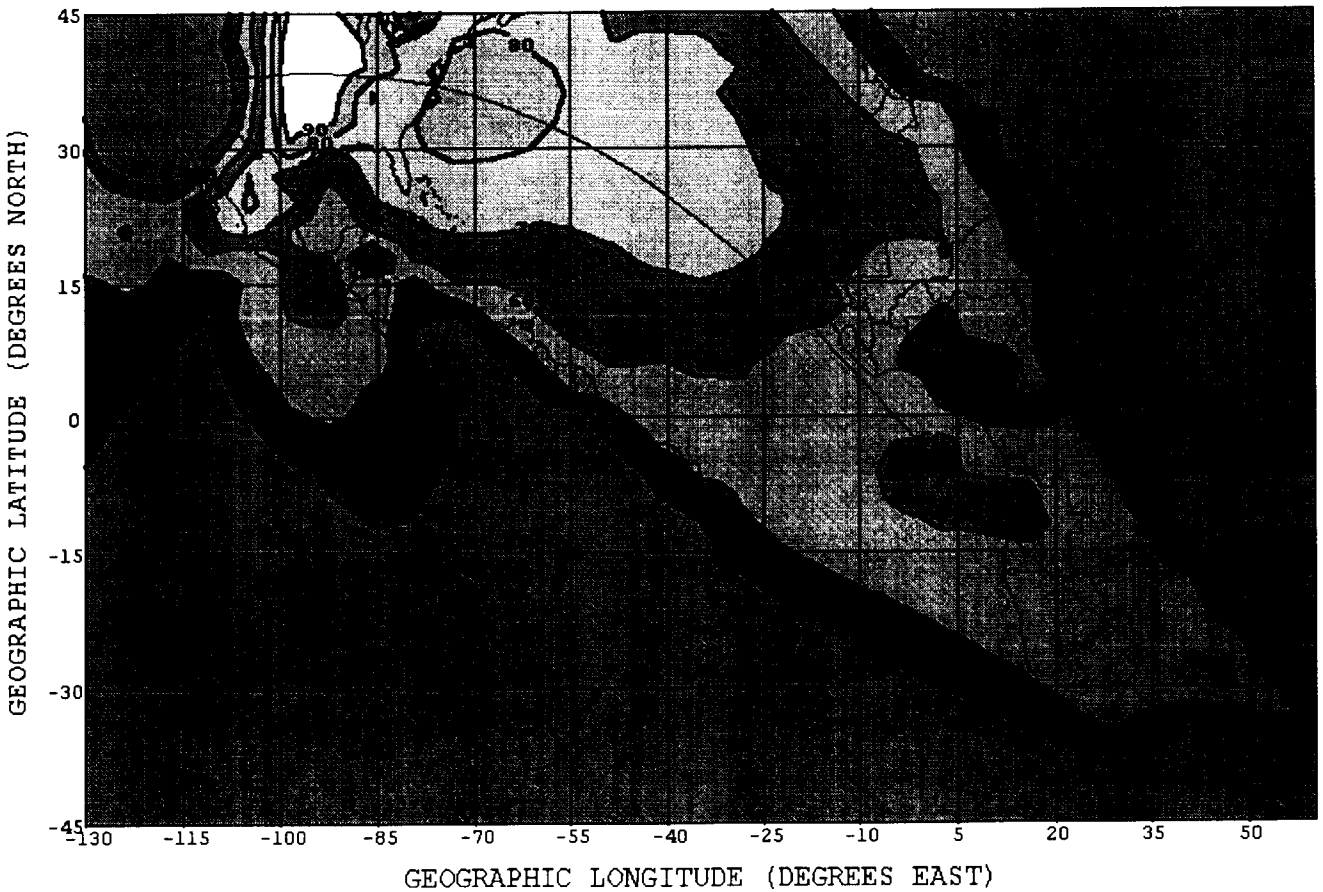

VOACAP

Signal-to-Noise
Median Decile
[dB]

	> 90
	> 80
	> 70
	> 60
	> 50
	> 40
	< 40

Min=-161.70
Max= 99.60

CCIR coefficients

NTIA/ITS

VOA/JPL DBS RADIO

DBS-R TECHNOLOGY APPLICATION TO HF BROADCASTING

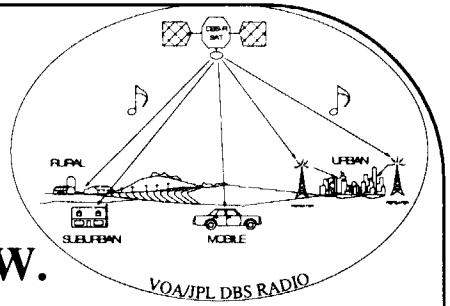

THE TEST EQUIPMENT CONFIGURATION IS SHOWN BELOW.

- A COMPUTER WAS USED TO GENERATE A TEST SIGNAL SEQUENCE
- MODULATION WAS ACCOMPLISHED AT THE TRANSMITTER EXCITER USING A D TO A CONVERTER AND ANALOG MULTIPLIER
- THE RECEIVER IF WAS LOWERED TO 13 KHZ
- BOTH THE IF AND THE AM DETECTOR OUTPUT WERE RECORDED ON A DAT
- RECEIVED SIGNAL PROCESSING ACCOMPLISHED IN NON-REAL TIME

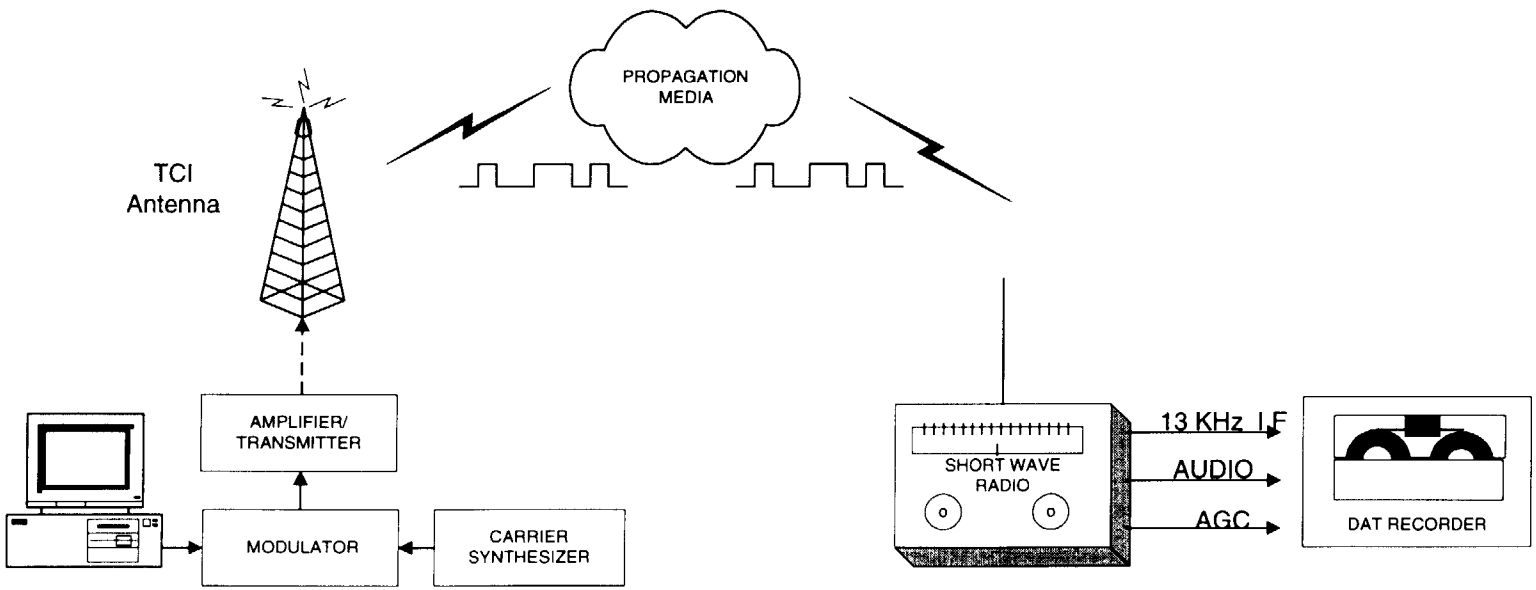

VOA/JPL DBS RADIO

DBS-R TECHNOLOGY APPLICATION TO HF BROADCASTING

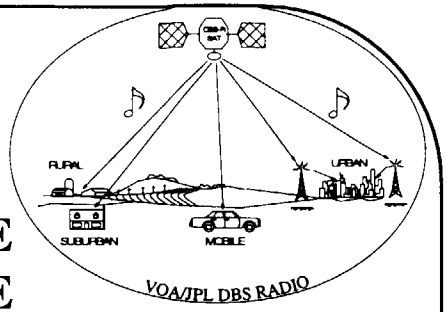

TIME EXPANDED SNAPSHOT OF PN CORRELATION OF THE THREE PATHS AT 15.2 MHZ WITH NOISE FREE REFERENCE

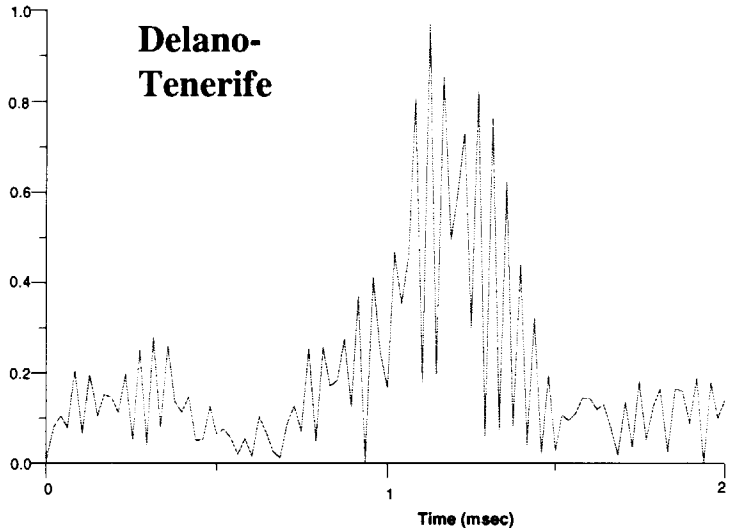

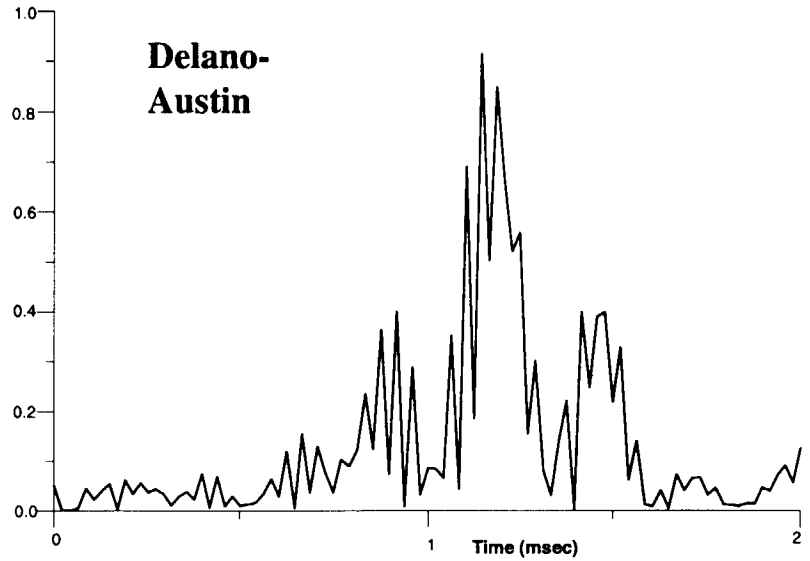

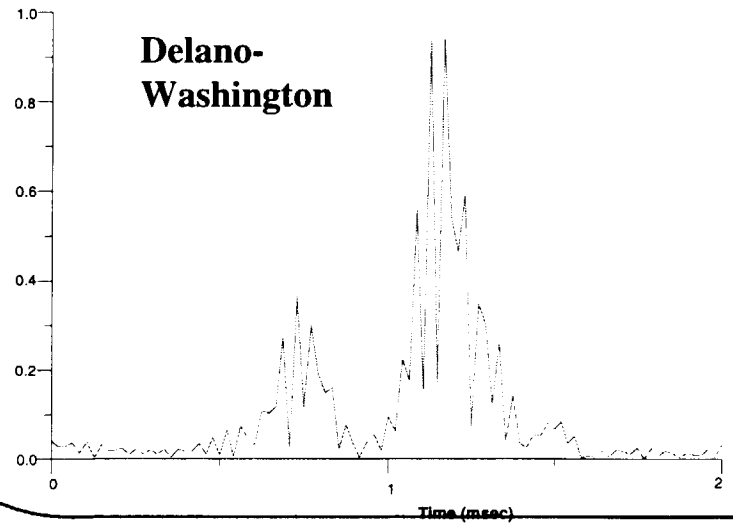

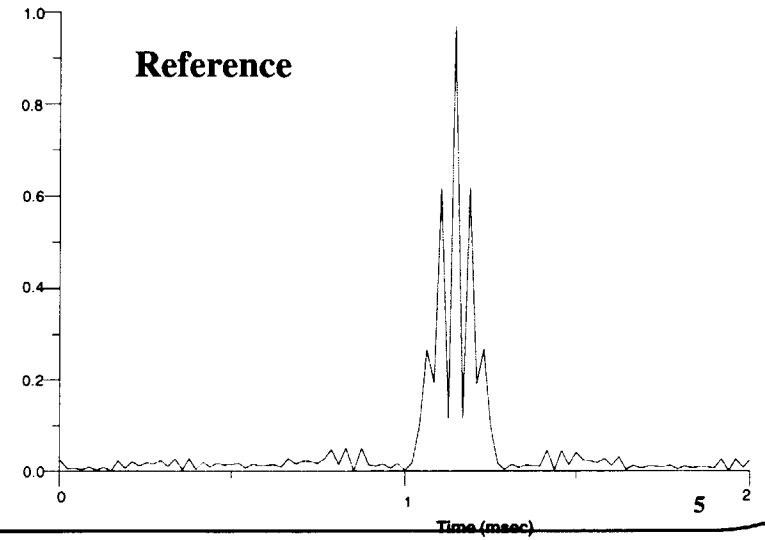

VOA/JPL DBS RADIO

DBS-R TECHNOLOGY APPLICATION TO HF BROADCASTING

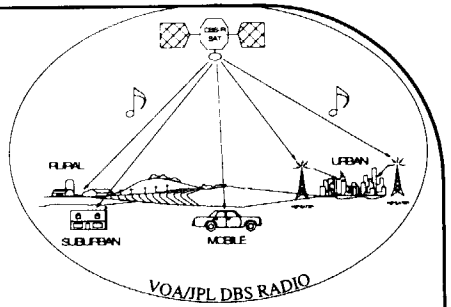

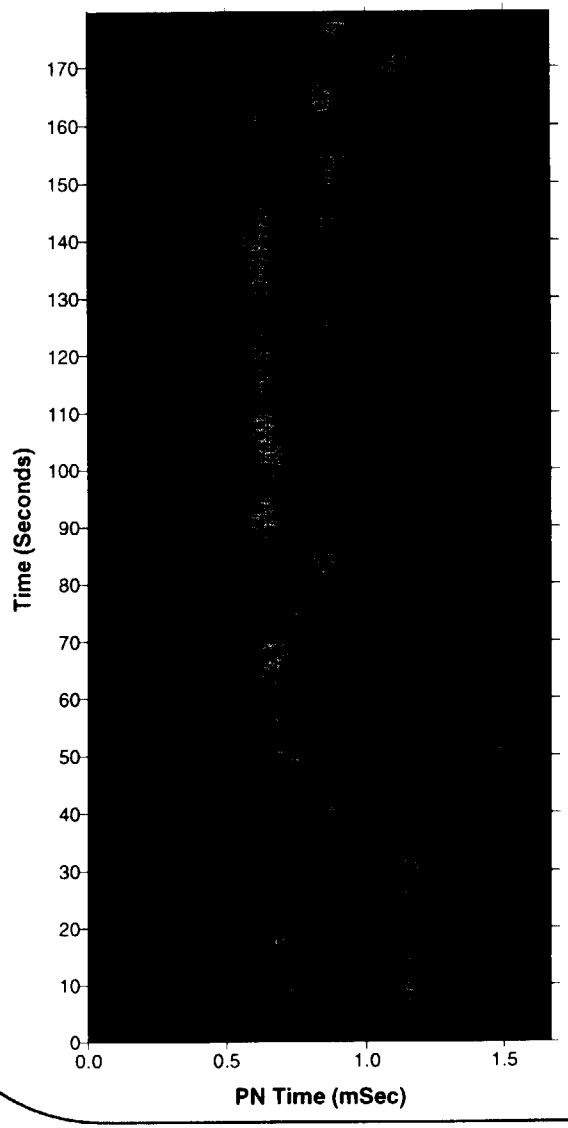

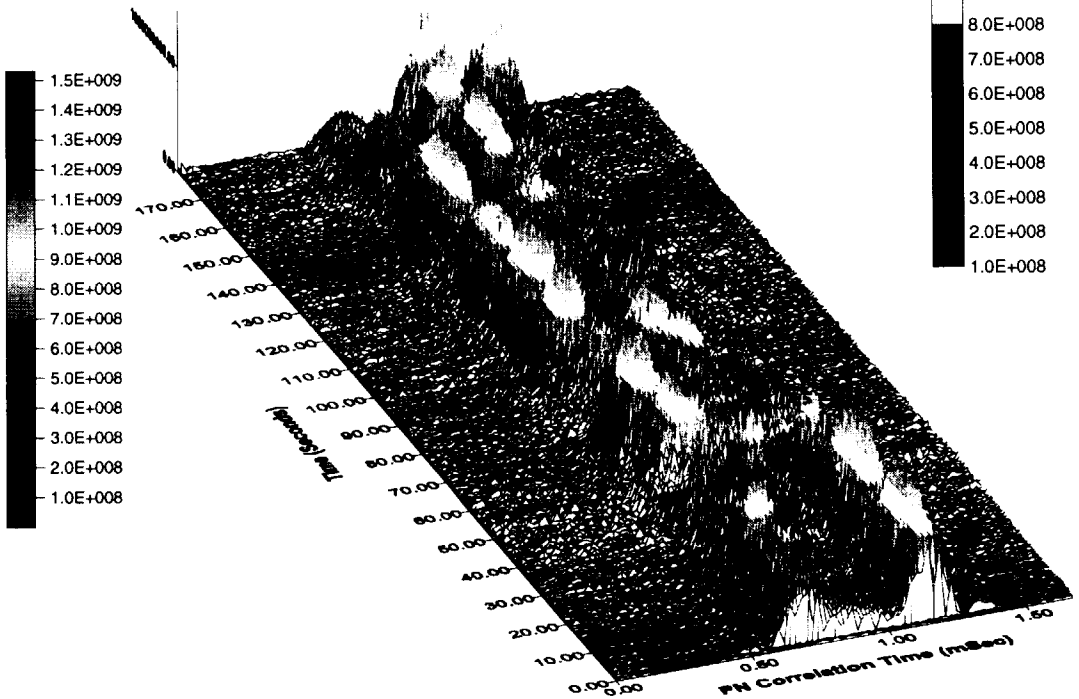

VOA/JPL DBS RADIO

DBS-R TECHNOLOGY APPLICATION TO HF BROADCASTING

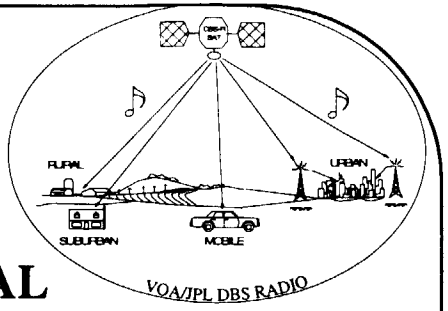

3 D SPECTRA PLOTS OF PN BPSK MODULATED SIGNAL

NOISE-FREE

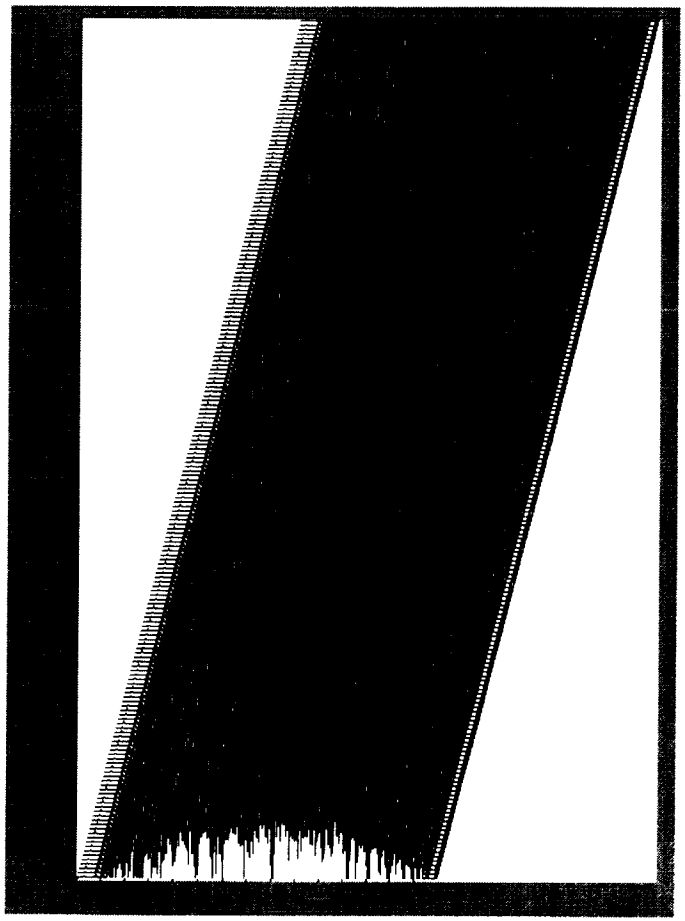

RECEIVED DELANO-WASHINGTON PATH

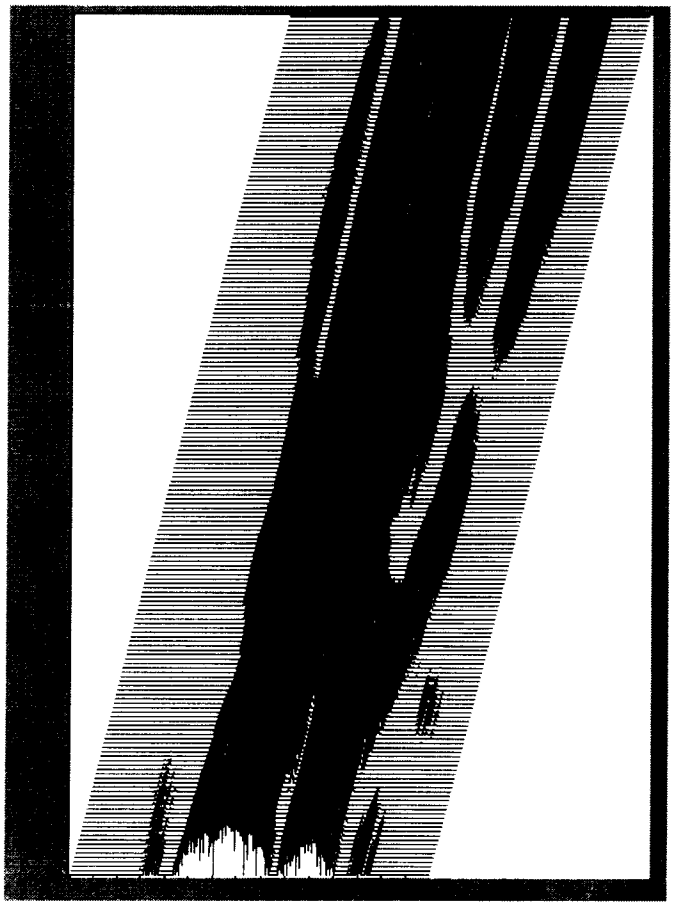

VOA/JPL DBS RADIO

DBS-R TECHNOLOGY APPLICATION TO HF BROADCASTING

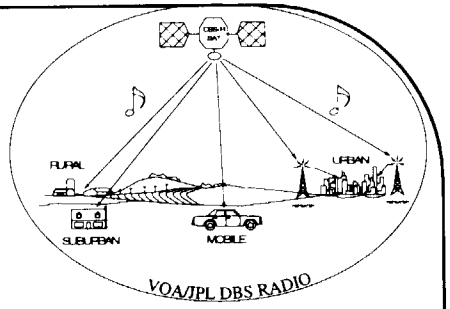

EXAMPLE OF MAN-MADE INTERFERENCE ON DELANO TO AUSTIN PATH (BPSK PN SPECTRUM)

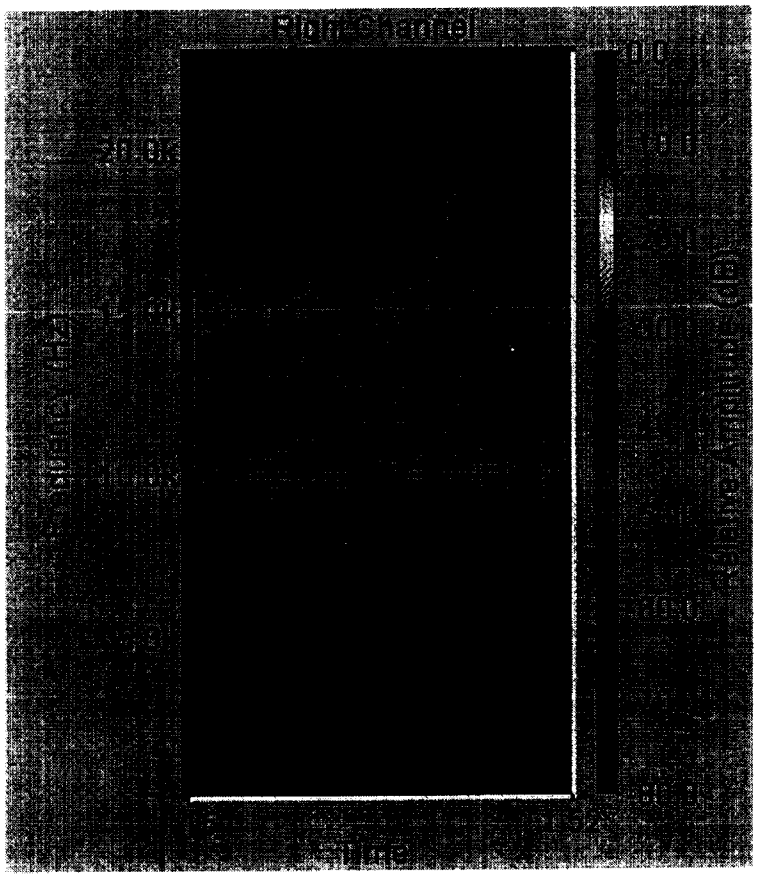

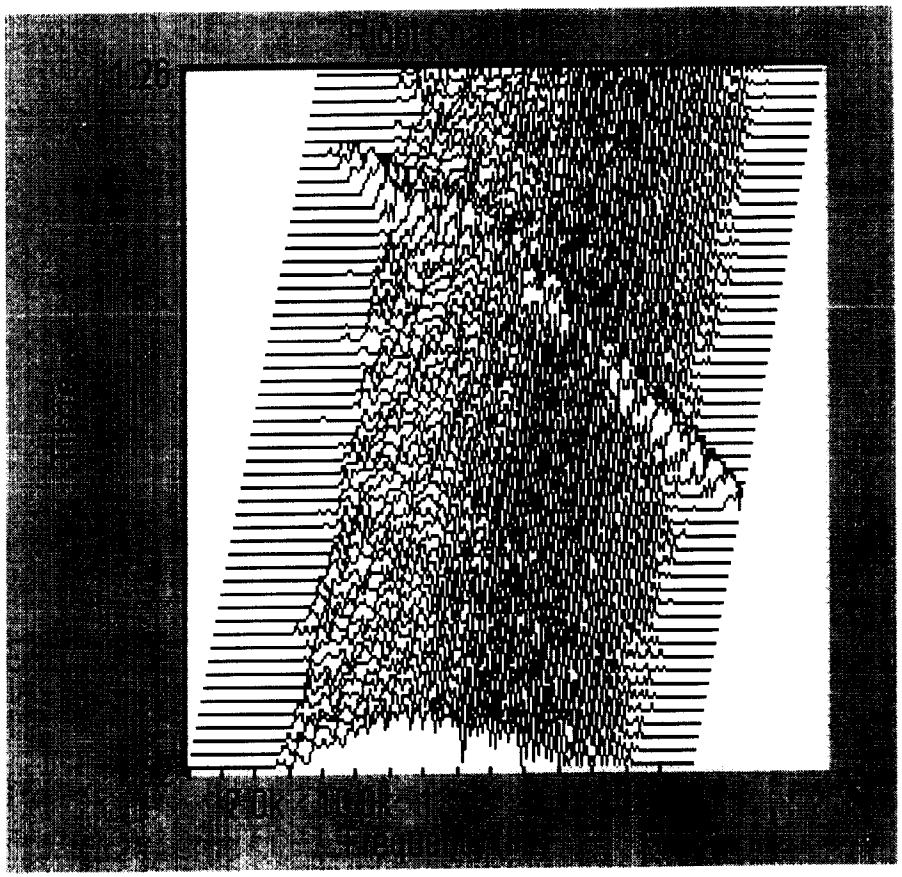

A DATABASE FOR PROPAGATION MODELS

Anil V. Kantak
and
James Rucker

Jet Propulsion Laboratory
California Institute of Technology
Pasadena, California 91109

1.0 Introduction

The Propagation Models Database is designed to allow the scientists and experimenters in the propagation field to process their data through many known and accepted propagation models. The database is an Excel 5.0 based software that houses user-callable propagation models of propagation phenomena. It does not contain a database of propagation data generated out of the experiments. The database not only provides a powerful software tool to process the data generated by the experiments, but is also a time- and energy-saving tool for plotting results, generating tables and producing impressive and crisp hard copy for presentation and filing.

2.0 The Software

The software has Excel 5.0 as the underlying application. Excel was selected to write the program for two different reasons. Excel software has

the needed sophistication in mathematical functionality for the database, and it is the software preferred by the industry. To make the software useful to the industry in their designs of systems, it was deemed necessary to generate the entire propagation models database in terms of the Excel-callable functions, otherwise known as the user-defined functions in Excel. Originally, it was decided that a combination of C and Excel should be used to generate the database software so that the high speed of the C compiler combined with the superior data handling and charting capabilities of the Excel software can be incorporated in the Propagation Models Software. Even though it seems to be the best way of using the best of both worlds, this software has an inherent disadvantage that the user will have to know the intricate workings of the C compiler and C language to make any changes/additions to the software. Another consideration is that industry needs to incorporate the database functions into their own Excel software and, from the surveys done in the past, it became clear that the industry does not want the software, or any part of the software, written in C or C++.

Considering all the requirements stated above, a decision was made to write the software in the Excel user-callable functions alone. The current version of the tool is self-sufficient and complete in terms of the user help and the guidance needed for the user to run the program successfully. The software is subdivided into the following six major categories of functions:

1. Ionospheric propagation models.
2. Tropospheric propagation models.
3. Land-mobile system propagation models.

4. Effects of small particles on propagation.
5. Rain models.
6. Radio noise models.

The user may select any model desired and compute the respective numbers. The user may call the model in his / her own program to return a value to the program.

3.0 Conclusions

It is felt that with industry as a partner, development of the database software is now on firm footing. It is also felt that proper steps have been taken that will result in the finished product in the near future. The finished database will have all the necessary features including a good graphics capability. Anyone desiring a copy of the software should contact the authors. Even if the programming is complete, the architecture is open-ended, easily allowing new additions, such as new models and help subroutines.

Propagation Models Database

Anil V. Kantak

James Rucker

3-78

Jet Propulsion laboratory

California Institute of Technology

Pasadena, California 91109

June 11, 1997.

PROPAGATION MODELS DATABASE

- A database of various propagation phenomena models which can be used by the telecommunications systems engineers to obtain the desired parameter values for systems design.
  - Propagation research
  - Ease of using the models
  - Passing the experimental data through the models
  - Comparison and checking of experimental data.

- An easy to use convenient tool, implemented on a PC to analyze the user propagation data.

PROPAGATION MODELS DATABASE

- Salient features of the software:
  - Microsoft Excel 5.0-based software, utilizing Excel's excellent spreadsheet features and charting functions.
  - Every model is written as Excel subroutine / Excel User-Defined Function.
  - The program produces output for the user in its own spreadsheet or the user may use the subroutines / functions in their own Excel program and transport the result to their program.
  - Every care is taken to avoid user-made errors in running the program models.

PROPAGATION MODELS DATABASE

- Every model of the database has the same overall instructions set and same operating procedure, making the user capable of using any model once the procedure is learned.
- Extensive charting procedures are available to the user and, where feasible, the charting procedures and workings are made transparent to the user. The program allows the user to vary any desired variable of the model and see its effects on the user-selected output variable via a chart. The user is allowed to loop back to obtain other combinations of outputs and independent variables without running the model again.
- Every chart produced may be saved or printed out.

PROPAGATION MODELS DATABASE

- The database is divided into six major categories
  - Ionospheric propagation models.
  - Tropospheric propagation models.
  - Land-Mobile system propagation models.
  - Effects of small particles on propagation.
  - Rain models.
  - Radio noise models.

PROPAGATION MODELS DATABASE

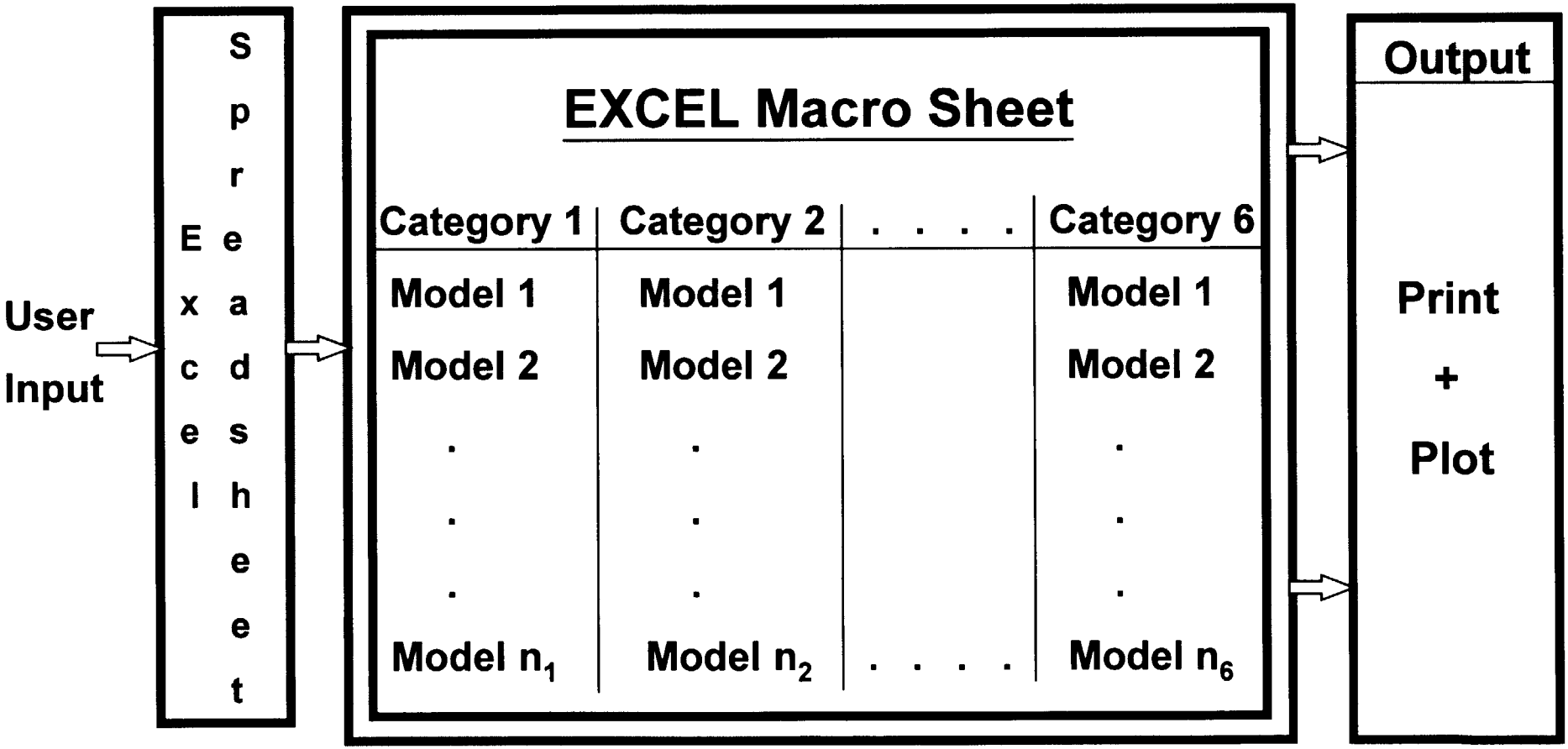

PROPAGATION MODELS DATABASE

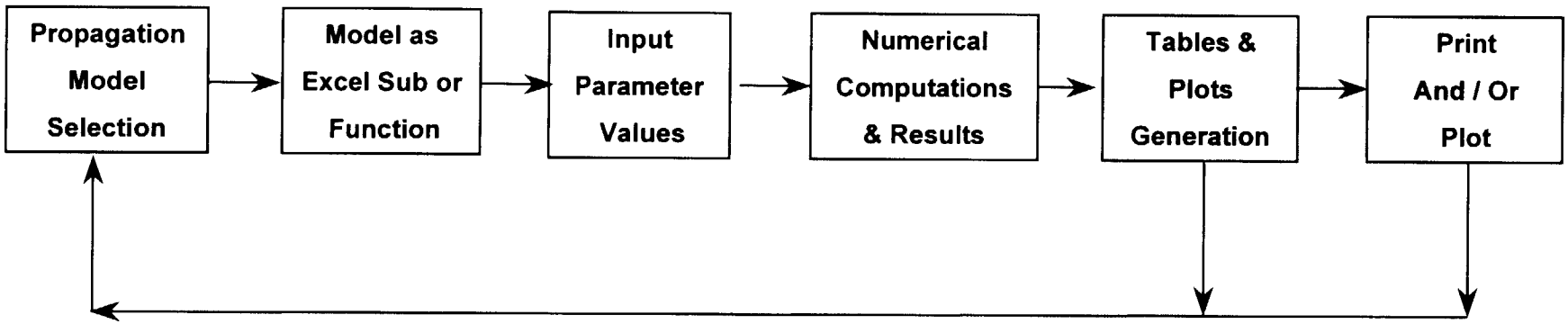

PROPAGATION MODELS DATABASE

- System Requirement:
  - Windows NT or Windows 95
  - At least 8 to 16 Mbytes of RAM
  - 2 Mbytes of disk space.
  - 486 or Pentium processor with at least 25 MHz clock rate.

PROPAGATION MODELS DATABASE

- Conversion of the Propagation Models Database from Excel environment to C++ environment.
- Design Concepts
  - Isolation of:
    - User Interface
    - Databases
    - Computational Engine.
  - Make the Propagation Database software more compatible with other software the user may have.
  - Make the Propagation Database software independently accessible from a server by remote users.
  - Make the Propagation Database software platform independent.

CD and VIDEO PRESENTATION ON NASA LEWIS RESEARCH CENTER IN-HOUSE RAIN FADE STUDIES

Jennifer J. Sibits

Two products were presented which resulted from a question posed by NASA Administrator Dan Goldin. These products are a Video and CD ROM.

In a conversation Mr. Goldin had with special Projects Manager, Nancy Horton, Mr. Goldin had expressed knowledge about the in-house Rain Fade studies being done at Lewis Research Center, and asked what was being done to get the information out to industry. At that time, there was no deliberate program in place, nor was there a formal method by which to notify interested parties that such information was available. The question was enough to stimulate an interest by Ms. Horton to pull together a Product Development Team to produce a response. Ultimately the response took the form of a Video and CD.

The video provides and overview of the research being done at Lewis Research Center and introduces viewers to three areas of technical expertise and knowledge. Presentations in the video include: Rain Attenuation Modeling by Dr. Robert Manning; System Performance by Thom Coney; and Compensation Techniques by Dr. Roberto Acosta.

The CD ROM provides in-depth information on these three research areas. Users are given an opportunity to listen to answers to critical questions, review reports generated on these topics, and preview seminar work. Additionally, the CD introduces users to other sources of information generated on the ACTS Propagation and Implementation Program. Web site addresses, listings of contacts and papers published are a few examples.

Because of the nature of the NAPEX organization, it was deemed appropriate to pre-view these new products with members of the NAPEX team. Associates of NAPEX were given opportunity to obtain copies of the finished video and were asked to comment on the content and use-ability of the CD. The CD was at an 80% completion point when demonstrated at NAPEX.

Meeting attendees who viewed the video and CD were asked to provide feedback in the form of survey response cards or email (acts@lerc.nasa.gov). Comments and suggestions were received and incorporated into the CD. Overall both products were well received. Twenty-seven copies of the video were provided to NAPEX members at the meeting. Approximately 30 requests for the finished CD were received and will be processed once all changes to the CD have been validated.

4. Workshop No. 1, ACTS Project Propagation Program Update

ACTS PROJECT & PROPAGATION PROGRAM UPDATE

Robert Bauer
NASA Lewis Research Center
ACTS Propagation Studies Workshop
June 13, 1997

ACTS PROJECT OFFICE

SPACECRAFT STATUS

- Spacecraft operations continue to be nominal.
- Ka-band license extended through 12/31/98. Modification to license for inclined orbit will be needed.
- Failed Telstar 401 missed ACTS in orbit during close encounter June 05 (by over 7 km, estimated.)

ACTS PROJECT OFFICE

INCLINED ORBIT

- Beginning of inclined orbit operations still set for July 1998 (through Sept. '00).
- Tracking modifications planned for T1VSATs, High Data Rate Terminals.
- Both Lockheed Martin and Comsat looking at needed changes to operations procedures and software.

ACTS PROJECT OFFICE

OTHER ACTS INFO

- ACTS inducted into US Space Foundation Space Technology Hall of Fame, Colorado Springs on April 3, 1997.
  - Honors individuals, orgs.& comp.'s responsible for "remarkable products developed from space technology."
- Ron Schertler, ACTS Experiments Manager, retired from NASA Jan. 1997 with 34 yrs. of service.

ACTS PROJECT OFFICE

EXPERIMENTS PROGRAM

- Total proposals received (05/07/97) 157
- Number of approved experiments: 85
  - Experiments started: 74
  - Experiments completed: 46
  - Experiments yet to start: 11

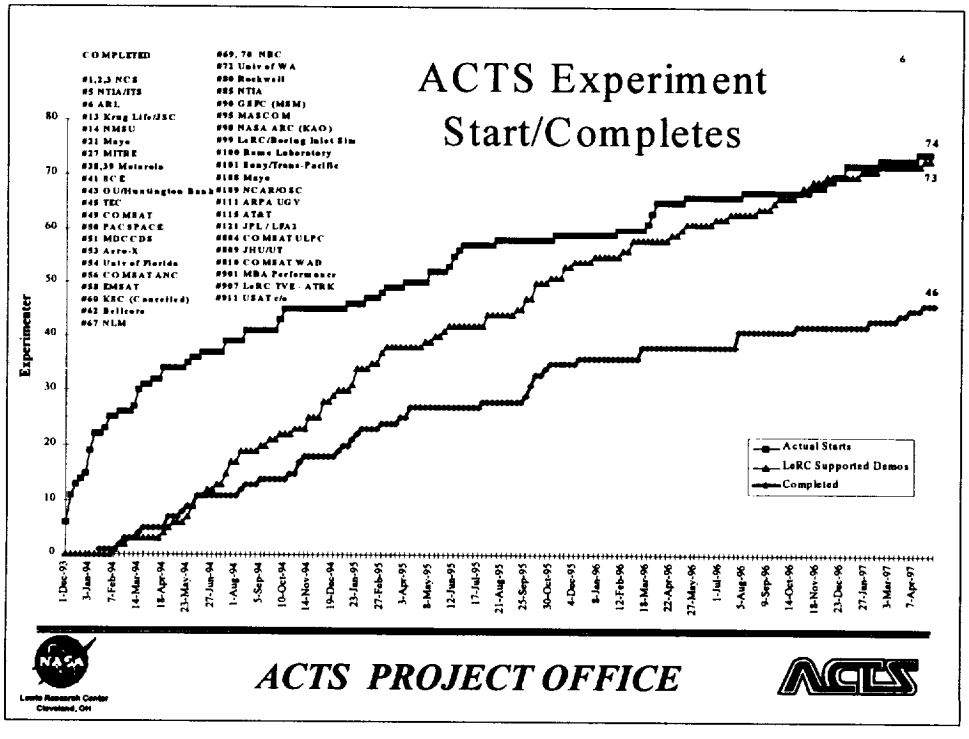

EXPERIMENTS PROGRAM

- ACTS Usage Policy
  - All new users must reimburse NASA for its expenses in operating ACTS & NASA terminals.
  - Based on general govt. policy of reimbursement to offset operations expenses of govt. facilities.
  - Policy effective immediately, evolving. First used in Jan. '97.
  - Current experimenters being worked one-on-one to transition to new policy.

ACTS PROJECT OFFICE

MAJOR ON-GOING/RECENT EXPERIMENTS

- AT&T first paying experimenter under new policy.
  - Voicespan filing withdrawn the week after ACTS experiment.

ACTS PROJECT OFFICE

MAJOR ON-GOING/RECENT EXPERIMENTS, cont.

- HPCC - High Data Rate (OC-3, OC-12)
  - Keck Observatory between Hawaii and JPL.
  - Goddard Global Climate Modelling on hold.

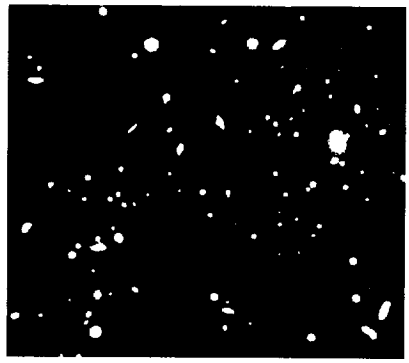

Image of Abell 963 obtained by the Keck II Telescope the night of February 7, 1997

MAJOR ON-GOING/RECENT EXPERIMENTS, cont.

- Latin America Distance Education
  - Program between Georgetown Univ. and So. America concludes end of June.
  - Cleveland Clinic and Quito still hold regular teleconferences. Interested in continuing through Dec. '97.

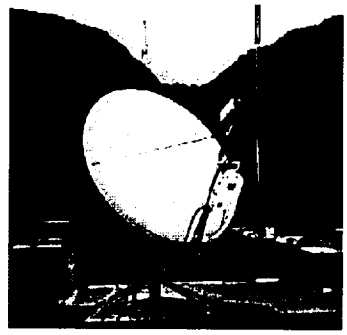

ACTS 2.4m Antenna Installed at Javeriana University, Bogota, Colombia

MAJOR ON-GOING/RECENT EXPERIMENTS, cont.

- "Live from Antarctica" - Interactive PBS broadcast; 3 live dates in Jan & Feb/97.
  - Multi-schools across the country.

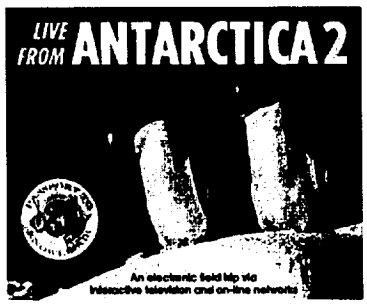

See web site @: http://quest.arc.nasa.gov/antarctica2/

MAJOR ON-GOING/RECENT EXPERIMENTS, cont.

- AAMNet - Several experiments using HDR terminals.
  - University of Kansas - TCP/IP protocol evaluation over ATM
  - Natl. Library Medicine - TCP data over ATM in delivery of medical text and imagery
  - GSFC - Tuning TCP over high speed sat. links

MAJOR ON-GOING/RECENT EXPERIMENTS, cont.

- Naval Research & Development (NRaD) - Ship-to-shore communications including video, voice, data, and internet protocol eval. at T1 (1.544 Mbps).

U.S. Navy cruiser USS Princeton (CG 59)

RECENT DEMOS

- Pacific Telecomm. Conf.
  - Feb.'97, Waikiki, HI
  - Lockheed Martin AstroLink product development demo with USAT.

F. Gargione tries the virtual reality demo at PTC '97

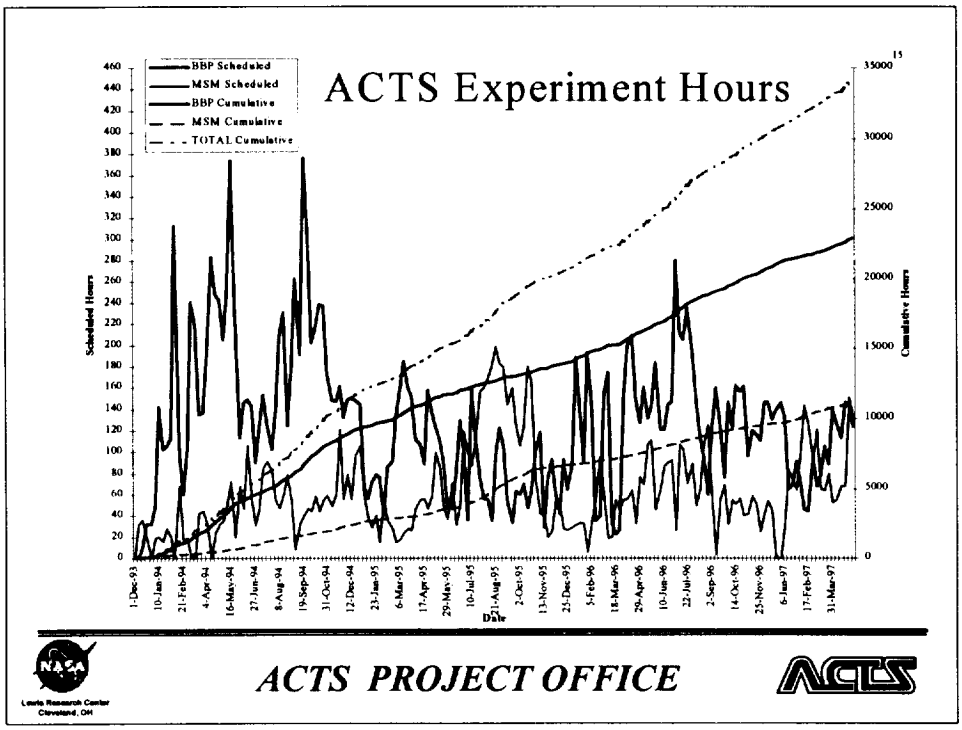
15
ACTS Experiment Hours
BBP Scheduled
MSM Scheduled
BBP Cumulative
MSM Cumulative
TOTAL Cumulative
Scheduled Hours
Cumulative Hours
Date
ACTS PROJECT OFFICE

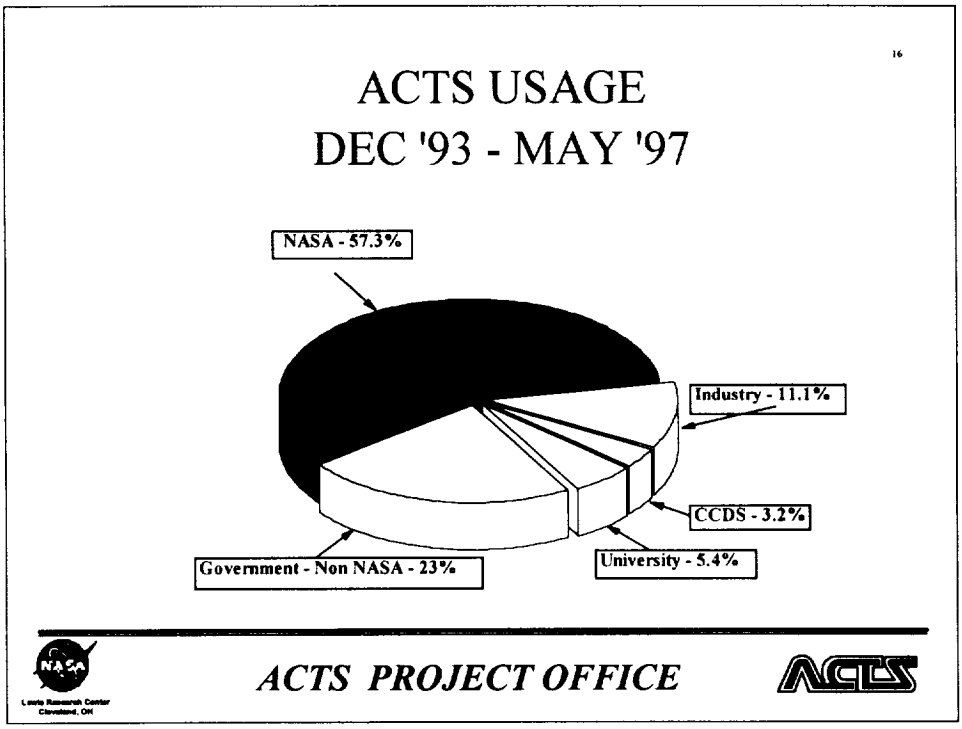
16
ACTS USAGE
DEC '93 - MAY '97
NASA - 57.3%
Industry - 11.1%
CCDS - 3.2%
University - 5.4%
Government - Non NASA - 23%
ACTS PROJECT OFFICE

17

PROPAGATION PROGRAM

- ACTS under considerable fiscal pressure for FY 98 due mostly to preparation for inclined orbit operations.
- Contract extensions being worked.
- 6 mos. extension through 3/98 to complete 4th year is well supported.
- Fifth year (collect data through 11/98) funding TBD.

18

PROPAGATION PROGRAM TIMELINE

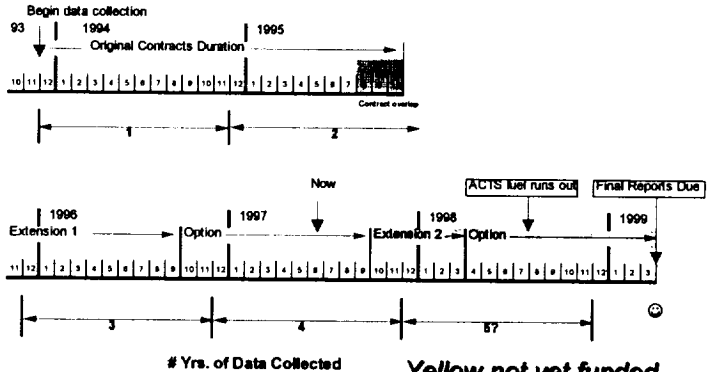

19

PROPAGTION CONTRACTS OUTLOOK

- Every effort being made to fund program's 5th year as best as possible.
- Some level of funding will be available!

Must look at options and priorities of data collection campaign.

20

PLANNED PATH

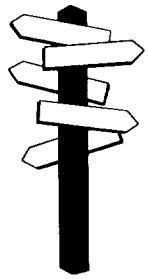

- Budget constraints greatest in FY 98.
- Cut of 25% in FY 98 must be worked.
- FORTUNATELY, our contracts will extend into FY 99.
- Shift FY98 budget shortage into FY 99.
- IMPACT:
  - Varying payment schedule.

FUNDING PROFILE

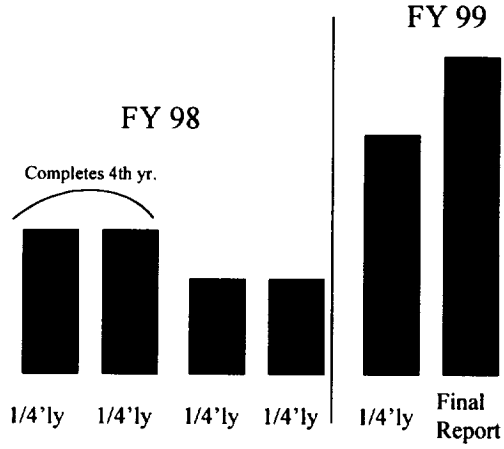

Funding Milestones

OPTIONS

- If 5th year funding pinched, what makes the most sense to do?
- Options I've considered:

1) Terminate program with 4 complete years of data (Mar. 98).

2) Find outside source to supplement program, either individually or as a group.

23

OPTIONS, cont.

De-scope work

3) No final report.

- Collect data/pre-process/send to TX only. Analyze later with separate contract?

4) Shorten contract duration (final report prep. time).

24

OPTIONS, cont.

6) Reduce number of sites.

7) Cut all contracts evenly by fixed %.

- Each site finds own ways to reduce costs.

8) Consolidate site operations (one contract operates multiple sites, or does all processing.)

Other options???

Two years ACTS Propagation Data in Cleveland

Roberto J. Acosta, Robert Manning
Tina Cox and Sandra Johnson

NASA Lewis Research Center
Cleveland Ohio, 44145

Outline

1. Description of Experiment
2. Motivation
3. Analysis
4. Summary
5. Future Work

Motivation

- Present fade availability curves for 95 & 96 in Cleveland
- Present availability curves including S/C MBA effects in Cleveland
- Compare results with the ACTS rain model prediction in Cleveland
- System margin determination from model or measurements ?
- Which effects are important to include in a fade availability model?

Experiment Description

Assumptions

- NGS beacon receiver - 30 dynamic range
- Ground station stability - amplitude corrected
- Ground station tracking errors - not corrected
- Ground station thermal distortions - not corrected
- Wet antenna effects - not corrected
- Data sampled at 150 m sec - average to 1 minute
- Clear sky corrected - over 2 years
- C0 measurements include all above plus S/C MBA effects

Experiment Description

Antenna Characteristics

- **F/D = 0.4**
- **D = 5.5 m**

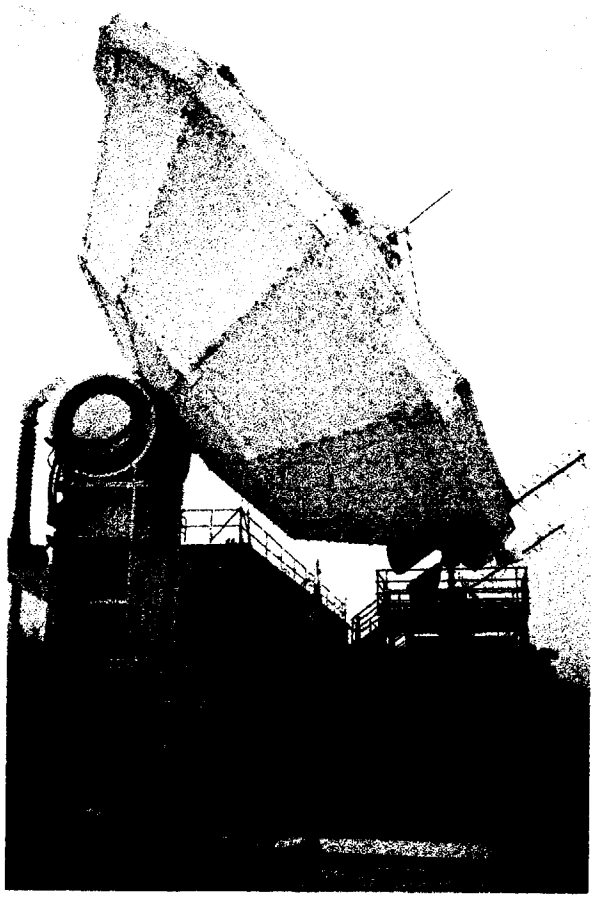

NASA Ground Station

ANALYSIS

1995 : 20 GHz Beacon Fades

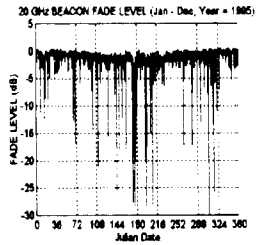

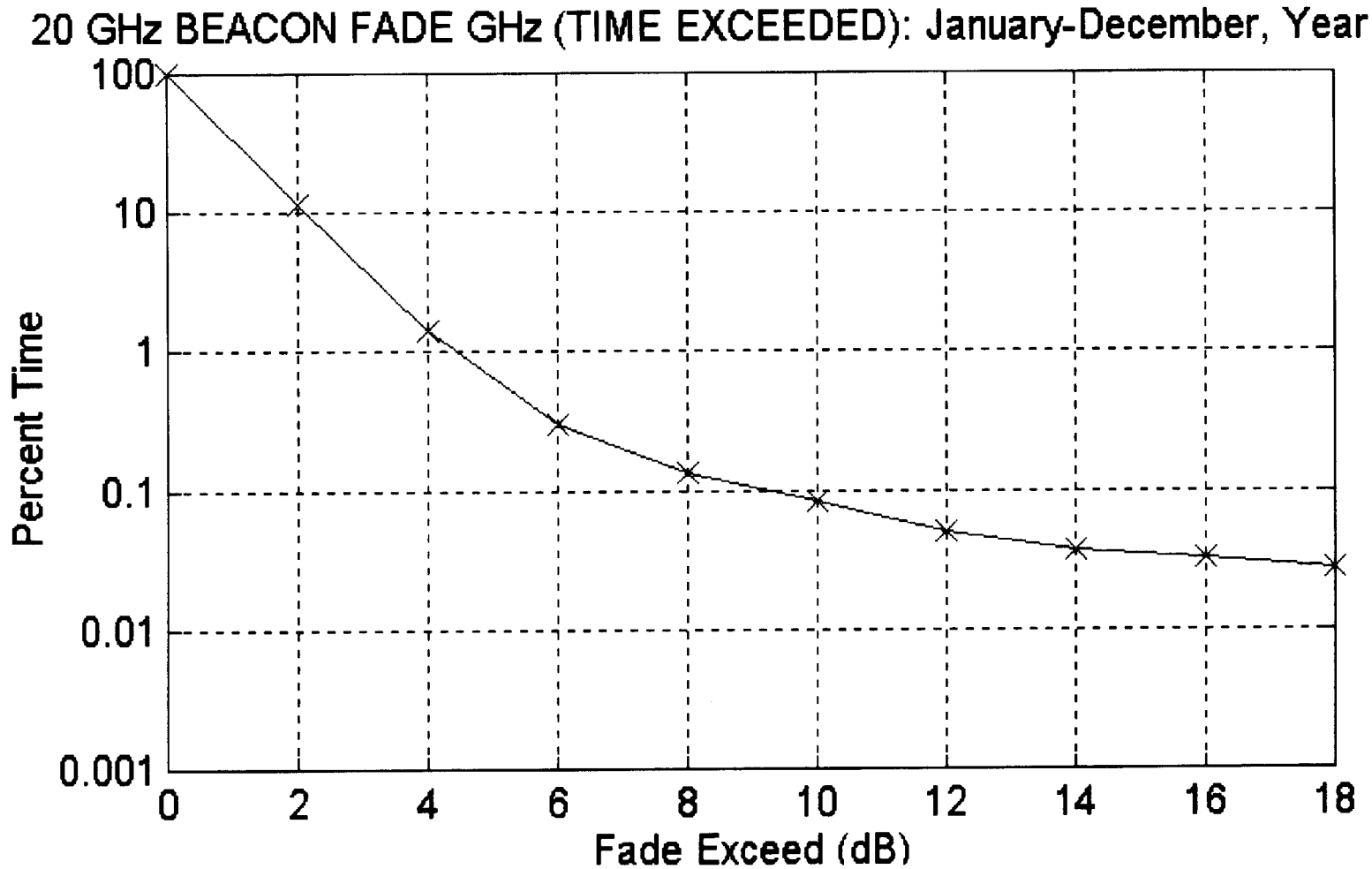

ANALYSIS

1996 : 20 GHz Beacon Fades

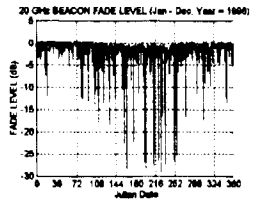

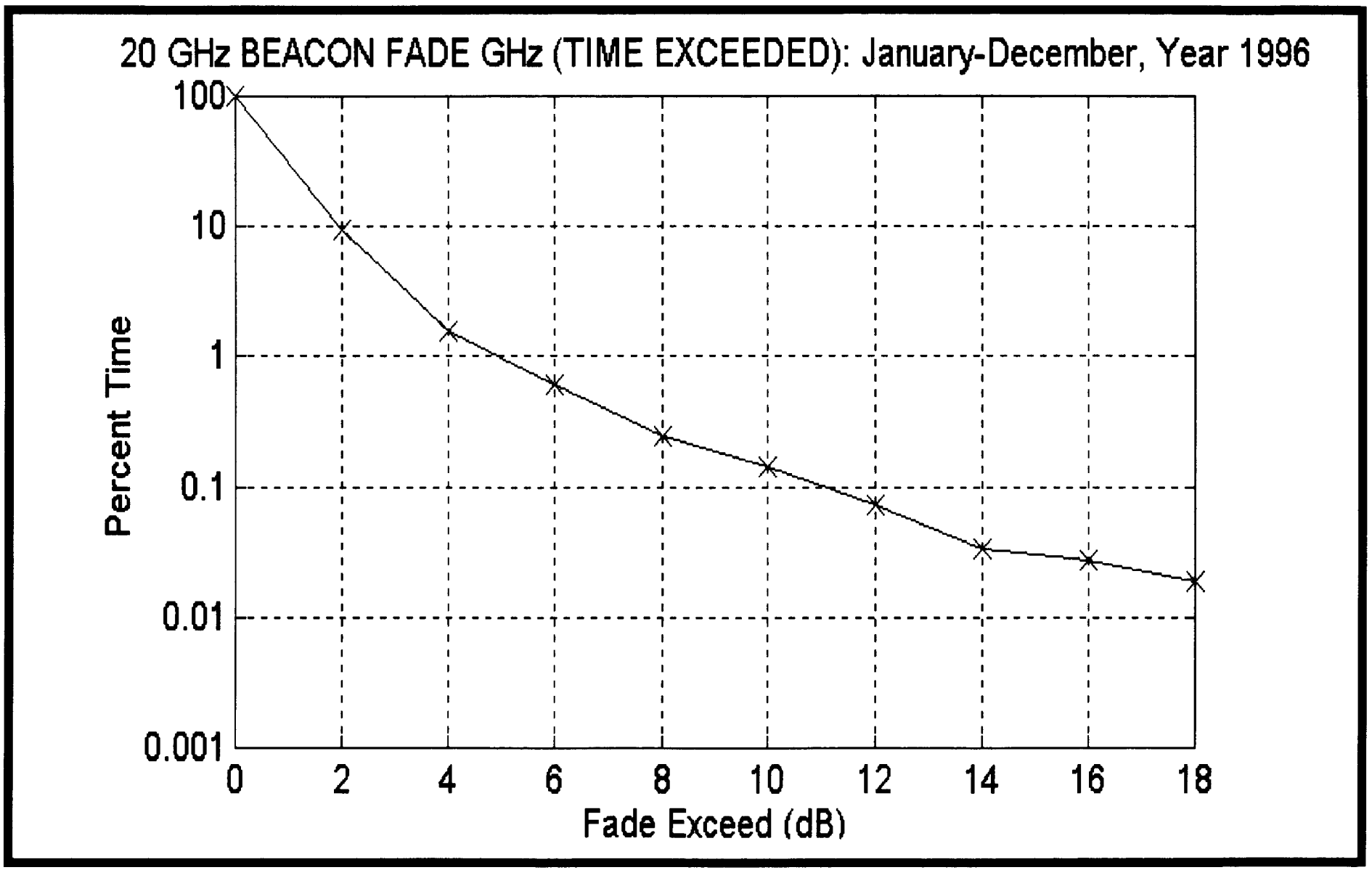

ANALYSIS

1995 : 30 GHz Beacon Fades

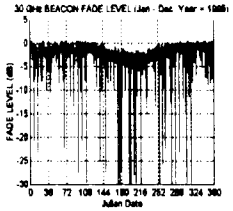

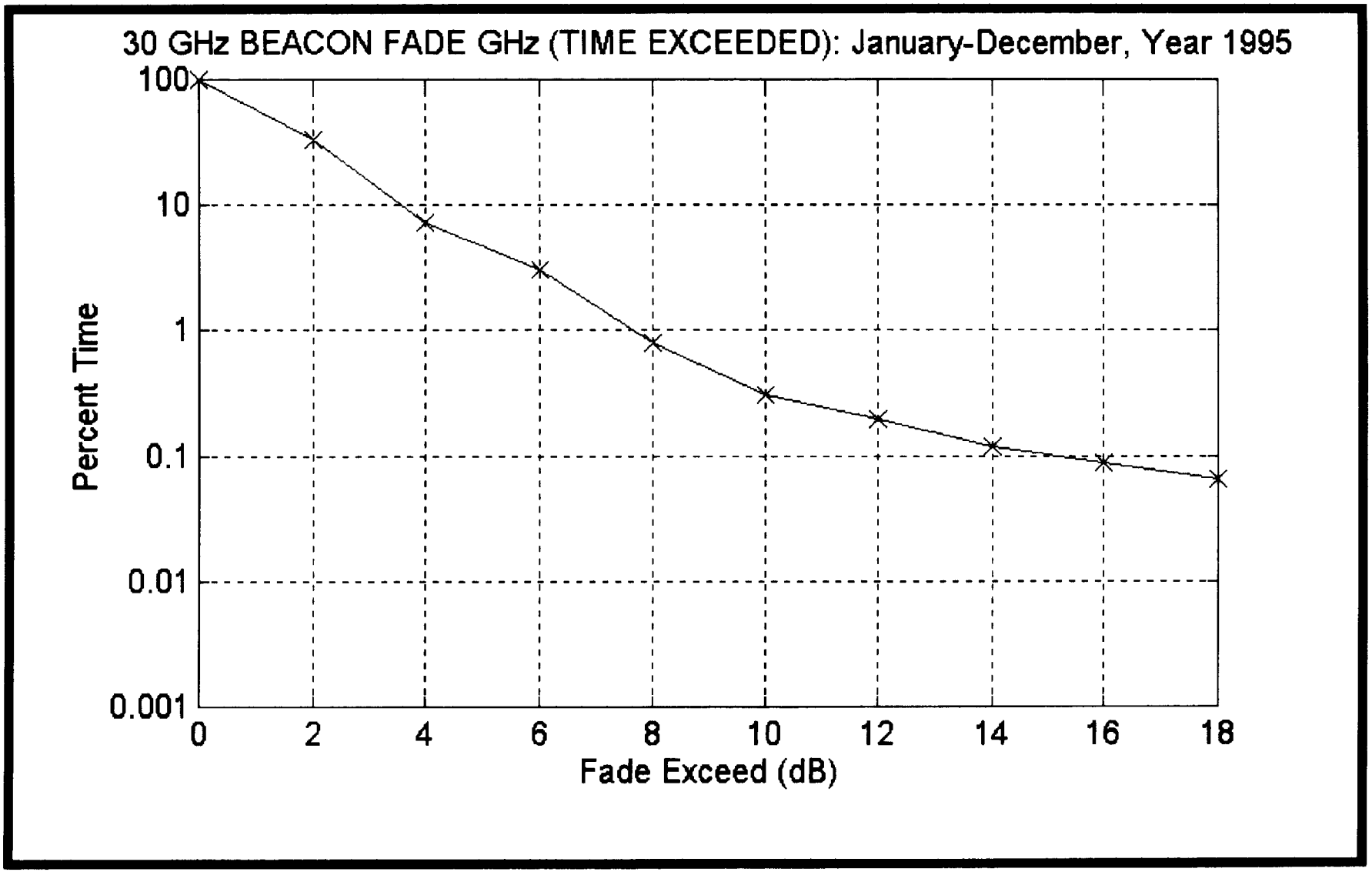

ANALYSIS

1996 : 30 GHz Beacon Fades

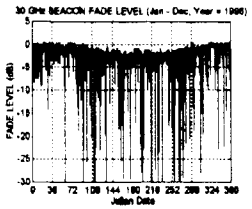

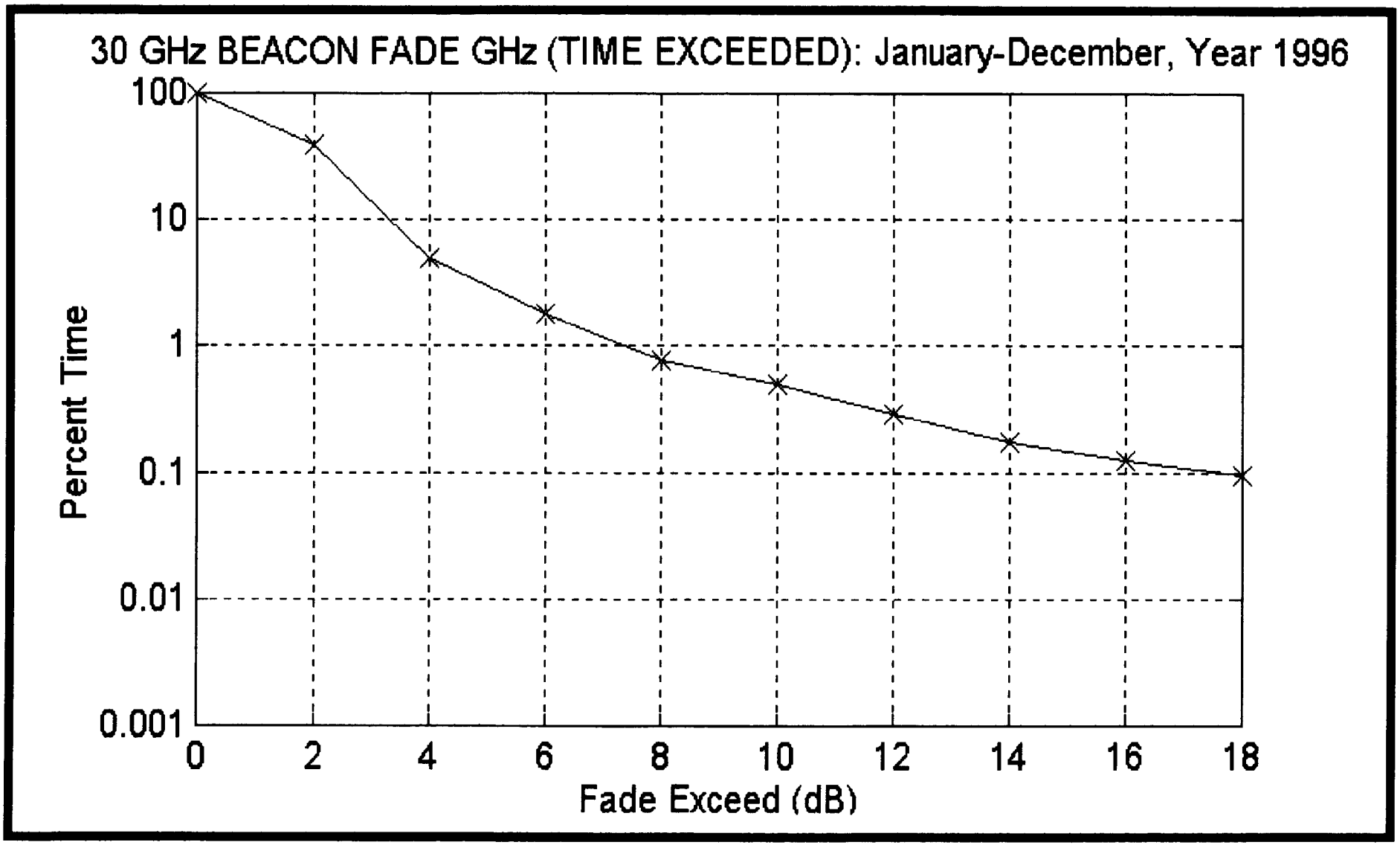

Analysis

Downlink (C0) Fade Availability 95, 96
Cleveland

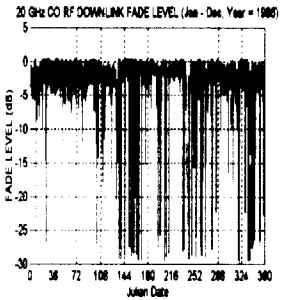

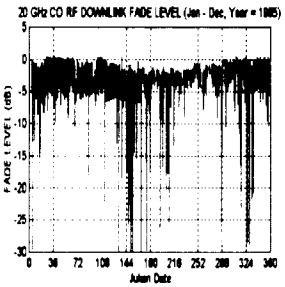

20 GHz C0 RF DOWNLINK (TIME EXCEEDED): January-December, Year 1996

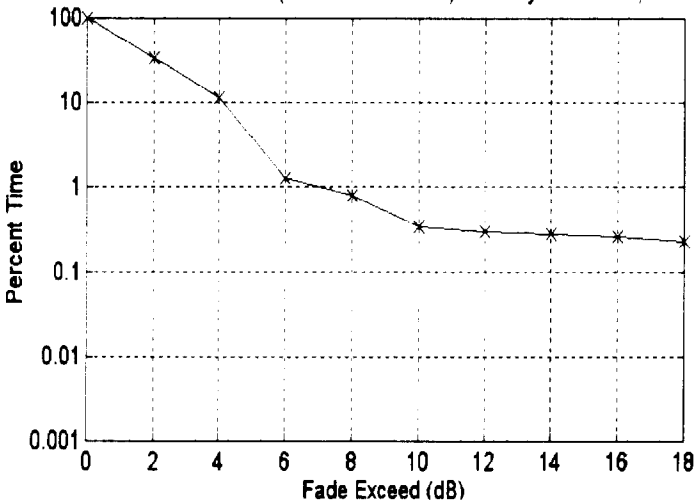

20 GHz C0 RF DOWNLINK (TIME EXCEEDED): January-December, Year 1995

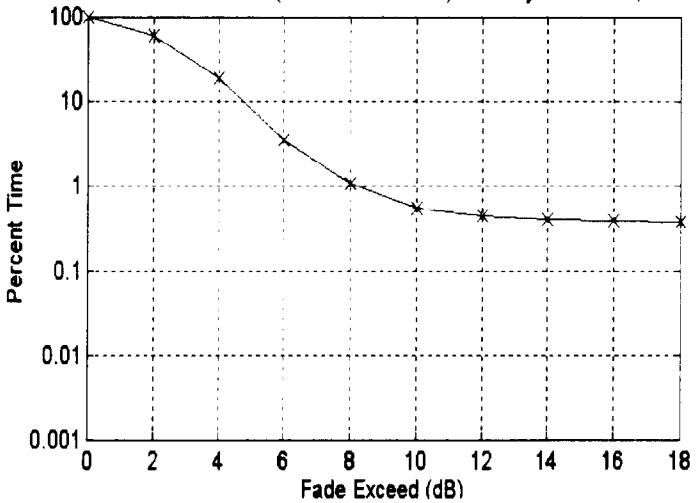

Analysis

ACTS Rain Model Predictions vs Measurements in Cleveland for 99.9 % Fade Availability for 95 and 96

Year	20 Ghz			30 Ghz		
	ACTS MODEL	Beacon Meas.	C0 Meas.	ACTS MODEL	Beacon Meas.	C0 Meas.
1995	4 dB	9 dB	> 18 dB	9 dB	15 dB	n.a.
1996	5 dB	11 dB	> 18 dB	10 dB	18 dB	n.a.

SUMMARY

- Wet antenna effects need to be taken out if only rain fade availability is of interest.
- System margin and system availability at minimum are a function of:
  - Wet antenna
  - Ground station stability
  - Ground station tracking (in rain)
  - Ground Station Thermal Distortions (De-Icers)
  - Spacecraft antenna pointing (Narrow beams)
  - Rain attenuation
  - Cloud attenuation
  - Rain and ice depolarization
  - Gaseous absorption

FUTURE WORK

- Analysis of 94 data - in progress
- Analysis of data using 150 msec - started in May 97.
- Network availability analysis in progress (T1VSAT - T. Cox and T. Coney (retired))
- Fade dynamics - experimental case in progress
- Analysis of 97 data -in progress
- Complete comparison between ACTS model and measurements in Cleveland - in progress

Acts Propagation Terminals

Engineering Support and Systems Upgrades

David Westenhaver

Westenhaver Wizard Works, Inc.
wwwinc@crl.com

June 11 - 13, 1997

Software Status / Deficiencies and Known Problems

DRX software status:

- Current version 17 of 4/25/96.
- Need to open beacon acquisition constraints.

DACS software status:

- Current version 10 of 4/01/96.
- Need to add force beacon reacquisition.
- Need to prevent repeating radiometer setups.

TSR software status:

- Current version 11 of 7/16/96 .
- Testing version 12.
- Need clear indication of DOS Critical-Errors.
- Works with Zip Drive except when operator error.
- Data missing from RV0; Defragment Disk.

ActsView software status:

- Current version 3 of 9/26/94.
- Testing version 4 progress.

Actspp PreProcessing software status:

- Current version 7.1 of 4/17/97.
- Testing version 7.2.
  - Fixed minor defects.
  - Making new user setup easier.
- Need input from users.

System Hardware Status / Deficiencies and Known Problems

LNB Failures.

20 GHz LNB at CSU was replaced March 28,1997.
20 GHz LNB at CSU failed May 27, 1997.
20 GHz LNB at NMSU may be causing data "jumps."
Have no spare 20 LNB.

Radiometer 0.25 -0.5 Volt Jumps

This effect is seen at several sites.
Cause is being investigated, This may be due to LNB.

Feed Horn Widow.

Problem: The windows crack and leak water.
Solution: Replace the feed horn.
Experimenters need to visually check windows often.

Summary plots of the Sites System Calibration to Date

All Sites Data Accumulation Summary

Rain Accumulation Calculated from Rain-Rate in EDF

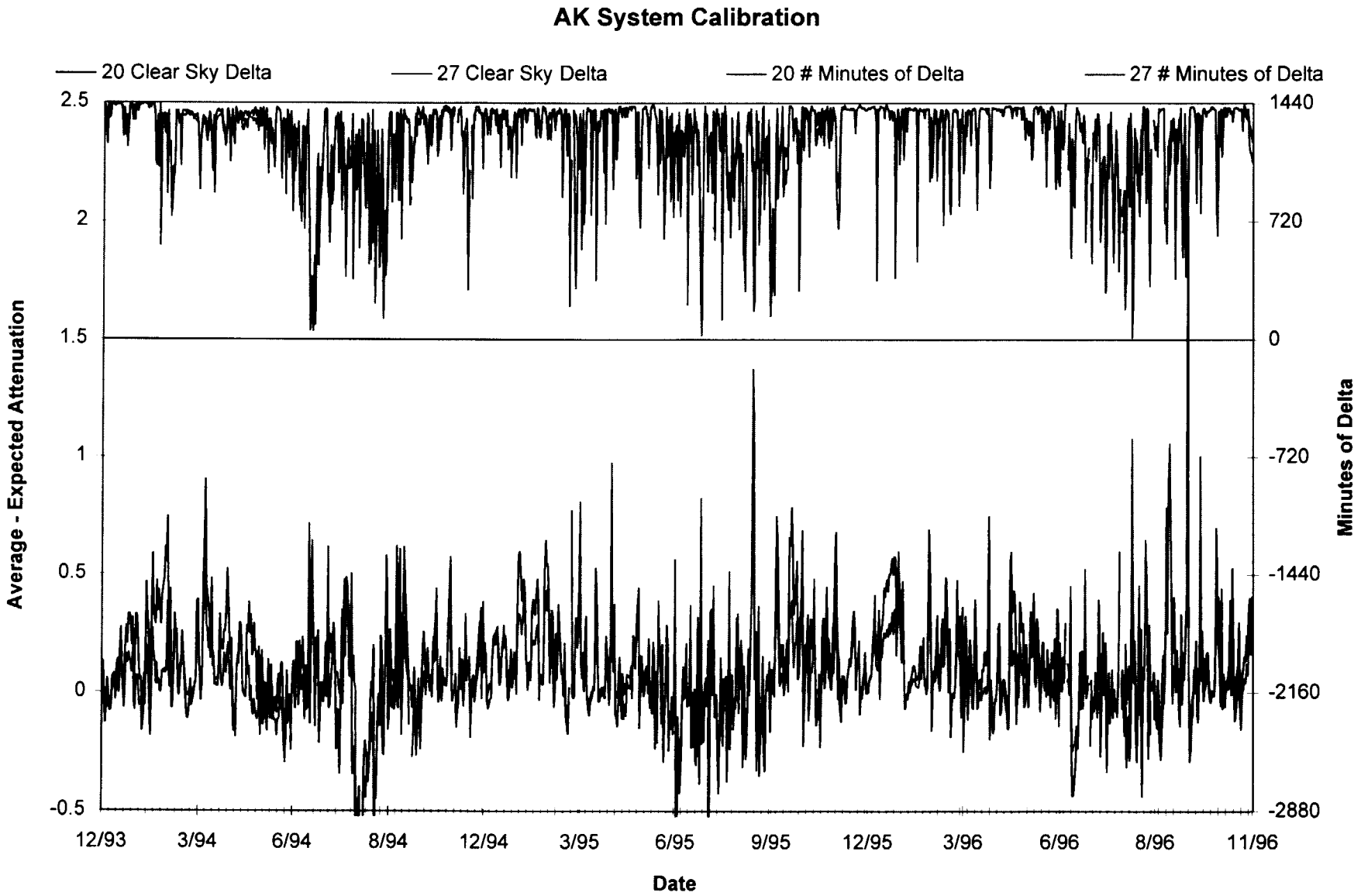
AK System Calibration
20 Clear Sky Delta
27 Clear Sky Delta
20 # Minutes of Delta
27 # Minutes of Delta
Average - Expected Attenuation
Minutes of Delta
Date
2.5
2
1.5
1
0.5
0
-0.5
1440
720
0
-720
-1440
-2160
-2880
12/93
3/94
6/94
8/94
12/94
3/95
6/95
9/95
12/95
3/96
6/96
8/96
11/96

LOG_AK1.XLS

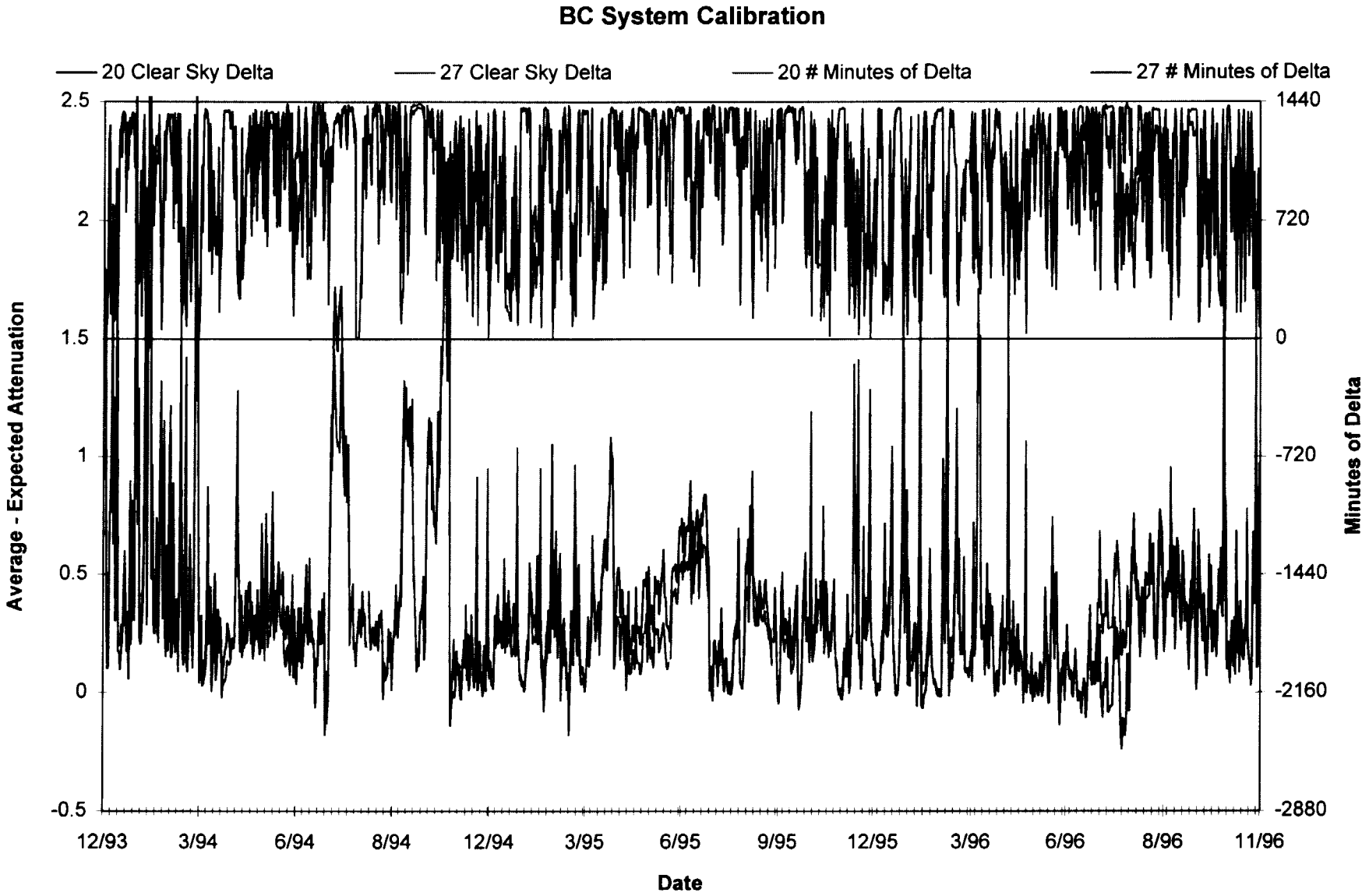
BC System Calibration
20 Clear Sky Delta
27 Clear Sky Delta
20 # Minutes of Delta
27 # Minutes of Delta
Average - Expected Attenuation
Minutes of Delta
2.5
2
1.5
1
0.5
0
-0.5
1440
720
0
-720
-1440
-2160
-2880
12/93
3/94
6/94
8/94
12/94
3/95
6/95
9/95
12/95
3/96
6/96
8/96
11/96
Date

LOG_BC1.XLS

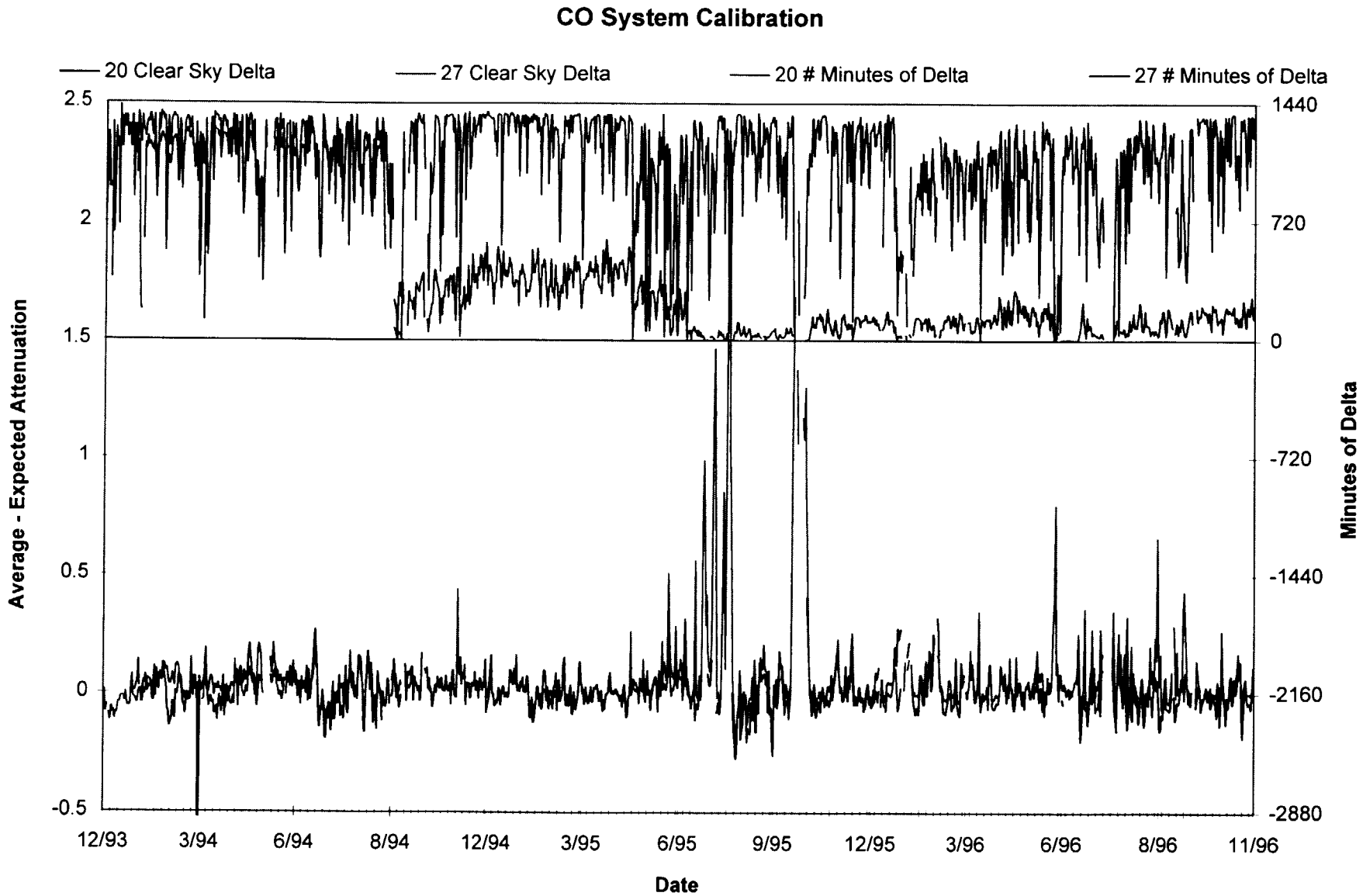
CO System Calibration
20 Clear Sky Delta
27 Clear Sky Delta
20 # Minutes of Delta
27 # Minutes of Delta
Average - Expected Attenuation
Minutes of Delta
2.5
2
1.5
1
0.5
0
-0.5
1440
720
0
-720
-1440
-2160
-2880
12/93
3/94
6/94
8/94
12/94
3/95
6/95
9/95
12/95
3/96
6/96
8/96
11/96
Date

LOG_CO1.XLS

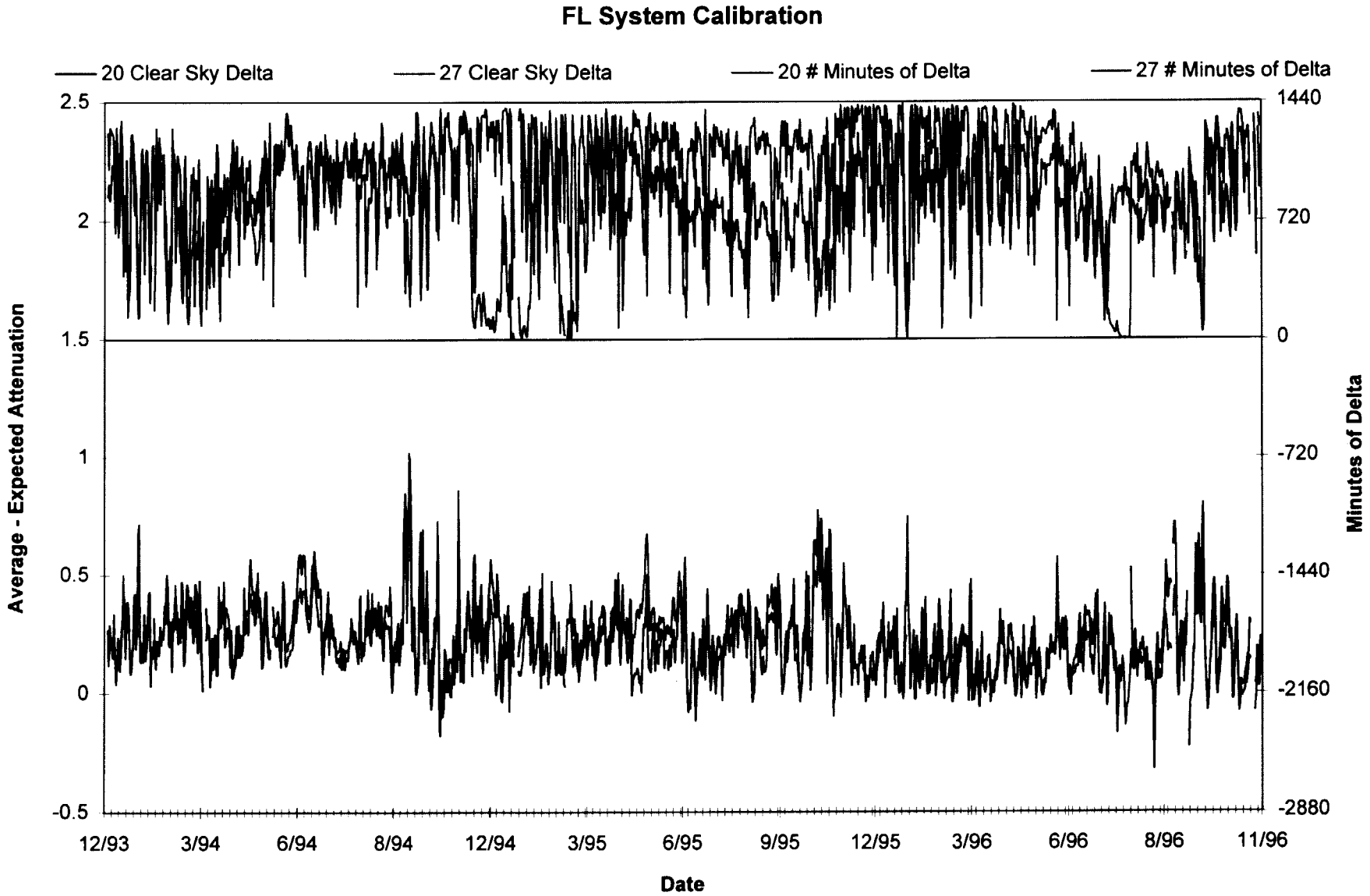
FL System Calibration
20 Clear Sky Delta
27 Clear Sky Delta
20 # Minutes of Delta
27 # Minutes of Delta
Average - Expected Attenuation
Minutes of Delta
2.5
2
1.5
1
0.5
0
-0.5
1440
720
0
-720
-1440
-2160
-2880
12/93
3/94
6/94
8/94
12/94
3/95
6/95
9/95
12/95
3/96
6/96
8/96
11/96
Date

LOG_FL1.XLS

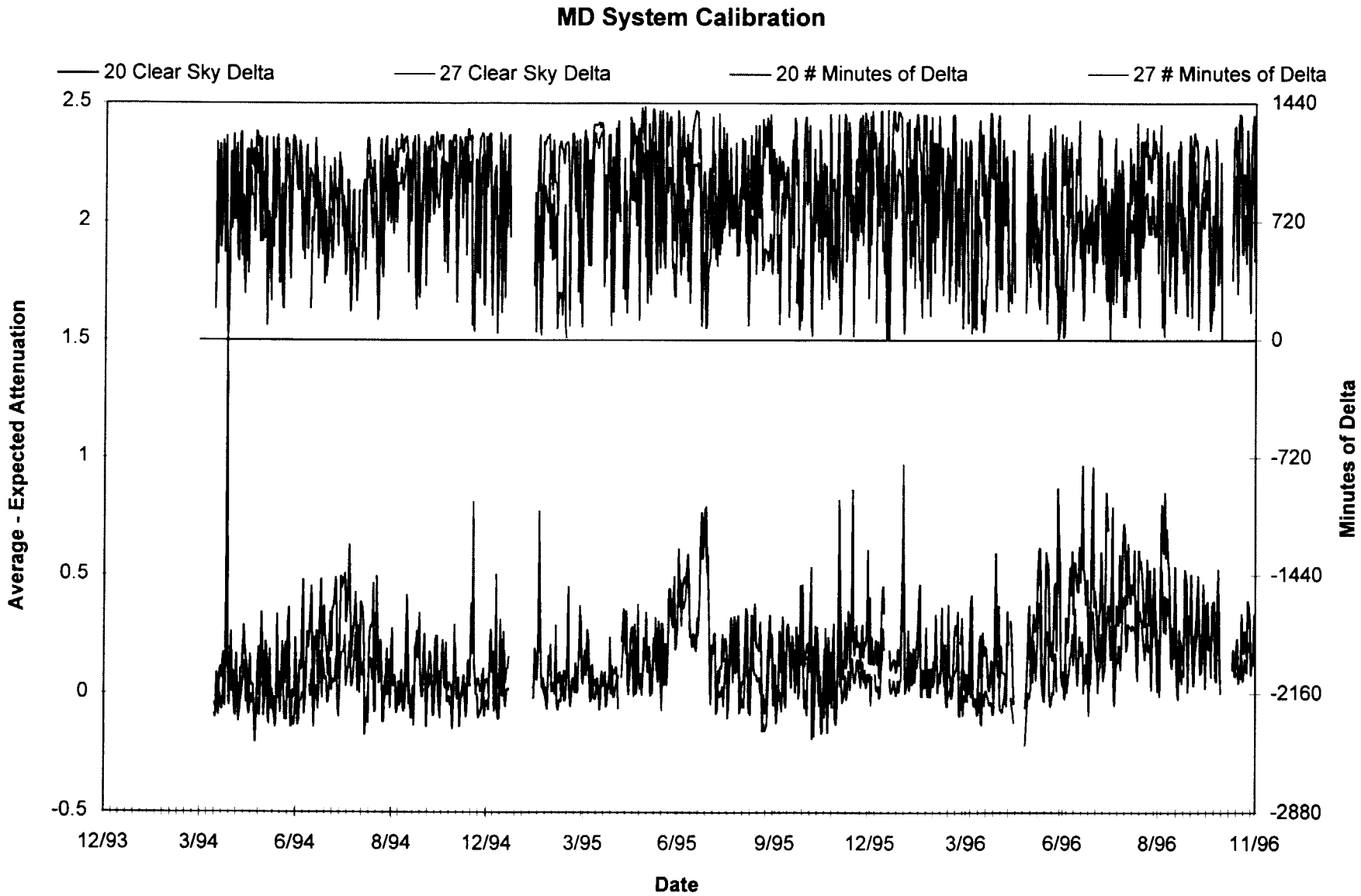
MD System Calibration
20 Clear Sky Delta
27 Clear Sky Delta
20 # Minutes of Delta
27 # Minutes of Delta
Average - Expected Attenuation
Minutes of Delta
Date
2.5
2
1.5
1
0.5
0
-0.5
1440
720
0
-720
-1440
-2160
-2880
12/93
3/94
6/94
8/94
12/94
3/95
6/95
9/95
12/95
3/96
6/96
8/96
11/96

LOG_MD1.XLS

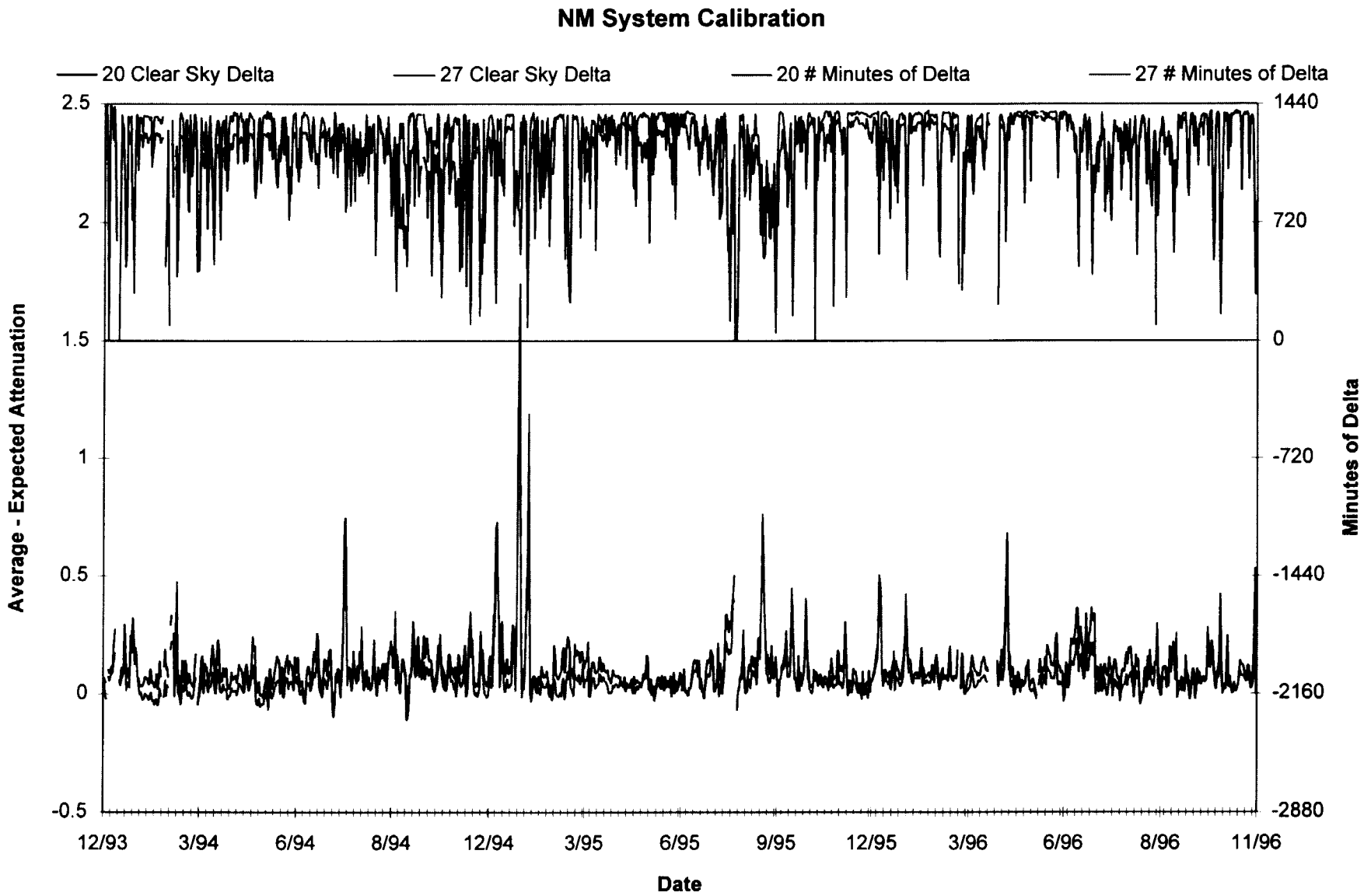
NM System Calibration
20 Clear Sky Delta
27 Clear Sky Delta
20 # Minutes of Delta
27 # Minutes of Delta
Average - Expected Attenuation
Minutes of Delta
2.5
2
1.5
1
0.5
0
-0.5
1440
720
0
-720
-1440
-2160
-2880
12/93
3/94
6/94
8/94
12/94
3/95
6/95
9/95
12/95
3/96
6/96
8/96
11/96
Date

LOG_NM1.XLS

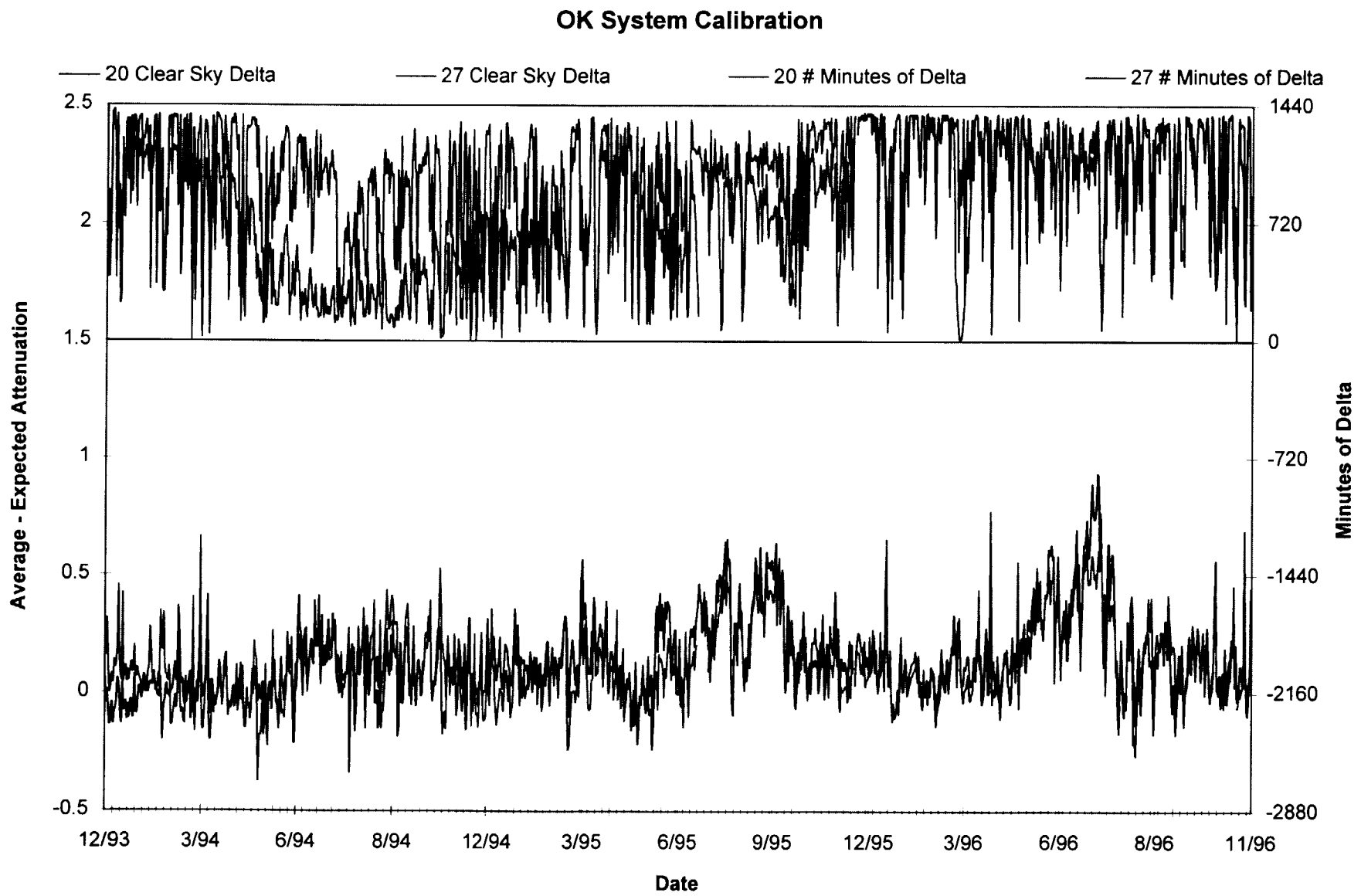
OK System Calibration
20 Clear Sky Delta
27 Clear Sky Delta
20 # Minutes of Delta
27 # Minutes of Delta
Average - Expected Attenuation
Minutes of Delta
2.5
2
1.5
1
0.5
0
-0.5
1440
720
0
-720
-1440
-2160
-2880
12/93
3/94
6/94
8/94
12/94
3/95
6/95
9/95
12/95
3/96
6/96
8/96
11/96
Date

LOG_OK1.XLS

Total Data Accumulation Summary

Site	Total Days	Total Days Collected		Lost Time During Collection		Total Good Days Collected		Total Lost or Missing Days	
AK	1096	1091.0	99.54%	2.5	0.23%	1088.4	99.31%	7.6	0.69%
3rd yr	366	365.8	99.93%	0.6	0.17%	365.1	99.76%	0.9	0.24%
BC	1096	1091.4	99.58%	2.3	0.21%	1089.1	99.37%	6.9	0.63%
3rd yr	366	365.7	99.92%	0.9	0.23%	364.8	99.68%	1.2	0.32%
CO	1096	1068.2	97.46%	8.5	0.77%	1059.7	96.69%	36.3	3.31%
3rd yr	366	350.6	95.80%	2.4	0.66%	348.2	95.14%	17.8	4.86%
FL	1096	1077.6	98.32%	8.7	0.79%	1068.9	97.53%	27.1	2.47%
3rd yr	366	360.9	98.60%	3.7	1.00%	357.2	97.60%	8.8	2.40%
MD	1006	938.3	93.27%	1.8	0.18%	936.5	93.09%	69.5	6.91%
3rd yr	366	340.3	92.99%	0.5	0.15%	339.8	92.84%	26.2	7.16%
NM	1096	1076.3	98.21%	6.5	0.59%	1069.9	97.61%	26.1	2.39%
3rd yr	366	356.0	97.28%	1.7	0.46%	354.4	96.82%	11.6	3.18%
OK	1096	1094.1	99.83%	2.7	0.24%	1091.5	99.59%	4.5	0.41%
3rd yr	366	366.0	100.0%	0.2	0.06%	365.8	99.94%	0.2	0.06%

ALL_UPT6.XLS

Rain Accumulation Calculated from Rain-Rate in EDF
For 12/1/95 to 11/31/96, (mm) accumulation

Site	Capacitive Rain Gauge	Tipping Bucket Rain Gauge
AK	225	na
BC	1475	665
CO	21	na
FL	1815	1481
MD	32056 (bad gauge)	964
NM	1061	209
OK	513 (no gauge connected)	560

Note: Rain Rate Data Must be Interpreted with Great Care

REPORT OF ACTS MINIWORKSHOP PLENARY MEETING

D.V. Rogers and W.J. Vogel

On June 13, 1997, the ACTS Working Groups held the customary joint Plenary meeting in El Segundo to address issues related to experiments being conducted with the NASA ACTS Propagation Terminals (APTs). Results of that meeting are reported here.

I. *Current Status/Future Focus*

N. Golshan, NASA/JPL coordinator for the ACTS Propagation Studies program, briefly addressed the Plenary at the start of the meeting, and suggested a change in focus is required at the present time. With the recent distribution of the first three years of preprocessed data for the seven sites, the emphasis should shift from collection, processing and distribution of data to analysis of these data. He proposed that experimenters take a more global view of all seven data sets and plan for the "big picture" with input from both industry and doers to identify concerns, rectify gaps in the data and data analyses (*e.g.*, low rain rate impairments, infrequent propagation events), *etc.*

Golshan emphasized the need for peer review of the results, and for a recommendation re continuity/quality of the results. This requirement will be met in part, of course, with the imminent publication of the Special Issue of the Proceedings of the IEEE, devoted to Ka-band earth-space propagation, which contains preliminary results of studies now being conducted with the ACTS data. There was broad agreement with Golshan's remarks.

II. *Technical Issues in the ACTS Experiments*

A. *Rain Rate Data*

During the NAPEX/ACTS presentations and discussions, it was observed that some of the rain gauge statistics in the recently-distributed data CDs were not fully valid. In cases, invalid data that had been (appropriately) included in the ACTS data archives were inadvertently also included in the preprocessed files, mainly because data flags were not always properly set in the electronic data (*e.g.*, if all relevant information had not been transferred from paper logs). Hence, statistics derived from the preprocessed data occasionally include data segments intended to be marked invalid.

In a wide-ranging discussion, a variety of options were proposed both to resolve the problem of mismarked data and to provide supporting rain data that might assist users of these data sets. H. Helmken stated there must be a diligent effort to mark any bad rain gauge data. W. Vogel observed that current practice is to assume the data are valid unless specifically marked otherwise; he suggested that a more reliable default procedure, which would also enforce a review of these data, would be to assume the data are invalid unless specifically marked otherwise. This approach would preserve the original intent that each experimenter maintain ultimate authority of the data set for the respective experiment site. R. Henning suggested incorporating auxiliary rain rate data from nearby weather services as available, such as the 15-min. rainfall accumulations.

D. Westenhaver said this problem is being addressed in the revised version of the processing software. He also noted that there is a program available now to assist the doers in checking their rain gauge(s), and further that there is a column in the EDF to enter the daily rainfall accumulation, which information is saved. In response to a question from J. Feil, he pointed out that the marking of data validity is independent for each gauge that may be available at a specific experimenter site.

C. Mayer stated that the rain rate data are a small subset of the otherwise excellent database, and that this issue should not detract from the utility of the other data. He also stated that each site should have at least one reliable rain gauge to supply data for eventual inclusion in the archives.

ACTIONS:

D. Westenhaver will address the issues regarding rain gauge data collection and preprocessing software, allow input of supplementary rain information (as available), and provide instructions for correct use of the new software. The ACTS Data Center will alert recipients of the latest CDs to the problem with the rain data, and supply CDs without the rain data to those who may request same.

B. *Inclined-Orbit Operation*

Several issues related to the anticipated transition to inclined-orbit operation of ACTS were addressed (contractual ramifications are discussed below). Present plans are to transition to inclined-orbit operation in July 1998, with a predicted increase in orbital inclination of about 0.8° per year in this mode. B. Bauer reiterated the prior conclusion that operation through the fifth year of data collection (*i.e.*, through November 1998) is feasible without antenna tracking. If measurements are pursued into the sixth year (considered unlikely), some form of tracking will be necessary.

D. Westenhaver remarked that the ACTS preprocessing software is already capable of removal of diurnal signal-level variations up to 3 dB. N. Golshan asked if the antenna pattern as viewed from each APT is site-specific; if so, the predicted diurnal variations in signal level are as well, and this fact must be taken into account.

ACTIONS:

By the time of the next ACTS meeting, B. Bauer will provide predictions of diurnal signal-level variations specific to each site.

C. *Antenna-Wetting Issue*

In response to presentations and discussions at this and previous meetings, issues related to characterizing and accounting for the apparent path losses caused by antenna wetting were once again deliberated. The discussion was framed by the questions of what are the goals of the effort and how might aspects such as correction for statistical and dynamic aspects be achieved. It was noted that several groups are investigating the problem. The dual-antenna investigations at COMSAT and Lewis Research Center appear promising to establish the practical significance of the effect.

C. Mayer pointed out that the configuration for the LeRC measurements did not include a rain gauge, and that one is required for that experiment. S. Horan noted the difficulty in reliably replicating artificial rain rates below 30 to 40 mm/h, an area still under study. J. Goldhirsh stated that the behavior of the signal level while the antenna surfaces are drying indicates that the loss effect may be important at lower rates and be intractable, and thus may require a caveat on the fade distributions. D. Rogers observed the related problem of dealing with fade dynamics.

ACTIONS:

J. Goldhirsh will try to locate a rain gauge and personal computer with software to loan to the group at LeRC for the antenna-wetting measurements at that location.

III. *ACTS Operations/Contract Issues and Concerns*

A. ***Site Support/Maintenance***

Concerns were voiced about an apparent reduction in site-support resources. N. Golshan identified several elements that had indeed contributed to reduced funding: the APTs are aging, and sometime require more maintenance; as three years of data have been collected, there is a need to progress to more modeling as well as updating of the NASA handbooks; and the original budget for the

program was for a 3-year effort, which has now been concluded. He stated that for site-support, the "glass is 80% full" but there are insufficient resources to do everything. He asked if elements of the effort might be prioritized to allow some activities to be dropped or deferred.

A wide-ranging discussion followed, where options such as the possibility of discontinuing measurements at some sites, continuing only partial data collection should, say, a low-noise amplifier fail at one of the beacon frequencies (perhaps filling the gaps with frequency scaling), *etc.* J. Beaver noted that data collection for the fourth year was already more than half completed, and that this phase at least should be finished. D. Rogers recalled that both the experimenters and the Satellite Industry Task Force had supported continuity of the measurements. C. Mayer said the goal should remain the collection of five years of data with full-up capabilities.

There was some brainstorming concerning the potential of seeking additional support from industry, especially those parties that have recommended continuation of the measurements program. L. Peronard suggested that those parties that had filed to the FCC for spectrum to offer services at Ka-band would be good candidates. J. Feil mentioned that at the Fairbanks meeting, some representatives of industry had indicated that their organizations might contribute, say, a low-noise block. B. Bauer stated that some industrial organizations might have discretionary funds for such purposes.

It was finally agreed that the preferred approach would probably be for experimenters at the individual sites to approach potential donors directly, with help from NASA in identifying candidates.

ACTIONS:

N. Golshan and B. Bauer will collaborate to plan an approach and draft an example letter that might serve to approach industrial organizations.

B. *Budget Issues Related to Inclined-Orbit Operation*

B. Bauer identified an anticipated experiments funding crunch in 1998 as a result of the need to prepare for inclined-orbit operation. Funds will likely have to be diverted to operational planning, revision of control software at the Master Control Station in Cleveland, *etc.*, to support operation in the inclined-orbit mode. He asked NASA-funded experimenters to consider deferring some contract funding requirements into the 1999 fiscal year. There is of course some risk, since the 1999 budget has not yet been finalized nor approved.

The funding of the (fixed-price) contracts would probably remain the same, but the program would benefit by shifting progress payments into 1999 as feasible. Individual experimenters offered support in addressing this difficulty.

ACTIONS:

B. Bauer will address the funding details for each site during individual contract negotiations.

C. *Project Emphasis*

The discussion on 1998 budget issues resurrected a general discussion regarding the priorities of the measurements and what is of maximum value to users of the information, similar to that reported in Item III.A above. B. Bauer asked if the current fundamental priority is collection of raw data or modeling/handbook activities. Z. Koro stated that the long-term benefits are maximized by continuing the measurements as long as possible.

N. Golshan stated that industry needs models now, and there are a lot of dollars at stake. L. Peronard concurred, noting that ground-station commitments are now in process, and Ka-band satellites will be in orbit by the year 2000. Analysis is required to provide results such as dynamics of fading, seasonal variations, impairment extremes, *etc.* Z. Koro agreed that numbers are needed at the moment,

but existing models already provide approximate impairment estimates. More certainty is preferred, but is only achievable by making long-term measurements, probably the greatest value of this project. As in previous deliberations, there seemed to be general agreement that additional effort must be applied to modeling and analysis activities, concurrent with continuation of the ACTS data collection efforts.

D. *General Operations*

As customary, near the end of the Plenary session the individual experimenters discussed operational issues at the sites. C. Mayer emphasized that critical spares are becoming more important as the equipment ages, and offered to purchase a spare feed horn if need be. He also noted that the custom-design low-noise blocks (LNBs) used in the APTs are critical, expensive long-lead items, and that the 20-GHz units have not been very reliable (a bench spare 27.5-GHz LNB is maintained by D. Westenhaver, probably sufficient as these units have been reliable).

B. Dow noted some unusual anomalies at UBC during the last few months which stopped data collection for over a day, but had not recurred (C. Mayer indicated that defragmenting the hard drive might fix this problem). He also reported a decrease in LNA gain and faulty siphoning of the capacitance rain gauge. UBC has purchased a new humidity sensor, but the sun shield isn't yet available.

J. Beaver reported that the Colorado 20-GHz LNA has failed, particularly unfortunate because June is normally the wettest month at his site. He is also using a temporary feedhorn cover to replace one damaged by hail, and noted this is not really a satisfactory solution.

R. Henning voiced concern about the lack of an on-shelf 20-GHz LNB spare, and stated that the site-support function had been essential in amalgamating and retaining expertise developed by the ACTS experimenter group. Similar views were expressed by J. Feil and S. Horan. X. Wang also noted the need for a spare 20-GHz LNA, although the existing one has been stable for a year.

A general conclusion of the overall discussions seemed to be that at least two spare 20-GHz LNBs and feedhorns would be needed for the program.

ACTIONS:

At the end of the Plenary session, Golshan remarked, based on overall discussions during the session, that he was convinced of the urgent need to address the sparing issue, and would request resources for these requirements, although he could make no guarantee of additional funds.

E. *Next Meetings*

The next ACTS Propagation Studies Workshop is planned for Boca Raton, Florida, during the week of November 17, 1996 (the week before U.S. Thanksgiving). The NAPEX XXII meeting is planned for Austin, Texas, during the first week of June 1998.

Appendix

List of Attendees

NAPEX XXI MEETING AND TENTH ACTS WORKSHOP

Lyle Abramowitz
The Aerospace Corporation
2350 E. El Segundo Blvd.
310-336-2657
310-336-6225 (FAX)
E-mail: abramowitz@courier8.aero.org

Roberto Acosta
NASA Lewis Research Center
2100 Brookpark Rd., MS 54-6
Cleveland, OH 44135
216-433-4460
216-433-6371 (FAX)
E-mail: R.Acosta@lerc.nasa.gov

Riza Akturan
Globalstar
3200 Zanker Road, MS-2
San Jose, CA 95164-0670
408-473-6113
408-473-6227 (FAX)
E-mail: Riza.Akturan@globalstar.com

Khamet Alkebulan
Jet Propulsion Laboratory, MS 264-538
4800 Oak Grove Drive
Pasadena, CA 91109
818-393-7722
818-393-3068 (FAX)
E-mail: Khamet.N.Alkebulan@
jpl.nasa.gov

Dick Astrom
Motorola
Satellite Communications Group
2501 S. Price Road MD OSC-N
Chandler, AZ 85248
602-732-3178
602-732-3171 (FAX)
E-mail: Dick_Astrom@sat.mot.com

Roy Axford
NRAD
53560 Hull St.
San Diego, CA 92152
619-553-3729
619-553-7190 (FAX)
E-mail: axfordra@nosc.mil

Robert Bauer
NASA Lewis Research Center
21000 Brookpark Rd., MS 54-6
Cleveland, OH 44135
216-433-3431
216-433-6371 (FAX)
E-mail: robert.bauer@lerc.nasa.gov

John Beaver
Colorado State University
EE Department
Ft. Collins, CO 80521
970-491-6758
970-491-2249 (FAX)
E-mail: beaver@engr.colostate.edu

Harvey Berger
TRW Space and Electronics Group
One Space Park
Redondo Beach, CA 90278
310-813-7692
E-mail: berger@emu.sp.trw.com

Scott Borgsmiller
Georgia Technology
5023 Ceylor Drive
Austell, GA 30001
770-739-7362
E-Mail: gt3681c@prism.gatech.edu

Atle Borsholm
New Mexico State University
Dept. of Elec. & Computer Engr.
Box 30001 - MSC 3-0
Las Cruces, NM 88003
505-646-3012
E-mail: aborshol@verdi.nmsu.edu

Greg Bostrom
NRAD
53560 Hull Street
San Diego, CA 92152
619-553-4422
E-mail: gbostrom@nosc.mil

Faramaz Davarian
Hughes Space & Communications
Bldg. S10, MS S352
2260 Imperial Highway
El Segundo, CA 90245
310-662-5375
310-662-7060 (FAX)
E-mail: fdavarian@ccgate.hac.com

Asoka Dissanayake
COMSAT Labs
22300 Comsat Drive
Clarksburg, MD 20871
301-428-4411
301-428-3638 (FAX)
E-mail: asoka.dissanayake@comsat.com

Bruce Dow
University of British Columbia
2356 Main Mall
Vancouver, British Columbia
Canada VGT 174
604-822-3980
604-822-5949 (FAX)
E-Mail: bdow@ee.ubc.ca

Carol Emrich
UCF/FSEC
1679 Clearlake Road
Cocoa, FL 32922
407-638-1507
E-mail: carol@fsec.ucf.edu

Julie Feil
Stanford Telecom
1761 Business Center Dr., Suite 300
Reston, VA 22090
703-438-7846
703-438-7921 (FAX)
E-mail: jfeil@sed.stel.com

Phillip Feldman
Rand
1700 Main Street, M-24
P.O. Box 2138
Santa Monica, CA 90407-2138
310-393-0411 - ext. 7273
E-mail: Phillip_Feldman@rand.org

Paul Flikkema
University of South Florida
4202 East Fowler Ave, ENB 118
Tampa, FL 33620
813-974-3940
813-974-5250 (FAX)
E-mail: flikkema@sunburn.eng.usf.edu

Julius Goldhirsh
Applied Physics Lab/JHU
Johns Hopkins Road
Laurel, MD 20723-6099
301-953-5042
301-953-5548 (FAX)
E-mail: julius_goldhirsh@jhuapl.edu

Nasser Golshan
Jet Propulsion Laboratory
4800 Oak Grove Drive, MS 161-260
Pasadena, CA 91109
818-354-0459
818-393-4643 (FAX)
Nasser.Golshan@jpl.nasa.gov

Henry Helmken
Florida Atlantic University
777 W. Glades Road, MS SE-456
Boca Raton, FL 33431
561-367-3452
561-367-2336 (FAX)
helmkenh@acc.fau.edu

Rudolph Henning
University of So. Florida, ENB 118
4202 E. Fowler Ave.
Tampa, FL 33620
813-974-4782
813-974-5250 (FAX)
E-mail: henning@eng.usf.edu

Hau Ho
TRW/Odyssey
One Space Park, E2/5063
One Space Park
Redondo Beach, CA 90278
310-812-1656
310-813-4719 (FAX)
E-mail: hau.ho@trw.com

Donald Hopkins
University of Alaska/EE Dept.
P.O. Box 755915
Fairbanks, AK 99775-5915
907-474-7815
907-474-6087 (FAX)
E-mail: fsdlh1@aurora.alaska.edu

Jerry Hopponen
Lockheed Martin Telecommunications
1272 Borregas Dr., MS O/GB-70, B/551
Sunnyvale, CA 94087
408-543-3194
E-mail: Jerry.Hopponen@lmco.com

Stephen Horan
Dept. of Elec. and Computer Engr.
New Mexico State University
Box 30001 - MSC 3-0
Las Cruces, NM 88003
505-646-3012
E-mail: shoran@nmsu.edu

Louis J. Ippolito
Stanford Telecom.
1761 Business Center Drive
Reston, VA 22090
703-438-8061
703-438-7921 (FAX)
E-mail: lippolito@sed.stel.com

Brad Jaeger
University of Alaska
Box 751705
Fairbanks, AK 99775
907-474-7815
907-474-6087 (FAX)
E-mail: fsbej1@aurora.alaska.edu

Jay Jones
Lockheed Martin Telecommunications
1272 Borregas Drive
Sunnyvale, CA 94087
408-543-3132
E-mail: Jay.Jones@lmco.com

Anil Kantak
Jet Propulsion Laboratory, MS 161-260
4800 Oak Grove Drive
Pasadena, CA 91109
818-354-3836
818-393-4643 (FAX)
E-mail: Anil.V.Kantak@jpl.nasa.gov

David Klemes
TRW Space & Electronics Group
MS R10/2352
One Space Park
Redondo Beach, CA 90278

Zlata Koro
Teledesic
2300 Carillon Point
Kirkland, WA 98033
206-602-6644
E-mail: zlata@teledesic.com

John Kurash
GTE Government Systems
15000 Conference Center Drive
Chantilly, VA 20151-3808
703-818-4341
703-818-5484
John.Kurash@gsc.gte.com

Richard Lilley
Harris Corporation
Box 91000, MS 1-5860
Melbourne, FL 32902
407-729-7588
E-mail: rlilley@harris.com

Patrick Loner
DirecTV, Inc.
2230 E. Imperial Highway
RE/R08/N353
El Segundo, CA 90245
310-726-4573
E-mail: pjloner@directv.com

Robert Manning
NASA Lewis Research Center
21000 Brookpark Road, MS 54-6
Cleveland, OH 44135
216-433-6750
215-433-6371 (FAX)
E-mail: robert.manning@lerc.nasa.gov

Remberto L. Martin
Hughes Communications
P.O. Box 9712
Long Beach, CA 90810-9928
310-525-5236
310-525-5250 (FAX)
E-mail: rlmarin@ccgate.hac.com

Ashok Mathur
DirecTV, Inc.
MS RE R8 N361
2230 Imperial Highway
El Segundo, CA 90245
310-726-4927
E-mail: amathur@directv.com

Charlie Mayer
University of Alaska, EE Dept.
P.O. Box 755915
Fairbanks, AK 99775-5915
907-474-6091
907-474-6087 (FAX)
E-mail: ffcem@aurora.alaska.edu

Azita Milanian
Telos Corporation/JPL
320 N. Halstead, Suite 260
Pasadena, CA 91107
818-306-6616
E-mail: amilanian@pop.jpl.nasa.gov

David Morabito
Jet Propulsion Laboratory
4800 Oak Grove Drive, MS 161-260
Pasadena, CA 91109
818-354-2424
818-393-4643 (FAX)
E-mail: David.D.Morabito@jpl.nasa.gov

Martin Parks
C.C.S.R. University of Surrey
Stag Hill
Guildford, Surrey GU25XH
+44 (0) 1483 300800, Ext. 2326
E-mail: Martin.Parks@ee.surrey.ac.uk

Eldad Perahia
TRW Inc.
One Space Park, MS/R10-1747
Redondo Beach, CA 90278
310-813-6038
E-mail: perahia@emu.sp.trw.com

Louis Peronard
Harris Corporation
P.O. Box 91000
Melbourne, FL 32902
407-729-3168
E-mail: lperonard@harris.com

Ken Peterson
Motorola
2501 S. Price Road, MS OSC-T
Chandler, AZ 85248
602-732-2997
602-732-2303 (FAX)
E-mail: P02983@email.mot.com

Robby Peterson
Hughes Information Technology Systems
16800 E. Centre Tech Parkway
MS 5M98
Aurora, CO 80011-9046
303-306-8167
E-mail: rpeterso@redwood.dn.hac.com

David V. Rogers
Communications Research Centre
3701 Carling Avenue
Ottawa, Ontario
Canada K2H 8S2
613-998-5174
613-998-4077 (FAX)
E-mail: dave.rogers@crc.doc.ca

Jim Rucker
Jet Propulsion Laboratory
4800 Oak Grove Drive, MS 161-260
Pasadena, CA 91109
818-354-0859
818-393-4643 (FAX)
E-mail: James.D.Rucker@jpl.nasa.gov

Kamran Shaik
ISCOMP Systems
5777 W. Century Blvd., #560
Los Angeles, CA 90045
310-641-3260
E-mail: kamran@spicenet.net

Fred Shimabukuro
Aerospace Corporation
2350 E. El Segundo Blvd.
El Segundo, CA 90245-4691
310-336-6903
310-336-6225 (FAX)
E-mail: shimabukuro@10.aero.org

Jennifer Sibits
NASA Lewis Research Center
MS 54-6
21000 Brookpark Road
Cleveland, OH 44135
216-433-6371 (FAX)

Paul Steffes
Georgia Institute of Technology
School of Elec. & Computer Engr.
Atlanta, GA 30332-0250
404-894-3128
E-mail: ps11@prism.gatech.edu

John Terry
Texas Instruments
6600 Chase Oaks Blvd., MS 8497
Plano, TX 75023
972-575-5884
972-575-6112 (FAX)
E-mail: J_Terry1@ti.com

Steve Townes
Jet Propulsion Laboratory, MS 238-420
4800 Oak Grove Drive
Pasadena, CA 91109
818-354-7525
818-354-6825 (FAX)
E-mail: Stephen.A.Townes
@jpl.nasa.gov

Arvydas Vaisnys
Jet Propulsion Laboratory, MS 161-260
4800 Oak Grove Drive
Pasadena, CA 91109
818-354-6219
818-393-4643 (FAX)
E-mail: Arvydas.Vaisnys@jpl.nasa.gov

Wolf Vogel
University of Texas
10100 Burnet Road
Austin, TX 78758
512-471-8608
512-471-8609 (FAX)
E-mail: Wolf_Vogel@mail.utexas.edu

Xuhe Wang
University of Oklahoma
100 E. Boyd, Rm. 1310
Norman, OK 73019
405-325-3658
405-325-7689 (FAX)
E-mail: xwang@tornado.gcn.ou.edu

Robert Weaver
University of Southern California
MC 2565 EEB 516
Los Angeles, CA 90089-2565
213-740-4686
213-740-8729 (FAX)
E-mail: rweaver@scf.usc.edu

David B. Westenhaver
WWW, Inc.
746 Lioness Ct. S.W.
Stone Mountain, GA 30087-2855
770-925-1091
707-931-3741 (FAX)
E-mail: wwwinc@crl.com

Allyson Yarbrough
The Aerospace Corporation
2350 E. El Segundo Blvd.
El Segundo, CA 90245
310-336-1499
310-336-6225 (FAX)
E-mail: yarbro@commsys.aero.org

Administrative Assistant
JPL:

Mardy Wilkins
818-354-7421
818-393-4643 (FAX)
E-mail: Mardith.J.Wilkins@jpl.nasa.gov

ACTS Electronic Mailing List
Address:
acts@java.jpl.nasa.gov